Proteomic and structural analysis of the Neuronal Src SH3 domain

Laura Christina West

PhD

University of York

Biology

January 2019

Abstract

The ubiquitous non-receptor tyrosine kinase C-Src functions in proliferation, migration and differentiation, and is well characterised in terms of the ligands, substrates and signalling pathways driving these functions. A neuronal-specific splice variant of C-Src, N1-Src, is formed by the insertion of six residues (RKVDVR) in the n-Src loop of the substrate binding SH3 domain. N1-Src is evolutionarily conserved in vertebrates and is expressed in both the developing and adult brain, where it is implicated in neuronal development, differentiation and morphology. However, the ligands and substrates through which N1-Src carries out these functions are unknown. This study aimed to assess the structural impact of the N1-Src insertion, and its effects upon the interactome and phosphoproteome of N1-Src.

The ligand and substrate specificity of C- and N1-Src were compared via mass spectrometry analysis of GST-SH3 domain pull-downs and a novel *in vitro* whole cell lysate kinase assay in a developmental neuronal lysate. Thirty three N1-Src SH3 domain ligands were identified as a lower affinity subset of the 176 C-Src ligands, suggesting that N1-Src could function as a tailored C-Src in neurons. Furthermore, N1-Src had 239 *in vitro* substrates, with the phosphorylation sites mapped in over 70 % of the proteins. The ligands and substrates of N1-Src enriched for Gene Ontology terms spanning neuronal development, differentiation, morphology and cytoskeletal regulation, in-line with its cellular functions. A number of the C- and N1-Src SH3 domain ligands were also *in vitro* substrates, providing strong candidates for follow up studies. Indeed, an uncharacterised neuronal isoform of the actin remodeller, Enah, was preferentially bound and phosphorylated by N1-Src.

The ligand consensus of the N1-Src SH3 domain was investigated by peptide arrays. Interestingly, the C- and N1-Src SH3 domains both selected for canonical Class I/II SH3 domain peptide ligands, and despite N1-Src interacting with a subset of C-Src ligands, they displayed differential peptide ligand binding profiles via nuclear magnetic resonance spectroscopy. The function of the N1-Src six residue insertion was investigated, and changes to the N1-Src SH3 domain were identified that could aid in explaining its tailored ligand binding, and importantly, N1-Src's increased catalytic activity. Taken together, these proteomic and structural studies have provided a solid basis for the structural and *in vivo* molecular characterisation of N1-Src.

Table of Contents

List of tables

Chapter 2

Chapter 3

Chapter 4

Chapter 5

List of figures

Chapter 1

Chapter 3

Chapter 4

Chapter 5

Acknowledgements

I would like to thank my supervisors Gareth and Jennifer, for their continual support and enthusiasm throughout this project. Thank you to my TAP panel, Michael and Harv for their support, and to the past and present lab members of the Evans and Potts groups. In particular, I wish to thank Dr Adam Dowle and Dr Alex Heyam for their expertise in mass spectrometry and NMR.

Declaration

I declare that this thesis is a presentation of original work and I am the sole author. This work has not previously been presented for an award at this, or any other University. All sources are acknowledged as references. All experiments were performed by the author, with the exception of LC-MS/MS, which was performed by Dr Adam Dowle (Metabolomics and Proteomics- Technology facility University of York).

Chapter 1

Introduction

Chapter 1 Introduction

1.1 Cellular signal transduction pathways and protein phosphorylation

Cellular signal transduction pathways are complex but controlled cascades that occur in response to external stimuli. Signalling pathways are comprised of a variety of small molecules and second messengers including calcium, cyclic adenosine monophosphate (cAMP) and lipids. They also comprise proteins, including enzymes (kinases, phosphatases, lipases, proteases), adapters/scaffolds, and diverse downstream targets including cytoskeletal regulators and DNA/RNA regulatory proteins. In addition, multiple points within a signalling pathway can be subject to positive or negative regulation, and there can be crosstalk between pathways. A key component of signal transduction is protein phosphorylation, which is the covalent addition of a phosphate group (PO_3^{2-}) onto the side chains of the residues serine, threonine, tyrosine, and less commonly, histidine and aspartate. Phosphorylation is a reversible post-translational modification (PTM) and is therefore tightly controlled by a balance between kinases, and their opposing phosphatases, which remove the phosphate by hydrolysis. The importance of this is highlighted in multiple diseases including cancers that are caused by dysregulated phosphorylation (Shchemelinin et al. 2006). Src kinase was first identified as its oncogenic mutant v-Src which contains an activating mutation (Sefton and Hunter 1986), and as such, kinases can also be considered druggable targets (Okamoto et al. 2010).

There are approximately 568 protein kinase domains in the human genome and up to 30 % of cellular proteins may be phosphorylated (Ardito et al. 2017). Thus, it is inevitable that phosphorylation impinges on most cellular processes. 518 human protein kinases have been classified as serine/threonine kinases, tyrosine kinases, or dual-specificity kinases that can phosphorylate all three residues (Ardito et al. 2017). Protein tyrosine phosphorylation was identified after serine and threonine phosphorylation, in part due to its lower abundance. It is estimated that the relative abundance of phospho-S/T/Y in vertebrate cells is 1800:200:1 respectively (Hunter 1998). The discovery of protein tyrosine phosphorylation was an accident, due to a change in pH of a chromatography buffer. Following acid hydrolysis from a ^{32}P- labelled *in vitro* kinase assay, chromatography revealed a product that resolved between the phosphoserine and phosphothreonine markers. This was identified as phosphotyrosine, which had

previously evaded detection by co-migrating with phosphothreonine (Eckhart et al. 1979).

Protein phosphorylation can exert its effects through several mechanisms and Src is an excellent example of this. Phosphorylation can act as molecular switch that activates or inhibits protein function. Src kinase activity is positively regulated by autophosphorylation of Y416, and negatively regulated by phosphorylation of Y527 (Roskoski 2004). Phosphorylation can also disrupt and/or create transient protein interactions. For example Src contains a phosphotyrosine binding Src homology 2 (SH2) domain, which forms an intramolecular interaction with its phosphorylated C-terminal residue Y527 (Murphy et al. 1993). Whereas in other instances, the phosphorylation of a residue that is structurally in proximity to an interaction motif may disrupt binding. The phosphorylation status of a protein might also regulate its subcellular distribution. Phosphorylation of Src has been shown to result in its translocation to a variety of structures including the cytoskeleton (Weernink and Rijksen 1995) and membrane ruffles (Hamadi et al. 2009). In addition, phosphorylation can prime neighbouring sites for processive phosphorylation. The protein Mint1 is tyrosine phosphorylated by Src, which then binds via its SH2 domain to carry out phosphorylation of a further two tyrosine residues (Dunning et al. 2016). Overall, the function of a protein's phosphorylation site can be diverse, and can have differing effects depending on the signalling context, therefore it must be assessed for each protein and scenario individually.

1.1.1 Receptor tyrosine kinases

Tyrosine kinases are broadly classified as receptor (RTKs) and non-receptor tyrosine kinases (nRTKs). Humans have 58 characterised RTKs that are classified into 20 subfamilies, all of which are cell surface receptors (Schlessinger 2000). Structurally, RTKs comprise an extracellular ligand binding domain, a transmembrane domain and a cytoplasmic region that provides the tyrosine kinase activity (Lodish et al. 2000). RTK's are activated by polypeptide growth factors binding to the extracellular domain, which induces receptor dimerisation, or in some cases oligomerisation. Ligand binding induces an active confirmation that stimulates the kinase activity and transphosphorylation of the kinase. Transphosphorylation in turn increases the catalytic efficiency and the kinase further auto-phosphorylates. Phosphotyrosine-rich patches are able to scaffold and

recruit interactors containing domains such as SH2 and phosphotyrosine binding (PTB) domains. These docking proteins can then interact with and accumulate more proteins, generating large multi-protein signalling complexes that are able to propagate the signal downstream (Lemmon and Schlessinger 2010; Ségaliny et al. 2015). Examples of receptor tyrosine kinases include the Epidermal growth factor receptor (EGFR), Fibroblast growth factor receptor (FGFR) and Platelet-derived growth factor receptor (PDGFR) (Schlessinger 2000), which are activated by their ligands EGF, FGF and PDGF respectively. Non-receptor tyrosine kinases are often found signalling alongside, or downstream of RTK's. For example the nRTK, C-Src, phosphorylates the EGF receptor (Biscardi et al. 1999; Stover et al. 1995), and mutation of one of the sites reduced the downstream DNA synthesis that is induced upon receptor activation (Kloth et al. 2003).

1.2 Non receptor tyrosine kinases: The Src family kinases

The Src family kinases (SFKs) are one of nine families of non-receptor protein tyrosine kinases (Gocek et al. 2014), which differ from RTK's due to their cytoplasmic localisation, however, some nRTKs, including the SFKs, associate with intracellular membranes. C-Src, the founding member of the SFKs, was first identified as its oncogenic mutant v-Src that was carried by the Rous sarcoma virus (RSV). Src was identified as a kinase via immunoprecipitation with viral anti-sera from RSV infected cells. The immunoprecipitated extract contained Src and resulted in the incorporation of ^{32}P, providing the first link between Src and kinase activity (Collett and Erikson 1978). The *in vivo* tyrosine kinase activity of Src was confirmed by ^{32}P labelling of RSV infected cells, which revealed a 7-8 fold increase in tyrosine phosphorylation in comparison to those uninfected (Hunter and Sefton 1980).

The SFKs are present only in multicellular animals (Brown and Cooper 1996) and C-Src is present in both vertebrates and invertebrates (Parker et al. 1985; Hoffmann et al. 1983). In humans the Src family consists of 11 members, Src, Fyn, Yes, Blk, Yrk, Frk, Fgr, Hck, Lck, Srm and Lyn (Manning et al. 2002). The SFKs can be broadly grouped based on their expression. Src is expressed in all cell types (Roskoski 2004) and Fyn and Yes are also in most tissues. However, expression varies between tissues and Src has 5-200 fold higher levels in platelets, neurons, and osteoclasts (Brown and Cooper 1996). Blk, Fgr, Hck, Lck and Lyn are primarily haematopoietic (Bolen and Brugge 1997) and

Frk in epithelial cells. Therefore a single cell type can express multiple SFKs, which has made deciphering their individual functions challenging. Further diversity is generated by splicing as Src and Fyn undergo splicing to generate neuronal isoforms termed N1-Src, N2-Src and FynB respectively (Rouer 2010; Goldsmith et al. 2002).

The SFKs have been intensely studied due to their participation in diverse cellular events including proliferation, differentiation, adhesion, migration and cytoskeletal remodelling (Thomas and Brugge 1997). The signalling pathways for many of these have been dissected, resulting in the assignment of a variety of ligands and substrates. The structure and function of the kinases' individual domains have also been investigated. The conserved domain architecture of the SFKs, termed Src homology domains (SH) is shown in Fig.1.1. The SFKs comprise an SH4, unique domain, SH3, SH2 and SH1/kinase domain, as well as a C-terminal tail containing a key regulatory residue (Y527). The function of each domain will be discussed in the proceeding sections.

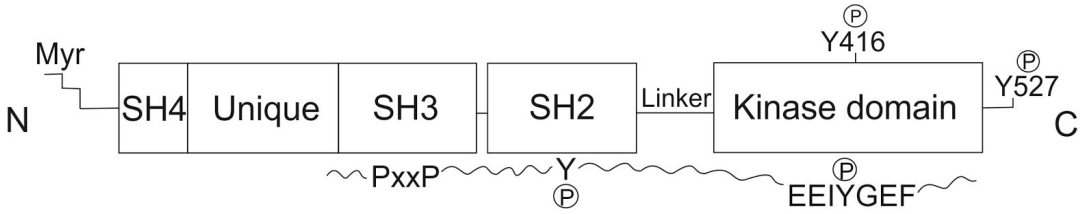

Figure 1.1 The domain structure of the Src family kinases and features of their substrates. The N-terminal SH4 domain undergoes myristoylation and then palmitoylation (excluding Src and Blk) to enable membrane association. The highly variable unique domain undergoes a number of post-translational modifications as well as interacting with the SH3 domain and lipids. The SH3 domain binds proline rich ligands within binding proteins and kinase substrates. The SH2 domain also binds the kinase ligands and substrates via phosphotyrosine motifs, which can enable processive phosphorylation by the kinase. The SH1/kinase domain provides the tyrosine kinase activity to enable substrate phosphorylation (ideal substrate sequence depicted). The domain also contains the residue Y416, which is auto- or trans- phosphorylated to stabilise the kinases active conformation.

1.2.1 The Src SH4 domain and membrane localisation

To participate in signalling, Src cycles between the plasma membrane and other intracellular membranes resembling late endosomes/lysosomes (Resh 1993). Src associates with membranes via its SH4 domain at the N-terminus of the protein. SH4 domains are approximately 15-17 amino acids and are myristoylated on the consensus motif of MGxxx(S/T/C). Myristoylation occurs via the formation of an amide bond between the N-terminal glycine residue (G2) and myristic acid, which occurs co-translationally after the initiating methionine is cleaved (Resh 1994). Myristoylation

is a permanent and essential modification as Src mutants lacking myristoylation do not associate with membranes or conduct downstream signalling (Kamps et al. 1985). In addition, SH4 membrane association is enhanced by three lysine residues interacting with negatively charged lipid headgroups (Resh 1999).

With the exception of Src and Blk, SFKs are also palmitoylated. Palmitoylation occurs after myristoylation and is the covalent addition of the fatty acid palmitate onto the side chains of the cysteine residues (C3, C5 or C6). Unlike myristoylation, palmitoylation is reversible, thus providing a means of regulation (Resh 1999). The SFKs vary in their ability to be mono or dual palmitoylated, and their palmitoylation status is important for cellular trafficking. Indeed, mutation of the palmitoylated cysteine residue in Lyn generated trafficking similar to Src (Kasahara et al. 2007). Similarly, chimeric SFKs generated by swapping their SH4 domains revealed three main pathways for trafficking depending on their lipid modifications (Sato et al. 2009). The authors proposed that i) myristoylation alone mediates late endosome/lysosome to plasma membrane cycling ii) mono-palmitoylation drives traffic from the Golgi to the plasma membrane via the secretory pathway, and iii) dual palmitoylation directly targets the kinase to the plasma membrane. This has since been assigned some molecular basis, for example Fyn localises to the Golgi due to palmitoyl acyl-transferase, and Src is concentrated at endosomes due to the UNC119 and Arl2/3 proteins, and electrostatic interactions of its SH4 domain with the endosome membrane (Konitsiotis et al. 2017).

The mechanism of Src translocation and cycling from endosomes/lysosomes to the plasma membrane was shown to require the cytoskeleton as the actin disrupting drug cytochalasin D prevented the translocation of C-Src to the cell periphery. Although kinase dead v-Src was able to translocate (Fincham and Frame 1998), the translocation process was shown to activate Src, so that it formed a gradient of activity from the perinuclear region to the plasma membrane where Src was most active (Sandilands et al. 2004). Knockout of the actin cytoskeletal regulatory protein RhoB in cells resulted in the loss of Src activation and translocation, and Src and RhoB were shown to co-localise in translocating intracellular structures, which was prevented by cytochalasin D. Thus it was concluded that Src resides in RhoB associated endosomes that utilise the actin cytoskeleton to enable Src translocation (Sandilands et al. 2004). The SH4 domain was shown to be responsible for this behaviour, as Src SH4 domain mutants that gained

palmitoylation behaved like Fyn, and were resident in RhoD associated endosomes. Similarly, Fyn mutants lacking wild-type palmitoylation behaved like C-Src, co-localising with RhoB endosomes that were required for both its activation and translocation (Sandilands et al. 2007). Thus the SH4 domain plays a key role in the activation and localisation of the SFKs.

Evidence for the regulation of membrane association beyond the SH4 domain was obtained by fusion proteins of Src with the cytoplasmic protein pyruvate kinase (PK) (Kaplan et al. 1990). The Src fusion proteins all contained the myristoylation sequence, but truncated at either the unique, SH3 or SH2 domain. Interestingly, the mutants resulted in variable distributions between cytoplasmic granules, the plasma membrane and perinuclear membranes, suggesting that other domains function alongside the SH4 domain to direct localisation (Kaplan et al. 1990). In line with this, recent literature has shown that both the C-Src unique and SH3 domain also bind lipids (Pérez et al. 2013).

1.2.2 The Src Unique domain

Amongst SFKs the variable SH4 domain defines unique functions via their differential lipid modifications and cellular trafficking. Further variation is generated by the proceeding unique domain, a 50–90 residue domain that is intrinsically disordered and displays the lowest sequence conservation amongst SFK domains. However, individual unique domains are conserved across species (Amata et al. 2014). The unique domain has been shown to regulate kinase activity, undergo post-translational modifications, interact with lipids and participate in intramolecular interactions with the Src SH3 domain (Pérez et al. 2009; Pérez et al. 2013; Shenoy et al. 1992).

Surprisingly, (Pérez et al. 2009) demonstrated an interaction between the Src SH4-unique domain and SH3 domain via NMR. Chemical shift perturbations (CSPs) were observed throughout the unique domain and in the n-Src and RT loops of the SH3 domain, which partake in ligand binding. Titrations of a proline-rich SH3 domain peptide ligand abolished the interaction between the SH3 and unique domain. However, this was through an allosteric effect as the unique domain was shown to bind on the opposite side to the canonical SH3 ligand binding site. Interestingly, the unique domain was also shown to bind lipids via the same region that interacts with the SH3 domain (Pérez et al. 2009). The authors suggested that interactions of the unique domain with

the SH3 domain and lipids may represent an additional layer of kinase regulation that will be further discussed in Section 1.2.7.

The Src SH4 and unique domain are phosphorylated on residues S12, S17, T37 and S75 (Pérez et al. 2009). To assess the function, an SH4-unique domain construct was *in vitro* phosphorylated at S17, T37 and S75 by protein kinase A (PKA) and cyclin dependent kinase 5 (CDK5). NMR analysis revealed that p-S17 abolished the SH4 domain interaction with lipids, but not the unique domain, whereas p-T37/p-S75 had no effect on the SH4 domain, but significantly reduced lipid binding by the unique domain. The CSPs of the phosphorylated constructs were local around the phosphorylated serine and threonine residues, suggesting that the effects were not conformational, and likely electrostatic, particularly for p-S17, which disturbed a positively charged patch that contributes to lipid binding (Pérez et al. 2013; Pérez et al. 2009).

Biological context has been assigned to the phosphorylation of the unique domain. For example, active Src translocates from the cell periphery to the cytoplasm upon stimulation of the PDGF receptor. The translocation correlated with the phosphorylation of serine/threonine residues in Src's N-terminus, and was blocked by a PKA inhibitor (Walker et al. 1993). The authors speculated that the translocation was caused by changes to electrostatic interactions, which was confirmed by the NMR study of the phosphorylated unique domain (Pérez et al. 2009). In addition, mutation of the serine/threonine phosphorylation sites prevented the increase in kinase activity observed for Src during mitosis (Shenoy et al. 1992). This suggests that the unique domain phosphorylation can also play an activatory role. Furthermore, a striking phenotype has been observed during the maturation of *Xenopus laevis* oocytes, where mutation of the conserved serine and threonine phosphorylation sites in Src resulted in defects and subsequently death in ~50 % of the mutants (Pérez et al. 2013). Thus SH4/unique domain phosphorylation modulates both the localisation and activation status of Src.

1.2.3 The Src SH3 domain

SH3 domains are approximately 60 amino acid residues in length and function as protein-protein interaction domains in eukaryotes (Kaneko et al. 2008). The human genome contains 296 SH3 domains (Kärkkäinen et al. 2006), which are present in diverse signalling proteins including the SFKs. The Src SH3 domain functions to

regulate kinase activity via intramolecular interactions, and importantly to direct intermolecular interactions with proline rich ligands and substrates.

The Src SH3 domain can act to scaffold and target the kinase to subcellular locations, often in cooperation with the phosphotyrosine-binding SH2 domain (Section 1.2.4). For example, peptides from focal adhesion kinase (FAK) that contained both the C-Src SH2 and SH3 domain ligand motifs bound Src with increased affinity, and activated Src *in vitro* (Thomas et al. 1998). The Src SH3 domain also has a key role in directing substrate phosphorylation. For example, mutation of the Src SH3 domain binding site in FAK reduced FAK phosphorylation by Src (Thomas et al. 1998). Similarly, the mutation of the Src SH3 domain binding site in Sam68, or competing concentrations of Sam68 proline rich peptides, prevented Sam68 phosphorylation by Src (Shen et al. 1999). The expression in cells of C-Src with an SH3 domain deletion also resulted in reduced phosphorylation of Src ligands (Weng et al. 1994). Thus the SH3 domain can be key for substrate interactions and subsequent phosphorylation. Other examples of Src ligands that contain SH2 and SH3 ligand motifs include p130Cas, paxillin and Sam68; all three of which are phosphorylated by Src (Sachdev et al. 2009).

The structure of the C-Src SH3 domain has been solved by crystallography (Musacchio et al. 1992) and NMR (Yu et al. 1992). The SH3 domain comprises five antiparallel beta strands that form two beta sheets, each sheet consists of three strands with one shared (Fig.1.2). There is also a 3-10 helix between the beta-strands B4 & B5, and in addition two variable loops termed the RT and n-Src loops (Fig.1.2). The ligand binding site has been identified by NMR with the C-Src SH3 domain and proline rich peptide ligands, which are generally low affinity (Kd ~ 1-100 μM) (Stamenova et al. 2007).

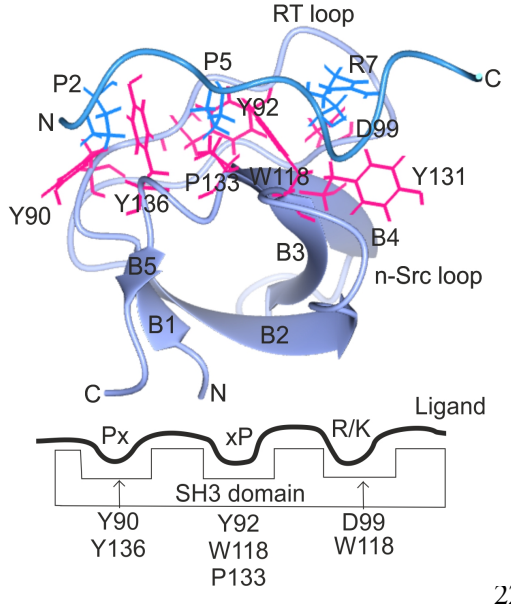

Figure 1.2: The C-Src SH3 domain in complex with a Class II ligand.
The solution structure of the C-Src SH3 domain (purple) in complex with a Class II peptide ligand (blue; PDB:1QWE). The C-Src beta strands (B1-B5) are shown, and the n-Src and RT loops. The residues contributing to the core binding pockets (Y90, Y92, D99, W118, Y131, P133 and Y136) are depicted in pink, and the peptide ligand (P2, P5 and R7) in blue.

The defining feature of the SH3 domain is its interaction with proline-rich ligands. Early studies identified PxxP as the minimal consensus for SH3 ligands via phage display and peptide ligand mutagenesis (Feng et al. 1994). The PxxP motif is present in two types of ligand, Class I (+xxPxxP) and Class II (PxxPx+) (+ is positively charged), which adopt a polyproline type II helix (PPII). The two classes of ligand bind the SH3 domain in reverse backbone orientations as the charged residue is N-terminal for Class I ligands and C-terminal for Class II ligands. The SH3-ligand interaction involves three core pockets. The specificity pocket is formed by D99 and W118 and it accommodates the positively charged residue, which flanks the PxxP motif via the formation of a salt bridge with the SH3 domain RT loop residue D99 (Feng et al. 1995a). There are also two hydrophobic pockets that each accommodate a proline residue as a xP di-peptide (Feng et al., 1994). The first pocket is formed by the residues Y90 and Y136, and the second by Y92, Y131, W118 and P133 of the SH3 domain. The importance of these residues in SH3-ligand interactions is clear as GST-SH3 domain alanine mutants of Y90, Y92, Y136, P133 and W118 all abolished ligand binding via pull-downs in a lysate (Erpel et al. 1995). Similarly, pull-downs with a D99N GST-C-Src SH3 domain mutant reduced binding to most proteins in a cellular lysate. Those that were retained were referred to as 'D99-independent' ligands, that appear to bind by alternative contacts (Weng et al. 1995). However, the simple model of SH3 domains binding PxxP motifs is not compatible with their diverse ligand specificity, which can be influenced by a number of factors that will be discussed in the proceeding sections.

The orientation of the conserved 'tryptophan switch' (W118 of the SH3 domain) is able to direct Class I/II ligand binding. Interestingly, the conformation of the tryptophan depends on the residue at position 131, and the aromatic amino acids (Y/W/F) at this position all enable the tryptophan to bind Class I/II ligands. A single point mutation to I or M hinders the movement of the tryptophan to direct Class II specificity (Fernandez-Ballester et al. 2004). However, 75 % of SH3 domains do not possess the restrictive amino acids, suggesting that the tryptophan switch is only a small element in determining specificity (Fernandez-Ballester et al. 2004).

The phage display technique has played a major role in determining SH3 domain ligand specificity, and has yielded motifs such as the Class I RPLPxxP (Cheadle et al. 1994). A large screen of 115 SH3 domains by phage display revealed that only 66 SH3 domains

bound Class I/II motifs. Thus, half of the SH3 domains bound non-canonical motifs (Teyra et al. 2017). The study included the C-Src SH3 domain and the SH3 domain of its neuronal splice variant N1-Src. C-Src was characterised as a Class I/II binder, in line with the literature. The N1-Src SH3 domain also interacted with Class I peptides, but surprisingly peptides from 'Class IX', which contained SH3 domains with diverse non-canonical specificities. The N1-Src SH3 domain was also more selective, and bound a total of 204 unique peptides, in contrast to 1364 by the C-Src SH3 domain (Teyra et al. 2017).

It has become increasingly clear that additional SH3-ligand interactions occur outside of the core ligand motif, in a region termed the 'specificity zone' (Saksela and Permi 2012). The specificity zone contains the D99 charge binding pocket, and can function alongside or without it. However, it also contains additional sub-pockets that make affinity and specificity contacts, and between SH3 domains the specificity zone is structurally diverse (Saksela and Permi, 2012). Unsurprisingly, the specificity zone is flanked by the variable n-Src and RT loops (Fig.1.3). The influence of the RT loop on ligand selection has been demonstrated using random hexapeptide mutants of the Hck SH3 domain RT loop, where mutants were generated that bound wild-type ligands with higher affinity, and in some instances novel ligands (Hiipakka and Saksela 2007).

The Eps8 family of SH3 domains highlights the function of the n-Src loop in determining ligand specificity. Due to a positively charged R/K residue in the n-Src loop (Fig.1.3), the SH3 domain selects a PxxDY motif, via the formation of a salt bridge with the aspartate residue. In addition, the Eps8L1 SH3 domain does not bind PPII helical peptides, and only the second hydrophobic binding pocket is utilised, as the first pocket is dysfunctional due to a distorted conformation (Aitio et al. 2008). Interestingly the Nck-a SH3 domain also binds PxxPxxDY motifs via a positively charged residue in its n-Src loop. However, unlike Eps8L1, Nck binds ligands that have a PPII helix (Santiveri et al. 2009). Thus, SH3 domains can bind similar motifs by different mechanisms.

Further examples of alternative binding modes by the n-Src loop include the amphiphysin II isoform that has an acidic insertion in its n-Src loop (Fig.1.3), which aids its interaction with basic residues in the dynamin I proline rich domain (Owen et al. 1998). A residue in the n-Src loop of the Csk SH3 domain also contributes to high affinity interactions with residues flanking the PPII helix (Ghose et al. 2001).

Interestingly, in the *Candida albicans* Rvs167-3 SH3 domain, which has a 10 residue n-Src loop insertion, mutation of only two residues abolished binding, whereas other conserved residues had no effect (Gkourtsa et al. 2016). In addition, the n-Src loop can also have steric effects, for example the Abl SH3 domain was unable to bind a Src SH3 domain peptide ligand due to steric clashes with its n-Src loop (Feng et al. 1995a).

The Mlk3 SH3 domain contains a six residue insert in the n-Src loop (Fig.1.3) that undergoes a large conformational change upon peptide binding. Interestingly, the Mlk3 SH3 domain bound a canonical proline rich peptide ligand via the characterised binding site, but also an atypical peptide ligand at a novel site formed by the n-Src loop and B3 strand (Kokoszka et al. 2018). The Fyn SH3 domain also binds Class I and an atypical RKxxYxxY motif (Kang et al. 2000), and the N1-Src SH3 domain has been reported as binding canonical and atypical motifs via phage display (Pérez et al. 2013; Teyra et al. 2017; Keenan et al. 2017). However, there is minimal literature on whether the atypical interactions are physiological.

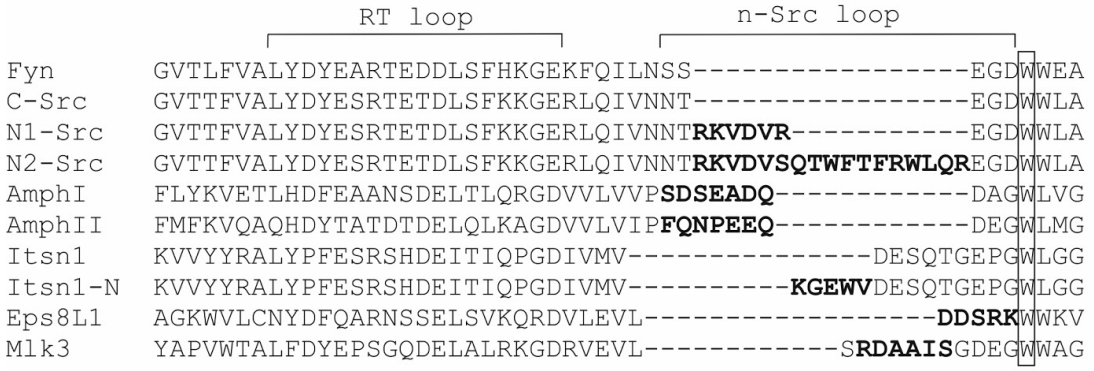

Figure 1.3: Sequence alignment of SH3 domain splice variants and isoforms. Alignment of the human SH3 domains Fyn, C-Src and its neuronal specific splice variants N1- and N2-Src, the Amphiphysin I and II isoforms, Intersectin 1 and its neuronal specific splice variant, Eps8L1 and Mlk3. The residues spanning the SH3 domains variable RT- and n-Src loops are indicated, and those from specific isoforms are shown in bold. The conserved tryptophan residue that is essential for ligand binding is boxed.

Due to their diverse binding capacity, it is unsurprising that some SH3 domains undergo splicing (Fig.1.3). Both the C-Src and intersectin I SH3 domains are spliced to generate neuronal specific variants. The splicing of intersectin I inserts five residues (KGEWV) into the start of the n-Src loop (Fig.1.3). This displaces negatively charged residues in the SH3 domain towards the interaction interface, which results in high affinity binding to ligands that have positively charged flanking residues (4-5 residues downstream of the PxxP motif) (Dergai et al. 2010). Intersectin I and its neuronal isoform vary in their

affinity for ligands (Tsyba et al. 2008). The neuronal splicing of the C-Src SH3 domain to generate N1- and N2-Src inserts 6 and 17 residues into the centre of the n-Src loop respectively (Fig.1.3), suggesting they could be directly involved in binding as opposed to a displacement mechanism.

Whilst amino acids flanking the core ligand motifs can function as specificity/affinity determinants, residues at an even greater distance have since been identified. (Luo et al. 2016) analysed the binding of the syndapin SH3 domain to the dynamin I proline rich domain (PRD) by NMR. Interestingly, CSPs were observed around the characterised PxxP ligand, however there were also CSPs of a similar magnitude in residues that were nine and > 50 residues away from the binding site. These two sites were termed short (SDE) and long distance elements (LDE) respectively. Point mutations of the SDE and LDE residues abolished binding, however neither site bound independently of the PxxP motif, suggesting that they provide an additional affinity element (Luo et al. 2016).

SH3 domains may also be regulated by tyrosine phosphorylation. The Y90 residue of the C-Src SH3 domain that forms the first proline binding pocket, has been found to be phosphorylated in cells (Hornbeck et al. 2015). The equivalent residue of the Cas SH3 domain is phosphorylated *in vivo,* and GST-SH3 domain pull-downs with its phosphomimetic mutant (Y12E) disrupted ligand binding, whereas the phospho-null (Y12F) had no effect (Janoštiak et al. 2011). The crystal structure of the tyrosine phosphorylated Abl1 SH3 domain has since been obtained, confirming that the phosphorylation sterically blocks the ligand binding pocket (Merő et al. 2019).

In summary SH3 domain ligand specificity is regulated by:

- Cellular context; the expression profile and cellular localisation of the SH3 domain containing protein and its ligand.
- A preference for Class I or II motifs (tryptophan switch), atypical motifs, and the sequence closely flanking these motifs.
- Structural determinants of the ligand; PPII helix or atypical ligands.
- SH3 domain structure including the utilisation of hydrophobic binding pockets, steric inhibition, and importantly the interactions with the structurally diverse specificity zone formed by the variable n-Src and RT loops.
- Additional long and short distance affinity elements within the ligand.

- Putative tyrosine phosphorylation of the SH3 domain.

The C-Src SH3 domain is also essential for the formation of intramolecular interactions that regulate kinase activity. The C-Src SH3 domain interacts with a linker between the SH2 and SH1 domain in order to inactivate the kinase (Roskoski 2005). The expression of Src mutants lacking the SH3 domain result in an upregulation of phosphotyrosine content (Erpel et al. 1995). Similarly, mutation of the linker elevates both auto- and substrate phosphorylation by the kinase (Briggs and Smithgall 1999). The SH3 domain can also activate the kinase upon forming ligand interactions to relieve the negative regulatory conformation (Fig.1.6).

1.2.4 The Src SH2 domain

Proceeding the SH3 domain is the non-catalytic SH2 domain. SH2 domains are approximately 100 residue phosphotyrosine-binding domains, there are 111 SH2-domain containing proteins in the human genome including kinases, phosphatases, cytoskeletal regulators and scaffold/adaptors (Kükenshöner et al. 2017; Liu et al. 2011). SH2 domain containing proteins are often found associated with the phosphotyrosine rich regions generated by receptor tyrosine kinases. Similar to the SH3 domain, the Src SH2 domain is multifunctional participating in the regulation of cellular localisation, kinase activity and substrate/ligand interactions.

One function of the Src SH2 domain is to bind the kinase's ligands and substrates. A number of phosphotyrosine containing proteins were identified following pull-down with the GST-Src SH2 domain from v-Src transformed cells (Koch et al. 1992). Phosphopeptide libraries revealed that the Src SH2 domain selects for a p-YEEI motif, and this resembles the consensus phosphorylation motif of the kinase domain (Songyang et al. 1993) (Section 1.2.5). Therefore, the SH2 domain can enable Src to anchor to its phosphorylated substrates and conduct multisite processive phosphorylation (Dunning et al. 2016; Pellicena et al. 1998).

The Src SH2 domain binds ligands via two hydrophobic pockets, the first accommodates the pY+3 residue, and the second is a deep pocket that binds phosphotyrosine. The acidic glutamate residues of the p-YEEI motif orientate towards basic residues on the surface of the SH2 domain (Waksman et al. 1993). Affinity and selectivity is obtained by the flanking residues, generally the 3-6 residues C-terminal to the phosphotyrosine

residue (Liu et al. 2006). Furthermore, residues that do not make direct contacts can also regulate binding through electrostatic repulsion and structural restrictions. SH2 domains are also highly selective, even towards conservative mutations, as the Crk SH2 domain bound leucine at pY+3 but not isoleucine or valine. Similarly, the Grb SH2 domain favoured glutamate at pY+1 but not aspartic acid (Liu et al. 2010).

In terms of negative regulation of kinase activity, the SH2 domain contributes to Src inactivation via its intramolecular interaction with the phosphorylated C-terminal residue p-Y527 (chicken Src numbering) to form the repressed conformation. The SH2 domain also contributes to positive regulation of kinase activity via the formation of interactions with phosphotyrosine ligands to relieve the negative regulatory conformation (Section 1.2.6/7) (Roussel et al. 1991; Seidel-Dugan et al. 1992).

1.2.5 The Src SH1/Kinase domain

The Src SH1/kinase domain possesses the catalytic tyrosine kinase activity. Active Src binds MgATP and its substrate, and the γ-phosphate of ATP provides the phosphoryl group (PO_3^{2-}) that is transferred to the substrate tyrosyl group, which is then released alongside MgADP (Roskoski 2004).

The Src catalytic domain consists of a small N-terminal (N), and large C-terminal (C) lobe, and together the lobes form the active site (Fig.1.4A). The bi-lobed structure is conserved in both serine/threonine and tyrosine kinases (Huse and Kuriyan 2002). The two lobes contain polypeptides that adopt active and inactive conformations. In the small lobe this is the ‘C-helix’, and in the large lobe, a loop termed the ‘activation loop’ that contains the activatory residue Y416 (Williams et al. 1997; Harrison 2003). A structure termed the regulatory spine is formed by residues from the N- and C-lobes, including the C-helix and activation loop. The spine can be made and broken to activate and inactive the kinase (Xu, Harrison, and Eck 1997).

The kinase domain contains four residues constituting the ‘K/E/D/D’ motif, which is critical for ATP, magnesium and substrate binding. The highly conserved K295 (**K**/E/D/D) of the N-lobe is a phosphate binding lysine that interacts with ATP. A glycine rich loop (G-rich loop) from the N-lobe, and residues from the C-lobe also support ATP docking (Roskoski 2004, 2015), including D404 of the activation loop that binds magnesium, which in turn orientates the ATP. The residue D386 of the C-lobe, is present

in a region termed the catalytic loop, and it functions to orientate and prepare the substrates tyrosyl group (Roskoski 2004; Huse and Kuriyan 2002; Roskoski 2015). In addition, K295 also forms a salt bridge with E310 of the C-helix that is essential for the formation of Src's active state (Fig.1.4B). As such, kinase dead mutants are generated by the mutation of this residue (K295M; (Florio et al. 1994).

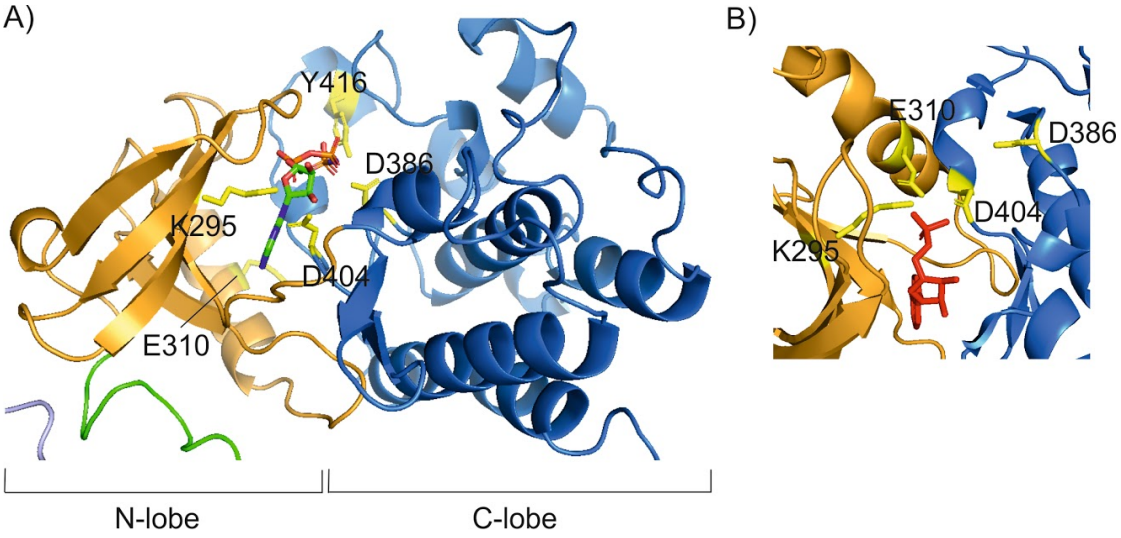

Figure 1.4: The structure of the inactive and active C-Src kinase domain. A) The structure of the inactive C-Src kinase domain in complex with adenylyl-imidodiphosphate (AMP-PNP). The N- (orange) and C-lobes (blue), K/E/D/D motif residues K295, E310, D386 and D404 and Y416 (yellow) that is auto-phosphorylated upon activation are shown (PDB 2SRC). This conformation orientates the C-helix to prevent the K295:E310 salt bridge that is essential for activity. B) The structure of the activated C-Src kinase domain (Thr338Ile) in complex with ATPgS (PDB 3DQW). The K/E/D/D motif residues K295, E310, D386 and D404 (yellow) are shown, including the salt bridge between K295:E310 that occurs upon activation.

The catalytic activity of Src involves two major conformational changes, the first is the generation of an active kinase from its inactive state (Fig 1.6), and the second is the activated kinase domain cycling between its open and closed forms, to bind substrate and ATP, and then release p-Y substrate and ADP. When inactive Src forms intramolecular interactions via its SH2 and SH3 domains, and the activation loop adopts a conformation whereby the side chain of Y416 is concealed. The activation loop also orientiates the C-helix to prevent the K295:E310 salt bridge and the regulatory spine assumes a 'broken' conformation (Fig.1.4A). Upon the disruption of the intramolecular interactions by the formation of SH2/SH3 domain-ligand interactions (Section 1.2.7), the activation loop and C-helix adopt active conformations, enabling the K295:E310 salt bridge (Fig.1.4B), and auto/trans-phosphorylation of Y416 to stabilise the regulatory

spine and lock the kinase in an active state (Xu et al. 1999; Roskoski 2004; Huse and Kuriyan 2002; Sugimoto et al. 1985; Roskoski 2015). The active kinase then cycles between open and closed conformations. The open kinase binds Mg-ATP and the protein substrate, and catalysis occurs during closing. Upon reopening, the phosphorylated substrate and Mg-ADP are released, ready for a new cycle (Roskoski 2015).

Peptide library screening identified EEEIY[G/E]EFD as an optimal v-Src substrate motif (Songyang and Cantley 1995). Interestingly, the acidic residues are selected for by some phosphatases, demonstrating that there was co-evolution to add and remove phosphate. Phosphorylation motifs can often tolerate amino acid substitutions, suggesting that whilst the kinase domain has sequence preference, the overall determinants go beyond this *in vivo* (Roskoski 2004). This likely includes factors such as phosphorylation site accessibility, and co-localisation/scaffolding to ligands.

1.2.6 The Src C-terminal domain (CTD)

The C-terminal domain (CTD) of Src contains a key regulatory residue, Y527, which is conserved in all other vertebrate Src family kinases and inhibits Src activity when phosphorylated. Y527 is phosphorylated by C-terminal Src kinase (Csk), which is expressed in most tissues, including high levels in the developing brain (Inomata et al. 1994). Csk is capable of regulating both C-Src and its neuronal isoform N1-Src (Inomata et al. 1994). A phosphopeptide library revealed that the Csk SH2 domain selected for a motif resembling Src's p-Y416 motif (Songyang et al. 1994), suggesting it could be a means of targeting Csk to activated Src. However, p-Y527 was readily detected in a Src Y416F mutant suggesting that SH2 domain docking via Csk is not the only means to achieve Y527 phosphorylation *in vivo* (Kmiecik and Shalloway 1987). The importance of negative regulation of the SFKs is apparent in mice deficient for Csk, which exhibit embryonic lethality, likely caused by an 11-fold increase in Src activity, and increased cellular protein tyrosine phosphorylation (Imamoto and Soriano 1993). Csk homologous kinase (Chk) also phosphorylates Y527, and interestingly, whilst Csk has a higher catalytic activity, Chk possesses greater inhibitory properties. This occurs by a non-catalytic mechanism, which involves high affinity binding of the Chk kinase domain to activated SFKs (Advani et al. 2017). In addition, Src may also autophosphorylate at Y527, which could form a negative feedback loop, however this has not been confirmed *in vivo* and could be an *in vitro* artefact (Osusky, Taylor, and Shalloway 1995).

The Src SH2 domain interacts with p-Y527 to induce a negative regulatory conformation that suppresses kinase activity. This was demonstrated using immobilised phospho- and dephospho Y527-containing peptides. C-Src interacted with the p-Y527 peptide, and this was abolished by an SH2, but not SH3 domain deletion. Furthermore, the phosphopeptide inhibited C-Src auto-phosphorylation in a kinase assay, suggesting it was also negatively regulating kinase activity (Roussel et al. 1991). Consistent with this, the mutation of Y527 to a serine or phenylalanine, or premature truncation of C-Src at residues 518 or 523, all stimulate *in vivo* tyrosine kinase activity, whereas truncation at residue 530 had no effect (Reynolds et al. 1987). Similarly, SH2 domain mutations also activate kinase activity in *vivo,* likely through the loss of interaction with p-Y527 (Seidel-Dugan et al. 1992).

p-Y527 is also dephosphorylated by phosphatases that activate Src. Phosphatases including Pest (Chellaiah and Schaller 2009), PTPα (Chen, Chen, and Pallen 2006), PTP1B (Dadke and Chernoff 2003), Syp (Peng and Cartwright 1995), and Shp1 (Somani et al. 1997) have all been identified, and integrate into signalling pathways to activate Src. For example, Src participates in EGFR signalling and PTPα is positively regulated in response to EGF stimulation (Wang et al. 2013).

1.2.7 Regulation of Src activity

The crystal structure of human C-Src revealed how the SH3 domain, SH2 domain and C-terminal tail all contribute to forming intramolecular interactions to regulate Src activity (Xu et al. 1999). In the inactive conformation, the SH2 domain interacts with the C-terminal p-Y527 residue (Williams et al. 1997; Roussel et al. 1991; Xu, Harrison, and Eck 1997), and the SH3 domain interacts with the linker between the SH2 and SH1 domains (Xu, Harrison, and Eck 1997; Briggs and Smithgall 1999). In this conformation the catalytic domain is locked and inactivated (Roskoski 2004) (Fig.1.5).

The inactive Src structure is destabilised by a number of mechanisms, including dephosphorylation of p-Y527 by activating phosphatases (Section 1.2.6) and high affinity SH3 and SH2 domain ligands (Section 1.2.3 & 1.2.4) that relieve the repressed structure to enable auto/trans-phosphorylation of Y416 in the activation loop (Section 1.2.5) (Fig.1.6A). This mechanism has been demonstrated by the addition of SH2/SH3 domain peptides and ligands to recombinant SFKs, which increases substrate

phosphorylation (Keenan et al. 2015). The combination of both SH2 and SH3 domain ligands generates maximal activity (Moarefi et al. 1997). Src can then be inactivated by phosphatases, such as PTP-BAS, which dephosphorylate p-Y416 (Roskoski 2005), and kinases such as Csk and Chk that phosphorylate Y527 (Section 1.2.6). However, this may represent a simplified model.

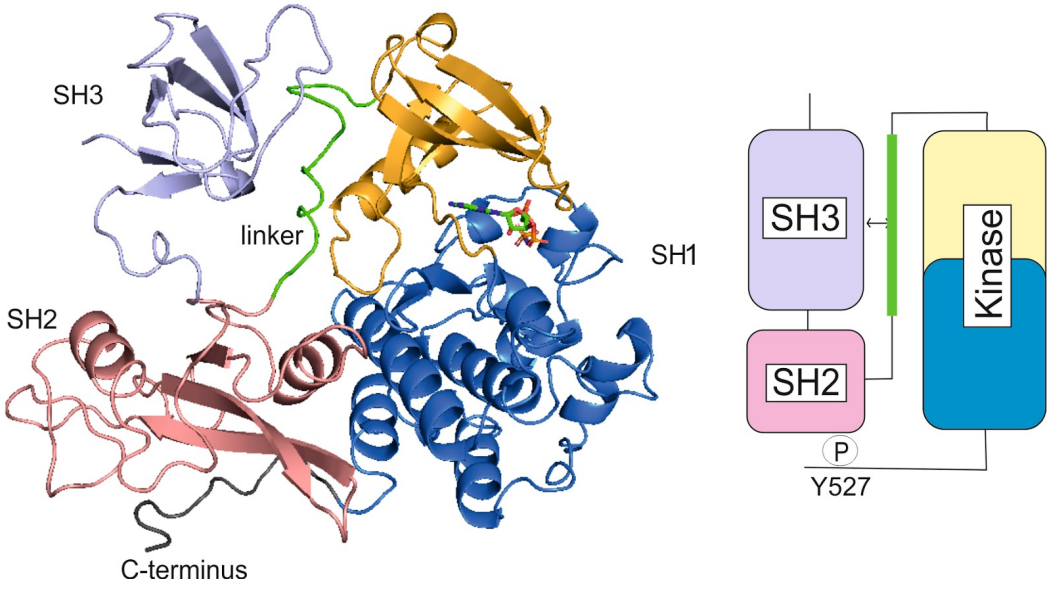

Figure 1.5: The crystal structure of inactive C-Src kinase. The SH3 domain (purple) interacts with the linker (green) between the SH2/SH1 domain, and the SH2 domain (pink) interacts with the C-terminal region (grey). The SH1 domain N- (orange) and C- (blue) lobes that form the catalytic site are shown (PDB: 2SRC).

Upon kinase activation, Y416 is auto-phosphorylated (Section 1.2.5), and auto-phosphorylated Src has an increased affinity for substrate peptide (Foda et al. 2015). However, p-Y416 has been detected in a mutant repressed Src, and the phosphorylation of a Src substrate has been weakly correlated with p-Y416 content (Irtegun et al. 2013). Similarly, in comparison to v-Src, C-Src had a 10-fold reduction in substrate phosphorylation, whereas its autophosphorylation was only reduced 1-2 fold (Coussens et al. 1985). Thus, the extent of auto-phosphorylation does not always correlate with catalytic activity and instead, the auto-phosphorylated state might 'prime' Src for further activation by other events such as ligand interaction.

The role of the SH3-domain in SFK activation was investigated using inactivated SFKs, generated by mutation of the C-terminal tail to p-YEEI. The mutant is locked in a SH2 domain-bound state, meaning that any kinase activation is only attributable to the SH3 domain (Moroco et al. 2014). Interestingly, all SFKs tested were catalytically activated

by a proline rich peptide (VSL12), and auto-phosphorylated C-Src was more susceptible to further activation by VSL12. This suggested that auto-phosphorylated Src was still regulated by its SH3 domain. This was confirmed by the mutation of the SH2:SH1 linker that interacts with the SH3 domain, which prevented the increase in activity by VSL12. Furthermore, this study suggests that the SH3 domain can activate Src without disrupting the SH2:C-terminal tail interaction, and that auto-phosphorylation and SH2/SH3 domain-ligand interactions can function somewhat independently in activating the kinase domain (Moroco et al. 2014).

The tyrosine kinase Abl is regulated like Src in that its SH3 domain interacts with the SH2:SH1 linker (Panjarian et al. 2013). However, the SH2 domain plays a key role in the allosteric regulation of the kinase domain. Interestingly, in contrast to an SH2-kinase domain construct, the Abl kinase domain alone was unable to auto-phosphorylate. The structure revealed that the SH2:kinase domain interaction was essential to generate an open activation loop to enable autophosphorylation (Lamontanara et al. 2014). Similarly, comparison of the C-Src kinase domain and a SH3-SH2-kinase domain construct, revealed that there were small CSPs in the kinase domain when expressed with the SH2 and SH3 domains, suggesting a transient interaction (Tong et al. 2017).

Recent studies have provided insight into the potential for a whole new layer of Src regulation by the intramolecular interactions of the SH4 and unique domains (Maffei et al. 2015). As discussed in Section 1.2.2 the Src SH3 domain interacts with the unique domain, which is abolished by the addition of a proline rich peptide ligand, due to allosteric competition (Pérez et al. 2009). Interestingly, in a Src SH4-unique domain construct, the addition of a proline rich peptide ligand did not affect binding by the SH4 domain. It was shown that the SH4 domain interacted with the n-Src loop of the SH3 domain, whereas the unique domain interacted with the RT loop. The interaction between the SH3 and SH4 domains was confirmed independently using a synthetic peptide of the SH4 domain. However, surprisingly, the CSP profile differed from that of the SH4-unique domain construct. Thus, the unique domain was directing the interaction of the SH4 domain with the n-Src loop of the SH3 domain, regardless of the unique domain's interaction status (Maffei et al. 2015). As the unique domain bind lipids via the same region that interacts with the SH3 domain, the authors propose that when Src is activated by SH3 domain ligands, the SH3 domain would no longer interact with the

unique domain, and this may feed back onto the unique domain to modulate its interactions with lipids (Pérez et al. 2013; Maffei et al. 2015) (Fig.1.6).

The studies described here demonstrate how Src activation is highly complex, and that auto-phosphorylation does not always correlate with activity, and that the kinase may still be under a degree of control by the SH2/SH3 domains. There is also the potential for additional allosteric control of kinase activity. Not only does the Src SH3 domain receive input from the SH2/SH1 linker and its proline-rich ligands, but also from the SH4 domain, unique domain, kinase domain and lipids (Maffei et al. 2015; Pérez et al. 2013). These interactions could generate myriad states of kinase activity, and modulate cellular localisation, however, this has not yet been investigated. It is also interesting to consider how the composition of the variable n-Src and RT loops of SH3 domains could regulate these interactions and contribute to functional diversity.

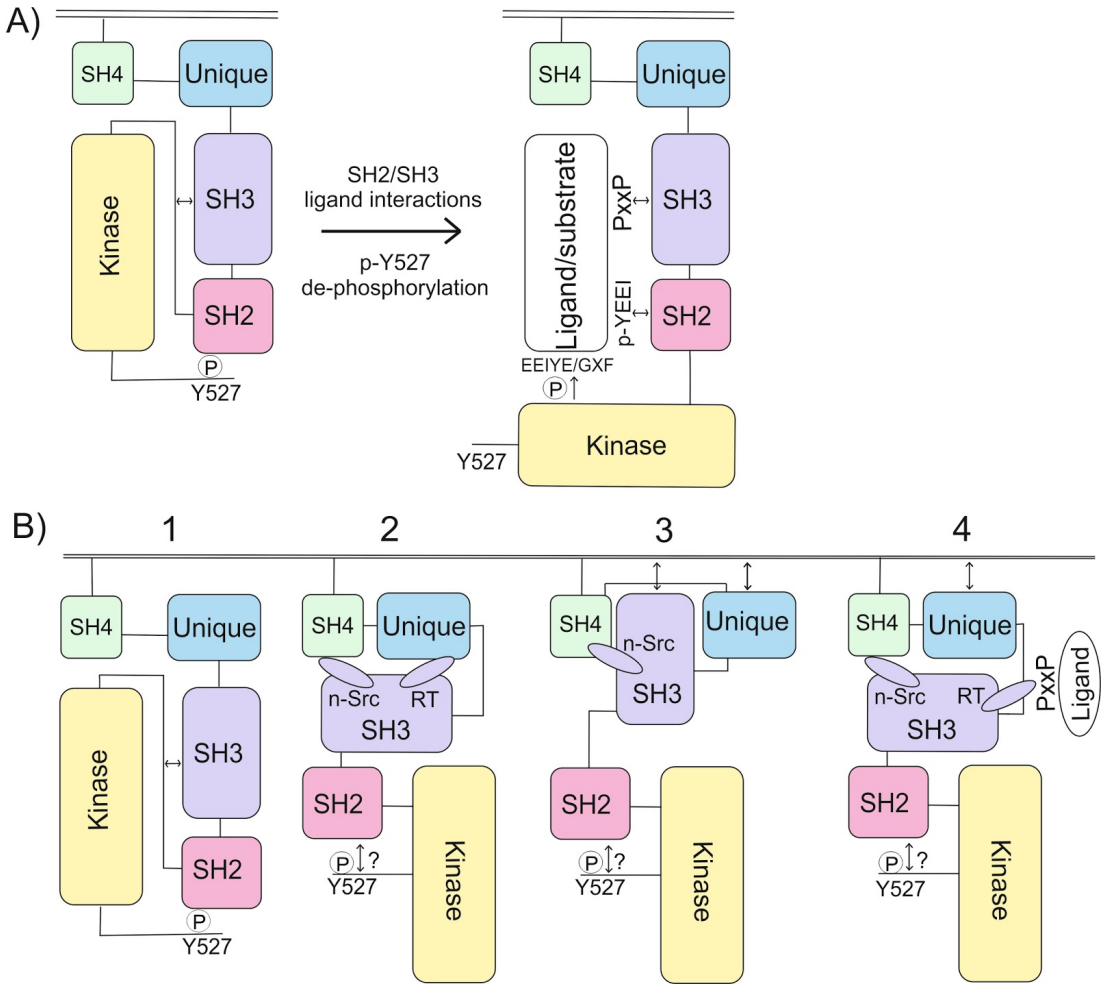

Figure 1.6: Regulation of Src activity by intra- and intermolecular interactions.
A) In the inactive conformation the Src SH3 domain interacts with a linker between the SH2 and kinase domain. The SH2 domain also interacts with p-Y527. Upon the formation of SH3/SH2 domain ligand interactions and/or p-Y527 de-phosphorylation, the inactive conformation is disrupted. The kinase domain can then autophosphorylate and conduct substrate phosphorylation. B) Schematic of intramolecular Src interactions identified by (Maffei et al. 2015; Pérez et al. 2013). 1) Current model of inactive Src as described in Section A). 2) The Src SH3 domain interacts with the SH4 and unique domain via its n-Src and RT loops respectively. 3) The Src SH3 and unique domain interact with each other and lipids via the same binding site. 4) In the presence of proline rich peptide ligands, the SH3 domain continues to interact with the SH4 domain. However, the interaction with the unique domain is lost due to allosteric modulation. This may feedback to the unique domain to regulate its interaction with lipids. 2-4 It is unknown how the SH4, unique and SH3 domain interactions relate to the SH3 domain:linker and SH2:p-Y527 interactions.

1.3 Functions of C-Src in the nervous system

C-Src signals alongside receptors in the immune system (FcμR, IL-2R), receptor tyrosine kinases (RTKs; PDGFR, EGFR, FGFR), G-protein coupled receptors (GPCRs), cell-adhesion molecules (integrins, cadherins) and channels (calcium, potassium, IP3R). Through these diverse signalling events, C-Src functions in proliferation, migration, apoptosis, differentiation and regulation of transcription (reviewed by (Thomas and Brugge 1997). In the developing and mature brain, C-Src has been associated with neurite extension, morphology, axon guidance and synaptic transmission. Unfortunately, many studies have utilised techniques such as Western blotting and immunofluorescence with Src antibodies against epitopes common to both C-Src and its neuronal variants, N1- and N2-Src (Section 1.4). Similarly, the use of broad specificity SFK inhibitors, such as PP1 and PP2, fail to distinguish between the isoforms. Thus, in many studies it is undetermined which SFK member or C-Src isoform is responsible.

Surprisingly a C-Src knockout mouse was not lethal and the main phenotype was osteoporosis (Soriano et al. 1991). The osteoporosis is not unexpected as C-Src has 5-200 fold higher levels in platelets, neurons, and osteoclasts compared to other cell types (Brown and Cooper 1996). However, there were no obvious abnormalities in the brain or platelets. This is believed to be due to functional redundancy, as a Fyn knockout mouse was also viable, whereas most Src/Fyn double mutants died perinatally (Stein et al. 1994). The embryonic Src/Fyn double mutants displayed axon pathfinding defects and defasciculation of the olfactory nerve (Morse et al. 1998).

During nervous system development, neurons send out axonal projections that sense attractive and repelling environmental cues (Plachez and Richards 2005). This complex process is mediated by axon guidance molecules residing in the growth cone at the tip of the axon. The growth cone also undergoes cytoskeletal remodelling, including filopodial and lamellipodial extensions, and the formation of stable and dynamic microtubule bundles (Dent et al. 2011). C-Src is present in growth cone membranes (Maness et al. 1988) where it phosphorylates tubulin (Maness and Matten 1990) and may modulate neurite extension. C-Src has also been implicated in dendritic morphogenesis (Skupien et al. 2014). A Src inhibitor prevented the rapid neurite outgrowth observed upon the transfection of the Src substrate p190 RhoGAP into neuroblastoma cells (Brouns et al. 2001). It was later shown that p190 RhoGAP promotes neurite outgrowth upon its

activation by Src and subsequent inhibition of RhoA (Jeon et al. 2012). Similarly, neurite outgrowth from a rat pheochromocytoma cell line (PC12) was concomitant with the association of activated Src with the cytoskeleton, and an increase in cellular protein tyrosine phosphorylation, which was prevented by the expression of dominant negative Src (Rusanescu et al. 1995). The induction of neurites in PC12 cells by NGF and FGF was also inhibited by microinjection of neutralising Src antibodies (Kremer et al. 1991). Thus, there is extensive evidence linking Src to neurite outgrowth. Aside from tubulin (Maness and Matten 1990) and p190 RhoGAP (Brouns et al. 2001), the cytoskeletal substrates of C-Src include Cortactin (Amanchy et al. 2008), Cofilin 1 (Yoo et al. 2010), Wasf1 (WAVE1) (Ardern et al. 2006), N-WASP (Park et al. 2005), Raph1 (Carmona et al. 2016) and RhoA (Kim et al. 2017). All of which have been associated with neurite outgrowth (Hall and Lalli 2010; Khodosevich and Monyer 2010; Hansen and Mullins 2015; Figge et al. 2012; Kinnunen et al. 1998).

C-Src interacts with axon guidance molecules and their ligands including the L1 cell adhesion molecule (L1-CAM), Ephrin receptors, and the Deleted in colorectal cancer receptor (DCC). Ephrin receptors are RTK's, and the SFKs are recruited to Ephrin receptors via their SH2 domains (Zisch et al. 1998; Knöll and Drescher 2004), where they regulate axon guidance and neuronal migration via phosphorylation of cytoskeletal regulators including N-WASP, cortactin and p190RhoGAP (Knöll and Drescher 2004). Netrin-1 is a secreted axon guidance cue that interacts with the DCC receptor to stimulate neurite outgrowth. C-Src was shown to interact with the intracellular region of DCC and phosphorylate the receptor, and both PP2 and kinase-dead Src prevented netrin-1 induced axon outgrowth (Li et al. 2004). L1-CAM is a cell adhesion molecule that participates in neuronal migration (Kiefel et al. 2012). Cerebellar neurons from Src knockout mice demonstrated impaired neurite outgrowth on L1-CAM in comparison to those from $Fyn^{-/-}$ and $Yes^{-/-}$ knockouts (Ignelzi et al. 1994). C-Src phosphorylates L1-CAM *in vitro*, and the phosphorylation prevents its interaction with the endocytic molecule AP-2 (Schaefer et al. 2002). The authors suggest that the disrupted trafficking of L1-CAM could explain the neurite outgrowth defects in Src knockout neurons. The neuronal splice variant of C-Src, N1-Src, has also been associated with neurite outgrowth on L1-CAM (Keenan et al. 2017).

C-Src also regulates neurotransmission, including the modulation of excitatory and inhibitory neurotransmitter receptors, and voltage-gated channels that regulate membrane potential. A role for the SFKs in the regulation of synaptic transmission was identified by PP2, as it enhanced calcium-dependent neurotransmitter release in primary neurons (Ohnishi et al. 2001). In-line with this observation, expression of v-Src suppressed neurotransmitter release, suggesting that Src negatively regulates neurotransmission (Ohnishi et al. 2001). Synapsin is a synaptic vesicle associated C-Src substrate and SH3 domain ligand, and its interaction with Src was shown to stimulate kinase activity, and tyrosine phosphorylation of synapsin. Inhibition of this interaction increased calcium-dependent neurotransmitter release, suggesting that synapsin might be the Src-regulated protein in neurotransmission (Onofri et al. 2007). In addition, Src also phosphorylates the synaptic vesicle-associated protein synaptophysin (Barnekow 1991; Evans and Cousin 2005), and dynamin I, which participates in synaptic vesicle endocytosis (Smillie and Cousin 2005; Ahn et al. 2002).

The N-methyl-D-aspartate (NMDA) receptor is a post-synaptic glutamate receptor that mediates excitatory synaptic transmission. NMDA receptor activation is central to synaptic plasticity and memory (Li and Tsien 2009). Upon membrane depolarisation, and the binding of glutamate and glycine to its extracellular region, the NMDA receptor gates sodium and calcium ions, which triggers signalling required for learning (Neveu and Zucker 1996). C-Src immunoprecipitates with the NMDA receptor, and its expression increases the NMDA receptors current in neurons. This was shown to be via the phosphorylation of the receptor's NR2A subunit, as its phosphorylation site mutant prevented regulation of the receptors current (Yu et al. 1997; Yang and Leonard 2001; Zheng et al. 1998). Infusion of the Src inhibitor PP2 into the hippocampus of rats prevented both short and long term memory formation (Bevilaqua et al. 2003). In addition, spatial maze learning in rats increased hippocampal Src activity, and the interaction of Src with synaptic proteins, including synapsin, synaptophysin and the NMDA receptor, increased (Zhao et al. 2000).

C-Src also regulates α-amino-3-hydroxy-5-methyl-4-isoxazole propionic acid (AMPA) receptors, which are also excitatory post-synaptic glutamate receptors that mediate synaptic transmission and plasticity. The AMPA receptor GluR2 (Gria2) subunit is phosphorylated *in vitro* by C-Src (Scholz et al. 2010), and *in vivo* by the SFKs, which

regulates its trafficking by promoting its internalization and is thus likely to inhibit communication at excitatory synapses (Hayashi and Huganir 2004).

C-Src regulates a host of other neurotransmitter receptors and voltage gated channels. For example, inhibitory GABA receptor currents were enhanced by v-Src phosphorylation (Moss et al. 1995). Similarly, C-Src phosphorylation of neuronal acetylcholine receptors enhanced the current (Wang et al. 2004). Conversely, v-Src phosphorylation of the neuronal voltage-gated potassium channel Kv1.3 suppressed the current (Fadool et al. 1997). Thus, C-Src regulates a variety of receptors and channels in the brain via the common mechanism of phosphorylation to modulate their currents.

1.4 Identification of N1- and N2-Src kinases

N1-Src kinase was initially referred to as pp60Src^{+} and was first identified due to its slightly slower electrophoretic mobility on SDS-PAGE, which occurred only for Src from neuronal tissues (Brugge et al. 1985). Many of the early experiments used the differential mobility of full-length Src or its peptides from partial proteolytic digestion to detect what is now known as N1-Src. Initial investigations into N1-Src focused on the cause of the electrophoretic shift, and its location within the Src protein. The location of the modification was mapped by partial proteolytic peptide mapping of Src by V8 protease. The digestion generated multiple fragments, including a fragment referred to as Vl, which was further cleaved to generate either the V3 or V4 peptide from the N-terminus of Src (Brugge et al. 1985). The V1, V3 and V4 peptides all showed differential electrophoretic mobility in comparison to non-neuronal Src and therefore established that the alteration was in the N-terminus of Src.

Differential phosphorylation was a candidate for the retarded mobility of N1-Src. However, partial digestion of ^{32}P-labelled Src did not reveal a phosphorylation stoichiometry in the V3 or V4 fragments that was capable of explaining the shift (Lynch et al. 1986). Similarly, phosphatase treatment of Src from neuronal cultures had no effect on the electrophoretic mobility (Brugge et al. 1987). A second possibility was a lack of N-terminal myristoylation. However, ^{3}H-mystric acid labelling revealed that N1-Src was also myristoylated (Brugge et al. 1987). Thus, it was speculated that N1-Src was modified at the level of the protein sequence. Initial evidence for this was obtained by the *in vitro* translation of polyA RNA from chicken embryo brain, as the translated Src

exhibited the same electrophoretic mobility as N1-Src (Brugge et al. 1987). Shortly after, using a cDNA library it was confirmed that there was an 18-base-pair insertion between exons 3 and 4 of C-Src (Levy et al. 1987). As final confirmation, a chimeric construct of C-Src containing the 18 base pairs (NI exon) was transfected into fibroblasts. Indeed, the expressed protein displayed the same mobility as N1-Src at the level of peptides and full length protein (Levy et al. 1987). As such, N1-Src was characterised as a 6 residue insert (RKVDVR) in the N-terminal SH3 domain (Fig.1.7).

A second Src splice variant was later identified by PCR from human cDNAs in the region containing the N1-Src insertion (Pyper and Bolen 1990). Three different sized products were amplified, and sequencing identified both C-Src and N1-Src. The third product, N2-Src, comprised the 18 bp NI exon, coupled to a second 33 bp exon, termed NII. This second splicing event inserted 17 residues (RKVDVSQTWFTFRWLQR) between exons 3 and 4 (Fig.1.7). The final arginine of the N1-Src insert is mutated to a serine in N2-Src due to the N1-NII exon splicing (Pyper and Bolen 1990).

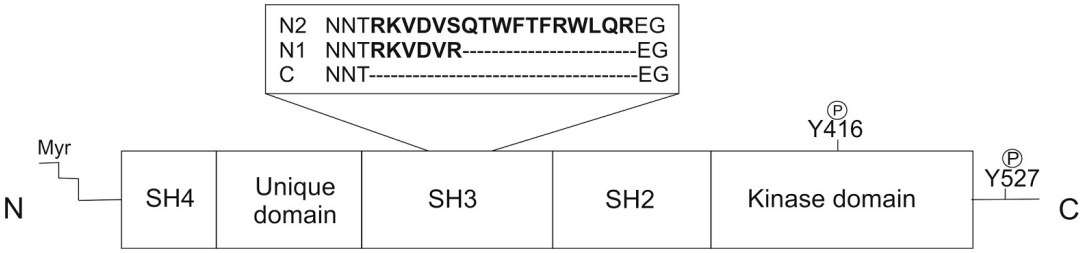

Figure 1.7 N1- and N2-Src are neuronal specific splice variants of C-Src. The N1- and N2-Src splice variants are formed by the insertion of 6 (RKVDVR) and 17 (RKVDVSQTWFTFRWLQR) residues respectively in the C-Src SH3 domains n-Src loop.

1.4.1 The evolution of neuronal Srcs

N1-Src is specifically expressed in neurons and has not been detected in non-neuronal cells or glia (Lynch et al. 1986; Brugge et al. 1987; Cotton and Brugge 1983; Brugge et al. 1985). Evolutionarily, N1-Src expression has been detected in vertebrates including the chicken, mouse and human (Levy et al. 1987; Martinez et al. 1987). The teleost fish *Xiphophorus* is a lower vertebrate that also has N1-Src, however the insertion encodes RKINCR, which deviates from the human, mouse, and chicken sequence of RKVDVR (Raulf, Robertson, and Schartl 1989). The two *Xenopus laevis* Src genes encode N1-Src as five residue insertions (RPDIR & RPDMR) (Collett and Steele 1992). However, overall all species contain the positively charged arginines at each end of the insert, and

with the exception of the fish, a central aspartic acid. In-line with the proposed vertebrate-specific expression of N1-Src, the insertion was not detected in *Drosophila* or hydra (Raulf, Robertson, and Schartl 1989). The N2-Src splice variant has been detected in the human brain, but not in avian cDNA clones, or *Xenopus* (Collett and Steele 1992), suggesting N2-Src is specific to mammalian species (Pyper and Bolen 1990), and could be important for higher brain functions.

1.4.2 Neuronal Src splicing mechanism and regulation

The splicing of C-Src to generate N1- and N2-Src occurs in the C-Src SH3 domain. As discussed in Section 1.2.3, the SH3 domain is involved in the regulation of Src kinase activity via intramolecular interactions and, importantly, intermolecular interactions with C-Src ligands and substrates.

The neuronal-specific splicing of C-Src to yield the N-Srcs is tightly regulated. The repression of the NI exon in non-neuronal cells is mediated by the polypyrimidine tract binding protein (PTB; PTBP1). PTB binds two conserved CUCUCU repeats within the N1 3' splice site and in a downstream intron, which blocks the assembly of the spliceosome (Fig.1.8). PTB was shown to be essential for the repression of N1-Src, as the addition of RNA containing the N1 exon 3' splice site to nuclear extract enabled N1-Src splicing. The repression was restored upon the addition of purified PTB, suggesting it was the trans-acting factor that was titrated out by the RNA competitor (Chan and Black 1997). Interestingly, hnRNPA1 also represses N1-Src splicing *in vitro*. However, this occurs through a different mechanism as mutation of the PTB binding sites did not prevent hnRNPA1-mediated inhibition (Rooke et al. 2003).

Upon neuronal differentiation, PTB is downregulated and replaced by *de novo* expression of neural PTB (nPTB; PTBP2), and thus the isoforms have mutually exclusive expression (Fig.1.8). A number of neuronal-specific exons, including that of N1-Src are repressed by PTB and are induced upon the switch to nPTB, which functions as a weaker repressor (Boutz et al. 2007). N1-Src splicing is also positively regulated by an enhancer element in a downstream intron, which binds the splicing activator FOX1 (Fig.1.8). The FOX proteins show tissue specific expression including in the brain, and like PTB, multiple neuronal-regulated exons contain the FOX enhancer element (Underwood et al. 2005; Black 1992). In addition, there is also an enhancer complex consisting of KH-type splicing regulatory protein (KHSRP), hnRNPH and hnRNPF

(Fig.1.8). KHSRP induces the assembly of the proteins on to the enhancer element, and its depletion from *in vitro* splicing reactions prevents N1-Src splicing. Similarly, the loss of hnRNPH also results in the partial inhibition of splicing, whereas the re-addition of both purified proteins rescues splicing (Chou et al. 1999; Min et al. 1997). Splicing factor 2 (SF2) has also been shown to stimulate N1 splicing (Rooke et al. 2003). Thus, the splicing is under tight positive and negative regulatory control by a number of proteins. Splicing of the NII exon has not been observed alone (Pyper and Bolen 1990), which is surprising as it would not disrupt the reading frame. The NII exon alone would generate an 11 residue insert, however, the serine that is generated at the N1-NII exon boundary would instead be a threonine.

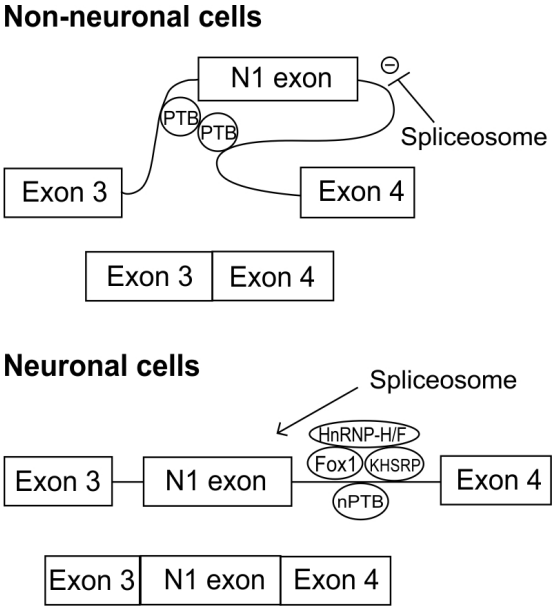

Figure 1.8: Schematic of Src splicing to generate neuronal Src. In non-neuronal cells PTB binds to the N1 exons 3' splice site and a downstream intron, which blocks the assembly of the spliceosomal complex. In neuronal cells PTB is replaced by neural PTB and N1-Src splicing is positively regulated by an enhancer complex consisting of the FOX1 protein, KHSRP, hnRNPH and hnRNPF.

1.4.3 N1-Src cellular expression and localisation

The expression profile of N1-Src implies a function in development. In the developing mouse brain, N1-Src was identified as the predominant form, and Western blotting revealed that Src expression increased upto ~ 15-fold between embryonic day 12 (E12) and postnatal day 1 (P1) in the forebrain and midbrain, and expression was maximal at P1 (Wiestler and Walter 1988). Src auto-phosphorylation also increased, suggesting that there were both high levels of activity and expression during this period. During the period E10-E18 there are diverse processes spanning the development of brain structures, neuronal migration, differentiation, and some neurons entering a post-mitotic state. The authors were unable to attribute the rise in N1-Srcs expression to a particular cell type or process (Wiestler and Walter 1988).

The cellular localisation of N1-Src in the developing spinal cord of chick embryos was assessed via an antibody raised against the N1-Src insertion. N1-Src was detected in the neuronal cell soma, surrounding the nucleus, and in developing dendrites. However, it was not detected within the nucleus. Electron microscopy revealed that N1-Src was associated with polysomes and the rough endoplasmic reticulum, where it is likely been translated. Interestingly, N1-Src was present at the presynaptic membrane of developing synapses, including synaptic vesicle membranes, as well as in the signalling hub of the post-synaptic density (Atsumi et al. 1993). In the adult rat forebrain, N1-Src has been shown to mostly associate with the presynaptic membrane, and C-Src with highly purified synaptic vesicles (Onofri et al. 2007). Whilst N1-Src was predominantly present at immature synapses, it was also found in mature synapses, suggesting it may function in both synapse development and their maintenance/general function (Atsumi et al. 1993). A surprising finding that goes against the neuronal specificity of N1-Src, was its detection in chick embryonic but not adult skeletal muscles. Therefore N1-Src may be expressed temporarily in early muscles (Atsumi et al. 1993), although its function is not clear and the finding has not been repeated in mammals.

In order to compare the relative expression of C-, N1- and N2-Src in the fetal and adult brain, RNAase protection assays were performed. Whilst N2-Src was found at comparable levels in fetal and adult brain, both C- and N1-Src were significantly higher in fetal brain (Pyper and Bolen 1990). This suggests that N1- and N2-Src could have unique functions. A similar study did not distinguish between the Src isoforms, however, they also noted that Src was most expressed in the human fetal brain, and that its kinase activity was increased ~ 3.5 fold in the fetal brain in comparison to the adult. However, kinase activity was raised in all fetal tissues assayed, consistent with a broad function of Src in development (Sorge et al. 1985).

In the adult rat nervous system, N1-Src was detected in all CNS tissues via Western blotting, including the forebrain, hippocampus and cerebellum. However, N1-Src was only detected in trace amounts in one peripheral nervous system (PNS) tissue (Le Beau, Wiestler, and Walter 1987), in comparison to C-Src, which was detectable in both the CNS and PNS. Similarly, via *in situ* hybridisation, N1-Src mRNA was shown to be pronounced in the CNS of 15-19 day old rat fetuses (Ross et al. 1988). It has been proposed that the CNS-specificity of N1-Src could suggest a function in neuronal

plasticity (Le Beau, Wiestler, and Walter 1987). Indeed, *in situ* hybridisation in the adult rat brain indicated N1-Src is most expressed in the hippocampus, olfactory bulb, and granule cell layer of the cerebellum, all of which are associated with synaptic plasticity (Ross et al. 1988). In addition, whilst the expression of C- and N1-Src mRNA was similar in the hindbrain, N1-Src was expressed at higher concentrations in the forebrain, and showed more 'pronounced regional variations' (Ross et al. 1988). A differential expression profile could also suggest unique functions by C- and N1-Src.

The localisation of N1-Src in adult rat neurons has also been investigated by an antibody against the N1-Src insert (Sugrue et al. 1990). Interestingly, N1-Src immunoreactivity was observed throughout the brain, although not in all neurons. The authors note a similar finding to the pronounced regional variations described by (Ross et al. 1988), in that N1-Src appeared to be expressed in populations of neurons, however there was no clear classification for them in terms of their morphology or neurotransmission. Thus, it could represent an uncharacterised system or specialised function. At the cellular level N1-Src was mostly detected in the cell body and dendrites and to a lesser extent in the axons and their terminals. However, there were some regions including the brain stem, where axonal N1-Src was increasingly detectable. Interestingly, the cerebellar Purkinje neurons and granule cells were some of the most intensely stained, in line with the *in situ* hybridisation by (Ross et al. 1988), and the phenotype observed upon N1-Src overexpression in Purkinje neurons (Kotani et al. 2007) (Section 1.4.4).

Lipid rafts are signalling hubs enriched in lipids, structural proteins, receptors and signal transduction molecules (Simons and Sampaio 2011). In the CNS, lipid rafts are associated with broad functions including cell adhesion, endo- and exocytosis, axon guidance, and regulation of neurotransmission (Korade and Kenworthy 2008). In total, 5-20 % of Src, with N1-Src as the dominant isoform, resided in lipid rafts in the embryonic and adult mouse brain, with the highest levels found in the adult brain. N1-Src only entered lipids rafts in the brain and not in fibroblasts, and this is believed to be due to their unique protein and lipid composition. Src was shown to enter lipid rafts via its myristoylated SH4 domain, and the isolated C-Src SH3 domain did not enter (Mukherjee et al. 2003). However, this does not rule out C- and N1-Src forming unique SH3 domain interactions and signalling events upon entry. Indeed, the N1-Src in lipid rafts was shown to be highly active with raised auto-phosphorylation and exogenous

substrate phosphorylation (Mukherjee et al. 2003), suggesting they could be a signalling platform for N1-Src.

In summary, N1-Src is the predominant form of Src during neuronal development and shows CNS specificity. In the adult brain, N1-Src is present throughout the neuron including the cell body, dendrites, axons, synaptic vesicles and post-synaptic density. Whilst differences have been observed between C- and N1-Src, including their expression in the forebrain, association with synaptic vesicles, and overall localisation within the brain, it is unclear what the cellular and developmental functions of N1-Src are.

1.4.4 The cellular functions of the neuronal Srcs

One of the first proposed functions of N1-Src was a role in differentiation, as N1-Src was the major Src isoform present upon retinoic acid induced neuronal differentiation of embryonal carcinoma cell lines (Lynch et al. 1986). Similarly, N1-Src mRNA was expressed upon neural induction in *Xenopus* (Collett and Steele 1993). However, in these studies it is unclear whether N1-Src was driving the differentiation process or was expressed as a result of neuronal differentiation. Evidence that N1-Src can drive neuronal differentiation was obtained from studies of neuroblastoma (NB). NB is commonly a childhood cancer, and is derived from immature neuroblasts from embryonic neural crest that fail to undergo neuronal differentiation (Ratner et al. 2016). A perplexing phenotype is the 'spontaneous regression' of neuroblastoma, for which it has the highest rate of any human cancer (Challis and Stam 1990). This could be mediated by the immune system (Kataoka et al. 1993) or the neuroblasts successfully undergoing neuronal differentiation. Interestingly, favourable prognosis NBs were shown to express high levels of Src mRNA. Therefore, the expression of C-, N1-, and N2-Src mRNAs were assayed in NB cell lines upon the induction of neuronal differentiation. The expression of N1-Src correlated with the ability to differentiate *in vitro*, in comparison to a cell line expressing only C-Src that did not show morphological changes upon induction of differentiation (Matsunaga et al. 1993). Good prognosis cases expressed high levels of N2-Src, in contrast to advanced cases, which expressed little or no N2-Src. Thus, whilst N1-Src induced a differentiated phenotype, N2-Src may be essential for complete maturation and differentiation (Matsunaga et al. 1993). The expression of N2-Src has been proposed as a prognostic marker for NB (Matsunaga et al.

1998). However, the molecular basis of N1- and N2-Src in NB differentiation is currently unknown, and their potential to be therapeutic targets remains ambiguous.

Studies in both heterologous cells and neurons have linked N1-Src to cytoskeletal remodelling and regulation of neurite outgrowth. For example, the expression of N1-Src and its constitutively active mutant (N1-Src Y527F) in a *Xenopus* epithelial cell line resulted in more than 60 % of the cells presenting elongated morphologies and 'neurite' like processes. In comparison, cells transfected with C-Src Y527F had flattened and round morphologies (Worley et al. 1997). Similarly, the overexpression of N1-Src in a COS7 fibroblast cell line resulted in a significant increase in both the average length of processes/neurite-like extensions, and the average number of neurites per cell (Keenan et al. 2017), thus generating a neuron-like morphology. The overexpression of C- and N1-Src in rat hippocampal and cerebellar granule neurons also generated differential morphologies. Whilst the overexpression of C-Src had no significant effects, the mean number of neurites, mean length of neurites, and the length of the longest neurite were all significantly reduced for N1-Src (Wetherill 2016; Keenan et al, 2017). Interestingly, the specific knockdown of N1-Src by shRNA mirrored the overexpression data by significantly reducing the neurite number and length (Wetherill 2016; Keenan et al, 2017). The equivalent effects of the knockdown and overexpression could be due to aberrant substrate phosphorylation and pathway modulation, or the sequestering/formation of promiscuous ligand interactions upon overexpression.

Transgenic mice expressing N1-Src or its constitutively active mutant (N1-Y527F) under the control of the Purkinje cell-specific L7 promoter, were generated to assess the role of N1-Src in neuronal development (Kotani et al. 2007). A number of phenotypes were observed, including abnormally localised Purkinje cells in cerebellar tissue sections, which was worse in the N1-Y527F transgenic. The dendrites also displayed defects, including multiple dendritic shafts and minimal neurite extension, which could be due to the microtubule cytoskeleton, as electron microscopy revealed that the microtubules from N1-Y527F were at a higher density, and had structural abnormalities, appearing intertwined and curved. Cerebellar cultures from the N1-Y527F transgenic also presented thick dendritic shafts, large growth cones, and minimal neurite outgrowth. This phenotype was rescued by the Src inhibitor, PP2, which produced a morphology comparable to control cells (Kotani et al. 2007). As discussed in Section 1.4.3,

endogenous N1-Src expression has been detected in the Purkinje neurons and granule cells of the cerebellum (Ross et al. 1988; Sugrue et al. 1990), and using strains of mutant mice that display cerebellar developmental abnormalities, a large loss of N1-Src expression occurred alongside cerebellar neurodegeneration (Brugge et al. 1987). In addition, one mutant had significantly reduced N1-Src expression from an early time point and the granule cells failed to migrate, although a causal relationship was not confirmed (Brugge et al. 1987).

The role of C-Src and N1-Src in axon guidance and neuronal differentiation was assayed in the developing *Xenopus* retina (Worley et al. 1997). Interestingly the overexpression of constitutively active C- or N1-Src (Y527F) resulted in fewer photoreceptors. However, there was not an increase in other differentiated cell types, suggesting that differentiation was inhibited as opposed to the cells adopting an alternative fate. The retinal ganglion cells (RGCs) were used as a model system for axon guidance as they sprout axons that travel along a characterised pathway to the optic tectum. A large percentage of the axons from cells overexpressing wild-type C- or N1-Src reached the optic tectum. However, none of the axons from the cells overexpressing the constitutively active mutants did. N1-Src-Y527F-expressing axons progressed further along the pathway than those expressing C-Src-Y527F, suggesting that active C-Src impaired axonogenesis to a greater extent. Overexpression of wild-type C- or N1-Src increased the phosphotyrosine content in the neuronal cell soma, dendrites and axons, and this was further increased by the constitutively active mutants, in particular N1-Src Y527F. Thus, the authors concluded that enhanced impairment of axonogenesis by C-Src could not be attributed to an increase in overall phosphorylation (Worley et al. 1997). However, this does not rule out the increased phosphorylation of a unique C-Src substrate(s). The authors also assessed the role of C- and N1-Src in neuritogenesis in *Xenopus* neuroepithelial cells. The C- and N1-Src Y527F mutants each decreased the average length of the longest neurite in comparison to their wild-type counterparts. However, wild-type N1-Src increased the average length of the longest neurite by 2.4-fold in comparison to C-Src, suggesting that N1-Src could promote axonogenesis (Worley et al. 1997). Thus, the extent of axonogenesis impairment, neurite outgrowth and phosphotyrosine content varied between C- and N1-Src. However, there was also

functional overlap in that both constitutively active mutants inhibited photoreceptor differentiation.

The function of C- and N1-Src have been studied in the context of *Xenopus* development. RNA encoding C-Src, N1-Src or their constitutively active mutants were injected into *Xenopus* embryos. In terms of lethality, the wild-type C-Src had no significant effect, whereas 27 % of embryos expressing wild-type N1-Src died. C-Src-Y527F yielded 70 % lethality, while embryos expressing N1-Y527F had a 100 % mortality rate (Worley et al. 1997). This again highlights that the kinases have differential functions, and suggests that lethality is proportional to kinase activity.

More recently, the role of N1-Src in *Xenopus tropicalis* development has been investigated in our laboratory through a collaboration with the laboratory of Dr Harry Isaacs (Lewis et al. 2017). The expression of N1-Src mRNA was shown by PCR to increase during both primary and secondary neurogenesis, and *in situ* hybridization revealed that N1-Src was enriched at the neural plate, a structure that gives rise to the nervous system. Next, the specific knockdown of N1-Src was achieved by antisense morpholinos directed to the NI exon splice site, selectively inhibiting N1-Src expression whilst maintaining C-Src expression. N1-Src knockdown generated morphological phenotypes in larval stage embryos and they also presented an abnormal dart response. The larvae did not swim away when a touch stimulus was applied, suggesting that there was a defect in the neuronal circuitry. The motor, sensory and interneurons of the *Xenopus* primary nervous system form a distinct pattern and can be identified by their expression of the neuronal-specific tubulin (tubb2b) protein. Interestingly, the knockdown of N1-Src was shown to almost completely ablate the tubb2b-positive neurons, thus explaining the loss of the touch reflex, and providing a role for N1-Src in primary neurogenesis in amphibian development (Lewis et al. 2017).

1.4.5 Regulation of N1-Src kinase activity

A commonly observed feature of N1-Src is its increased autophosphorylation of Y416, which has been detected for endogenous N1-Src in neurons (Brugge et al. 1985) and upon overexpression of N1-Src in COS7 fibroblasts (Keenan et al. 2017) and B104 neuroblastoma cell lines (Keenan et al. 2015). Furthermore, Src from neuronal lysates incorporated ^{32}P with an 8-10 fold increase, and phosphorylated the exogenous substrate

enolase with a 6-fold increase, in comparison to Src from cultured astrocytes (Brugge et al. 1985). The increased autophosphorylation of N1-Srcs is suspected to be a result of a weakened interaction between its SH3 domain and the SH2:SH1 linker that forms the negative regulatory conformation (Keenan et al. 2015).

In addition, serine phosphorylation has been detected in the N-terminal 16 kDa of N1-Src in neurons. The modification was not present in Src from astrocytes (Brugge et al. 1987) or N1-Src overexpressed in chicken embryo fibroblasts (CEFs) (Levy and Brugge 1989), confirming its neuronal specificity and the possibility that it is phosphorylated by a neuronal kinase. However, the authors did not identify the function of the phosphorylation event, or whether the phosphorylation was unique to only N1-Src and not C-Src in neurons (Brugge et al. 1987). As the N-terminal 16 kDa encompases the SH4, unique and SH3 domain, it is possible that the phosphoserine is one of the SH4/unique domain modifications discussed in Section 1.2.2 that has roles in activation and localisation.

The kinase activity and regulation of N1-Src has been assayed in heterologous cells. The expression of C-Src, v-Src and N1-Src in CEFs resulted in whole cell lysate phosphotyrosine levels of C-Src < N1-Src < v-Src, suggesting that N1-Src may be a partially activated C-Src (Levy and Brugge 1989). Interestingly, despite the raised substrate phosphorylation by N1-Src, its p-Y527 phosphopeptide was detected but not its p-Y416 phosphopeptide (Levy and Brugge 1989). This could suggest that the activity was not representative of neuronally expressed N1-Src. Conversely, (Keenan et al. 2017) successfully identified raised autophosphorylation of N1-Src in COS7 fibroblasts. Thus some caution should be taken when assaying N1-Src in heterologous cells due to variations in autophosphorylation and N-terminal serine phosphorylation.

The role of the SH2 and SH3 domains in N1-Src kinase regulation were assessed by the expression of mutants in HEK cells (Groveman et al. 2011). In comparison to the wild-type N1-Src, its constitutively active mutant (Y527F) had increased p-Y416 immunoreactivity. However, upon coupling the Y527F mutation to inactivating SH3 domain (D101N; human equivalent of D99N) and SH2 domain (R183K) mutations, p-Y416 content was slightly and greatly reduced respectively. The *in vitro* phosphorylation of Src substrate peptides was also reduced for the kinase mutants,

correlating with the reduced auto-phosphorylation. The equivalent experiments were not conducted for C-Src, however, it suggests that N1-Src might require SH2 and/or SH3 domain-ligand interactions to enable autophosphorylation *in vivo*. As the Y527F mutation relieves the negative regulation of the SH2:p-Y527 interaction, the fact that the Y527F/SH2 domain mutant possessed reduced auto-phosphorylation suggests that the SH2 domain-ligand interactions do not simply relieve the negative regulation, and there could be allosteric effects on kinase activity as discussed in Section 1.2.7.

1.4.6 Neuronal Src SH3 domain ligands and substrates

C-Src is well characterised in terms of its SH2 and SH3 domain ligands, substrates, phosphorylation sites, and their downstream functional effects. However, a huge gap in the field remains with regards to the interactors and substrates of N1-Src. To date the N1-Src SH3 domain has only 5 *in vitro* ligands, dynamin I (Abdelhameed 2010), Ena/VASP like protein (Evl) (Lambrechts et al. 2000), Delphilin (Miyagi et al. 2002), hyperpolarization-activated cyclic nucleotide-gated channel 1 (HCN1) (Santoro et al. 1997), and the NMDA receptor (Groveman et al. 2011). Only the NMDA receptor was phosphorylated as well as interacting with N1-Src *in vitro* (Groveman et al. 2011). N2-Src is even less understood and currently has no SH3 domain ligands or *in vivo* substrates.

The N1-Src six residue insertion (RKVDVR) occurs in the SH3 domain n-Src loop. As discussed in Section 1.2.3, the n-Src loop participates in ligand binding and contributes to the structurally diverse specificity zone. As the specificity zone forms additional affinity/specificity contacts, it is extremely likely that the six residue insertion in some way alters ligand binding. Indeed, other SH3 domain splice variants in the n-Src loop have modulated ligand binding (Tsyba et al. 2008). Thus far, the neuronal insertion has been shown to raise N1-Src autophosphorylation (Brugge et al. 1985) and this may be the cause of its increased catalytic activity (Section 1.4.5). However, unique N1-Src ligands could explain the differential cellular localisation (Section 1.4.3) and cellular functions (Section 1.4.4) via the generation of unique substrates and signalling pathways.

To date, no structure of the N1- or N2-Src SH3 domain has been obtained, and the mechanism of ligand binding is unknown. Despite this, early studies pointed towards

differential binding by N1-Src, as GST pull-downs with the C- and N1-Src SH3 domains demonstrated that multiple C-Src SH3 domain ligands including synapsin (Foster-Barber and Michael Bishop 1998), tau (Reynolds et al. 2008), FAK (Messina et al. 2003), Snp70 (Craggs et al. 2001), Asap1 (Brown et al. 1998), and Rich (Richnau and Aspenström 2001) do not bind, or very weakly bind the N1-Src SH3 domain. Furthermore, pull-downs from lysates demonstrated that N1-Src had an overall reduced SH3 domain interactome (Weng et al. 1993).

Yeast-2-hybrid with the N1-Src SH3 domain identified the HCN1 channel (Santoro et al. 1997) as the only interactor from a screen of 5×10^5 independent clones. HCN1 is one of four members of the HCN family of cation channels that are found in excitable cells (Biel et al. 2009). The HCN1 channel is a voltage gated potassium channel that is exclusive to the brain, and functions in the regulation of action potentials (Magee 1998, 1999). However, there has been no follow up to confirm the interaction, and since the Yeast-2-hybrid technique can generate false positives it remains a questionable ligand. However, the HCN4 channel is a C-Src substrate, and the phosphorylation sites (Y531/Y554) (Li et al. 2008) are conserved in HCN1, thus it has the potential to be an N1-Src substrate.

Delphilin was also identified as an N1-Src SH3 domain ligand by Yeast-2-hybrid (Miyagi et al. 2002). Delphilin is a neuronal-specific formin that interacts with the GluRδ2 receptor in the dendrites of Purkinje neurons, thus it potentially correlates with N1-Src expression (Sugrue et al. 1990). The GluRδ2 receptor is associated with synaptic plasticity and motor learning (Zanjani et al. 2016). However, Delphilin is poorly characterised, although it is known to have actin nucleating and capping abilities (Dutta et al. 2017; Silkworth et al. 2018), and is suspected to function as a post-synaptic scaffolding protein that partakes in cytoskeletal remodelling and downstream signal propagation from the glutamate receptor (Miyagi et al. 2002). However, like the HCN1 channel, the interaction between N1-Src and Delphilin was not confirmed beyond Yeast-2-hybrid.

Ena/VASP-like protein (EVL) of the Ena/VASP family was identified as an N1-Src SH3 domain interactor via GST-SH3 domain pull-down (Lambrechts et al. 2000). The Ena/VASP proteins regulate the actin cytoskeleton through direct interactions with actin

and the actin binding protein profilin (Krause et al. 2003). The Ena/VASP proteins are associated with neurite initiation, dendritic morphology and axon guidance via signalling downstream from plasma membrane receptors, and the formation of growth cone filopodia (Drees and Gertler 2008). The interaction between the N1-Src SH3 domain and EVL was abolished by PKA phosphorylation of EVL on a site adjacent to its proline rich motifs. Furthermore, the N1-Src SH3 domain was shown to compete with profillin for EVL binding, but only binding to the N1-Src SH3 domain was disrupted by PKA phosphorylation. The authors speculate that profilin could function to compete away bound N1-Src SH3 domain, or interact with EVL upon the loss of its interaction with N1-Src by PKA phosphorylation (Lambrechts et al. 2000). Thus EVL is an attractive N1-Src SH3 domain ligand, however, this has not been investigated *in vivo.*

Dynamin I was initially identified as interacting with the C-Src SH3 domain, and the interaction between full length C-Src and dynamin I was confirmed by immunoprecipitation (Onofri et al. 2007). The N1-Src SH3 domain was later identified as interacting with dynamin I via mass spectrometry analysis of GST-C- and N1-Src SH3 domain pull-downs from rat brain synaptosomes (Abdelhameed 2010).

Dynamin I is an endocytic protein and the 100 kDa dynamin GTPases are known for their role in vesicle membrane fission to complete endocytosis, which occurs due to the formation of a dynamin helix at the vesicle neck and subsequent GTP hydrolysis. Dynamin I is highly expressed in neurons and is abundant in nerve terminals, where it participates in synaptic vesicle recycling (Cao et al. 1998). The conserved structure of dynamin comprises an N-terminal GTPase domain, a stalk that mediates oligomerisation, a pleckstrin homology (PH) domain which binds lipids, a GTPase effector domain (GED) that promotes GTPase activation, and a C-terminal proline rich domain (PRD), which has 13 PxxP motifs, mediating protein-protein interactions with a plethora of SH3 domain-containing proteins (Ferguson and De Camilli 2012).

Dynamin oligomerises into tetramers, rings and helices, and its GTPase activity increases with oligomerisation. Utilising *in vitro* assays (Krishnan et al. 2015) demonstrated that a panel of SH3 domains differentially bound dynamin I and modulated its oligomerisation and GTPase activity. Interestingly, oligomerisation did not always correlate with the ability to stimulate GTPase activity, and it was proposed that SH3 domains may induce unique dynamin oligomers with unique GTP hydrolysis rates.

In unpublished data in a PhD thesis, dynamin I was shown to differentially bind the C- and N1-Src SH3 domains (Abdelhameed 2010). In resting neurons, the dynamin I PRD is constitutively phosphorylated at S774/S778. However, upon synaptic stimulation and calcium influx, the calcium dependent phosphatase calcineurin is activated. This results in the de-phosphorylation of dynamin at S774/S778, and dynamin is then directed to the membrane, where it is later re-phosphorylated by CDK5. Thus the dephosphorylation of dynamin I is a major event upon nerve terminal stimulation. Interestingly, via GST-SH3 domain pull-downs, the N1-Src SH3 domain preferentially bound dynamin I lacking the phospho-S774 modification (Abdelhameed 2010). This suggested that the C- and N1-Src SH3 domains could differentially interact with dynamin I in a synaptic stimulation-dependent manner. This hypothesis requires further investigation, but in support of the proposed mechanism, both the syndapin and amphiphysin II SH3 domain interactions with the dynamin I PRD are regulated by serine phosphorylation in response to synaptic activity (Anggono et al. 2006; Huang et al. 2004).

A variety of truncation and substitution mutants of the dynamin-I PRD were used to identify the N1-Src SH3 domain binding site. However, mutation of several sites independently reduced binding (Abdelhameed 2010), suggesting that N1-Src could be utilising additional affinity elements like the syndapin SH3 domain (Luo et al. 2016) (Section 1.2.3). Alternatively, like the C-Src SH3 domain (Solomaha et al. 2005), N1-Src might bind multiple sites within the dynamin I PRD *in vitro*.

Dynamin I is phosphorylated by C-Src *in vitro* and *in vivo* (Ahn et al. 2002). Tyrosine phosphorylation is required for receptor mediated endocytosis of the EGF receptor, as the dynamin I phosphorylation site mutant (Y597F) reduced receptor internalization by 60 %. Electron microscopy revealed that tyrosine phosphorylated dynamin I formed oligomerised rings, that in turn promoted GTP hydrolysis and enabled receptor internalisation (Ahn et al. 2002). C-Src phosphorylation of dynamin has also been reported in the internalisation of the β2-adrenergic receptor (Ahn et al. 1999), and the endocytosis of the transferrin receptor by dynamin II (Cao et al. 2010).

The function of the NMDA receptor is discussed in Section 1.3. The C-tail fragment of the NMDA receptor NR2A subunit is the only *in vitro* N1-Src SH3 domain ligand that is also a substrate (Groveman et al. 2011). Furthermore, upon the addition of NMDA to HEK cells co-expressing the NMDA receptor and constitutively active N1-Src, the

receptor currents were enhanced. Thus like C-Src (Zheng et al. 1998), N1-Src appears to activate the NMDA receptor *in vivo*.

The synaptic vesicle protein synaptophysin was also *in vitro* phosphorylated by N1-Src, however, it was to a lesser extent than by C-Src (Keenan et al. 2015). A caveat of *in vitro* phosphorylation assays is that some proteins possess Src substrate motifs and are phosphorylated without SH2/SH3 domain mediated interactions, whereas substrates with SH2/SH3 domain docking motifs are considered more likely to be physiological. An example of this is enolase, as its phosphorylation by Src was unaffected by the addition of proline rich peptides, in contrast to the *in vivo* Src substrate Sam68, where phosphorylation was abolished (Shen et al. 1999). It remains unclear whether the NR2A subunit and synaptophysin represent physiological substrates.

The N1-Src SH3 domain has only a few *in vitro* ligands, and none of the interactions have been confirmed by further assays such as immunoprecipitation, pull-down, NMR or SPR, or investigated *in vivo* with full length N1-Src in heterologous or neuronal cells. As such the putative N1-Src SH3 domain ligands have no characterised *in vivo* effects, with the exception of the NR2A subunit (Groveman et al. 2011), and it remains unclear which are the physiological ligands and substrates of N1-Src. Furthermore, the current small number of candidates is unlikely to explain the diverse functions of N1-Src (Section 1.4.4).

1.4.7 Neuronal Src SH2 domain ligands

The N1-Src SH2 domain-ligand interactions are easily overlooked as the domain is identical to C-Src's. However, N1-Src differs in its developmental expression, cellular localisation and activation status (Section 1.4.4/6). Thus the differential processes driven by the SH3 domain are likely to result in the SH2 domain receiving exposure to distinct ligands that could further enhance functional diversity between C- and N1-Src. Indeed, the isolated N1-Src SH3 domain does not interact with focal adhesion kinase (FAK) (Messina et al. 2003). However, FAK was able to promote the phosphorylation of Cas by N1-Src in COS-7 fibroblasts, and the phosphorylation was prevented by a FAK mutant that cannot be bound by the Src SH2 domain (Ruest et al. 2001). Thus the N1-Src SH2 domain also appears to drive protein-interactions and substrate phosphorylation (Ruest et al. 2001). However, the authors did not confirm a direct interaction between N1-Src and

FAK, and N1-Src could be recruited through another protein that interacts with the FAK SH2 ligand motif.

1.5 Aims

There is a dearth of literature on N1-Src kinase. However, the limited cellular and model organism-based studies that have been undertaken have identified a function for N1-Src in neuronal development, specifically, neurogenesis, migration, neuronal differentiation, and neurite outgrowth/morphology. The signalling pathways, SH2/SH3 domain ligands and substrates underlying these functions are poorly characterised, and only a few putative *in vitro* ligands and substrates have been proposed. Therefore the aims of this project were to investigate the ligand and substrate specificities of N1-Src and compare them to C-Src.

The three major aims were to:

1. **Identify novel N1-Src SH3 domain ligands:**

GST-C- and N1-Src SH3 domain pull-downs in postnatal day 1 rat brain homogenates were analysed by LC-MS/MS in order to identify, compare and contrast the C- and N1-Src SH3 domain interactomes in a relevant neuronal background. Bioinformatics analyses were used to functionally characterise the SH3 domain ligands and how they relate to the functions of C- and N1-Src.

2. **Investigate the mechanism of ligand binding by the N1-Src SH3 domain:**

Peptide arrays were employed to identify N1-Src SH3 domain binding motifs within the ligands identified in Aim 1, and to provide insight into the overall motif preference of the N1-Src SH3 domain. Furthermore, NMR studies were used to compare the chemical environments of the C- and N1-Src SH3 domains and also to assess the mechanism of peptide ligand binding by the N1-Src SH3 domain. Mutagenesis of the N1-Src SH3 domain n-Src and RT loops was also used to investigate their functions in ligand binding.

3. **Identify novel N1-Src substrates in the developing brain:**

The postnatal day 1 rat brain homogenate that yielded novel N1-Src SH3 domain ligands, was also employed to determine the N1-Src phosphoproteome. A novel *in vitro* kinase assay was conducted using recombinant C- and N1-Src kinase, and their *in vitro* substrates and specific phosphorylation sites were identified via LC-MS/MS. These data enabled a comparison of the N1-Src interactome and phosphoproteome in a neuronal background and identified candidates for future studies of N1-Src function in the brain.

Chapter 2

Materials and Methods

Chapter 2 Materials and Methods

2.1 Materials

2.1.1 Molecular biology reagents

SYBR®Safe DNA stain was from Life Technologies, Nucleospin plasmid mini- and midi-prep kits were obtained from Macherey-Nagel, DNA HyperLadder I was from Bioline, XL10 Gold supercompetent *E. coli* were purchased from Stratagene and BL21-DE3 *E. coli* were a gift from Dr. D. Ungar. The pGEX-6P-1 plasmids containing the rat N1-Src SH3 domain mutants R1insA, K2insA, V3insA, D4insA, V5insA, R6insA, D99N and W118A and C-Src SH3 domain D99N mutant were synthesised as codon optimised for *E. coli* and cloned via BamHI and SalI restriction sites by General Biosystems (Gene synthesis service). The pEGFP-C1 plasmid containing full length rat Neuronal Enah was codon optimised for mammalian cells and cloned via BglII and BamHI restriction sites by General Biosystems. The wild-type rat C- and N1-Src SH3 domains in pGEX-6P-1 were described previously (Keenan et al, 2017). C- and N1-Src-FLAG plasmids were made in-house by replacing the EGFP gene in the pEGFP-N1 vector with a FLAG tag separated by a glycine/serine rich linker (Keenan et al., 2015).

2.1.2 Biochemistry reagents

Protein Biochemistry: Precision Plus Protein All Blue Standards protein ladder was from BioRad, 2X Laemmli SDS sample buffer and His-Select Nickel affinity gel were from Sigma. Protease inhibitor cocktail (P8849) was from Sigma. Glutathione agarose resin was from Genscript and 3C Prescission protease was from GE Healthcare. Zeba spin desalting columns (7K MWCO, 0.5mL) and Slide-A-Lyzer dialysis cassettes (3,500 MWCO) were from Thermo Scientific Pierce. Vivaspin 20 (3,000 MWCO) centrifugal concentrators were from Sartorius. Spin-X Centrifuge Tube Filters 0.45µm Pore CA Membrane Nonsterile were from Corning Life Sciences. 5′-4-Fluorosulfonylbenzoyl adenosine (FSBA) was from Santa Cruz Biotechnology.

Peptides: The Dynamin I B8 peptide (PFGPPPQVPSRPNRA) lyophilised at a purity of >90 %, with N-terminal acetylation and C-terminal amidation was synthesised by Genscript. Custom-made peptide arrays from Kinexus were designed with 15-mer peptides with a frame shift of four residues that were N-terminally acetylated and C-terminally conjugated onto a trioxatridecanediamine (TOTD) membrane.

Western blotting: PVDF membrane and chemiluminescent HRP substrate were purchased from Millipore. UltraCruz Autoradiography Film was from from Santa Cruz Biotechnology.

Antibodies: Phosphotyrosine (clone PY20; BD Bioscience Cat no. 610000), Dynamin I p-S774 (St John's Laboratory Ltd), Polyhistidine HRP conjugate (Sigma Cat no. A7058-1VL), Dynamin I (Santa Cruz Biotechnology Cat no. sc-6402), agarose conjugated anti-PY20 (Enzo Life Sciences Cat no. BML-SA241-0500), Enah/Mena (Bethyl Laboratories Cat no. A301-500A), Raph1 (Novus Biologicals), SF1 (Bethyl Laboratories), N-WASP (Santa Cruz Biotechnology Cat no. sc-20770), Nono (Bethyl Laboratories Cat no. A300-587A), Anti-Flag M2 affinity gel (Sigma Cat no. A2220), anti-mouse, rabbit and goat HRP conjugate (Sigma), agarose conjugated anti-4G10 (Millipore Cat no. 16-101), Actin B (ProteinTech Cat no. 60008-1-Ig), Src p-Y416 and Src p-Y527 (Cell Signalling Technologies Cat no. 2101 and 2105).

2.1.3 Cell culture reagents

Dulbecco's Modified Eagle Medium and penicillin/streptomycin were from Gibco, Ecotransfect was from Oz Biosciences, Hygromycin B was obtained from Thermo Fisher, foetal bovine serum and trypsin/EDTA were from Invitrogen, doxycycline was obtained from Santa Cruz Biotechnology. Tetracycline-inducible Flp-in T-Rex HeLa cell lines that stably express C-terminal FLAG tagged C- or N1-Src kinase were generated in-house by Dr Philip Lewis. B104 and COS7 cells were obtained from ECACC.

2.2 Molecular Biology

2.2.1 Agarose gel electrophoresis

DNA was resolved via agarose gel electrophoresis. In order to prepare the gels 0.7-2 % (w/v) agarose was added to 60 ml of TAE buffer (40 mM Tris, 20 mM acetic acid, 1 mM EDTA). The suspension was heated via microwave and upon cooling SYBR®Safe DNA stain was added at 1:20,000 (v/v). Once set in a cassette, the gel was submerged in TAE buffer and the DNA samples were loaded in Orange G buffer (3 % (v/v) glycerol, 0.04 % (w/v) Orange G dye). The DNA was sufficiently resolved at ~ 80 V and then visualised under blue safelight.

2.2.2 Bacterial transformation

Bacterial transformations were conducted using 50 µl of competent *E. coli* XL-10 gold or BL21 DE3. One hundred nanograms of plasmid DNA was added to the bacteria and incubated on ice for 15-30 min. The bacteria were heat shocked for 45 s at 42 ℃, and then incubated on ice for 2 min. Three hundred microlitres of lysogeny broth (LB) media (1 % NaCl, 1 % tryptone, 0.5 % yeast extract w/v) was added to the transformed bacteria and incubated for 30 min at 37 ℃ and 200 rpm. The bacteria were plated at volumes of 50-200 µl on LB agar plates (1 % NaCl, 1 % tryptone, 0.5 % yeast extract, 2 % agar w/v) containing the required antibiotic of kanamycin (50 µg/ml) or ampicillin (100 µg/ml) and incubated overnight at 37 ℃.

2.2.3 Preparation of plasmid DNA from bacterial cultures

A single colony of transformed XL-10 *E. coli* grown under antibiotic selectivity on LB agar plates was used to inoculate 5 ml (mini) or 100 ml (midi) of LB media containing the required antibiotic. The cultures were incubated overnight at 37 ℃ and 200 rpm. The bacteria were pelleted by centrifugation at 5000 x g for 10 min at 4 ℃, and the plasmid DNA was purified from the pellets as per the manufacturer's instructions. The DNA was eluted in 10 mM Tris, pH 8.5 and stored at -20 °C. The DNA concentration and quality was determined via the absorbance at A260 using a NanoDrop spectrophotometer.

2.2.4 DNA sequencing

The sequencing of plasmid DNA was conducted by the Genomics unit in the Technology Facility at the University of York. One hundred nanograms of plasmid DNA and 3.2 µM of vector specific primer was submitted as a pre-mix. DNA sequence analysis was conducted using Sequence Scanner software.

2.2.5 Preparation of glycerol stocks

For storage at -80 ℃, transformed *E. coli* XL-10 or BL21 DE3 were stored in cryovials in LB media with 25 % filter sterilised glycerol.

2.3 Protein Biochemistry

2.3.1 Sodium dodecyl sulphate-polyacrylamide gel electrophoresis (SDS-PAGE)

Proteins were resolved via SDS-PAGE gel electrophoresis using BioRAD Mini-PROTEAN® Tetra Vertical Electrophoresis Cell equipment. Resolving gels were prepared in 5 ml with (7.5 – 15 % (v/v) acrylamide, 0.05 % (w/v) ammonium

persulphate (APS), 0.1 % (v/v) tetramethylethylenediamine (TEMED), 0.1 % (w/v) SDS and 375 mM Tris pH 8.8). Stacking gels were subsequently prepared in 2.5 ml with (4 % acrylamide, 0.05 % APS, 0.1 % TEMED, 0.1 % SDS and 125 mM Tris pH 6.8) and were set with a 10 well comb. Protein samples were loaded in Laemmli sample buffer (2 % SDS, 10 % glycerol, 5 % beta-mercaptoethanol, 0.002 % bromophenol blue, 125 mM Tris.HCl pH 6.8) after heating at 95 °C for 10 min. The gel was submerged in SDS-PAGE buffer (25 mM Tris, 192 mM glycine, 0.1 % (w/v) SDS) and ran at ~ 200 V until sufficiently resolved. The gels were then utilised in Western blotting (Section 2.3.2) or stained with Coomassie Blue (15 % methanol, 10 % acetic acid (v/v), 0.2 % w/v Coomassie Brilliant Blue) for 1 h and subsequently de-stained (40 % methanol, 10 % (v/v) glacial acetic acid) for visualisation of proteins and downstream applications such as protein quantification by densitometry analysis (Section 2.14.1).

2.3.2 Western blotting

Proteins were transferred to polyvinylidene fluoride (PVDF) membranes via wet transfer. The membranes were activated in 100 % methanol for 1 min and then pre-equilibrated in transfer buffer (25 mM Tris, 192 mM glycine, 20 % (v/v) methanol). The SDS-PAGE gel and PVDF membrane were assembled into the BioRad transfer apparatus cassette as per the manufacturer's instructions, and transferred at 66 V for 1 h or 20 V overnight. Ponceau stain (5 % (v/v) acetic acid, 0.1 % (w/v) Ponceau S) was used to confirm the successful transfer of proteins. The membranes were then blocked for 1 h at room temperature in 3 % (w/v) Marvel skimmed milk powder (marvel) in PBS (142 mM NaCl, 2 mM KCl, 8 mM Na_2HPO_4, 1.5 mM KH_2PO_4 pH 7.4) or overnight at 4 °C. The membranes were then incubated with the appropriate primary antibody (Table 2.1) in PBS for 3 h at room temperature or overnight at 4 °C with agitation. The membranes were washed for 3 x 5 min in 0.5 % (v/v) Tween-20 in PBS before incubation with the secondary antibody of anti-mouse, rabbit or goat HRP (Table 2.1) in 3 % marvel and 0.5 % Tween-20 in PBS, for a 1 h incubation at room temperature. The membranes were washed for 3 x 10 min in 0.5 % Tween-20 in PBS and then incubated with enhanced chemiluminescence reagent for visualisation with autoradiography film at the necessary exposure times.

Table 2.1: Primary and Secondary antibodies utilised in Western Blotting.

Primary antibody		Secondary antibody	
Antibody and source	**Concentration**	**Antibody**	**Concentration**
Dynamin I	1:200	α-Goat HRP	1:150,000
N-WASP	1:200	α-Rabbit HRP	1:5000
Nono	1:1000	α-Rabbit HRP	1:5000
Raph1	1:400	α-Rabbit HRP	1:5000
Sf1	1:1000	α-Rabbit HRP	1:5000
Enah	1:1000	α-Rabbit HRP	1:5000
PY20	1:1000	α-Mouse HRP	1:5000
His-HRP	1:20,000-120,000	N/A	N/A
Dynamin I S774	1:500	α-Rabbit HRP	1:5000
Flag	1:1000-10,000	α-Mouse HRP	1:5000
Src p-Y416	1:1000	α-Rabbit HRP	1:5000
Src p-Y527	1:1000	α-Rabbit HRP	1:5000
Actin	1:1000	α-Mouse HRP	1:5000

2.4 Protein expression and purification

2.4.1 Protein expression in LB media

GST- and His-tagged fusion proteins were expressed in BL21 *E. coli*. LB media (1 % NaCl, 1 % tryptone and 0.5 % (w/v) yeast extract) containing antibiotic at the required dilution (100 µg/ml ampicillin, 34 µg/ml chloramphenicol or 50 µg/ml kanamycin), was inoculated with an overnight starter culture (50 ml) of transformed *E. coli* BL21 DE3 to a starting OD of 0.05. The culture was incubated at 37 ℃ and 200 rpm until the OD reached 0.7-1.0 before induction with isopropyl β-D-1-thiogalactopyranoside (IPTG) (0.3-1 mM) to induce expression for 3-4 h at 37 ℃ or overnight at 22 ℃. The bacteria were then pelleted by centrifugation for 15 min at 5000 x g, and when required the bacteria pellets were stored at -80 ℃.

2.4.2 Expression of ^{15}N labelled proteins

An *E. coli* colony from a fresh transformation was used to inoculate 10 ml of LB media with the required antibiotic. The culture was incubated at 37 ℃ and 200 rpm for 8 h. The bacteria were then pelleted by centrifugation and resuspended in 1 ml of M9 base (42 mM Na_2HPO_4, 22 mM KH_2PO_4 and 8.5 mM NaCl) and used to inoculate 50 ml of minimal media (0.4 % (w/v) glucose, 2 mM $MgSO_4$, 200 µM $CaCl_2$, 20 mM NH_4Cl, trace metals (50 µM $FeCl_3$, 20 µM $CaCl_2$, 10 µM $MnCl_2$, 10 µM $ZnSO_4$, 2 µM $CoCl_2$, 2 µM $CuCl_2$, 2 µM $NiCl_2$, 2 µM Na_2MoO_4 , 2 µM Na_2SeO_3, 2 µM H_3BO_3), vitamins (2.6 µM riboflavin, 8.1 µM nicotinamide, 5.9 µM pyridoxine, 3.7 µM thiamine), and the required antibiotic in M9 base) for incubation overnight at 37 ℃ and 200 rpm. The overnight culture was pelleted by centrifugation for 15 min at 5,000 x g, and resuspended in M9 base and used to inoculate 1L of minimal media, whereby in order to enable uniform ^{15}N incorporation (*U*-^{15}N), NH_4Cl was substituted with 1 g of $^{15}NH_4Cl$. The litre was inoculated to a starting OD of 0.05, and incubated at 37 ℃ and 200 rpm before induction at OD 0.7-1.0 with 0.3 mM IPTG for incubation overnight at 22 ℃ and 200 rpm. The bacteria were then pelleted by centrifugation for 15 min at 5,000 g and subsequently used in protein purification (Section 2.4.3) followed by cleavage of the GST- fusion tag (Section 2.4.4).

2.4.3 Purification of His- and GST-tagged recombinant proteins

The bacteria that were pelleted by centrifugation and stored at -80 ℃ were thawed on ice and resuspended in 1 mM phenylmethylsulfonyl fluoride (PMSF), 1x protease inhibitor cocktail, lysozyme at 13.3 mg/L of induction culture, 1.5 % (v/v) Triton X-100 and 6.5 mM dithiothreitol (DTT) in PBS and incubated on ice for 30 min. The suspension was sonicated every 30 s for a total of 5 min 30 s at 12 kHz. The lysate was clarified by centrifugation for 30 min at 4 ℃ and 17,000 x g. For the purification of GST-tagged proteins, the supernatant was incubated with 200-500 µl of glutathione agarose resin for 1-2 h at 4 ℃ with agitation. Following the incubation, the resin was washed 7 x in at least 10 vols of PBS and once in 1.2 M NaCl via centrifugation at 720 x g for 2 min at 4 ℃. The proteins were stored on glutathione agarose resin at - 20 ℃ in 50 % glycerol in PBS, for use in pull-down assays (Section 2.7/8). Alternatively, the GST tag was cleaved (Section 2.4.4) followed by dialysis and concentration (Section 2.4.5).

His-tagged fusion proteins were purified as above. However, protease inhibitor cocktail

specific for the purification of histidine-tagged proteins was utilised. In addition, after clarification of the lysate, the supernatant was incubated for 1-2 h at 4 ℃ with 200-500 µl of His-select Nickel affinity resin with agitation. The resin was washed 7 x in at least 10 vols (50 mM sodium phosphate, 0.3 M NaCl, 10 mM imidazole pH 8.0). The proteins were then eluted from the resin a total of three times in at least one resin volume of elution buffer (50 mM sodium phosphate, 0.3 M NaCl, 250 mM imidazole pH 8.0) via incubation for 10 min with agitation, followed by centrifugation for 5 min at 5000 g to extract the supernatant. The elutions were then combined and dialysed overnight into the required buffer (Section 2.4.5).

2.4.4 Cleavage of the GST tag from GST fusion proteins

Purified GST fusion proteins were prepared on glutathione agarose resin in PBS. In order to cleave the GST tag, the resin was incubated overnight at 4 ℃ with agitation with GST-tagged 3C prescission protease (one unit of protease was used per 100 µg of GST-fusion protein) in 50 mM Tris, 150 mM NaCl, 1 mM EDTA, 1 mM DTT pH 7.0. The resin was pelleted by centrifugation for 5 min at 16,000 x g and 4 ℃, and the supernatant containing the cleaved protein was removed. The resin was then resuspended in buffer and this step was repeated three times to isolate maximal cleaved protein. The supernatants were then combined and dialysed overnight (Section 2.4.5).

2.4.5 Protein dialysis and concentration

Proteins were dialysed into PBS or 20 mM sodium phosphate, 100 mM NaCl pH 6 overnight at 4 ℃ using Slide-A-Lyzer™ Dialysis Cassettes with a 3,500 Dalton MWCO, and subsequently concentrated to an appropriate volume and concentration using Vivaspin® 20 columns with a 3,000 Dalton MWCO as per manufacturer's instructions.

2.4.6 Protein quantification

The protein concentration of a cell/tissue lysate used for downstream applications such as immunoprecipitation or pull-down assays was determined by Bradford assay (Kruger 1994). Bovine serum albumin (BSA) was used as a standard to calibrate the protein concentration (mg/ml) using 300 µl of Bradford reagent (5 % methanol, 10 % (v/v) orthophosphoric acid, 0.01 % (w/v) Coomassie Brilliant blue G) for each reaction in a 96 well plate.

The concentration of recombinant purified proteins was determined using a NanoDrop

spectrophotometer. The absorbance measured at 280 nm (A) was converted to concentration with the Beer-Lambert law (A = ε * b * c), where ε is the extinction coefficient (calculated with ExPASy ProtParam tool; www.web.expasy.org/protparam/), b is the path length, and c is the molar concentration. Coomassie stained SDS-PAGE gels were also used as a semi-quantitative method to compare amounts of protein, using BSA as a protein standard and analysis by densitometry (Section 2.14.1).

2.5 Preparation of cell and tissue lysates

2.5.1 Preparation of postnatal day 1 rat brain homogenate

Postnatal day 1 (P1) and adult rat brain tissue was provided by Dr Sangeeta Chawla and Dr Christopher Ugbode (University of York). The animals had been euthanised according to Schedule 1 of the UK Home Office Animals (Scientific Procedures) Act. Brains were homogenised using seven up down strokes of a dounce homogeniser at full speed. The homogenisation was performed in ice cold RIPA buffer (50 mM Tris, 150 mM NaCl, 1 % (v/v) Triton-X-100, 0.5 % (w/v) sodium deoxycholate, 0.1 % (w/v) SDS, 1 mM EDTA, 1 mM Na_3VO_4, 0.1 % (v/v) beta mercaptoethanol, 0.5 % (v/v) PMSF and 1x protease inhibitor cocktail) at a ratio of 1 g tissue / 5 ml buffer. The homogenates were incubated for 1 h at 4 °C with agitation, and clarified by centrifugation for 30 min at 20,000 g and 4 °C. The supernatant was then retained for direct use in assays.

2.5.2 Preparation of synaptosomal lysates

Isolated adult rat brain nerve terminals (synaptosomes) were prepared previously in collaboration with Dr Sangeeta Chawla according to the method of Evans, 2015. Synaptosomes (10 mg/ml protein) were lysed in 1x RIPA buffer and incubated for 15 min at 4 °C with agitation, before centrifugation for 10 min at 4 °C at 16,000 x g to remove insoluble material. The supernatant was then retained for direct use in assays.

2.6 *In vitro* kinase assays

2.6.1 *In vitro* whole cell lysate kinase assays with recombinant and cellular purified Src

Preliminary *in vitro* whole cell lysate kinase assays were conducted with purified recombinant Δ80 His-C- and N1-Src kinases (Keenan et al. 2015) and 1 mg of P1 rat brain lysate (Section 2.5.1) in RIPA buffer per condition. The P1 lysate was incubated

with 5 mM FSBA (solubilised in DMSO) for 1 h at 30 ℃ in order to inhibit endogenous kinases. The lysate was then centrifuged for 10 min at 16,000 x g, and the supernatant desalted by Zeba spin desalination columns (7,000 MWCO) as per the manufacturer's instructions, in order to remove any unbound FSBA. 1x protease inhibitor cocktail, kinase assay buffer (100 mM Tris, 25 mM $MgCl_2$, 1 mM Na_3VO_4 , pH 7.5), 3 µg (285 nM) Δ80 His-C- and N1-Src kinases, and 800 µM ATP were added to the lysates and incubated for 1.5-3 h at 30 ℃, before termination with Laemmli sample buffer for analysis by Western blotting.

In vitro whole cell lysate kinase assays were conducted as described above with purified full length C- and N1-Src-FLAG from stable HeLa cell lines. The C-terminal FLAG-tagged Src kinases were immunoprecipitated from confluent 75 cm^2 flasks using agarose conjugated anti-flag resin (Section 2.8.2). The immunoprecipitated kinases on resin were then supplemented into the described assay above and incubated for 1 h 30 at 30 ℃.

2.6.2 *In vitro* whole cell lysate kinases assays in P1 rat brain homogenate for LC-MS/MS analysis

The triplicate *in vitro* whole cell lysate kinase assays submitted for LC-MS/MS analysis were conducted as described in Section 2.6.1. However, following FSBA treatment and subsequent desalting, 2.6 mg of P1 lysate was utilised per condition. The kinase assays were conducted with 240 nM of Δ80 His-C- and N1-Src kinases, and 1 mM ATP, for a 3 h incubation at 30 ℃. Upon completion of the assay, the samples were precipitated in acetone via the addition of 4x the sample volume of cold acetone, followed by vortexing for 1 min, and incubation overnight at - 20 ℃. The following day the samples were centrifuged for 10 min at 15,000 g and 4 ℃. The supernatants were discarded and the precipitated protein pellets were air dried for 3 min at room temperature, followed by resuspension in 150 µl of 4 % (w/v) SDS, 100 mM Tris, 100 mM DTT pH 7.6 and 10 min of boiling at 95 ℃ to aid protein solubilisation in preparation for on-filter tryptic digestion (Section 2.10.2) and subsequent LC-MS/MS analysis (Section 2.10.3).

2.6.3 *In vitro* kinase assays with purified recombinant proteins

In vitro kinase assays with GST tagged-Src substrate peptide (Keenan et al. 2015) were conducted in kinase assay buffer (100 mM Tris, 25 mM MgCl, 1 mM Na_3VO_4 pH 7.5)

with 60 nM Δ80 His-C- and N1-Src kinases, 7 µM of GST-tagged Src substrate peptide and 0.5 mM ATP. The assays were incubated for 1.5 h at 30 ℃ before termination with Laemmli sample buffer for analysis by Western blotting.

2.7 Protein-protein interaction assays via pull-downs with fusion tags

2.7.1 Pull-down assays with recombinant proteins and cell lysates

Protein pull-downs from cell lysates were conducted with immobilised GST and GST-fusion proteins on glutathione agarose resin. An equal molar concentration of GST- and GST-fusion proteins were incubated with an equal quantity of P1 or synaptosome lysate (Section 2.5) for 1-2 h at 4 ℃ with agitation. Post-incubation the resin was pelleted by centrifugation for 2 min at 16,000 x g and 4 ℃. The supernatant was removed and the resin was transferred to spin-X centrifuge columns that were pre-equilibrated with wash buffer. The resin was then washed 6-8 times in 800 µl wash buffer (Table 2.2) for 1 min at 16,000 x g and 4 ℃, before a 10 min incubation with Laemmli sample buffer, and subsequent elution via centrifugation for 10 min at 16,000 x g.

Table 2.2: Protein concentrations and incubation conditions utilised for pull-downs with recombinant proteins in cell lysates.

Interaction assay	Lysate (mg)	GST or GST-SH3 domain concentration (µM)	Wash buffer
GST-SH3 domain pull downs for LC-MS/MS analysis (3.3.1)	2 mg P1	12.5 µM	PBS
Dynamin I and Dynamin I-S774 pull downs (4.3.4)	1 mg synaptosome	13 µM	RIPA
N1-Src SH3 domain insertion alanine mutants (4.3.11)	0.5 mg synaptosome	5 µM	RIPA
C- and N1-Src SH3 domain D99N mutats (4.3.12)	1 mg P1	7 µM	RIPA

2.7.2 Pull-down assays with purified recombinant proteins

Interaction assays with two purified recombinant proteins were conducted with one of the interactors immobilised on glutathione agarose resin via its GST fusion tag. An equal

molar concentration of GST- and GST-fusion protein were incubated with an equal concentration of His-tagged interactor in PBS for 1-2 h at 4 ℃ with agitation. Post-incubation the resin was pelleted by centrifugation for 2 min at 16,000 x g and 4 ℃. The supernatant was removed and the resin was transferred to pre-equilibrated spin-X centrifuge columns. The resin was then washed 6-8 times in 800 µl wash buffer (Table 2.3) for 1 min at 16,000 x g and 4 ℃, before a 10 min incubation with Laemmli sample buffer, and subsequent elution via centrifugation for 10 min at 16,000 x g.

Table 2.3: Protein concentrations and incubation conditions utilised for pull-downs with recombinant proteins.

Interaction assay	Protein concentrations (µM)	Wash buffer
GST-Dyn1 PRD and His-tagged N1-Src SH3 domain (4.3.4)	GST-Dyn1 PRD- 17 µM His-N1-Src SH3 domain- 20 µM	PBS

2.8 Immunoprecipitation

2.8.1 Phosphopeptide immunoprecipitation for LC-MS/MS analysis

The *in vitro* kinase assays (Section 2.6.2) were subjected to on-filter tryptic digestion (Section 2.10.2) and the tryptic peptides were dried by vacuum (by Dr Adam Dowle). In order to immunoprecipitate the phosphopeptides, the peptides were resuspended in 350 µl of 100 mM Tris pH 7.4 by vortexing. In total 80 µl of pre-washed agarose conjugated 4G10 (50 µl) and PY20 (30 µl) slurry was added to the suspension and incubated overnight at 4 ℃ with agitation. The following day the resin was pelleted by centrifugation for 5 min at 16,000 x g and 4 ℃. The supernatant was removed and the resin applied to a pre-equilibrated spin-X column. The resin was then washed 3 times in 750 µl Tris 100 mM pH 7.4 and 3 times in PBS for 1 min at 16,000 x g and 4 ℃. The immunoprecipitated peptides were eluted twice (90 µl and 60 µl) in (60 % acetonitrile and 0.15 % trifluoroacetic acid) via centrifugation for 10 min at 16,000 x g.

2.8.2 Immunoprecipitation of FLAG-tagged Src kinases

C-terminal FLAG-tagged full length C- and N1-Src kinases were immunoprecipitated from confluent 75 cm^2 flasks of stable HeLa cell lines that were treated with doxycycline (1 µg/ml) for 48 h to induce expression. As controls the same cell lines were utilised but

without doxycycline treatment. The culture media was removed and the cells washed in PBS, followed by lysis in 1 ml of cold RIPA buffer. The cells were incubated on ice for 5 min, scraped from the bottom of the flask, and then incubated on ice for a further 5 min. The lysate was then clarified by centrifugation for 10 min at 16,000 g and 4 ℃ to pellet the insoluble material. The supernatant was retained, including a small fraction as input. The remaining supernatant was added to 20 µl of agarose-conjugated anti-Flag M2 resin (pre-washed in RIPA) per condition. The resin was incubated overnight at 4 ℃ with agitation. The following day the resin was pelleted by centrifugation for 10 min at 16,000 x g and 4 ℃. The supernatant was removed and the resin washed eight times with 1.5 ml of RIPA buffer for use in *in vitro* kinase assays (Section 2.6.1).

2.9 Peptide arrays

2.9.1 Detection of C- and N1-Src SH3 domain ligands via peptide arrays

Custom made peptide arrays were designed as 15-mer N-terminally acetylated peptides that were conjugated to trioxatridecanediamine (TOTD) membranes via their C-terminus. The membranes were activated in 100 % methanol for 10 min and then washed 3 x 5 min in PBS. The membranes were blocked for 1 h at room temperature in 4 % (w/v) marvel in PBS and controls for non-specific binding by the antibody were conducted by subsequently incubating the membrane with anti-His-HRP (1:120,000 v/v) for 2 h at room temperature in 4 % marvel in PBS. The membrane was then washed 3 x 10 min in 0.5 % Tween-20 (v/v) in PBS and incubated with enhanced chemiluminescent reagent for visualisation with autoradiography film at the required exposure times. Following confirmation that there was not non-specific binding by the antibody, the membrane was reactivated in methanol and blocked as previously, and then incubated with 0.5 µM His-tagged C-Src SH3 domain in blocking buffer for 2 h at room temperature or 1 µM His-tagged N1-Src SH3 domain in PBS overnight at 4 ℃. The membranes were then washed 3 x 10 min in 0.5 % Tween-20 in PBS, before incubation with anti-His-HRP (1:120,000) for 2 h at room temperature in 4 % marvel in PBS. The membrane was then washed 3 x 10 min in 0.5 % Tween-20 in PBS and incubated with chemiluminescent reagent for visualisation with autoradiography film. All incubations were conducted with agitation at room temperature, unless stated otherwise.

2.10 Mass spectrometry

2.10.1 In gel tryptic digestion

Following SDS-PAGE gel electrophoresis of the GST-C- and N1-Src SH3 domain pull-downs, the gel was excised into two fractions ~ < 40 kDa and > 40 kDa to separate the GST-SH3 domain bait and the remainder respectively. The gel pieces were then further excised into 1 mm pieces. The gel was washed twice with 25 mM ammonium bicarbonate in 50 % (v/v) acetonitrile for 20 min, and then once with acetonitrile for 5 min, followed by drying for 20 min under vacuum. The gel was then incubated with 10 mM DTT in 100 mM ammonium bicarbonate for 1 h at 56 ℃. The supernatant was removed, and the gel incubated with 50 mM iodoacetamide in 100 mM ammonium bicarbonate in the dark for 30 min at room temperature. The supernatant was removed and the gel washed in 100 mM ammonium bicarbonate for 15 min, then with 25 mM ammonium bicarbonate in 50 % acetonitrile for 15 min, and acetonitrile for 5 min. The supernatant was removed and the gel dried for 20 min under vacuum. The gel samples were incubated with trypsin at 25 µg/ml in 25 mM ammonium bicarbonate overnight at 37 ℃. The following day the supernatant containing the digested peptides was retained, and any remaining peptide was extracted by incubation with 50 % acetonitrile for 15 min, this was repeated twice and the extracts pooled with the supernatant. The combined supernatant was then dried under vacuum, and the peptides reconstituted in 0.1 % trifluoroacetic acid for analysis by LC-MS/MS (Section 2.10.3).

2.10.2 On filter tryptic digestion

The described method was conducted and provided by Dr Adam Dowle (Metabolomics and Proteomics, Bioscience Technology facility, The University of York).

The solubilised protein was diluted to 2 mL with aqueous 8 M urea in 100 mM Tris pH 8.5 before loading onto a 4 mL, 30 kDa cut-off, regenerated cellulose Amicon spin filter. Protein was washed on-filter twice with 2 mL aqueous 8 M urea, 100 mM Tris pH 8.5 before alkylating at room temperature for 30 min with 2 mL of 40 mM iodoacetamide in the same urea solution. Protein was washed once more with 2 mL 8 M urea, 100 mM Tris pH 8.5 before transferring into aqueous 50 mM ammonium bicarbonate with 4 x 2 mL washes. Centrifugation was performed at 14,000 g for 20 min after all washes. Protein was digested on-filter with 20 µg sequencing grade modified trypsin and incubation at 37 ℃ for 16 h. Resulting peptides were recovered from the filter with centrifugation at 14,000 g for 20 min pre- and post-addition of 1 mL water. A 5 %

aliquot was taken from each sample for analysis of non-enriched peptide before drying all samples under vacuum.

2.10.3 LC-MS/MS

The described method was conducted and provided by Dr Adam Dowle (Metabolomics and Proteomics, Bioscience Technology facility, The University of York).

Samples were loaded onto an UltiMate 3000 RSLCnano HPLC system equipped with a PepMap 100 Å C_{18}, 5 µm trap column (300 µm x 5 mm) and a PepMap, 2 µm, 100 Å, C_{18} EasyNano nanocapillary column (75 m x 500 mm). The trap wash solvent was aqueous 0.05 % (v/v) trifluoroacetic acid and the trapping flow rate was 15 µL/min. The trap was washed for 3 min before switching flow to the capillary column. Separation used gradient elution of two solvents: solvent A, aqueous 1 % (v/v) formic acid; solvent B, aqueous 80 % (v/v) acetonitrile containing 1 % (v/v) formic acid. The flow rate for the capillary column was 300 nL/min and the column temperature was 30 °C. The linear multi-step gradient profile was: 3-10 % B over 7 min, 10-35 % B over 30 min, 35-99 % B over 5 min and then proceeded to wash with 99 % solvent B for 4 min. The column was returned to initial conditions and re-equilibrated for 15 min before subsequent injections. The nanoLC system was interfaced with an Orbitrap Fusion hybrid mass spectrometer with an EasyNano ionisation source. Positive ESI-MS and MS2 spectra were acquired using Xcalibur software (version 4.0). Instrument source settings were: ion spray voltage, 1,900 V; sweep gas, 0 Arb; ion transfer tube temperature; 275 °C. MS1 spectra were acquired in the Orbitrap with: 120,000 resolution, scan range: m/z 375-1,500; AGC target, $4e^5$; max fill time, 100 ms. Data dependant acquisition was performed in top speed mode using a fixed 1 s cycle, selecting the most intense precursors with charge states 2-5. Easy-IC was used for internal calibration. Dynamic exclusion was performed for 50 s post precursor selection and a minimum threshold for fragmentation was set at $5e^3$. MS2 spectra were acquired in the linear ion trap with: scan rate, turbo; quadrupole isolation, 1.6 m/z; activation type, HCD; activation energy: 32 %; AGC target, $5e^3$; first mass, 110 m/z; max fill time, 100 ms. Acquisitions were arranged by Xcalibur to inject ions for all available parallelizable time.

2.11 Nuclear magnetic resonance spectroscopy

2.11.1 NMR sample preparation

All [*U*-^{15}N] labelled protein samples were dialysed overnight into 20 mM sodium phosphate, 100 mM NaCl pH 6. The samples were 600 µl in final volume containing 10 % D_20, and were analysed in 5 mm diameter NMR tubes (Wilmad). All spectra were acquired at 25 °C on a Bruker Avance NEO 700 MHz spectrometer with a liquid nitrogen cooled triple resonance cryoprobe, and the data processed with TopSpin version 4. Spectral referencing values relative to the internal standard 4,4-dimethyl-4-silapentane-1-sulfonic acid (DSS) were provided by Dr Alex Heyam.

2.11.2 Backbone assignment of the N1-Src SH3 domain

0.5 mM *U*-^{13}C ^{15}N labelled N1-Src SH3 domain was expressed and purified into 20 mM sodium phosphate, 100 mM NaCl pH 6 by the Potts lab (Dr Andrew Brentnall). The spectra were acquired at 25 °C on a Bruker Avance 700 MHz spectrometer with a liquid nitrogen cooled triple resonance cryoprobe at the National Institute for Medical Research (NIMR). The spectra were processed in NMRPipe and referenced to DSS by Dr Andrew Brentnall.

The acquired pairs of CBCA(CO)NNH / HNCACB, and HNCO / HN(CA)CO spectra facilitated the triple resonance backbone assignment of the N1-Src SH3 domain in CCPN software. Resonance assignment was conducted manually, primarily using the CBCA(CO)NNH / HNCACB spectra. The assignment was made utilising spin systems, which contain all resonances belonging to an amino acid. The 3D HNCACB spectrum correlated each NH group to the Cα and Cβ of a particular residue (n) and those of the preceding residue (n-1) via magnetisation transfer. In addition, the CBCA(CO)NNH spectrum correlated each NH group to the Cα and Cβ of the preceding residue (n-1). These spectra were superimposed to identify sequential and intra residue correlations, which enabled the spin systems of individual residues to be linked (excluding prolines which cause a break in the sequence). The primary sequence was then mapped onto the chains, and amino acids such as alanine, serine, and threonine were readily identifiable as they have distinct Cβ chemical shifts, and glycine does not have a Cβ.

2.11.3 Peptide ligand titrations with the C- and N1-Src SH3 domains

U-^{15}N labelled C- and N1-Src SH3 domains were expressed and purified into 20 mM sodium phosphate, 100 mM NaCl pH 6 with 10 % D_2O. The lyophilised 15 mer Dynamin I B8 peptide (PFGPPPQVPSRPNRA) was resuspended in milliQ pH 6. The

peptide was aliquoted and lyophilised overnight to achieve the SH3:peptide molar concentration ratios of 1:0.1, 0.25, 0.5, 0.75, 1, 1.5, 2 and 4 for 150 µM C-Src, and 1:0.25, 0.75, 1.5, 2.5, 4.5, 8.4, 14.4 and 24.3 for 185 µM N1-Src. A 2D (^{1}H-^{15}N) heteronuclear single quantum coherence (HSQC) spectrum was obtained for each SH3 domain in the absence of peptide, and then upon the resuspension of the lyophilised peptide at each titration point. The pH was monitored for consistency throughout. The spectra were acquired and processed as described (Section 2.11.1), and the titration series spectra were superimposed in CCPN software for chemical shift perturbation analysis (Section 2.11.4). The C-Src SH3 domain was referenced to the assignments from the Biological Magnetic Resonance Bank (BMRB) source 3433 (Yu et al. 1993) and the N1-Src SH3 domain was referenced to the manual assignment (Section 2.11.2).

2.11.4 Chemical shift analysis in CCPN software

Chemical shift perturbations between individual 2D (^{1}H-^{15}N) HSQC spectra were calculated using CCPN software (Vranken et al. 2005). The data analysis 'shift differences' tool was used to calculate the change in the hydrogen (ΔδH) and nitrogen shifts (ΔδN) (ppm) for each cross-peak/ SH3 domain backbone residue, with the exception of prolines. The compound chemical shift perturbations were then calculated for each residue by inserting the (ΔδH) and (ΔδN) into the below formula (Schumann et al. 2007):

$$\delta = \left[(\Delta\delta H)^2 + (\Delta\delta N/5)^2\right]^{1/2}$$

2.12 Cell biology Techniques

2.12.1 Culture of mammalian cell lines

Mammalian cell lines were cultured in a Class 2 biological safety cabinet. Cell lines were cultured in high glucose DMEM containing glutamine and pyruvate, with 10 % foetal bovine serum (FBS) and 1 % penicillin-streptomycin. Cells were incubated at 37 ˚C with 5 % CO2 in a humidified atmosphere. Hygromycin B (500 µg/mL) was used to maintain selectivity in the stable C- and N1-Src-FLAG HeLa cell lines.

2.12.2 Bringing up and storage of cells

Cell were stored in cryovials at - 80 ℃ in FBS containing 10 % DMSO. The cells were thawed and immediately resuspended in complete media. The suspension was then

centrifuged at 200 x g for 2 min at room temperature, and the cell pellet resuspended in fresh media for transfer to a 25 cm^2 culture flask containing pre-warmed media.

2.12.3 Passage of cell lines

Cells were passaged upon approaching confluency. The media was removed and the cells were washed in sterile PBS. One millilitre of 1x trypsin-EDTA was incubated with the cells for 2-5 min at 37 ℃. Upon dislodging of the cells the trypsin was inhibited by the resuspension of the cells in fresh media. The cells were then split according to their proliferation rates into new 25 or 75 cm^2 flasks containing pre-warmed media.

2.12.4 Plating of cells

Cells were quantified using a haemocytometer and plated into 6 or 24 well plates at appropriate densities for transfection the following day. Oven sterilised 13 mm coverslips were added to 24 well plates to enable cell imaging via microscopy (Section 2.12.7), and 6 well plates were used to analyse transfected cells by Western blotting (Section 2.12.6). COS7 cell were plated at 50,000 cells per well of a 24 well plate, and 25,000 HeLa and B104 cells.

2.12.5 Transient transfection of cells

Mammalian cells were transfected the day after plating using Ecotransfect reagent as per the manufacturer's instructions. Cells were transfected with a DNA:Ecotransfect reagent ratio of 1µg:2µl. Six well plates were transfected with 3 µg of mini- or midi- prepped plasmid DNA, and 24 well plates were transfected with 0.5-1 µg of DNA. Co-transfections in a six well plate were conducted with 1.5 µg of each plasmid. The DNA and Ecotransfect reagent were prepared separately in DMEM, and then combined and incubated for 20 min at room temperature, before being added to the wells dropwise. The cells were then incubated for 48 h at 37 ℃.

2.12.6 Lysis of transfected cells for Western blotting

Following transient transfection and incubation of the cells for 48 h at 37 ℃, the media was aspirated from the cells, and the cells washed 3x in PBS. The cells were then lysed and scraped from the wells in 100 µl (for a 6 well plate) of Laemmli Sample buffer for analysis by SDS-PAGE after boiling for at least 10 min at 95 ℃.

2.12.7 Cell imaging via fluorescence microscopy

Following plating and transfection (Section 2.12.3/4), the media was aspirated from the cells, and the cells were washed 3x in PBS and then fixed in 4 % paraformaldehyde in PBS for 20 min at room temperature. The cells were washed a further three times in PBS and once in distilled water. The coverslips were then removed from the wells and air dried, before mounting onto microscope slides via mowial containing 4′,6-diamidino-2-phenylindole (DAPI). The slides were imaged at 40x objective using a Nikon TE200 epifluorescence inverted microscope with a RoleraXR CCD camera controlled by SimplePCI Software. All image analysis was conducted in ImageJ software.

2.13 Bioinformatics analysis

2.13.1 STRING protein-protein interaction networks and pathway analysis

Protein-protein interaction networks were generated in STRING. All proteins were inputted by their gene name and searched against *Homo Sapiens*. Interactions were obtained from the sources 'Experiments' and 'Databases' with a high confidence interaction score. Functional enrichment GO term analysis of the proteins was conducted using the whole genome as the statistical background by Fishers Exact test with Benjamini–Hochberg correction.

2.13.2 FuzzPro

The rat protein sequences of the GST, GST-C- and N1-Src SH3 domain ligands were inputted into FuzzPro as FASTA format. The search pattern tool was utilised to identify Class I (R/KxxPxxP) and Class II (PxxPxR/K) motifs within the proteins, which were reported as the number of proteins containing the motif, and the total number of motifs within the sequences.

2.13.3 BioGRID and PhosphoSite

In order to identify characterised C-Src ligands within the proteomics datasets the BioGRID database was utilised. The C-Src interactors were filtered to those identified from either 'Affinity capture-MS, Affinity Capture-Western, Two-hybrid, Reconstituted Complex, or Biochemical Activity'. The PhosphoSite database was used to obtain known substrates of C-Src including their specific tyrosine phosphorylation sites.

2.13.4 PRATT motif analysis

PRATT software was used to identify motifs common to the N1-Src SH3 domain peptide ligands from the arrays. The fifteen 15-mer peptide ligands were inputted as FASTA format and motifs were generated that were present in 100, 90, 80, 70 and 60 % of the peptides.

2.13.5 Weblogo motifs

Weblogo motifs were generated by the input of all significantly upregulated C-Src phosphopeptides ($p < 0.05$) with a significant localisation score ($p < 0.05$). The 9 mer peptides were aligned via their central phosphorylated tyrosine residue and inputted as FASTA format.

2.14 Data analysis

2.14.1 Densitometry analysis of SDS-PAGE gels and Western blots

Densitometry was performed on all Western blots and SDS-PAGE gels using ImageJ software. Firstly, densitometry was conducted on SDS-PAGE gels. The density of all bait proteins (C- and N1-Src SH3 domains and mutants) was obtained, and one was set as a standard (usually the wild-type C- or N1-Src). The density of the remaining bait proteins were then calculated as a percentage of the standard. The percentage differences between the bait proteins and the standard were then used to adjust the densitometry values obtained from the accompanying Western blots displaying ligand interactions, in order to account for any differences in the amount of bait protein. This was conducted for the triplicate replicates, and the normalised Western blot density values were then used to express ligand binding as an average percentage of the wild-type.

2.14.2 Statistical analysis

Statistical analysis was performed on all triplicate data. The GST-SH3 domain pull-downs and *in vitro* Src kinase assays that were analysed by LC-MS/MS (Fig.3.2 and Fig.5.3) are biological replicates having utilised brain homogenate from three independent rat litters. The remaining GST-SH3 domain pull-downs (Fig.4.5, 4.14, 4.15) are technical replicates. The proteins spectral counts from the GST-C- and N1-Src SH3 domain pull-downs were analysed by Fishers Exact test with Benjamini-Hochberg correction in Scaffold 4 software. The phosphopeptides peak areas from the C- and N1-Src phosphoproteomics study were analysed by the Peaks Q significance model in PEAKS software by Dr Adam Dowle. The remaining statistical analysis (ANOVA,

T-test) was conducted in SigmaPlot software. The data are presented as the mean plus the standard error of the mean (SEM), and significance is considered at $p < 0.05$.

The C- and N1-Src SH3 domain peptide ligand titration curves (Fig.4.10B) were produced in GraphPad Prism 8 software. The K_d was calculated using the 'One site specific binding' function and model $y = \delta_{max}*x/(K_d + x)$, where x is the ligand concentration (μM), y is the specific binding (CSP (ppm), and δ_{max} the extrapolated maximum specific binding in ppm.

Chapter 3

Identification of novel neuronal Src SH3 domain ligands in the developing brain

Chapter 3: Identification of novel neuronal Src SH3 domain ligands in the developing brain

3.1 Introduction

The only feature distinguishing N1-Src from C-Src is the insertion of six residues (RKVDVR) into the n-Src loop of the SH3 domain. The n-Src and RT loops of SH3 domains are highly variable and to date a small number of SH3 domain isoforms in the n-Src loop have been identified, including N1-Src, Intersectin 1 and Amphiphysin II (Pyper and Bolen 1989; Tsyba et al. 2008; Ramjaun et al. 1997). The neuronal splice variant of Intersectin 1 inserts 5 residues into the n-Src loop, and this modulates ligand binding by both lowering and raising the affinity for Intersectin ligands (Tsyba et al. 2008). Similarly, multiple GST-C-Src SH3 domain ligands including Tau (Reynolds et al., 2008), Focal adhesion kinase (Messina et al., 2003), Snp70 (Craggs et al., 2001) and Rich (Richnau and Aspenström, 2001) do not bind the N1-Src SH3 domain, suggesting that the neuronal insert may have affected the affinity, specificity or ligand consensus of N1-Src.

The C-Src SH3 domain functions in the negative regulation of kinase activity via intramolecular interactions and positive regulation via ligand/substrate interactions (Section 1.2.3/7). The C-Src SH3 domain interacts with two canonical proline rich ligands termed Class I (+xxPxxP) and Class II (PxxPx+), whereby the PxxP motif is flanked by an N- or C-terminal charged residue respectively (Feng et al. 1994). However, it is now accepted that this is a simplified model and SH3 domains can possess atypical ligand motifs, and diverse mechanisms of ligand binding (Section 1.2.3) (Saksela and Permi 2012) and this will be further investigated in the context of N1-Src in Chapter 4.

Identifying N1-Src SH3 domain ligand interactions is key to substrate identification due to the role of the SH3 domain in directing phosphorylation. For example, the C-Src SH3 domain ligands pl30Cas, Paxillin and Sam68 are all phosphorylated by C-Src (Sachdev et al., 2009), and mutation of the Sam68 SH3 domain binding site abolished its phosphorylation (Shen et al., 1999). Similarly, transfection of cells with C-Src containing an SH3 domain deletion, resulted in the identification of SH3 domain ligands via a GST-Src SH3 domain pull-down, however they lacked tyrosine phosphorylation (Weng et al., 1994), indicating that the SH3 domain can be key for substrate interactions and subsequent phosphorylation *in vitro* and *in vivo*.

Few cellular studies have directly compared the functions of C- and N1-Src, however, N1-Src has been shown to initiate 'neurite like' protrusions in fibroblasts (Keenan et al. 2017), as well as differential functions to C-Src in axonogenesis and photoreceptor differentiation (Worley et al. 1997). The SH3 domain must be directly or indirectly driving the function of N1-Src. To date a number of screens have been employed to identify N1-Src SH3 domain ligands, but have only identified a few proteins. Yeast-2-hybrid identified the HCN1 channel (Santoro et al. 1997) and Delphillin (Miyagi et al. 2002). An affinity purification approach with GST-tagged C- and N1-Src SH3 domains was also attempted (Abdelhameed 2010). However, mass spectrometry was not conducted on the entire sample, and only a single N1-Src SH3 domain ligand, Dynamin I, was identified. Other N1-Src SH3 domain ligands include the NMDA receptor (Groveman et al. 2011) and Ena/Vasp like protein (Lambrechts et al. 2000) (Section 1.4.6). However these interactions have only been studied *in vitro*, and only the NMDA receptor was shown to be *in vitro* phosphorylated as well as interacting with the N1-Src SH3 domain. Overall there are significantly fewer characterised N1-Src SH3 domains ligands than C-Src, and currently no *in vivo* substrates. Furthermore, the identification of only five putative N1-Src SH3 domain ligands is unlikely to be sufficient to explain its roles in neurogenesis, cytoskeletal remodelling, neurite outgrowth and neuronal differentiation (Lewis et al. 2017; Kotani et al. 2007; Keenan et al. 2017; Matsunaga et al. 1994). Thus, identifying novel interactors is key to providing a mechanistic basis for the cellular functions of N1-Src.

Alternative approaches to identify N1-Src SH3 domain ligands include immunoprecipitation and pull-down assays. Immunoprecipitation, whilst physiologically relevant can encounter issues including scale up requirements, which would be furthered by the transfection and overexpression of N1-Src in neurons. Affinity purification via GST-pull-downs is preferable as GST-SH3 domain fusions often express as soluble high yield proteins in *E. coli*. However, the primary disadvantage is that the method enriches for stable high affinity interactions, with the lower affinity ligands lost during wash steps. Despite this, affinity purification via GST-SH3 domain pull-downs coupled to mass spectrometry has been utilised successfully to identify a number of SH3 domain ligand interactions including CrkL (Cheerathodi and Ballif, 2011), Nck (Lettau et al., 2010) and Hck (Scott et al., 2002). These mass spectrometry analyses identified 22, 26

and 101 proteins for Nck, Hck and CrkL respectively. The interactors were validated *in vivo* by immunoprecipitation, and also lead to the identification of ligand phosphorylation events (Scott et al., 2002).

3.2 Aims

The aim of this chapter was to identify the N1-Src SH3 domain interactome and compare it to that of the C-Src SH3 domain. To achieve this, postnatal day 1 (P1) rat brain lysates, which provide a developmental neuronal lysate relevant to N1-Src's expression and activity, were utilised in GST pull-downs with the C- and N1-Src SH3 domains. The pull-downs were subjected to proteomic identification by shotgun mass spectrometry (LC-MS/MS). Putative SH3 domain ligands were analysed by various bioinformatic approaches to determine the N1-Src SH3 domains ligand consensus motif, and any physical and functional associations. Furthermore, several ligands were validated by orthogonal techniques and one binding partner, a neuronal splice variant of Enah, was studied in greater detail. The outcome of these analyses is i) that the identified N1-Src SH3 domain interactome is a subset of the C-Src SH3 domain interactome and ii) the identified ligands could account for the characterised cell biology of N1-Src and should be considered as candidate N1-Src substrates.

3.3 Results

3.3.1 Optimisation of neuronal lysates for LC-MS/MS analysis of GST-C- and N1-Src SH3 domain pull-downs

The only feature distinguishing C- and N1-Src is the six residue insertion in the N1-Src SH3 domain. Therefore, the ligand specificity of the isolated SH3 domains were assayed on a proteome wide scale via GST pull-downs. The C- and N1-Src SH3 domains were expressed with an N-terminal GST-tag in BL21 *E. coli,* and purified via glutathione agarose resin in order to conduct affinity purification interaction assays.

Firstly, an optimal neuronal lysate for the pull-downs was selected via binding analysis on SDS-PAGE. GST-pull downs were conducted with GST, GST-C- and N1-Src SH3 domains in both synaptosomes and postnatal day 1 rat brain cortices (P1) homogenate. Adult rat brain synaptosomes were previously utilised to screen for C- and N1-Src SH3 domain ligands (Abdelhameed 2010). The P1 lysates were screened as N1-Src has high expression and activity at this developmental stage in the mouse fore- and midbrain (Wiestler and Walter 1988). Furthermore, cellular studies have shown that N1-Src's function is not limited to the synapse. Therefore, whole cell lysates are preferable over synaptosomes. The pull-down eluates were analysed by Coomassie staining of SDS-PAGE gels in order to identify the extent of protein association with the GST-Src SH3 domains against the GST control. Qualitatively, the P1 lysates provided a differential subset of interactions than the synaptosome (Fig.3.1B).

The P1 rat brains were homogenised to yield a protein concentration of ~10 mg/ml in radioimmunoprecipitation assay buffer (RIPA), which extracts nuclear proteins, membrane proteins and cytoskeletal components, whilst also supporting protein-protein interactions. The GST fusions were immobilised on glutathione agarose resin and the pull downs were repeated in triplicate, with GST (26 kDa), GST-C-Src and GST-N1-Src SH3 domains (~35 kDa) and P1 lysates obtained from three independent rat litters. Twelve micromolar GST and GST-SH3 domains were incubated with 2 mg of P1 lysate protein for 1 h at 4 °C. Subsequent wash steps were used to remove non-specific binding and the bait and interactors were eluted via Laemmli sample buffer. The sample was resolved via SDS-PAGE and the gel excised into two fractions of above and below ~ 40 kDa, which were analysed separately to avoid quenching via the abundant GST-SH3 domains. In-gel trypsin digestion was conducted on the gel fractions and the peptides

were analysed via LC-MS/MS on an Orbitrap Fusion mass spectrometer by staff at the York Technology facility. The peptide spectra were then pooled for data analyses and cross-referenced against the rat subset of the UniProt database using both Mascot and X!Tandem (Fig.3.1A).

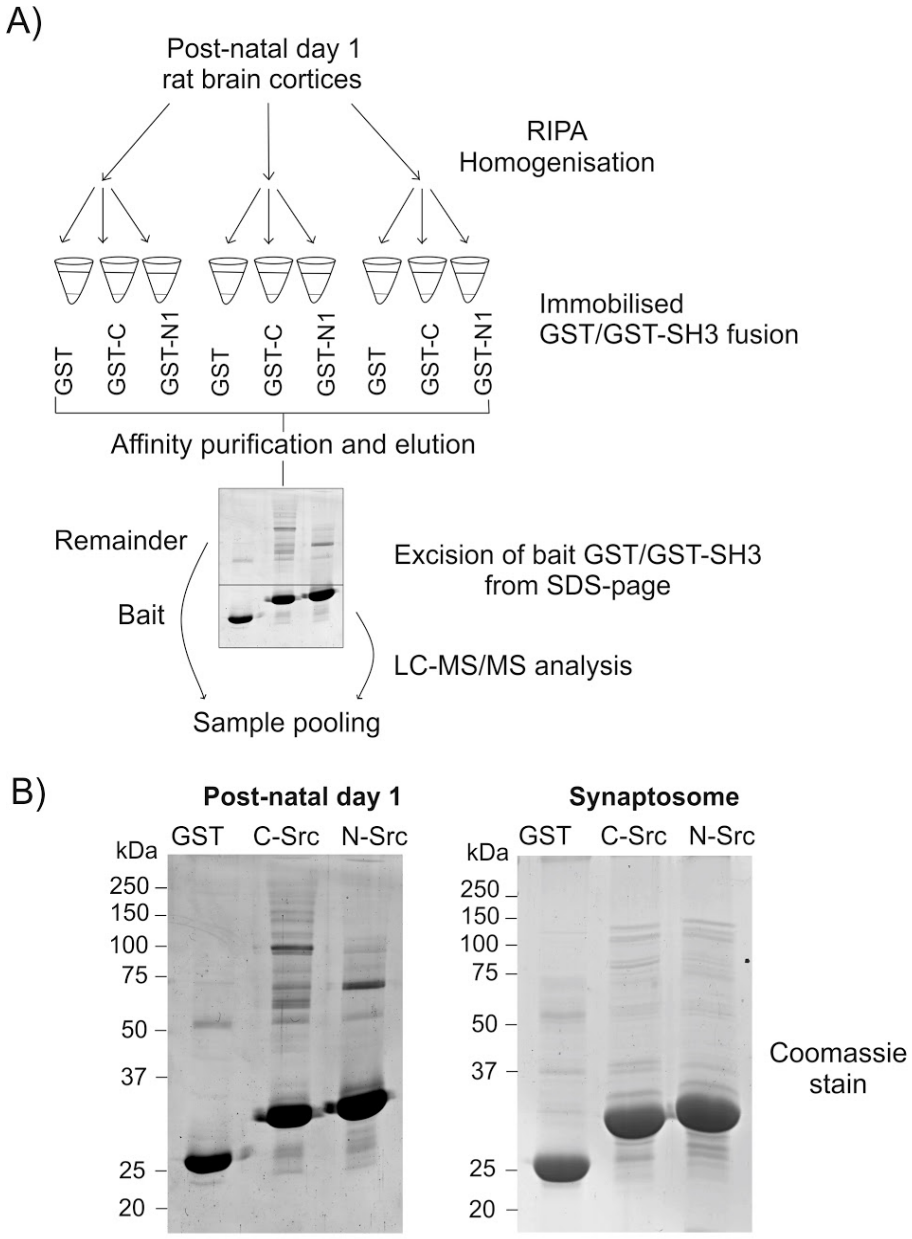

Figure 3.1: Methodology for LC-MS/MS based ligand identification from the GST-C- and N1-Src SH3 domain pull-downs in P1 rat brain homogenate. A) Three independent post-natal day 1 (P1) rat brain cortices were homogenised with RIPA buffer. The pull-downs were conducted in triplicate with 12 µM GST, GST-C- and N1-Src SH3 domains and 2 mg of P1 rat brain homogenate. The pull-down eluates were excised from an SDS-PAGE gel and analysed via LC/MS-MS involving separate analysis of two gel fractions that were above and below ~ 40 kDa to avoid quenching by the GST-SH3 domain bait. The identified peptides/proteins were subsequently pooled for data analyses. B) Coomassie stained 12.5 % SDS-PAGE gels of GST, GST-C-Src and N1-Src SH3 domain pull downs in P1 rat brain homogenate and adult rat brain synaptosomes.

3.3.2 Processing of C- and N1-Src SH3 domain LC-MS/MS results

The GST control served to identify proteins that are non-specific binders that associated with the glutathione agarose resin and/or the GST fusion tag (Fig.3.2). Therefore, statistical analysis was conducted using Scaffold 4 software (Searle 2010) to identify GST-C- and N1-Src SH3 domain binding proteins that were significantly increased above binding to the the GST-only control.

The LC-MS/MS was conducted and analysed in the absence of stable isotope labelling or additional tag incorporation that are necessary for absolute quantification. Label-free semi-quantitative relative abundance estimates can be obtained indirectly by spectral counting or directly by measuring the signal intensity of the peptide precursor ion (Dowle et al. 2016). We employed spectral counting, which measures the total number of peptide spectra that map to each protein and has been shown to be accurate for determining the label-free relative abundance of proteins (Cooper et al. 2010, Dowle et al. 2016).

Using Scaffold 4, pairwise comparisons were conducted between the total spectral counts data from the triplicate GST, GST-C-Src, and N1-Src SH3 domain pull-downs by Fisher's Exact test with a Benjamini-Hochberg correction for multiple testing. This revealed 176 and 33 proteins with significantly increased total spectral counts for C- and N1-Src respectively, compared to the GST control (Table 3.1).

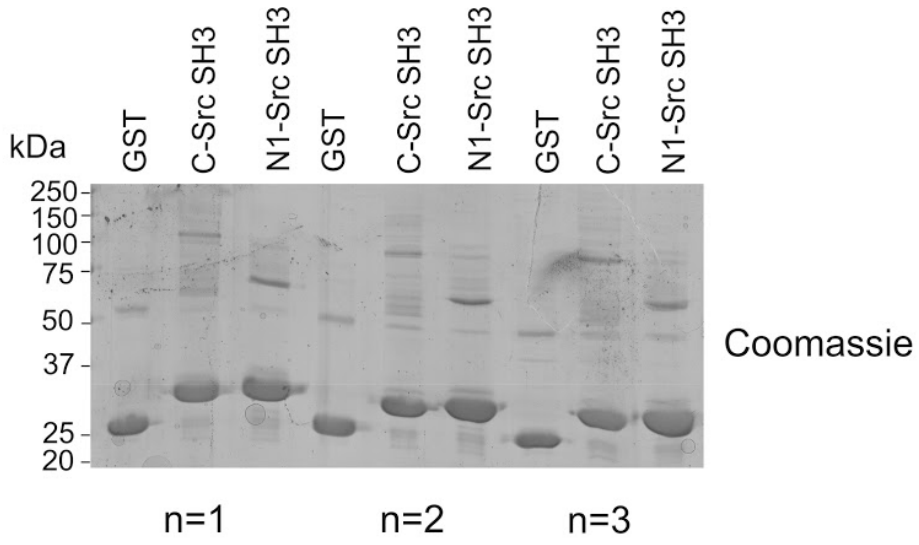

Figure 3.2 Triplicate GST-C- and N1-Src SH3 domain pull-downs submitted for LC-MS/MS analysis. Coomassie stained 12.5 % SDS-PAGE gel of 12 µM GST, GST-C-Src and N1-Src SH3 domain pull-downs in 2 mg of P1 rat brain homogenate. Each of the three replicates submitted for LC-MS/MS analysis are shown.

Table 3.1: Pairwise comparisons of proteins total spectral counts from the GST, GST-C-Src, and N1-Src SH3 domain triplicate pull-downs via Fisher's Exact test with Benjamini-Hochberg correction. The number of proteins at the level of significance for each pairwise comparison is shown, alongside the p value for significance.

	No. of proteins at level of significance		
Pairwise comparison	**GST**	**C**	**N1**
GST vs C ($p < 0.01923$)	191	176	-
GST vs N1 ($p < 0.00311$)	26	-	33
C vs N1 ($p < 0.01045$)	-	128	78

3.3.3 Identification of canonical SH3 domain ligand motifs and characterised C-Src ligands and substrates within the datasets

As non-specific binding proteins were eliminated by the statistical analysis, the remaining C- and N1-Src datasets should contain direct SH3 domain ligands and indirect interactors isolated as part of a complex. (Cheerathodi and Ballif, 2011) demonstrated that the CrkL SH3 domain ligand motif was enriched within a GST-SH3 CrkL pull-down dataset. Therefore, this rationale was applied to the C- and N1-Src datasets. To validate the screen and confirm the successful identification of C-Src SH3 domain ligands, a FuzzPro consensus motif search (Rice et al. 2000) was employed to identify Class I (+xxPxxP) and Class II (PxxPx+) ligands within the C-Src dataset. Of the 176 C-Src ligands, 63 % contained a Class I motif, and 60 % a Class II motif, in comparison to 32 % of proteins in the control GST-only interactome. Whilst the ligand preference of the N1-Src SH3 domain is unknown, surprisingly, of the 33 N1-Src ligands, 69 % contained a Class I motif, and 72 % a Class II motif, in comparison to 30 % of the GST control proteins (Fig.3.3A).

The total number of Class I and Class II motifs were normalised to the number of proteins from which they were derived. For C- and N1-Src the Class I containing proteins had on average 2.4 and 2.8 motifs per protein respectively. Whereas the Class II containing proteins had on average 3.2 and 3.9 motifs per protein for C- and N1-Src respectively (Fig.3.3B).

The unrelated PKD phosphorylation consensus motif [L/I]xRxx[S/T] was utilised as a negative control. 61 % of the C-Src SH3 domain ligands contained the motif in comparison to 46 % in the GST control. Whereas for N1-Src 60 % of the ligands contained the motif in comparison to 61 % of the GST control (Fig.3.3C). Total sequence length would affect the probability of identifying any given motif. However, this was controlled for as the total length of all the N1-Src SH3 domain ligand protein sequences was 76 % the length of the GST control. The C-Src proteins total sequence length was increased by only 0.5 % that of the GST control. Taken together this suggests that the SH3 domains were enriching for Class I and II motifs with specificity.

Identifying characterised Src ligands and substrates within the datasets is another means of validation. Therefore, the datasets were screened for known Src ligands and substrates from the BioGRID (Chatr-Aryamontri et al., 2017) and Phosphosite (Hornbeck et al., 2004) databases. This revealed that 11 % of the C-Src dataset are C-Src ligands and 13

% are known C-Src substrates. Within the N1-Src dataset the proteins Evl (Lambrechts et al. 2000) and Dynamin I (Abdelhameed 2010) are previously identified N1-Src SH3 domain ligands. Furthermore, 27 % of the N1-Src proteins are characterised C-Src ligands, and 33 % C-Src substrates (Fig.3.3D).

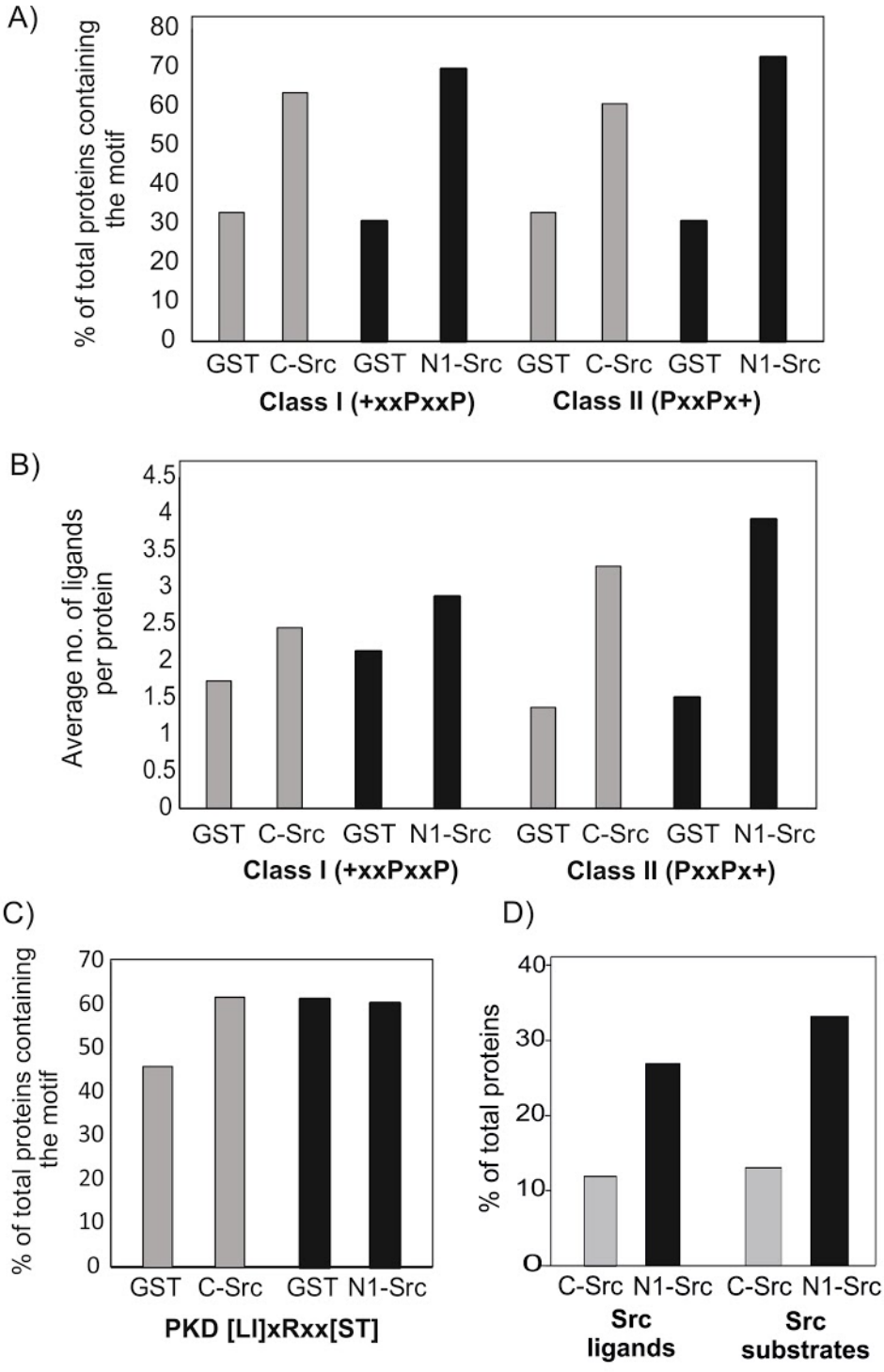

Figure 3.3: The C- and N1-Src SH3 domain pull-downs ligands contain canonical SH3 domain Class I and II ligand motifs and known Src ligands and substrates.
A) FuzzPro was used to identify the percentage of C- and N1-Src SH3 domain ligands containing Class I and Class II motifs in comparison to the GST controls. B) The total number of Class I and II motifs were normalised to the number of proteins from which they were derived. C) As described in A) however the unrelated PKD phosphorylation consensus motif was utilised as a negative control. D) The percentage of C- and N1-Src SH3 domain ligands that are characterised C-Src ligands (BioGrid) or substrates (Phosphosite).

3.3.4 The semi quantitative relative abundance of the N1-Src SH3 domain ligands

Surprisingly, the 33 N1-Src SH3 domain ligands also bound the C-Src SH3 domain. Thus N1-Src appears to bind a subset of C-Src ligands, as opposed to a unique interactome. The average total spectral counts were used to assess the semi-quantitative relative abundance of the 33 N1-Src SH3 domain ligands against C-Src (Fig.3.4). The proteins Asap1, Caskin1, Cbl, Evl, Nckap1, Nono, Sf3b2, Sfpq, Sh3pxd2b, Sos1 and Syn1 all had significantly increased spectral counts for C-Src compared to N1-Src, whereas only Wipf2 was significantly increased for N1-Src. This difference is likely due to factors such as relative binding affinity and whether proteins are direct or indirect (via complexes) interactors. As spectral counts are dependent on the abundance of a protein within a sample, but also the protein's size and the number of tryptic peptides it yields, they cannot be directly compared between proteins. Instead, normalisation of peptide counts can be calculated using emPAI (Section 3.3.5). Therefore, contrary to the spectral count data in Fig.3.4, Dynamin I and Synapsin I are not the most and least abundant N1-Src SH3 domain ligands respectively.

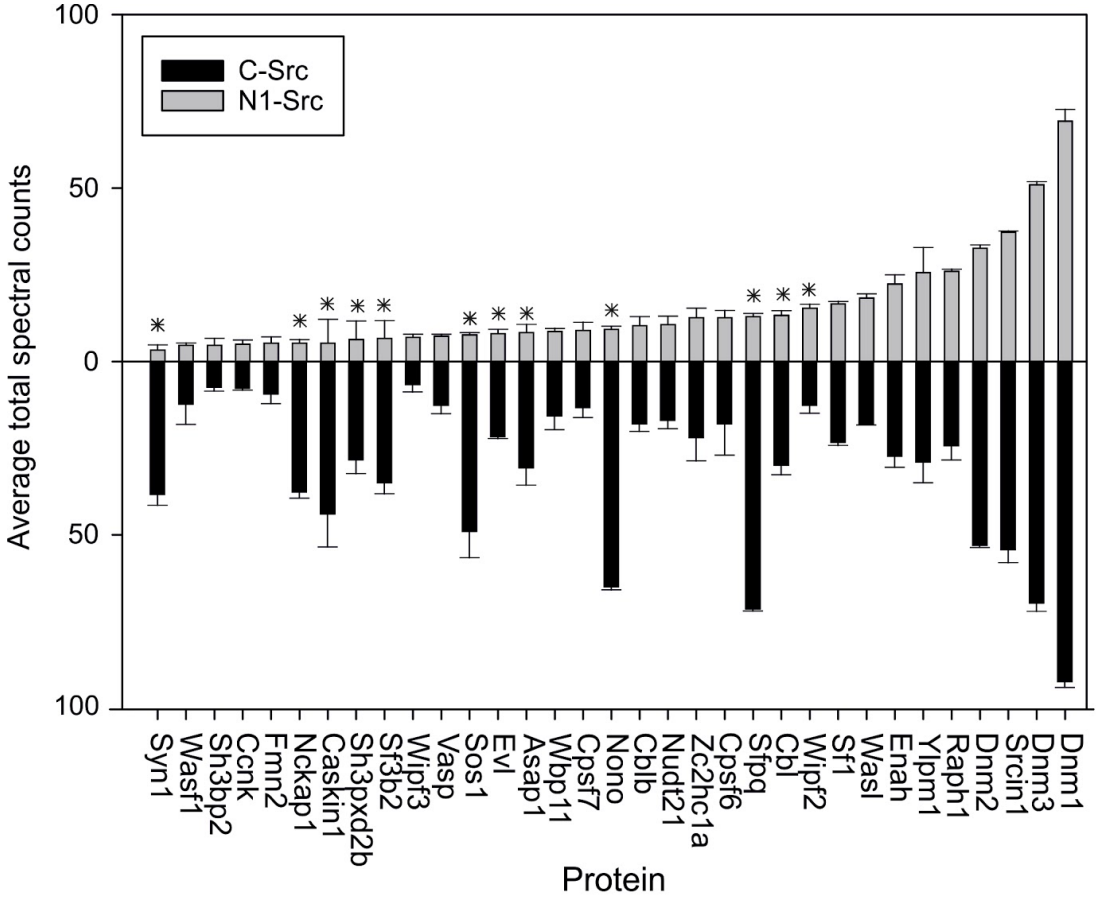

Figure 3.4: The semi-quantitative relative abundance of the 33 N1-Src SH3 domain ligands against C-Src. The average total spectral counts from the triplicate replicates is shown for each of the 33 N1-Src SH3 domain ligands/complexes against C-Src. The

error bars show the SEM and the asterisk (*) indicates statistical significance by Fisher's Exact test with Benjamini-Hochberg correction at ($p < 0.01045$).

3.3.5 The relative sample abundance of the C- and N1-Src SH3 domain ligands

In order to quantify the relative abundance of the SH3 domain ligands within the pull-downs, the protein abundance index (PAI) was utilised. The PAI of a protein is calculated by dividing the number of identified peptides by the number of theoretical observable tryptic peptides. Thus PAI takes into account protein size by considering that smaller and larger proteins will give rise to fewer and more tryptic peptides respectively (Ishihama et al. 2005). EmPAI (exponentially modified protein abundance index) is the base 10 logarithm of PAI (10PAI-1) and has been shown to be directly proportional to protein abundance (Ishihama et al. 2005).

emPAI can be used to calculate the molar percentage (% mol), which represents the concentration of a protein within a sample (de Souza et al. 2011, Yang et al. 2007, Cabral et al. 2017). The % mol for each protein is calculated by normalising the emPAI to the sum of the sample's emPAI (protein content in % mol = emPAI/ΣemPAI x 100). The % mol was therefore used to assess the relative abundance of the C- and N1-Src SH3 domain ligands within the samples.

Table 3.2 shows the average % mol for the C- and N1-Src SH3 domain ligands listed in order of decreasing abundance, with the most abundant interacting proteins for C- and N1-Src, Nono (0.97 mol %) and Dynamin I (0.31 mol %) respectively. Dynamin I was also the second most abundant interactor for C-Src (0.5 mol %). The GST and SH3 domains are also included and as shown via SDS-PAGE these bait proteins comprise the majority of the sample protein (Fig.3.2) at 77 mol % and 84 mol % for C- and N1-Src respectively. The GST-C-Src SH3 bait likely makes up a smaller fraction of the sample due to C-Src's increased number of ligand interactions. In addition, the proteins that bound the C-Src SH3 domain but not the N1-Src SH3 domain are highlighted in grey (Table 3.2). It is striking that abundant C-Src interacting proteins such as HnrnpK and Dpysl2 did not interact with the N1-Src SH3 domain.

Table 3.2: The relative sample abundance of the GST-C- and N1-Src SH3 domain ligands as determined by their average percentage molarity. The SH3 domain ligands are listed in order of decreasing sample abundance and the ligands that were unique to C-Src are highlighted in grey. The GST and SH3 domain bait are also included.

N1-Src		C-Src			
Protein	**Avg % mol**	**Protein**	**Avg % mol**	**Protein**	**Avg % mol**
Dnm I	0.31	Nono	0.97	Arhgef7	0.04
Dnm III	0.14	Dnm I	0.50	Asap1	0.04
Enah	0.09	HnrnpK	0.60	Asap2	0.04
Cpsf5	0.08	Dpysl2	0.40	Abi1	0.04
Wasl	0.07	Sfpq	0.32	Dtx3	0.04
Wipf2	0.07	Dpysl3	0.32	Vps37b	0.04
Dnm II	0.07	Crmp1	0.30	Prr36	0.04
Srcin1	0.06	Dnm III	0.24	Prrc2a	0.04
Zc2hc1a	0.06	Cpsf5	0.19	Wbp11	0.04
Sf1	0.05	Zc2hc1a	0.15	Cyfip2	0.04
Raph1	0.04	Syn1	0.14	Rbmx	0.03
Cpsf6	0.04	Dnm II	0.14	Snrpd2	0.03
Ylpm1	0.03	Evl	0.15	Myb12b	0.03
Evl	0.03	Sf3a1	0.12	Raph1	0.03
Nono	0.03	Enah	0.11	Ylmp1	0.03
Sfpq	0.03	Srcin1	0.11	Satb1	0.03
Vasp	0.03	Sf3a3	0.08	Pabpc1	0.03
Cpsf7	0.03	Sf3b2	0.08	Diaph1	0.03
Wbp11	0.02	Ppp1cb	0.08	Git1	0.03
Wipf3	0.02	Sf1	0.07	Tsg101	0.03
Cbl	0.02	Khdrbs1	0.07	Wdr5	0.03
Cblb	0.01	Synj1	0.07	Wasf1	0.03
Asap1	0.01	Sos1	0.07	Pabpc1	0.03
Sf3b2	0.01	Vasp	0.07	Afdn	0.03
Sh3pxd2b	0.01	Nckap1	0.06	Raver1	0.03
Wasf1	0.01	Cpsf6	0.06	Cblb	0.03
Sh3bp2	0.01	Caskin1	0.06	Pak2	0.03
Sos1	0.008	Cbl	0.06	Snrpb2	0.03
Ccnk	0.008	Sh3pxd2b	0.06	Phf5a	0.03
Syn1	0.007	Brk1	0.06	Sf3b3	0.02
Fmn2	0.006	Wasl	0.06	Abi2	0.02
Caskin1	0.005	Pspc1	0.05	Snrpa	0.02
Nckap1	0.0003	Cpsf7	0.05	Brks1	0.02
		Sf3b1	0.05		
GST	42.05	Wipf2	0.05	GST	38.49
N1-Src SH3	42.02	Snrpa1	0.05	C-Src SH3	38.46
Remaining	14.51	Vps28	0.04	Remaining	15.94

3.3.6 Validation of the C- and N1-Src SH3 domain ligands via Western blotting

The mass spectrometry analysis of the GST-SH3 domain pull-downs was confirmed via Western blotting. The assay was repeated under the same experimental conditions with 12 μM GST and GST-SH3 domains and 2 mg of P1 lysate, followed by Western blotting for a number of interactors. Fig.3.5 presents the input P1 brain homogenate, GST control and GST-C- and N1-Src SH3 domain pull-downs. A Coomassie stained SDS-PAGE loading control for the GST and GST-SH3 domains is also shown. The Western blots were consistent with the proteomic quantification for Dynamin I, N-WASP, Raph1, Sf1 and Enah enrichment above GST for both C- and N1-Src. Nono was identified in the N1-Src data set, however, it was initially not detected via Western blot. The C- and N1-Src average % mol for Nono was 0.97 and 0.03 respectively (Table 3.2), thus its sample abundance for N1-Src is ~32-fold lower. Upon increasing the amount of pull-down eluate assayed by Western blotting, Nono was detected as binding to the N1-Src SH3 domain via GST-SH3 pull-downs (Chapter 4).

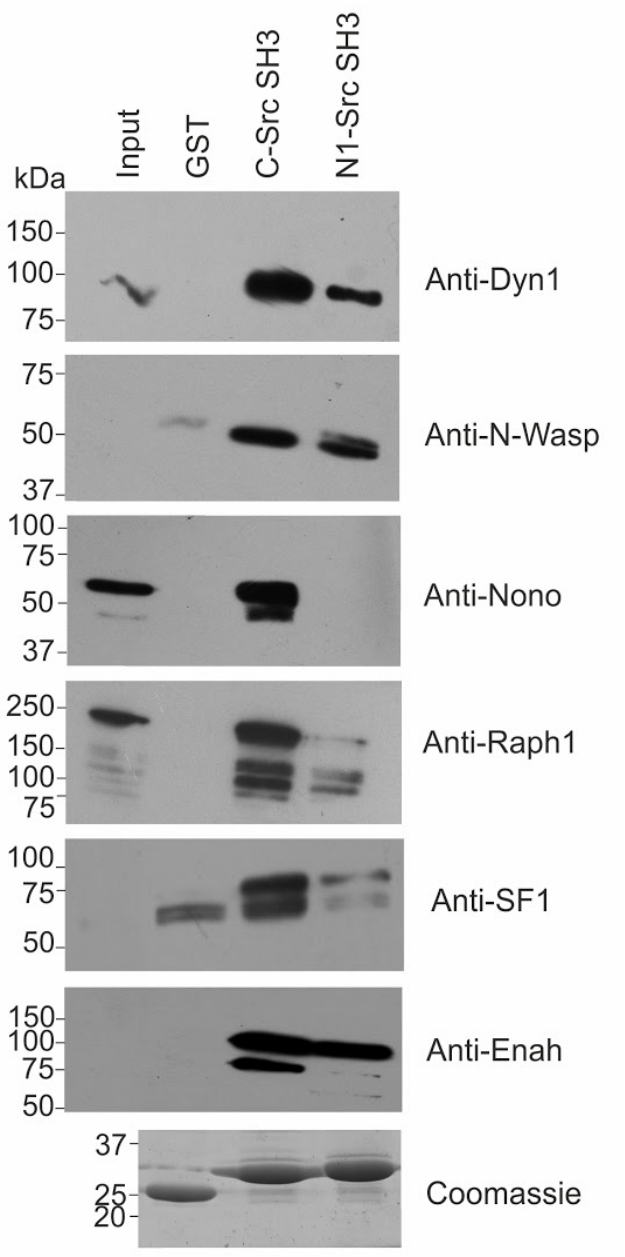

Fig.3.5: Confirmation of the C- and N1-Src SH3 domain ligands from P1 rat brain via Western blotting. GST and GST-C- and N1-Src SH3 domain pull-downs were conducted in P1 rat brain lysates and the eluates assayed by Western blotting for the putative SH3 domain ligands Dynamin I, N-WASP, Nono, Raph1, Sf1 and Enah. The input brain lysate (1 %) is shown and a 12.5 % Coomassie stained SDS-PAGE gel loading control.

3.3.7 Identification of the Neuronal-Enah splice variant as a C- and N1-Src SH3 domain ligand

The Western blot to confirm Enah binding to the GST-C- and N1-Src SH3 domains revealed two bands, the first at ~75 kDa and the second between 100-150 kDa (Fig.3.5). Enah has a predicted mass of 66 kDa, but migrates at ~ 80 kDa by Western blotting, and hence the additional band at ~140 kDa could represent non-specific binding by the antibody or a larger protein isoform possessing the same epitope. Indeed, there is a neuronal splice variant of Enah which migrates at 140 kDa by SDS-PAGE (Gertler et al., 1996), however its peptides were not detected in the LC-MS/MS analysis. This was found to be due to the isoform being absent from the Uniprot rat database. However, the manual addition of the rat protein sequence to the Mascot database, revealed peptides unique to the neuronal splice variant in the samples. The identified peptides are highlighted on the Neuronal Enah (N-Enah) insert sequence in bold in Fig.3.6A. Pairwise comparisons revealed the N-Enah variant was significantly increased for both C- and N1-Src against the GST control.

The domain structure of Enah and N-Enah from the N- to C-termini comprises an EVH1 domain, tandem repeats and then a proline rich and EVH2 domain (Fig.3.6A). The EVH1 domain directs intracellular localisation and interacts with proline-rich sequences found in signal transduction proteins and cytoskeletal regulators. The tandem repeats likely function as a protein interaction interface. The central proline-rich domain interacts with SH3 and WW domain containing proteins and the actin binding protein Profilin (Sechi and Wehland 2004; Kwiatkowski et al. 2003). In addition, the proline-rich domain is the site of the 249 residue rat N-Enah insertion as shown in Fig.3.6A (Gertler et al. 1996). The C-terminal EVH2 domain is involved in oligomerisation, and interacts with actin, recruiting Enah to filopodia and lamellipodia extensions (Nisticò and Di 2011).

The relative abundance of the Enah variants for C- and N1-Src were quantified using their ‘exclusive unique spectrum counts’. This identifies distinct spectra for related proteins, on the basis of changes such as in the protein sequence. C-Src had increased spectral counts for both Enah and N-Enah in comparison to N1-Src. The fold difference between the counts for Enah and Neuronal-Enah was 3.8 for C-Src, in comparison to 17 for N1-Src (Fig.3.6B). This suggests that the N1-Src SH3 domain has a preference for

the neuronal variant as borne out by the Western blot where N-Enah is clearly detectable and Enah is barely visible. Conversely, for C-Src, Enah is readily detectable (Fig.3.5).

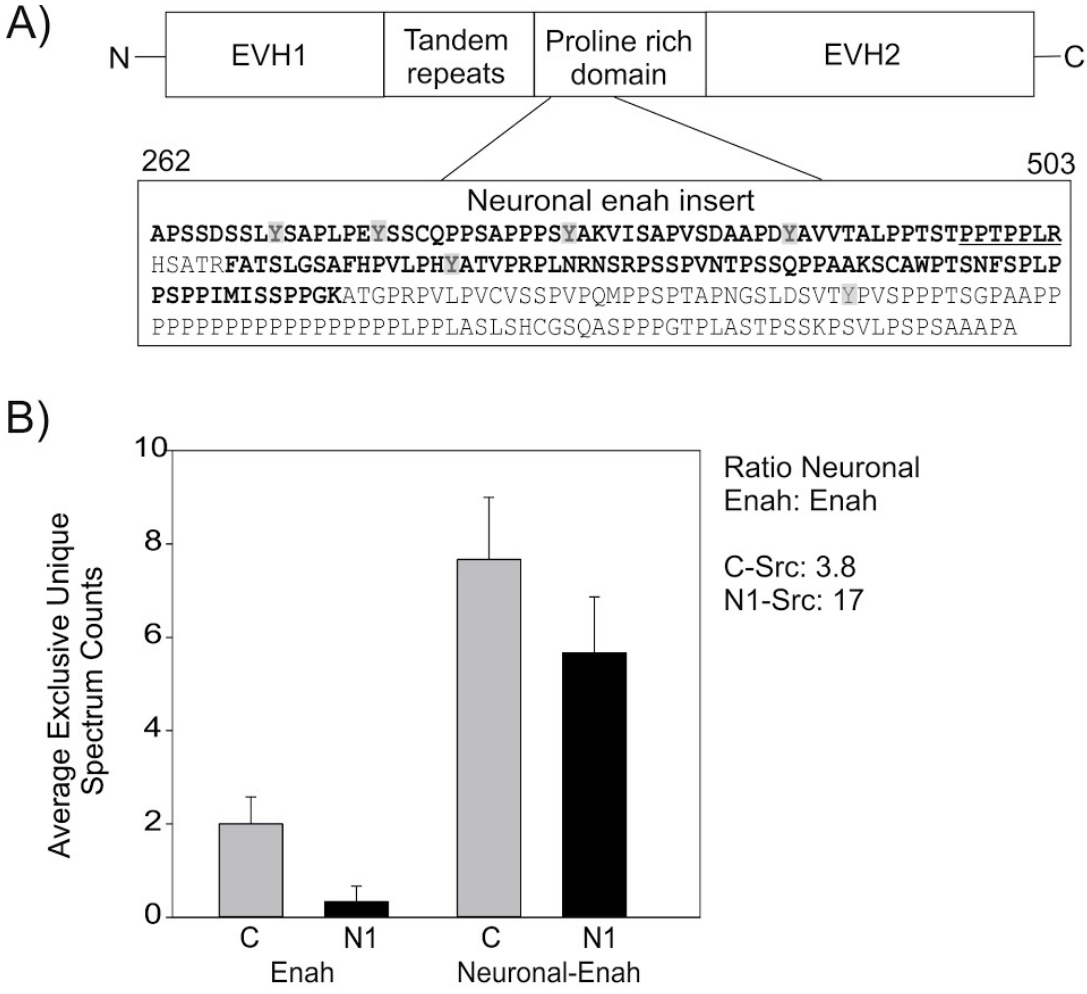

Figure 3.6: Identification of the Neuronal Enah splice variant within the C- and N1-Src SH3 domain pull-downs.
A) Domain structure of Enah and the Neuronal-Enah splice variant. The EVH1 domain, tandem repeats, proline rich and EVH2 domains are shown. The sequence of the N-Enah insertion is shown with the tyrosine residues highlighted in grey and the Class II SH3 domain ligand motif underlined. The peptide sequences from the neuronal insert that were identified via mass spectrometry are highlighted in bold. B) Mass spectrometry quantification of the Enah splice variants in the C- and N1-Src datasets. The average exclusive unique spectrum counts are shown for Enah and Neuronal Enah for C- and N1-Src. Error bars show the SEM. The ratio of Enah:Neuronal-Enah is also indicated for C- and N1-Src.

3.3.8 Functional enrichments and protein-protein interactions by the C- and N1-Src SH3 domain ligands

As the GST-SH3 domain pull-downs were conducted in RIPA buffer under non-denaturing conditions it is likely that intact protein complexes were isolated, which might provide clues to the cellular functions of the SH3 domains ligand interactions. Thus, STRING was used to generate protein-protein interaction networks from the lists of putative SH3 interactors (von Mering et al., 2003). In addition, to further assign biological function to the ligands, they were also analysed for Gene Ontology (GO) term enrichment in STRING. This was conducted using the whole genome as the statistical background and analysed by a Fisher's exact test with multiple test correction (Szklarczyk et al. 2016).

All of the C- and N1-Src SH3 domain ligands with significantly upregulated spectral counts compared to GST, were analysed by STRING. STRING was used to generate interaction networks based on high confidence physical or functional associations derived from experiments and curation databases. A selection of the significantly enriched GO terms spanning biological processes and cellular components were used to annotate the networks and highlight proteins within the terms. The gene counts from the C- and N1-Src datasets and the false discovery rate (FDR) for each GO term is shown. In addition, the networks were also manually annotated with characterised C-Src substrates (Phosphosite database) marked with an asterisk (*) and C-Src ligands (BIOGRID database) within a square box (Fig.3.7A/B).

As the C-Src SH3 domain had 176 direct or indirect interactors, it yielded a more complex network than for the N1-Src SH3 domain interactors. Prominent features from the C-Src network (Fig.3.7A) include the entire complexes or multiple components from:

- SCAR complex (Cyfip1, Abi2, Abi1, Ncakp1, Wasf1, Wasf2, Brk1). FDR 1.78e-11.
- Spliceosomal complex (Rbm22, Snrpa1, Srrm2, Sf3b3, Phf5a, Sf3b1, Sf3a3, Sf3b2, Hnrnpk, Snrpa, Snrpb2, Sf3a1, Sf3a2, Sf1). FDR 4.63e-09.
- Paraspeckle complex (Sfpq, Nono, Pspc1, Nudt21, Cpsf6). FDR 2.84e-08.
- ESCRT I complex (Vps28, Vps37, Fam125b, Tsg101). FDR 1.67e-05.
- SET1C/COMPASS complex (Setd1b, Cxxc1, Wdr5, Rbbp5). FDR 2.74e-05.

- mRNA cleavage factor complex (Cpsf7, Nudt21, Cpsf6, Fip1l1). FDR 9.25e-05.
- Cyclin K/CDK13 complex (Cdk13, Ccnk). FDR 2.08e-03.

The C-Src dataset significantly enriched for proteins within diverse GO terms including cytoskeletal organisation (FDR 6.16e-16), mRNA processing (FDR 1.39e-14), neuron projection morphogenesis (FDR 4.5e-12) and endocytosis (FDR 1.65e-10). In addition the molecular function GO term of SH3 domain binding was enriched (FDR 1.87e-10), supporting the identification of an abundance of Class I and II SH3 domain ligand motifs (Fig.3.3A) and characterised C-Src ligands (Fig.3.3D).
Serving as positive controls, the C-Src network highlighted a number of characterised C-Src ligands (Khdrbs1, Crebbp, Crmp1, Pak2, Sh3kbp1, Evl, Tnk2, Asap2, Map2), substrates (Sf3b2, Sfpq, Git1, Sh3pxd2a, Sh3pxd2b, Wasf1, Abi1), and both ligands and substrates (HnrnpK, Cbl, Ctnnd1, Dnm1, Dnm2, Abl1, Bcar1, Wasl1, Asap1) (Fig.3.7A).

The N1-Src SH3 domain network contained fewer complexes (Fig.3.7B) but also contained the:

- Paraspeckle complex (Sfpq, Nono, Nudt21, Cpsf6). FDR 1.13e-07.
- mRNA cleavage factor complex (Cpsf7, Nudt21, Cpsf6). FDR 3.41e-04.
- SCAR complex (Wasf1, Nckap1). FDR 0.011.

The N1-Src dataset significantly enriched for proteins within the GO term ‘actin polymerisation and depolymerisation’ (FDR 6.93e-05) including the actin cytoskeletal regulatory proteins Wasl, Evl, Enah, Vasp and Wasf1. Similarly, the actin-based ‘lamellipodium’ (FDR 1.13e-07) and ‘positive regulation of Arp2/3 complex mediated actin nucleation’ (FDR 3.68e-04) were also enriched. Furthermore, N1-Src enriched for proteins involved in ‘axonogenesis’ (FDR 3.11e-03) and neuron projection development and morphogenesis (FDR 2.89e-03 and 1.42e-03), alluding to a broad theme of cytoskeletal remodelling and neurite morphology. In addition, N1-Src enriched for the GO terms ‘mRNA processing’ (FDR 3.68e-04) and ‘RNA splicing’ (FDR 1.16e-03) including the proteins Sfpq, Nono, Wbp11, Cpsf7, Cspf6, Nudt21, Sf3b2 and Sf1, some of which form the ‘paraspeckle’ (FDR 1.13e-07) and ‘mRNA cleavage factor complexes’ (3.41e-04), highlighting regulation of RNA as a putative function of N1-Src.

Contained within the N1-Src interactome were Asap1, Raph1, Sh3pxd2b, Syn1, Wasfl, Wasl, Sf3b2, Sfpq, Dnm1, Dnm2 and Cbl, all of which have been identified as C-Src substrates. The proteins Wasl, Evl, Dnm1, Dnm2, Cbl, Syn1, Srcin1, Sh3bp2 and Asap1 have all been identified as C-Src interactors. Thus in total, 14 (42 %) of the N1-Src SH3 domain ligands are associated with C-Src through interactions, phosphorylation or both.

A)

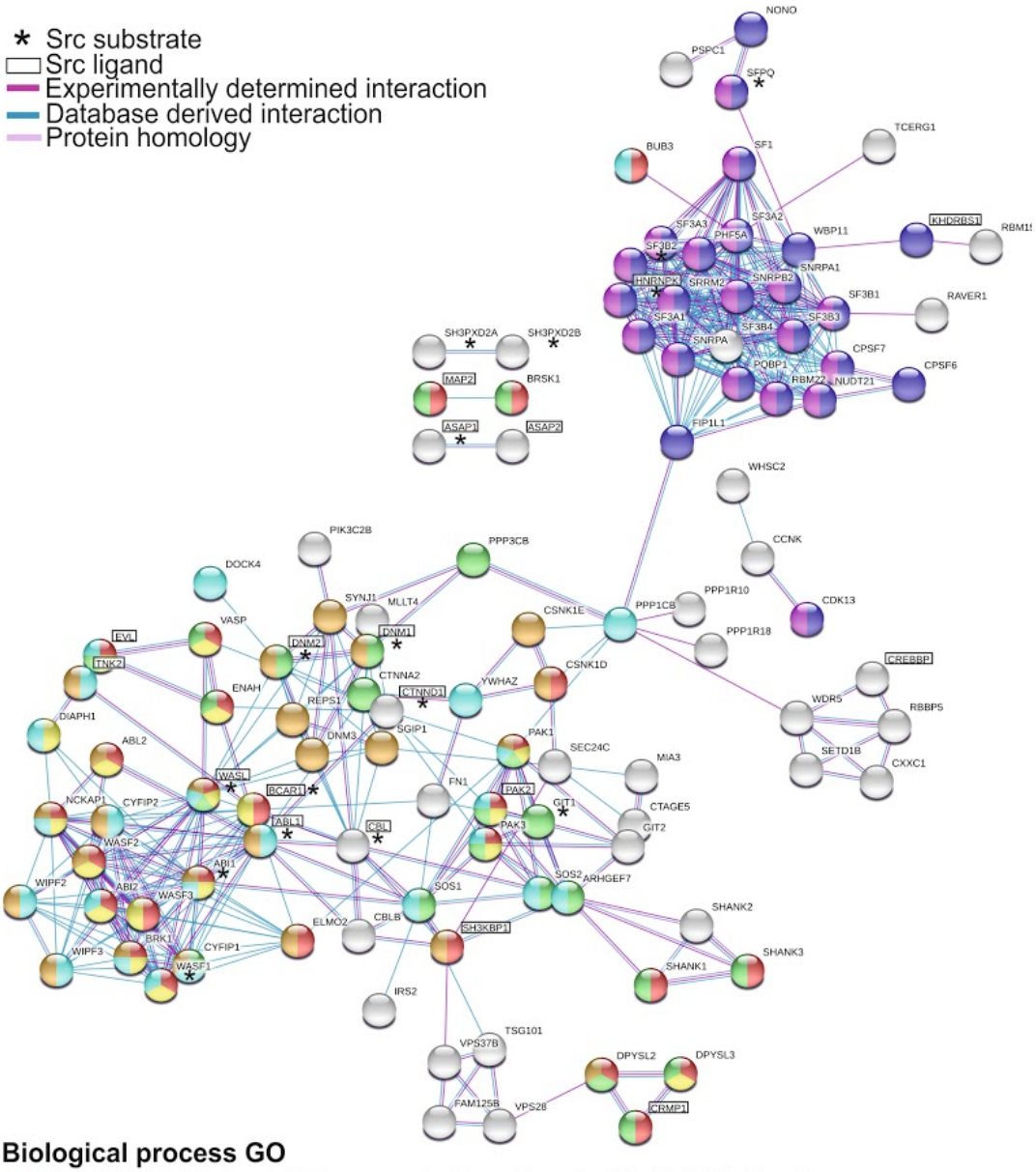

Biological process GO

- GO:0007010 Cytoskeleton organization, Counts 39, FDR 6.16e-16
- GO:0006397 mRNA processing, Counts 28, FDR 1.39e-14
- GO:0030036 Actin cytoskeleton organization, Counts 25, FDR1.54e-12
- GO:0000398 mRNA splicing, via spliceosome, Counts 20, FDR 1.85e-12
- GO:0048812 Neuron projection morphogenesis, Counts 28, FDR 4.5e-12
- GO:0007264 Small GTPase mediated signal transduction, Counts 30, FDR 1.05e-11
- GO:0006897 Endocytosis, Counts 25, FDR 1.6e-10
- Unassigned node

Molecular function GO

GO:0044822 Poly(A) RNA binding, Counts 40, FDR 1.8e-11
GO:0017124 SH3 domain binding, Counts 11, FDR 1.87e-10

Cellular component GO

GO:0030027 Lamellipodium, Counts 19, FDR 1.81e-13
GO:0031209 SCAR complex, Counts 7, FDR 1.78e-11
GO:0045202 Synapse, Counts 27, FDR 3.85e-10
GO:0005681 Spliceosomal complex, Counts 14, FDR 4.63e-09
GO:0042382 Paraspeckles, Counts 5, FDR 2.84e-08

B)

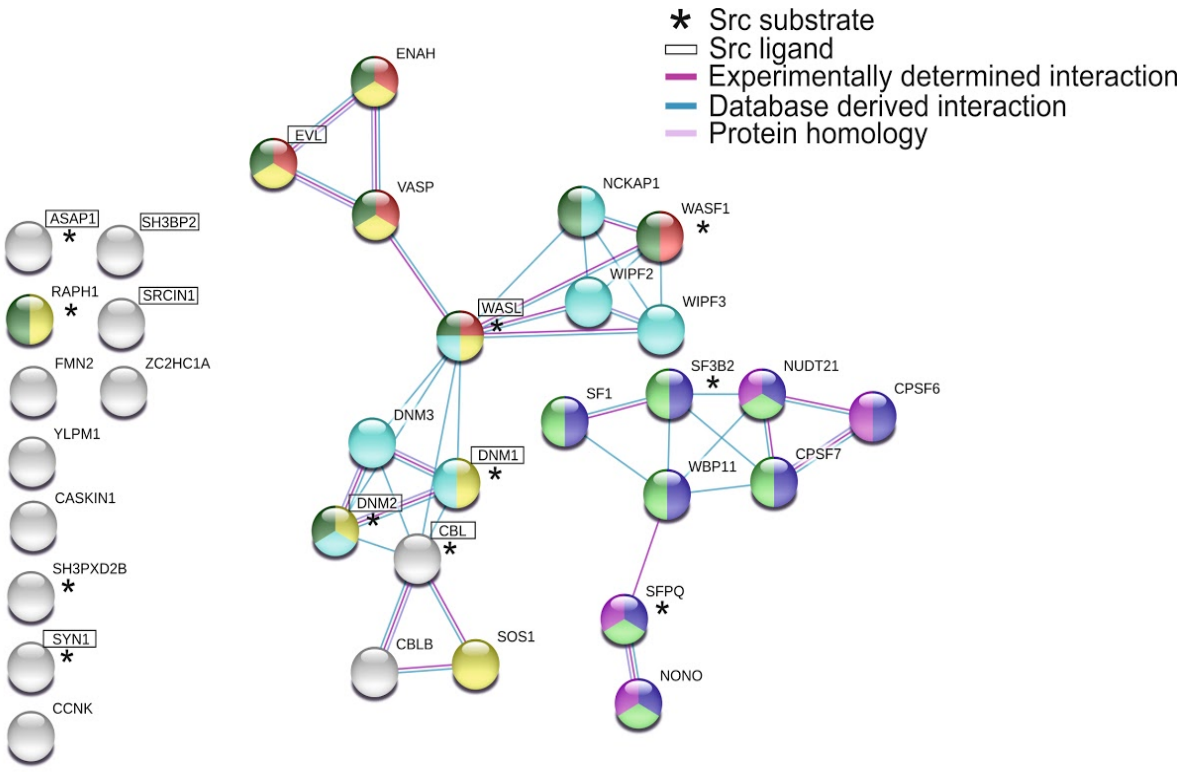

Biological process GO

GO:0008154 Actin polymerization or depolymerization, Counts 5, FDR 6.93e-05
GO:0006397 mRNA processing, Counts 8, FDR 3.68e-04
GO:0030030 Cell projection organization, Counts 11, FDR 3.68e-04
GO:2000601 Positive regulation of Arp2/3 complex actin nucleation, Counts 3, FDR 3.68e-04
GO:0008380 RNA splicing, Counts 7, FDR 1.16e-03
GO:0048812 Neuron projection morphogenesis, Counts 8, FDR 1.42e-03
GO:0031175 Neuron projection development, Counts 8, FDR 2.89e-03
GO:0006897 Endocytosis, Counts 7, FDR 3.11e-03
GO:0007409 Axonogenesis, Counts 7, FDR 3.11e-03
Unassigned node

Cellular component GO

GO:0030027 Lamellipodium, Counts 8, FDR 1.13e-07
GO:0042382 Paraspeckles, Counts 4, FDR 1.13e-07
GO:0031252 Cell leading edge, Counts 8, FDR 2e-05
GO:0005849 mRNA cleavage factor complex, Counts 3, FDR 3.41E-04
GO:0016604 Nuclear body, Counts 6, FDR 3.68E-03

Figure 3.7: GO term pathway analysis and protein-protein interaction networks from the C- and N1-Src SH3 domain ligands.

The GST-C- and N1-Src SH3 domain ligands were analysed in STRING. The proteins were searched against *Homo Sapiens* to generate high confidence interaction networks derived from 'experiments' (dark pink connection) and 'databases' (blue connection) sources. Proteins with sequence homology are also indicated by a light pink connection. The proteins are annotated with an asterisk (*) for a characterised Src substrate, or within a box for a characterised Src ligand. A selection of the significantly enriched GO terms are listed, including the counts from the datasets and the false discovery rate (FDR). The proteins from the enriched GO terms that are mapped onto the interaction networks are colour coded. The network and pathway analysis for C-Src is shown in A and N1-Src in B.

3.3.9 Preliminary characterisation of the N-Enah splice variant

The poorly characterised N-Enah splice variant was an interesting SH3 domain ligand due to its preference for the N1-Src SH3 domain over the canonical Enah (Fig.3.5/6). N-Enah expression peaks in the developing brain from embryonic day 15 (E15) to P1 (Lanier et al. 1999), a period in which axonal migration occurs. Furthermore, N-Enah was identified as the major tyrosine phosphorylated form of Enah in the developing brain (Gertler et al. 1996). The putative N1-Src:N-Enah interaction could provide mechanistic insight into the role of N1-Src in axon elongation (Keenan, et al. 2017; Worley et al. 1997). Cell-based assays were conducted to investigate the interaction further.

No commercial N-Enah vectors were available, thus N-Enah was codon optimised for mammalian cells and cloned into pEGFP-C1, fused to an N-terminal GFP tag. An N-terminal GFP tag was selected as it has been used successfully in functional assays fused to canonical Enah (Geese et al. 2002; Balsamo et al. 2016). Firstly, the successful cellular expression and detection of N-Enah was confirmed. GFP alone and GFP-N-Enah were transfected into COS7 monkey fibroblast cells, and the cells were imaged for GFP fluorescence 48 h post-transfection. GFP transfected cells revealed green fluorescence in the nucleus and throughout the cytoplasm, whereas GFP-N-Enah formed cytoplasmic puncta in all transfected cells (Fig.3.8A). In order to investigate the properties of the N-Enah puncta, the transfected COS7 cells were treated with 0.1 % Triton X-100 for 5 min prior to fixation (Fig.3.8A). Triton is a nonionic surfactant that permeabilises the plasma membrane and extracts soluble proteins. Thus Triton-insoluble proteins such as cytoskeletal and associated proteins are retained. The N-Enah puncta were retained following Triton treatment, suggesting the puncta are insoluble (Fig.3.8A). Further investigations are required to establish the nature of the N-Enah puncta and whether they are physiologically relevant.

Western blot analysis of the GFP-N-Enah transfected COS7 cells with an anti-Enah antibody identified a protein with a molecular weight of approximately 170 kDa, in-line with the electrophoretic mobility of N-Enah (140 kDa) with a 27 kDa GFP-tag. The antibody also detected what is likely to be endogenous expression of the 80 kDa canonical Enah variant (Fig.3.8B).

As described in Chapter 5, N-Enah was identified as an *in vitro* C- and N1-Src substrate. Therefore, preliminary experiments were conducted to assess if N-Enah was

phosphorylated by N1-Src in cells. A rat neuroblastoma cell line (B104) was employed, which possesses the ability to undergo neuronal differentiation and expresses many neuronal proteins (Shastry et al. 2001). GFP-N-Enah and N1-Src-FLAG were co-transfected into B104 cells, and 48 h post-transfection the cells were lysed in Laemmli sample buffer for Western blot analysis. N1-Src was successfully detected as a 60 kDa band by an anti-FLAG antibody and as observed in Fig.3.8B, the GFP-N-Enah migrated just above 150 kDa. Upon the co-expression of N-Enah and N1-Src a ~150 kDa phosphotyrosine containing protein was observed in both experimental replicates. Importantly, it was not present upon the expression of N1-Src or N-Enah alone, suggesting that it could be tyrosine phosphorylated N-Enah. This represents the first tentative evidence that N1-Src is a N-Enah kinase in cells.

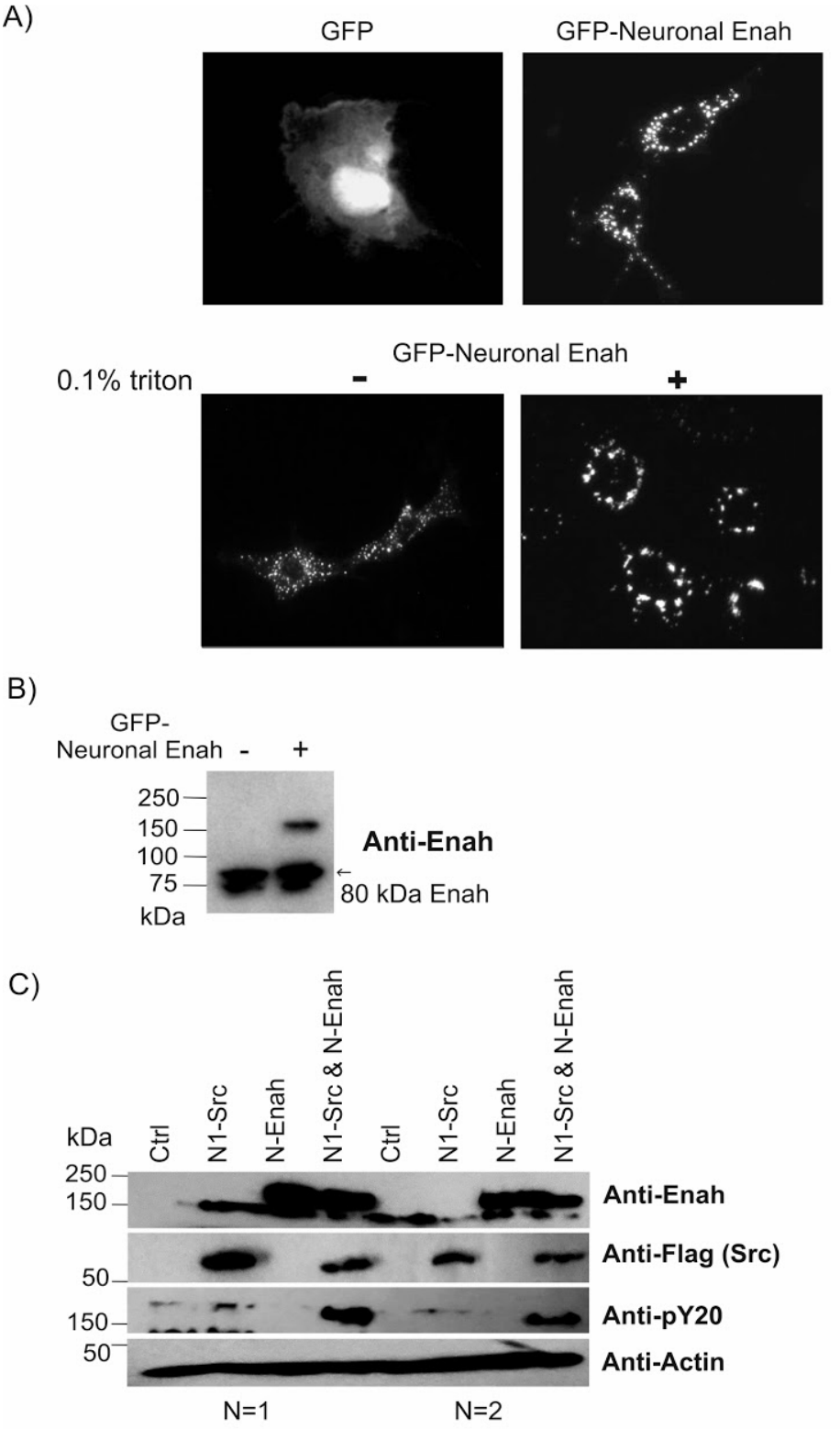

Figure 3.8: Characterisation of the N-Enah splice variant. A) Expression and localisation of GFP and GFP-N-Enah in COS7 cells, after 48 h of transfection. The solubility of the Neuronal-Enah puncta was assessed by incubation with 0.1 % Triton for 5 min prior to fixation. B) Detection of transfected GFP-N-Enah in COS7 cells by anti-Enah Western blotting. C) B104 cells were co-transfected with N1-Src-FLAG and GFP-Neuronal Enah. The cells were transfected for 48 h before Laemmli lysis and analysis by Western blotting.

3.4 Discussion

The primary aim of this chapter was to compare the C- and N1-Src SH3 domain interactomes in a neuronal background. The secondary aim was to conduct bioinformatics analysis on the N1-Src interactome to assess if the proteins could be potential substrates and shed light on the functions of N1-Src in neurite outgrowth (Worley et al., 1997), cytoskeletal remodelling (Kotani et al., 2007) and neuronal differentiation (Cartwright et al., 1987). Overall this study identified 33 N1-Src SH3 domain ligands, 31 of which were novel. Surprisingly, the N1-Src SH3 domain interacted with a subset of C-Src ligands as opposed to a unique interactome. In line with this, the N1-Src SH3 domain ligands were rich in canonical Class I/II SH3 domain ligand motifs, suggesting that N1-Src could interact with similar motifs to C-Src. Furthermore, the N1-Src SH3 domain ligand interactions appeared to be lower affinity, in line with the literature. To date, N1-Src has no characterised *in vivo* substrates, thus it was encouraging to obtain tentative evidence that N1-Src phosphorylates N-Enah *in vivo*, alongside the identification of N-Enah as an *in vitro* substrate in Chapter 5.

Identification of C- and N1-Src SH3 domain ligands via GST-pull downs

In order to identify C- and N1-Src SH3 domain ligands, GST-SH3 domain pull-downs coupled to LC-MS/MS analysis were utilised as described in the literature (Cheerathodi et al. 2015; Lettau et al., 2010; Scott et al. 2002). As N1-Src is a neuronal specific kinase, it was essential to screen for ligands in a neuronal background. P1 rat brain homogenate was selected due to N1-Src's high levels of expression and activity in the P1 mouse brain (Wiestler and Walter 1988), and its developmental functions (Lewis et al. 2017). The C-Src SH3 domain was used for comparative purposes, and as a positive control. The 176 C-Src SH3 domain ligands enriched for its characterised Class I and II ligand motifs (Fig.3.3). Furthermore, 11 % of the ligands were characterised C-Src SH3 domain ligands, and 13 % were characterised C-Src substrates (Fig.3.3). In addition, two of the previously identified N1-Src SH3 domain ligands, Evl and Dynamin 1, were identified in the N1-Src SH3 domain pull-downs. Taken together this suggests that the assay was functioning with specificity.

A caveat of the analysis is that some ligands could be *in vitro* artefacts which may not encounter C- or N1-Src *in vivo.* The C- and N1-Src interaction networks highlight multiple proteins that are homologous (Fig.3.7). Thus some interactors could share a

common SH3 domain ligand motif, however not be exposed to Src within the cell. Therefore follow up studies in cells are essential. In addition, the pull-downs were conducted in RIPA buffer which contains SDS and sodium deoxycholate. These ionic detergents enable the extraction of cytoskeletal components, which is important as N1-Src has been linked to cytoskeletal regulation (Kotani et al. 2007; Keenan et al. 2017), however they can also disrupt low affinity protein-protein interactions. Despite this, the method was successful in identifying 176 C-Src SH3 domain ligands and 33 N1-Src SH3 domain ligands, in comparison to the 22, 26 and 101 SH3 domain ligands identified for Nck, Hck and CrkL respectively via similar methodology (Cheerathodi and Ballif, 2011; Lettau et al., 2010; Scott et al., 2002).

N1-Src SH3 domain ligand specificity

Previous studies demonstrated that the N1-Src SH3 domain had weak or abolished interactions with C-Src ligands (Reynolds et al., 2008; Messina et al., 2003; Craggs et al., 2001; Richnau and Aspenström, 2001), suggesting that N1-Src may have a unique interactome. However, this is the first high throughput study to assess the N1-Src SH3 domain ligand specificity on a proteome wide scale. Most striking was that N1-Src had no unique interactors, and instead its 33 ligands also interacted with the C-Src SH3 domain (Fig.3.4). This suggests that N1-Src may function as a tailored version of C-Src in neurons. It is logical for C-Src to possess more SH3 domain ligands due to its ubiquitous expression and broad functions (Section 1.3). However, N1-Src could have unique SH3 domain ligands that were too low abundance or affinity for detection via pull-down.

Eleven of the thirty three N1-Src SH3 domain ligands had a significantly increased interaction with the C-Src SH3 domain (Fig.3.4). Furthermore, Western blotting of the pull-downs demonstrated that Dynamin I, N-WASP, Nono, Raph1 and Sf1 all interacted with N1-Src to a lesser extent than C-Src (Fig.3.5). Thus this data supports the previous observations that the N1-Src SH3 domain ligand interactions are lower affinity. (Onofri et al., 1997) reported negligible binding of the N1-Src SH3 domain to Synapsin in comparison to C-Src, and in line with this, Synapsin was a significantly increased interactor for C-Src (Fig.3.4). It is unknown if the lowered affinity still renders Synapsin physiologically relevant to N1-Src, and to expand this study the N1-Src SH3 domain interactions need to be confirmed *in vivo* by techniques such as immunoprecipitation,

preferably in a neuronal related cell line. The 33 % of N1-Src SH3 domain ligands that are characterised C-Src substrates (Fig.3.7B) should also be assessed for *in vivo* phosphorylation by N1-Src, as C- and N1-Src possess identical catalytic domains.

Given that N1-Src interacted with a subset of C-Src ligands, it was unsurprising that like C-Src, the N1-Src SH3 domain ligands enriched for both Class I and II motifs (Fig.3.3A). This suggests that the N1-Src SH3 domain could interact with similar motifs to C-Src. Indeed, (Teyra et al. 2017) detected binding of the N1-Src SH3 domain to Class I ligand motifs by phage display. However they also reported the binding of N1-Src to diverse atypical motifs, and (Keenan et al. 2017) proposed an atypical motif of +xPxxT/Vx+ for N1-Src derived from phage display and mutagenesis assays. The ligand motif preference of the N1-Src SH3 domain was therefore further investigated in Chapter 4.

The three most abundant N1-Src SH3 domain ligands were Dynamin I, Dynamin III and Enah respectively. The most abundant C-Src ligand was Nono, followed by Dynamin I and HnrnpK (Table 3.2), the two latter are characterised C-Src SH3 domain ligands and substrates (Ahn et al. 1999; Cans et al. 2002). The interaction between the C- and N1-Src SH3 domains and Dynamin I was further investigated in Chapter 4. The abundance of the SH3 domain ligands is not necessarily reflective of affinity, and is likely a combination of both affinity and relative expression within the P1 lysates. Interestingly, N1-Src fails to interact with a number of abundant C-Src ligands such as HnrnpK and Dpysl2 (Table 3.2). The loss of these interactions could be due to a change in the ligand consensus motif of N1-Src. As discussed, atypical N1-Src SH3 domain ligand motifs have been identified by phage display (Keenan et al. 2017; Teyra et al. 2017). However, as N1-Src enriched for ligands containing Class I/II motifs, and interacted solely with a subset of C-Src ligands, it would be surprising for it to possess a highly diverse binding motif. Although N1-Src could have additional filtering of C-Src ligands, for example the Abl SH3 domain was unable to bind a Src SH3 domain peptide ligand due to steric clashes by its n-Src loop (Feng et al. 1995). Thus the N1-Src insertion could be involved in steric repulsion. Alternatively, or in conjunction with this, the overall affinity of the N1-Src SH3 domain could be lowered so that it no longer interacts with the lowest affinity C-Src ligands. Peptide arrays of the unique C-Src SH3 domain ligands could be used to identify if the specificity is at the level of the amino

acid sequence. In addition, when applicable techniques such as surface plasmon resonance or isothermal titration calorimetry could be used to assess if the unique C-Src ligands are the lowest affinity. The identification of the N1-Src SH3 domain structure and mechanism of ligand binding is key to understanding its tailored interactome, and this was further investigated in Chapter 4.

Functional enrichments and protein-protein interactions by the C- and N1-Src SH3 domain ligands

The C- and N1-Src SH3 domain ligands were analysed in STRING in order to generate protein-protein interaction networks, and to conduct GO term enrichment analysis. The C-Src network highlights a number of characterised C-Src ligands and substrates identified by the pull-down (Fig.3.7A). In addition, there were multiple complexes linked to the functions of Src. For example the Escrt complex is involved in the transport of Src to focal adhesions (Tu et al. 2010). The SCAR complex regulates the actin cytoskeleton through the Arp2/3 complex, and is present in dynamic structures including the lamellipodia. C-Src phosphorylates Wasf1 in the SCAR complex, which regulates both the stability and activation of the complex (Pollitt and Insall 2009).

Surprisingly, nuclear and RNA regulatory proteins complexes were enriched for both C- and N1-Src including the spliceosome, paraspeckle complex and mRNA cleavage factor complex. The most prominent complex within the C-Src network is the mRNA processing/spliceosome complex (Fig.3.7A), which contains two characterised C-Src substrates, HnrnpK and Sf3b2. The mRNA cleavage factor complex participates in the 3' processing of mRNA including regulation of polyadenylation and cleavage (Shi et al. 2009). However, there is overlap as the mRNA cleavage factor complex proteins Cspf7 and Nudt21 (Cpsf5) are also associated with Paraspeckles (Naganuma et al. 2012). Paraspeckles are relatively new to the literature and are defined as ribonucleoprotein bodies that regulate gene expression by nuclear RNA retention (Bond and Fox 2009). They have since been associated with RNA regulation at most levels (Knott et al. 2016). The minimal complex is described as containing Nono, Sfpq, Pspc1 and the long non-coding RNA *NEAT1* (Bond and Fox 2009). Interestingly, all three core Paraspeckle proteins were identified as C-Src SH3 domain ligands, whereas N1-Src pulled down Nono and Sfpq (Fig.3.7). Sfpq has been detected outside of the nucleus, in the axons and growth cones of sensory neurons (Cosker et al. 2016). Sfpq promotes axon survival via

the regulation of mRNA pools (Cosker et al. 2016), and functions as a coactivator with the FOX3 protein to enhance neuronal specific alternative splicing (Kim et al. 2011). Furthermore, in a zebrafish Sfpq mutant, structural brain abnormalities were observed and some classes of neurons failed to differentiate (Lowery et al. 2007). Similarly, Nono deficient mice present defects at inhibitory synapses (Mircsof et al. 2015), and upon NGF induced c-Jun N-terminal kinase (JNK) mediated neuronal differentiation, JNK interacted with both Sfpq and Nono in an RNA dependent manner (Sury et al. 2015). Sfpq was significantly upregulated in a C-Src phosphoproteomics study (Amanchy et al. 2008), and *in vitro* phosphorylated by N1-Src (Chapter 5), thus it should be considered as a potential target for both kinases. Nono was the most abundant C-Src SH3 domain ligand making up nearly 1 % mol of the sample (Table 3.2). However, there is currently no functional link between Src and Nono or Sfpq in the literature. Only a few studies have detected Src in the nucleus, one of which identified nuclear tyrosine phosphorylation activity (Paladino et al. 2016). Thus is it currently unknown whether these nuclear and RNA regulatory protein ligands are *in vitro* artefacts or represent a physiological role for Src in RNA regulation.

The most enriched GO term for the C-Src SH3 domain ligands was cytoskeletal organisation, one of its highly cited functions in the literature (Destaing et al. 2008; Weernink and Rijksen 1995; Tehrani et al. 2007). N1-Src also enriched for the regulation of actin polymerisation and depolymerisation, neuron projection morphogenesis, and the actin based structure of the lamellipodia. N1-Src generates a ‘neuronal like’ morphology upon overexpression in fibroblasts (Keenan et al. 2017) and has been associated with the regulation of microtubule morphology in Purkinje neurons (Kotani et al. 2007) (Section 1.4.4). Thus these ligands are relevant to the characterised functions of N1-Src.

Identification of the N-Enah splice variant as an N1-Src SH3 domain ligand and putative substrate

The canonical Enah and Neuronal Enah (N-Enah) splice variants interacted with both the C- and N1-Src SH3 domains. However, there was differential binding whereby the N1-Src SH3 domain showed preference for the neuronal variant (Fig.3.5). The lack of binding by the N1-Src SH3 domain to canonical Enah has previously been observed by GST-SH3 domain pulldowns (Gertler et al., 1996).

Enah is an actin-binding cytoskeletal regulatory protein in the Enabled/Vasodilator stimulated phosphoprotein (Ena/VASP) gene family, also consisting of Vasp and Evl, both of which also interacted with the C- and N1-Src SH3 domains. As the N-Enah variant is formed by a 249 residue insert in the Enah proline-rich domain, it's speculated to have altered interactions with SH3 and WW domain containing proteins (Gertler et al. 1996). Interestingly, the N-Enah insertion contains a Class II motif (Fig.3.6A), whereas the canonical Enah contains no Class I or II motifs. As the N1-Src SH3 domain ligands enriched for Class I and II motifs, it is interesting to consider whether this could be the cause of N1-Src's preference for N-Enah. This could be investigated via mutagenesis of the motif in full length N-Enah, or a peptide containing the putative binding site.

Enah has been detected in growth cone filopodia (Lanier et al. 1999), and functions downstream of axon guidance receptors (Menzies et al. 2004; Lanier et al. 1999). More recently Enah has been associated with the regulation of mRNA translation in neurons (Vidaki et al. 2017). N-Enah research has similarities to that of N1-Src in that studies utilising Enah knockouts, or Enah antibodies in neurons have failed to distinguish between the isoforms. The few studies on N-Enah have identified that it's enriched in the developing nervous system and is present in neurons but not glia. In the embryonic mouse brain N-Enah expression peaked between E15 and P1, coinciding with rapid neurite outgrowth and axonal migration. In the adult brain, N-Enah was detected in all brain regions. Immunocytochemistry identified N-Enah in growth cone filopodia (Lanier et al. 1999) and its expression in RAT2 fibroblasts induced actin cytoskeletal remodelling (Gertler et al. 1996). The authors reported enhanced actin remodelling abilities by N-Enah over the canonical isoform. Interestingly, immunoprecipitation of Enah from embryos identified only N-Enah as tyrosine phosphorylated (Gertler et al. 1996), however, a responsible kinase was not identified. It is suspected that tyrosine phosphorylated N-Enah could have a role in axon guidance (Gertler et al. 1996).

Upon overexpression in COS7 cells, GFP-N-Enah formed triton insoluble puncta that were dispersed throughout the cell (Fig.3.8). It is unclear if the puncta are N-Enah associating with the actin cytoskeleton or a signalling complex, and this could be assessed by phalloidin staining. Indeed, other cytoskeletal regulators including N-WASP, Arp2/3 and Cortactin have been shown to localise at actin-rich puncta (Yu and Machesky 2012). Alternatively, the puncta could be protein aggregates, as overexpression of some

proteins has been reported to result in cytoplasmic puncta (Smalley 2005). Thus this construct requires further characterisation. Interestingly, upon the co-expression of N1-Src and N-Enah in B104 cells, a prominent phosphotyrosine band at the electrophoretic mobility of N-Enah was present (Fig.3.8). This suggests that N-Enah may be tyrosine phosphorylated by N1-Src, or that signalling has been induced resulting in the phosphorylation of a protein at the same electrophoretic mobility as N-Enah. However, considering the scale of phosphorylation, and that N-Enah was identified as an *in vitro* C- and N1-Src substrate (Chapter 5), it is likely that of N-Enah. The phosphorylation could be confirmed following optimisation of N-Enah immunoprecipitation, as preliminary experiments suggest that upon RIPA lysis a substantial amount of Enah is lost to the insoluble fraction (data not shown). Alternatively, mass spectrometry could be used to reveal the *in vivo* phosphorylation sites. As phosphorylated N-Enah is suspected to play a role in axon guidance this could be assayed via morphological analysis upon overexpression and knockdown of N1-Src in neurons alongside N-Enah phospho-null and -mimetic mutants. In addition, it would be interesting to assess if C-Src also phosphorylates N-Enah *in vivo*, and if so, how it relates to N1-Src.

***In vivo* implications of a lower affinity SH3 domain**

The N1-Src SH3 domain has a weakened intramolecular interaction with the SH2:SH1 regulatory linker (Keenan et al. 2015). This could relieve the SH3 domains negative regulation and promote auto- and substrate phosphorylation. N1-Src also appears to have lower affinity intermolecular interactions, however it is unclear how much of an effect this would have upon the exposure of N1-Src to high local concentrations of cellular ligands and substrates. The N1-Src SH3 domain could be less likely to participate in stable interactions, and this could result in a higher substrate turnover. Indeed, peptide based studies have shown that high affinity substrates compete with and reduce phosphorylation of low affinity substrates, and with increasing affinity, specific activity was reduced (Sommese and Sivaramakrishnan 2016). Thus N1-Src could be more promiscuous, in line with cellular studies that have reported raised substrate phosphorylation by N1-Src (Worley et al. 1997; Levy and Brugge 1989). Following confirmation that N-Enah is phosphorylated by N1-Src, it could provide a means to assess the regulation of phosphorylation events by C- and N1-Src. For example, N1-Src

SH3 domain mutants that disrupt ligand binding (Chapter 4) could be used to assess if the N1-Src SH3 domain is also directing ligand interactions and subsequent substrate phosphorylation *in vivo.*

Chapter 4
Mechanism of ligand binding by the N1-Src SH3 domain

Chapter 4: Mechanism of ligand binding by the N1-Src SH3 domain

4.1 Introduction

The data in Chapter 3 demonstrated using GST-Src SH3 domain pull-downs in postnatal day 1 rat brain, that the N1-Src SH3 domain interacted with only a subset of C-Src ligands, and the interactions appeared to be of reduced affinity. This is consistent with reports of the N1-Src SH3 domain failing to interact or only weakly interacting with C-Src SH3 domain ligands (Reynolds et al. 2008; Messina et al. 2003; Craggs et al. 2001; Brown et al. 1998). In contrast to C-Src, N1-Src kinase has high levels of constitutive auto-phosphorylation (Brugge et al. 1985), and this is suspected to be due to a weakened interaction between the SH3 domain and the SH2:SH1 negative regulatory linker (Keenan et al. 2015). Thus, the N1-Src insertion might disrupt both intra- and intermolecular interactions, tailoring the ligand interactions and activation status of N1-Src.

SH3 domain structures have been successfully determined by nuclear magnetic resonance (NMR) spectroscopy and X-ray crystallography, in both the peptide bound and unbound forms (Morton et al. 1996; Musacchio et al. 1994; Yu et al. 1992; Musacchio et al. 1992; Yu et al. 1994). The structure of the C-Src SH3 domain is described in Section 1.2.3, and a schematic of the peptide-bound C-Src SH3 domain is shown in Fig.4.1. The C-Src SH3 domain interacts with Class I (+xxPxxP) and Class II (PxxPx+) ligand motifs via three core pockets. The first pocket is formed by the n-Src and RT loops, including the residues D99, W118 and Y131 (Feng et al. 1995b). The D99 residue of the RT loop forms a salt bridge with the charged residue flanking the PxxP motif in the Class I and II ligands. The D99N mutant has reduced affinity for peptide ligands, and via GST-SH3 domain pull-downs, the C-Src D99N mutant failed to interact with the majority of ligands, a subset that were retained were referred to as D99N independent ligands (Weng et al. 1995). The second and third pockets each bind proline residues as xP dipeptides. The SH3 domain residues that form these pockets are Y90, Y92, W118, Y131, P133 and Y136 (Feng et al. 1994) (Section 1.2.3). As W118 contributes to both the charge binding and xP binding pockets, the W118A mutant is used as a means of SH3 domain inactivation (Erpel et al. 1995).

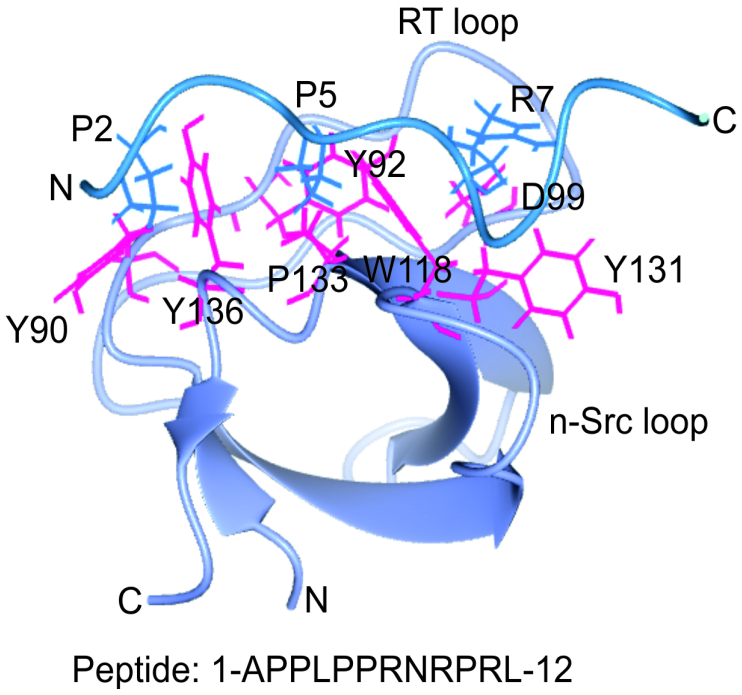

Figure 4.1: The solution structure of the C-Src SH3 domain in complex with a Class II peptide ligand. The sequence of the 12 mer peptide ligand (blue) is shown and the peptides interacting residues from the PPLPPR Class II motif P2, P5 and R7 (blue) are mapped onto the structure. The C-Src SH3 domain (purple) n-Src and RT loops are labelled, including the interacting residues Y90, Y92, D99, W118, Y131, P133 and Y136 (pink). PDB:1QWE, drawn using CCP4mg.

As discussed in Section 1.2.3, the mechanism of SH3 domain ligand binding has since shown to go well beyond this simplified model, including interactions with atypical ligand motifs that contain only a single proline, or none at all (Kokoszka et al. 2018; Kang et al. 2000). A recent phage display study found that half of the 115 SH3 domains analysed had diverse and atypical specificities. The N1-Src SH3 domain was identified as one of these, as well as binding canonical Class I ligand motifs (Teyra et al. 2017). Furthermore, a phage display study conducted in our laboratory proposed the atypical motif of +xPxxT/Vx+ for the N1-Src SH3 domain (Keenan et al. 2017). However, neither study has validated this atypical interaction beyond phage display.

The 'specificity zone' is a region flanked by the SH3 domains n-Src and RT loops, which makes additional flanking contacts that determine affinity and specificity (Saksela & Permi 2012). Considering that the n-Src and RT loops are highly variable between SH3 domains, and that there are also a number of isoforms and SH3 domain splice variants that occur in these loops, including N1-Src (Tsyba et al. 2008; Gkourtsa et al. 2016; Owen et al. 1998; Kokoszka et al. 2018), it makes sense that this region is important for controlling binding affinity and specificity.

NMR spectroscopy can provide a wealth of information on a protein of interest. As discussed, it has been utilised to determine the structures of SH3 domains, and to identify peptide binding sites (Yu et al. 1992). It can also be utilised to obtain the K_d for an interaction, study the dynamics of a protein, and provide information regarding the effects of mutations or isoforms/splice variants on the structure/stability of a protein, which in turn could explain features such as differential binding or loss of interactions.
A simple NMR experiment utilises *U*-^{15}N labelled protein to acquire a 2D (^{1}H-^{15}N) Heteronuclear single quantum coherence spectroscopy (HSQC) spectrum. The spectrum displays ^{1}H-^{15}N correlations with each cross-peak corresponding to each backbone residue, with the exception of prolines, and cross-peak(s) are also observed for the side chains of tryptophan, glutamine, arginine and asparagine residues. The HSQC spectrum can be considered as the fingerprint of the protein, and the cross-peaks are able to undergo chemical shift perturbations (CSPs), on a change in the chemical environment that can be measured accurately. CSPs can occur due to changes in buffer conditions such as salt and pH, the formation of protein-protein interactions, or mutation in a protein. CSPs can be observed without the backbone assignment of a protein, however, the assignment adds power by enabling the region of the protein that is perturbed to be mapped, if the structure is available (Williamson 2013).

NMR has been utilised to identify the interaction interface of the C-Src SH3 domain with peptide ligands (Katyal et al. 2013; Yu et al. 1992). The basis of this experiment is the exchanging system of the protein [P] and ligand [L], which undergo a reversible reaction of [P]+[L] <=> [PL]. Utilising uniformly ^{15}N labelled protein, the protein is titrated with increasing concentration of ligand, ideally to achieve saturation of peptide-protein binding, or as close as possible. A HSQC is recorded for each titration point, while also maintaining constant conditions. Due to the sensitivity of chemical shift, any real protein-peptide interaction should generate changes that progress in a ligand concentration-dependent manner, and are classified as fast, slow and intermediate exchange (Fig.4.2) with respect to the chemical shift timescale. A protein-ligand interaction generates two distinct states that undergo interconversion: ligand-free (A) and ligand-bound (B), and the exchange rate (k*ex*) is represented by k(*A*) + k(*B*). Fast exchange ($k_{ex} > \Delta\delta^{(\delta Free-\delta bound)}$) is indicative of weaker interactions as the protein-ligand complex only exists for a fraction of the time taken to record the experiment. As such,

the cross-peak generated is representative of a weighted average of the free and complexed species, and the cross-peak shifts across the titration series. Slow exchange ($k_{ex} < \Delta\delta^{(\delta Free-\delta bound)}$) occurs for stronger interactions, and results in two cross-peaks at distinct chemical shifts representing the free and complexed molecule, as throughout the recording a protein is either free or bound. As the ligand concentration increases, the bound cross-peak increases in intensity, whilst the unbound decreases. Intermediate exchange ($k_{ex} \approx \Delta\delta^{(\delta Free-\delta bound}$) falls between the two, where the cross-peaks undergo shifts whilst reducing in intensity, and a cross-peak may reappear upon saturation (Fig.4.2) (Williamson 2013).

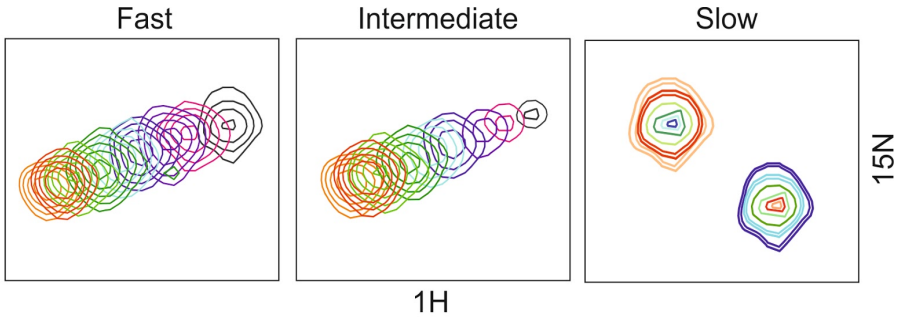

Figure 4.2: Schematic of peak exchange regimes upon ligand interactions. Cross-peaks can enter slow, fast or intermediate exchange upon ligand interactions. Fast exchange results in the cross-peak shifting in a concentration-dependent manner. Intermediate exchange cross-peaks shift in a concentration dependent manner whilst also reducing in intensity, and a cross-peak may reappear upon saturation. Slow exchange produces two cross-peaks, and as the ligand concentration increases the bound cross-peak increases in intensity, whilst the unbound cross-peak reduces.

When a protein undergoes an interaction, the resonance frequency of a given signal becomes perturbed. The perturbation can be measured accurately by calculating the chemical shift change of a cross-peak, and this can be applied to all the residues of a protein. Cross-peaks undergoing a change in chemical shift upon ligand binding are considered to correspond to either the binding site or nearby residues, or be affected by a conformational change induced by ligand binding. If the structure of the protein is known, the residues undergoing CSPs can be mapped to aid interpretation. Furthermore, by plotting the CSPs of cross-peaks in fast exchange vs the ligand concentration, a titration curve can be generated to obtain a K_d for the interaction (Williamson 2013). As NMR spectroscopy has successfully yielded SH3 domain structures and peptide binding sites, and can also provide information regarding affinity, it was selected as an experimental system to explore the structural and functional properties of the N1-Src SH3 domain in comparison to C-Src.

4.2 Aims

The data from Chapter 3 demonstrated that the N1-Src SH3 domain ligands are a subset of C-Src ligands, and these ligands are enriched in Class I/II proline rich motifs. Furthermore, the N1-Src SH3 domain appeared to be of reduced affinity. It is therefore hypothesised that the N1-Src SH3 domain has a lower affinity than the C-Src SH3 domain, but retains a similar substrate specificity. The aim of this chapter was to address this hypothesis and to 1) Investigate the N1-Src SH3 domains ligand consensus sequence by peptide arrays 2) Identify the structural determinants of N1-Src SH3 domain ligand binding by NMR spectroscopy and binding assays with GST-SH3 domain mutants, including the function of the N1-Src six residue insertion.

4.3 Results

4.3.1 Optimisation of peptide arrays for SH3 domain binding assays

The peptide array is an established technique for assessing SH3 domain ligand motifs, and identifying binding sites within proteins of interest (Rouka et al. 2015; Rufer et al. 2009). Therefore, this approach was adopted to identify the ligand consensus sequence(s) that bind His-tagged C- and N1-Src SH3 domains. To first optimise the detection of SH3:peptide interactions, a positive control array containing known C-Src SH3 domain peptide ligands was utilised (Fig.4.3). The arrays were designed with 15-mer peptides, which were N-terminally acetylated and C-terminally conjugated to the membrane. The peptides were acetylated to reduce their overall charge and be more representative of the native protein. The C-Src binding peptides were obtained from phage display (A1) (Weng et al. 1994), putative binding sites from a surface plasmon resonance experiment (A3 and A5) (Solomaha et al., 2005), a peptide competition assay (A7) (Taylor et al. 1995) and a peptide array (A9) (Sun et al. 2012). In order to confirm the specificity of binding, negative control peptides were included in which all proline residues were mutated to alanine (A2/A4/A6/A8/B1; Fig.4.3).

The assay enables the detection of SH3:peptide interactions via anti-His-HRP immunoreactivity following incubation of the arrays with the His-C- and N1-Src SH3 domains. Firstly, the detection of SH3:peptide interactions was optimised in terms of SH3 domain concentration, buffer conditions and incubation times. As shown in Table 4.1, reduced stringency conditions were necessary to detect N1-Src binding, as C-Src peptide binding was detectable at 0.1 μM, whereas N1-Src binding remained undetectable at 2 μM, until incubation overnight at 1 μM in PBS. This suggests that the N1-Src SH3 domain has lower affinity. Utilising these conditions, firstly an antibody-only control was conducted to detect any non-specific binding. The membranes were blocked and incubated with anti-His-HRP for 2 h, and then visualised by anti-His-HRP Western blotting (Fig.4.3A). Following conformation that there was no non-specific binding by the antibody, the experiment was then repeated to include the C- and N1-Src SH3 domains. The peptide array membrane was blocked and then incubated with the relevant His-SH3 domain (0.5 μM His-C-Src SH3 domain in blocking buffer for 2 h at room temperature and 1 μM His-N1-Src SH3 domain overnight at 4 °C in PBS),

and bound SH3 domain was detected using anti-His-HRP via Western blotting, as described for the antibody-only control.

The C-Src SH3 domain bound the peptides A1, A5 and A7 (Fig.4.3). As the peptides A1 and A7 generated white spots, qualitatively these peptides are likely to be higher affinity ligands, as this occurs due to an excessive signal and rapid consumption of the chemiluminescent substrate. Surprisingly the N1-Src SH3 domain bound all of the C-Src peptide ligands (A1, A3, A5, A7, A9), and C- and N1-Src both bound A1, A5, and A7. The A1 peptide also generated a white spot for N1-Src, suggesting this could also be a higher affinity ligand (Fig.4.3A). Indeed, the A1 peptide was the only binder detected upon incubation with N1-Src at 1 μM overnight in blocking buffer (Table 4.1). The proline-alanine mutant peptides all resulted in loss of binding to the C- and N1-Src SH3 domains, suggesting the observed binding to the experimental peptides was specific (Fig.4.3B). However, as the arrays were incubated with C- and N1-Src at different concentrations and buffer conditions, direct comparisons of affinity or ligand preference cannot be made.

Table 4.1: The experimental conditions under which the peptide arrays were conducted in order to optimise peptide binding by the C- and N1-Src SH3 domains

SH3 domain concentration (μM)	Incubation	C-Src binding	N1-Src binding
0.1	Blocking buffer-2h	Y	N
0.3	Blocking buffer- 2h	-	N
0.5	Blocking buffer-2h	Y: Same as 0.1 μM plus Enah A5	N
2	Blocking buffer- 2h	-	N
1	Blocking buffer-overnight	-	Y: Only to control peptide A1
1	PBS-overnight	-	Y

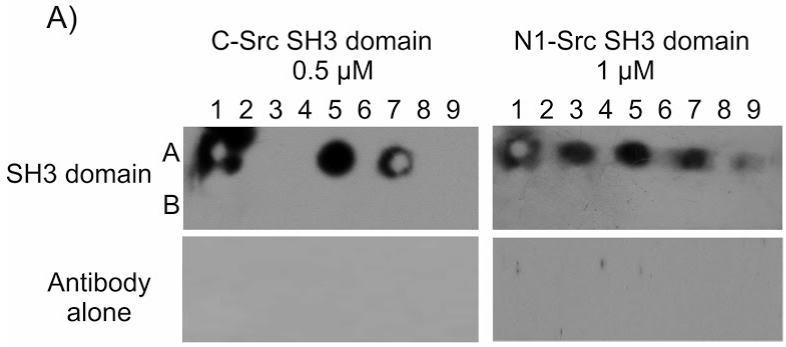

B)

	Peptide sequence	C-Src	N1-Src	Class I/II motif
A1	AERSSRPLPPIPGGK	+	+	I/II
A2	AERSSRALAAIAGGK	−	−	
A3	QRRAPAVPPARPGSR	−	+	I/II
A4	QRRAAAVAAARAGSR	−	−	
A5	FGPPPQVPSRPNRAP	+	+	II
A6	FGAAAQVASRANRAA	−	−	
A7	IQRIPLPPPPAPETY	+	+	I
A8	IQRIALAAAAAAETY	−	−	
A9	SQLLRPKPPIPAKPQ	−	+	I/II
B1	SQLLRAKAAIAAKAQ	−	−	

Figure 4.3: Optimisation of a peptide array assay to identify C- and N1-Src SH3 domain binding motifs. A) Binding of His tagged-C- and N1-Src SH3 domains to canonical 15-mer C-Src peptide ligands and their proline to alanine mutants. Membranes were probed with 0.5 μM C-Src SH3 domain for 2 h at room temperature in blocking buffer or 1 μM N1-Src SH3 domain overnight at 4 °C in PBS (labelled 'SH3 domain'). An antibody-only control membrane (labelled 'Antibody') was also conducted to detect non-specific binding. Peptide and non-specific binding was detected via anti-His-HRP (1:120,000 v/v). B) The peptide sequences (Class I/II) and their proline to alanine mutants are shown, including the presence or absence of C- and N1-Src SH3 domain binding.

4.3.2 Identification of C- and N1-Src SH3 domain ligand motifs

Following the successful optimisation and identification of the C- and N1-Src SH3 domains binding to the control peptides (Fig.4.3), the assay was expanded to identify C- and N1-Src SH3 domain ligand motifs within the interacting proteins identified in Chapter 3. The proteins Dynamin I/III, N-WASP and Enah were selected for this analysis, as the N1-Src SH3 domain directly interacts with the proline rich domain (PRD) of Dynamin I (Fig.4.5B), and it was the most abundant N1-Src SH3 domain interactor (Chapter 3). Actin polymerisation was the most enriched GO term for the N1-Src SH3 domain ligands (Fig.3.7B), therefore the cytoskeletal regulators N-WASP and Enah were also selected. The proteins all contain PRDs or proline rich regions (PRR), that often harbour SH3 domain ligands. Therefore, arrays of 15 mer peptides with an offset of 5 amino acids were generated to span these regions. This relied on the assumption that N1-Src bound the proline rich domains. However, the preference of N1-Src for proline was suggested by the control array (Fig.4.3) and the interaction of N1-Src with the Dynamin I PRD (Fig.4.5). Therefore, a limitation of this assay is that any atypical or PxxP motifs outside of these domains have been overlooked.

As described in Section 4.3.1, an antibody only control was used to confirm the absence of non-specific binding by the antibody prior to incubation with the SH3 domains (Fig.4.4). The arrays were then incubated with 0.5 μM His-tagged C-Src SH3 domain for 2 h in blocking buffer, or 1 μM His-N1-Src SH3 domain overnight at 4 °C in PBS, followed by visualisation with anti-His-HRP. The C- and N1-Src SH3 domains bound at least one peptide from each protein, and Dynamin I/III, and N-WASP contained multiple peptide ligands. The peptides bound by the SH3 domains are underlined in red in the protein sequences (Fig.4.4), and motifs that were present in multiple bound peptides are highlighted in bold. Interestingly all of these contained a Class II motif. The C-Src SH3 domain bound peptides corresponding to two regions in the Dynamin I PRD (B4 and B8), and the N1-Src SH3 domain bound peptides spanning three regions (A8, A9, B4, B8, B9). The C- and N1-Src SH3 domains both bound the peptides B2, B3, B4 and B8 in Dynamin III (Fig.4.4A). The binding to N-WASP appeared to be the most differential as C-Src bound peptides A5 and A6 corresponding to a single site, whereas N1-Src bound A1, A2, A6 and B3 (Fig.4.4B). It is interesting that N1-Src bound A6 but not A5, and its possible that it holds some information regarding N1-Src's ligand preference. However,

as previously stated, due to the differential concentrations and binding conditions utilised for C- and N1-Src, peptides should not be categorised as unique to either SH3 domain. C-Src arrays under the same conditions as N1-Src were not attempted due to technical challenges including high background. Enah was the only protein for which a single peptide was bound (A5) by C- and N1-Src (Fig.4.4B). The Enah A5 peptide was only detected upon increasing the C-Src SH3 concentration from 0.1 to 0.5 µM, suggesting it's likely lower affinity (Table 4.1). This is consistent with the peptide containing no Class I or II motifs. Overall this data mimic Fig.4.3, whereby in many instances the C- and N1-Src SH3 domains bound the same peptide ligands.

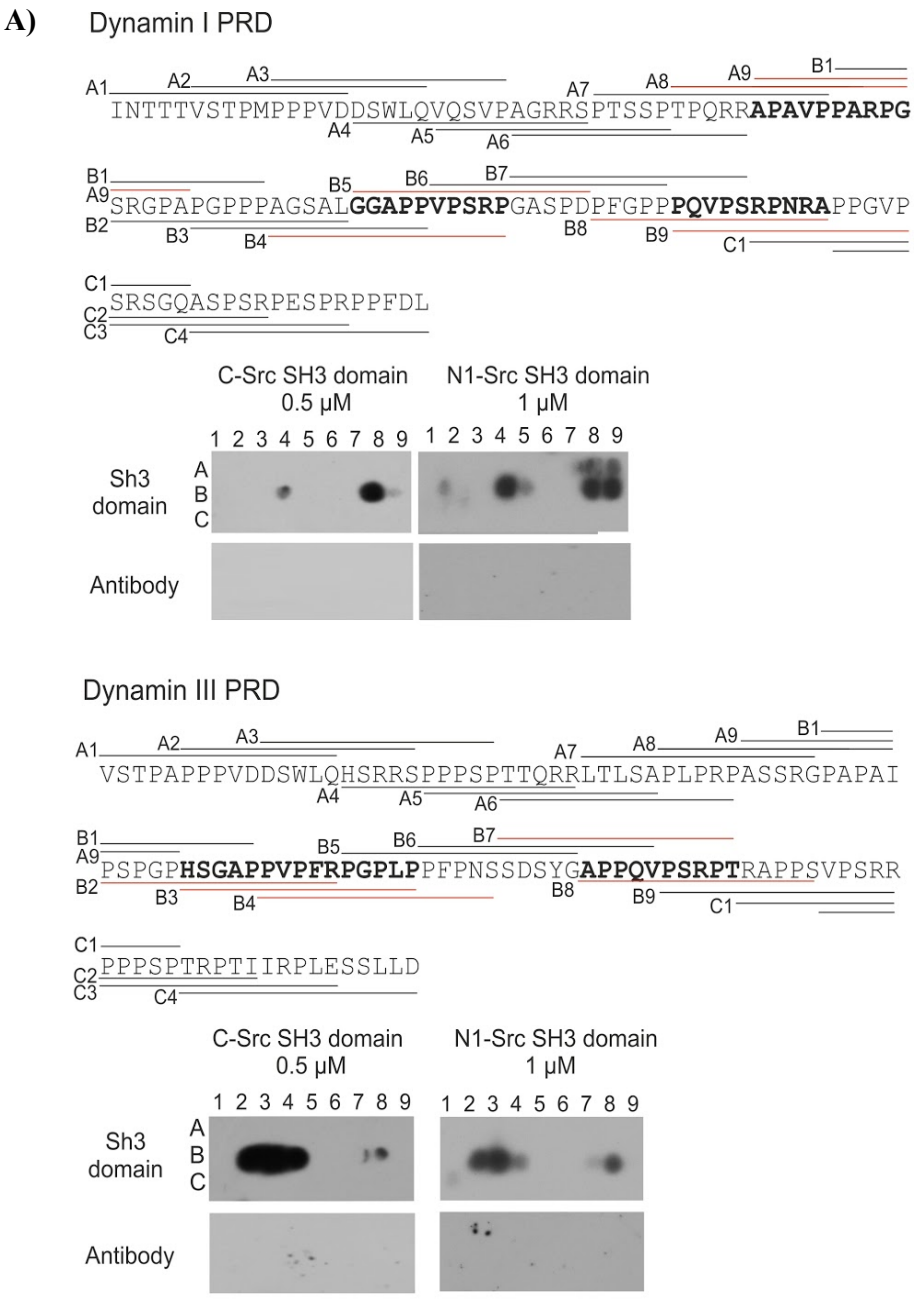

B)

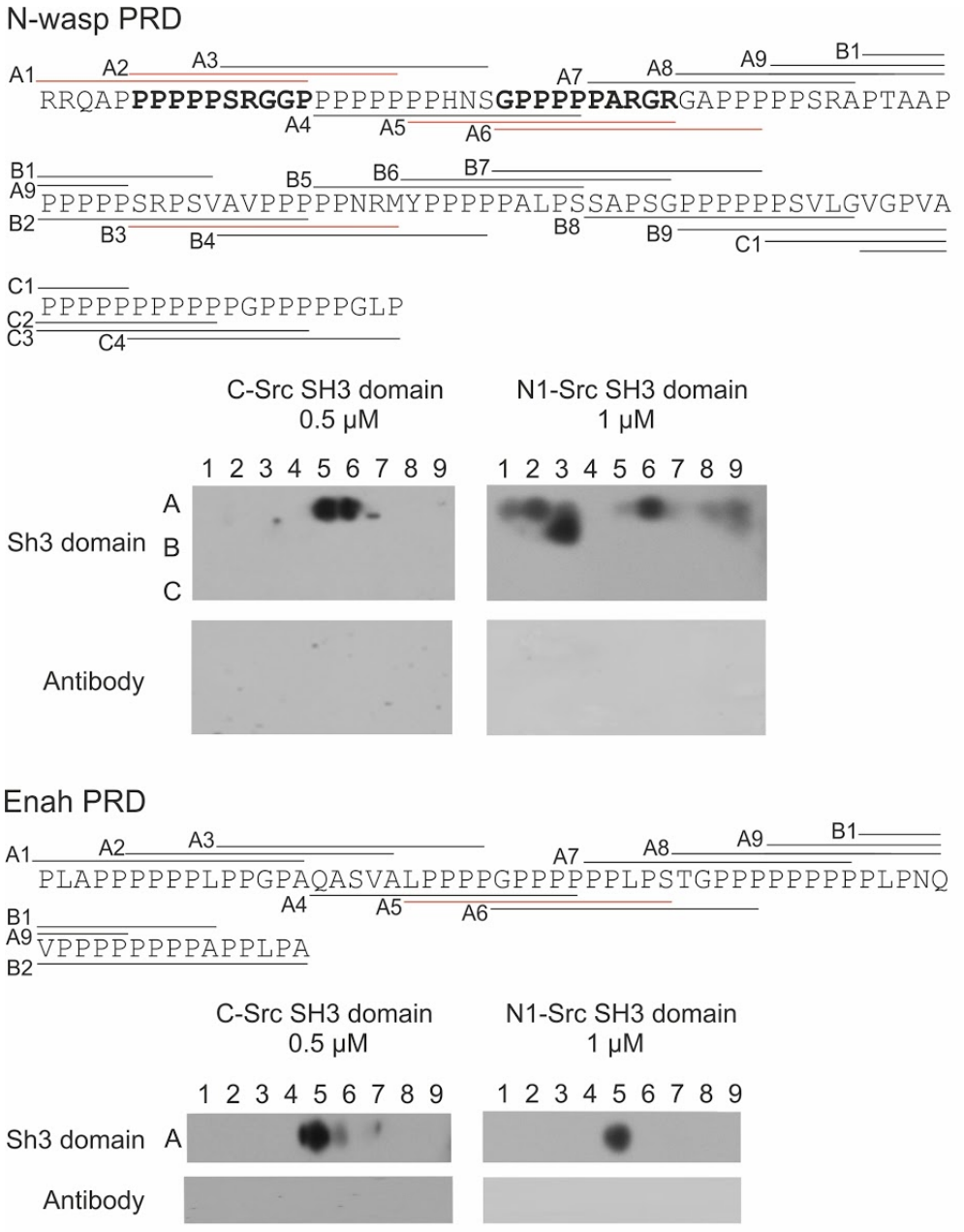

Figure 4.4: Utilisation of peptide arrays to identify C- and N1-Src SH3 domain binding motifs within the GST-SH3 domain ligands Dynamin I/III, Enah and N-WASP. The arrays consist of 15 mer overlapping peptides with an offset of 5 amino acids from the proline rich domains/regions of Dynamin I/III, Enah and N-WASP. The arrays were incubated with 0.5 µM His-tagged-C-Src SH3 domain for 2 h at room temperature in blocking buffer or 1 µM N1-Src SH3 domain in PBS overnight at 4 °C. A control membrane with the antibody alone was used to detect non-specific binding. SH3:peptide binding was detected via anti-His-HRP at the same concentration (1:120,000 v/v). A) The protein sequences and 15-mer peptides from Dynamin I and III. Bound peptides are highlighted in red, and motifs common to overlapping peptides are highlighted in bold. The His-immunoreactivity is shown for the array alone (antibody) and the array incubated with SH3 domain. B) The equivalent of A, but for the proteins N-WASP and Enah.

4.3.3 The N1-Src SH3 domain bound peptides containing Class I and Class II motifs

In total the C- and N1-Src SH3 domains bound 10 and 15 peptides, respectively, from the peptide arrays of their SH3 domain ligands (Fig.4.4). The N1-Src SH3 domain peptide ligands are shown in Table 4.2 and all Class I and II SH3 domain ligand motifs within each peptide are highlighted in red. The putative 'unique' peptides that were only bound by the N1-Src SH3 domain are underlined. However, this is only speculative as the assay was not conducted with the equivalent conditions for the C-Src SH3 domain.

In order to provide insight into the N1-Src SH3 domain ligand consensus, PRATT motif analysis was used to identify common features in the peptide ligands. This confirmed that all peptides were proline rich and that 70 % contained a Class II motif (Table 4.3). The abundance of Class II motifs is in line with the enrichment observed in the N1-Src SH3 domain ligands in Chapter 3.

In order to demonstrate that the C- and N1-Src SH3 domains were selectively binding Class I/II motif containing peptides, the peptides were classified based on their sequences. In total, the arrays spanning the four proteins contained 77 peptides (Table 4.4). There were 10 peptides that did not contain a PxxP motif, and none of these peptides were bound. Furthermore, there were 34 peptides that contained a PxxP motif but no flanking charge, and only one was bound (3 %), which was the Enah A5 peptide. There were 6 peptides that contained a Class I motif, 17 with a Class II motif, and 10 peptides with both a Class I and II motif, ie. +xxPxxPxx+ or PxxPxRxPxxP (Table 4.4). C-Src bound 7 (41 %) of the Class II peptides, and N1-Src 9 (52 %), both SH3 domains bound 1 Class I peptide (17 %), and C-Src bound 10 % of the Class I/II containing peptides in comparison to N1-Src's 40 % (Table 4.4).

As the arrays contained 34 peptides with just a PxxP motif (no flanking charge), and 33 peptides with a Class I and/or II motif, the arrays were not biased, and suggest that the C- and N1-Src SH3 domains were selecting for Class I/II motifs with specificity.

Table 4.2: The N1-Src SH3 domain peptide ligands. The Class I and II SH3 domain motifs with the N1-Src SH3 domain peptide ligands from the proteins Dynamin I, III, N-WASP and Enah. The peptides underlined are those which were not detected as binding to the C-Src SH3 domain.

		N1-Src	
Protein	Peptide	Class I motifs	Class II motifs
Dynamin I	A8	TPQRRAPAVPPARPG TPQRRAPAVPPARPG	TPQRRAPAVPPARPG
	A9	-	APAVPPARPGSRGPA APAVPPARPGSRGPA
	B4	-	AGSALGGAPPVPSRP
	B5	-	GGAPPVPSRPGASPD
	B8	-	PFGPPPQVPSRPNRA PFGPPPQVPSRPNRA
	B9	PQVPSRPNRAPPGVP	PQVPSRPNRAPPGVP PQVPSRPNRAPPGVP
Dynamin III	B2	-	PSPGPHSGAPPVPFR
	B3	-	HSGAPPVPFRPGPLP
	B4	PVPFRPGPLPPFPNS	-
	B8	-	APPQVPSRPTRAPPS APPQVPSRPTRAPPS
N-wasp	A1	RRQAPPPPPPSRGGP	RRQAPPPPPPSRGGP
	A2	PPPPPSRGGPPPPPP	PPPPPSRGGPPPPPP
	A6	-	GPPPPPARGRGAPPP
	B3	-	SRPSVAVPPPPNRM
Enah	A5	n/a	n/a

Table 4.3: PRATT motif analysis of the N1-Src SH3 domain peptide ligands. The motifs that were present in 60-100 % of the 15 N1-Src SH3 domain peptide ligands are shown.

PRATT motif	% of peptides conforming
P-P-x(1,2)-P	100
P-x-[PV]-P-x(0,2)-P	90
P-x-[PV]-P-x(0,2)-P-[AGNPS]	80
P-[PS]-x-P-x-R	70
P-x(0,1)-V-P-x(1,2)-R-P	60

Table 4.4: Categorisation of the peptides presented in the arrays. The types of peptides (Class I/II, PxxP, no PxxP) presented in the array are categorised, and the number of each peptide type bound by the C- and N1-Src SH3 domains are shown.

	No. of peptides bound by C-Src	% of peptides bound from each category	No. of peptides bound by N1-Src	% of peptides bound from each category
Class I peptides (n=6)	1	16.7%	1	16.7%
Class II peptides (n=17)	7	41.2%	9	52.9%
Class I and II peptides (n=10)	1	10%	4	40%
PxxP peptides (no charge) (n=34)	1	2.9%	1	2.9%
None PxxP peptides (n=10)	0	0%	0	0%
Total peptides = 77	**N=10**		**N=15**	

4.3.4 Differential Dynamin I binding by the C- and N1-Src SH3 domains

It was previously observed that there was differential binding to synaptosomal Dynamin I by the C- and N1-Src SH3 domains. Whereby N1-Src bound Dynamin I lacking the p-S774 modification, suggesting the interaction with N1-Src may be regulated by serine phosphorylation (Abdelhameed 2010). As S774 is dephosphorylated upon synaptic stimulation (Anggono et al. 2006), it was speculated that this could be a means of linking the N1-Src:Dynamin I interaction to synaptic vesicle endocytosis regulation. However this was not confirmed to be causal, and it could be due to another modification/protein interaction occurring alongside the loss of p-S774. Whilst attempts were made to isolate the N1-Src SH3 domain binding site using a variety of Dynamin I PRD mutants, the data was inconclusive as multiple sites significantly reduced binding (Abdelhameed 2010) (Section 1.4.6).

To confirm this observation, GST-Src SH3 domain pull-downs were conducted with the C- and N1-Src SH3 domains in synaptosome lysate. The pull-down eluates were analysed by Western blotting for total Dynamin I and Dynamin I p-S774. Dynamin did not bind to the GST-only control, and bound both the GST-C- and N1-Src SH3 domains with specificity (Fig.4.5A). Densitometry analysis was conducted on the Dynamin I and Dynamin I p-S774 Western blots for the triplicate replicates, and the ratio of p-S744 Dyn I:Total Dyn1 was calculated. The C- and N1-Src ratios were then analysed by T-test revealing a significant reduction ($p < 0.01$) in the ratio of p-S744 Dyn I:Dyn1 for the N1-Src SH3 domain, thus corresponding to a reduction in N1-Src binding to p-S774 Dynamin I (Fig.4.5A).

In addition, the direct interaction between the N1-Src SH3 domain and Dynamin I was demonstrated by GST-pull-downs with purified His-tagged N1-Src SH3 domain and GST-tagged Dynamin I proline rich domain. As a control for non-specific binding the His-tagged N1-Src SH3 domain was incubated with the equivalent concentration of GST-only (Fig.4.5B). Confirmation of the direct interaction supports the identification of N1-Src SH3 domain peptide ligands in the Dynamin I peptide array (Fig.4.4A).

The protein sequence of the Dynamin I PRD, including the serine phosphorylation sites of S774, S778 and S857 that are de-phosphorylated by synaptic activity (Anggono et al. 2006; Xie et al. 2012) are shown in Fig.4.5B. The Class I and II SH3 domain ligand

motifs that were identified in the Dynamin I peptide arrays with the C- and N1-Src SH3 domains (Fig.4.4A) are also mapped onto the sequence (Fig.4.5B).

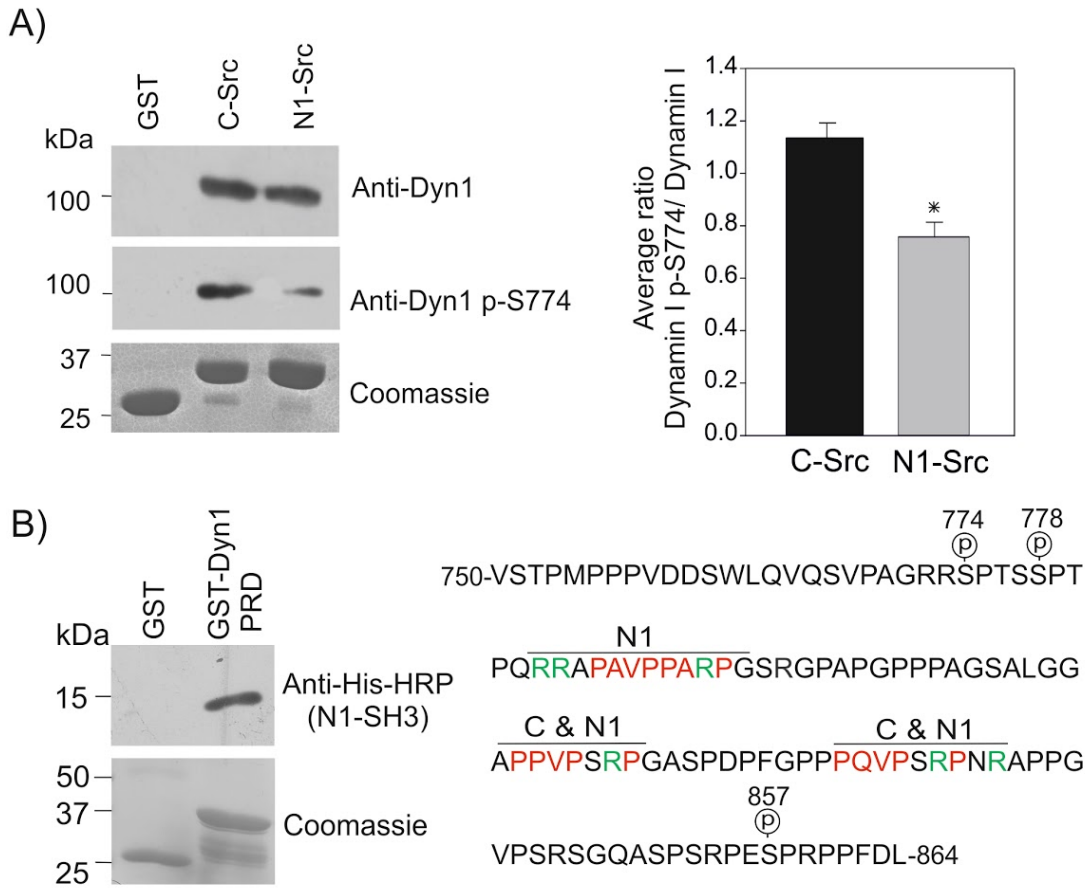

Figure 4.5: The C- and N1-Src SH3 domains differentially interact with full length synaptosomal dynamin I and the interaction can be specifically isolated to the dynamin I proline rich domain. A) Pull down of full length synaptosomal Dynamin I by 12.5 µM of GST, and GST-tagged C- and N1-Src SH3 domains. A 12.5 % SDS-PAGE Coomassie stained loading control is shown. Densitometry of the Dynamin 1 and Dynamin I p-S774 Western blots was used to calculate the average ratio of Dynamin I p-S774/Dynamin I in the C- and N1-Src SH3 domain pull downs. The n=3 experiments were statistically analysed by T-test, and the asterisk indicates significance at $p < 0.01$. The error bars show the SEM. B) Pull down of His-N1-Src SH3 domain by GST-Dynamin I proline rich domain. A 12.5 % SDS-PAGE Coomassie stained loading control is shown. The sequence of the Dynamin I proline rich domain (750-864) is shown, including the serine phosphorylation sites (774, 778 and 857) that are de-phosphorylated by synaptic activity. The C- and N1-Src SH3 domain Class I/II peptide ligand motifs that were identified via peptide array of the Dynamin I PRD are shown on the sequence in red and green.

4.3.5 NMR assignment of the N1-Src SH3 domain backbone

The triple resonance backbone resonance assignment of the N1-Src SH3 domain was conducted using 3D HNCACB, CBCA(CO)NH, HNCO and HNCACO spectra collected by the Potts lab using a double labelled N1-Src SH3 domain in 20 mM sodium phosphate, 100 mM sodium chloride pH 6.

The assignment was conducted using CCPN software, and the entire backbone of the N1-Src SH3 domain was assigned (Fig.4.6) with the exception of proline residues, as they do not produce a cross-peak in the 2D (^{1}H-^{15}N) HSQC spectrum. The ^{1}H-^{15}N chemical shift assignment of the N1-Src SH3 domain is included in Appendix 3. The N1-Src SH3 domain side chains were not assigned, however the 18 cross-peaks from the two tryptophans, three glutamines, three asparagines and four arginines are observable in the bottom left, top right and centre right of the HSQC spectrum, respectively. The six residues of the N1-Src insertion (RKVDVR) were identified centrally on the spectrum and are shown in red (Fig.4.6). The 102F and 129T cross-peaks occur at the same chemical shift and therefore overlap.

A schematic of the assignment process is shown in Fig.4.6. The 3D HNCACB spectrum correlates each NH group to the Cα and Cβ of the residue itself (referred to as i) and the Cα and Cβ of the preceding residue (referred to a i-1). Whereas the CBCA(CO)NH spectrum correlates each NH group to the Cα and Cβ of only the preceding residue. The spectra can therefore be superimposed to identify sequential and intra residue correlations, which enables the spin systems of individual residues to be linked sequentially, and then mapped onto the protein sequence (Section 2.11.2).

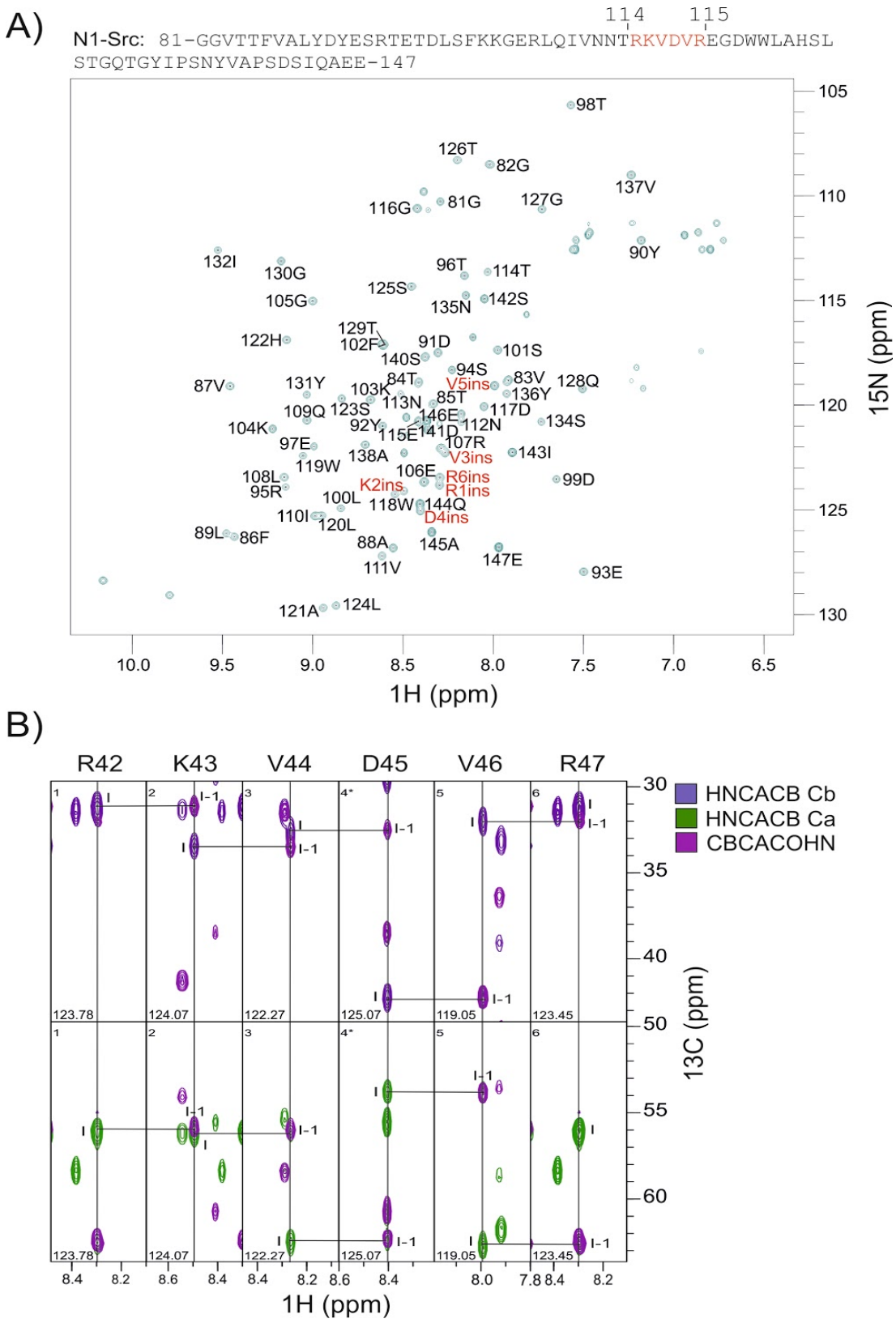

Figure 4.6: Triple resonance backbone assignment of the N1-Src SH3 domain. A) The protein sequence of the N1-Src SH3 domain is shown alongside its assignment onto a 2D (^{1}H-^{15}N) HSQC spectrum. The N1-Src insert (RKVDVR) is highlighted in red. B) The assignment theory via the Cα and Cβ chemical shifts from the superimposed HNCACB and CBCACONH spectra is shown for the six residue N1-Src insertion (R1ins-R6ins).

4.3.6 Chemical shift perturbations between the C- and N1-Src SH3 domains

The C- and N1-Src SH3 domains (~ 9 kDa) were expressed as [*U*-^{15}N] labelled (Section 2.4.2) in 20 mM sodium phosphate, 100 mM sodium chloride pH 6.

The C-Src SH3 domain cross-peaks were assigned using previously published data (BMRB:3433) and the N1-Src SH3 domain via the manual assignment in Section 4.3.5. The Schreiber lab C-Src SH3 domain construct terminated at 140S. Therefore, the 2D C-Src cross-peaks 141D-147E are only tentatively assigned based on being present at the same shift as the N1-Src SH3 domain. The 2D ^{15}N-TOCSY spectrum correlates each NH group to hydrogen atoms in the residue's side chain, and this can aid in assigning amino acid types. The C-Src SH3 domain ^{15}N-TOCSY spectrum also supported the tentative assignment of 141D-147E (data not shown). The only discrepancy with the C-Src SH3 domain assignment was the 140S cross-peak, as it occurred at the same shift as N1-Src 143I. The C-Src TOCSY spectrum confirmed the cross-peak was not a serine and was probably C-Src 143I. This likely occurred due to 140S being the C-terminal residue in the Schreiber construct. As the C-Src 140S cross-peak could not be identified, and the residues 141D-147E were only tentatively assigned, analysis was not conducted beyond 139P.

In order to compare the C- and N1-Src SH3 domains, their HSQC spectra were superimposed (Fig.4.7), and the hydrogen (^{1}H) and nitrogen (^{15}N) shift differences for each amino acid from 81G-139P were calculated (excluding prolines) in CCPN analysis software. Residues 141-147 were not analysed due to their tentative assignment for C-Src, however these cross-peaks were not shifted. The chemical shift perturbation between each amino acid of the C- and N1-Src SH3 domains was calculated via the formula: $\Delta\delta = (\Delta\delta H^2 + (\Delta\delta N/5)^2)^{½}$, and are displayed graphically (Fig.4.7). The largest CSPs occur for the residues 112N and 118W (1 ppm), that flank the N1-Src insertion (R1ins-R6ins). In addition, the n-Src loop and flanking residues 113N, 114T, 116G, 117D and 119W were perturbed (> 0.4 ppm). The third largest CSP was observed in the RT loop residue R95 (0.61 ppm), and 96T, 97E (0.48 ppm), 98T, 99D and 100L of the RT loop were also perturbed. Thus the N1-Src insertion has altered the local chemical environment of the n-Src loop, but also that of the RT loop, both of which are important for ligand binding.

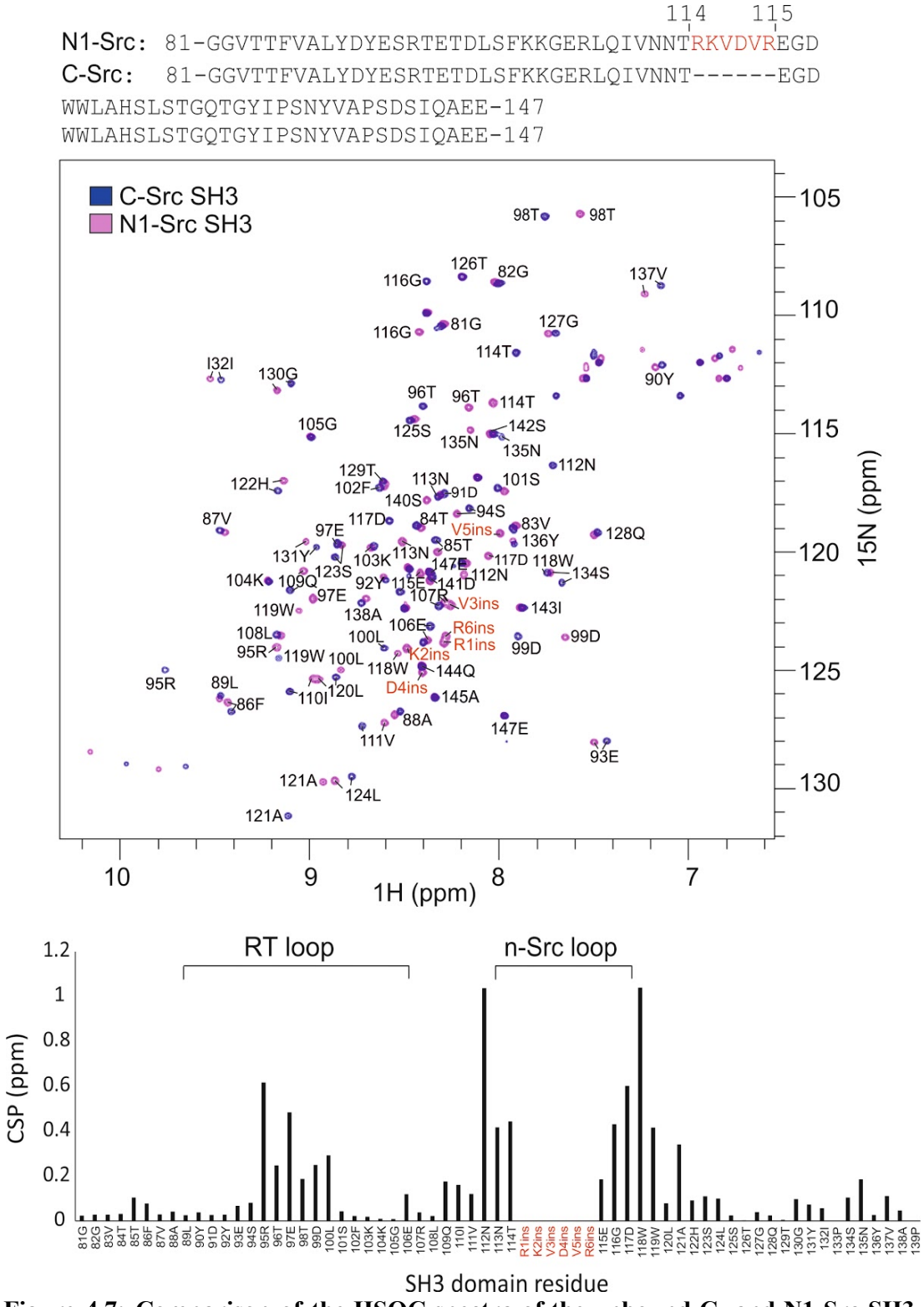

Figure 4.7: Comparison of the HSQC spectra of the unbound C- and N1-Src SH3 domains. Superimposed 2D (^{1}H-^{15}N) HSQC spectra of the C- (blue) and N1-Src (pink) SH3 domains. The N1-Src SH3 domain backbone residues were manually assigned via triple resonance spectra and the C-Src SH3 domain assignment was obtained from BMRB:3433. The graph shows the chemical shift perturbations (ppm) of each SH3 domain residue from 81G-139P with the exception of prolines, calculated by the formula $\Delta\delta = (\Delta\delta H^2 + (\Delta\delta N/5)^2)^{1/2}$. The residues spanning the SH3 domain RT and n-Src loops are shown, including the location of the N1-Src insertion which is highlighted in red.

4.3.7 The interaction of the C-Src and N1-Src SH3 domains with a Dynamin I peptide ligand

NMR spectroscopy was utilised to compare the mechanism of peptide ligand binding by the C- and N1-Src SH3 domains. The Dynamin I B8 peptide from the peptide arrays (Section 4.2.2) was selected as it bound both the C- and N1-Src SH3 domains, and was of interest due to the differential Dynamin I interactions by the C- and N1-Src SH3 domains (Section 4.2.4). The 15-mer peptide (PFGPPPQVPSRPNRA) contains two canonical Class II (PxxPx+) SH3 domain ligand motifs.

The *U*-^{15}N labelled C- and N1-Src SH3 domains were expressed and purified as described in Section 4.3.6. The lyophilised Dynamin I B8 peptide was resuspended to achieve the N1-Src SH3 (185 μM):peptide molar concentration ratios of 1:0.25 to 1:24, and C-Src SH3 domain (150 μM) 1:0.1 to 1:4. A HSQC spectrum was acquired for the C- and N1-Src SH3 domains in the absence of peptide, and then for each subsequent peptide titration. The HSQC spectra of the unbound SH3 domains and following each peptide ligand titration were superimposed and analysed using CCPN software. As described in Section 4.3.6 the formula $\Delta\delta = (\Delta\delta H^2 + (\Delta\delta N/5)^2)^{½}$ was used to calculate the CSPs of the SH3 domain residues at each titration against the no peptide control.

The C-Src SH3 domain peptide ligand titrations are shown in Fig 4.8. The HSQC spectrum demonstrates that a number of cross-peaks are not affected by peptide ligand binding, serving as an internal control. However, some cross-peaks enter fast exchange, as they shift in a ligand concentration dependent manner without a reduction in intensity, thus indicating a weak interaction between the C-Src SH3 domain and peptide ligand. The 95R cross-peak from the RT loop, and the side chain cross-peak from 118W, that flanks the n-Src loop, did not have a detectable cross-peak after the first peptide titration, suggesting that these residues entered intermediate exchange. The graph shows the CSPs of the C-Src SH3 domain residues 81G-139P at the SH3:peptide titration ratio of 1:4 against the 'no peptide' control. The C-Src SH3 domain RT loop residues (89L-106E) and n-Src loop residues (113N-117D) are highlighted on the sequence (Fig.4.8). Overall, CSPs occur in three regions of the C-Src SH3 domain, the RT loop, n-Src loop and C-terminus. The largest CSPs occur in the RT loop residues 97E (0.5 ppm) and 100L (0.32 ppm). The flanking residues 96T, 98T and 99D were also perturbed (> 0.16 ppm). As R95 entered intermediate exchange at the first peptide titration, the CSP could not be

measured and this is indicated by an asterisk. The third largest CSP was 114T (0.31 ppm) of the n-Src loop, and the flanking residues 116G, 118W and 119W were also perturbed (> 0.18 ppm). The C-terminal 131Y, 132I and 134S were also perturbed (> 0.13 ppm), and this is consistent with the characterised ligand binding site (Feng et al. 1995b). For example, D99 of the RT loop forms a salt bridge with the charged residue in Class I/II ligands, and W118 that flanks the n-Src loop contributes to the D99 charge binding pocket and also one of the proline binding pockets. The C-terminal CSPs surround Y131 and P133 which also contribute to the proline binding pockets (Feng et al. 1994; Feng et al. 1995) (Section 1.2.3).

The equivalent experiment for the N1-Src SH3 domain is shown in Fig.4.9. The HSQC spectrum demonstrates that some cross-peaks enter fast exchange, confirming that the N1-Src SH3 domain also weakly interacts with the Dynamin I peptide ligand. The graph shows the CSPs of the N1-Src SH3 domains residues 81G-147E at the SH3:peptide titration ratio of 1:14 against the no peptide control. Overall, the CSPs dominate the n-Src loop and C-terminal region. The largest perturbations occur for 118W (0.32 ppm) and 112N (0.25 ppm) that flank the N1-Src insertion. Interestingly, these are also the two most perturbed residues between the unbound C- and N1-Src SH3 domains (Fig.4.7), suggesting that the N1-Src insertion has modulated the chemical environment of residues involved in peptide ligand binding. The following most perturbed residues are R1ins, V3ins, D4ins, 116G, and 117D (0.21-0.25 ppm) of the n-Src loop. Interestingly, R1ins, V3ins, and D4ins are three of the residues of the N1-Src insertion. 2D (^{1}H-^{15}N) HSQC sub-spectra are shown for the six residue N1-Src insertion, demonstrating that all the residues (R1ins-R6ins) undergo fast exchange shifts in a concentration-dependent manner (Fig.4.9). The C-terminal 134S was also perturbed (0.2 ppm), but strikingly, minimal perturbations were observed in the N1-Src SH3 domain RT loop.

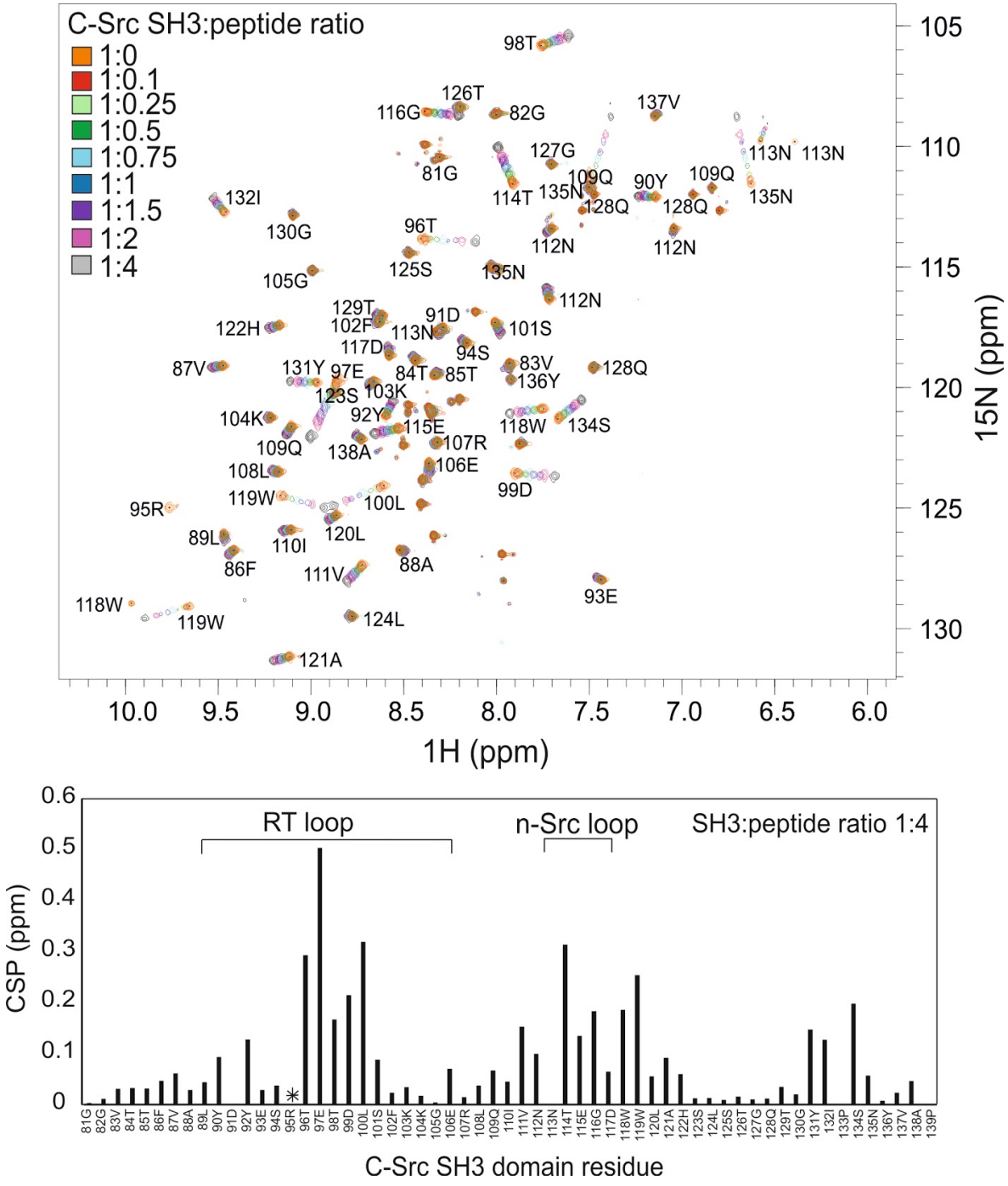

Figure 4.8: Interaction of the C-Src SH3 domain with the Dynamin I B8 peptide (PFGPPPQVPSRPNRA). The superimposed HSQC spectra are shown for the unbound C-Src SH3 domain (1:0) and at the SH3:peptide concentration ratios of 1:0.1, 1:0.25, 1:0.5, 1:0.75, 1:1, 1:1.5, 1:2 and 1:4 via colour coding. The graph shows the CSPs (ppm) of each SH3 domain residue at the SH3:peptide ligand titration of 1:4. The residues spanning the SH3 domain RT and n-Src loops are shown.

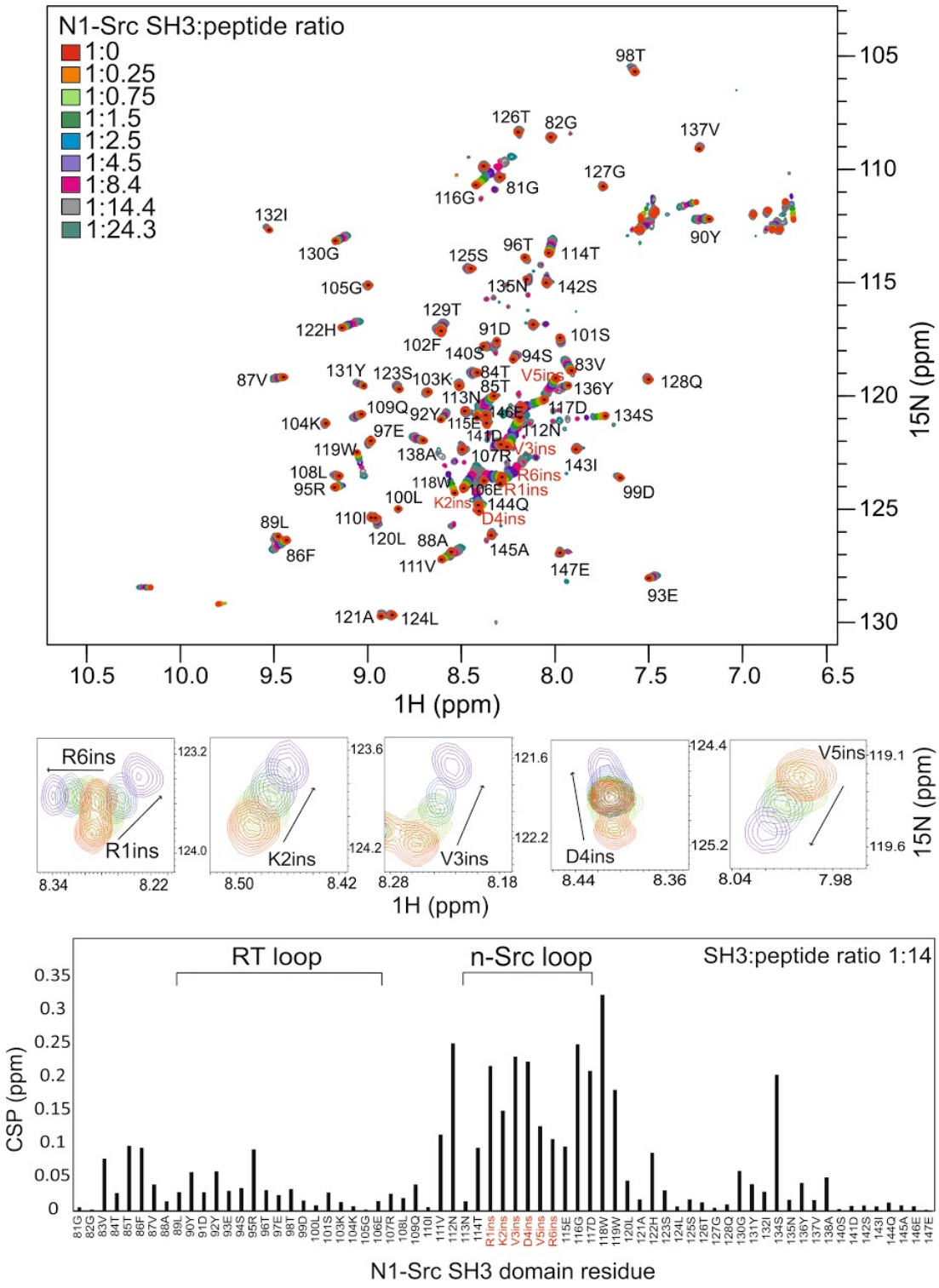

Figure 4.9: Interaction of the N1-Src SH3 domain with the Dynamin I B8 peptide (PFGPPPQVPSRPNRA). The superimposed HSQC spectra are shown for the unbound N1-Src SH3 domain (1:0) and at the SH3:peptide concentration ratios of 1:0.25, 1:0.75, 1:1.5, 1:2.5, 1:4.5, 1:8.4, 1:14.4 and 1:24.3 via colour coding. The individual panels are HSQC sub-spectra, demonstrating the fast exchange shifts observed in the N1-Src insertion residues R1ins-R6ins at the ratios of 1:0 to 1:4.5. The graph shows the CSPs (ppm) of each SH3 domain residue at the SH3:peptide ligand titration of 1:14. The N1-Src insertion is highlighted in red and the residues of the RT and n-Src loops are also shown.

4.3.8 Comparison of the mechanism of peptide ligand binding by the C- and N1-Src SH3 domains

The chemical shift perturbations of the C- and N1-Src SH3 domains upon Dynamin I peptide ligand binding were analysed in Section 4.3.7. Whilst the C-Src SH3 domains CSPs were largely in the RT- and n-Src loops (Fig.4.8), the N1-Src SH3 domains CSPs largely occured in the n-Src loop, with minimal shifts in the RT loop (Fig.4.9). For ease of comparison, the CSPs of the C- and N1-Src SH3 domain residues 81G-139P at the SH3:peptide ratios of 1:4 and 1:14 respectively, are plotted against each other (Fig.4.10A). The C-Src SH3 domain R95 cross-peak entered intermediate exchange which is indicated by an asterisk, and the N1-Src SH3 domain insertion residues (R1ins-R6ins) are shown in red. The graph clearly highlights the differential binding by the SH3 domain RT loops in terms of both the magnitude of CSPs, and relatively to the rest of the SH3 domain. In contrast, more comparable shifts are observed in the n-Src loops and C-terminal region (Fig.4.10A).

The SH3:peptide ligand titrations can also be used to obtain the equilibrium dissociation constant (K_d) of the interaction. The K_d is defined as the concentration of ligand required to achieve 50 % saturation, and because the experiment assays an exchanging system that can be brought to saturation, the K_d can be obtained by plotting titration curves that display an individual fast exchange cross-peaks CSPs as a function of peptide ligand concentration. The CSPs of the 119W cross-peaks from the C- and N1-Src SH3 domain peptide ligand titrations were used to generate titration curves (Fig.4.10B). However, as the titrations did not reach saturation an exact K_d cannot be obtained. Assuming 1:1 binding, saturation curve fitting estimates the K_d of C-Src (306-436 μM; δ_{max}= 0.36-0.43; 95% CI) to be approximately 4.5 fold smaller than that of N1-Src (1361-2096 μM; δ_{max}= 0.27-0.32 95% CI). In addition, the titration curves support the comparison of the C- and N1-Src SH3 domain CSPs at the SH3:peptide ratios of 1:4 (600 μM peptide) and 1:14 (2500 μM peptide) respectively (Fig.4.10A), as the SH3 domains are comparable in terms of saturation. Thus, direct comparisons can be made between the magnitude of shifts unlike those at highly different saturation states.

The relative CSPs of the N1-Src SH3 domain upon peptide ligand binding were mapped onto the C-Src SH3 domain solution structure (PDB:1QWE) via colour coding (second and third image), and onto a putative model of the N1-Src SH3 domain (first image)

produced by Dr G.J.O Evans (Fig.4.10C). This further highlights the minimal change to the N1-Src SH3 domain RT loop upon ligand binding.

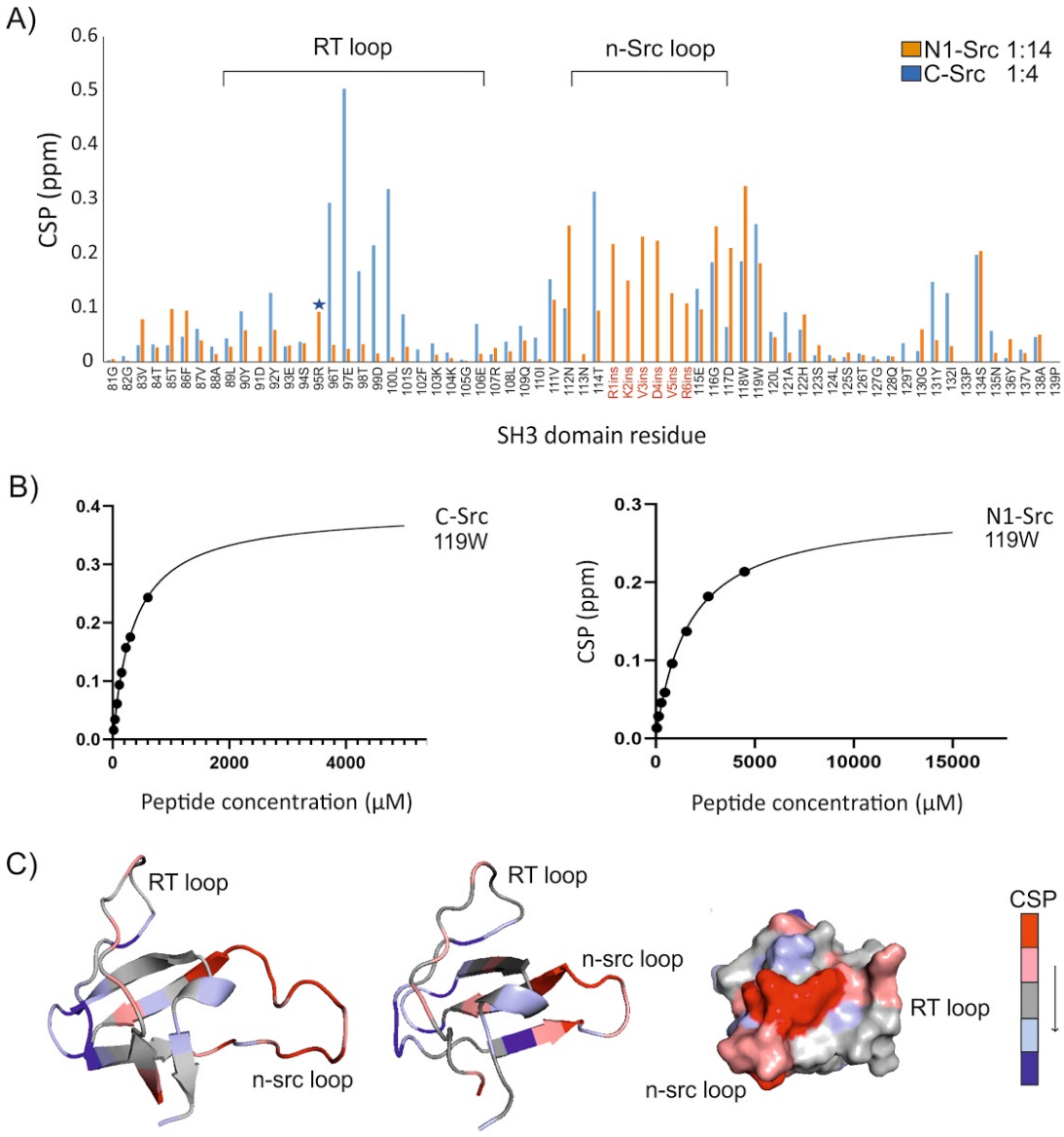

Figure 4.10: Comparison of the chemical shift perturbations and affinity of the C- and N1-Src SH3 domains upon peptide ligand binding. A) The CSPs of the C- and N1-Src SH3 domain residues (81G-139P) at the peptide ligand ratios of 1:4 and 1:14 respectively. The R95 residue that entered intermediate exchange in C-Src is indicated with an asterisk (*). The location of the RT and n-Src loops within the SH3 domain sequence are indicated, and the residues of the N1-Src insert (RKVDVR) are highlighted in red. B) The chemical shift perturbation (ppm) of the fast exchange cross-peak 119W against peptide ligand concentration (µM) for the C- and N1-Src SH3 domains. C) The relative chemical shift perturbations of the N1-Src SH3 domain upon peptide ligand binding are colour coded by magnitude onto a putative structure of the N1-Src SH3 domain (first), and the characterised solution structure of the C-Src SH3 domain (second and third) PDB:1QWE. The largest CSPs are indicated in dark red, and the smallest in dark blue.

4.3.9 The chemical environment of the N1-Src SH3 domain RT loop resembles that of the C-Src SH3 domain upon ligand binding

The CSP profile of the C-Src SH3 domain RT loop upon peptide ligand binding (Fig.4.8) resembled the difference observed between the unbound C- and N1-Src SH3 domains (Fig.4.7). The CSPs of the RT loop residues (89L-106E) from both experiments are plotted together in Fig.4.11. The CSPs for 95R cannot be compared as this cross-peak entered intermediate exchange upon the first peptide titration (Fig.4.8). The graph demonstrates that both the relative CSPs of the RT loop residues, and the magnitude of the shifts are highly comparable. As the C-Src SH3 domain was approaching saturation at the peptide titration ratio of 1:4 (Fig.4.10), the CSPs of the cross-peaks are representative of the unbound N1-Src SH3 domain.

Whilst the similar CSP profiles are compelling, they do not hold much meaning without assessing the chemical environment of the cross-peaks. Superimposed 2D (^{1}H-^{15}N) HSQC sub-spectra highlight the RT loop residues R95-L100 (Fig.4.11). The spectra contain the unbound C-Src SH3 domain, the eight C-Src SH3 domain peptide ligand titrations (1:0.1 to 1:4), and the unbound N1-Src SH3 domain, labelled as '-N1' for each cross-peak. The spectra clearly demonstrate that upon peptide ligand binding the C-Src SH3 domain RT loop cross-peaks 96T-100L undergo concentration-dependent shifts towards the chemical shift of the equivalent N1-Src SH3 cross-peaks in spectra of the unbound domain. This could not be demonstrated for R95 as the cross-peak entered intermediate exchange (Fig.4.8).

Taken together, this data suggests that upon peptide ligand binding, the C-Src SH3 domain RT loop enters a chemical environment similar to that of the unbound N1-Src SH3 domain. Thus the N1-Src insertion appears to modulate the RT loop so that it adopts a constitutively 'bound' conformation. The high degree of similarity between the unbound N1-Src SH3 domain, and the peptide bound C-Src SH3 domain, could also explain why the N1-Src SH3 domain RT loop underwent minimal CSPs upon peptide ligand binding (Fig.4.9).

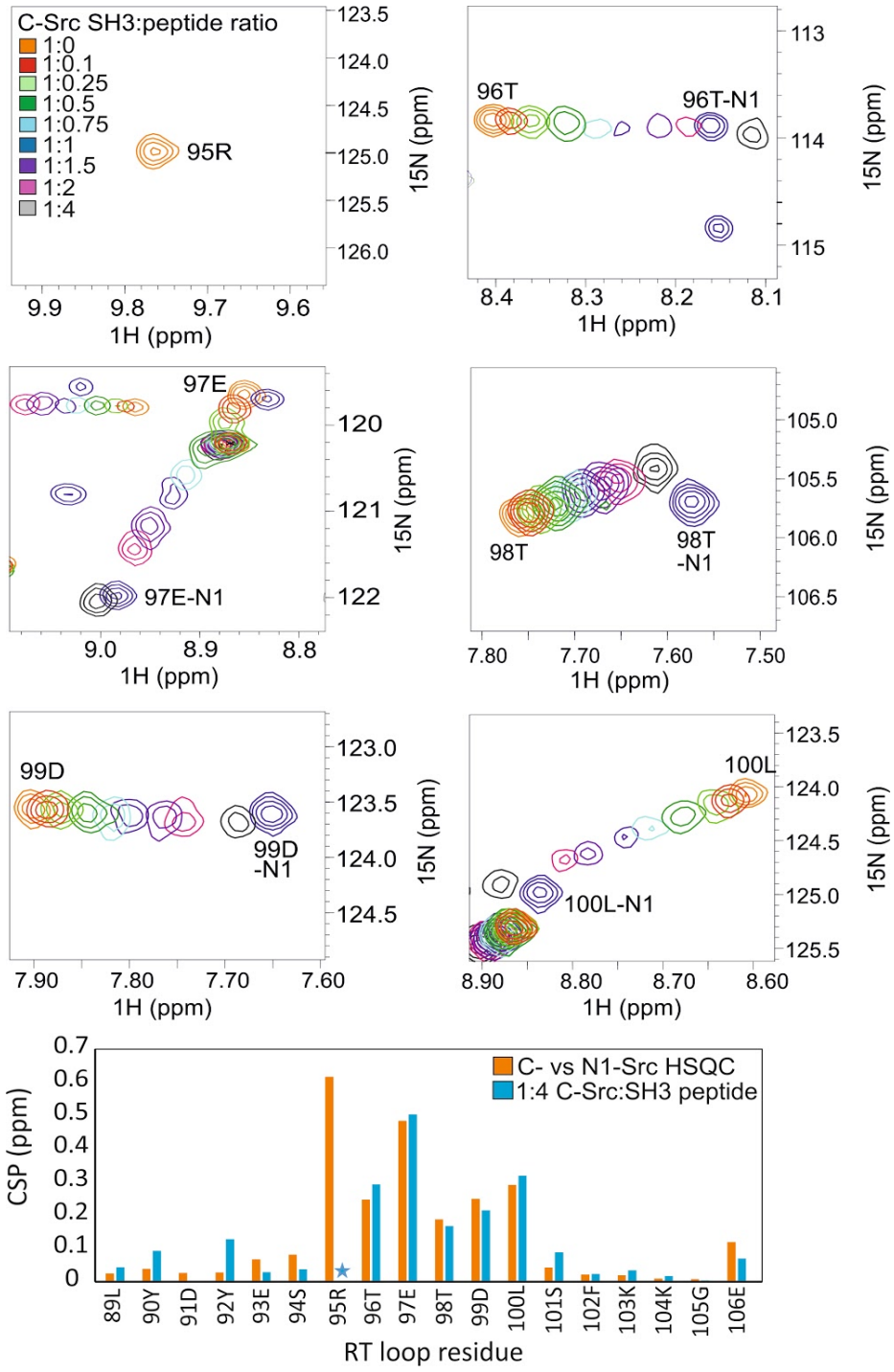

Figure 4.11: The interaction of the C-Src SH3 domain with the Dynamin I B8 peptide ligand results in the RT loop residues adopting a chemical environment similar to that of the unbound N1-Src SH3 domain. The HSQC sub-spectra show the C-Src SH3 domain RT loop residues 95R, 96T, 97E, 98T, 99D and 100L at the SH3:peptide titration ratios of 1:0, 1:0.1, 1:0.25, 1:0.5, 1:0.75, 1:1, 1:1.5, 1:2 and 1:4. The equivalent unbound N1-Src SH3 domain cross-peaks are shown in dark blue, and are labelled '-N1'. The graph shows the CSPs (ppm) of the Src SH3 domain RT loop residues (89L-106E) at the C-Src SH3:peptide titration of 1:4 (blue) in comparison to those observed between the unbound C- and N1-Src SH3 domains (orange).

4.3.10 The N1-Src SH3 domain mutant R1insA results in the loss of the RT loop bound environment

The unbound N1-Src SH3 domain RT loop adopts a chemical environment similar to that of the ligand-bound C-Src SH3 domain RT loop (Fig.4.11). Therefore, alanine mutagenesis of the N1-Src insertion was used to assess how it modulates the RT loop. *U*-^{15}N labelled N1-Src SH3 domain mutants R1insA, D4insA and R6insA (***R***KV***D***V***R***) were expressed and purified as described in Section 4.3.6. These mutants were selected as the arginine residues are evolutionarily conserved in vertebrates, and the aspartate residue also shows high levels of conservation (Section 1.4.2).

The HSQC spectra of the three mutants were superimposed with the wild-type N1-Src SH3 domain spectra. The protein sequence of the N1-Src SH3 domain is shown for all three mutants, including the mutated residue (red, underlined and bold) and the N1-Src insertion cross-peaks (R1ins-R6ins) which are highlighted in red on the spectra. Unfortunately, due to the crowded central regions of the spectra, it was not possible to confidently track cross-peak movement, and as such the CSPs of the individual residues could not be measured. Therefore, as preliminary analysis CSPs are only reported qualitatively.

The R1insA and D4insA mutant spectra are shown in Fig.4.12. The majority of cross-peaks occur at the same chemical shift as the wild-type N1-Src SH3 domain. However, there are cross-peaks that have undergone CSPs, in addition to the mutated residues. The CSPs seem to occur mainly in the n-Src loop and flanking regions, thus the effects appear to be local.

The R6insA mutant (Fig.4.13) results in a large CSP in one of the tryptophan side chains (bottom left). In addition to residues in the n-Src loop and flanking region showing perturbations, the RT loop residues 93E, 95R, 96T, 97E, 98T, 99D and 100L all underwent CSPs. The new position of the cross-peaks cannot be confirmed in this experiment, however, it is unlikely to be coincidental that these cross-peaks were all perturbed between the unbound C- and N1-Src SH3 domains (Fig.4.7), and have undergone CSPs in the R6insA mutant towards the position of those of the C-Src SH3 domain. This is illustrated by the HSQC sub-spectra of the RT loop residues (93E-100L), containing the wild-type C- and N1-Src SH3 domains, and the R6insA mutant (Fig.4.13). Thus this data provides strong preliminary evidence that R6ins of the N1-Src

insert is responsible for inducing the 'bound' chemical environment of the N1-Src SH3 domain RT loop (Fig.4.11).

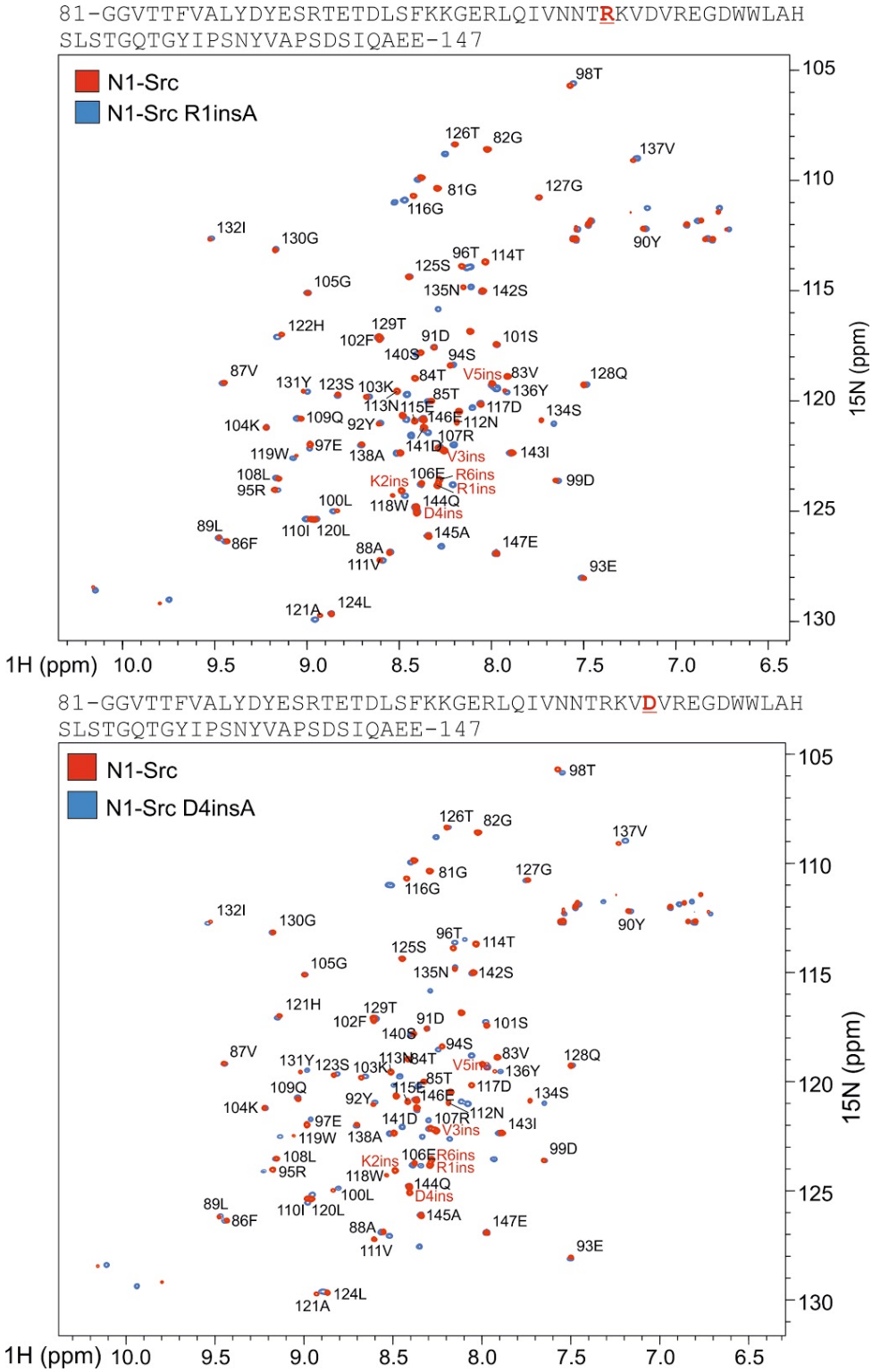

Figure 4.12: Comparison of the chemical environments of the N1-Src SH3 domain and the R1insA and D4insA insertion mutants. Superimposed HSQC spectra of the N1-Src SH3 domain (red) and alanine mutants (blue) R1insA (first panel) and D4insA (second panel). The sequence of the N1-Src SH3 domain is shown, including the locations of the mutations (red, underlined and bold). The six residue N1-Src insert (R1ins-6ins) is highlighted in red on the spectra.

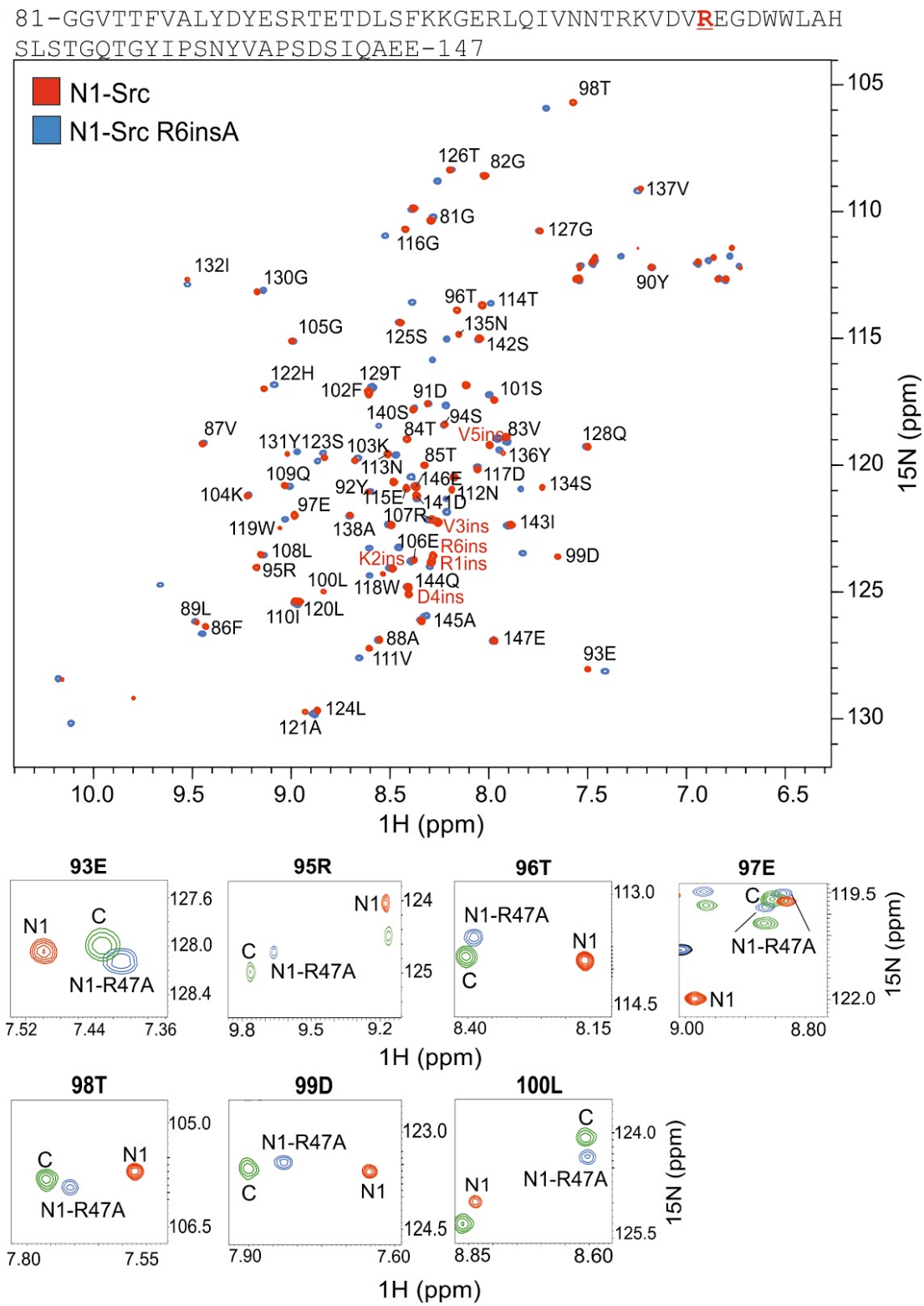

Figure 4.13: The N1-Src SH3 domain insertion mutant R6insA results in the loss of the RT loop 'bound' environment. Superimposed HSQC spectra of the N1-Src SH3 domain (red) and R6insA alanine mutant (blue). The sequence of the N1-Src SH3 domain is shown, including the location of the mutation (red, underlined and bold). The six residue N1-Src insert (R1ins-R6ins) is highlighted in red on the spectra. The superimposed HSQC sub-spectra show the RT loop residues 93E, 95R, 96T, 97E, 98T, 99D and 100L, for the wild-type C- (green) and N1-Src (red) SH3 domains and the N1-Src R6insA mutant (blue).

4.3.11 The role of the N1-Src SH3 domain insertion in Dynamin I binding

The N1-Src insertion perturbs the local chemical environment of the n-Src loop (Fig.4.7), and upon Dynamin I peptide ligand binding, the N1-Src insertion residues underwent some of the largest CSPs (Fig.4.9), suggesting that they could be directly involved in ligand binding, or were in close proximity to the interaction interface. Therefore, the role of the N1-Src SH3 domain insert (RKVDVR) in ligand binding was further assessed via alanine scanning mutagenesis.

The N1-Src SH3 domain alanine mutants were N-terminally GST-tagged and immobilised on glutathione agarose resin for utilisation in pull-downs as described in Chapter 3. The binding to the C- and N1-Src SH3 domain ligand Dynamin I was assessed by 5 μM GST and GST- SH3 domain pull-downs from 500 μg of adult rat brain synaptosome. The binding was assessed via an anti-Dynamin I Western blot (Fig.4.14A). This includes the GST control for non-specific binding, the GST-C-Src SH3 domain as a positive control, the wild-type N1-Src SH3 domain, and the N1-Src SH3 domain insertion alanine mutants R1insA, K2insA, V3insA, D4insA, V5insA and R6insA. A Coomassie stained SDS-PAGE gel loading control is also shown.

The assay was conducted in triplicate, and the extent of Dynamin I binding for each mutant was quantified by densitometry analysis of the Western blot. In order to normalise the extent of Dynamin I binding to the amount of each SH3 domain mutant, densitometry analysis of the Coomassie stained SDS-PAGE gel loading control was also conducted. The wild-type N1-Src SH3 domain was set as the standard, and the Dynamin I binding by each mutant was expressed as percentage of the wild-type N1-Src SH3 domain (Fig.4.14B). The data was analysed by One-way ANOVA, which revealed that Dynamin I binding was significantly reduced for the V5insA ($p < 0.05$) and R6insA mutants ($p < 0.01$) to the wild-type N1-Src SH3 domain. The HSQC spectrum of the R6insA mutant revealed that it induced the ‘bound’ chemical environment of the N1-Src SH3 domain RT loop (Fig.4.13), thus it was interesting that this mutant also significantly reduced ligand binding.

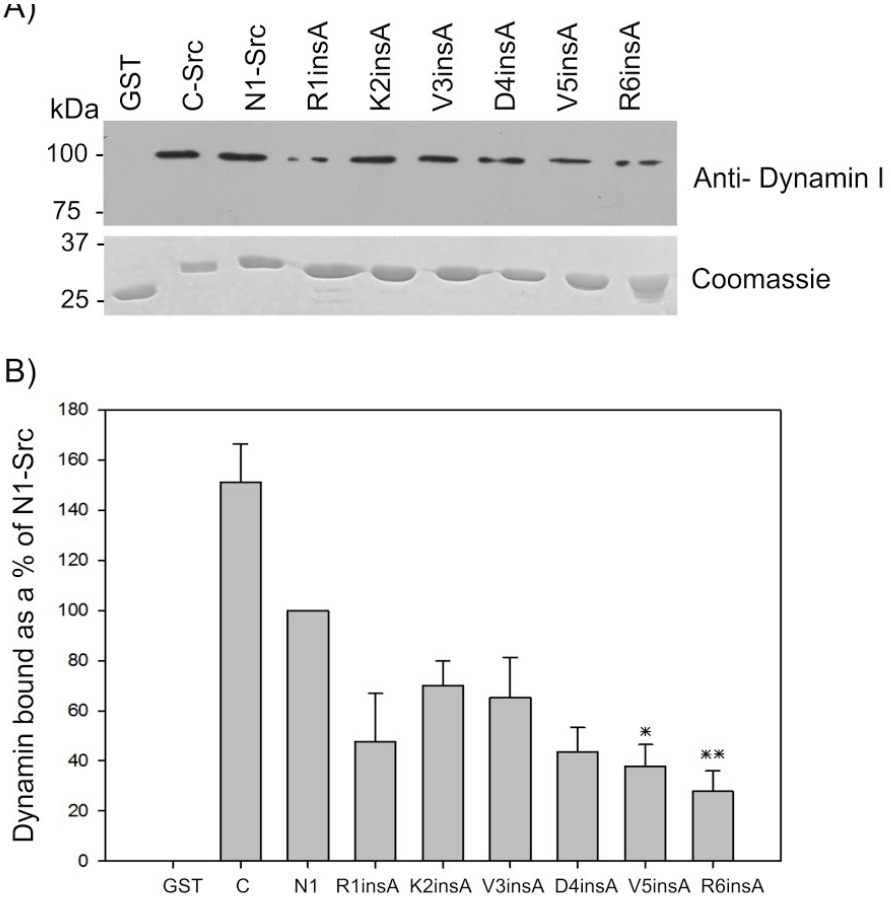

Figure 4.14: Dynamin I binding is significantly reduced by the N1-Src SH3 domain insertion alanine mutants V5insA and R6insA. A) GST-SH3 domain pull-down of Dynamin I from 500 µg of adult rat brain synaptosomes by 5 µM GST, GST-C- and N1-Src SH3 domains and the N1-Src insertion alanine mutants R1insA-R6insA. The samples were resolved on a 12.5 % SDS-PAGE gel and subjected to Western blotting with anti-Dynamin I. A 12.5 % Coomassie stained SDS-PAGE gel loading control is shown. B) Densitometry was used to normalise the Dynamin I Western blot to the SDS-PAGE loading control, and average Dynamin I bound as a percentage of the wild-type N1-Src SH3 domain is shown. The experiment was performed 3 times and statistical significance was assessed by one way ANOVA (*$p < 0.05$; **$p < 0.01$). Error bars show the SEM.

4.3.12 The role of the C- and N1-Src SH3 domains RT loop in ligand binding

The unbound N1-Src SH3 domain RT loop adopts a chemical environment similar to that of the ligand bound C-Src SH3 domain RT loop (Fig 4.11). However, the role of the N1-Src SH3 domain RT loop in ligand binding remains unclear, as it underwent minimal CSPs upon peptide ligand binding (Fig 4.9), which is speculated to be due to it already been present in the 'bound' conformation. The C-Src SH3 domain RT loop residue D99 forms a salt bridge with the charged residue flanking the Class I/II SH3 domain ligand motifs (Feng et al. 1995b). The C-Src SH3 domain D99N mutant abolishes the majority of interactions, and only a small subset are retained that are referred to as D99 independent ligands (Weng et al. 1995). The C- and N1-Src SH3 domains both interacted with Class I and II motif containing peptide ligands (Table 4.2/4), and the C-Src SH3 domain D99 residue underwent CSPs upon peptide ligand binding (Fig.4.8). Therefore the D99N mutation was selected in order to assay the role of the RT loop in ligand binding, and to identify D99 dependent and independent C- and N1-Src SH3 domain ligands. As a positive control the conserved tryptophan W118 was mutated to alanine as this abolishes SH3 domain ligand binding (Erpel et al. 1995).

The C- and N1-Src SH3 domain mutants were expressed N-terminally GST-tagged and were immobilised on glutathione agarose resin in order to conduct pull-downs in postnatal day 1 rat brain lysate. The pull-downs were conducted with 7 μM GST and the GST-C- and N1-Src SH3 domain mutants in 1 mg of postnatal day 1 rat brain homogenate. The pull-down eluates were subjected to Western blotting for a number of the identified C- and N1-Src SH3 domain ligands including Dynamin I, N-WASP, Nono and Neuronal Enah (Chapter 3). As described in Section 4.3.11, the assays were conducted in triplicate and densitometry of the Western blots and Coomassie stained SDS-PAGE loading controls was used to normalise ligand binding as quantified by Western blot, to the amount of SH3 domain present.

The wild type C- and N1-Src SH3 domains were set as standards, and the ligand binding of the SH3 domain mutants was expressed as an average percentage of the wild-type (Fig.4.15). The data was analysed by T-test, which revealed that the C-Src D99N mutant significantly reduced binding to Dynamin I ($p < 0.05$) (Fig.4.15A). This could suggest that the C-Src SH3 domains interactions with Neuronal Enah, Nono and N-WASP are 'D99 independent'. Indeed, Nono does not contain any Class I/II SH3 domain ligand

motifs. The D99N N1-Src SH3 domain mutant significantly reduced binding to Dynamin I, Neuronal Enah ($p < 0.01$) and N-WASP ($p < 0.05$) (Fig.4.15B), and the N1-Src SH3 domain W118A mutant significantly reduced binding to all four ligands assayed in comparison to the wild-type N1-Src SH3 domain ($p < 0.01$) (Fig 4.15B).

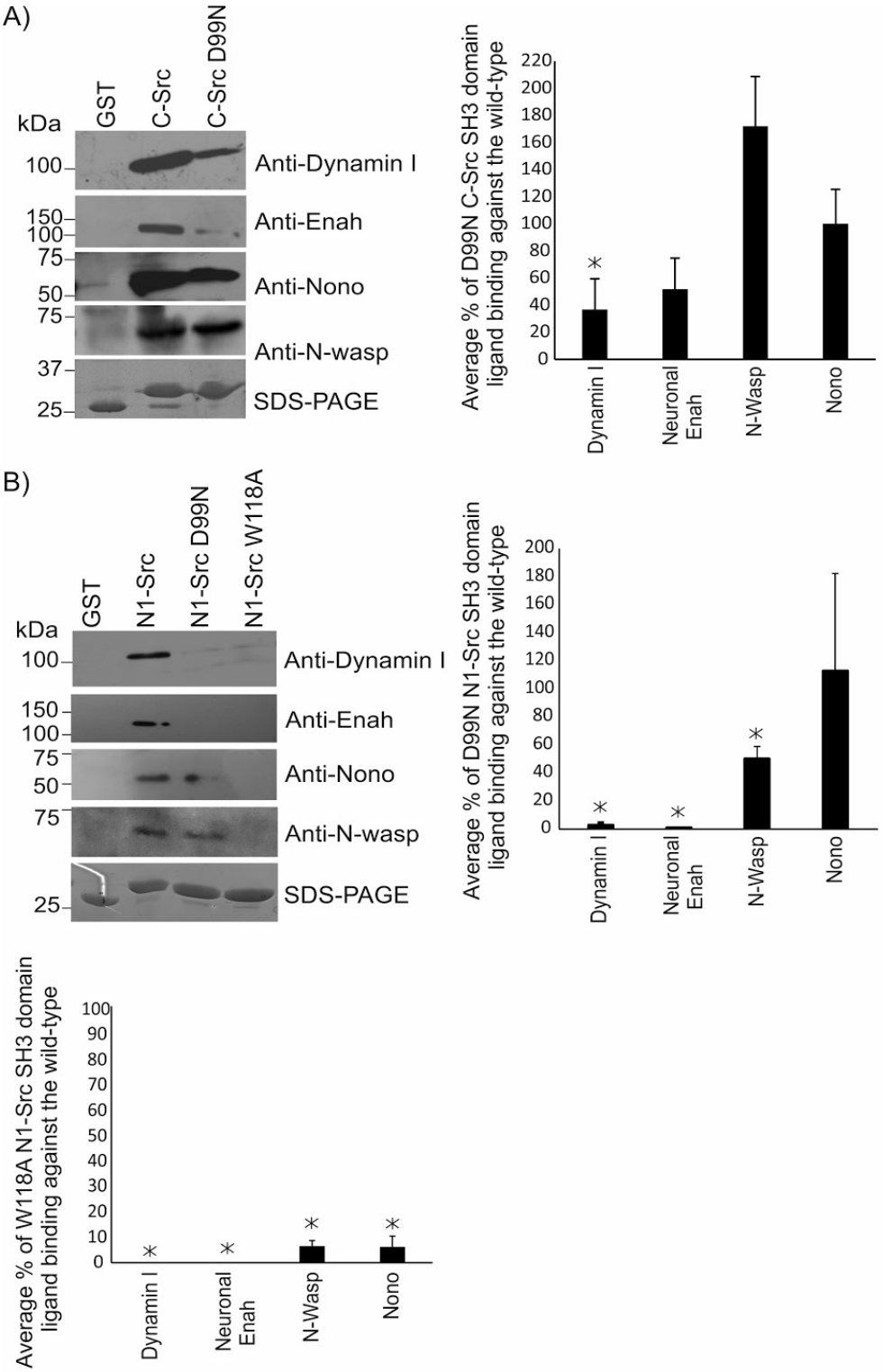

Figure 4.15: The D99N C- and N1-Src SH3 domain mutation modulates ligand binding. GST pull-downs were conducted with 7 µM GST, wild-type GST-C- and N1-Src SH3 domains, and the GST-SH3 domain mutants D99N and W118A in 1 mg of postnatal day 1 rat brain homogenate. The samples were resolved by SDS-PAGE and subjected to Western blotting for Dynamin I, Neuronal Enah, N-WASP and Nono. A Coomassie stained 12.5 % SDS-PAGE gel loading control is also shown. Densitometry was utilised to quantify the extent of ligand binding via Western blot, and normalise it to the amount of SH3 domain present via densitometry analysis of the SDS-PAGE gels.

The average ligand bound for each mutant is expressed as a percentage of the wild-type SH3 domain. The experiment was performed 3 times and statistical significance was assessed by T-test (*$p < 0.05$). Error bars show the SEM.

4.4 Discussion

The aims of this chapter were to 1) determine the ligand consensus motif of the N1-Src SH3 domain 2) compare the mechanism of ligand binding by the C- and N1-Src SH3 domains and 3) assess the structure-function determinants of the six residue N1-Src insertion. The N1-Src SH3 domain appears to show preference for canonical Class I/II SH3 domain ligand motifs. However, interestingly, the C- and N1-Src SH3 domains presented differential ligand binding profiles. In particular, the N1-Src SH3 domain RT loop failed to undergo CSPs upon peptide ligand binding and this is believed to be due to a conserved arginine of the N1-Src insertion causing the RT loop to adopt a constitutive 'bound like' chemical environment in the absence of ligand. The N1-Src SH3 domain RT loop was shown to be involved in ligand binding as mutation of the salt bridge forming aspartate D99, was able to abolish ligand interactions. Although the overall impact of the 'bound' RT loop is unclear. Furthermore, upon peptide ligand binding the N1-Src SH3 domain CSPs dominated the n-Src loop, including the six residues of the N1-Src insertion. The mutation of two of the insert residues significantly reduced ligand binding and suggest that the N1-Src insert could be directly involved in ligand interactions.

Identification of N1-Src SH3 domain binding sites and peptide ligands

Peptide arrays were employed to rapidly screen for binding sites within N1-Src SH3 domain ligands and also provide insight into the ligand consensus motif. In total the N1-Src SH3 domain bound 15 peptides from the proline rich domains/regions of its ligands (Dynamin I/III, N-WASP and Enah) and a further five peptides from the control array comprising characterised C-Src SH3 domain peptide ligands. Any putative binding sites should now be confirmed in the context of the full length protein via techniques such as pull-downs and immunoprecipitation. The mutation of SH3 domain binding sites within ligands has previously been used to demonstrate the role of SH3 domain docking in directing substrate phosphorylation (Shen et al. 1999). Furthermore, introducing binding site mutants into N1-Src ligands overexpressed in cells, could be used in the future to dissect the signalling pathways of N1-Src. Similarly, cell penetrating peptides containing the binding site could also be used to disrupt *in vivo* interactions. In addition,

N1-Src SH3 domain peptide ligands could be utilised for assaying *in vitro* SH3 domain based activation kinetics as described by (Moroco et al. 2014).

Analysis of the peptide sequences bound by the N1-Src SH3 domain provided insight into its ligand consensus motif. Interestingly, all but one of the peptide ligands contained a canonical Class I/II SH3 domain ligand motif, and this is consistent with the enrichment of Class I/II motifs in N1-Src SH3 domain binding proteins (Chapter 3). Furthermore, analysis of the peptide ligands with overlapping sequences revealed that the common sequences all contained Class II motifs, and proline to alanine mutants within a selection of the peptides all abolished binding to the N1-Src SH3 domain. Thus, these data suggest that like C-Src, the N1-Src SH3 domain may also bind canonical Class I/II ligand motifs. Indeed, the C-Src SH3 domain bound 9/15 of the N1-Src SH3 domain peptide ligands, although this might be an underestimate since the C-Src arrays were conducted under more stringent conditions (Fig 4.4). The arrays contained an equivalent number of Class I/II motif peptides and PxxP-only motifs (without flanking charge), suggesting that a PxxP type II helix and flanking basic charge represent determinants of specificity for N1-Src SH3 domain ligands.

The N1-Src SH3 domain ligand consensus motif has also been investigated by phage display. (Teyra et al. 2017) identified the binding of Class I peptides, as well as peptides possessing diverse non-canonical specificities, and a previous study from the Evans lab proposed an atypical motif of +xxPxxT/Vxx+ (Keenan et al. 2017). To date however, *in vivo* N1-Src ligands containing this motif have not been identified. Although, the Mlk3 and Fyn SH3 domains are both able to bind canonical and atypical peptide ligand motifs (Kokoszka et al. 2018; Kang et al. 2000). However, the interaction of the N1-Src SH3 domain with atypical motifs has not been validated beyond phage display, and SH3 domains can generate false positives by binding diverse motifs without true affinity (Kleino et al. 2015), thus it would be interesting to confirm these interactions by NMR. It would be peculiar for N1-Src to bind a subset of C-Src ligands via a differential motif, however if physiological, the atypical motifs could be present in ligands that were not identified by the pull-downs in Chapter 3. The motif preference of the N1-Src SH3 domain could be further refined by peptide arrays with alanine mutagenesis across entire peptides, and conservative and non-conservative mutations. In addition, arginine/lysine mutants of the Class I/II peptide ligands are essential to confirm if N1-Src is interacting

with these motifs. The peptide arrays also suggested that the N1-Src SH3 domain has a lower binding affinity than C-Src, as an increased SH3 domain concentration and reduced stringency conditions, were required to detect its peptide interactions. This is in-line with the N1-Src SH3 domain ligand interactions in Chapter 3, the NMR peptide ligand titrations in Fig 4.10 and those reported in the literature (Messina et al. 2003; Craggs et al. 2001; Reynolds et al. 2008). A precise K_d could be obtained by extending the peptide titration series to a higher concentration of peptide ligand, or preferably by isothermal titration calorimetry.

The interaction of the C- and N1-Src SH3 domains with dynamin I

The endocytic GTPase Dynamin I is a characterised C-Src substrate (Ahn et al. 1999; Ahn et al. 2002) and the most abundant interactor of the N1-Src SH3 domain (Chapter 3). It was previously proposed in a PhD thesis that the interaction of the N1-Src SH3 domain with Dynamin I may be regulated by serine phosphorylation (Abdelhameed 2010). This observation was confirmed and it was shown that the ratio of p-S774 Dynamin I/ total Dynamin I was significantly reduced for N1-Src in comparison to C-Src (Fig.4.5B). Thus N1-Src was selecting for Dynamin I lacking phosphorylated S774, however the phosphorylation event has not been shown to be causal in disrupting N1-Src binding. The proline rich domain of Dynamin I was analysed by peptide array (Fig 4.4). Encouragingly, the peptide ligands (B4/B8) that bound the C-Src SH3 domain have previously been identified as distinct C-Src binding sites in the Dynamin I PRD (Solomaha et al. 2005). The N1-Src SH3 domain bound six Dynamin I peptides corresponding to three sites (Fig 4.5B). Interestingly, (Abdelhameed 2010) identified six mutations across the Dynamin I PRD that significantly reduced binding to the N1-Src SH3 domain *in vitro*, and four of these mutations were found within the peptide array ligands (B5/B8/B9). The peptide binding sites could also explain how the N1-Src-dynamin I interaction is modulated by serine phosphorylation, as the A8/A9 and B8/B9 peptides contain binding sites utilised by the Syndapin and Amphiphysin II SH3 domains, which are both positively regulated by serine de-phosphorylation at p-S774 and p-S857 respectively, in response to synaptic activity (Huang et al. 2004; Anggono et al. 2006). Thus an N1-Src interaction with both or either of these sites could explain its regulation by serine phosphorylation in response to synaptic stimulation.

As N1-Src potentially binds multiple sites across the Dynamin I PRD, truncation mutants could be used to distinguish the individual binding sites and phosphorylation sites with phospho-null and phospho-mimetic mutations, as utilised by (Luo et al. 2016). Cell-based assays employing immunoprecipitation could also be conducted with full length Dynamin I containing serine phospho-null and -mimetic mutants with C- and N1-Src kinases. Dynamin I and Enah/Neuronal Enah (Chapter 3) both exemplify how the C- and N1-Src SH3 domains can interact with the same ligands differentially *in vitro*.

The N1-Src SH3 domain has a novel mode of ligand binding, and regulates the RT loop via its n-Src loop insertion

This study conducted the first NMR assignment of the N1-Src SH3 domain backbone in order to assess the effect of the N1-Src insertion on the conformation of the SH3 domain and upon ligand binding. NMR spectroscopy revealed that the N1-Src SH3 domain insert transmits effects throughout the SH3 domain, modulating the local chemical environment of the n-Src loop, but also that of the RT loop, both of which are involved in ligand binding.

Considering that the N1-Src SH3 domain interacts with a subset of C-Src SH3 domain ligands (Chapter 3), and has a preference for canonical Class I/II motifs, it was surprising that the C- and N1-Src SH3 domains had differential contributions of n-Src and RT loop residues to binding the same peptide ligand. The ligand-induced CSPs of the C-Src SH3 domain occurred in the RT loop, n-Src loop and C-terminal region, which are consistent with the previously characterised C-Src SH3 binding pockets (Feng et al. 1995b) and peptide ligand titrations described in the literature (Wu et al. 2015). In contrast, following introduction of the dynamin I B8 peptide to the N1-Src SH3 domain, the CSPs were concentrated in the n-Src loop, including the six residues of the N1-Src insertion, and unexpectedly there were minimal shifts in the RT loop.

There is a precedence in the literature for n-Src loop insert residues making critical interactions with ligand peptides (Section 1.2.3). Upon ligand binding to the Eps8L1 SH3 domain, the CSPs of greatest magnitude were observed in the n-Src loop and flanking region. The n-Src loop contains an arginine residue that forms a salt bridge with an aspartate in the peptide ligand (Aitio et al. 2008). Similarly, the n-Src loop of the Mlk3 SH3 domain undergoes a large conformational change upon peptide ligand binding (Kokoszka et al. 2018). Thus the N1-Src insertion residues could be directly involved in

ligand binding, in close proximity to, or affected by, a ligand-dependent conformational change. In support, two mutants of the N1-Src insertion, V5insA and R6insA significantly reduced binding to dynamin I in a GST-N1-Src SH3 domain pull-down (Fig 4.14).

The striking lack of CSPs in the RT loop of the N1-Src SH3 domain upon peptide ligand binding is a novel observation and suggests the loop does not participate in peptide ligand interactions. Canonical SH3 domain-ligand binding is critically dependent on residues in the RT loop, such as Y90, Y92 and D99 (Feng et al. 1994), and highlighted by the loss of ligand binding by mutations such as D99N (Weng et al. 1995). A comparison of the structures of several unbound and ligand-bound SH3 domains highlights a highly conserved switch mechanism involving the RT loop. In the unbound state, D99 (or the equivalent residue), makes an intramolecular interaction with the peptide backbone of the RT loop, which is broken upon binding to form a salt bridge with the flanking basic residue in Class I or Class II motifs (+xxPxxP or PxxPx+; Fig.4.16A). From here on, this conformational change is referred to as the 'aspartate switch'. Loss of the RT loop 'aspartate switch' in the N1-Src SH3 domain was explained by HSQC spectra of the unbound SH3 domain, and upon peptide ligand titrations, revealing that in an unbound state, the N1-Src RT loop residues were adopting a chemical environment similar to that of the ligand-bound RT loop residues in the C-Src SH3 domain (Fig.4.11). It is therefore hypothesised that the RT loop 'binding switch' is constitutively in the bound state in N1-Src (Fig.4.16C).

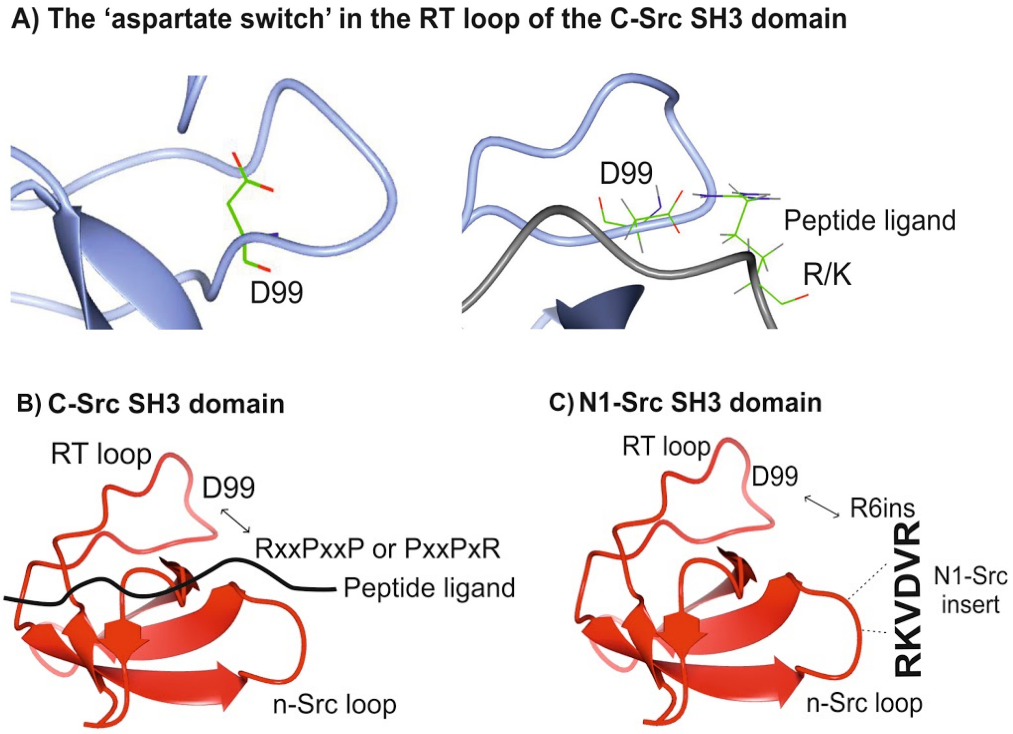

Figure 4.16: Putative model of how the N1-Src SH3 domain RT loop interacts with the n-Src loop. A) The C-Src SH3 domain RT loop residue D99 forms an intramolecular interaction with the RT loop peptide backbone in the absence of ligand (first image). Upon ligand interactions D99 forms a salt bridge with the charged residue flanking PxxP motifs in Class I/II ligands (second image). We refer to this conformational change as the 'aspartate switch'. B) Schematic of the C-Src SH3 domain D99 residue interacting with charged residues flanking Class I/II PxxP motifs. C) Putative model of how the N1-Src SH3 domain aspartate switch may be lost via an intramolecular salt bridge between R6ins of the N1-Src insertion and D99, resulting in the RT loop 'binding switch' being constitutively in the bound state.

A mutagenic screen of the N1-Src insert strengthened the binding switch hypothesis, by showing that in the N1-Src SH3 R6insA mutant (but not R1insA or D4insA), the RT loop residues underwent CSPs (in comparison to the wild type SH3 domain) that mapped onto those observed in the unbound C-Src SH3 domain (Fig.4.13). A caveat is that double labelling of the mutant is required to assign the backbone and confidently identify the new position of the cross-peaks. However, it is tempting to speculate that R6ins in the N1-Src insert forms an intramolecular salt bridge with D99, triggering the aspartate switch and causing the RT loop to adopt a bound state (Fig.4.11).

The N1-Src SH3 domain mutants D99N and R6insA both resulted in the loss of ligand interactions (Fig.4.14/15). This suggests that the putative salt bridge could position the RT- and n-Src loop for ligand interactions. Indeed, (Arold et al. 1998) demonstrated that the Hck SH3 domain RT loop was highly flexible and readily adopted the bound

environment which raised affinity. The putative D99:R6ins salt bridge contradicts the enrichment of Class I/II motifs by the N1-Src SH3 domain (Table 4.4). However, the N1-Src SH3 domain could have selected for these peptides on the basis of their optimal PxxP motifs. Therefore, Class I/II peptide ligands with arginine mutations are essential to determine if N1-Src is binding the flanking charge. The lack of interactions with the flanking charged residue could explain the reduced affinity of N1-Src, since the loss of the D99 salt bridge reduces the affinity for C-Src ligands (Weng et al. 1995). Alternatively, an aspartate in the n-Src loop of the Mlk3 SH3 domain forms a salt bridge with arginine residues in the peptide ligands (Kokoszka et al. 2018). Therefore, D4ins of the N1-Src insertion could replace D99 in binding the flanking charge. Indeed, D4ins underwent a CSP upon peptide ligand binding, and the D4insA mutant although not significant, bound dynamin I by an average of 40 % of the wild-type N1-Src SH3 domain (Fig.4.15). It is unlikely that an arginine-containing peptide ligand would compete with the D99:R6ins salt bridge, as there is no change in the chemical environment of D99 upon peptide ligand binding by N1-Src (Fig.4.9).

The lowered affinity of the N1-Src SH3 domain could also be explained by steric clashes with its n-Src loop, as described for the Abl SH3 domain (Feng et al. 1995a). In addition, the C-Src residue N135 makes side chain contacts with ligands via the second xP binding pocket (Feng et al. 1994). A large CSP is observed for the C-Src SH3 domain N135 side chain cross-peaks upon peptide ligand binding (Fig.4.8), and whilst the N1-Src SH3 domains side chains were not assigned, they have much smaller CSPs upon ligand binding (Fig.4.9). Thus there could be changes to the core binding pockets that are lowering the affinity.

Solving the structure of the N1-Src SH3 domain, including in the peptide bound form, would reveal the conformation of the n-Src and RT loops, including whether there is a constitutive salt bridge between them. This would also overcome the limitations of pull-downs in terms of a lack of clarity with regards to whether the mutations are directly or indirectly influencing ligand binding. In addition, mutagenesis experiments have been used to disrupt salt bridges by reversing the residues charges (e.g R6insD and D99R mutants), and double mutants (R6insD/D99R) with swapped charges to potentially restore the salt bridge (Venkatachalan and Czajkowski 2008; Jiang et al. 2010). The R6insA mutant resulted in the loss of the RT loop ‘bound’ environment, and

if D99 forms a salt bridge with R6ins to generate the RT loops environment, the D99N mutant should also do the same. It would also be useful to compare the mechanism of C- and N1-Src SH3 domain ligand binding to other peptides from the arrays, in order to confirm if the mechanism of ligand binding is universal.

Concluding remarks

This study proposes a novel mechanism for how an SH3 domain n-Src loop insertion switches the RT loop into a ligand-bound state. The C-Src SH3 domain RT loop is critical for ligand interactions, but also negative regulatory interactions with the kinase domain and SH2:SH1 linker (Xu et al. 1997; Xu et al. 1999), which could explain why N1-Src has increased auto-phosphorylation and catalytic activity. This will be further discussed in Chapter 6.

Chapter 5

Identification of novel Src substrates in the developing brain

Chapter 5: Identification of novel Src substrates in the developing brain

5.1 Introduction

Fundamental to understanding the function of N1-Src is to identify its SH3 domain ligands (Chapter 3), and importantly its substrates, presumably by which N1-Src carries out its cellular functions in neuronal development, differentiation and neurite outgrowth (Kotani et al. 2007; Worley et al. 1997; Lewis et al. 2017). As the Src SH3 domain ligand interactions can direct substrate phosphorylation (Shen et al. 1999), identifying N1-Src SH3 domain ligands that are also phosphorylated should provide meaningful candidates for deciphering the *in vivo* signalling events of N1-Src.

Studies in neurons have observed enhanced constitutive auto-phosphorylation by N1-Src compared to C-Src (Brugge et al. 1985). The expression of N1-Src in *Xenopus* retinal neurons and chicken embryo fibroblasts raised cellular phosphotyrosine levels above that mediated by C-Src (Worley et al. 1997; Levy and Brugge 1989), suggesting that N1-Src has altered regulatory control and is more active. N1-Src currently has only two *in vitro* substrates, synaptophysin and the NMDA receptor NR2A subunit (Section 1.4.6). Interestingly, synaptophysin was phosphorylated by N1-Src to a lesser extent than C-Src (Keenan et al. 2015). The NR2A subunit is the most convincing *in vitro* substrate as it also interacts with the N1-Src SH3 domain, and N1-Src enhances NMDA receptor currents (Groveman et al. 2011). The only *in vivo* substrate of N1-Src is Crk-associated substrate ($p130^{Cas}$). Cas is a characterised C-Src substrate at focal adhesions (Harte et al. 1996), and was also also shown to be phosphorylated by N1-Src in heterologous cells (Ruest et al. 2001). The phosphorylation appeared to be mediated by focal adhesion kinase and the N1-Src SH2 domain (Section 1.4.7), however, it is unknown whether Cas is an N1-Src substrate in neurons. Thus, there are only a few poorly characterised putative N1-Src substrates, and like the N1-Src SH3 domain interactome, a gap remains in the field regarding the substrates of N1-Src in the adult and developing brain, and how they integrate into signalling pathways to enable N1-Src's cellular functions.

Phosphoproteomics is the large scale study of phosphorylation, including kinases substrates. The coupling of phosphoproteomics to mass spectrometry is crucial for the quantification and identification of substrates and their phosphorylation sites. A typical phosphoproteomics workflow is depicted in Figure 5.1. Following experimental

manipulation such as kinase overexpression or inhibition, the cell/tissue lysate of interest is digested into peptides via an enzyme, commonly trypsin. However, analysis at this stage is unfavourable as peptides from abundant proteins may overshadow lower abundance peptides. In addition, as phosphorylation is even less abundant, it becomes increasingly challenging to detect phosphopeptides. Therefore, phosphopeptide enrichment is essential. Phosphotyrosine can be enriched by antibodies, whereas immobilised metal ion-affinity chromatography (IMAC) is preferred for phosphoserine and phosphothreonine due to the high specificity of phosphoserine/threonine antibodies (Thingholm and Larsen 2016).

The enriched phosphopeptides are then analysed by LC-MS/MS, which acquires two mass spectra. The first spectrum (MS^1) identifies the phosphopeptide precursor ion. Phosphopeptides are identifiable due to a mass shift of +79.97 Da for each phosphate present in the peptide. The MS^2 spectrum is generated from a second ionisation process that fragments the peptide. The spectrum consists of N- and C-terminal fragments of the peptide ions at the amide bond, referred to as b- and y- ions respectively (Olsen et al., 2004). The fragmentation of the phosphopeptide enables the identification of the specific phosphorylation site(s), which is important as peptides can contain multiple serine, threonine and tyrosine residues.

Comparing the abundance of phosphopeptides between samples can be achieved by labelled or label-free methods. The latter is less costly but is only considered semi-quantitative. Labelling can be achieved metabolically or *in vitro*. Metabolic labelling is conducted by stable isotope labelling with amino acids in cell culture (SILAC) (Ong and Mann 2006), whereas *in vitro* labelling is conducted with isobaric amine-specific tandem mass tags, which include iTRAQ and TMT reagents (Ross et al. 2004). Label-free quantification can be conducted using spectral counting, which is the number of spectra containing the phosphopeptide (Dowle et al. 2016). Alternatively, a more direct measurement is the peptide peak area. Plotting a peptide's intensity versus retention time generates a bell-shaped curve and the area beneath the curve is proportional to the peptide's abundance (Zhang et al., 2013). The quantified phosphopeptides are then compared against a control experiment to determine those that are significantly up- or downregulated. This provides a list of putative kinase substrates, or in some cases where a specific kinase is not assayed, databases and tools such as

Phosphosite and Netphos can enable the prediction of the kinase responsible. The kinase and substrate(s) will then require further confirmatory assays *in vivo* (Kosako and Nagano 2011).

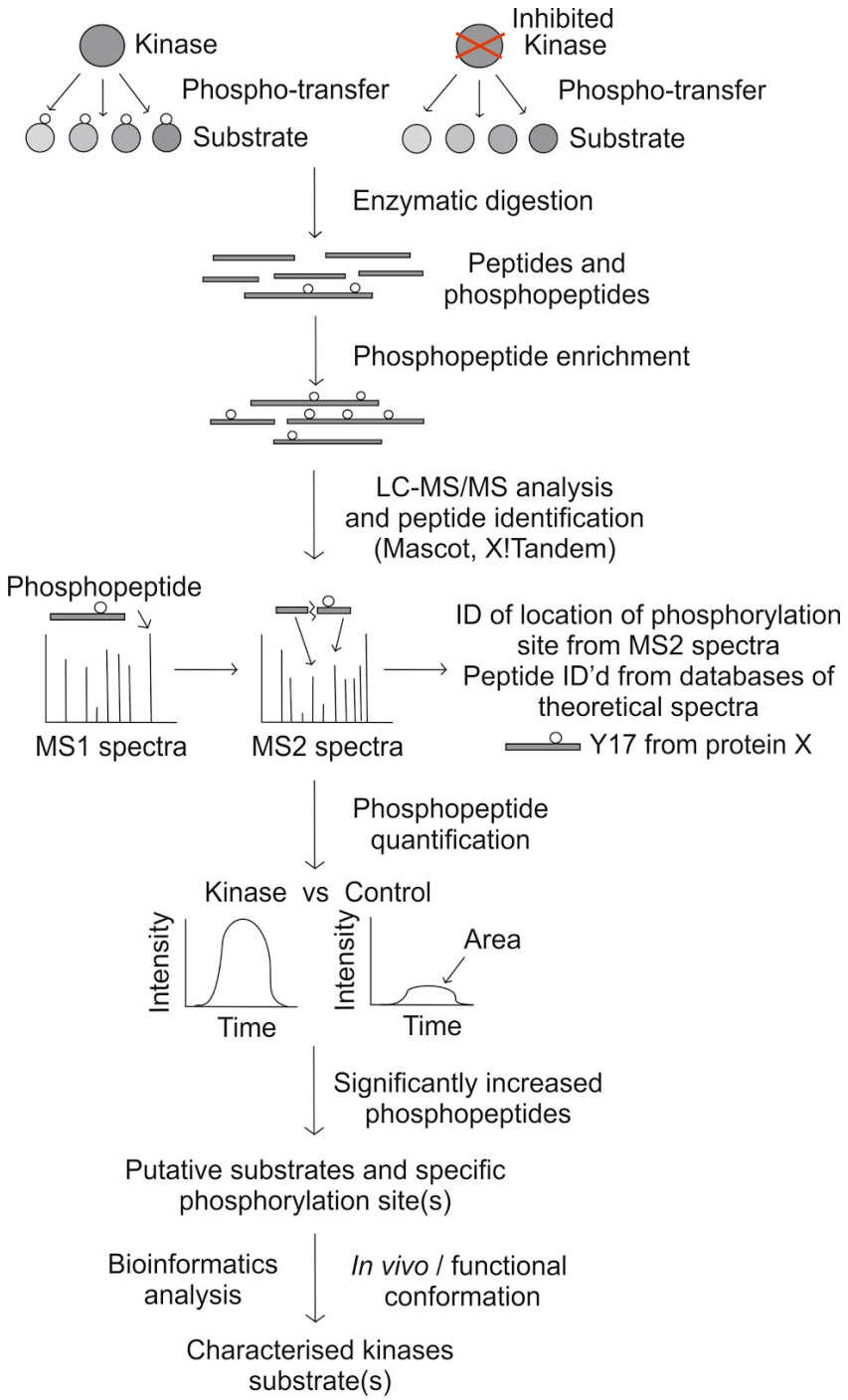

Figure 5.1: Schematic of phosphoproteomics methodology. A general phosphoproteomics methodology consists of the following steps, kinase manipulation (overexpression, inhibition), enzymatic digestion, phosphopeptide enrichment, and acquisition of MS^1 and MS^2 spectra. The phosphopeptide is identified by database searching (Mascot, X!Tandem), and the location of the specific phosphorylation site by the MS^2 spectra. The phosphopeptides are then quantified against a control experiment

by spectral counts or peak area, and those that are significantly changed are considered putative kinase substrates, which require further *in vivo* characterisation.

A number of *in vitro*, *in vivo*, and bioinformatics prediction techniques exist to identify kinase substrates. These include *in vitro* kinase assays with purified kinases and substrates, lysate kinase assays, protein/peptide arrays, and cellular manipulation of kinases including shRNA knockdown, mutants (kinase dead, constitutively active), inhibitors, and genetic knockouts. The advantages and disadvantages of each method are reviewed in detail by (Johnson and Hunter 2005). *In vitro* assays are beneficial as they can reveal direct phosphorylation events, however, they lack cellular context. Whereas *in vivo* assays provide cellular context, however, it is harder to infer direct phosphorylation due to downstream signalling. Thus, characterisation will likely involve a combination of the two.

Regarding Src phosphoproteomics, studies have utilised techniques such as activation of receptors upstream of Src to study its signalling pathways (Amanchy et al., 2009), however, this can result in cascades of direct and indirect phosphorylation events. Similarly, as a single cell type can express multiple SFKs, ATP-competitive Src inhibitors such as PP1/PP2 lack specificity as they target a broad range of Src family kinases; for example, C-, N1- and N2-Src have identical kinase domains (Brandvold et al., 2012). Thus, it is possible that some neuronal substrates and signalling pathways have been wrongly assigned to C-Src. SU6656 is considered a more selective inhibitor of Src-family tyrosine kinases, however, at high concentrations it also produces off target effects (Amanchy et al. 2009). Alternative techniques include kinase mutants, such as kinase dead C-Src vs constitutively active C-Src (Amanchy et al. 2008). Furthermore, a Src kinase domain mutant was engineered to accept a non-native ATP analogue, to enable the identification of direct phosphorylation events (Liu et al. 1998). Additional kinase domain mutants include R390A, which has reduced catalytic activity that is rescued by imidazole to ~ 40 % of the wild-type. The imidazole functions in cell culture, thus enabling the identification of *in vivo* substrates, and is believed to rescue activity without affecting selectivity (Ferrando et al. 2012). A method has recently been developed to covalently crosslink Src to its substrates upon phosphorylation via a reactive nucleotide based analog of ATP (ADP-methacrylate; (Wong et al. 2019).

In vitro kinase assays with recombinant or cellular purified C-Src and its substrates are abundant in the literature (Dunning et al. 2016; Keenan et al. 2015; Amanchy et al. 2008; Wang et al. 2018). However, a limitation is that proteins can be phosphorylated simply due to their Src substrate-like motifs, whereas substrates that interact with Src via its SH2/SH3 domains are more likely to be physiological (Shen et al. 1999). Thus *in vivo* characterisation is essential.

In vitro kinase assays with cell lysates were previously challenging due to the activation and high background from endogenous kinases, making phosphorylation events unattributable to a specific kinase. However, (Knight et al., 2012) developed an *in vitro* lysate kinase assay using the ATP analogue, and universal kinase inhibitor, 5'-4-fluorosulphonyl-benzoyl adenosine (FSBA). FSBA irreversibly inhibits the endogenous kinases in the lysate via the covalent modification of a conserved catalytic lysine in the ATP binding site (Fox et al., 1999), this is K295 in C-Src (Section 1.2.5) (Miller and Taunton 2014). FSBA therefore generates a kinase inactivated cell lysate. Thus, upon removal of unbound FSBA by desalting, and the addition of a recombinant exogenous kinase of interest, it enables the identification of kinase-specific direct phosphorylation events (Knight et al., 2012). The FSBA method enables the use of wild-type kinases, and is non-denaturing, which is preferable over methods such as heat inactivation of kinases. The FSBA-based method has been successfully utilised to identify *in vitro* p38 MAPK substrates. The 94 substrates included those previously characterised, and enriched for the p38 MAPK phosphorylation consensus motif (Knight et al., 2012). This methodology has since been applied to identify substrates of the tyrosine kinases Abl1 (Müller et al. 2016) and Syk (Xue et al. 2013), and was adopted in this study to identify novel N1-Src substrates in postnatal day 1 (P1) rat brain lysate. The P1 lysate is relevant to N1-Src's developmental expression and catalytic activity (Wiestler and Walter, 1988), and avoids the use of heterologous cells. However, orthogonal studies to validate candidate substrates in cells is essential.

5.2 Aims

C-Src has been assigned diverse substrates, and for many the specific phosphorylation site(s) and cellular effects have been deciphered. N1-Src has been linked to core neuronal functions including neurogenesis, neurite outgrowth and differentiation, however, it currently has no characterised *in vivo* substrates. Therefore, the primary aim of this chapter was to identify C- and N1-Src substrates in the developing brain via LC-MS/MS analysis of an FSBA-based *in vitro* whole cell lysate kinase assay. The secondary aims were to, i) identify specific Src phosphorylation sites to enable follow up studies with phospho-null and phospho-mimetic mutants, ii) identify if any of the C- and N1-Src SH3 domain ligands are also substrates, as these should be considered strong candidates for *in vivo* characterisation and iii) utilise bioinformatics to assess the cellular functions of the C- and N1-Src substrates.

5.3 Results

5.3.1 Optimisation of Src kinase substrate phosphorylation in P1 rat brain lysates

The FSBA-based *in vitro* whole-cell lysate kinase assay developed by (Knight et al. 2012), was applied to recombinant C- and N1-Src kinases, in order to identify their substrates in P1 rat brain lysate. First, in order to reduce the background tyrosine phosphorylation that occurred upon the addition of ATP to the lysate, the concentration of FSBA required to inhibit endogenous tyrosine kinases within the P1 lysate was optimised. The P1 lysate was incubated with 0-5 mM FSBA for 1 h at 30 °C. The FSBA was removed by desalting and 1 mM ATP was added and incubated for 1 h at 30 °C. Western blotting with anti-phosphotyrosine revealed there was a concentration-dependent inhibition from 0-5 mM and at 5 mM FSBA background phosphotyrosine signals were no longer identified (Fig.5.2A). Therefore, 5 mM FSBA was carried forward to enable the identification of C- and N1-Src phosphorylation events with minimal background phosphorylation.

His-Δ80 C- and N1-Src were utilised for the *in vitro* kinase assays, as the first 80 N-terminal residues of Src are not required for phosphorylation *in vitro* (Keenan et al. 2015). Thus the constructs comprise the SH3-SH2-SH1 domain and C-terminal region, but lack the N-terminal SH4 and unique domain. The catalytic activity of the purified recombinant C- and N1-Src kinases was assessed via the *in vitro* phosphorylation of a purified GST-tagged ideal Src substrate peptide motif (AEEEIYGEFF). The assay was conducted with 65 nM kinase, 7.5 μM substrate and 0.5 mM ATP for 1.5 h at 30 °C and assessed by Western blotting for phosphotyrosine. Approximately equal substrate phosphorylation by the two kinases was observed (Fig.5.2B) and confirmed they were catalytically active.

Having optimised the FSBA concentration, and confirmed catalytic activity for both C- and N1-Src, the experiment was then conducted with C- and N1-Src in the P1 rat brain lysate. Fig.5.2C, lane 1 shows that by Western blotting for phosphotyrosine there was undetectable basal tyrosine phosphorylation in the untreated lysate, which is not unexpected due to the low abundance of tyrosine phosphorylation in the absence of specific stimuli *in vivo* (Section 1.1), and the tight regulation of kinase signalling. Upon the addition of 1 mM ATP and incubation for 1 h at 30 °C, there were high levels of activation of endogenous tyrosine kinases (Fig 5.2C, lane 2), demonstrating the necessity

for endogenous kinase inhibition. The endogenous tyrosine kinase activity was prevented by pre-incubation of the lysate with 5 mM FSBA for 1 h at 30 °C (Fig.5.2C, lane 3). Following desalting to remove the FSBA, 300 nM of C- or N1-Src and 1 mM ATP were incubated with the P1 lysate for 1 h at 30 °C. In addition, to determine if any of the tyrosine phosphorylation was attributable to autophosphorylation of the kinases, 300 nM C- and N1-Src were incubated with 1 mM ATP for 1 h at 30 °C without P1 lysate. Phosphotyrosine immunoblotting revealed that overall N1-Src displayed largely reduced phosphorylation in the lysate in comparison to C-Src, and had only a single band at ~ 100 kDa (Fig.5.2C, lanes 4&5). In addition, no tyrosine phosphorylation was detected for the kinases incubated without P1 lysate, suggesting that all detectable phosphorylation was that of substrates. Due to the low levels of phosphorylation by N1-Src, the assay was optimised to increase substrate phosphorylation. The phosphorylation of substrate(s) at ~100 kDa and 150 kDa increased over time, with maximal phosphorylation at 3 h (Fig.5.2D).

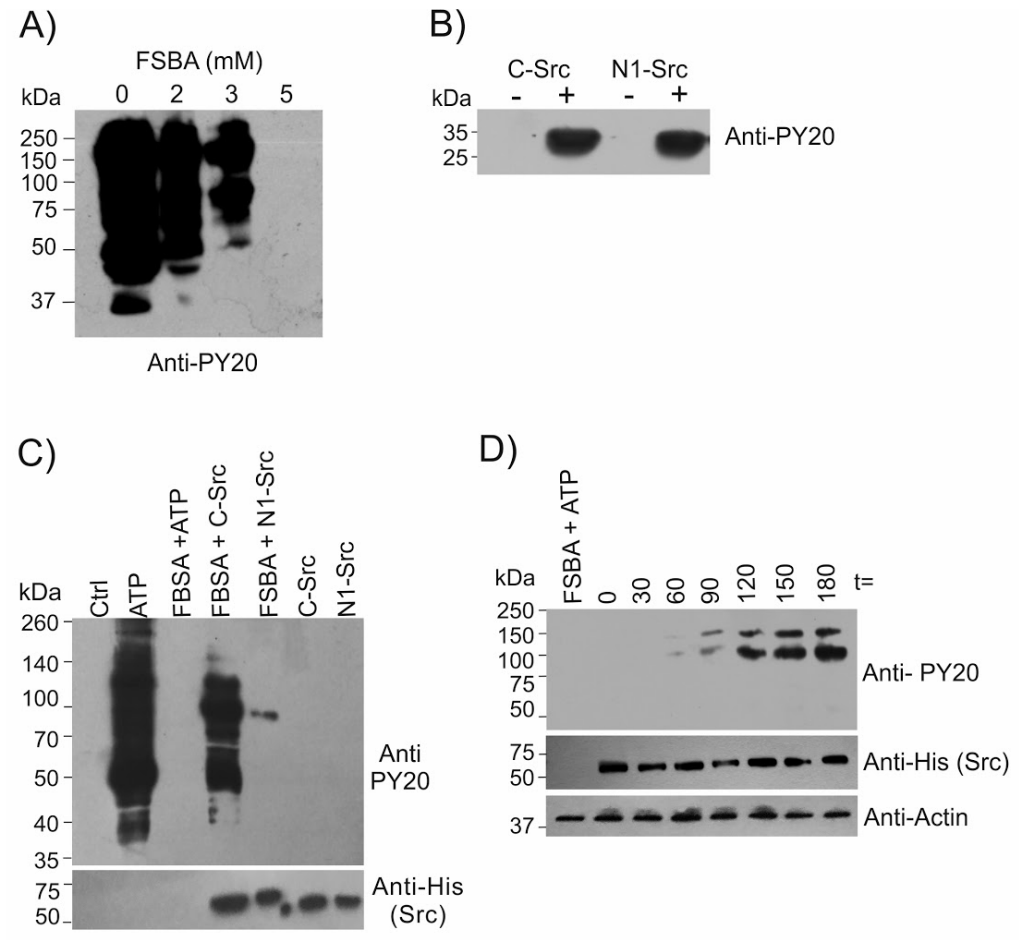

Figure 5.2: Identification of *in vitro* C- and N1-Src phosphorylation events in P1 rat brain homogenate. A) Optimisation of FSBA concentration for endogenous tyrosine kinase inhibition. The P1 lysates were incubated with 0-5 mM FSBA for 1 h at 30 °C. The samples were then desalted and incubated with 1 mM ATP for 1 h at 30 °C, followed by phosphotyrosine Western blotting (anti-PY20). B) Phosphorylation of 7.5 μM recombinant GST-fusion Src peptide substrate by 65 nM recombinant C- and N1-Src kinase for 1 h at 30 °C. Samples were denatured in Laemmli sample buffer and resolved via 12.5 % SDS-PAGE gel before Western blotting with anti-PY20. C) P1 rat brain lysate prior to any treatment (Ctrl), the incubation of P1 lysate with 1 mM ATP for 1 h at 30 °C (ATP), P1 lysate was treated with 5 mM FSBA for 1 h at 30 °C. The lysate was then desalted to remove the FSBA and reconstituted in kinase assay buffer and 1 mM ATP (FSBA + ATP), and with 300 nM recombinant C and N1-Src kinases (FSBA + C/N1-Src) for incubation at 30 °C for 1 h. 300 nM recombinant C- and N1-Src kinases incubated in kinase assay buffer and 1 mM ATP for 1 h at 30 °C in the absence of P1 lysate (C/N1-Src). Samples were denatured in Laemmli sample buffer and resolved by SDS-PAGE (10 % gel) before Western blotting with anti-PY20, the anti-His loading control shows the His-tagged recombinant kinases. D) Time course of N1-Src phosphorylation in P1 rat brain lysate. As described in Section C, however, samples were incubated for a total of 3 h at 30 °C with a fraction removed every 30 min for analysis by Western blotting. The anti-His loading control shows the recombinant kinases, the anti-actin is a loading control for the amount of P1 lysate, and the anti-PY20 shows substrate phosphorylation within the lysate.

5.3.2 Src phosphoproteomics methodology for LC-MS/MS analysis

A schematic of the phosphoproteomics workflow is shown in Fig.5.3A. The final experiment for LC-MS/MS analysis was conducted in triplicate, using P1 lysates from three independent rat litters. Each replicate contained an FSBA-only control for background tyrosine phosphorylation, and C- and N1-Src kinase. The endogenous kinases within the lysate were inhibited via incubation with 5 mM FSBA for 1 h at 30 °C. To avoid inhibition of the exogenous C- and N1-Src kinases, the unbound FSBA was removed by desalting (Fig.5.3A, Step 1). The P1 lysates (2.5 mg per condition) were then supplemented with kinase buffer, 1 mM ATP and either 250 nM of C- or N1-Src kinase and incubated for 3 h at 30 °C (Fig.5.3A, Step 2). Prior to further analysis, the triplicate reactions were analysed by Western blotting for phosphotyrosine content and His-tag immunoreactivity to confirm equal levels of kinase and tyrosine phosphorylation between replicates (Fig.5.3B). A Coomassie stained SDS-PAGE lysate loading control is also shown. The protein lysates were then precipitated with acetone overnight at 4 °C and resuspended for filter aided sample preparation (FASP) tryptic digestion (by Adam Dowle; Metabolomics and Proteomics Lab, CoEMS, Technology Facility, University of York). A phosphotyrosine peptide immunoprecipitation was then conducted overnight using a combination of agarose-conjugated PY20 and 4G10 antibodies to enable the enrichment of tyrosine phosphopeptides (Fig.5.3A, Step 3), which were then analysed by LC-MS/MS (Fig.5.3A, Step 4).

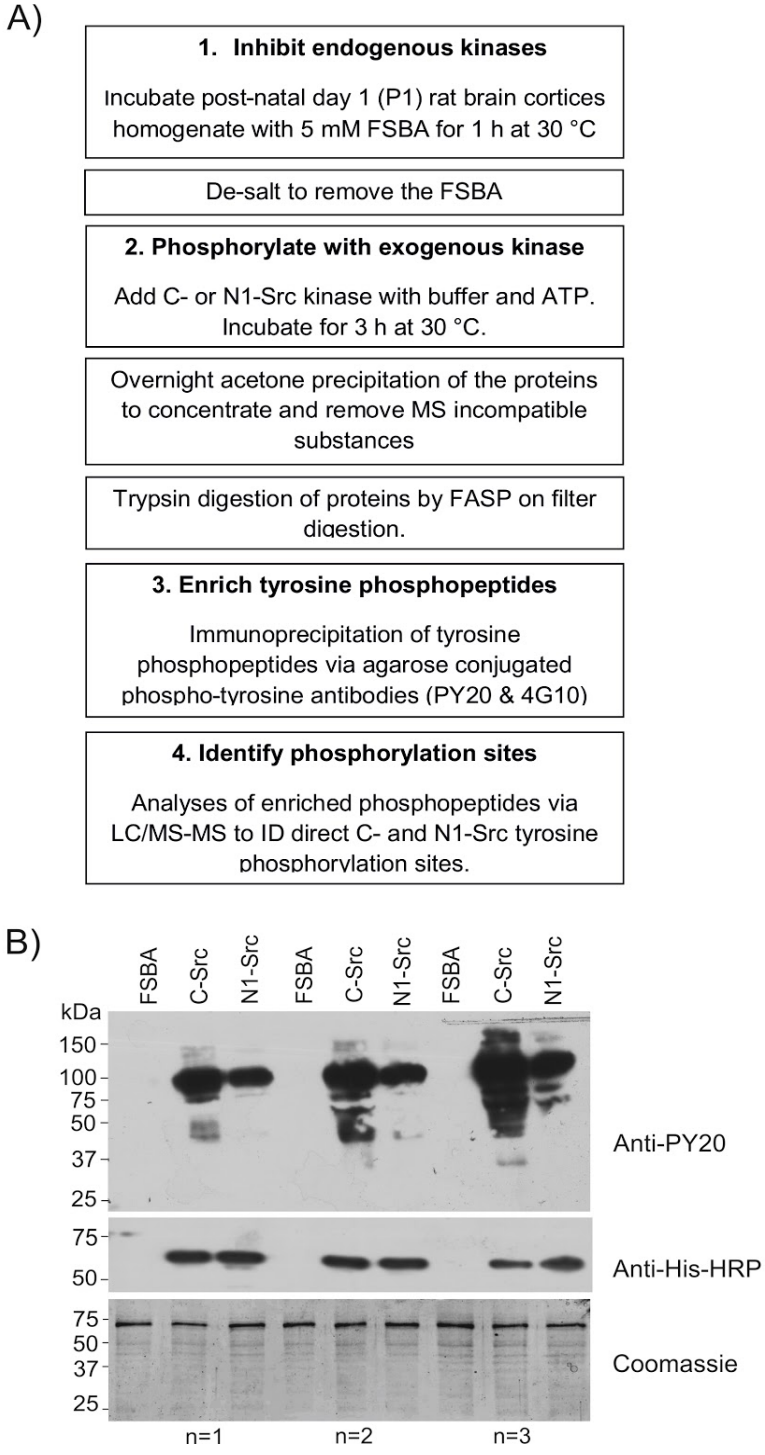

Figure 5.3: Schematic of methodology for the C- and N1-Src phosphoproteomics and characterisation of the triplicate samples that were submitted for LC-MS/MS analysis A) In brief, the endogenous kinases within the lysate were inhibited by 5 mM FSBA for 1 h at 30 °C. Exogenous C- and N1-Src was then added to the lysate and incubated for 3 h at 30 °C to elicit specific phosphorylation events. The protein lysates were then concentrated by acetone precipitation and digested with trypsin, and phosphotyrosine immunoprecipitation was used to enrich the phosphopeptides for LC-MS/MS analysis. B) N=3 replicates of the C- and N1-Src *in vitro* lysate phosphorylation assays. Anti-PY20 revealed the tyrosine phosphoproteins, anti-His-HRP the kinase loading control, and the Coomassie stained SDS-PAGE gel is a P1 lysate loading control.

5.3.3 Processing LC-MS/MS phosphoproteomics data

The phosphotyrosine immunoprecipitated peptides (enriched), and a fraction of each replicate taken prior to immunoprecipitation (non-enriched) were loaded onto an UltiMate 3000 RSLCnano HPLC system. The HPLC system was interfaced with an Orbitrap Fusion hybrid mass spectrometer and MS^1 and MS^2 spectra were acquired.

PEAKS Studio software was used to combine the enriched and non-enriched MS data. The peptides were searched against the rat Uniprot proteome and PEAKS was used to identify post translational modifications within the peptides. The location of the phosphorylation site within the peptide was identified by the MS^2 spectra, and the confidence in the identified phosphorylation site(s) were communicated by a localisation score p-value, with significance at the level of 0.05. The label-free semi-quantitative relative abundance of the phosphopeptides was determined using peak area based quantification (by Adam Dowle). Peak area is considered to be both accurate and sensitive for the detection of small fold changes (Dowle et al. 2016). Therefore, pairwise statistical analysis of the phosphopeptides peak areas between FSBA, C- and N1-Src was conducted using the PEAKS Q significance model.

Overall, there were two levels of analysis, the first assessed whether the phosphopeptides abundance was significantly upregulated against the FSBA-only control, and the second determined whether the specific phosphorylated tyrosine residue(s) within the peptide could be identified (localisation p-value < 0.05). Further complexity arose from variable peptide cleavage products. Trypsin cleaves after arginine and lysine residues, however if aspartic and glutamic acids are present at the cleavage site, or if there are consecutive lysine and/or arginine residues, this can result in a miscleavage (Šlechtová et al., 2015). Thus, there were many examples within the dataset of the same phosphosites contained within peptides of varying length (Appendix 4). In most instances miscleavage products had the same direction of statistical significance. However, there were a small number where the miscleavage products varied in their significance. Therefore, to avoid carrying over significant phosphopeptides that only occurred due to a low abundance cleavage product, a threshold was set, and miscleavage products were excluded from further analysis unless they were greater than 5 % of the total abundance of the phosphopeptides. In addition, peptides were only carried through if they were quantified in at least two of three experimental replicates.

The phosphopeptides were therefore selected for analysis based on the following criteria:

1. Significantly upregulated against the FSBA-only control ($p < 0.05$)
2. Detectable in at least 2/3 sample replicates
3. Miscleavage products must be greater than > 5 % of the total abundance

Using these criteria there were 363 and 340 significantly upregulated phosphopeptides for C- and N1-Src respectively. These corresponded to 260 *in vitro* protein substrates for C-Src and 239 for N1-Src. Of these proteins, 182 and 170 were assigned a specific phosphorylation site (localisation score $p < 0.05$) within the peptide for C- and N1-Src respectively (Fig.5.4A).

Serving as positive controls, previously published C-Src phosphorylation sites described in the PhosphoSite database were identified in the proteins EnoA, Celf2, Cof1, EfnB1, Ewsr1, Gab1 and Gria2 (localisation score $p < 0.05$), and in the phosphopeptides from the proteins Acp1, Arhgap5, Fubp1, Hnrnpk, H-Ras and Khsrp (localisation score $p > 0.05$) (Fig.5.4B). Furthermore, novel phosphorylation sites were identified in the Src substrates Arhgdia, Atxn2l, Mapt, Pag1, Sh3glb1, Sh3pxd2b, Ywhaz, Plcg1, RhoA, Gapdh and Sfpq (Appendix 5). The Src autophosphorylation site (Y419) that occurs upon activation was significantly upregulated for both C- and N1-Src against FSBA (Fig.5.4B).

In addition, to confirm the specificity of the phosphorylation events, all significantly increased phosphopeptides for C-Src with a localisation score $p < 0.05$, were aligned as 9 mers via the phosphorylated tyrosine residue to generate a phosphorylation consensus motif in WebLogo (Crooks et al., 2004). Fig.5.4C shows the central phosphotyrosine residue, and the four flanking residues either side. The phosphorylation motif conforms to a previously published Src consensus motif, derived from a peptide array:
−−φpY[φ/−]Xφ, where '−' is acidic and φ is hydrophobic and X is any amino acid (Miller et al., 2008).

A)

	C-Src	N1-Src
No. of signifcantly increased peptides (p < 0.05) against FSBA including miscleavages (Peptides must be quantified in 2/3 samples and be > 5% in MS response)	363	340
The corresponding no. of proteins	260	239
The no. of proteins with at least one tyrosine phosphorylation site localisation score (p < 0.05)	182	170

B)

Protein	Significantly upregulated tyrosine phosphorylation site or tyrosine containing phosphopeptide (p < 0.05)
Acp1	QLIIEDPY*YGNDSDFEVVYQQCLR
Arhgap5	GYPDEIY*VVPDDSQNR
Celf2	Y67
Cof1	Y68
EfnB1	Y323, Y328
EnoA	Y44
Ewsr1	Y284
Fubp1	1.QQAAY*YAQTSPQGMPQHPPAPQGQ 2.IGGDAGTSLNSNDY*GYGGQK
Gab1	Y285
Gria2	Y876
Hnrnpk	GSY*GDLGGPIITTQVTIPK
Hras	QVVIDGETCLLDILDTAGQEEY*SAMR
Hsp90ab1	NPDDITQEEY*GEFYK
Khsrp	AAAAATDPNAAWAAYYSHY*YQQPPGPVPGPAP APAAPPAQGEPPQPPPTGQSDYTK
Src	Y419

C)

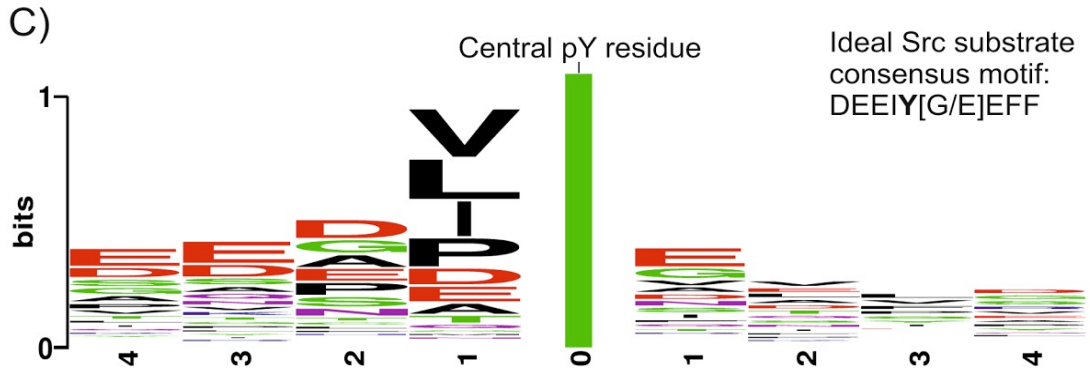

Figure 5.4: Identification of *in vitro* C- and N1-Src substrates, characterised phosphorylation sites and consensus motifs. A) The number of statistically increased phosphopeptides for C- and N1-Src against the FSBA control and the corresponding number of proteins, including those with a specific phosphorylation site identification (localisation score $p < 0.05$) B) Identification of characterised C-Src phosphorylation sites within the datasets via PhosphoSite. The specific phosphorylation site, or phosphopeptide that contains the phosphorylation site (marked with an *) are listed for each characterised C-Src substrate. C) The significantly increased C-Src phosphopeptides with a localisation score $p < 0.05$, were aligned via the phosphotyrosine residue to generate a 9 mer Weblogo consensus motif. An ideal Src substrate motif (DEEIY[G/E]EFF) is also shown.

5.3.4 Summary of *in vitro* C- and N1-Src substrates

A summary of all the identified C- and N1-Src phosphoproteins based on the set criteria (Section 5.3.3) is shown in Table 5.1. Proteins containing phosphopeptides for which a phosphorylation site assignment was not significant (localisation p value > 0.05) are marked with an asterisk (*), the remainder have an assigned specific tyrosine phosphorylation site(s) within the rat protein (Appendix 5).

In total there were 193 shared *in vitro* substrates and 67 and 46 unique proteins for C- and N1-Src respectively. Proteins are classified based on whether or not they were phosphorylated and not on a shared phosphorylation site. However, the majority of C- and N1-Src phosphorylation sites were shared (Appendix 5), and the differences appeared to be the phosphorylation of additional sites on top of these. This is not unexpected as C- and N1-Src have identical catalytic domains. There are some instances where neighbouring residues were phosphorylated and this could be indicative of processive phosphorylation, whereby the SH2 domain docks to promote further phosphorylation. Examples include Akap1 (Y419/425), Cnrip1 (Y85/89), Dek (Y354/360), S1p1r (Y20/23) and Zc2hc1a (Y119/124) (Appendix 5).

Previously published C-Src substrates (PhosphoSite) in the datasets are shown in bold. In addition, as Src SH3 domain ligand interactions can drive substrate phosphorylation (Shen et al. 1999), the proteins that were identified in the GST- C- and N1-Src SH3 domain interaction screen (Chapter 3) are underlined for a C-Src ligand or double underlined for a C- and N1-Src SH3 domain ligand. Six of the previously identified N1-Src SH3 domain interactors; Caskin1, Neuronal Enah, Sh3pxd2b, Srcin1, Sfpq and Zc2hc1a were phosphorylated, with the specific phosphorylation site(s) identified for Sh3pxd2b, Srcin1, Sfpq and Zc2hc1a. Another N1-Src SH3 domain interactor, Sf1, was only identified as phosphorylated by C-Src. In addition, the C-Src SH3 domain ligands Caskin1, Cep170b, Ctnnd1, Dpysl2, Dpysl3, Hnrnpk, Map2, Neuronal-Enah, Sf3a1, Sfpq, SH3pxd2b, Snrpa1, Srcin1, Ywhaz and Zc2hc1a were all tyrosine phosphorylated. The substrates were also screened against the BioGRID database for additional Src interactors and substrates, and these are labelled with a dotted line (Table 5.1). Thus, in total 49 of the *in vitro* C- and N1-Src and substrates are previously linked to C-Src through interactions or phosphorylation events.

A caveat of the analysis is that some phosphopeptides, in particular for C-Src, had a larger average abundance than N1-Src, but were not significant against FSBA, possibly as a result of variation between replicates. A number of 'unique' proteins were also phosphorylated by the other kinase but only in a single replicate, and were therefore excluded from further analysis. Therefore, the 'unique' assignments should be treated with caution, and with a larger replicate size, some proteins could be reclassified. Considering this, there were only 2 N1-Src substrate phosphoproteins that were not detected in any C-Src replicates, Gng3 and Tex2, and 26 C-Src phosphoproteins that were not detected for N1-Src. However, the equivalent phosphorylation site of Gng3, is phosphorylated in Gng2 by C-Src, suggesting that it is not a stand-out novel N1-Src substrate.

An example of a PEAKS software MS^2 spectrum used to assign the specific phosphorylation site p-Y124 in the C- and N1-Src SH3 domain ligand Zc2hc1a is shown in Fig.5.5. Interestingly, the PhosphoSite database does not contain any reports of Zc2chc1a tyrosine phosphorylation, suggesting that it is a novel C- and N1-Src SH3 domain ligand (Chapter 3), *in vitro* Src substrate, and tyrosine phosphoprotein.
The spectrum show the B- (blue) and Y- ions (red), and the mass difference between the ions reveals the location of the phosphorylation site. The fragmented peptide ions enable the peptide to be scanned one residue at a time from both termini, until a residue is identified that also contains a mass change indicative of phosphorylation. For example, the mass difference between the Y3 and Y4 ions corresponds to the addition of a tyrosine residue, plus a phosphate (+79.97) (Fig.5.5). Thus, specific site identification relies on the quality of the MS^2 spectra. However, in practise, fragmentation events are somewhat random, and some occur more often others.

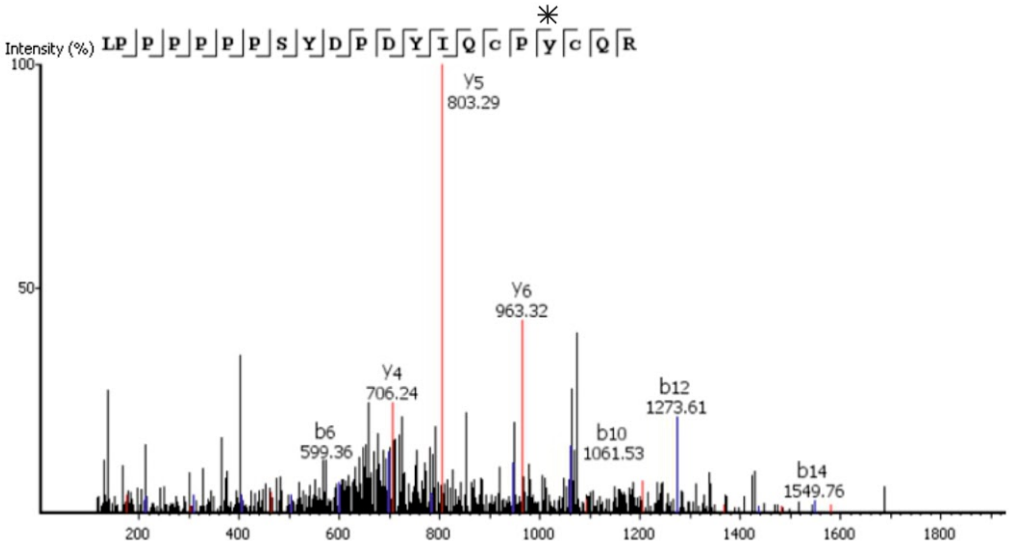

#	b	Seq	y	#
1	114.09	L		21
2	211.30	P	2527.05	20
3	308.23	P	2429.99	19
4	405.23	P	2332.94	18
5	502.29	P	2235.89	17
6	599.13	P	2138.83	16
7	696.46	P	2041.78	15
8	783.91	S	1944.73	14
9	946.23	Y	1857.70	13
10	1061.39	D	1694.63	12
11	1158.58	P	1579.80	11
12	1273.65	D	1482.58	10
13	1436.48	Y	1367.56	9
14	1549.88	I	1204.37	8
15	1677.82	Q	1091.24	7
16	1837.85	C(+57.02)	963.35	6
17	1934.90	P	803.30	5
18	2177.93	Y(+79.97)	706.30	4
19	2337.96	C(+57.02)	463.08	3
20	2466.02	Q	303.17	2

Figure 5.5: Identification of p-Y124 within the Zc2hc1a phosphopeptides.
The MS^2 spectrum utilised by PEAKS software to assign the specific phosphorylation site of p-Y124 in the C- and N1-Src SH3 domain ligand and *in vitro* substrate Zc2hc1a. The sequence of the phosphopeptide is shown, and the B- (blue) and Y- (red) ions on the MS^2 spectra and fragment ion table.

Table 5.1: C- and N1-Src *in vitro* substrates

Proteins are statistically classified as shared, C-Src or N1-Src specific substrates via their significantly up-regulated phosphopeptide(s). Asterisk (*) indicates a localisation score ($p > 0.05$) for which the specific phosphorylation site was not assigned. The remainder have a specific phosphorylation site assigned ($p < 0.05$), see Appendix 5. Proteins labelled in bold are characterised C-Src substrates (PhosphoSite database). Proteins identified in the GST-C- and N1-Src SH3 domain ligand screen (Chapter 3) are underlined once for a C-Src ligand and double underlined for a C and N1-Src SH3 domain ligand, and those underlined with a dotted line are C-Src ligands/substrates from the BioGRID database.

C and N1-Src phosphoproteins						
Acp1	Cep170b	**Ewsr1**	M6pr *	Nolc1	RGD1306271	Stip1
Agl *	**Cfl1**	Fnbp1l	Magi1	Nsfl1c	RGD1311703	Sugt1 *
Akap1	Cherp	**Fubp1 ***	Magi2	Nsrp1	RGD1560065	Tbr1
Alb	Chl1 *	Gab2	Map1b	Ntmt1	Rnf113a1	Tcea1
Aldh2	Cic	Glcci1	Map2 *	Nucb2 *	Rpsa *	Timp2
Aldoc	Cisd1	Gmds	Map6	Nyap1	Rrm1	Tkt
Anks1a *	Ckap4	Gnpda1 *	**Mapt**	Nyap2 *	Rtn4	Tlk2 *
Anxa6 *	Clasp1	Gpbp1 *	Mast4	**Pag1**	S1pr1	Tmem106b
Apool *	Clasp2	Gpc4	Mavs *	Pcbp2 *	Sar1a	Tmem35a *
Arhgdia	Cnpy3	Gpx1	Mcrip1	Pdha1l1 *	Scamp1	Tmpo
Arpc3	Cnrip1	Grpel1	Mdga1	Pdia3	Sephs1 *	Tomm34 *
Ashwin	Cops7a	Gyg1	Mdh2 *	Pgrmc1	Serpina10	Tsn
Atn1	Cox4i1 *	Hcfc1	Micall1	Pithd1	Sf3a1 *	Tuba1a
Atp5o	Cpe *	Hepacam	Mlip	Pitpna	Sh3bgrl	Wbp2 *
Atxn2	Cs	Hnrnph1	Myl6	Pitpnb *	**Sh3glb1**	Wdr70
Atxn2l	**Ctnnd1 ***	Hsp90aa1	Naca *	Plcb1	Sh3glb2	Xpnpep1
Bcan *	Cxadr	Hspa8	Nacad	Plppr3	**Sh3pxd2b**	Xrn2 *
Cab39 *	Dcx	Hspe1	Napa	Poldip3	Sin3a	Yars
Cacng8	Dek	Hsph1	Napb	Ppp1r14b	Sirpa	Ywhaq
Cadm3	Denr	Igfbp5 *	Naxe	Ppp2r5d	Slc4a1ap *	**Ywhaz**
Canx	Dlg2	Itga5	Ncam1	Prkrip1	Snap91	Zc2hc1a
Caskin1 *	Dlg3	Itgb1	Nectin1	Prrc2b	Snrpa1 *	Zc3h14 *
Casp3	Dlgap4	Itpa	Nelfe	Psmd9	Snrpc *	Zfp608 *
Ccdc177	Dnajc5	**Khsrp ***	N-Enah *	Psme1	Snw1	Zfp609
Cd34 *	Dpysl2	Kng1	Nfasc *	Psmg1 *	Sox11 *	Zfp706 *
Cdc37 *	Eef1a1	Lancl1	Nfya	Ptpn1	Spata2	
Cdh2 *	**Efnb1**	Letm1	Nfyb	Pym1	**Src**	
Cdv3	Efnb3	Lin7c	Nipsnap1	Rab1b *	Srcin1	**Total = 193**

C-Src phosphoproteins						
A1m	Cat *	Fam213a	Lemd3 *	Pcdh1 *	Rab4b	Tcf3
Actg1 *	Cct8	**Gab1**	Magi3	Pcyox1	RGD1305178	Thrap3 *
Actr1a *	Cops4	Gng2	Mcm3	Pdap1 *	**RhoA**	Tmed9
Apcs *	Cops7b *	Gprc5c	Mdga2	Pfdn1	Rps21 *	Uba1
Apoo	Ddx41	Hist1h4b *	Memo1 *	Pfn2	Scg2 *	Ubap2
Arhgap5 *	Dpysl3	Hivep2 *	Mpi *	Pgrmc2	Sema6d	Ubap2l *
Atp1a3 *	Eef2	**Hnrnpk ***	Mpzl1 *	**Plcg1**	Sf1	Uqcr10
Cadm2	Eif4enif1	**Hras ***	Ndufv3 *	Prag1 *	Sgta	
Cap1	Eno1	Hspa5 *	Nucks1 *	Prdx4	Shb	
Casd1	Ensa	Klc2	Paics	Psma7	Stmn2 *	**Total = 67**

N1-Src phosphoproteins						
Ambp	Crip2 *	Gnao1	Mapk3 *	Nme1	Raver1 *	Tex2
Apc	Dcbld2	Gng3	Mat2a *	Park7 *	RGD1561636	Txnl1 *
Arhgap12	Dcc	**Gria2**	Me2 *	Pdcd10	Rilpl2	Uqcrb
Atp6v1a *	Dctn2 *	Hspd1 *	Mgrn1 *	Pgk1	Romo1 *	Zhx3
Celf2	Epha3 *	**L1cam ***	Mtdh *	Plrg1	Sf3b1 *	
Clstn1	Erp29	Lamc1 *	Mtnd3	Ppp1r13b *	**Sfpq**	
Cpd	**Gapdh**	Lgalsl	Mug1 *	Rap1gap *	Sugp2	**Total = 46**

5.3.5 Functional enrichments within the C- and N1-Src substrates

STRING was used to generate protein-protein interaction networks and to identify functional enrichments within the N1-Src dataset (Fig.5.6). The interaction network might identify N1-Src substrates that co-cluster in functional protein complexes, which would strengthen any conclusions relating to the cellular functions of N1-Src. Furthermore, the inclusion of N1-Src itself in the network, due to its auto-phosphorylation, might reveal known Src interactors that were phosphorylated. All 239 proteins that had significantly upregulated phosphopeptides for N1-Src against FSBA were analysed. The interaction network was filtered for high confidence interactions derived from experiments and curation databases. Only the N1-Src network is presented as C- and N1-Src phosphorylate the majority of the same proteins. The GO term enrichment analysis was also conducted in STRING using the whole genome as the statistical background.

The network was annotated to highlight proteins within the significantly enriched GO terms; Neuron projection morphogenesis (FDR 2.77E-11), Neuron differentiation (FDR 1.06E-09), Axonogenesis (FDR 3.89E-09), Neuron development (FDR 1.44E-08), Neurogenesis (FDR 6.59E-07) and PolyA RNA binding (FDR 1.48E-10). The gene count and false discovery rate for each GO term is also shown (Fig.5.6A). The enrichment of these terms demonstrates that *in vitro* N1-Src is phosphorylating proteins involved in the development, differentiation and morphology of neurons. The Src interactors from the STRING database that were phosphorylated include Itgb1, Itga5, Hsp90, EfnB1, EfnB3, EphA3, S1p1r, Gnao1, Dcc, Ctnnd1 and Ptpn1. The C- and N1-Src SH3 domain interactors that were identified via the pull-downs (Chapter 3) and BIOGRID database are underlined, and characterised Src substrates (PhosphoSite) are marked with an asterisk (Fig.5.6A). A standout feature of the network was a cluster of interacting proteins that were classified within the GO term PolyA RNA binding. Interestingly the cluster shares proteins from the mRNA processing/splicing cluster present in the STRING network for the C-Src SH3 domain pull-downs (Chapter 3), including Snrpa1, Sf3a1, Sf3b1 and Raver1.

The functional enrichment analysis including the GO terms highlighted in the interaction network is shown in Fig.5.6B. Each significantly enriched GO term and its false discovery rate for C- and N1-Src is shown. As C- and N1-Src phosphorylated a similar

number of proteins, and the majority were shared, it is unsurprising that the FDRs for many GO terms are comparable. Besides the abundance of enriched GO terms spanning neuron/nervous system development, differentiation, neurite/axon morphology, there were also those including the neuronal structures of the synapse, myelin sheath, axon and growth cone (Fig.5.6). Therefore, phosphoproteins have been identified with relevance to the cellular expression and functions of N1-Src. In support of the validity of this analysis, C-Src enriched for proteins at focal adhesions, one of its highly cited signalling pathways within the literature (McLean et al. 2000; Schaller et al. 1999; Ferrando et al. 2012). The focal adhesion associated proteins Arpc3, Cap1, Cdh2, Cfl1, ItgA5, ItgB1 RhoA, Ywhaq and Ywhaz were all phosphorylated by C-Src (Table 5.1).

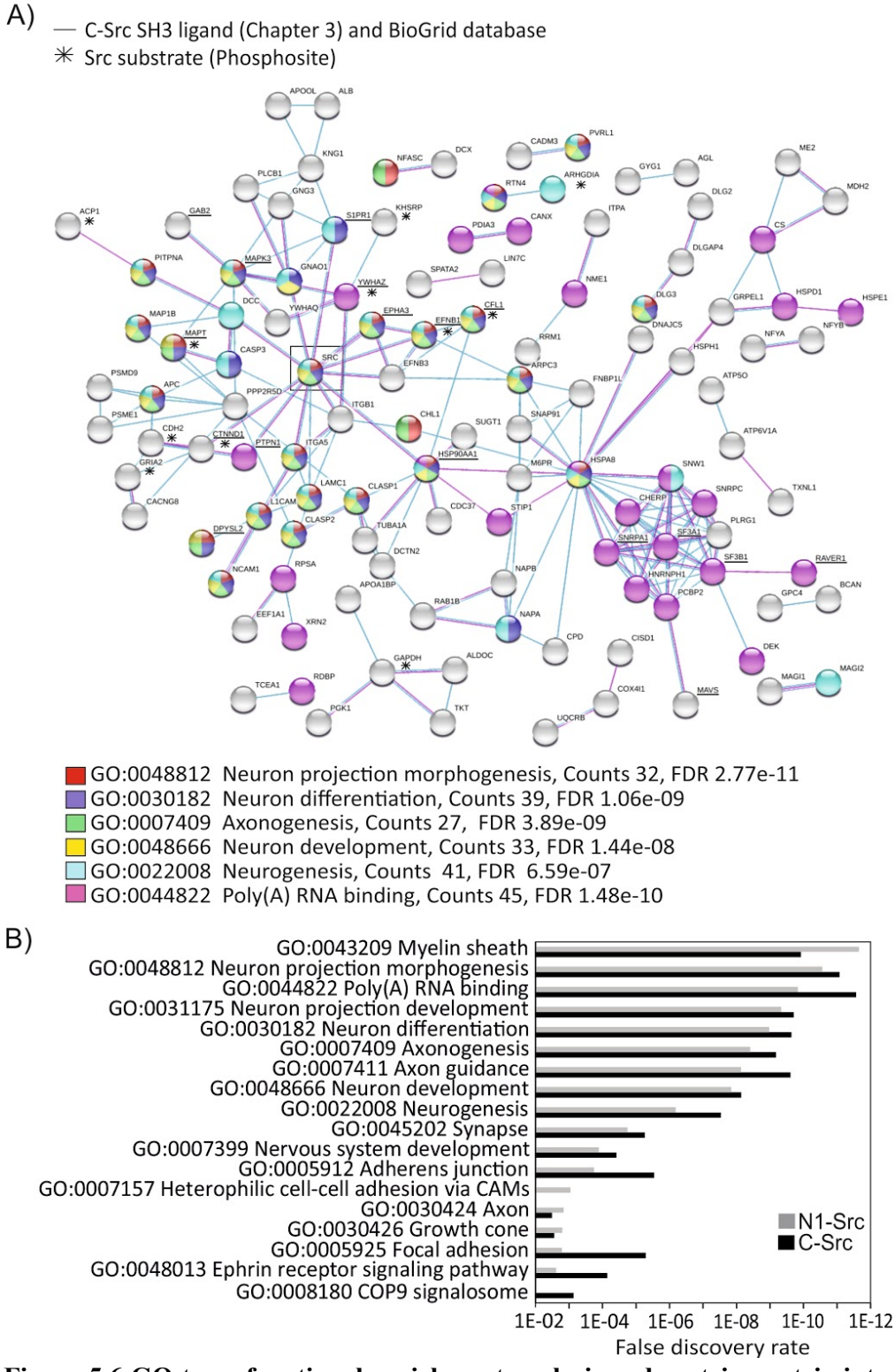

Figure 5.6 GO term functional enrichment analysis and protein-protein interaction network of the *in vitro* N1-Src substrates. A) STRING protein-protein interaction network of the 239 significantly upregulated N1-Src phosphoproteins. The interaction network is annotated with the listed GO terms, including their gene counts and false discovery rates. The characterised C-Src substrates (*), and SH3 domain ligands (underlined) are also annotated onto the network. B) GO term functional enrichment analysis of the C- (260) and N1-Src (239) phosphoproteins. The FDR for C- and N1-Src is shown for each GO term.

5.3.6 Assessment of activity within the *in vitro* kinase assays

Cellular studies have reported enhanced auto- and substrate phosphorylation by N1-Src compared to C-Src (Worley et al. 1997; Brugge et al. 1985). However, recombinant His-Δ80 N1-Src *in vitro* phosphorylated synaptophysin to a lesser extent than C-Src (Keenan et al. 2015), and the same was observed on a lysate wide scale in this *in vitro* assay.

Qualitatively, N1-Src had reduced substrate phosphorylation in the P1 lysates in comparison to C-Src via phosphotyrosine Western blotting (Fig.5.2/3), and this was mirrored by the semi-quantitative mass spectrometry analysis. A heat map of all the phosphopeptides that were significantly upregulated for N1-Src against FSBA is shown in Fig.5.7A. The average peptide peak area for FSBA, C- and N1-Src were summed for each phosphopeptide and then expressed as a percentage of the total in order to display the peptides' relative abundance. The relative abundance of all FSBA phosphopeptides was 0 %, likely due to the low abundance of tyrosine phosphorylation in the untreated lysate (Fig.5.3B), and the statistical analysis eliminating phosphopeptides present in the control. In addition, the majority of phosphopeptides were greater in abundance for C- than N1-Src (Fig.5.7A), and the average relative abundance of all the phosphopeptides was 1:2.7 for N1:C-Src respectively.

Only two of the significantly upregulated N1-Src phosphopeptides (0.6 %) were not identified for C-Src, and 42 (12 %) of the significantly upregulated C-Src phosphopeptides were not identified for N1-Src. This confirms that there is little difference in phosphorylation site (Appendix 5), or substrate selectivity (Table 5.1) between C- and N1-Src *in vitro*. Thus, N1-Src appears to be functioning as a lower activity C-Src in these assays, and the few phosphopeptides unique to C-Src are likely a result of its increased activity (Fig.5.3).

In order to explain the reduced substrate phosphorylation by N1-Src, the core regulatory phosphotyrosine residues (p-Y419 and p-Y527) were investigated. Autophosphorylation of Y419 in the kinase domain is necessary for the stabilisation of Src's catalytically active conformation (Meng and Roux 2014) (Section 1.2.5). Thus, lack of autophosphorylation could equate to reduced substrate phosphorylation. The pY419 phosphopeptide was detected by LC-MS/MS and was significantly increased for both C- and N1-Src against FSBA. However, whilst not significant, the relative abundance

between C- and N1-Src was 83:17 respectively, thus N1-Src autophosphorylation was reduced (Fig.5.7B). Surprisingly, two other phosphopeptides from the kinase domain were identified. The p-Y439 peptide was identified in all three C- and N1-Src replicates, and was significantly increased against FSBA, with a relative abundance of 81:19 for C:N1-Src (Fig.5.7C). The second phosphopeptide containing p-Y338 was significantly increased for C-Src against FSBA, however it was only identified in one experimental replicate (Fig.5.7C). Therefore, it does not pass the stringent criteria outlined in Section 5.5.3, but is acknowledged in this context.

The Src C-terminal Y527 residue is phosphorylated by Csk and Chk to negatively regulate kinase activity (Advani et al. 2017) via its intramolecular interaction with the SH2 domain (Section 1.2.4). There is also evidence to suggest that Y527 is autophosphorylated by Src *in vitro* (Osusky et al. 1995). The auto-phosphorylation of Y527 would generate the inactive conformation of Src (Section 1.2.7), and reduce auto-phosphorylation of Y416, and in turn substrate phosphorylation. The non-phosphorylated peptide containing Y527 was identified via LC-MS/MS, however, the phosphopeptide was not. It is possible that the phosphopeptide was not identified due to factors such as the peptide flying poorly, or being insoluble. Non-phosphorylated peptides can be used to quantify changes in phosphorylation sites, via their reduction in intensity upon kinase incubation. However, this was not feasible as the FSBA only control does not contain recombinant Src. Therefore, in order to confirm the lack of p-Y527, an *in vitro* kinase assay was conducted with the same concentrations of N1-Src and ATP (Section 5.3.2), for 3 h at 30 °C. The assay was analysed by Western blotting, which did not detect p-Y527 immunoreactivity (Fig. 5.7D). Ideally, this experiment requires a positive control of Src p-Y527, although, taken together with the LC-MS/MS, suggests that p-Y527 is not likely to be the cause of the reduced auto- and substrate phosphorylation.

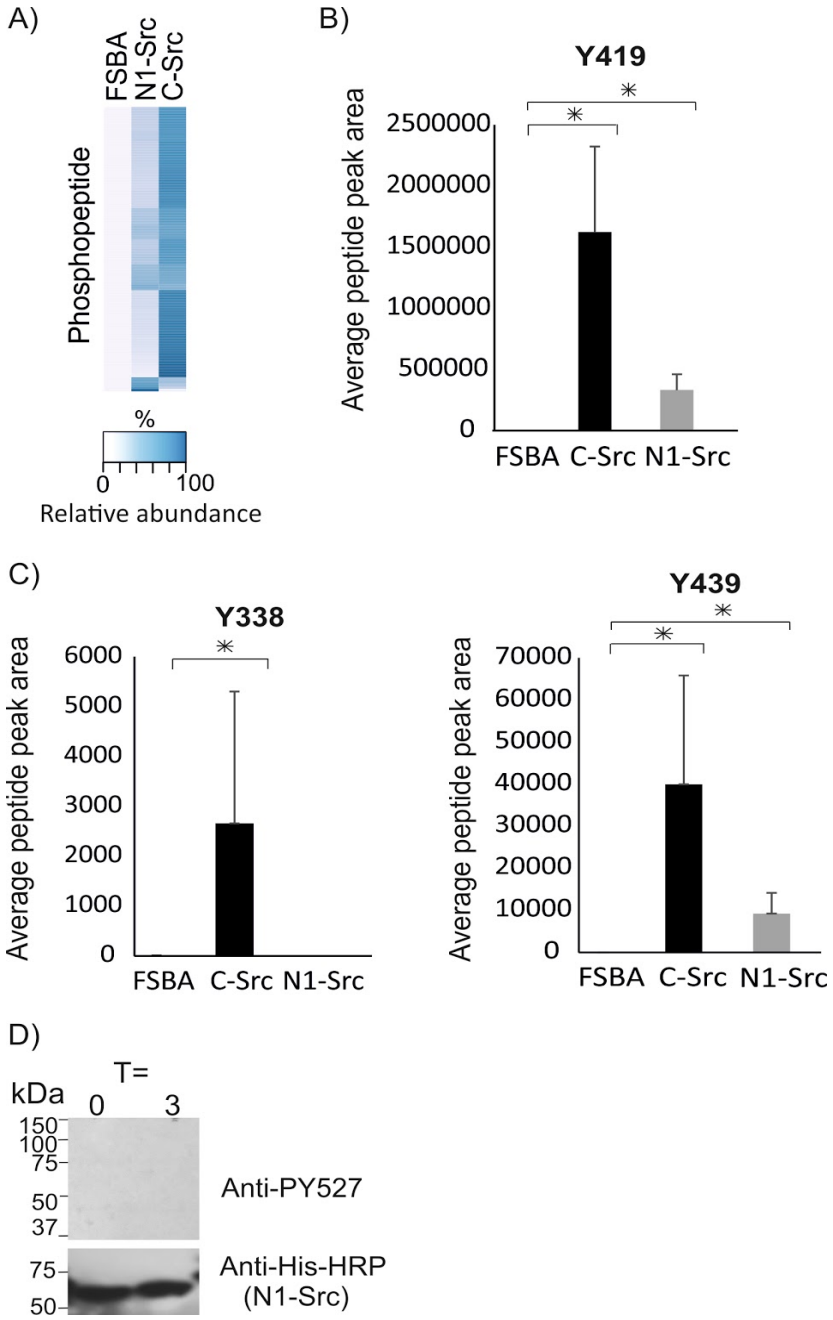

Figure 5.7: Recombinant N1-Src has reduced auto- and substrate phosphorylation. A) Heat map showing the relative percentage abundance of all significantly upregulated N1-Src phosphopeptides against C-Src and FSBA. B/C) LC-MS/MS quantification of phosphopeptide peak area for the phosphopeptides containing p-Y419/Y439/Y338 between C-, N1-Src and FSBA. The error bars show the SEM, and * indicates statistical significance at $p < 0.05$ via PEAKS Q significance model. D) Assessment of N1-Src auto-phosphorylation via incubation of 250 nM N1-Src for 3 h at 30 °C with 1 mM ATP. The Western blots shown an anti-His-HRP kinase loading control, and anti-pY527 for the Src C-terminal phosphorylation site.

5.3.7 *In vitro* phosphorylation by purified cellular N1-Src

The recombinant Δ80 N1-Src kinase yielded unexpected results in terms of its low auto- and substrate phosphorylation (Fig.5.3/7). Therefore, the catalytic activity of full length cellular purified C- and N1-Src-FLAG were compared in the P1 lysate.

A preliminary assay was conducted to assess if the Src-FLAG constructs could be successfully utilised in an *in vitro* kinase assay. C- and N1-Src were immunoprecipitated from stable inducible HeLa cells using anti-FLAG agarose-conjugated resin and stringent washing was applied to remove any endogenous kinases. The kinase on resin was incubated with a GST-tagged ideal Src substrate peptide for 1 h at 30 °C. The supernatant was then removed and the kinase eluted from the resin with Laemmli sample buffer. The ~ 60 kDa kinases are shown via anti-FLAG immunoblotting (Fig.5.8A), and tyrosine phosphorylation of the GST-tagged peptide substrate was increased by both C- and N1-Src as shown by the anti-PY20 Western blot. However, background tyrosine phosphorylation was detected in the control lysates, suggesting that the washing was not stringent enough to remove all endogenous kinase (Fig.5.8A).

Having confirmed that the cellular purified kinases were viable for *in vitro* kinase assays (Fig.5.8A), the assay was then extended to the FSBA treated P1 lysates (Fig.5.8B). The FSBA method was conducted as previously described (Section 5.3.1/2), however, the immunoprecipitated kinases on resin were utilised as oppose to recombinant kinase. The kinases were incubated with the P1 lysate for 1 h at 30 °C, and not 3 h due to concerns regarding high levels of background tyrosine phosphorylation. The assay was terminated via Laemmli sample buffer and analysed via Western blotting. As expected background tyrosine phosphorylation was observed (anti-PY20 Fig.5.8B), however, C-Src-FLAG raised the lysate phosphorylation content above that of the background. Surprisingly, with the exception of a single band ~ 75 kDa, N1-Src did not raise the tyrosine phosphorylation above the background (Fig.5.8B). However, the anti-FLAG immunoblot showed that less N1-Src was present than C-Src, thus the extent of phosphorylation cannot be directly compared. Encouragingly, p-Y416 was identified for both C- and N1-Src (Fig.5.8B). However, it was increased for C-Src, and despite there been more C-Src in the assay, suggests that N1-Src is not auto-phosphorylated in excess of C-Src as shown in previous experiments in our lab (Keenan et al. 2015; Keenan 2012). Thus, the full length cellular purified kinases mimic the recombinant kinases (Fig.5.3/7). The

p-Y416 content of the kinases was assessed prior to their addition to the P1 lysates (Fig.5.8C). However, as p-Y416 immunoreactivity was only detected for C-Src, it was not possible to compare the ratios of Src p-Y416:Total Src for C- and N1-Src via densitometry analysis, although qualitatively N1-Src is not autophosphorylated in huge excess of C-Src in HeLa cells.

In order to demonstrate that N1-Src possess high levels of catalytic activity *in vivo*, a B104 neuroblastoma cell line was utilised. C- and N1-Src-FLAG were transfected into the B104 cells for 48 h prior to lysis in Laemmli sample buffer and analysis by Western blotting. Unfortunately a poor transfection efficiency was achieved for C-Src, as evident via the anti-FLAG Western blot (Fig.5.8D). However, N1-Src raises cellular phosphotyrosine content above that of the control cells (anti-PY20), and auto-phosphorylation of p-Y416 by N1-Src was detectable (Fig.5.8D).

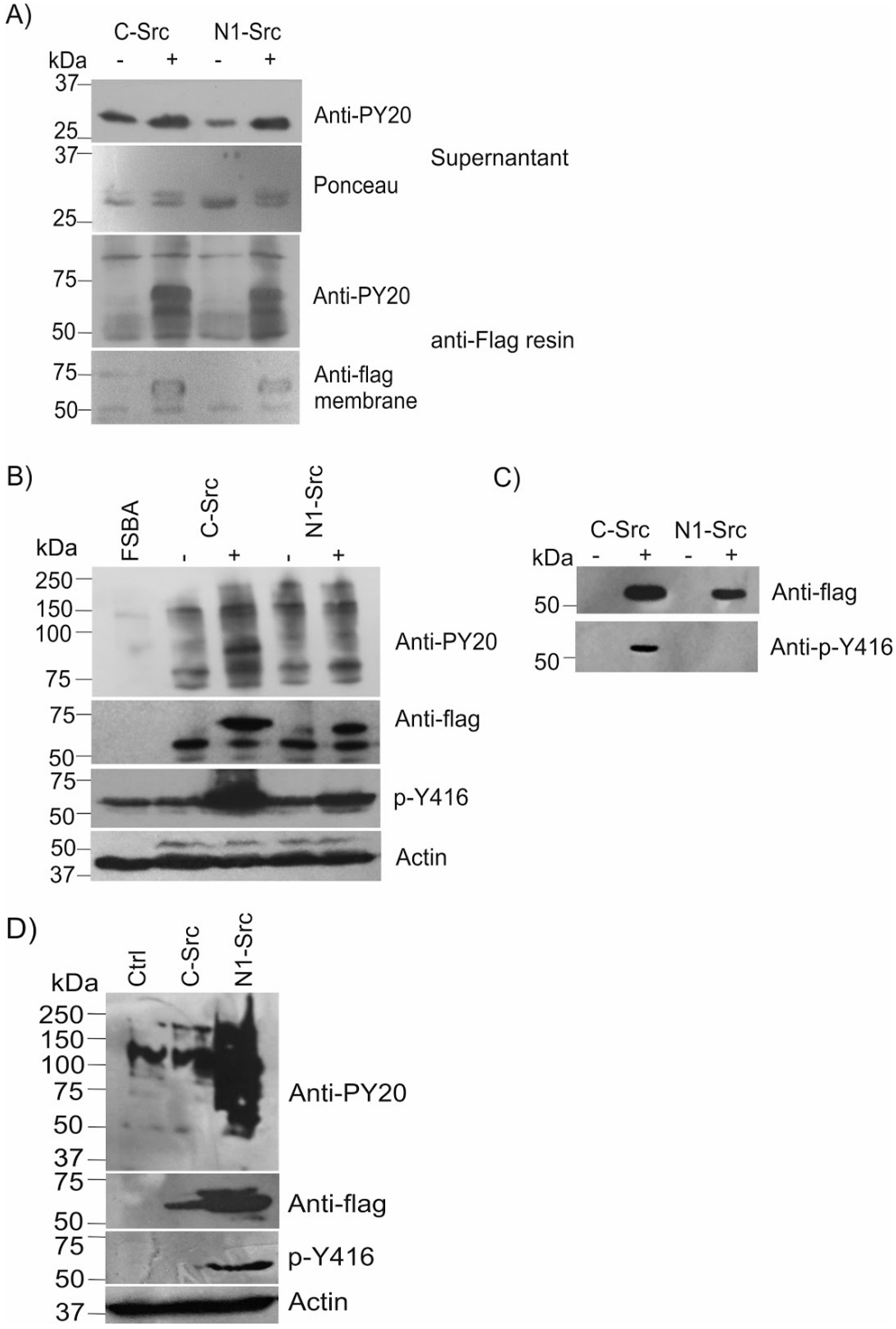

Figure 5.8 *In vitro* kinase assays with purified cellular C- and N1-Src kinases. A) *In vitro* phosphorylation of a GST-tagged Src peptide substrate by C- and N1-Src-FLAG immunoprecipitated from HeLa cells. The kinases were immobilised on anti-Flag agarose conjugated resin and incubated with the GST-tagged ideal Src substrate peptide for 1 h at 30 °C. The resin was then pelleted by centrifugation, and the supernatant removed for analysis by phosphotyrosine Western blotting. The kinases were eluted off the resin in Laemmli sample buffer for analysis via Western blotting. B) *In vitro* phosphorylation in P1 rat brain lysates by C- and N1-Src-FLAG immunoprecipitated from HeLa cells. The P1 rat brain lysates were treated with FSBA, and the kinase assay conducted as described in Section 5.3.1. However, the immunoprecipitated C- and

N1-Src-FLAG kinases on anti-Flag agarose-conjugated resin were supplemented into the assay as oppose to the recombinant kinases, and incubated for 1 h at 30 °C. The assay was terminated with Laemmli sample buffer, and assayed via Western blotting. C) Assessment of C- and N1-Src-FLAG p-Y416 content upon purification from HeLa cells, and prior to supplementation into the *in vitro* kinase assay described in Section B. A fraction of kinase on resin was added to Laemmli sample buffer to enable analysis via Western blotting for Src (anti-Flag) and p-Y416 content. D) C- and N1-Src-FLAG were transfected into B104 cells for 48 h followed by lysis in Laemmli sample buffer. The lysate was assessed via Western blotting for phosphotyrosine (anti-PY20), Src p-Y416 content, Src expression (anti-Flag), and actin as a loading control.

5.4 Discussion

The primary aim of this chapter was to identify the substrates of C- and N1-Src kinase in the developing brain as N1-Src has no characterised *in vivo* substrates, and only three putative substrates. The secondary aims were to compare and contrast the C- and N1-Src SH3 domain interactomes with their phosphoproteomes to assess whether any SH3 ligands were also phosphorylated. In addition, bioinformatics analyses were utilised to identify functional enrichments within the N1-Src phosphoproteins that may explain or shed further light on the function of N1-Src in neurons.

In total, 260 and 239 *in vitro* substrates were identified for C- and N1-Src respectively, and these proteins enriched for GO terms spanning neuronal functions that included morphology, differentiation and development. Furthermore, a number of C- and N1-Src SH3 domain ligands (Chapter 3) were tyrosine phosphorylated, and these should be considered primary candidates for follow up studies. Indeed, one of these proteins, Neuronal Enah, appeared to be phosphorylated by N1-Src *in vivo* (Chapter 3). While N1-Src overexpressed in neuroblastoma cells was highly active, and raised cellular substrate phosphorylation, the *in vitro* activity of recombinant N1-Src, and N1-Src purified from HeLa cells, was less than that of C-Src, and this is likely reflective of differential regulation and activation in neuronal and non-neuronal cells.

FSBA-based detection of *in vitro* kinase substrates

The FSBA-based method pioneered by (Knight et al. 2012), has since been adopted in other studies (Xue et al. 2013; Müller et al. 2016). In this study, FSBA enabled the direct identification of N1-Src substrates and their phosphorylation sites in a developmental neuronal lysate. Whereas cellular studies would require N1-Src expression in heterologous cells, resulting in the loss of neuronal structures and neuronal specific proteins. FSBA was an effective inhibitor of endogenous kinases, and combined with the low levels of basal tyrosine phosphorylation in the lysate (Fig.5.2), and the small amount of lysate required (2.5 mg), this paradigm proved to be ideal for the identification of Src substrates. The identification of many previously characterised C-Src substrates validated the approach (Fig.5.4B), and a Weblogo motif of the C-Src phosphorylation sites identified a Src-like consensus motif (Miller 2003), suggesting that the kinase domain was functioning with specificity (Fig.5.4C).

A caveat, as observed by (Knight et al. 2012), is that the specificity of phosphorylation appears to be determined only by the catalytic domain and not the SH2/SH3 domain ligand interactions, as C- and N1-Src phosphorylated the majority of the same proteins, despite the limited SH3 domain interactome of N1-Src (Chapter 3). As the C- and N1-Src SH2 domains are identical, they could direct equivalent protein interactions, however, it would be surprising for all substrates to possess a Src SH2 ligand motif. Thus, the assay appears to override the *in vivo* requirements of SH2/SH3 docking. This is not surprising, as the *in vitro* phosphorylation of Src substrates, such as enolase, are unaffected by manipulation of the Src SH3 domain (Shen et al., 1999). Thus the method appears to be an excellent tool for identifying a kinase's *in vitro* substrates but not for discriminating between isoforms with identical catalytic domains.

Improvements to the method could include the pre-incubation of C- and N1-Src with ATP to enhance auto-phosphorylation, and in turn substrate phosphorylation. However, this was not hugely detrimental as C- and N1-Src were still assigned 260 and 239 *in vitro* substrates respectively, and specific tyrosine phosphorylation site(s) were identified for more than 70 % of these. The PhosphoSite database contains 298 Src substrates, a number that is rivalled by this single study. This is unsurprising, given the ubiquitous expression and broad functions of C-Src (Section 1.3). However, it's possible that some proteins are *in vitro* artefacts, or phosphorylated due to sharing a common kinase substrate motif. A unique N1-Src phosphoproteome was not identified, however, it is likely that C- and N1-Src have differential substrates *in vivo* due to their variable developmental expression and cellular localization within neurons (Section 1.3.7), resulting in exposure to unique substrate pools. This was also observed by (Knight et al., 2012) as the MAPK isoforms (p38 alpha/beta) did not have unique substrates *in vitro*, but showed clear differential localisation in cells.

Phosphorylation of Src SH3 domain ligands by C- and N1-Src

Src substrates containing SH2/SH3 domain ligand motifs are considered more likely to be physiological substrates due to the potential of the kinase to dock and subsequently phosphorylate (Shen et al. 1999). Excitingly, a number of C- and N1-Src SH3 domain ligands in the P1 lysate (Chapter 3) were also phosphorylated (Table 5.1).

Fifteen C-Src SH3 domain ligands (8.5 %) were phosphorylated and six of the N1-Src SH3 domain ligands (18 %), Caskin1, Neuronal-Enah, Sfpq, Sh3pxd2b, Srcin1 and

Zc2hc1a (Table 5.1). Sfpq has been detected as a Src substrate in a cellular phosphoproteomics study (Amanchy et al. 2008). Interestingly, Zc2hc1a has not been reported as tyrosine phosphorylated in curated phosphoproteomic databases (PhosphoSite) and the protein is uncharacterised. Neuronal-Enah is also poorly characterised, however it was identified as the tyrosine phosphorylated form of Enah in the embryonic brain (Gertler et al. 1996). While the *in vitro* phosphorylation site(s) for Enah were not identified, preliminary assays in B104 cells identified it as potentially phosphorylated by N1-Src (Chapter 3). Thus, proteins that are both SH3 domain ligands and *in vitro* substrates, can successfully yield *in vivo* substrates.

A further nine N1-Src SH3 domain ligands, Asap1, Cbl, Dnm I, Dnm II, N-WASP, Raph1, Sf3b2, Syn1 and Wasf1 are bona fide Src substrates (Brown et al. 1998; Miyazaki et al. 2004; Ahn et al. 2002; Ahn et al. 1999; Suetsugu et al. 2002; Carmona et al. 2016; Amanchy et al. 2008; Messa et al. 2010; Ardern et al. 2006), but were not detected in this assay. This might be due to factors such as low abundance and phosphorylation stoichiometry, in addition, the phosphopeptides may not be sufficiently ionised, or the phosphorylation site might not be flanked by trypsin cleavage sites. Despite this, 45 % of the N1-Src SH3 domain ligands have the potential to be phosphorylated by Src. Considering N1-Src's enhanced constitutive kinase activity in neurons, it could be speculated that N1-Src has evolved for a prominent role in phosphorylation, over functions such as scaffolding and directing cellular localisation. However, it is unclear how many of the GST-C-Src SH3 domain ligands are direct interactors, as opposed to part of a complex (Fig.3.7). Thus it is unknown whether C-Src is capable of phosphorylating an equivalent percentage of SH3 domain ligands.

To further highlight *in vivo* N1-Src targets, neuroblastoma or primary neurons cells transfected/infected with N1-Src could be treated with cAMP or retinoic acid and induced to differentiate. The significantly up-regulated phosphopeptides in comparison to the control cells could be identified via LC-MS/MS. Furthermore, in order to identify direct N1-Src phosphorylation events, a fraction of the control lysate could be treated with phosphatase (if required), and then FSBA, followed by incubation with recombinant N1-Src for LC-MS/MS analysis. Direct phosphorylation events that were identified *in vitro* and *in vivo* would be considered strong candidates for follow up studies. A similar approach is described by (Knight et al. 2012) whereby FSBA and

recombinant kinase was utilised on kinase inhibitor treated cell lysates to rescue phosphorylation events observed in the control.

Additional auto-phosphorylation within the Src kinase domain

Interestingly, two other phosphorylation sites within the kinase domain, Y439 and Y338 were identified. As endogenous kinases within the lysate were inhibited by FSBA, the phosphorylation is likely via autophosphorylation by the Src kinases, especially as both phosphorylation sites are increased for C-Src, in line with the trend of the dataset, and despite C- and N1-Src been at equal concentrations. The phosphorylation sites have been previously detected, however neither have been confirmed as auto-phosphorylation. The p-Y338 modification on its own did not appear to promote catalytic activity (Barker et al. 1995), and p-Y439 was significantly increased by C-Src expression in cells (Ferrando et al. 2012), although a function has not been assigned.

Functional enrichment of neuronal processes and phosphoproteins

GO term enrichment analysis of the phosphoproteins was conducted in an unbiased manner as no information was provided regarding the cell/tissue lysate of analysis. Therefore, it was encouraging to see core neuronal functions significantly enriched by both C- and N1-Src, including neuronal structures (myelin sheath, synapse, axon, growth cone) (Fig.5.6), consistent with N1-Src's neuronal-specific expression and localisation in dendrites and axons (Sugrue et al., 1990), as well as the increase of phosphoproteins in the dendrites, cell body and axon upon N1-Src expression in retinal neurons (Worley et al., 1997). The GO terms 'neuron differentiation' and 'neuron development' are in-line with N1-Src's function in neuroblastoma differentiation (Section 1.4.4) (Matsunaga et al. 1993). Furthermore, our lab recently implicated N1-Src in primary neurogenesis (Lewis et al., 2017), and this GO term was enriched (FDR 6.59E-07). The *in vitro* substrate Sox11 is an interesting candidate as the transcription factor is essential for neurogenesis (Wang et al. 2013; Haslinger et al. 2009; Bergsland et al. 2006).

N1-Src induces morphological changes to neurites upon overexpression and knockdown in neurons and heterologous cells (Keenan et al. 2017; Wetherill 2016; Worley et al. 1997) (Section 1.4.4). Furthermore, the cerebellar Purkinje neurons from a constitutively active N1-Src transgenic mouse presented morphological abnormalities of the microtubules (Kotani et al., 2007). Thus, it was encouraging to identify a number of

microtubule associated phosphoproteins including Mapt, Map2, Map6, Map1b, Tuba1a, Clasp1/2 and Cep170b. Map6 possesses multiple calmodulin binding sites, and calmodulin binding inhibits its microtubule stabilising activity (Lefèvre et al. 2013). The Map6 phosphorylation site p-Y539 is found within one of the calmodulin binding motifs (Bosc et al. 2001). The sites p-Y521 and p-Y299 of Clasp1/2 respectively, are also found within domains that interact with microtubule dimers (Al-Bassam and Chang 2011).

Actin cytoskeletal regulators were also *in vitro* phosphorylated including Actg1, Arhgdia, Arpc3, Cfl1, Fnbp1l, RhoA and Pfn2 (Table 5.1, Fig.5.9). The phosphorylation site p-Y68 of Cofilin 1 promotes its degradation and prevents actin cytoskeletal remodelling that leads to cell spreading (Yoo et al. 2010). Additional morphological regulators include TMEM106B, an integral membrane glycoprotein which controls dendritic morphogenesis through lysosome trafficking (Schwenk et al. 2014). Interestingly, the Src *in vitro* phosphorylation site (p-Y51) has been detected *in vivo* (PhosphoSite), and occurs within the cytosolic domain which mediates interactions with cytoskeletal and trafficking proteins (Kang et al. 2018). Rtn4, an inhibitor of neurite outgrowth was also phosphorylated (Sepe et al. 2014).

Proteins that regulate Src splicing and catalytic activity were also phosphorylated, including Khsrp1 and HnrnpH1 both of which are implicated with positive regulation of N1-Src splicing (Section 1.4.3). Whilst these proteins have diverse roles in splicing, it is interesting to consider if N1-Src could regulate its own splicing through such phosphoproteins. In addition, PTPn1, also known as PTP-1B, is a phosphatase that positively regulates Src activity by dephosphorylation of p-Y527 (Section.1.2.6).

The role of C-Src in signalling downstream of neuronal channels and receptors was discussed in Section 1.3. A number of these molecules were *in vitro* phosphorylated by N1-Src, including the DCC receptor, neural cell adhesion molecule 1 (NCAM1), the ephrin receptor Epha3, and the ephrin receptor ligands EfnB1/B3. Furthermore, the AMPA receptor subunit Gria2 was phosphorylated, as well as the AMPA receptor regulator, Cacng8. L1-CAM was also detected as tyrosine phosphorylated, and N1-Src has been implicated in neurite outgrowth by L1-CAM (Keenan et al. 2017) (Table 5.1, Fig.5.9). Thus, many of the phosphoproteins are in-line with the cellular functions of Src in the brain and, as discussed in Section 1.3, a number of early studies failed to

distinguish between C-Src and N1/N2-Src, thus it is possible that some of the functions are attributable to N1-Src.

Interestingly, the C- and N1-Src phosphoproteins enriched for the GO term Poly(A) RNA binding, consistent with the GST-C- and N1-Src SH3 domain pull-downs (Chapter 3). Furthermore, the mRNA processing and spliceosome proteins, Snrpa1, Sf3b1, Sf3a1, Sf1, Hnrnpk, Raver1 and Sfpq were identified in both the phosphoproteomics and SH3 domain ligand screen. Sf3b2 and Sfpq were identified in an *in vivo* C-Src phosphoproteomics study (Amanchy et al. 2008). N1-Src has not been detected in the nucleus by immunocytochemistry, and it remains unclear whether the interaction and phosphorylation of these proteins is an *in vitro* artefact or if N1-Src is impinging on RNA regulation and splicing. A high frequency of splicing occurs during nervous system development and differentiation (Su et al. 2018), and considering the cellular functions of N1-Src in neurogenesis and differentiation (Lewis et al. 2017), it is not unreasonable to predict that N1-Src could be regulating RNA. The Evans lab is currently investigating the role of N1-Src in splicing using mini-gene reporters.

A summary of the 170 N1-Src phosphoproteins that were assigned a specific phosphorylation site are shown in Fig.5.9. The proteins were manually classified into categories spanning cellular functions and compartments via their Uniprot, GeneCards and STRING annotations. The phosphorylation sites that have been identified *in vivo* (PhosphoSite) are underlined. Encouragingly, many of the *in vitro* phosphorylation sites have been identified *in vivo* (Fig.5.9). Overall the *in vitro* Src substrates span signal transduction, cytoskeletal dynamics (Rho GTPases, actin and tubulin), axon guidance (L1-CAM, N1-CAM, Ephrin) and RNA regulation (Fig.5.9).

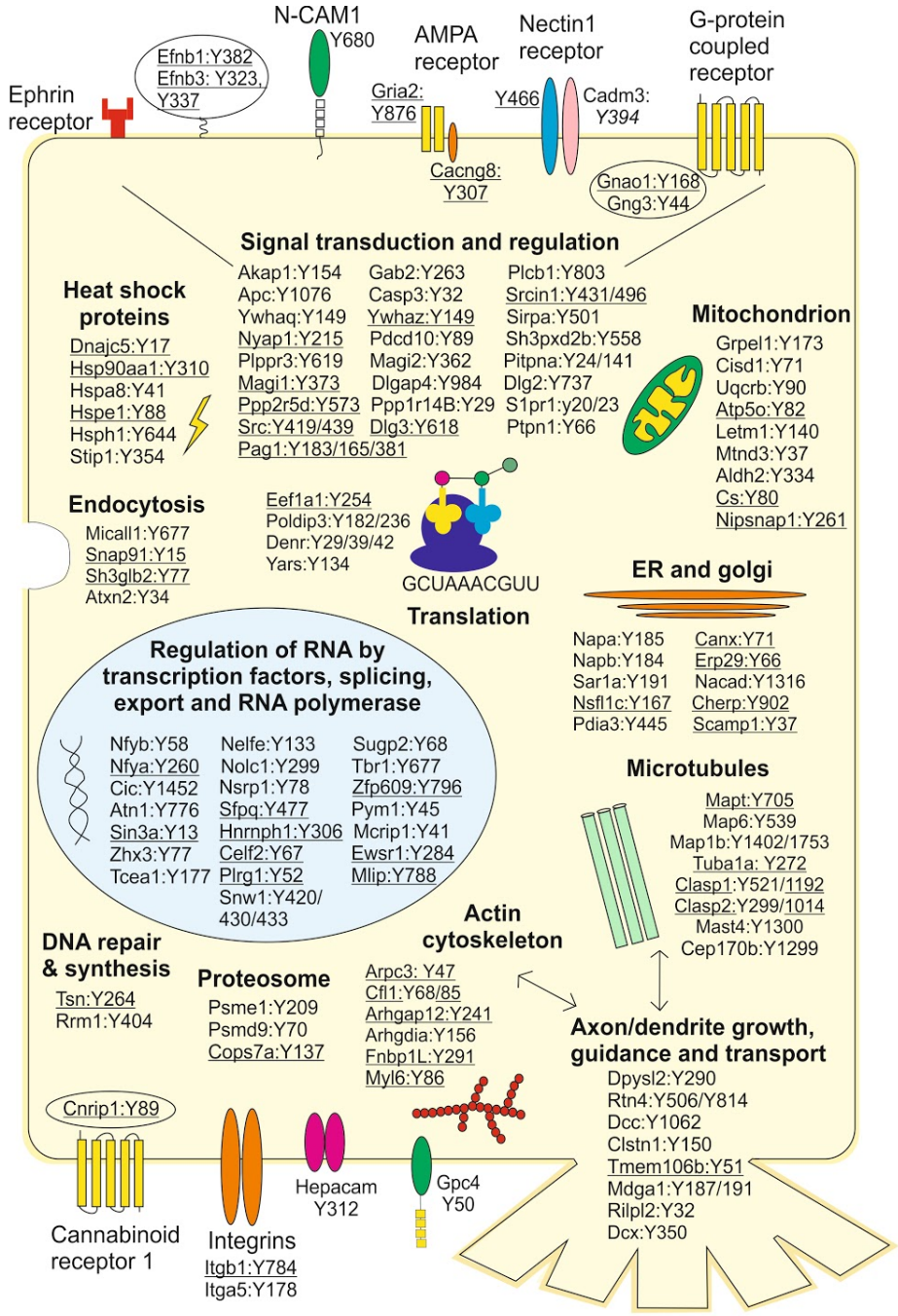

Unassigned

Acp1:Y143, Alb:Y419/425, Aldoc:Y357, Ambp:Y343, Ashwin:Y53, Atxn2l:Y116, Ccdc177:Y131 Cdv3:Y213, Ckap4:Y53, Cnpy3:Y76, Cpd:Y1372, Cxadr:Y318,Dcbld2:Y744, Dek:Y354, Gapdh:Y92 , Glcci1:Y64, Gmds:Y159, Gpx1:Y147, Gyg1:Y315, Hcfc1:Y111, Itpa:Y164, Kng1:Y72, Lancl1:Y13, Lgalsl:Y25, Lin7c:Y58, Naxe:Y279, Nme1:Y151, Ntmt1:Y215/218, Pgk1:Y161, Pgrmc1:Y113, Pithd1:Y96, Prkrip1:Y82, Prrc2b:Y1496,RGD1306271:Y1157, RGD1311703:Y84,RGD1560065:Y131,RGD1561636:Y43,Rnf113A:Y118,Serpina10:Y400,SH3bgrl:Y92, Sh3glb1:Y80/100, Spata2:Y478,Tex2:Y299,Timp2:Y62, Tkt:Y202, Tmpo:Y350, Wdr70:Y619,Xpnpep1:Y412, Zc2hc1a:Y119/124

Figure 5.9 Functional characterisation of the *in vitro* N1-Src substrates assigned a specific phosphorylation site. The 170 N1-Src proteins that were assigned a specific phosphorylation site are shown. The proteins were categorised based on their functional annotations in Uniprot, GeneCards and STRING. Proteins for which the phosphorylation site was identified *in vivo* (PhosphoSite) are underlined. Diverse multi-functional proteins and uncharacterised proteins are listed as unassigned.

Reduced auto- and substrate phosphorylation by N1-Src

N1-Src phosphorylated substrates in the P1 lysates to a lesser extent than C-Src (Fig.5.2/3/7). This was surprising as N1-Src displays high levels of autophosphorylation in neurons (Brugge et al. 1985) and upon expression in heterologous cells raises tyrosine phosphorylation above C-Src (Worley et al. 1997; Levy and Brugge 1989). However, the Δ80 recombinant N1-Src lacks the SH4 and unique domain, and wild-type regulation as it is bacterially expressed. Whilst the phosphorylation activity of recombinant N1-Src may not be fully representative of its *in vivo* behaviour, it does not explain why its phosphorylation is reduced in comparison to C-Src, as both kinases are Δ80, thus the only difference is the six residue N1-Src insertion in the SH3 domain.

Autophosphorylation of Y419 stabilises Src's catalytically active state (Section 1.2.5), and reduced autophosphorylation could decrease substrate phosphorylation. Indeed, whilst not statistically significant, the relative abundance of the auto-phosphorylated peptide was 83:17 for C:N1-Src respectively. As C- and N1-Src are purified fused to a phosphatase (PTP1B), and do not have detectable auto-phosphorylation following purification (Keenan et al. 2015), this is not believed to be due to differences in auto-phosphorylation prior to the P1 assay.

An unlikely explanation is an inhibitory factor within the P1 lysate with selectivity for N1-Src. For example Chk inhibits active SFKs through protein-protein interactions (Advani et al. 2017). However, as N1-Src does not have any unique SH3 domain interactors (Chapter 3) and the SH2, kinase and C-terminal tail are identical to C-Src, it is unclear how N1-Src would be targeted selectively. In addition, the FSBA treatment, and phosphatase inhibitor vanadate should have suppressed endogenous kinases and phosphatases that regulate Src. However, an alternative cellular lysate could be trialled to assess if there is a factor within the P1 lysates. Despite having an identical kinase domain to C-Src, N1-Src could be increasingly sensitive to any residual FSBA that is not removed by desalting, as it has a reduced affinity SH3:linker interaction (Keenan et al. 2015), and this is proposed to result in a less restrained catalytic domain. Thus the N1-Src kinase domain may be more accessible to FSBA. In addition, N1-Src could be negatively regulated by the *in vitro* autophosphorylation of Y527 to promote the negative regulatory conformation. However, it is unclear why N1-Src would show preference to this site over C-Src. Furthermore, the p-Y527 phosphopeptide was not

detected for C- or N1-Src by mass spectrometry or for N1-Src by Western blotting of an *in vitro* kinase assay (Fig.5.7D).

The assay does not appear to require SH2/SH3 docking to direct substrate phosphorylation. However, the addition of SH2/SH3 domain peptide ligands to recombinant SFKs increases substrate phosphorylation (Keenan et al. 2015; Moarefi et al. 1997) via activatory interactions, that relieve the negative regulatory conformation and promote auto-phosphorylation (Section 1.2.7). As the C- and N1-Src SH2 domains are identical, and p-Y527 was not detected in the Src constructs, the main mode of negative regulation is likely that of the SH3:linker. As the N1-Src SH3 domain has both less and weaker interactions than C-Src (Chapter 3/4), this could result in less positive regulation by the SH3 domain. Indeed, (Moroco et al. 2014) showed that C-Src was activated by a SH3 domain peptide ligand, which continued to activate the auto-phosphorylated kinase as it remained under allosteric control by the linker. Thus, the raised auto- and substrate phosphorylation of C-Src could be a result of its higher affinity SH3 domain interactions. To investigate the role of the SH3 domain on N1-Src activity, the kinase assay could be conducted with mutants including the SH2:SH1 linker, inactivating SH2 and SH3 domain mutants, and SH2/SH3 domain activatory peptide ligands. This could also explain why the GST-tagged ideal Src substrate did not show as great difference in phosphorylation by C- and N1-Src (Fig.5.3B), as the phosphorylation of the micromolar concentration substrate could be reflective of the affinity of the kinase domain, whereas at lower concentrations in the P1 lysate, other regulatory interactions may be at play.

Interestingly, full length N1-Src purified from HeLa cells also did not raise substrate phosphorylation in the P1 lysate kinase assay (Fig.5.8B). This could support the proposal of a N1-Src inhibitory factor within the lysate, or an increased sensitivity to FSBA. However, the auto-phosphorylation of N1-Src did not appear to be in excess of C-Src directly after purification from the HeLa cells (Fig.5.8C). Previously studies have failed to identify raised auto-phosphorylation by N1-Src in heterologous cells (Wetherill 2016; Levy and Brugge 1989). This could be due to factors such as a varying regulation by kinases and phosphatases (Section 1.2.6/7), or even that auto-phosphorylation is dependent on expression levels. N1-Src purified from cultured neurons or neuronal cell lines would be more appropriate as its activity is more representative of that in the brain

(Fig.5.8D). This reaffirms that caution should be exercised when studying N1-Src in heterologous cells.

Concluding remarks

This study has provided a detailed catalogue of Src substrates in the developing brain, and has taken the number of putative N1-Src *in vitro* substrates from three to two hundred and thirty nine. In addition, two potentially novel auto-phosphorylation sites within the kinase domain were identified. Regarding candidate substrates to investigate further, proteins that were also identified as SH3 domain binders should be given more weight due to their potential to dock and recruit the kinases *in vivo*, as exemplified by Neuronal Enah and N1-Src (Chapter 3). Initial lines of enquiry would likely include confirmation of the interactions via immunoprecipitation, and *in vivo* phosphorylation, followed by functional assays which could include phospho-null and -mimetic mutants.

Furthermore, this study identified both reduced *in vitro* auto- and substrate phosphorylation by N1-Src in the P1 brain lysate, and this is likely reflective of differential regulation of N1-Src, for example it could be lacking SH3 domain-based activatory interactions.

Chapter 6

Conclusions and future directions

Chapter 6 Conclusions and future directions

N1-Src possesses diverse cellular functions including neuronal differentiation, cytoskeletal remodelling, neurite outgrowth and neurogenesis (Lewis et al. 2017; Kotani et al. 2007; Matsunaga et al. 1993; Keenan et al. 2017). However, it is poorly characterised in terms of the SH2/SH3 domain ligands, substrates and signalling pathways driving these cellular functions. This study therefore investigated three core features regarding the function of N1-Src in comparison to C-Src. These were i) the SH3 domain ligands of N1-Src, ii) the substrates of N1-Src, and iii) the N1-Src SH3 domain ligand consensus and mechanism of ligand binding. The outcomes of which are discussed below.

6.1 The N1-Src SH3 domain interacts with a subset of C-Src ligands

Prior to this study, the N1-Src SH3 domain interactome was poorly characterised, with only five putative *in vitro* ligands, which were unlikely to explain its diverse neuronal functions. As the N1-Src SH3 domain contains a six residue insertion (RKVDVR) in its ligand binding n-Src loop, it was hypothesised that N1-Src has unique ligands and substrates that in turn drive unique cellular functions. LC-MS/MS analysis of the GST-C- and N1-Src SH3 domain pull-downs from postnatal day 1 rat brain revealed that surprisingly N1-Src had no unique SH3 domain ligands, and instead its 33 ligands were a subset of the 176 C-Src ligands. It is possible that some unique low affinity ligands were overlooked as pull-downs enrich for high affinity interactions. However, it is logical for N1-Src to have a reduced set of ligands considering its neuronal-specific expression in comparison to the ubiquitous expression of C-Src. Furthermore, the N1-Src ligands were enriched for actin cytoskeletal remodelling factors, in-line with its cellular functions in neurite outgrowth (Keenan et al. 2017; Kotani et al. 2007), and contained two of its previously identified interactors dynamin I and EVL (Abdelhameed 2010; Lambrechts et al. 2000).

Possessing equivalent SH3 domain ligands does not necessarily equate to C- and N1-Src having the same functions, and it was discussed in Chapter 1 how C- and N1-Src have differential development expression and cellular localisation (Wiestler and Walter 1988; Atsumi et al. 1993; Pyper and Bolen 1990; Ross et al. 1988; Sugrue et al. 1990). Thus, they may not encounter the same ligands despite having the capacity to interact, alternatively, they might encounter the same ligand but under different signalling

contexts. Indeed, cellular studies comparing C- and N1-Src have demonstrated that the kinases possess differential functions in axon guidance and neurite outgrowth (Keenan et al. 2017; Wetherill 2016; Worley et al. 1997). In addition, this study provided evidence that C- and N1-Src can interact with the same ligands differentially *in vitro*. For example, while C- and N1-Src both bound Enah and Neuronal Enah, N1-Src showed a preference for the Neuronal Enah variant. Similarly, the N1-Src SH3 domain selected for dynamin I lacking phosphorylated S774, which occurs upon synaptic stimulation, however the phosphorylation event has not yet been shown to be casual in disrupting binding. Thus, differential binding could define unique signalling events for the two kinases. As the peptide arrays identified C- and N1-Src SH3 domain interacting motifs within the ligands dynamin I/III, N-WASP and Enah, mutation of these sites could potentially be used to abolish the interactions with C- and N1-Src and aid in dissecting their signalling pathways.

6.2 N1-Src splicing reduces the affinity of the SH3 domain

Previous studies demonstrated that the N1-Src SH3 domain bound weakly with, or failed to interact with, C-Src SH3 domain ligands (Messina et al. 2003; Craggs et al. 2001; Richnau and Aspenström 2001; Reynolds et al. 2008), suggesting it was tailored and possessed a lower affinity. Multiple experimental approaches used in this study support this finding. Firstly, the GST-C- and N1-Src SH3 domain pulldowns revealed that via LC-MS/MS label-free quantification, 11 of the 33 N1-Src SH3 domain ligands had a significantly enhanced interaction with the C-Src SH3 domain. Western blotting of a selection of the C- and N1-Src SH3 domain ligands also confirmed that they interacted with N1-Src to a lesser extent. In addition, in order to detect binding by the N1-Src SH3 domain to arrayed peptides, its concentration had to be increased and the incubations conducted under less stringent conditions in comparison to C-Src. Direct evidence that the N1-Src SH3 domain is lower affinity was obtained by NMR, in which titrations of the same peptide ligand with the C- or N1-Src SH3 domain, demonstrated that the N1-Src SH3 domain had a larger K_d.

Interestingly, (Keenan et al. 2015) utilised an *in vitro* kinase assay with C- and N1-Src in order to investigate SH3 domain interactions via a read-out of substrate phosphorylation. The coupling of a Src substrate motif to Class I/II SH3 domain ligand motifs enhanced phosphorylation by C-Src but not N1-Src, which in part led to the hypothesis of the

N1-Src SH3 domain having a unique interactome. However, this result was likely due to N1-Src having a lower affinity for these motifs.

It is interesting to consider the *in vivo* implications of a lower affinity SH3 domain, for example, could N1-Src be less likely to participate in stable interactions and have a higher substrate turnover? Indeed, N1-Src has an enhanced constitutive kinase activity *in vivo* (Levy and Brugge 1989; Worley et al. 1997). The N1-Src SH3 domain has a reduced affinity interaction with the SH2:SH1 regulatory linker peptide compared to C-Src (Keenan et al. 2015), which could relieve its negative regulation and explain its increased auto-phosphorylation. Thus the main purpose of the SH3 domain insertion could be to render N1-Src a 'primed' kinase, and reduced ligand affinity occurs at the expense of this.

The reduction in affinity and interactome of the N1-Src SH3 domain might impose increased control on N1-Src by its SH2 domain. Indeed, the N1-Src Y527F mutant had enhanced cellular phosphorylation (Worley et al. 1997) and an N1-Src SH2 domain mutant greatly reduced kinase autophosphorylation (Groveman et al. 2011), suggesting that N1-Src is under both positive and negative regulatory control by its SH2 domain. Thus, it is essential to consider the N1-Src SH3 domain in conjunction with the SH2 domain with regard to kinase activity and ligand binding. C- and N1-Src kinase mutants spanning the SH3, SH2 and C-terminal region could be used to compare parameters including p-Y416, p-Y527, and relative substrate phosphorylation on a lysate wide scale or using a specific transfected substrate in cells, in order to compare the relative contributions of the SH2 and SH3 domains between the kinases.

The *in vitro* phosphoproteomics study (Chapter 5) also provided evidence for differential regulation of C- and N1-Src kinase, as recombinant N1-Src failed to auto-phosphorylate and conduct substrate phosphorylation in excess of C-Src (Fig.5.5), contrary to previous studies in the literature. The main mode of kinase regulation in the assay would likely be via the SH3 domain as Y527 is not phosphorylated in the purified kinases. As the N1-Src SH3 domain was shown to bind ligand with a lowered affinity, it may be a result of reduced SH3 domain based activation via ligand interactions.

6.3 The N1-Src SH3 domain appears to show preference for canonical Class I and II SH3 domain ligand motifs

Indirect evidence that the N1-Src SH3 domain binds canonical Class I/II SH3 domain ligand motifs was obtained by the GST-N1-Src SH3 domain pulldowns, as the ligands were rich in Class I/II motifs in comparison to the GST control. This was further supported by the peptide arrays as all but one of the peptides bound by the N1-Src SH3 domain contained either a Class I/II motif or both. Furthermore, mutation of the proline residues to alanine within the Class I/II peptides was able to abolish binding to the N1-Src SH3 domain, suggesting that N1-Src was selecting for proline to at least some extent. NMR analysis also confirmed a direct interaction between the N1-Src SH3 domain and dynamin I B8 peptide that contains two Class II SH3 domain motifs. Thus, these data are in-line with a recent phage display study that demonstrated N1-Src interacts with canonical Class I motifs (Teyra et al. 2017).

Peptide arrays or NMR analysis could be conducted with alanine scanning mutagenesis of peptides including those with arginine mutations to remove the Class I/II motifs. This could provide insight into the overall motif preference of N1-Src and whether it is selecting for Class I/II motifs. Solving the structure of the peptide bound N1-Src SH3 domain would also demonstrate if and how N1-Src is binding Class I/II motifs. However, considering that N1-Src interacts with a subset of C-Src ligands, it is not unreasonable to suggest that they interact with a similar motif, and that the neuronal insertion might slightly alter binding as opposed to conferring a unique consensus.

6.4 N1-Src SH3 domain ligands are phosphorylated by N1-Src *in vitro* and *in vivo*

The pull-down experiment identified Caskin1, Neuronal Enah, Sh3pxd2b, Sfpq, Srcin1 and Zc2hc1a as N1-Src SH3 domain ligands. The role of SH3 domain ligand interactions in directing Src substrate phosphorylation is well-documented (Shen et al. 1999; Weng et al. 1994), thus it was exciting to also identify these proteins as *in vitro* N1-Src substrates. Furthermore, the specific tyrosine phosphorylation site(s) were mapped for Sfpq, Zc2hc1a and Sh3pxd2b, thus enabling follow up studies with phospho-null and phospho-mimetic mutants of these putative N1-Src substrates.

While the specific *in vitro* phosphorylation site(s) were not identified for Neuronal Enah, preliminary assays in B104 cells identified a prominent phosphotyrosine signal at the electrophoretic mobility of GFP-Neuronal Enah, which only occured upon

co-transfection of Neuronal Enah and N1-Src. This either represents direct phosphorylation of Neuronal Enah or signalling by N1-Src and Neuronal Enah that induced the phosphorylation of a protein at the same electrophoretic mobility as Neuronal Enah. Either explanation represents an exciting preliminary result in terms of an *in vivo* interaction between the two. Neuronal Enah is poorly characterised but is predicted to have a role in axon guidance (Gertler et al. 1996), which is also one of the functions of N1-Src (Worley et al. 1997), and this could be an initial line of investigation via neurite outgrowth assays. Identification of the *in vivo* Neuronal Enah phosphorylation sites via LC-MS/MS would also aid in the introduction of phosphorylation site mutants into such assays. Interestingly, the Neuronal Enah phosphopeptides that were significantly upregulated in the *in vitro* phosphoproteomics were those from the Neuronal Enah insertion in the proline rich domain. While the ligands of the Neuronal Enah PRD are currently unknown, it could represent a mechanism for phosphorylated Neuronal Enah to modulate its interactions with SH3 domain containing proteins, including C- and N1-Src and/or cytoskeletal regulators that also contain proline binding domains.

6.5 A putative function of N1-Src in RNA regulation

The N1-Src SH3 domain interacted with the paraspeckle and mRNA cleavage factor complex, and its ligands significantly enriched for the GO term ‘mRNA processing’. Interestingly, the *in vitro* N1-Src substrates mirrored this result as they significantly enriched for the GO term ‘poly(A) RNA binding’. C-Src has been associated with RNA regulation via the slowing down of splicing reactions, and the regulation of RNA export (Neel et al. 1995). Interestingly, via a C-Src ΔSH3/Y527F mutant, it was proposed that the SH3 domain did not direct RNA regulation (Gondran and Dautry 1999). However, it's possible that the overexpression of constitutively active Src is able to override some physiological requirements. Furthermore, C-Src enters the nucleus to carry out substrate phosphorylation (Paladino et al. 2016), and C-Src can impinge on RNA regulation through its substrate Sam68 as the *in vitro* interaction of the C-Src SH3 domain with Sam68 prevents its interaction with RNA (Taylor et al. 1995). Whilst it remains unknown whether the *in vitro* interactions and phosphorylation events of nuclear and RNA regulatory proteins by N1-Src are a physiological, as N1-Src has been implicated in neuronal differentiation and neurogenesis (Lewis et al. 2017) it would make sense for

N1-Src to have ligands and substrates involved in gene expression regulation. The Evans lab is currently collaborating to assess the role of N1-Src on the transcriptional landscape via knockdown of N1-Src and RNA sequencing in *Xenopus tropicalis* embryos. Preliminary data from these studies have revealed that N1-Src knockdown led to the upregulation of a cluster of RNA splicing genes and there are many examples of alternative or mis-splicing events in these embryos.

The paraspeckle protein Sfpq has been detected outside of the nucleus where it has been associated with promoting neuronal axon survival via regulation of RNA pools (Cosker et al. 2016). Sfpq has been identified as an *in vivo* C-Src substrate (Amanchy et al. 2008), and *in vitro* N1-Src substrate in this study, suggesting it is a strong follow-up candidate. The tyrosine phosphorylation of Sfpq by the non-receptor tyrosine kinase Brk promoted its cytoplasmic localisation, and prevented its interactions with RNA (Lukong et al. 2009). Thus preliminary analysis with N1-Src and Sfpq could involve immunocytochemical analysis of localisation, and immunoprecipitation with phosphorylation site mutants could be used to assess if N1-Src interacts with and phosphorylates Sfpq *in vivo*. Pulldowns with poly (U) Sepharose could also be used to determine if N1-Src affects the interaction of Sfpq with RNA.

6.6 The role of the N1-Src SH3 domain in kinase regulation

The N1-Src insertion was shown to perturb the chemical environments of both the n-Src and RT loops via NMR analysis of the SH3 domain. The N1-Src SH3 domain RT loop adopts a similar chemical environment to that of the ligand-bound C-Src SH3 domain RT loop, and the conserved N1-Src insert residue R6ins was shown to be responsible for this. This led to the hypothesis that an intramolecular salt bridge between R6ins of the N1-Src insertion and D99 of the RT loop, results in the RT loop 'binding switch' being constitutively in the bound (Chapter 4). These data could explain some of the regulatory features of N1-Src, such as its raised auto-phosphorylation (Brugge et al. 1987), and catalytic activity (Worley et al. 1997), and reduced affinity interaction with the SH2:SH1 regulatory linker (Keenan et al. 2015). The C-Src SH3 domain n-Src loop residue D117, and the RT loop residues R95 and T96, all make direct negative regulatory contacts with the kinase domain, and are perturbed between the C- and N1-Src SH3 domains. In addition, R95 also contacts the SH2:SH1 regulatory linker (Xu et al. 1997). Thus it is possible that these negative regulatory interactions are disrupted in N1-Src. The RT loop

is essential for kinase regulation as replacement of R95 or T96, or mutation of R95 to a variety of amino acids, raises Src kinase activity *in vivo* (Kato et al. 1986; Potts et al. 1988). This could suggest that the RT loop 'bound' environment is a means of mimicking the ligand-bound SH3 domain, in order to disrupt the negative regulatory contacts with the kinase domain and SH2:SH1 linker, pushing N1-Src into a higher state of activity. Interestingly (Moroco et al. 2014) showed that *in vitro* auto-phosphorylated C-Src was still under negative regulatory control by the SH3:linker. Therefore, if the N1-Src SH3 domain interaction with the linker is disrupted, this could also explain how the autophosphorylated kinase is less regulated, and highly active. It is also tempting to speculate that reduced negative regulation could lower the activation threshold of N1-Src, and this could be why the N1-Src SH3 domain functions with lower affinity ligands. As the R6insA mutant results in the loss of the RT loop bound conformation, it would be interesting to introduce this mutation into full length N1-Src in cells, as it could be predicted to lower the auto- and substrate phosphorylation by the kinase. In addition, an R95 mutant would be expected to activate C-Src to a greater extent than N1-Src.

6.7 Why has neuronal splicing of Src evolved?

Neuronal development including neurite outgrowth and synapse formation are under tight transcriptional and post-translational control, and alternative splicing is prevalent in the vertebrate nervous system. Micro-exons are often found in protein-protein interaction domains in order to modulate ligand interactions for neuronal functions (Raj and Blencowe 2015) and splicing of the C-Src SH3 domain to yield N1-Src is a prime example. Neuronal splicing of proteins has been reported to alter their interactions (Irimia et al. 2014; Laurent et al. 2015; Tsyba et al. 2008), and neuronal splicing of intersectin 1 results in the isoform having both lowered and raised affinity for various intersectin 1 ligands (Tsyba et al. 2008). N1-Src also interacts with a subset of C-Src ligands, however in contrast, all of its interactions appear to be lower affinity. The *in vitro* N1-Src interactome comprises cytoskeletal remodelers and RNA regulatory proteins, and its *in vitro* substrates are those involved in the development, differentiation and morphology of neurons, in-line with its cellular functions (Lewis et al. 2017; Wetherill 2016; Kotani et al. 2007; Keenan et al. 2017). However, the purpose of its lowered affinity is less clear. As discussed, it could be responsible for N1-Src having a

higher substrate turnover, alternatively, it could be a means to regulate substrate phosphorylation. C-Src is ubiquitously expressed and has an abundance of SH2 and SH3 domain ligands and broad cellular functions. Therefore, it is not surprising that during neuronal development, a process essential for the function of an organism, whereby tightly controlled and timed signalling cascades occur, that a less promiscuous isoform of C-Src may take precedent. N1-Src might also be a means of temporal regulation of Src, as its splicing is positively regulated by neuronal PTB, which is expressed upon neuronal differentiation and controls ~25 % of neuronal alternative splicing events (Coutinho-Mansfield et al. 2007). Thus the purpose of N1-Src might be to link Src expression to the neuronal PTB-regulated cascade of transcripts that are required for neuronal differentiation and function, whilst also having N1-Src as a tailored Src that is optimal for sensitive neuronal functions. Furthermore, if N1-Src regulates neuronal splicing, it could have positive feedback on its own splicing, and possibly function in maintaining neuronal identity.

The evolution of the N2-Src splice variant is unclear. However, it is only expressed in mammals, suggesting that it has evolved for higher brain functions. Unlike N1-Src, N2-Src expression was not skewed towards the developing brain (Pyper and Bolen 1990), and upon neuroblastoma differentiation, N2-Src was proposed to have a role in the maturation of differentiated neurons (Matsunaga et al. 1993). This suggests that N2-Src may have a function in mature neurons. Furthermore, the auto- and substrate phosphorylation activity of N2-Src is higher than N1-Src (Keenan et al. 2015), and upon expression in *Xenopus*, N2-Src generated the most prominent larvae phenotype in comparison to C- and N1-Src (Lewis 2014). Thus X*enopus* may be lacking the means to regulate N2-Src. It is curious that the kinase activity of Src increases alongside nervous system complexity, for example, C-Src (invertebrates) < N1-Src (vertebrates) < N2-Src (mammals). The N2-Src SH3 domain interactome is likely further tailored from C- and N1-Src, and possibly even unique. Interestingly, R6ins, which is responsible for the 'bound' N1-Src RT loop, is mutated to serine at the NI-NII exon boundary, although N2-Src also contains an arginine residue at both ends of the 17 residue insert.

6.8 Final conclusions and future directions

This is the first study to employ high throughput screens to assess the neuronal interactome and phosphoproteome of N1-Src. In total, 31 novel *in vitro* N1-Src SH3

domain ligands and 239 *in vitro* substrates of N1-Src were identified, providing a foundation for the *in vivo* molecular characterisation of N1-Src. In particular, the SH3 domain ligands that were also substrates should be considered as strong candidates for follow-up studies. Indeed, preliminary evidence was obtained to suggest that the *in vitro* N1-Src SH3 domain ligand and substrate Neuronal Enah, is phosphorylated by N1-Src in cells. Furthermore, phosphoproteins found within the GO term 'neuron differentiation' could be candidates for investigating the signalling of N1-Src in neuroblastoma differentiation. The NMR analysis has provided insight into how the N1-Src insertion affects the RT loop, with implications for ligand binding and kinase activity. However, solving the structure of the N1-Src SH3 domain would now complement these data, and enable the characterisation of the binding site, including the function of the N1-Src insertion and how R6ins is impacting on the RT loop.

Advances in proteomics have provided a variety of techniques for the in depth characterisation of N1-Src, including *in vivo* phosphoproteomics, fusion proteins to enable proximity-dependent mapping and analysis of cellular localisation (Roux et al. 2012), and also the identification of *in vivo* interactions via photoreactive amino acids (Okada et al. 2011). Studies with full length N1-Src kinase are essential to understand how the SH3 domain functions in the context of the entire kinase, and in particular with the SH2 domain. This could include assays such as immunoprecipitation of ligands, and analysis of activation kinetics with SH2/SH3 domain ligands and kinase mutants. Sortase-mediated ligation has also been used to isotopically label single domains of Src, and this could be used to assess the N1-Src SH3 domain ligand interactions in the context of the entire kinase (Refaei et al. 2011).

Overall there is a vast amount to be discovered regarding the cellular substrates and signalling pathways of N1-Src, and in particular the role of the SH3 domain in these functions. The enhanced auto-phosphorylation of N1-Src suggests that its regulatory mechanism is altered, and recent literature has demonstrated that the C-Src SH3 domain is a hub for forming interactions throughout the kinase, including the SH2:SH1 regulatory linker, unique domain, SH4 domain, kinase domain and also with its proline-rich ligands and lipids. Thus it is important to consider how these interactions could differ for N1-Src and tailor both its activation status and function.

Appendix 1: Table of proteins total spectral counts from the GST-C and N1-Src SH3 domain pulldowns in postnatal day 1 rat brain homogenate

		Total spectrum count									GST vs N1-Src	GST vs C-Src	C vs N1-Src
		C-Src replicates			GST replicates			N1-Src replicates			(p < 0.00311)	(p < 0.01923)	(p < 0.01045)
Gene name	Accession												
2900026A02Rik	A0A0G2JZ88_RAT	2									1	0.29	0.35
Abcb1	MDR1_RAT							2			0.21	1	0.17
Abi1	ABI1_RAT	15	11	11						1	0.45	< 0.00010	< 0.00010
Abi2	F1LYA6_RAT	12	6	12				1	2	3	0.0086	< 0.00010	0.0016
Abi3	Q6AYC6_RAT	2	1	2							1	0.047	0.071
Abl1	E9PT20_RAT	9	5	5							1	< 0.00010	1
Abl2	F1M0N1_RAT	16	7	10							1	< 0.00010	1
Ablim1	F1LWK7_RAT			1		2	1			1	0.39	0.25	0.65
Acin1	E9PST5_RAT	1	1	2		4	4			4	0.3	0.12	0.43
Aco1	ACOC_RAT				4			1			0.25	0.044	0.41
Actb	ACTB_RAT	26	16	30	37	43	52	25	27	45	0.2	< 0.00010	< 0.00010
Actl6a	Q4KM87_RAT	5	4	2	5	11	9	4	3	5	0.079	0.0035	0.19
Actl6b	ACL6B_RAT	6	4	2	6	11	12	7	4	6	0.16	0.0011	0.043
Adgrl1	AGRL1_RAT	2	1			1				1	0.7	0.38	0.46
Adgrl3	AGRL3_RAT				2						0.3	0.21	1
Afap1	AFAP1_RAT	2	2	3		1	1			1	0.57	0.14	0.095
Aff2	A0A0G2KA99_RAT				2						0.3	0.21	1
Aftph	D3ZQQ1_RAT				1	4	2	2	1	4	0.46	0.0042	0.002
Agap2	AGAP2_RAT	5	1								1	0.025	0.042
Agfg1	AGFG1_RAT	5	6	4	7	9	6	5	4	5	0.27	0.066	0.27
Ago1	D4AC38_RAT	2	1	2	4	10	10	1	1	2	0.00054	< 0.00010	0.55
Ago2	AGO2_RAT	1		3	2	9	6	2			0.0014	0.0011	0.52
Akap8	AKAP8_RAT	2		2	1	6	2	2	3	2	0.55	0.078	0.11
Alg2	G3V6U3_RAT				4	3	3				0.0024	0.0004	1
Ank2	A0A0G2KBB9_RAT			3		6	0			1	0.1	0.18	0.46
Ankrd17	A0A0G2JVW3_RAT	3	2	5	7	20	18	3	3	11	0.003	< 0.00010	0.018

		Total spectrum count									GST vs N1-Src	GST vs C-Src	C vs N1-Src
		C-Src						N1-Src					
Gene name	Accession	replicates			GST replicates			replicates			(p < 0.00311)	(p < 0.01923)	(p < 0.01045)
Anxa11	Q5XI77_RAT	1	1	2	5	3	3	1	2	1	0.12	0.029	0.43
Anxa7	Q6IRJ7_RAT	2	2	5	4	7	10	4	4	6	0.33	0.0064	0.044
Ap1m1	AP1M1_RAT	1	0		2	1		1	1	1	0.56	0.25	0.19
Ap2a2	AP2A2_RAT	7	6	7	2	5	4	2	1	3	0.28	0.17	0.044
Ap2b1	AP2B1_RAT		4	4		2	3			3	0.47	0.4	0.27
Ap2m1	AP2M1_RAT	3	1	1	2	2	1	2		3	0.5	0.52	0.4
Ap2s1	AP2S1_RAT	1	1	2	2	2	2	1	1	1	0.35	0.28	0.6
Ap3b2	D4AE00_RAT			1	2	1				1	0.39	0.25	0.65
Apbb1ip	D3ZDZ1_RAT	3	2								1	0.047	0.071
Arf4	ARF4_RAT					2					0.3	0.21	1
Arhgap17	RHG17_RAT	2	1	2							1	0.047	0.071
Arhgap21	F1LXQ7_RAT	21	16	19			1				0.55	< 0.00010	< 0.00010
Arhgap23	F1M2D4_RAT	4		6							1	0.0022	0.005
Arhgap31	D4A987_RAT	2	2	2		2		1			0.57	0.21	0.14
Arhgap33	D4A9G6_RAT	15	9	6		2	1	3	1	2	0.17	< 0.00010	0.0016
Arhgap44	RHG44_RAT	3									1	0.16	0.2
Arhgef7	ARHG7_RAT	23	18	10							1	< 0.00010	< 0.00010
Arid1a	D4A3E3_RAT	13	11	19	23	43	47	19	20	24	0.0066	< 0.00010	0.00011
Arid1b	F1LNP1_RAT	11	11	6	16	32	28	12	9	22	0.027	< 0.00010	0.00073
Arl8b	ARL8B_RAT			1			2				0.3	0.44	0.59
Armcx4	D3ZV39_RAT			1	3	4	8	4	2	3	0.29	< 0.00010	0.0021
Arnt2	ARNT2_RAT				3	1	1			2	0.31	0.02	0.17
Arpp21	A0A0G2JVX9_RAT					2					0.3	0.21	1
Asap1	ASAP1_RAT	37	27	28				8	11	6	< 0.00010	< 0.00010	< 0.00010
Asap2	A0A0G2K808_RAT	29	19	25	3	2	2	2	2	2	0.58	< 0.00010	< 0.00010
Ash2l	A0A0G2JT90_RAT	2		2							1	0.086	0.12
Atad3	ATAD3_RAT	10	9	4	3	3	3	3	1	3	0.55	0.032	0.033
Atat1	ATAT_RAT	12	8	6							1	< 0.00010	< 0.00010
Atn1	ATN1_RAT	1	4	6		2	4			2	0.22	0.27	0.049

		Total spectrum count									GST vs N1-Src	GST vs C-Src	C vs N1-Src
		C-Src						N1-Src					
Gene name	Accession	replicates			GST replicates			replicates			(p < 0.00311)	(p < 0.01923)	(p < 0.01045)
Atp1a3	AT1A3_RAT	1	5	3	16	17	13	7	7	6	0.0092	< 0.00010	0.0023
Atp1b1	AT1B1_RAT			1	1	3	2			2	0.22	0.039	0.37
Atp2a2	AT2A2_RAT		1		7	6	7		2	3	0.0079	< 0.00010	0.046
Atp2b1	AT2B1_RAT	1			1	2				2	0.59	0.25	0.37
Atp2b1- Cluster	AT2B1_RAT	1	1	1	1	2	1	1	1	2	0.53	0.41	0.31
Atp2b2	AT2B2_RAT	1	1	2	1	2	1		1	1	0.44	0.54	0.52
Atp2b3	AT2B3_RAT	1		1	1					2	0.43	0.56	0.54
Atp2b4	AT2B4_RAT			1					1	2	0.093	0.54	0.19
Atp4a	ATP4A_RAT			1		2	2		3		0.6	0.14	0.19
Atp5a1	ATPA_RAT	16	12	12	21	21	21	15	16	23	0.46	0.0012	0.001
Atp5b	ATPB_RAT	1	4	5	8	14	12	4	3	10	0.056	< 0.00010	0.018
Atp5c1	ATPG_RAT	1	2	1	2		3			1	0.16	0.4	0.32
Atp5f1	AT5F1_RAT	1		4	1	2	3	1	1	1	0.35	0.39	0.57
Atp5h	ATP5H_RAT	1			1	1	2	2		1	0.6	0.14	0.19
Atp5o	ATPO_RAT	2	1	4	3	2	2	2		2	0.39	0.48	0.5
Atp6v0a1	VPP1_RAT	3	2		3	5	3			1	0.0079	0.055	0.22
Atp6v1a	D4A133_RAT				3	2	3	1		4	0.42	0.0019	0.012
Atp6v1h	A0A0G2K9J2_RAT			1	4	6	2	1		2	0.04	0.00063	0.19
Atxn10	ATX10_RAT				2	3	2	1	1	1	0.26	0.0042	0.07
Atxn2	F1M049_RAT	10	7	7	11	21	17	10	5	15	0.12	0.00019	0.023
Atxn2l	A0A0G2JYE0_RAT	20	16	25	18	32	24	19	15	22	0.34	0.021	0.083
Auts2	F1M388_RAT	1	1	2	1	3	1	1		3	0.61	0.4	0.43
Bag4	F1M3K6_RAT	1	1	1	1	1	1	2	1	1	0.4	0.57	0.31
Basp1	BASP1_RAT	1	1	3	6		2	6	3	8	0.019	0.19	0.00063
Bcar1	BCAR1_RAT	9	6	5							1	< 0.00010	< 0.00010
Bcl11a	D3ZSY3_RAT	1	2	2	6	14	11	5	3	8	0.079	< 0.00010	0.0012
Bcl11b	D4A0W4_RAT						2		1	1	0.61	0.21	0.17
Bcl9	D4A7D6_RAT	11	9	7	3	11	11	6	8	7	0.54	0.42	0.41
Bcl9l	D4A0D9_RAT	10	4	2	3	4	8	2	2	3	0.15	0.45	0.2
Birc6	A0A0G2JZ53_RAT				2						0.3	0.21	1

		Total spectrum count									GST vs N1-Src	GST vs C-Src	C vs N1-Src
Gene name	Accession	C-Src replicates			GST replicates			N1-Src replicates			(p < 0.00311)	(p < 0.01923)	(p < 0.01045)
Blk	Q4KM97_RAT										1	1	0.59
Brd4	D3ZGX8_RAT	8	7	7							1	< 0.00010	< 0.00010
Brk1	D3ZUP5_RAT	3	3	2							1	0.0075	0.014
Brsk1	BRSK1_RAT	17	10	12							1	< 0.00010	< 0.00010
Brsk2	BRSK2_RAT	2	3								1	0.047	0.071
Bsn	BSN_RAT	10	2	2	2	10	9	1		7	0.04	0.064	0.41
Bub3	D4A567_RAT	13	10	8						1	0.45	< 0.00010	< 0.00010
C1qbp	C1QBP_RAT	1	5	5			1	1			0.7	0.0072	0.016
Calm1	CALM_RAT			3	2	2	1	1		1	0.31	0.28	0.66
Camk2b	KCC2B_RAT	11	11	3	7	9	10	6	8	11	0.34	0.27	0.13
Camsap1	CAMP1_RAT	1	3	1							1	0.047	0.071
Camsap3	D3ZXQ2_RAT	2	3	2		4	2			3	0.35	0.6	0.35
Cand1	CAND1_RAT	1			1		1			2	0.61	0.44	0.37
Canx	CALX_RAT		1	2	2	3	2	1		2	0.26	0.11	0.48
Caprin1	CAPR1_RAT	1		2	2	7	11	2	2	4	0.054	< 0.00010	0.035
Capza1	CAZA1_RAT	2	2	5	1		3			1	0.25	0.21	0.04
Capza2	CAZA2_RAT	1	1	3			4				0.09	0.6	0.071
Capzb	CAPZB_RAT	2	3	5			3				0.16	0.084	0.005
Carm1	CARM1_RAT	8	4	8	13	16	14	11	7	11	0.23	0.00026	0.0081
Carmil3	CARL3_RAT	7	5	5							1	< 0.00010	0.00012
Casc3	CASC3_RAT					2					0.3	0.21	1
Caskin1	CSKI1_RAT	55	35	42				4	6	6	< 0.00010	< 0.00010	< 0.00010
Caskin2	D4A9T0_RAT	3	7	5							1	0.0001	0.00035
Cbl	D3ZV15_RAT	35	22	33				15	12	13	< 0.00010	< 0.00010	0.0095
Cblb	CBLB_RAT	22	15	17				12	10	9	< 0.00010	< 0.00010	0.22
Cbr1	CBR1_RAT	39	22	33	37	39	37	20	22	16	0.0016	0.0065	0.25
Ccar1	D4A2P1_RAT	6	3	8	9	19	23	12	10	13	0.23	< 0.00010	0.00012
Ccar2	F1LM55_RAT	10	3	6	1	10	8	2		8	0.16	0.36	0.3
Ccdc6	D4AEK9_RAT		2								1	0.29	0.35
Ccnk	A1L1L5_RAT	10	7	6					7	3	0.00036	< 0.00010	0.14

		Total spectrum count									GST vs N1-Src	GST vs C-Src	C vs N1-Src
Gene name	Accession	C-Src replicates			GST replicates			N1-Src replicates			(p < 0.00311)	(p < 0.01923)	(p < 0.01045)
Ccnt1	D3ZC98_RAT	1	0	2							1	0.16	0.2
Cct6a	Q3MHS9_RAT									2	0.21	1	0.17
Cdc5l	CDC5L_RAT			1		3	0			1	0.39	0.25	0.65
Cdh2	CADH2_RAT	4	2	0			1		1		0.7	0.095	0.14
Cdk13	F1M1X9_RAT	12	15	15		1		2		0	0.43	< 0.00010	< 0.00010
Cdk20	CDK20_RAT										1	1	1
Cdkn2aip	CARF_RAT				0	2	4			1	0.1	0.0092	0.41
Celf1	CELF1_RAT	1			5	2	3			1	0.013	0.0026	0.65
Celf2	CELF2_RAT	1	1	5	9	9	9	2	4	4	0.018	< 0.00010	0.11
Celf3	D4A916_RAT	1		2	1	3	1	1	1	4	0.37	0.28	0.11
Celf4	F1M6I9_RAT				3	3	2	1			0.037	0.0019	0.41
Celf5	D4A8V0_RAT			1	2	2	1			1	0.16	0.075	0.65
Celf6	D4ABS9_RAT					3				3	0.56	0.096	0.07
Cep170b	D4A1G8_RAT	18	9	7					0		1	< 0.00010	< 0.00010
Cherp	D3ZAX5_RAT	1	1	1		1	2			3	0.56	0.57	0.48
Chka	CHKA_RAT	2	1	1							1	0.086	0.12
Chtf8	CTF8A_RAT	3	2								1	0.047	0.071
Cic	D4A853_RAT	3		1							1	0.086	0.12
Clasp1	A0A0G2JUI5_RAT	1	3	2		0	1	1			0.7	0.095	0.14
Clint1	A0A0G2JW94_RAT	2	3	4	10	10	10	6	6	8	0.27	< 0.00010	0.0023
Cltc	CLH1_RAT	2	1	6	13	8	8	5	8	14	0.38	0.00012	< 0.00010
Cnot1	G3V7M0_RAT	2	3	3	5	6	5	2	1	5	0.17	0.032	0.32
Cnot4	Q498M7_RAT			1	1	4	1	1	1	1	0.35	0.039	0.19
Cntn1	CNTN1_RAT	1	2	3	4	6	7	2		4	0.048	0.0059	0.36
Cobl	COBL_RAT	2	1								1	0.16	0.2
Col18a1	F1LR02_RAT		3	2							1	0.047	0.071
Col4a1	F1MA59_RAT	2	1								1	0.16	0.2
Col4a5	F1LUN5_RAT										1	1	1
Copa	G3V6T1_RAT	1		2	33	26	25	1	1	6	< 0.00010	< 0.00010	0.035
Copb2	COPB2_RAT				19	15	20				< 0.00010	< 0.00010	1

		Total spectrum count									GST vs N1-Src	GST vs C-Src	C vs N1-Src
Gene name	Accession	C-Src replicates			GST replicates			N1-Src replicates			(p < 0.00311)	(p < 0.01923)	(p < 0.01045)
Cope	G3V8Q1_RAT				4	1	3				0.008	0.0019	1
Copg1	COPG1_RAT	1			1	1		2		1	0.41	0.44	0.19
Copg2	COPG2_RAT										1	1	1
Coro1c	G3V624_RAT					2	2			1	0.25	0.044	0.41
Cpeb3	D4AD99_RAT	1		3	3	8	6	2	4	2	0.13	0.0011	0.067
Cpeb4	A0A0G2K3Y6_RAT	2		1	3	4	2	2	1	3	0.44	0.04	0.11
Cpsf1	B5DEL2_RAT	7	5	2	1	5	2	2	2	3	0.56	0.25	0.31
Cpsf2	D3Z9E6_RAT	3	3	1	1	2	1	1	4	2	0.18	0.38	0.34
Cpsf6	D3ZPL1_RAT	18	17	19		1	1	12	15	11	< 0.00010	< 0.00010	0.53
Cpsf7	CPSF7_RAT	16	10	14	1	5	3	7	10	10	0.00028	< 0.00010	0.5
Crebbp	CBP_RAT	21	18	12	1	6	6	1	3	8	0.47	< 0.00010	0.00017
Crmp1	DPYL1_RAT	49	48	47	12	10	11	3	5	7	0.034	< 0.00010	< 0.00010
Csnk1d	KC1D_RAT	10	3	4						1	0.45	< 0.00010	0.00098
Csnk1e	Q99PS2_RAT	13	6	6				1	2	1	0.042	< 0.00010	0.0015
Csnk2a1	CSK21_RAT	3	4	1	3	2	2				0.015	0.57	0.014
Ctage5	A0A0G2K2J9_RAT	8	4	3							1	0.0001	0.00035
Ctnna1	Q5U302_RAT	2	1	3	0		1	1	2	1	0.13	0.095	0.6
Ctnna2	D4A6H8_RAT	5	4	2	0	1		2	3		0.071	0.0072	0.3
Ctnnb1	CTNB1_RAT	9	10	3	3	4	5	7	5	5	0.1	0.15	0.44
Ctnnd1	D3ZZZ9_RAT	4	4						1		0.45	0.0075	0.062
Ctnnd2	CTND2_RAT	4	4	2					1	1	0.21	0.0022	0.072
Cttnbp2	CTTB2_RAT	18	16	9						0	1	< 0.00010	< 0.00010
Cxadr	CXAR_RAT		1	1	4	6	5	3		4	0.15	0.00036	0.029
Cxxc1	A1A5S2_RAT	6		1							1	0.014	0.025
Cyc1	D3ZFQ8_RAT		1	2		1	1			1	0.57	0.58	0.46
Cyfip1	D4A8H8_RAT	9	13	15	1		1		2	1	0.41	< 0.00010	< 0.00010
Cyfip2	A0A0G2JT63_RAT	21	21	31	3			3	3	2	0.063	< 0.00010	< 0.00010
Daam1	D4ABM3_RAT	5	4	3							1	0.00065	0.0017
Dab2	DAB2_RAT	3	5	3	1	1		4	2	1	0.052	0.024	0.52

		Total spectrum count									GST vs N1-Src	GST vs C-Src	C vs N1-Src
Gene name	Accession	C-Src replicates			GST replicates			N1-Src replicates			(p < 0.00311)	(p < 0.01923)	(p < 0.01045)
Dab2ip	DAB2P_RAT	19	11	2							1	< 0.00010	< 0.00010
Dad1	DAD1_RAT				2			1			0.57	0.21	0.41
Dazap1	Q4KLZ3_RAT	11	5	6	8	6	9	5	6	4	0.29	0.28	0.54
Dbn1	DREB_RAT	1	1	8	5	24	15	3	3	9	0.0013	< 0.00010	0.044
Dcaf7	B2RZ68_RAT	2		6			8			1	0.037	0.46	0.062
Dcps	DCPS_RAT	4	2	2							1	0.0075	0.014
Dctn1	DCTN1_RAT			1	1	2	2	1	1	2	0.61	0.075	0.096
Dcx	DCX_RAT	7	4	6	2	3	3	4	2	3	0.35	0.12	0.32
Ddb1	DDB1_RAT	1	1	1	1		1	2	3		0.16	0.58	0.19
Ddost	OST48_RAT			1	1		2				0.16	0.25	0.59
Ddx1	DDX1_RAT			1	1	2	1			2	0.44	0.14	0.37
Ddx17	A0A096MIX2_RAT	16	8	15	10	18	18	9	7	15	0.22	0.075	0.34
Ddx39b	DX39B_RAT					3				1	0.39	0.096	0.41
Ddx3x	A0A0G2K719_RAT			3	1	4	3	2	1	1	0.3	0.067	0.31
Ddx5	Q6AYI1_RAT	7	6	12	13	25	19	10	12	17	0.21	< 0.00010	0.0011
Ddx6	D3ZD73_RAT	11	10	6	10	16	18	10	8	12	0.24	0.0044	0.052
Dennd1a	A0A0G2K6J1_RAT	5	3	4		1		1		2	0.25	0.0042	0.077
Dennd2a	D3ZLQ1_RAT	3									1	0.16	0.2
Dhcr7	DHCR7_RAT				1	1	2				0.09	0.044	1
Dhx15	D3ZD97_RAT	4	7	6	1	4	5	1		2	0.09	0.24	0.012
Dhx30	DHX30_RAT	1		1	1	7	5	1	1	4	0.17	0.0013	0.057
Dhx36	D4A2Z8_RAT			1	2	5	6	1		3	0.057	0.00031	0.096
Dhx9	D4A9D6_RAT	3	4	20	13	28	28	8	2	33	0.084	< 0.00010	0.00048
Diaph1	F1M775_RAT	37	27	19							1	< 0.00010	< 0.00010
Dido1	D3ZWL9_RAT	6	1	1		0					1	0.0075	0.014
Dmd	DMD_RAT		1	2	0			0			1	0.16	0.2
Dnaja1	DNJA1_RAT			1	1	2			1		0.39	0.25	0.65
Dnaja2	DNJA2_RAT				2	1	1		1		0.25	0.044	0.41
Dnajc13	D3ZN27_RAT					2					0.3	0.21	1
Dnm1	DYN1_RAT	106	74	97	3		5	73	79	56	< 0.00010	< 0.00010	0.23

		Total spectrum count									GST vs N1-Src	GST vs C-Src	C vs N1-Src
Gene name	Accession	C-Src replicates			GST replicates			N1-Src replicates			(p < 0.00311)	(p < 0.01923)	(p < 0.01045)
Dnm2	DYN2_RAT	61	50	48			3	39	37	22	< 0.00010	< 0.00010	0.18
Dnm3	DYN3_RAT	76	66	67			3	61	48	44	< 0.00010	< 0.00010	0.35
Dock1	D3ZZW1_RAT	2	3								1	0.047	0.071
Dock3	F1M4N6_RAT	14	8	5							1	< 0.00010	< 0.00010
Dock4	F1LZ81_RAT	10	5								1	0.0001	0.00035
Dopey2	A0A0G2JXD9_RAT	3	2	3	2	3	1	1	3	3	0.36	0.52	0.43
Dpf1	DPF1_RAT		1	2	1	5	4	1	1	1	0.09	0.023	0.48
Dpf2	A0A0G2K948_RAT				1	4	3			1	0.037	0.0019	0.41
Dpysl2	DPYL2_RAT	57	52	42	6	3	4	2	4	4	0.52	< 0.00010	< 0.00010
Dpysl3	DPYL3_RAT	54	54	41	13	7	9	5	5	9	0.26	< 0.00010	< 0.00010
Dtx3	F1LY78_RAT	13	11	9				2			0.21	< 0.00010	< 0.00010
Dync1h1	DYHC1_RAT	13	19	17	60	68	60	24	17	38	< 0.00010	< 0.00010	< 0.00010
Dync1i1	DC1I1_RAT				2		1	1		2	0.56	0.096	0.07
Dync1i2	DC1I2_RAT		1	1	4	5	5	4	3	2	0.35	0.0007	0.0074
Dync1li1	DC1L1_RAT	1	1	2	9	8	6	3	5	6	0.23	< 0.00010	0.0018
Dync1li2	DC1L2_RAT		2	1	2	3	6	1	2	4	0.38	0.013	0.064
Dynll1	DYL1_RAT					0					1	1	1
Dynll2	DYL2_RAT	1	1	1	1	2	1		1	2	0.6	0.41	0.48
Ece2	D4A4U1_RAT		2								1	0.29	0.35
Eea1	A0A0G2K051_RAT			2							1	0.29	0.35
Eef1b2	B5DEN5_RAT	1	1	1	2	1	1	1		1	0.44	0.41	0.66
Eef1g	EF1G_RAT	7	4	4	10	7	8	7	7	8	0.47	0.025	0.019
Eftud2	F1LM66_RAT			2	1	9	4			2	0.0062	0.0007	0.54
Eif3b	EIF3B_RAT				1	2		1			0.39	0.096	0.41
Eif3f	D4AC36_RAT	1	1	2				1	1	1	0.093	0.086	0.6
Eif3l	G3V7G9_RAT	0	1		3	2	3	2		1	0.19	0.01	0.19
Eif4a1	Q6P3V8_RAT										1	1	1
Eif4a2	IF4A2_RAT	2								1	0.45	0.29	0.63
Eif4a2- Cluster	IF4A2_RAT	2		1						1	0.45	0.16	0.46
Eif4a3	IF4A3_RAT	1	1	5	1	7	4	2	2	3	0.31	0.098	0.34

		Total spectrum count									GST vs N1-Src	GST vs C-Src	C vs N1-Src
Gene name	Accession	C-Src replicates			GST replicates			N1-Src replicates			(p < 0.00311)	(p < 0.01923)	(p < 0.01045)
Eif4e	IF4E_RAT			2			1			1	0.7	0.56	0.63
Eif4e2	A0A0G2K933_RAT						2				0.3	0.21	1
Eif4enif1	D4ACF1_RAT	4	2	2		1	1		1	2	0.41	0.091	0.27
Eif4g1	D3ZU13_RAT			1	5	7	5	1		6	0.082	< 0.00010	0.01
Eif4g3	A0A0G2JY73_RAT	2		3	5	10	8	4	4	12	0.49	< 0.00010	< 0.00010
Elavl1	ELAV1_RAT	1	1	5	1	2	8		1	4	0.19	0.14	0.055
Elavl2	ELAV2_RAT	7	6	12	17	17	21	9	5	12	0.011	< 0.00010	0.099
Elavl3	Q76IJ9_RAT	4	5	8	9	8	17	5	4	12	0.18	0.0021	0.59
Elmo2	G3V982_RAT	7	4	3							1	0.00019	0.0006
Eln	ELN_RAT					1				2	0.43	0.46	0.17
Enah	A0A0G2K6I4_RAT	33	25	24				26	23	18	< 0.00010	< 0.00010	0.19
Ep400	A0A0G2JU09_RAT	3									1	0.16	0.2
Eprs	A0A0G2JZI2_RAT	2			1		1	1	1	4	0.091	0.62	0.057
Erc2	ERC2_RAT	3				2	2				0.09	0.41	0.2
Evl	EVL_RAT	23	17	25				8	9	7	< 0.00010	< 0.00010	0.0038
Ewsr1	A0A140UHY3_RAT	6	5	6	7	8	8	8	8	13	0.084	0.092	0.0022
Exoc4	EXOC4_RAT			1		1	1			2	0.61	0.44	0.37
Fam110a	M0RB04_RAT	2	2	1							1	0.047	0.071
Fam110b	F110B_RAT	2	2	2							1	0.025	0.042
Fam120a	D4AB03_RAT	1	1		1	4	2		1		0.061	0.055	0.63
Fam171a2	D3ZT47_RAT					1				3	0.25	0.46	0.07
Fam195b	F195B_RAT	2			2	3	2	1	2	3	0.58	0.055	0.057
Farp1	FARP1_RAT							1		3	0.042	1	0.029
Farsa	SYFA_RAT	2	2	1	1	1	2		1	2	0.6	0.6	0.57
Fbxl19	A0A0G2KB30_RAT	2		2							1	0.086	0.12
Fgd1	F1LQ56_RAT	3	1								1	0.086	0.12
Fgfr1	FGFR1_RAT										1	1	1
Fgfr2	F1LSG7_RAT										1	1	1
Fgfr3	A0A0G2K210_RAT										1	1	0.59
Fgfr4	FGFR4_RAT			1							1	0.54	1

		Total spectrum count									GST vs N1-Src	GST vs C-Src	C vs N1-Src
Gene name	Accession	C-Src replicates			GST replicates			N1-Src replicates			(p < 0.00311)	(p < 0.01923)	(p < 0.01045)
Fgr	FGR_RAT										1	1	1
Fhdc1	D3ZL83_RAT		0				2				0.3	0.21	1
Fip1l1	FIP1_RAT	5	2	3		1				1	0.7	0.012	0.026
Fmn2	A0A0G2JZ27_RAT	11	9	8				7	4	5	< 0.00010	< 0.00010	0.32
Fmnl2	A0A0G2K132_RAT	14	8	4							1	< 0.00010	< 0.00010
Fmr1	FMR1_RAT	1	1	4	2	9	3	2	1	3	0.12	0.025	0.36
Fn1	FINC_RAT	2	2	3							1	0.014	0.025
Foxp1	FOXP1_RAT	3		5	8	12	6	6	5	5	0.22	0.00026	0.01
Foxp4	A0A0G2JXI7_RAT				2	2	1				0.049	0.02	1
Frmd4a	D3ZU85_RAT	1			2	1	2		1	3	0.61	0.075	0.096
Fubp1	FUBP1_RAT	19	14	22	26	37	45	22	22	28	0.088	< 0.00010	0.00028
Fubp3	G3V829_RAT	6	7	8	19	17	15	10	9	10	0.064	< 0.00010	0.012
Fus	Q5PQK2_RAT	3	3	4	3	9	8	5	4	7	0.53	0.017	0.029
Fxr1	FXR1_RAT			1	3	6	3	2	1	5	0.4	0.00063	0.0047
Fxr2	B1H2A6_RAT	6	2	4	7	18	12	5	2	5	0.0022	< 0.00010	0.25
Fyn	FYN_RAT					1					0.55	0.46	< 0.00010
G3bp1	D3ZYS7_RAT			1	1	4	4			2	0.063	0.0052	0.37
G3bp2	Q6AY21_RAT	2	1	4	1	6	4	2	1	4	0.38	0.14	0.34
G3P	M0R660_RAT	14	18	29	19	23	37	17	9	18	0.02	0.0072	0.47
Gap43	NEUM_RAT			1	3	1	1	1		2	0.47	0.075	0.19
Gatad2b	Q4V8E1_RAT	0			4	1	1	4		3	0.36	0.0092	0.002
Gigyf1	D3ZQJ3_RAT				1	2	1			1	0.25	0.044	0.41
Gigyf2	A0A096MKC0_RAT	4	2	3	7	5	11	6	4	3	0.17	0.0025	0.068
Git1	GIT1_RAT	21	18	13							1	< 0.00010	< 0.00010
Git2	Q66H91_RAT	10	10	7							1	< 0.00010	< 0.00010
Gna12	GNA12_RAT							2			0.21	1	0.17
Gna12- Cluster	GNA12_RAT							2			0.21	1	0.17
Gna13	GNA13_RAT										1	1	1
Gnao1	GNAO_RAT	3	7	7	4	4	11	2	1	4	0.044	0.25	0.16

		Total spectrum count									GST vs N1-Src	GST vs C-Src	C vs N1-Src
Gene name	Accession	C-Src replicates			GST replicates			N1-Src replicates			(p < 0.00311)	(p < 0.01923)	(p < 0.01045)
Gnb1	GBB1_RAT	5	5	8	6	2	11	2		4	0.024	0.3	0.078
Gorasp2	GORS2_RAT	3	3	2							1	0.0075	0.014
Gpm6a	GPM6A_RAT	1	2	2			2			2	0.61	0.3	0.4
Grpel1	GRPE1_RAT			1	1	1	3	7	3	1	0.051	0.075	0.00042
Gse1	F1M4A7_RAT		2	1			1	1			0.7	0.38	0.46
Gstm1	GSTM1_RAT	35	33	37	34	33	49	31	31	19	0.13	0.026	0.095
Gstm3	GSTM4_RAT	45	42	43	43	37	51	36	34	24	0.16	0.084	0.42
Gstm4	Q5BK56_RAT	18	15	21	20	18	24	18	12	7	0.068	0.058	0.27
Gstm5	GSTM5_RAT	24	22	26	22	18	25	17	14	7	0.052	0.38	0.51
Gstp1	GSTP1_RAT	19	19	30	34	25	37	21	21	15	0.027	0.00067	0.18
GST-SH3 domain	-	787	645	692	694	630	717	960	974	972	< 0.00010	< 0.00010	< 0.00010
Hadha	ECHA_RAT	1		1	3	1		2		1	0.6	0.27	0.34
Hba1	HBA_RAT	3	4	4	5	4	3	5	4	6	0.19	0.34	0.066
Hbb	HBB1_RAT	4	4	5	4	7	3	7	4	12	0.029	0.33	0.0049
Hck	HCK_RAT	1									1	0.54	< 0.00010
Hcn4	HCN4_RAT	14	13	15				1	1	1	0.093	< 0.00010	< 0.00010
Hdac2	F7ENH8_RAT				1	3	2	1	1		0.22	0.0092	0.17
Hdac3	HDAC3_RAT					3					0.16	0.096	1
Helz	D4ADZ6_RAT	2		1							1	0.16	0.2
Hgs	HGS_RAT	2	4	5	12	8	8	8	8	11	0.33	0.00089	0.00018
Hist1h2ak	D3ZVK7_RAT			1		2	1			1	0.39	0.25	0.65
Hist1h2ba	H2B1A_RAT			3		3	2				0.049	0.28	0.2
Hist1h2bd	D3ZWM5_RAT					3	2				0.049	0.02	1
Hist1h2bh	D3ZLY9_RAT										1	1	1
Hist1h4b	H4_RAT					2	1			1	0.39	0.096	0.41
Hist2h2be	D4A817_RAT										1	1	1
Hist3h2bb	M0RBQ5_RAT			3		2				1	0.57	0.58	0.46
Hist3h2bb- Cluster	M0RBQ5_RAT			3		3	2	1		1	0.31	0.28	0.66
Hivep2	ZEP2_RAT					2				1	0.57	0.21	0.41

		Total spectrum count									GST vs N1-Src	GST vs C-Src	C vs N1-Src
Gene name	Accession	C-Src replicates			GST replicates			N1-Src replicates			(p < 0.00311)	(p < 0.01923)	(p < 0.01045)
Hnrnpa0	F1M3H8_RAT	1		6	1		8	1		3	0.22	0.28	0.5
Hnrnpa1	ROA1_RAT	4	3	17	7	9	23	2	2	13	0.016	0.0072	0.54
Hnrnpa2b1	ROA2_RAT	2		18	2	11	26			3	< 0.00010	0.0013	0.0038
Hnrnpa3	ROA3_RAT	3	2	6	2	16	16	1	3	4	0.00035	< 0.00010	0.55
Hnrnpab	Q9QX81_RAT	1	1	6	2	5	5	3	2	6	0.48	0.15	0.11
Hnrnpc	HNRPC_RAT		1	8	3	8	17			5	0.00026	0.00021	0.45
Hnrnpd	HNRPD_RAT	7	4	8	4	17	11	4	6	8	0.12	0.011	0.22
Hnrnpdl	HNRDL_RAT						3			2	0.59	0.096	0.17
Hnrnpf	HNRPF_RAT	2	2	3	5	6	5	2	2	3	0.11	0.018	0.34
Hnrnph1	HNRH1_RAT	4	4	8	11	17	13	5	5	8	0.015	< 0.00010	0.11
Hnrnph2	HNRH2_RAT	3		3	6	11	8	3	3	2	0.011	< 0.00010	0.17
Hnrnph3	D4ABK7_RAT			2		1	9				0.0024	0.0091	0.35
Hnrnpk	HNRPK_RAT	109	69	90	10	14	15	9	13	15	0.31	< 0.00010	< 0.00010
Hnrnpl	HNRPL_RAT	5	3	12	6	33	25	5	6	20	0.0081	< 0.00010	0.0036
Hnrnpm	HNRPM_RAT	6	5	9	20	40	32	10	7	22	0.0002	< 0.00010	< 0.00010
Hnrnpr	Q566E4_RAT	5	2	8	3	19	8	2	1	11	0.049	0.0038	0.27
Hnrnpu	A0A0G2JZ52_RAT	4	5	5	4	15	12	6	5	17	0.42	0.0015	0.00073
Hnrnpul1	D4A962_RAT	17	8	14	16	29	20	17	16	15	0.31	0.00043	0.0056
Hnrnpul2	D4ABT8_RAT	2	1	1	1	15	7		2	5	0.011	< 0.00010	0.11
Hsp90ab1	HS90B_RAT	2	3	6	15	9	9	9	9	9	0.54	< 0.00010	0.00018
Hspa5	GRP78_RAT	17	10	11	11	14	7	7	10	8	0.47	0.55	0.46
Hspa8	HSP7C_RAT	36	29	29	26	32	24	27	25	22	0.32	0.44	0.24
Hspa9	GRP75_RAT	10	11	8	3	9	8	8	5	5	0.46	0.29	0.41
Hspd1	CH60_RAT	2	1	1	6	4	6	2	5	4	0.39	0.0019	0.012
Ick	ICK_RAT										1	1	1
Igf2bp1	IF2B1_RAT			1	3	6	5			5	0.074	0.00015	0.046
Igf2bp2	D3ZWZ6_RAT			1	2	2	2			1	0.1	0.039	0.65
Igf2bp3	A0A0G2K0Y2_RAT			1	1	7	2			3	0.09	0.0026	0.19
Ilf2	ILF2_RAT	1	1	4	3	8	10	2	2	5	0.065	0.00071	0.11
Ilf3	ILF3_RAT	1	2	2	1	18	9			10	0.013	< 0.00010	0.041

		Total spectrum count									GST vs N1-Src	GST vs C-Src	C vs N1-Src
Gene name	Accession	C-Src replicates			GST replicates			N1-Src replicates			(p < 0.00311)	(p < 0.01923)	(p < 0.01045)
Immt	MIC60_RAT				3	4	2		1	1	0.063	0.00088	0.17
Ina	AINX_RAT	10	4	27	33	55	34	21	4	33	0.00023	< 0.00010	0.00033
Inf2	E9PT22_RAT	2	2								1	0.086	0.12
Inppl1	SHIP2_RAT	2	2	1			1				0.55	0.15	0.071
Ipo9	D4A857_RAT				1	2					0.16	0.096	1
Iqsec2	A0A0G2JZX5_RAT	13	6	7				1		1	0.21	< 0.00010	< 0.00010
Irf2bp1	D4AAZ8_RAT	5	3	2						2	0.21	0.0022	0.072
Irf2bp2	M0R9Z5_RAT	5	1								1	0.025	0.042
Irf2bpl	I2BPL_RAT	13	13	7							1	< 0.00010	< 0.00010
Irs2	F1MAL5_RAT	5	3	1							1	0.0041	0.0085
Jup	PLAK_RAT	3	2	2	4	3	3	4	3	1	0.57	0.2	0.24
Kalrn	KALRN_RAT	1	2	1							1	0.086	0.12
Kars	Q5XIM7_RAT				2	0					0.3	0.21	1
Kdm1a	F1MA31_RAT	1		1			2	1		1	0.61	0.62	0.54
Khdrbs1	KHDR1_RAT	22	17	18		1	2	3	1	1	0.27	< 0.00010	< 0.00010
Khdrbs3	KHDR3_RAT	6	5	8		1					0.55	< 0.00010	< 0.00010
Khsrp	FUBP2_RAT	27	25	32	46	55	61	42	30	31	0.02	< 0.00010	< 0.00010
Kpnb1	IMB1_RAT	3	3	7	8	13	12	7	5	4	0.05	0.00032	0.089
Krt1	K2C1_RAT	18	12	14	34	32	35	37	27	24	0.39	< 0.00010	< 0.00010
Krt10	K1C10_RAT	28	31	19	45	42	41	37	30	24	0.15	< 0.00010	0.00055
Krt2	K22E_RAT	6	6	7	8	7	10	7	8	6	0.54	0.094	0.097
Krt71	D3ZXB7_RAT		1				2	1			0.57	0.44	0.65
Krt71- Cluster	D3ZXB7_RAT		1				3	1			0.39	0.25	0.65
Krt72	K2C72_RAT		1				3				0.16	0.25	0.59
Krt83	A7M746_RAT						2				0.3	0.21	1
L1cam	L1CAM_RAT					2	2			1	0.25	0.044	0.41
Lama2	F1M614_RAT					0	2		1		0.57	0.21	0.41
Lancl1	LANC1_RAT	2			3					1	0.39	0.42	0.63
Larp1	F1M062_RAT					5	4				0.0044	0.00088	1
Larp4b	D3ZF45_RAT	0				4	4			1	0.037	0.0019	0.41

		Total spectrum count									GST vs N1-Src	GST vs C-Src	C vs N1-Src
Gene name	Accession	C-Src replicates			GST replicates			N1-Src replicates			(p < 0.00311)	(p < 0.01923)	(p < 0.01045)
Lats1	F1M2K4_RAT	1	2			0					1	0.16	0.2
Lck	LCK_RAT										1	1	1
Ldb1	A0A0G2JVQ2_RAT	4	2	2	4	8	3	3	1	3	0.15	0.048	0.43
Ldb2	E9PTQ0_RAT	4		1		4		1		2	0.6	0.6	0.57
Lmnb1	LMNB1_RAT		1	1	5	7	5			4	0.012	< 0.00010	0.2
Lmo3	LMO3_RAT				1	2	2	2		1	0.47	0.02	0.07
LOC100359563	D3ZZK1_RAT	1	1	2			2		1	2	0.41	0.43	0.6
LOC100359563- Cluster	D3ZZK1_RAT	1	1	2			2	1	1	2	0.26	0.43	0.43
LOC100360057	Q6PDV8_RAT	1	1	2	1	2	1	1	1	2	0.53	0.54	0.43
LOC100360413	M0R757_RAT	12	9	12	21	17	16	13	14	13	0.34	0.0016	0.013
LOC100361180	D3ZHU9_RAT			2	1	4	4				0.0044	0.017	0.35
LOC100362298	D3ZM33_RAT	2	1	5	4	7	9	2	2	9	0.31	0.0054	0.044
LOC100362339	D4A6G6_RAT	2	3	4	5	4	4	6	4	5	0.24	0.15	0.028
LOC100362366	D3ZFA8_RAT			2	1	4	4			1	0.022	0.017	0.63
LOC100362366- Cluster	D3ZFA8_RAT					4	4			1	0.037	0.0019	0.41
LOC100362814	F1LXC7_RAT	0			2	2	2		1		0.1	0.0092	0.41
LOC100362987	M0RA26_RAT					2	1			1	0.39	0.096	0.41
LOC100363452	M0R7Q5_RAT			4			3			0	0.16	0.59	0.12
LOC100910255	A0A0G2K9I4_RAT	1	1	1	2	6	6	2		4	0.12	0.0023	0.11
LOC100912534	G3V678_RAT	1			2	2	1	1	1	2	0.61	0.075	0.096
LOC502176	Q7TP86_RAT	3	1	3		2	3	2			0.31	0.51	0.21
LOC685590	A0A0G2K5T3_RAT	2	0		0			1			0.45	0.29	0.63
LOC686066	D3ZW57_RAT		1			2					0.3	0.44	0.59
LOC691716	D3ZLL8_RAT	1	1	1	1	2	2	1	1	4	0.37	0.28	0.11
Lsm12	D4A8G0_RAT	2	2	2	3	3	3	2	3	2	0.55	0.2	0.26
Lsm14a	B2GV58_RAT	5	5	3		1		1			0.7	0.0024	0.0065
Lyn	LYN_RAT										1	1	1
Maged1	MAGD1_RAT	2		2	5	7	6	2	2	3	0.06	0.00059	0.11
Mak	MAK_RAT										1	1	1
Map1a	MAP1A_RAT	5	4	3							1	0.00065	0.0017

		Total spectrum count									GST vs N1-Src	GST vs C-Src	C vs N1-Src
Gene name	Accession	C-Src replicates			GST replicates			N1-Src replicates			(p < 0.00311)	(p < 0.01923)	(p < 0.01045)
Map1b	MAP1B_RAT	10	9	14	18	22	20	12	8	16	0.075	0.00021	0.041
Map2	MTAP2_RAT	22	17	15	6	1	8	6	4	16	0.015	< 0.00010	0.071
Map3k7	M3K7_RAT	2	2								1	0.086	0.12
Map4	MAP4_RAT	9	8	4			1			1	0.7	< 0.00010	0.00014
Map4k3	M4K3_RAT	7	5	5							1	< 0.00010	0.00012
Map6	MAP6_RAT	15	16	11	7	11	7	6	6	10	0.47	0.1	0.17
Marcks	MARCS_RAT	3	3	4	6	4	3	8	6	9	0.019	0.2	0.00085
Mark1	MARK1_RAT	3	1	1	1	3			1	2	0.6	0.6	0.57
Mast1	MAST1_RAT	5	5	3							1	0.00035	0.001
Matr3	MATR3_RAT	7	6	20	14	37	29	7	8	29	0.017	< 0.00010	0.0033
Mcm3ap	A0A0G2JV99_RAT					2					0.3	0.21	1
Med14	D4A020_RAT	1				2	1		1	2	0.56	0.25	0.19
Med15	G3V684_RAT	1	1	2	3	6	6	3	1	1	0.053	0.0034	0.29
Med17	D4ABU0_RAT					3	1			1	0.25	0.044	0.41
Med25	D3ZJW8_RAT	2	2	1							1	0.047	0.071
Mef2c	A0A096MJY4_RAT	2	2	1	2	3	3	2	2	1	0.42	0.19	0.4
Mex3a	A0A0G2KAA1_RAT				1	2	1	1		2	0.6	0.044	0.07
Mia3	A0A0G2JVM2_RAT	19	11	10					0		1	< 0.00010	< 0.00010
Mical3	D3ZGN7_RAT	4	2	1							1	0.014	0.025
Mllt4	AFAD_RAT	47	36	24		0					1	< 0.00010	< 0.00010
Mn1	D4AAP6_RAT	1		2		4	4			2	0.096	0.067	0.66
Morc2	A0A0G2JWF7_RAT	3	1								1	0.086	0.12
Mprip	MPRIP_RAT			2		4	1			2	0.31	0.16	0.54
Msi1	MSI1H_RAT				1	1	2			1	0.25	0.044	0.41
Mvb12b	D4A732_RAT	10	8	6							1	< 0.00010	< 0.00010
Myef2	A0A0G2K402_RAT	2	2	5	7	15	14	5	4	10	0.07	< 0.00010	0.0039
Myh10	MYH10_RAT	18	4	72	58	165	112	23	4	84	< 0.00010	< 0.00010	0.00011
Myh15	A0A0G2JY53_RAT		1			2				0	0.3	0.44	0.59
Myl12b	ML12B_RAT			4		5	6	1		2	0.061	0.029	0.6
Myl6	MYL6_RAT	1		2	2	5	6	2		4	0.17	0.0041	0.11

		Total spectrum count									GST vs N1-Src	GST vs C-Src	C vs N1-Src
Gene name	Accession	C-Src replicates			GST replicates			N1-Src replicates			(p < 0.00311)	(p < 0.01923)	(p < 0.01045)
Myo16	MYO16_RAT	4	1								1	0.047	0.071
Myo18a	A0A0G2JY08_RAT			0		4	2				0.027	0.0092	1
Myo1b	MYO1B_RAT	2		2	2	9	6			3	0.0046	0.0011	0.6
Myo3b	F1LWJ6_RAT			2	1					1	0.7	0.56	0.63
Myo5a	MYO5A_RAT	7	1	9	16	39	30	6	2	18	< 0.00010	< 0.00010	0.0081
N4bp2	D3ZLS6_RAT			1		2	2	1		1	0.44	0.14	0.37
Naa15	D3ZD89_RAT				1	2	1	4	2	2	0.12	0.044	0.00082
Naa15- Cluster	D3ZD89_RAT	1		0	1	2	1	4	2	2	0.12	0.14	0.0047
Naa16	M0RC73_RAT										1	1	1
Nav1	D4A5I4_RAT	9	2	3	0	2					0.3	0.0056	0.0006
Ncam1	NCAM1_RAT	6	3	6	13	13	12	7	9	11	0.32	0.00012	0.002
Nckap1	NCKP1_RAT	52	35	26				4	6	6	< 0.00010	< 0.00010	< 0.00010
Nckap5l	D3Z9A7_RAT		2							0	1	0.29	0.35
Ncl	NUCL_RAT	1	1	4	4	9	5	3	3	6	0.35	0.0035	0.026
Ncoa1	D4A3Q3_RAT	3	0	5	5	7	7	6	6	6	0.4	0.0086	0.0035
Ncoa2	NCOA2_RAT	0			2	1		1			0.39	0.096	0.41
Ncoa5	D3ZEI6_RAT			1		7	1				0.008	0.01	0.59
Ncoa6	NCOA6_RAT	2		1							1	0.16	0.2
Ncor2	D3ZXN9_RAT	4	4	1		2	1			1	0.39	0.12	0.04
Ndufa4	B2RZD6_RAT				2	1	1	2		2	0.53	0.044	0.029
Ndufs1	NDUS1_RAT					2	2			1	0.25	0.044	0.41
Negr1	NEGR1_RAT				1		2				0.16	0.096	1
Nelfa	Q5U2N1_RAT	4	2	3							1	0.0041	0.0085
NEWGENE_1565481	A0A0G2K6D0_RAT	1	1			1	2	0			0.16	0.42	0.35
Nf1	NF1_RAT			2			1				0.55	0.56	0.35
Nfib	O70185_RAT	13	8	8	9	18	22	10	5	15	0.12	0.0018	0.083
Nhsl1	A0A0G2JZL4_RAT	4	3	1		0					1	0.0075	0.014
Nipbl	A0A0G2K0J4_RAT	1	1	0		1	2	2	1	2	0.27	0.42	0.11
Nlgn3	NLGN3_RAT			1	3	2	2		1	1	0.15	0.02	0.37
Nono	NONO_RAT	75	61	59	2	2	4	8	6	14	< 0.00010	< 0.00010	< 0.00010

		Total spectrum count									GST vs N1-Src	GST vs C-Src	C vs N1-Src
Gene name	Accession	C-Src replicates			GST replicates			N1-Src replicates			(p < 0.00311)	(p < 0.01923)	(p < 0.01045)
Nova1	NOVA1_RAT					2	1	1	1	1	0.56	0.096	0.07
Nova2	F1M4H5_RAT					2	1	1	1	1	0.56	0.096	0.07
Npepps	F1M9V7_RAT				2	1					0.16	0.096	1
Nptn	NPTN_RAT				1			1		2	0.25	0.46	0.07
Nsf	NSF_RAT			1	2	3	1			3	0.35	0.039	0.19
Nudt21	CPSF5_RAT	22	12	17	1	1	3	14	10	8	< 0.00010	< 0.00010	0.36
Nufip2	D3ZC82_RAT	2	2	2	4	4	1	2	2	2	0.44	0.2	0.36
Nup153	NU153_RAT	7	3	10	17	27	24	14	14	20	0.23	< 0.00010	< 0.00010
Nup214	D4ACK1_RAT	5	2	9	17	21	18	11	11	10	0.057	< 0.00010	0.00031
Nup54	NUP54_RAT	4	2	4	6	12	11	7	3	10	0.32	0.00027	0.0042
Nup58	NUP58_RAT	3		4	7	7	8	4	5	6	0.34	0.00097	0.0095
Nup62	NUP62_RAT	2	3	2	8	9	7	5	2	4	0.068	0.00033	0.07
Nup88	NUP88_RAT	1		2	5	6	6		1	2	0.0046	0.00035	0.48
Nup98	NUP98_RAT	4	1	4	5	10	11	4	6	10	0.46	0.00058	0.0023
Nyap1	D3ZDP7_RAT	1	2	2	1						0.55	0.15	0.071
Nyap2	F1M3A4_RAT	3	1	1							1	0.047	0.071
Ogt	OGT1_RAT	7	1	6	7	15	16	10	4	11	0.22	< 0.00010	0.0032
Ophn1	OPHN1_RAT	3	3	2							1	0.0075	0.014
Osgepl1	OSGP2_RAT			1		2	1			1	0.39	0.25	0.65
Otud4	F1M7Q7_RAT			1	3	10	9	2	1	5	0.029	< 0.00010	0.0047
Pabpc1	PABP1_RAT	19	13	17	26	41	39	24	18	26	0.057	< 0.00010	0.00015
Pak1	PAK1_RAT	12	9	7							1	< 0.00010	< 0.00010
Pak2	PAK2_RAT	13	7	9							1	< 0.00010	< 0.00010
Pak3	PAK3_RAT	9	4	3							1	< 0.00010	0.00021
Pak7	PAK7_RAT	2	1					0		1	0.45	0.16	0.46
Parp1	PARP1_RAT				1	2	2	1	1		0.31	0.02	0.17
Pcbp2	Q6AYU5_RAT	1	1	5	4	3	7	2		4	0.12	0.044	0.46
Pclo	PCLO_RAT	8	3	1	1	2	1	1		3	0.53	0.076	0.14
Pdzd8	D3ZXY2_RAT	5	4								1	0.0041	0.0085
Phb	PHB_RAT	1	1	3	2		5			1	0.061	0.28	0.22

		Total spectrum count									GST vs N1-Src	GST vs C-Src	C vs N1-Src
		C-Src						N1-Src					
Gene name	Accession	replicates			GST replicates			replicates			(p < 0.00311)	(p < 0.01923)	(p < 0.01045)
Phb2	PHB2_RAT	2	3	5	3		6	1		2	0.13	0.53	0.15
Phf5a	PHF5A_RAT	1	2	4							1	0.014	0.025
Phldb1	PHLB1_RAT	8	5	3							1	< 0.00010	0.00021
Picalm	PICAL_RAT	1	1	3	2	5	6		1	5	0.17	0.021	0.27
Pik3c2b	D3ZVF3_RAT	17	15	9				1	1		0.21	< 0.00010	< 0.00010
Pik3r1	P85A_RAT	3	2	1							1	0.025	0.042
Pkp4	F1M2K6_RAT	6	3	2		1		2	3	1	0.037	0.0072	0.41
Plaa	PLAP_RAT				3		2				0.049	0.02	1
Pnpt1	G3V6G7_RAT	1				1	1			3	0.41	0.44	0.19
Polr2a	D4A5A6_RAT	6	3	12	13	25	19	7	7	14	0.014	< 0.00010	0.56
Polr2b	G3V8Y5_RAT	6	2	6	3	12	9		1	9	0.044	0.023	0.017
Polr2c	Q5EB90_RAT	1		2	1		4	1		1	0.31	0.28	0.66
Polr2e	RPAB1_RAT			1			2				0.3	0.44	0.59
Polr2j	D3ZQI0_RAT	1			1	2	2				0.049	0.075	0.59
Pom121	PO121_RAT				1	4	2			1	0.061	0.0042	0.41
Ppp1cb	PP1B_RAT	17	15	27			7	2	2	3	0.46	< 0.00010	< 0.00010
Ppp1r10	PP1RA_RAT	8	5	6							1	< 0.00010	< 0.00010
Ppp1r18	G3V629_RAT	4	3	3							1	0.0022	0.005
Ppp1r9b	NEB2_RAT	3	2	1							1	0.025	0.042
Ppp2r1a	Q5XI34_RAT	3	3	2	4	5	1	2	1	3	0.36	0.27	0.55
Ppp3cb	PP2BB_RAT	4	4	4	0			1			0.45	0.00065	0.01
Pqbp1	PQBP1_RAT	1	3	5						1	0.45	0.0041	0.04
Prkar2b	KAP3_RAT			1	2	1	1	1	1	2	0.53	0.14	0.096
Prkra	PRKRA_RAT		1	4			5	1		2	0.47	0.52	0.57
Prmt9	D3ZDR5_RAT	5	4	1							1	0.0022	0.27
Prpf19	PRP19_RAT			4	2	9	8		1	5	0.024	0.00032	0.19
Prpf40b	F1LTJ8_RAT	3	1								1	0.086	0.12
Prpf8	G3V6H2_RAT			5		12	8			2	0.00031	0.0005	0.4
Prr12	A0A0G2K5M6_RAT	27	16	16		6	3	2		7	0.43	< 0.00010	< 0.00010
Prr36	D3ZUH5_RAT	28	22	24				3		2	0.019	< 0.00010	< 0.00010

		Total spectrum count									GST vs N1-Src	GST vs C-Src	C vs N1-Src
Gene name	Accession	C-Src replicates			GST replicates			N1-Src replicates			(p < 0.00311)	(p < 0.01923)	(p < 0.01045)
Prrc2a	PRC2A_RAT	54	42	46	2	20	13	14	15	18	0.019	< 0.00010	< 0.00010
Prrc2b	D3ZZ51_RAT	17	12	14	10	28	17	9	8	14	0.052	0.025	0.49
Psmc2	PRS7_RAT		2		2		2		1	1	0.44	0.27	0.54
Psmc4	PRS6B_RAT	1	2	1	3		1				0.09	0.54	0.12
Psmc5	PRS8_RAT			0	5	4	1	1	1	3	0.25	0.0004	0.012
Psmd2	PSMD2_RAT		1	1	4	4	1	3	2	4	0.43	0.017	0.0074
Psmd3	Q5U2S7_RAT	1	1	1	4	6	4		2	4	0.12	0.0023	0.11
Pspc1	PSPC1_RAT	21	14	12	1	1			2	2	0.26	< 0.00010	< 0.00010
Ptbp1	PTBP1_RAT	1	1	2	3	9	7	1	2	4	0.044	0.00032	0.11
Ptbp2	PTBP2_RAT			4	3	3	5	2		5	0.38	0.029	0.11
Ptk2	FAK1_RAT	1	1	3	1	2	1	1	1		0.44	0.6	0.4
Ptpn23	PTN23_RAT	20	11	5		1					0.55	< 0.00010	< 0.00010
Puf60	PUF60_RAT		1	1	2	3	2	1		1	0.15	0.055	0.54
Pum1	D3Z8L5_RAT	3	2	7	12	17	14	8	6	10	0.075	< 0.00010	0.0017
Pum2	D3ZQL8_RAT	2	1	3	6	20	14	6	6	6	0.019	< 0.00010	0.0008
Pura	PURA_RAT	1	1	1		2	2			2	0.44	0.41	0.66
Purb	PURB_RAT						3				0.16	0.096	1
Pygo2	B5DFG8_RAT	4	1	1	1	3	4	1		1	0.096	0.28	0.29
R3hdm1	F1LNT3_RAT	4	2	1	1	1	3		2	2	0.61	0.51	0.5
R3hdm2	A0A0G2K4E8_RAT				2	1	3	1		1	0.22	0.0092	0.17
Rab10	RAB10_RAT	2	5	8	5	4	14	1	1	6	0.021	0.048	0.35
Rab11a	RB11A_RAT		1	1	2		1				0.16	0.42	0.35
Rab15	RAB15_RAT	2									1	0.29	0.35
Rab18	RAB18_RAT			3			1			2	0.43	0.38	0.66
Rab25	B5DEP2_RAT										1	1	1
Rab2a	RAB2A_RAT	1	3	4			4		1	3	0.53	0.29	0.41
Rab33b	F1LW77_RAT	2									1	0.29	0.35
Rab42	A0A0G2K201_RAT		3	2	1		4	1		4	0.5	0.52	0.4
Rab5c	B0BNK1_RAT		1	4	1		3			1	0.25	0.6	0.22
Rab7a	RAB7A_RAT		1	1			3			1	0.39	0.42	0.63

		Total spectrum count									GST vs N1-Src	GST vs C-Src	C vs N1-Src
Gene name	Accession	C-Src replicates			GST replicates			N1-Src replicates			(p < 0.00311)	(p < 0.01923)	(p < 0.01045)
Rae1	RAE1L_RAT	1	1	1	5	9	11		2		< 0.00010	< 0.00010	0.66
Rala	RALA_RAT		1	1			3	1		1	0.59	0.42	0.54
Ralb	RALB_RAT										1	1	1
Ralbp1	RBP1_RAT	2	2								1	0.086	0.12
Raly	E9PTI6_RAT			2		1	8			1	0.022	0.017	0.63
Ran	RAN_RAT	1		4	1		3	1	1	2	0.53	0.6	0.55
Ran- Cluster	RAN_RAT	1		4	1	1	3	1	1	2	0.61	0.52	0.55
Ranbp2	M0R3M4_RAT	19	9	18	38	36	33	24	18	23	0.028	< 0.00010	0.00015
Rangap1	F1MAA5_RAT	2	4	5	6	12	5	4	7	4	0.29	0.0083	0.066
Raph1	D4ADX8_RAT	26	20	27				27	30	21	< 0.00010	< 0.00010	0.0056
Raver1	RAVR1_RAT	19	10	12		3	2		1	4	0.5	< 0.00010	< 0.00010
Rbbp4	B5DFB2_RAT	2		1	1	1	2	1	1	3	0.39	0.41	0.19
Rbbp5	D3ZC01_RAT	7	3	4							1	0.00019	0.0006
Rbfox3	D4A2H6_RAT	1		3	4	8	6	5	2	6	0.43	0.00059	0.0034
Rbm12	Q6XLI7_RAT	22	13	9							1	< 0.00010	< 0.00010
Rbm14	M0R9Q1_RAT	9	7	9	14	22	16	9	6	13	0.04	< 0.00010	0.056
Rbm15	M0R3Z8_RAT	10	10	11							1	< 0.00010	< 0.00010
Rbm17	Q6AY02_RAT		2	1	1	2	3	1			0.1	0.18	0.46
Rbm22	RBM22_RAT	7	2	3							1	0.00065	0.0017
Rbm25l1	D3Z8R4_RAT	5	4	3		2	4			7	0.36	0.21	0.45
Rbm26	D3ZRG7_RAT	14	4	6							1	< 0.00010	< 0.00010
Rbm27	F1M1R4_RAT	8	3	5							1	< 0.00010	0.00021
Rbm33	D3ZTA8_RAT	11	9	7							1	< 0.00010	< 0.00010
Rbm39	Q5BJP4_RAT					2				1	0.57	0.21	0.41
Rbm42	RBM42_RAT	2		1							1	0.16	0.2
Rbm4b	RBM4B_RAT				2	3	5			1	0.013	0.0004	0.41
Rbm8a	RBM8A_RAT			2			3			3	0.56	0.42	0.34
Rbmx	RBMX_RAT	10	5	11	4	20	15	4	3	9	0.01	0.015	0.41
Rc3h2	D3ZBM2_RAT					2				1	0.57	0.21	0.41
Reps1	A0A0G2JZY3_RAT	7	5	1							1	0.00035	0.001

		Total spectrum count									GST vs N1-Src	GST vs C-Src	C vs N1-Src
		C-Src replicates			GST replicates			N1-Src replicates					
Gene name	Accession										(p < 0.00311)	(p < 0.01923)	(p < 0.01045)
Reps2	A0A0G2K1L4_RAT	2	2	1							1	0.047	0.071
Rere	RERE_RAT	2			1	1	2			1	0.25	0.27	0.63
RGD1306195	Q66H11_RAT			4	1		3	1		2	0.6	0.54	0.6
RGD1563947	D3ZVN8_RAT	1		1	2	2	1	2	1	2	0.5	0.16	0.11
Rims1	RIMS1_RAT	2		2		1					0.55	0.24	0.12
Rita1	RITA1_RAT						2				0.3	0.21	1
Rnf149	D3ZI66_RAT						2				0.3	0.21	1
Robo1	ROBO1_RAT	3									1	0.16	0.2
Robo2	A0A0G2JZA1_RAT	10	4	2	3	2	4	2		1	0.13	0.22	0.018
Rpl11	RL11_RAT				1		3	1		1	0.44	0.044	0.17
Rpl12	RL12_RAT	1	2	2	1	2	5	2		3	0.42	0.19	0.4
Rpl23	RL23_RAT	2		2	2	3	1		1	2	0.35	0.28	0.6
Rpl27	RL27_RAT	1	1	1	1	2	1	1		1	0.44	0.41	0.66
Rpl30	RL30_RAT	2		1	1	1	1	2	2	2	0.17	0.57	0.11
Rplp0	RLA0_RAT	1	2	4	1	2	5		1	1	0.096	0.37	0.21
Rplp1	RLA1_RAT	1			1	2	1	1	3	1	0.39	0.14	0.046
Rpn1	RPN1_RAT	2	3	2	6	10	6	2	2	9	0.21	0.00097	0.027
Rpn2	RPN2_RAT		1	1	2	4	2	2	3	5	0.26	0.031	0.0036
Rps11	RS11_RAT			1			5				0.049	0.075	0.59
Rps13	RS13_RAT		1	8	2	6	6	3		6	0.35	0.11	0.3
Rps14	RS14_RAT				2	5	4	2	2	3	0.38	0.00018	0.002
Rps15	RS15_RAT	1			1	2	3			2	0.22	0.039	0.37
Rps16	RS16_RAT	5	1	6	4	10	6	4	1	6	0.18	0.043	0.33
Rps25	RS25_RAT	1		1	1	2	2	1		2	0.47	0.16	0.34
Rps28	RS28_RAT					3	1	1		3	0.53	0.044	0.029
Rps3	RS3_RAT	5	4	7	4	5	10	4		5	0.11	0.2	0.38
Rps3a	RS3A_RAT	2	0	5			7			3	0.26	0.48	0.35
Rps4x	RS4X_RAT	1		3			7			1	0.061	0.19	0.32
Rps5	RS5_RAT			2			5				0.049	0.16	0.35
Rps7	RS7_RAT			3			2			1	0.57	0.58	0.46

		Total spectrum count									GST vs N1-Src	GST vs C-Src	C vs N1-Src
Gene name	Accession	C-Src replicates			GST replicates			N1-Src replicates			(p < 0.00311)	(p < 0.01923)	(p < 0.01045)
Rtcb	RTCB_RAT					2	1				0.16	0.096	1
Rtn1	RTN1_RAT	1	1	1	4	3	2	2	4	2	0.54	0.04	0.035
Rtn4	RTN4_RAT	4	6	3	6	3	1	5	2	6	0.19	0.5	0.23
Ruvbl1	RUVB1_RAT	4	3	1	1		1				0.3	0.091	0.014
Ruvbl2	G3V8T5_RAT	3	2							1	0.45	0.047	0.22
Safb	SAFB1_RAT			1		6	4			4	0.16	0.0026	0.096
Satb1	Q5U2Y2_RAT	20	14	12		1	1	2	3	3	0.029	< 0.00010	< 0.00010
Satb2	D3ZJ19_RAT	13	4	11	3	6	7	3	4	8	0.43	0.13	0.25
Scaf8	SCAF8_RAT	2	3	1							1	0.025	0.042
Scamp1	SCAM1_RAT		2	1						1	0.45	0.16	0.46
Scyl2	A0A0G2JVC2_RAT	1	1	3	7	15	10	6	3	8	0.088	< 0.00010	0.00063
Sec13	SEC13_RAT	1		1			2				0.3	0.62	0.35
Sec16a	D3ZN76_RAT	16	5	14	20	42	32	13	11	20	0.00089	< 0.00010	0.0062
Sec23a	B5DFC3_RAT	16	4	6	8	12	9	6	7	10	0.5	0.18	0.25
Sec23ip	G3V8Q8_RAT	16	15	17	9	18	16	13	10	16	0.38	0.43	0.27
Sec24b	D3ZW15_RAT	5	3	6	8	12	11	4	6	12	0.34	0.0015	0.012
Sec24c	B5DEG8_RAT	17	10	10	4	5	1	1	1	5	0.46	0.00043	0.00031
Sec31a	SC31A_RAT	1	3	3	5	5	2		2	8	0.58	0.098	0.11
Setd1b	F1LWJ1_RAT	18	8	7							1	< 0.00010	< 0.00010
Sf1	F1LSC3_RAT	28	20	22	3	9	3	20	18	12	< 0.00010	< 0.00010	0.49
Sf3a1	D3ZQM0_RAT	48	39	37				1		2	0.093	< 0.00010	< 0.00010
Sf3a2	SF3A2_RAT	7	5	6							1	< 0.00010	< 0.00010
Sf3a3	Q4KLI7_RAT	26	23	14						1	0.45	< 0.00010	< 0.00010
Sf3b1	G3V7T6_RAT	27	35	47		8	7		2	11	0.52	< 0.00010	< 0.00010
Sf3b2	D3ZMS1_RAT	48	31	26		3	1	5	3	12	0.00015	< 0.00010	< 0.00010
Sf3b3	E9PT66_RAT	10	24	28		5	1	1	1	2	0.5	< 0.00010	< 0.00010
Sf3b4	SF3B4_RAT	5	5	7					2		0.21	< 0.00010	0.0041
Sf3b5	D4A5T1_RAT			2							1	0.29	0.35
Sf3b6	M0R835_RAT	1	2	1							1	0.086	0.12
Sfpq	A0A0G2K8K0_RAT	89	59	66	5	2	5	10	12	17	< 0.00010	< 0.00010	< 0.00010

		Total spectrum count									GST vs N1-Src	GST vs C-Src	C vs N1-Src
Gene name	Accession	C-Src replicates			GST replicates			N1-Src replicates			(p < 0.00311)	(p < 0.01923)	(p < 0.01045)
Sfxn3	SFXN3_RAT			1			4			1	0.25	0.14	0.65
Sgip1	SGIP1_RAT	17	5	4							1	< 0.00010	< 0.00010
Sh3bp2	F1LS93_RAT	8	6	8				5	6	3	< 0.00010	< 0.00010	0.46
Sh3d19	D3Z8S0_RAT	4	2						0		1	0.025	0.042
Sh3kbp1	SH3K1_RAT	5	3	9							1	< 0.00010	0.00012
Sh3pxd2a	A0A0G2JX92_RAT	3	3	3				1	1	1	0.093	0.0041	0.2
Sh3pxd2b	D3ZAF9_RAT	31	23	31				9	5	5	< 0.00010	< 0.00010	< 0.00010
Shank1	SHAN1_RAT	22	11	11							1	< 0.00010	< 0.00010
Shank2	SHAN2_RAT	4	2	2							1	0.0075	0.014
Shank3	SHAN3_RAT	9	5	4							1	< 0.00010	< 0.00010
Shtn1	SHOT1_RAT	2									1	0.29	0.35
Sik3	M0RD40_RAT			1	1	3	2			1	0.1	0.039	0.65
Slain2	G3V6A2_RAT	2									1	0.29	0.35
Slc1a3	EAA1_RAT	1	1	1	2	1	1	2		2	0.53	0.41	0.31
Slc25a12	F1LX07_RAT	1		2	4	3	4	3	1	3	0.38	0.013	0.064
Slc25a3	MPCP_RAT	1	1	4	1	1	3	1		2	0.47	0.61	0.45
Slc25a4	ADT1_RAT	6	4	7	4	4	9	1	3	7	0.33	0.37	0.5
Slc3a2	4F2_RAT	1	1	2	2	3		1	1		0.31	0.4	0.52
Smap1	M0RC57_RAT			2	1	3	2	2	3	2	0.36	0.096	0.029
Smap2	B1WBX6_RAT	4	1	4	4	6	6	1	4	4	0.23	0.052	0.3
Smarca4	SMCA4_RAT	11	6	12	4	48	26	9	1	25	0.0013	< 0.00010	0.019
Smarcb1	Q4KLI0_RAT	2	2	3	7	14	6	4	1	6	0.03	< 0.00010	0.07
Smarcc2	D4A510_RAT	19	12	15	25	37	37	27	17	29	0.25	< 0.00010	< 0.00010
Smarcd1	D3ZBS9_RAT	5	7	13	12	22	22	13	13	16	0.35	< 0.00010	0.0003
Smarce1	SMCE1_RAT	4	4	5	7	11	10	7	7	8	0.49	0.003	0.0077
Snap91	AP180_RAT		1	1	1		3	1		3	0.53	0.27	0.2
Snrnp200	U520_RAT	2		4	1	5	5	1		3	0.12	0.093	0.6
Snrpa	Q5U214_RAT	3	5	6						3	0.093	0.00019	0.038
Snrpa1	D3ZZR5_RAT	1	7	11							1	< 0.00010	< 0.00010
Snrpb	RSMB_RAT	2	5	6			4			2	0.44	0.052	0.022

		Total spectrum count									GST vs N1-Src	GST vs C-Src	C vs N1-Src
		C-Src replicates			GST replicates			N1-Src replicates					
Gene name	Accession										(p < 0.00311)	(p < 0.01923)	(p < 0.01045)
Snrpb2	B5DEQ4_RAT	2	5	6							1	0.00035	0.001
Snrpd1	B2RZB7_RAT	1	1	2	1	2	3	1	1	2	0.5	0.28	0.43
Snrpd2	B5DES0_RAT	1	1	5		1				1	0.7	0.058	0.095
Snrpd3	M0R907_RAT	3	4	5	2	3	2	4	2	1	0.46	0.29	0.45
Snrpf	D4AAT4_RAT	3	2	3		3	2			1	0.16	0.4	0.062
Snrpn	RSMN_RAT	2	5	6			4			2	0.44	0.052	0.022
Snw1	D4A8G7_RAT			1		2	1			1	0.39	0.25	0.65
Sobp	SOBP_RAT	6	3	2						1	0.45	0.0012	0.016
Soga3	D4A0A1_RAT	20	10	12	1	3	6	4		3	0.46	< 0.00010	< 0.00010
Sos1	D4A3T0_RAT	49	53	45				7	10	6	< 0.00010	< 0.00010	< 0.00010
Sos2	F1MAI3_RAT	16	12	15				1	1	1	0.093	< 0.00010	< 0.00010
Sox5	F1M8W4_RAT	1			5	7	5	3	2	3	0.13	< 0.00010	0.0047
Sptan1	SPTN1_RAT	1	1	31	1	78	45			34	< 0.00010	< 0.00010	0.07
Sptbn1	A0A0G2K8W9_RAT	1	0	20	2	62	38		1	26	< 0.00010	< 0.00010	0.024
Sptbn2	SPTN2_RAT	0	0	4		20	8			9	0.0071	< 0.00010	0.039
Srcin1	SRCN1_RAT	66	51	46	3	6	5	49	39	24	< 0.00010	< 0.00010	0.47
Srrm2	A0A0G2K2M9_RAT	3	1	3				1			0.45	0.014	0.095
Srsf7	D4A720_RAT		1	3		1	1			1	0.57	0.43	0.32
Ss18l1	CREST_RAT	1			1	3	1	2	2	1	0.5	0.075	0.046
Ssb	LA_RAT	1		3		4	1				0.049	0.4	0.12
Ssbp2	F1M3J3_RAT	6	2	5	6	12	8	6	5	7	0.33	0.0069	0.042
Ssr4	SSRD_RAT				1	2					0.16	0.096	1
Stam	B5DF55_RAT	3	1	1	5	6	4	5	6	3	0.44	0.0078	0.0041
Stam2	STAM2_RAT				5	4	5	3	2	5	0.44	< 0.00010	0.00014
Stau2	STAU2_RAT	4	1	5	7	12	11	6	3	8	0.13	0.00016	0.018
Strbp	STRBP_RAT				1	6	2				0.0044	0.00088	1
Stx12	STX12_RAT			1			2				0.3	0.44	0.59
Stx1b	STX1B_RAT		1	1	1	1	2			2	0.44	0.27	0.54
Stx7	STX7_RAT	1		1	1	2	1			3	0.6	0.27	0.34
Stxbp1	STXB1_RAT	2	4	5	5	8	7	4	3	6	0.31	0.028	0.14

		Total spectrum count									GST vs N1-Src	GST vs C-Src	C vs N1-Src
Gene name	Accession	C-Src replicates			GST replicates			N1-Src replicates			(p < 0.00311)	(p < 0.01923)	(p < 0.01045)
Sucla2	F1LM47_RAT				2						0.3	0.21	1
Sugp2	D3ZJH2_RAT					2	2			1	0.25	0.044	0.41
Sv2a	SV2A_RAT			0	2	3	1			1	0.1	0.0092	0.41
Syn1	SYN1_RAT	46	37	32				2	4	4	0.00036	< 0.00010	< 0.00010
Syn2	SYN2_RAT	9	4	4				1			0.45	< 0.00010	0.00098
Syn3	SYN3_RAT	4	7	3	4	4	5		1	5	0.17	0.48	0.22
Syncrip	HNRPQ_RAT	3	2	3	3	12	3	1		6	0.06	0.014	0.43
Syngap1	SYGP1_RAT	5	2	2		1		0	1	1	0.43	0.021	0.1
Synj1	SYNJ1_RAT	66	49	52					1	1	0.21	< 0.00010	< 0.00010
Synrg	SYNRG_RAT	2	1	1	6	8	10	4	5	10	0.51	< 0.00010	< 0.00010
Syt1	SYT1_RAT					1	2	1	1	1	0.56	0.096	0.07
Tab1	A0A0U1RRU5_RAT	1		2							1	0.16	0.2
Tab3	F1M1D2_RAT	5	2	2							1	0.0041	0.0085
Tanc2	A0A0G2K9J0_RAT	12	5	3							1	< 0.00010	< 0.00010
Tardbp	I6L9G6_RAT	7	2	4	8	13	10	5	5	8	0.14	0.00081	0.042
Tbl1xr1	D3ZNF4_RAT	6	4	3	6	9	7	4	6	3	0.21	0.031	0.23
Tbr1	D4A6N8_RAT	10	5	12	15	23	20	12	12	16	0.22	< 0.00010	0.0016
Tcerg1	D3ZTL0_RAT	11	5	4							1	< 0.00010	< 0.00010
Tcf4	ITF2_RAT			2	2			1	1	2	0.26	0.62	0.2
Tdrd3	TDRD3_RAT	2	0	1		2	1				0.16	0.57	0.2
Tenm2	TEN2_RAT	13	5	1					1		0.45	< 0.00010	0.00037
Tep1	TEP1_RAT			0						2	0.21	1	0.17
Tet3	D3ZQT7_RAT	1				2	2				0.09	0.14	0.59
Tfg	Q6AYR1_RAT	3	4	6	9	20	14	4	3	7	0.001	< 0.00010	0.17
Tia1	Q5PQR7_RAT	7	3	5	8	9	8	7	8	10	0.3	0.025	0.0051
Tial1	Q5BJN3_RAT	8	4	4	7	8	14	8	6	7	0.37	0.009	0.04
Tle3	TLE3_RAT	3	2	3	3	6	4	3	5	1	0.42	0.1	0.23
Tm9sf2	TM9S2_RAT						2				0.3	0.21	1
Tmod2	TMOD2_RAT			1	1	2	2				0.049	0.075	0.59
Tmpo	LAP2_RAT	3	6	2	10	7	8	3	2	5	0.033	0.0035	0.35

		Total spectrum count									GST vs N1-Src	GST vs C-Src	C vs N1-Src
		C-Src replicates			GST replicates			N1-Src replicates					
Gene name	Accession										(p < 0.00311)	(p < 0.01923)	(p < 0.01045)
Tmx4	G3V912_RAT		1							2	0.21	0.54	0.37
Tnik	A0A0G2K490_RAT	7	8	8		0					1	< 0.00010	< 0.00010
Tnk2	ACK1_RAT	5	2	2							1	0.0041	0.0085
Tnrc6a	A0A0G2JZJ3_RAT				2	2	4				0.008	0.0019	1
Tnrc6b	F1LV37_RAT	3	2	2	4	9	7	3	1	4	0.054	0.0027	0.24
Tnrc6c	D3ZRA6_RAT	3	2	2	8	16	14	3	2	7	0.0015	< 0.00010	0.044
Tpm3	TPM3_RAT						2				0.3	0.21	1
Tra2b	TRA2B_RAT		2	1		2	2			2	0.44	0.41	0.66
Trim3	TRIM3_RAT	2	3	1							1	0.025	0.042
Trim33	D3ZUK4_RAT	2	1	1							1	0.086	0.12
Trim46	A0A0G2JXN2_RAT	1	3								1	0.086	0.12
Trim67	D3ZTX1_RAT	14	7	7							1	< 0.00010	< 0.00010
Tsg101	TS101_RAT	9	9	8	3	2	3	1	2	5	0.45	0.0064	0.025
Ttc3	D3ZSP7_RAT	1		1		1		1		2	0.25	0.56	0.34
Ttc9b	D3ZTK0_RAT	4	2	3							1	0.0041	0.0085
Tuba4a	TBA4A_RAT	75	62	80	77	114	89	54	59	90	0.08	< 0.00010	0.0015
Tubb3	TBB3_RAT	114	98	106	139	143	164	93	111	139	0.16	< 0.00010	< 0.00010
Tufm	EFTU_RAT					1	2				0.16	0.096	1
Tulp4	D3ZFM2_RAT	4	3								1	0.014	0.025
U2af1	Q3KR55_RAT			4			6			2	0.22	0.28	0.52
U2af2	F2Z3T9_RAT					2	1				0.16	0.096	1
U2surp	D3ZAI0_RAT		1			2	3			2	0.31	0.075	0.37
Ubap2	A0A0G2JYI7_RAT	7	4	5	12	19	19	9	8	10	0.045	< 0.00010	0.0034
Ubap2l	E9PTR4_RAT	13	9	16	23	27	35	12	19	23	0.074	< 0.00010	0.00049
Ubb	UBB_RAT		1	2	3	4	3	1	1		0.04	0.023	0.66
Uckl1	D3ZYQ8_RAT	2						2	3		0.019	0.29	0.11
Uncharacterized protein	M0RBS7_RAT	4	1		5	6	4	3	1	2	0.092	0.0078	0.005
Uncharacterized protein	M0RBV9_RAT				1	2		1	1	1	0.56	0.096	< 0.00010
Uncharacterized protein	A0A0G2K315_RAT	22	20	13					1		0.45	< 0.00010	0.17
Uncharacterized protein	A0A0G2K6L6_RAT	1		2			2				0.3	0.58	0.07

		Total spectrum count									GST vs N1-Src	GST vs C-Src	C vs N1-Src
Gene name	Accession	C-Src replicates			GST replicates			N1-Src replicates			(p < 0.00311)	(p < 0.01923)	(p < 0.01045)
Uncharacterized protein	A0A0G2K7R1_RAT										1	1	0.2
Uncharacterized protein	A0A0G2JY03_RAT	3	1	4			1	1	3	1	0.071	0.035	0.54
Uncharacterized protein	A0A0G2JY70_RAT	1		1			1			2	0.43	0.56	0.54
Uncharacterized protein	A0A0G2K5E6_RAT							2			0.21	1	1
Uncharacterized protein	F1M5B1_RAT										1	1	1
Upf1	A0A0U1RS25_RAT	8	6	8	12	20	17	9	3	12	0.021	< 0.00010	0.085
Uqcrc1	QCR1_RAT			1	2	2					0.09	0.14	0.59
Uqcrc2	QCR2_RAT	1		3	1	2	2	1		3	0.61	0.4	0.43
Usp9x	A0A0G2K2C7_RAT	0			2	3	5		1		0.013	0.0004	0.41
Vamp2	VAMP2_RAT			2	1		1		2	2	0.26	0.62	0.2
Vamp3	VAMP3_RAT	1		2	1		1	1	2	2	0.16	0.58	0.19
Vamp3	VAMP3_RAT	1		2	1		1	1	2	2	0.16	0.58	0.19
Vapa	VAPA_RAT										1	1	1
Vapb	VAPB_RAT	1	2	1							1	0.086	0.12
Vasp	A0A0G2K9C0_RAT	13	11	14				8	8	6	< 0.00010	< 0.00010	0.29
Vat1	VAT1_RAT				3	2		2		2	0.61	0.02	0.029
Vdac1	VDAC1_RAT	4	11	7	6	9	10	6	5	9	0.52	0.19	0.24
Vdac2	VDAC2_RAT	2	5	5	4	7	8	2	3	3	0.073	0.06	0.55
Vdac3	VDAC3_RAT		3	1		1	4				0.049	0.4	0.12
Vim	VIME_RAT	9	12	26	27	40	38	17	14	35	0.045	< 0.00010	0.00015
Vps28	VPS28_RAT	3	7	10							1	< 0.00010	< 0.00010
Vps37b	D3ZU64_RAT	6	6	10							1	< 0.00010	< 0.00010
Was	M0RBE8_RAT	1	1						2		0.21	0.29	0.54
Wasf1	WASF1_RAT	17	11	9	1			3	5	6	0.00013	< 0.00010	0.031
Wasf2	A0A0G2K5T9_RAT	7	4	3							1	0.00019	0.0006
Wasf3	M0R7F3_RAT	5	3	2							1	0.0022	0.005
Wasl	WASL_RAT	19	17	18				21	17	17	< 0.00010	< 0.00010	0.03
Wbp11	WBP11_RAT	23	13	11				8	9	9	< 0.00010	< 0.00010	0.2
Wdr33	F1LT09_RAT	2	1			1				1	0.7	0.38	0.46
Wdr5	WDR5_RAT	10	7	7	2	2	1	1		2	0.47	0.0013	0.00073
Wipf1	WIPF1_RAT	1		1				1	2	3	0.0086	0.29	0.057

		Total spectrum count									GST vs N1-Src	GST vs C-Src	C vs N1-Src
Gene name	Accession	C-Src replicates			GST replicates			N1-Src replicates			(p < 0.00311)	(p < 0.01923)	(p < 0.01045)
Wipf2	D3ZUD3_RAT	12	13	13				17	16	13	< 0.00010	< 0.00010	0.0079
Wipf3	WIPF3_RAT	8	6	6				8	8	5	< 0.00010	< 0.00010	0.12
Wwp2	F7EYF1_RAT	3	2	3		0		2	1		0.093	0.0075	0.27
Xrn1	D4ABN8_RAT	1		1	1	4	1			4	0.5	0.096	0.2
Xrn2	D4A914_RAT	3	2			1	4	2	2	4	0.18	0.52	0.11
Ybx1	YBOX1_RAT	6	6	8	5	11	9	9	6	11	0.25	0.12	0.025
Yes1	YES_RAT		3						2	3	0.019	0.16	0.19
Yes1- Cluster	YES_RAT	1	3	1		1			2	3	0.071	0.15	0.4
Ylpm1	YLPM1_RAT	32	29	26	4	16	10	30	28	19	< 0.00010	< 0.00010	0.075
Ythdf1	Q4V8J6_RAT	8	4	7	8	14	10	5	3	6	0.029	0.011	0.51
Ythdf2	E9PU11_RAT	7	4	5	5	10	10	6	3	6	0.2	0.036	0.26
Ythdf3	D3ZIY3_RAT	5	5	7	8	13	13	5	4	10	0.11	0.0021	0.11
Ywhaz	1433Z_RAT	5	3	10			5	1	1	2	0.61	0.016	0.021
Zc2hc1a	A0A0G2K782_RAT	28	17	21	3	2	3	18	10	10	< 0.00010	< 0.00010	0.2
Zc3h4	D3ZVW3_RAT	2	2								1	0.086	0.12
Zcchc11	A0A0G2JZ04_RAT				1	2	4		2	2	0.39	0.0042	0.029
Zeb2	E9PTC3_RAT		1		3	5	2	3	4	6	0.19	0.0026	< 0.00010
Zfp207	Q498C9_RAT	4	3	2							1	0.0041	0.0085
Zfp598	D3ZR64_RAT	3	2	1							1	0.025	0.042
Zfp638	D4A0U3_RAT	1	1		0	2					0.3	0.62	0.35
Zfr	ZFR_RAT	4	2	2	5	10	11	4	2	8	0.12	0.00026	0.028
Zmiz1	D4AE97_RAT	2	2		2	3	3	1	1	1	0.19	0.12	0.6
Zmiz2	G3V9C9_RAT	2	2		4	2	4	1		1	0.04	0.048	0.52
Zswim8	A0A0G2K9R0_RAT			1		4	3	1	1	2	0.39	0.02	0.096

Appendix 2: 15 mer peptide sequences from the Dynamin I, III, Enah, and N-WASP proline rich domains utilised for the peptide arrays

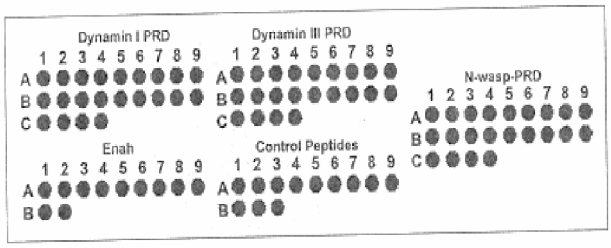

Dynamin I PRD

Nr.	Pos.	Sequence
1	A 1	INTTTVSTPMPPPVD
2	A 2	VSTPMPPPVDDSWLQ
3	A 3	PPPVDDSWLQVQSVP
4	A 4	DSWLQVQSVPAGRRS
5	A 5	VQSVPAGRRSPTSSP
6	A 6	AGRRSPTSSPTPQRR
7	A 7	PTSSPTPQRRAPAVP
8	A 8	TPQRRAPAVPPARPG
9	A 9	APAVPPARPGSRGPA
10	B 1	PARPGSRGPAPGPPP
11	B 2	SRGPAPGPPPAGSAL
12	B 3	PGPPPAGSALGGAPP
13	B 4	AGSALGGAPPVPSRP
14	B 5	GGAPPVPSRPGASPD
15	B 6	VPSRPGASPDPFGPP
16	B 7	GASPDPFGPPPQVPS
17	B 8	PFGPPPQVPSRPNRA
18	B 9	PQVPSRPNRAPPGVP
19	C 1	RPNRAPPGVPSRSGQ
20	C 2	PPGVPSRSGQASPSR
21	C 3	SRSGQASPSRPESPR
22	C 4	ASPSRPESPRPPFDL

Dynamin III PRD

Nr.	Pos.	Sequence
1	A 1	VSTPAPPPVDDSWLQ
2	A 2	PPPVDDSWLQHSRRS
3	A 3	DSWLQHSRRSPPPSP
4	A 4	HSRRSPPPSPTTQRR
5	A 5	PPPSPTTQRRLTLSA
6	A 6	TTQRRLTLSAPLPRP
7	A 7	LTLSAPLPRPASSRG
8	A 8	PLPRPASSRGPAPAI
9	A 9	ASSRGPAPAIPSPGP
10	B 1	PAPAIPSPGPHSGAP
11	B 2	PSPGPHSGAPPVPFR
12	B 3	HSGAPPVPFRPGPLP
13	B 4	PVPFRPGPLPPFPNS
14	B 5	PGPLPPFPNSSDSYG
15	B 6	PFPNSSDSYGAPPQV
16	B 7	SDSYGAPPQVPSRPT
17	B 8	APPQVPSRPTRAPPS
18	B 9	PSRPTRAPPSVPSRR
19	C 1	RAPPSVPSRRPPPSP
20	C 2	VPSRRPPPSPTRPTI
21	C 3	PPPSPTRPTIIRPLE
22	C 4	TRPTIIRPLESSLLD

N-wasp-PRD

Nr.	Pos.	Sequence
1	A 1	RRQAPPPPPPSRGGP
2	A 2	PPPPPSRGGPPPPPP
3	A 3	SRGGPPPPPPPPPHNS
4	A 4	PPPPPPPPHNSGPPPP
5	A 5	PPHNSGPPPPPARGR
6	A 6	GPPPPPARGRGAPPP
7	A 7	PARGRGAPPPPPSRA
8	A 8	GAPPPPPSRAPTAAP
9	A 9	PPSRAPTAAPPPPPP
10	B 1	PTAAPPPPPPSRPSV
11	B 2	PPPPPSRPSVAVPPP
12	B 3	SRPSVAVPPPPPNRM
13	B 4	AVPPPPPNRMYPPPP
14	B 5	PPNRMYPPPPPALPS
15	B 6	YPPPPPALPSSAPSG
16	B 7	PALPSSAPSGPPPPP
17	B 8	SAPSGPPPPPPSVLG
18	B 9	PPPPPPSVLGVGPVA
19	C 1	PSVLGVGPVAPPPPP
20	C 2	VGPVAPPPPPPPPPP
21	C 3	PPPPPPPPPPPGPPP
22	C 4	PPPPPPGPPPPPGLP

Enah

Nr.	Pos.	Sequence
1	A 1	PLAPPPPPPLPPGPA
2	A 2	PPPPLPPGPAQASVA
3	A 3	PPGPAQASVALPPPP
4	A 4	QASVALPPPPGPPPP
5	A 5	LPPPPGPPPPPPLPS
6	A 6	GPPPPPPLPSTGPPP
7	A 7	PPLPSTGPPPPPPPP
8	A 8	TGPPPPPPPPPLPNQ
9	A 9	PPPPPPLPNQVPPPP
10	B 1	PLPNQVPPPPPPPPA
11	B 2	VPPPPPPPPAPPLPA

Control Peptides

Nr.	Pos.	Sequence
1	A 1	AERSSRPLPPIPGGK
2	A 2	AERSSRALAAIAGGK
3	A 3	QRRAPAVPPARPGSR
4	A 4	QRRAAAVAAARAGSR
5	A 5	FGPPPQVPSRPNRAP
6	A 6	FGAAAQVASRANRAA
7	A 7	IQRIPLPPPPAPETY
8	A 8	IQRIALAAAAAAETY
9	A 9	SQLLRPKPPIPAKPQ
10	B 1	SQLLRAKAAIAAKAQ
11	B 2	WHRMPAYTAKYP
12	B 3	WHRMAAYTAKYA

Appendix 3: ^{1}H-^{15}N backbone resonance assignment (ppm) of the N1-Src SH3 domain

Residue	1H	15N
8G	8.29	110.27
9G	8.01	108.5
10V	7.91	118.81
11T	8.41	118.91
12T	8.33	119.93
13F	9.43	126.28
14V	9.45	119.09
15A	8.55	126.82
16L	9.47	126.12
17Y	7.17	112.12
18D	8.3	117.49
19Y	8.61	120.99
20E	7.49	127.95
21S	8.22	118.31
22R	9.14	123.91
23T	8.15	113.81
24E	8.99	121.96
25T	7.57	105.66
26D	7.64	123.53
27L	8.84	124.92
28S	7.97	117.36
29F	8.61	117.11
30K	8.67	119.74
31K	9.22	121.13
32G	8.99	115.02
33E	8.38	123.66
34R	8.28	122.06
35L	9.15	123.44
36Q	9.03	120.72
37I	8.98	125.29
38V	8.61	127.19
39N	8.17	120.8
40N	8.51	119.46
41T	8.03	113.63
42R	8.29	123.82
43K	8.49	124.09
44V	8.26	122.26
45D	8.4	125.04
46V	7.99	119.06
47R	8.29	123.44
48E	8.41	120.77
49G	8.42	110.6
50D	8.05	120.06
51W	8.54	124.25
52W	9.05	122.41

Residue	1H	15N
53L	8.95	125.27
54A	8.94	129.68
55H	9.14	116.88
56S	8.83	119.68
57L	8.87	129.57
58S	8.45	114.33
59T	8.19	108.29
60G	7.73	110.64
61Q	7.5	119.22
62T	8.61	117.08
63G	9.17	113.11
64Y	9.03	119.5
65I	9.52	112.59
66P	-	-
67S	7.73	120.78
68N	8.15	114.75
69Y	7.92	119.45
70V	7.23	109
71A	8.7	121.88
72P	-	-
73S	8.11	116.75
74D	8.36	121.17
75S	8.04	114.92
76I	7.89	122.25
77Q	8.4	124.72
78A	8.34	126.06
79E	8.36	120.74
80E	7.96	126.78

Appendix 4: Table of C- and N1-Src phosphopeptides from the *in vitro* whole cell lysate kinase assays. The peptides quantitative areas, and specific phosphorylation site assignments are shown.

Peptide sequence and modification (phospho-S/T/Y) & Carbamidomethylation	Gene name	Modification A-score (≥ 13 = p < 0.05)	Quantitative Area								p-value		
			FSBA replicates			N1-Src replicates			C-Src replicates			FSBA vs N1-Src	FSBA vs C-Src	N1-Src vs C-Src
KC(+57.02)VEEAYSLLNEYGDDMY(+79.97)GPEK	A0A0G2JZB6	C2:1000, Y18:30.64	0	0	0	0	0	0	0	0	0	4140	1	1E-06	0.154
KC(+57.02)VEEAY(+79.97)SLLNEYGDDMYGPEK	A0A0G2JZB6	C2:1000.0, Y7:11.06	0	0	0	0	0	0	0	0	0	5870	1	1E-06	1E-06
TIAQDY(+79.97)GVLKADEGISFR	A0A0G2K3Z9	Y6:7.26	0	0	0	0	0	0	0	0	0	14700	1	1E-06	1E-06
QLNYQHSDGSY(+79.97)STFGDR	A1m	Y11:14.02	0	0	0	0	0	0	0	0	29700	23900	1	1E-06	0.114
AIYDIERPDLITY(+79.97)EPFYTSGYEDKQDR	Ablim1	Y13:14.02	0	0	0	0	0	0	0	0	0	65000	1	1E-06	1E-06
IDSAATSTY(+79.97)EVGNPPDYR	Acp1	Y9:12.28	0	0	0	6E+05	8E+05	0	2E+06	3E+06	9E+05	1E-06	1E-06	0.547	
QLIIEDPY(+79.97)YGNDSDFEVVY(+79.97)QQC(+57.02)LR	Acp1	Y8:0.00, Y19:53.33 C22:1000.0	0	0	0	39400	8610	0	44300	40000	23300	1E-06	1E-06	1	
QLIIEDPYYGNDSDFEVVY(+79.97)QQC(+57.02)LR	Acp1	Y19:73.05, C22:1000	0	0	0	4E+05	3E+05	4E+05	1E+06	7E+05	4E+06	1E-06	1E-06	0.262	
EDFATFDY(+79.97)ILC(+57.02)MDESNLR	Acp1	Y8:0.0, C11:1000	0	0	0	0	0	0	0	0	13800	1	1E-06	1E-06	
TTGIVMDSGDGVTHTVPIY(+79.97)EGYALPHAILR	Actg1	Y19:11.12	0	0	0	0	0	27400	2E+05	0	8E+05	1	1E-06	0.086	
LC(+57.02)Y(+79.97)VALDFEQEMATAASSSSLEK	Actg1	C2:1000, Y3:30.57	0	0	0	0	0	0	0	0	17100	1	1E-06	1E-06	
TTGIVMDS(+79.97)GDGVTHTVPIYEGY(+79.97)ALPHAILR	Actg1	S8/Y22:0.00	0	0	0	0	0	0	0	0	60800	1	1E-06	1E-06	
DLY(+79.97)ANTVLSGGTTMYPGIADR	Actg1	Y3:9.42	0	0	0	1520	0	0	0	0	9120	1	1E-06	1E-06	
SY(+79.97)ELPDGQVITIGNER	Actg1	Y2:0.00	2460	0	1450	8040	9510	0	10800	16600	37400	0.348	0.061	0.839	
TTGVVLDSGDGVTHAVPIY(+79.97)EGFAMPHSIMR	Actr1a	Y19:4.45	0	0	0	0	0	0	0	31700	1E+05	1	1E-06	1E-06	
LEGGVAY(+79.97)NVVPATMSAC(+57.02)FDFR	Acy1a	Y7:56.47, C17:1000	0	0	0	0	0	0	0	0	6860	1	1E-06	0.292	
KPGDGDSFY(+79.97)SDFPPGGSADSASSSK	Adam22	Y9:0.00	0	0	0	0	343	0	0	0	16600	1	1E-06	1	
MAQQPLSLVGC(+57.02)DVLPDPSPDHLY(+79.97)SFR	Afap1l2	C11:1000, Y23:0.0	0	0	0	0	0	0	0	0	5880	1	1E-06	1E-06	
TLDPDDMVYC(+57.02)GVY(+79.97)DNALDNDNYNLAR	Agl	C10:1000, Y13:0.0	0	0	0	11000	0	9660	2E+05	98100	9710	1E-06	1E-06	0.26	
TLDPDDMVY(+79.97)C(+57.02)GVYDNALDNDNYNLAR	Agl	Y9:5.55, C10:1000	0	0	0	36700	0	0	73600	17200	9900	1E-06	1	1E-06	
SSEVVLSGDDEDY(+79.97)QRIY(+79.97)TTK	Ahnak	Y13:6.67, Y17:7.21	0	0	0	5070	0	0	13500	28800	0	1E-06	1	1E-06	
SS(+79.97)EVVLSGDDEDY(+79.97)QRIYTTK	Ahnak	S2/Y13:0.00	0	0	0	0	0	0	6660	0	0	1	1E-06	1E-06	
DLSFPY(+79.97)EAVEGC(+57.02)K	Akap1	Y6:28.36, C12:1000	0	0	0	2450	848	0	52600	1E+05	4690	1E-06	1E-06	0.163	
C(+57.02)C(+57.02)AEGDPPAC(+57.02)Y(+79.97)GTVLAEFQPLV EEPK	Alb	C1/C2/C10:1000.0 Y11:12.81	0	0	0	1E+05	0	31200	4E+05	3E+05	42700	1E-06	1E-06	0.137	
LGEY(+79.97)GFQNAVLVR	Alb	Y4:1000.0	0	0	0	43900	0	12400	61500	1E+05	8020	1E-06	1E-06	0.404	
TNC(+57.02)ELY(+79.97)EKLGEYGFQNAVLVR	Alb	C3:1000, Y6:15.48	0	0	0	20500	0	1E+05	3E+05	33000	66000	1E-06	1E-06	0.512	
DVFLGTFLYEY(+79.97)SR	Alb	Y11:0.00	0	0	0	0	0	0	44400	13300	18100	1	1E-06	1E-06	
TNC(+57.02)ELY(+79.97)EKLGEY(+79.97)GFQNAVLVR	Alb	C3:1000.0, Y6:2.87 Y12:26.12	0	0	0	5970	0	0	0	0	0	1E-06	1	0.483	
TFVQEDVY(+79.97)DEFVER	Aldh2	Y8:83.89	0	0	0	3E+05	1E+05	1E+05	6E+05	1E+06	3E+05	1E-06	1E-06	0.404	

Peptide sequence and modification (phospho-S/T/Y) & Carbamidomethylation	Gene name	Modification A-score (≥ 13 = p < 0.05)	FSBA replicates			N1-Src replicates			C-Src replicates			FSBA vs N1-Src	FSBA vs C-Src	N1-Src vs C-Src
YTPSGQSGAAASESLFISNHAY(+79.97)	Aldoa	Y22:25.70	0	0	0	7690	0	0	0	0	75400	1	1E-06	1E-06
YEGSGDGGAAAQSLY(+79.97)VANHAY	Aldoc	Y15:26.31	0	0	0	3E+05	3E+05	2E+05	8E+05	1E+06	5E+05	1E-06	1E-06	0.565
YEGSGDGGAAAQSLYVANHAY(+79.97)	Aldoc	Y21:53.33	0	0	0	0	0	0	0	0	5440	1	1E-06	0.511
EYC(+57.02)GVPGDGY(+79.97)EELTRS	Ambp	C3:1000, Y10:22.37	0	0	0	32900	22300	10400	1E+05	0	32900	1E-06	1	0.406
MQGSAPQEEEEHPY(+79.97)ELLLTAETK	Anks1a	Y14:10.19	0	0	0	3E+05	1430	62400	4E+05	3E+05	1E+05	1E-06	1E-06	0.218
GSVHDFADFDANQDAEALY(+79.97)TAMK	Anxa6	Y19:12.28	0	0	0	0	40200	24100	0	75600	1E+05	1E-06	1E-06	0.028
SQNTNFPVY(+79.97)SENTDDKHLK	Apc	Y9:14.02	0	0	0	16700	0	6370	0	0	16900	1E-06	1E-06	0.493
HKQNLY(+79.97)GDYVFDASR	Apc	Y6:24.24	0	0	0	0	0	0	0	0	23600	1	1E-06	0.343
SSPSIVLGQEQDTY(+79.97)GGGFDK	Apcs	Y14:8.14	0	0	0	25700	0	0	29000	98700	10300	1	1E-06	1E-06
EAAGEGPVLY(+79.97)EDPPDQK	Apex1	Y10:1000.0	1920	0	1040	34000	26900	5030	99000	2E+05	13200	0.184	0.09	0.855
IDELSLY(+79.97)SVPEGQSK	Apoo	Y7:33.98	3E+05	1E+05	1E+05	2E+06	2E+06	1E+06	6E+06	1E+07	3E+06	0.175	0.025	0.058
QLVRPEQLPIY(+79.97)TAPPLHSK	Apool	Y11:7.21	0	0	0	6E+05	2E+05	5E+05	1E+06	2E+06	1E+06	1E-06	1E-06	0.136
ATT(+79.97)PPNQGRPDS(+79.97)PVY(+79.97)ANLQELK	Arhgap12	T3:8.14, S12:21.30 Y15:33.02	0	0	0	1E+05	89500	49600	3E+05	4E+05	62800	1E-06	1	0.533
NEEENIY(+79.97)SVPHDSTQGK	Arhgap35	Y7:7.65	0	0	0	0	0	0	3E+05	0	0	1	1E-06	0.162
GYPDEIY(+79.97)VVPDDSQNR	Arhgap5	Y7:8.39	0	0	0	10800	2960	0	29000	61200	0	1	1E-06	0.44
AEEY(+79.97)EFLTPMEEAPK	Arhgdia	Y4:42.68	0	0	0	35300	16800	11100	1E+05	2E+05	0	1E-06	1E-06	0.486
DTDIVDEAIY(+79.97)YFK	Arpc3	Y10:30.46	0	0	0	61600	31200	49700	2E+05	3E+05	47800	1E-06	1E-06	0.923
ETKDTDIVDEAIY(+79.97)YFK	Arpc3	Y13:12.28	0	0	0	0	0	1E+05	0	0	2E+05	1E-06	1E-06	0.622
KVQY(+79.97)APERPGPQPTAETTR	Arrb1	Y4:13.77	0	2510	0	0	0	0	0	0	0	1E-06	1E-06	0.656
DFVDHIDLVDPVDGVVLVDPEY(+79.97)LKER	Arrb1	Y22:1000.0	0	0	0	0	0	0	0	0	14300	1	1E-06	1E-06
VNKDNLTDLY(+79.97)VQHAIPLPQR	Ashwn	Y10:9.42	0	0	0	0	9760	13400	0	2E+05	1E+05	1E-06	1E-06	0.175
DNLTDLY(+79.97)VQHAIPLPQR	Ashwn	Y7:26.52	0	0	0	62300	0	50600	35700	95800	82400	1E-06	1E-06	0.411
IAPLVLY(+79.97)SSLPMNNK	Ashwn	Y7:8.69	0	0	0	0	0	0	2E+05	0	0	1	1E-06	1E-06
SDLY(+79.97)FVPLEGSK	Atn1	Y4:41.59	0	0	0	30700	37300	18300	73000	2E+05	77400	1E-06	1E-06	0.442
NHPFYVPLGAVDPGLLGYNVPALY(+79.97)SSDPAAR	Atn1	Y24:11.06	0	0	0	0	0	0	0	0	4340	1	1E-06	1E-06
TVNDLEDSY(+79.97)GQQWTYEQR	Atp1a3	Y9:0.00	0	0	0	0	0	0	1880	0	1500	1	1E-06	1E-06
KGSITSVQAIY(+79.97)VPADDLTDPAPATTFAHLDATTVLSR	Atp5f1b	Y11:10.87	0	0	0	0	0	0	0	0	11300	1	1E-06	1
LASGGPVDTGPEY(+79.97)QQEVDRELFK	Atp5j	Y13:19.86	0	2490	0	0	0	0	2E+05	9320	46500	1	0.098	0.53
YATALY(+79.97)SAASK	Atp5o	Y6:0.00	0	0	0	0	0	0	2390	4230	0	1	1E-06	0.597
VSLAVLNPY(+79.97)IK	Atp5o	Y9:128.65	0	0	0	28900	5530	13800	22400	2E+05	22600	1E-06	1E-06	0.796
LVRPPVQVY(+79.97)GIEGR	Atp5o	Y9:1000.0	0	0	0	20700	2940	67700	5580	2E+05	97100	1E-06	1E-06	0.596
VSLAVLNPY(+79.97)IKR	Atp5o	Y9:77.80	0	0	0	5420	0	4990	0	0	9230	1	1E-06	0.506
VGSHITGGDIY(+79.97)GIVNENSLIK	Atp6v1a	Y11:6.74	0	0	0	18000	11000	26600	0	0	1E+05	1E-06	1E-06	0.132

Peptide sequence and modification (phospho-S/T/Y) & Carbamidomethylation	Gene name	Modification A-score (≥ 13 = p < 0.05)	FSBA replicates			N1-Src replicates			C-Src replicates			FSBA vs N1-Src	FSBA vs C-Src	N1-Src vs C-Src
VALENDDRSEEEKY(+79.97)TAVQR	Atxn2	Y14:0.00	0	0	0	60500	0	30500	0	1E+05	78300	1E-06	1E-06	0.384
Y(+79.97)NEENYGVVS(+79.97)TYDSSLSSYTVPLER	Atxn2	Y1:5.81, S10:7.65	0	0	0	5900	14600	0	22200	1E+05	51600	1E-06	1	0.577
GLPQPTISFDGIY(+79.97)ANVR	Atxn2	Y13:45.16	0	0	0	5E+05	2E+05	2E+05	1E+06	1E+06	4E+05	1E-06	1E-06	0.414
Y(+79.97)NEENYGVVSTYDSSLSSYTVPLER	Atxn2	Y1:4.75	0	0	0	2E+05	3E+05	2E+05	4E+05	1E+06	5E+05	1E-06	1	0.787
NSS(+79.97)KGLPQPTISFDGIY(+79.97)ANVR	Atxn2	S3:0.00, Y17:39.44	0	0	0	11400	0	0	0	0	0	1E-06	1	1E-06
GPPQSPVFEGVY(+79.97)NNSR	Atxn2l	Y12:19.27	0	0	0	2E+05	87500	45900	6E+05	7E+05	1E+05	1E-06	1E-06	0.389
QRPYSVAVPAFSQGLDDY(+79.97)GAR	Baiap2	Y18:55.13	0	0	0	0	0	0	0	0	28400	1	1E-06	1E-06
GAIY(+79.97)SIPITEDGGGGSSTPEDPAEAPR	Bcan	Y4:7.65	0	0	0	39800	10200	2440	1E+05	2E+05	30500	1E-06	1E-06	0.4
FAMPSSTPLY(+79.97)HDAIK	Bcl9	Y10:19.27	0	0	0	0	0	0	0	0	2660	1	1E-06	1E-06
TEDEQFNDEKTY(+79.97)LVK	Cab39	Y12:7.21	0	0	0	43800	3210	5430	12600	2E+05	0	1E-06	1E-06	0.538
EDFASNEVVY(+79.97)YNAK	Cacna2d1	Y10:20.00	0	0	0	4400	0	0	6590	27400	1280	1E-06	1	0.931
YQDLY(+79.97)TVEPNNAR	Cacna2d1	Y5:24.44	0	0	0	0	0	0	3040	0	0	1	1E-06	1E-06
HLEEDYADAY(+79.97)QDLYQPHR	Cacnb3	Y10:49.79	0	0	0	0	0	0	0	0	46600	1	1E-06	0.693
DASPGGPGGPGFASTDISMY(+79.97)TLSR	Cacng8	Y20:17.01	2490	0	0	66400	62600	29700	2E+05	3E+05	91600	1E-06	0.029	0.459
GADDAADADTAIINAEGGQNNSEEKKEY(+79.97)FI	Cadm1	Y28:10.92	0	0	0	0	0	0	3E+05	0	0	1	1E-06	0.247
GAEDAPDADTAIINAEGSQVNAEEKKEY(+79.97)FI	Cadm2	Y28:16.06	0	0	0	4E+05	3E+05	2E+05	2E+06	9E+05	4E+05	1	1E-06	0.798
GSDDAPDADTAIINAEGGQSGGDDKKEY(+79.97)FI	Cadm3	Y28:36.81	0	0	0	26200	4E+05	0	3E+06	35700	5200	1E-06	1E-06	0.433
VFDKDGNGY(+79.97)ISAAELR	Calm2	Y9:18.23	0	0	0	1830	0	0	0	0	10300	1	1E-06	1E-06
EVY(+79.97)PHVSTIINIC(+57.02)LK	Cand1	Y3:7.28, C13:1000	0	2E+05	0	0	0	0	0	0	0	1E-06	1E-06	0.522
APVPTGEVY(+79.97)FADSFDR	Canx	Y9:28.70	0	0	0	30200	6210	0	49000	98200	35500	1E-06	1E-06	0.519
LEAVSHTSDMHC(+57.02)GY(+79.97)GDSPSK	Cap1	C12:1000, Y14:18.88	0	0	0	0	0	0	0	40300	9400	1	1E-06	1E-06
GHGFITPADGGPDIFLHISDVEGEYVPVEGDEVTY(+79.97)K	Carhsp1	Y35:14.02	0	0	0	0	0	0	0	0	93200	1	1E-06	1E-06
GHGFITPADGGPDIFLHISDVEGEY(+79.97)VPVEGDEVTY(+79.97)K	Carhsp1	Y25:6.67, Y35:8.69	0	0	0	0	0	0	0	0	56600	1	1E-06	0.392
GHGFITPADGGPDIFLHISDVEGEY(+79.97)VPVEGDEVTYK	Carhsp1	Y25:0.00	0	0	0	0	0	0	0	0	5E+05	1	1E-06	1E-06
QELIALY(+79.97)GYDIR	Casc3	Y7:0.00	0	0	0	0	0	0	0	0	11000	1	1E-06	1E-06
TSDVYWVLQDPVY(+79.97)EDLLSENR	Casd1	Y13:36.20	0	0	0	0	0	0	15400	19600	25500	1	1E-06	1E-06
TSDVYWVLQDPVY(+79.97)EDLLSENRK	Casd1	Y13:32.94	0	0	0	0	0	0	0	0	1E+05	1	1E-06	1E-06
YAASDSEPERDELLVPAAAGPY(+79.97)ATVQR	Caskin1	Y22:5.99	0	0	0	1E+05	16100	70700	0	3E+05	3E+05	1E-06	1	1E-06
YAASDS(+79.97)EPERDELLVPAAAGPY(+79.97)ATVQR	Caskin1	S6:0.00, Y22:5.99	0	0	0	29000	0	0	6960	0	15000	1	1E-06	1E-06
TIHGSKS(+79.97)MDSGIY(+79.97)LDSSYK	Casp3	S7:0.00, Y13:12.33	0	0	0	2690	0	0	0	5150	8780	1	1E-06	1E-06
SMDSGIY(+79.97)LDSSYK	Casp3	Y7:46.91	0	0	0	32100	33500	11100	2E+05	2E+05	34500	1E-06	1E-06	0.302

Peptide sequence and modification (phospho-S/T/Y) & Carbamidomethylation	Gene name	Modification A-score (≥ 13 = p < 0.05)	FSBA replicates			N1-Src replicates			C-Src replicates			FSBA vs N1-Src	FSBA vs C-Src	N1-Src vs C-Src
IPVEADFLY(+79.97)AYSTAPGYYSWR	Casp3	Y9:32.28	0	0	0	0	0	22900	0	0	1E+05	1E-06	1E-06	0.001
TIHGSKSMDS(+79.97)GIY(+79.97)LDSSYK	Casp3	S10:5.81, Y13:13.03	0	0	0	5910	0	0	0	0	2920	1E-06	1	0.183
NAIHTY(+79.97)VQAGSHIAAK	Cat	Y6:9.34	0	0	0	11900	0	0	0	20600	14200	1E-06	1E-06	0.352
YVDSEGHLY(+79.97)TVPIR	Cav1	Y9:0.00	0	0	0	6120	8380	0	0	0	99400	1	1E-06	0.665
VATGLY(+79.97)EAYEAER	Ccdc177	Y6:42.00	0	0	0	16000	3060	2740	0	96100	16500	1E-06	1E-06	0.052
HTPEFSGGSASGDNYY(+79.97)YEDGGMK	Ccdc50	Y16:17.01	0	0	0	12700	0	0	0	6800	5630	1E-06	1	0.138
KIGDEY(+79.97)FTFITDC(+57.02)KDPK	Cct3	Y6:6.59, C13:1000	0	0	0	0	0	0	0	0	56300	1	1E-06	1E-06
HFSGLEEAVY(+79.97)R	Cct8	Y10:52.22	0	0	0	5780	0	0	0	4750	11300	1	1E-06	0.274
LGEDPY(+79.97)YTENGGGQGYSSGPGTSPETQGK	Cd34	Y6:0.00	0	0	0	22900	11800	0	74800	94300	10300	1E-06	1E-06	0.305
KAQNAADSY(+79.97)SWIPER	Cd93	Y9:8.14	0	0	0	4920	0	0	0	0	3010	1E-06	1	1E-06
LGPGGLDPVEVY(+79.97)ESLPEELQK	Cdc37	Y12:8.22	0	0	0	2E+05	35500	57600	0	3E+05	73700	1E-06	1E-06	0.719
ETIATY(+79.97)QLFVETTDASGR	Cdh13	Y6:0.00	0	0	0	0	0	0	0	0	1810	1	1E-06	0.478
TLDRETIATY(+79.97)QLFVETTDASGR	Cdh13	Y10:14.02	0	0	0	0	0	10400	0	0	71200	1	1E-06	0.546
TGFPEDVY(+79.97)SAVLPK	Cdh2	Y8:9.34	0	0	0	4E+05	3E+05	2E+05	7E+05	1E+06	4E+05	1E-06	1E-06	0.863
KVQYESSEPADFKVDEDGTVY(+79.97)AVR	Cdh2	Y21:5.47	0	0	0	23700	0	22900	0	0	97100	1E-06	1E-06	0.27
VQYESSEPADFKVDEDGTVY(+79.97)AVR	Cdh2	Y20:0.00	0	0	0	0	0	0	63500	0	0	1	1E-06	1E-06
TPQGPPEIY(+79.97)SDTQFPSLQSTAK	Cdv3	Y9:20.00	0	0	0	2E+06	2E+06	24500	5E+06	5E+06	1E+06	1E-06	1E-06	0.071
KTPQGPPEIY(+79.97)SDTQFPSLQSTAK	Cdv3	Y10:12.79	11400	87200	7870	3E+07	3E+07	2E+07	7E+07	1E+08	3E+07	0.265	0.091	0.514
TALVQAPPAPVTVTETPEPAMPSGVY(+79.97)RPPGAR	Cdv3	Y26:0.00	0	0	0	0	1E+05	0	6E+05	0	0	1E-06	1E-06	0.328
ELFEPYGAVY(+79.97)QINVLR	Celf2	Y10:31.56	0	0	0	20700	0	5890	0	0	8840	1E-06	1E-06	0.42
ELKELFEPYGAVY(+79.97)QINVLR	Celf2	Y13:42.68	0	0	0	0	0	0	0	0	5070	1	1E-06	1E-06
DTDDDEEEPDPY(+79.97)GFIVQTAEIAEIAR	Cep170b	Y12:21.30	0	0	0	3760	14600	0	15300	21100	10100	1E-06	1E-06	1
NIILEEGKEILVGDVGQTVDDPY(+79.97)TTFVK	Cfl1	Y23:12.28	0	0	0	7E+05	3E+05	5E+06	6E+06	0	1E+07	1E-06	1E-06	0.515
EILVGDVGQTVDDPY(+79.97)TTFVK	Cfl1	Y15:17.01	0	0	0	7E+05	4E+05	3E+05	2E+05	2E+06	6E+05	1E-06	1E-06	0.337
KNIILEEGKEILVGDVGQTVDDPY(+79.97)TTFVK	Cfl1	Y24:7.65	0	0	0	0	0	0	0	0	24500	1	1E-06	1E-06
YALY(+79.97)DATYETK	Cfl1	Y4:34.76	0	0	0	31300	37300	12200	7E+05	2E+05	50600	1E-06	1E-06	0.075
YALYDATY(+79.97)ETKESK	Cfl1	Y8:0.00	0	0	0	2E+05	3900	1E+05	8000	9E+05	2E+05	1	1E-06	1E-06
QILVGDIGDTVEDPY(+79.97)TSFVK	Cfl2	Y15:14.04	0	0	0	0	0	0	61000	0	0	1E-06	1E-06	0.261
GVGVALDDPY(+79.97)ENYR	Cherp	Y10:20.70	0	0	0	29200	0	7760	56600	1E+05	36700	1E-06	1	0.212
GVGVALDDPY(+79.97)ENYRR	Cherp	Y10:17.81	0	0	0	2E+05	68600	1E+05	7090	4E+05	3E+05	1	1E-06	1E-06
GAGPESEPY(+79.97)IFQTPEGVPEQPSFLK	Chl1	Y9:0.00	0	0	0	26200	69500	20100	25000	99000	43600	1E-06	1E-06	0.581
NDY(+79.97)C(+57.02)C(+57.02)FAAFPK	Chl1	Y3/C4/C5:1000.0	0	0	0	0	0	0	0	5790	0	1	1E-06	1E-06

Peptide sequence and modification (phospho-S/T/Y) & Carbamidomethylation	Gene name	Modification A-score (≥ 13 = p < 0.05)	FSBA replicates			N1-Src replicates			C-Src replicates			FSBA vs N1-Src	FSBA vs C-Src	N1-Src vs C-Src
TGTETEDVLGELEY(+79.97)EKVPYSSLR	Cic	Y14:33.54	0	0	0	4E+05	3E+05	4E+05	1E+06	2E+06	4E+05	1E-06	1E-06	2E-04
VVHAFDMEDLGDKAVY(+79.97)C(+57.02)R	Cisd1	Y16/C17:1000.0	0	0	0	58000	0	3E+05	3E+05	26500	1E+06	1E-06	1E-06	0.614
SSLQTMESDVY(+79.97)TEVR	Ckap4	Y11:14.02	0	0	0	99600	62900	0	1E+05	5E+05	1E+05	1E-06	1E-06	0.488
VLTPELY(+79.97)AELR	Ckb	Y7:67.69	11500	0	6530	4E+05	1E+05	1E+05	5E+05	8E+05	3E+05	0.08	0.058	0.088
HGGYQPSDEHKTDLNPDNLQGGDDLDPNY(+79.97)VLSSR	Ckb	Y29:26.52	0	0	0	0	0	0	0	0	2E+05	1	1E-06	1E-06
EAEHLY(+79.97)HTLESSYQK	Clasp1	Y6:14.63	0	0	0	23400	0	19000	0	10400	78800	1E-06	1E-06	0.504
SYS(+79.97)PSMLDYDTENLNSEEIY(+79.97)SSLR	Clasp1	S3:0.0, Y20:17.01	0	0	0	17100	32900	0	21300	79400	30200	1E-06	1E-06	1E-06
SYSPSMLDYDTENLNSEEIY(+79.97)SSLR	Clasp1	Y20:17.01	0	0	0	2E+05	4E+05	1E+05	5E+05	7E+05	3E+05	1E-06	1E-06	0.685
EYNPYPY(+79.97)SDTINTYDK	Clasp1	Y7:17.01	0	0	0	15200	8770	3610	31800	1E+05	26000	1	1E-06	0.109
RSYSPSMLDYDTENLNSEEIY(+79.97)SSLR	Clasp1	Y21:10.11	0	0	0	0	0	2080	0	0	33200	1	1E-06	1E-06
RYEPY(+79.97)GMYSDDDANSDASSVC(+57.02)SER	Clasp1	Y5:5.77, C21:1000	0	0	0	0	0	0	0	2820	0	1	1E-06	0.53
SRDYNPY(+79.97)NYSDSISPFNK	Clasp2	Y7:16.66	0	0	0	73100	9130	67300	0	3640	2E+05	1E-06	1E-06	0.485
NHFPGEAETLY(+79.97)NSLEPSYQK	Clasp2	Y11:45.01	0	0	0	2E+06	1E+06	1E+06	4E+06	3E+06	2E+06	1E-06	1E-06	0.612
SPANWSSPLTSPTNTSQNTLSPSAFDYDTENMNSEDIY(+79.97)SSLR	Clasp2	Y38:12.28	0	0	0	2E+05	3E+05	2E+05	3E+05	9E+05	3E+05	1E-06	1E-06	0.205
DYNPY(+79.97)NYSDSISPFNK	Clasp2	Y5:20.41	0	0	0	1E+05	2E+05	1E+05	3E+05	8E+05	3E+05	1E-06	1E-06	0.962
SPANWSS(+79.97)PLTSPTNTSQNTLSPSAFDYDTENMNSEDIY(+79.97)SSLR	Clasp2	S7:0.00, Y38:14.02	0	0	0	0	17100	0	0	19400	0	1E-06	1	0.372
NHFPGEAETLYNSLEPSY(+79.97)QK	Clasp2	Y18:0.00	0	0	0	4720	0	0	0	1510	0	1	1E-06	1E-06
ATVHIQVNDVNEY(+79.97)APVFK	Clstn1	Y13:88.86	0	0	0	8880	0	6420	0	0	36900	1E-06	1E-06	0.016
HKPWLEPTY(+79.97)HGIVTENDNTVLLDPPLIALDKDSPLR	Clstn1	Y9:0.00	0	0	0	0	0	0	37100	0	0	1	1E-06	1E-06
DIY(+79.97)DQKLTLQPVDNSTISLQMGTNK	Cnn3	Y3:12.35	0	0	0	0	0	0	0	0	53500	1	1E-06	1
TKEVIDTGY(+79.97)GILDR	Cnpy3	Y9:19.68	0	0	0	30000	0	5080	0	34800	50200	1E-06	1E-06	0.178
EVIDTGY(+79.97)GILDRK	Cnpy3	Y7:22.85	0	0	0	27700	0	8310	0	58400	48100	1E-06	1E-06	0.679
EVIDTGY(+79.97)GILDR	Cnpy3	Y7:22.85	0	0	0	3E+05	2E+05	1E+05	7E+05	1E+06	4E+05	1E-06	1E-06	0.162
VVY(+79.97)TGIYDTEGVAPTK	Cnrip1	Y3:40.00	0	0	0	0	0	0	2880	3530	0	1	1E-06	0.435
VVYTGIY(+79.97)DTEGVAPTK	Cnrip1	Y7:22.85	0	0	0	2E+05	2E+05	91100	5E+05	9E+05	2E+05	1E-06	1E-06	0.484
GAAQQYHSPVNLY(+79.97)HSPDAFR	Cntn5	Y13:32.28	0	0	0	2830	0	0	0	0	36900	1E-06	1E-06	0.168
LYLEDDDPVQAEAY(+79.97)INR	Cops4	Y14:35.28	0	0	0	0	0	0	0	2920	3020	1	1E-06	1E-06
GYKPPDEGPSEY(+79.97)QTIPLNK	Cops5	Y12:20.41	7100	14000	0	1E+06	3E+05	7E+05	1E+06	4E+06	8E+05	0.117	0.18	0.745
GYKPPDEGPSEY(+79.97)QTIPLNKIEDFGVHC(+57.02)K	Cops5	Y12:0.0, C27:1000	0	0	0	0	0	47400	0	0	9E+05	1	1E-06	1E-06
GY(+79.97)KPPDEGPSEYQTIPLNK	Cops5	Y2:19.61	0	0	0	0	0	0	8790	0	0	1	1E-06	1E-06

Peptide sequence and modification (phospho-S/T/Y) & Carbamidomethylation	Gene name	Modification A-score (≥ 13 = p < 0.05)	FSBA replicates			N1-Src replicates			C-Src replicates			FSBA vs N1-Src	FSBA vs C-Src	N1-Src vs C-Src
GY(+79.97)KPPDEGPSEYQTIPLNKIEDFGVHC(+57.02)K	Cops5	Y2:6.77, C27:1000	0	0	0	0	0	0	50400	0	0	1	1E-06	1E-06
QLEDLVIEAVY(+79.97)ADVLR	Cops7a	Y11:1000.0	0	0	0	21700	15700	68900	2E+05	3E+05	2E+05	1E-06	1E-06	0.778
ELEDLIIEAVY(+79.97)TDIIQGK	Cops7b	Y11:11.06	0	0	0	0	0	0	28500	20200	28700	1	1E-06	0.589
SEDY(+79.97)ALPSYVDRR	Cox4i1	Y4:19.86	0	0	0	0	4780	0	3E+05	1E+05	0	1E-06	1E-06	0.333
SEDYALPSY(+79.97)VDRR	Cox4i1	Y9:11.06	864	0	0	3E+05	1E+05	3E+05	2E+06	4E+06	3E+05	1E-06	1E-06	0.91
SEDY(+79.97)ALPSY(+79.97)VDRR	Cox4i1	Y4:29.32, Y9:0.00	0	0	0	22800	7800	2750	66400	2E+05	11600	1E-06	1	0.046
AHGSVVKSEDY(+79.97)ALPSYVDR	Cox4i1	Y11:32.69	14900	21500	0	2E+05	28800	4E+05	6E+05	2E+05	3E+05	0.135	0.082	0.183
SEDY(+79.97)ALPSYVDR	Cox4i1	Y4:41.59	4E+05	4E+05	2E+05	1E+06	9E+05	7E+05	3E+06	6E+06	6E+05	0.478	0.07	0.026
SYVY(+79.97)GPIPHTFDRDWVAMQTK	Cox4i1	Y4:9.42	0	0	0	0	0	0	0	0	19200	1	1E-06	1E-06
SLLSHEFQDETDTEEET(+79.97)LY(+79.97)SSKH	Cpd	T17:0.0, Y19:22.09	0	0	0	53100	0	24500	0	0	49200	1E-06	1	0.458
AYPFVLSANLHGGSLVVNYPY(+79.97)DDNEQGVATYSK	Cpd	Y21:11.10	0	0	0	0	0	0	0	0	43200	1	1E-06	1E-06
SGTAHEY(+79.97)SSC(+57.02)PDDAIFQSLAR	Cpe	Y7:12.28, C10:1000	0	0	0	2E+05	8520	78300	2080	2E+05	2E+05	1E-06	1E-06	0.632
GVNIGGAGSYIY(+79.97)EKPPTEAPQVTGPIEVPVVR	Crip2	Y12:0.00	0	0	0	2E+05	0	5E+05	0	2E+05	8E+05	1E-06	1	0.257
GVNIGGAGS(+79.97)Y(+79.97)IYEKPPTEAPQVTGPIEVPVVR	Crip2	S9/Y10:0.00	16200	57900	77100	1E+05	2E+05	74200	0	4E+05	2E+05	0.395	0.194	0.916
GVNTGAVGS(+79.97)Y(+79.97)IYDKDPEGTVQP	Crip2	S9:7.77, Y10:9.40	6770	6820	34900	18900	77700	24000	93300	2E+05	70600	0.982	1	0.729
GVNIGGAGSY(+79.97)IYEKPPTEAPQVTGPIEVPVVR	Crip2	Y10:0.00	0	5360	0	9E+05	0	0	0	0	21900	1E-06	0.566	1
TLTPGGHAEHDGQPY(+79.97)C(+57.02)HKPC(+57.02)YGILFGPK	Crip2	Y15:0.00 C16/C20:1000.0	0	0	0	0	0	0	0	0	16700	1	1E-06	1E-06
TLTPGGHAEHDGQPYC(+57.02)HKPC(+57.02)Y(+79.97)GILFGPK	Crip2	C16/C20:1000.0 Y21:7.99	0	0	0	0	0	0	2E+05	0	0	1	1E-06	1E-06
TLTPGGHAEHDGKPFC(+57.02)HKPC(+57.02)Y(+79.97)ATLFGPK	Crip2	C16/C20:1000.0 Y21:6.59	0	0	0	0	0	0	3E+05	0	0	1	1E-06	1E-06
GVNTGAVGSYIY(+79.97)DKDPEGTVQP	Crip2	Y12:18.53	0	0	0	0	8640	0	8640	0	0	1	1E-06	1E-06
YRPASASVSALIGGNQEGSHPQPLGGPEPGPY(+79.97)AQPSVNTPL PNLQNGPIYAR	Crk	Y32:0.00	0	0	0	0	0	0	0	0	2E+05	1	1E-06	0.01
GMYDGPVY(+79.97)EVPATPK	Crmp1	Y8:76.17	15100	4490	17100	8E+05	9E+05	3E+05	3E+06	3E+06	9E+05	0.169	0.089	0.8
GMYDGPVY(+79.97)EVPAT(+79.97)PK	Crmp1	Y8:0.00, T13:21.00	0	0	0	7930	28300	0	56300	38100	7580	1	1E-06	0.369
IINDDQSFY(+79.97)ADVYLEDGLIK	Crmp1	Y9:18.53	0	0	0	0	0	0	0	0	2E+05	1	1E-06	0.077
TVVGQITVDMMY(+79.97)GGMR	Cs	Y12:56.99	0	0	0	0	32100	0	0	11100	59400	1E-06	1E-06	0.511
GLVY(+79.97)ETSVLDPDEGIR	Cs	Y4:67.96	0	0	0	2E+05	3E+05	2E+05	4E+05	2E+06	5E+05	1E-06	1E-06	0.178
HYEDGYPGGSDNY(+79.97)GSLSR	Ctnnd1	Y13:11.10	0	0	0	71900	0	11400	22200	1E+05	54600	1E-06	1E-06	0.001
LNGPQDHNHLLY(+79.97)STIPR	Ctnnd1	Y12:12.28	0	0	0	70100	0	98800	0	0	2E+05	1	1E-06	0.407
VDQVIILYSGDKIYDNY(+79.97)YPDLK	Cxadr	Y17:0.00	0	0	0	2E+05	0	3E+05	0	37700	7E+05	1E-06	1	0.962

Peptide sequence and modification (phospho-S/T/Y) & Carbamidomethylation	Gene name	Modification A-score (≥ 13 = p < 0.05)	FSBA replicates			N1-Src replicates			C-Src replicates			FSBA vs N1-Src	FSBA vs C-Src	N1-Src vs C-Src
VDQVIILYSGDKIY(+79.97)DNYYPDLK	Cxadr	Y14:6.63	0	0	0	0	1E+05	0	0	1E+06	20400	1E-06	1E-06	0.608
TQY(+79.97)NQVPSEDFER	Cxadr	Y3:14.04	0	0	0	1750	3040	0	30200	46400	0	1E-06	1	0.11
TQY(+79.97)NQVPSEDFERAPQSPT(+79.97)LAPAK	Cxadr	Y3:14.04, T19:0.00	0	0	0	0	0	0	15500	11200	0	1	1E-06	0.332
SYIGSNHSSLGSMSPSNMEGY(+79.97)SK	Cxadr	Y21:8.69	0	0	0	0	0	0	1E+05	0	0	1	1E-06	1E-06
TQPTDEEMLFIY(+79.97)SHFK	Dbi	Y12:0.00	0	0	13700	33000	8980	76700	0	52300	3E+05	0.259	0.136	0.551
GGKPAAAPEELVY(+79.97)QVPQSTQEASGAGRDEK	Dcbld2	Y13:23.70	0	0	0	88500	0	66800	0	1E+05	2E+05	1E-06	1	0.195
GGKPAAAPEELVY(+79.97)QVPQSTQEASGAGR	Dcbld2	Y13:80.35	0	0	0	66900	0	37000	0	1E+05	1E+05	1E-06	1	0.871
GGKPAAAPEELVY(+79.97)QVPQSTQEASGAGRDEKFDAFK	Dcbld2	Y13:14.62	0	0	0	0	0	0	0	0	68100	1	1E-06	0.458
HGDGGY(+79.97)WPVDTNLIDR	Dcc	Y6:76.17	0	0	0	45800	0	28400	0	0	1E+05	1E-06	1E-06	0.437
TGY(+79.97)ESGDYEMLGEGLGVK	Dctn2	Y3:0.00	0	0	0	22700	4720	0	25500	75800	21700	1E-06	1	0.908
TGYESGDY(+79.97)EMLGEGLGVK	Dctn2	Y8:22.69	29800	9050	0	3E+05	3E+05	1E+05	1E+06	1E+06	3E+05	0.152	0.151	0.757
RTGYESGDY(+79.97)EMLGEGLGVK	Dctn2	Y9:7.38	0	0	0	15200	0	1930	0	0	13500	1E-06	1	0.296
HKDLY(+79.97)LPLSLDDS(+79.97)DSLGDSM	Dcx	Y5:28.70, S13:0.00	0	0	0	12000	0	0	0	10600	27800	1E-06	1E-06	1E-06
HKDLY(+79.97)LPLSLDDSDSLGDSM	Dcx	Y5:42.68	0	0	0	83300	0	1E+05	8E+05	38700	3E+05	1E-06	1E-06	0.366
TNEAT(+79.97)AGGSRSEDEDEDDEDY(+79.97)VPYVPLR	Ddx41	T5:0.00, Y21:22.45	0	0	0	20400	11800	12700	67900	52000	8210	1	1E-06	0.748
EVYENYPAY(+79.97)DLTER	Dek	Y9:28.36	0	0	0	7340	0	0	10500	33600	0	1	1E-06	0.199
EVY(+79.97)ENYPAYDLTER	Dek	Y3:28.36	0	0	0	47000	18300	18200	1E+05	2E+05	34700	1E-06	1E-06	0.63
VLYC(+57.02)GVC(+57.02)SLPTEYC(+57.02)EY(+79.97)MPDVAK	Denr	C4/C7/C14:1000.0 Y16:47.09	0	0	0	52700	11800	0	2E+05	0	35700	1E-06	1	0.463
VLYC(+57.02)GVC(+57.02)SLPTEY(+79.97)C(+57.02)EYMPDVAK	Denr	C4/C7/C14:1000.0 Y13:22.85	0	0	0	1E+06	1E+06	5E+05	76100	5E+06	1E+06	1E-06	1E-06	0.41
VLY(+79.97)C(+57.02)GVC(+57.02)SLPTEYC(+57.02)EYMPDVAK	Denr	Y3:30.64 C4/C7/C14:1000.0	0	0	0	29100	54800	25400	6E+06	3E+05	56100	1E-06	1	0.349
FIEAGQYNDNLY(+79.97)GTSVQSVR	Dlg2	Y12:26.31	0	0	0	1E+05	60400	64300	3E+05	6E+05	2E+05	1E-06	1E-06	0.885
HMLVEDDYTRPPEPVY(+79.97)STVNK	Dlg2	Y16:11.06	0	0	0	29600	3E+05	6500	5E+05	5E+05	3E+05	1E-06	1E-06	0.278
GDIPGLGDDGY(+79.97)GTK	Dlg2	Y11:5.47	0	0	0	0	0	0	4730	0	0	1	1E-06	1E-06
DFPGLSDDY(+79.97)YGAK	Dlg3	Y9:17.01	0	0	0	25500	17600	4520	66600	95300	19100	1E-06	1E-06	0.456
DFPGLSDDYY(+79.97)GAK	Dlg3	Y10:0.00	0	0	0	23700	12000	4190	77200	1E+05	26500	1E-06	1E-06	0.916
RDNEVDGQDY(+79.97)HFVVSR	Dlg3	Y10:15.48	0	0	0	0	0	0	0	0	6080	1	1E-06	1E-06
QNSAT(+79.97)ESADSIEIY(+79.97)VPEAQTR	Dlgap4	T5:12.81, Y14:11.75	0	0	0	0	3080	122	36600	43900	4690	1E-06	1	0.203
QNSATESADSIEIY(+79.97)VPEAQTRL	Dlgap4	Y14:27.19	0	0	0	10200	0	9320	2400	42000	11100	1E-06	1E-06	0.345
QNSATESADSIEIY(+79.97)VPEAQTR	Dlgap4	Y14:36.87	0	0	0	0	2640	5630	13600	0	0	1E-06	1E-06	0.733

Peptide sequence and modification (phospho-S/T/Y) & Carbamidomethylation	Gene name	Modification A-score (≥ 13 = p < 0.05)	FSBA replicates			N1-Src replicates			C-Src replicates			FSBA vs N1-Src	FSBA vs C-Src	N1-Src vs C-Src
QNS(+79.97)ATESADSIEIY(+79.97)VPEAQTRL	Dlgap4	S3:0.00, Y14:34.75	0	0	0	0	0	0	9790	0	0	1	1E-06	1E-06
SLS(+79.97)TSGESLY(+79.97)HVLGLDK	Dnajc5	S3:0.00, Y10:14.04	0	0	0	26000	0	8930	0	41200	21500	1E-06	1E-06	0.499
APEGEETEFY(+79.97)VSPEDLEAQLQSDER	Dnajc5	Y10:32.28	4E+05	2E+05	4E+05	5E+06	5E+06	3E+06	1E+07	2E+07	4E+06	0.108	0.047	0.139
SLSTSGESLY(+79.97)HVLGLDK	Dnajc5	Y10:5.99	0	0	0	0	0	4740	0	0	19000	1E-06	1	1E-06
APEGEETEFY(+79.97)VSPEDLEAQLQSDEREATDTPIVIQPASATETT QLTADSHPSYHTDGFN	Dnajc5	Y10:9.42	0	0	0	0	0	0	0	0	4E+05	1	1E-06	1E-06
LIDSKEDPIY(+79.97)DEPEGLAPAPLR	Dok1	Y10:13.13	0	0	0	0	0	0	0	0	15900	1	1E-06	1E-06
GTVVY(+79.97)GEPITASLGTDGSHYWSK	Dpysl2	Y5:3.29	0	0	0	40500	0	21400	0	15100	98700	1E-06	1E-06	0.106
GLY(+79.97)DGPVC(+57.02)EVSVT(+79.97)PK	Dpysl2	Y3:29.67, T13:4.64, C8:1000.0	0	0	0	3740	0	0	51100	6700	0	1	1E-06	1E-06
GTVVYGEPITASLGTDGSHY(+79.97)WSK	Dpysl2	Y20:14.04	0	0	0	48500	0	19000	33100	13700	80500	1E-06	1E-06	1E-06
SITIANQTNC(+57.02)PLY(+79.97)VTK	Dpysl2	C10:1000, Y13:8.18	0	0	0	59200	16300	10300	2E+05	2E+05	30400	1E-06	1E-06	0.006
GLY(+79.97)DGPVC(+57.02)EVSVTPK	Dpysl2	Y3:45.51, C8:1000	0	0	0	26000	0	0	1E+05	91700	14900	1	1E-06	1E-06
THNSALEY(+79.97)NIFEGMEC(+57.02)R	Dpysl2	Y8:19.86, C16:1000	0	0	0	10300	0	0	0	0	99300	1E-06	1E-06	0.003
IVNDDQS(+79.97)FYADIY(+79.97)MEDGLIK	Dpysl2	S7:0.00, Y13:28.74	0	0	4170	0	32800	0	23300	0	77300	1	0.112	1E-06
IVNDDQSFY(+79.97)ADIYMEDGLIK	Dpysl2	Y9:45.01	0	0	0	0	54500	0	0	0	4E+05	1	1	1E-06
IVNDDQSFY(+79.97)ADIY(+79.97)MEDGLIK	Dpysl2	Y9:0.00, Y13:10.92	5270	4450	0	0	46200	0	0	0	1E+05	1	0.179	0.574
NHQSVAEY(+79.97)NIFEGMELR	Dpysl3	Y8:33.81	0	0	0	0	7490	0	49800	12200	0	1E-06	1E-06	0.861
FIPC(+57.02)SPFSDY(+79.97)VYKR	Dpysl3	C4:1000, Y10:4.64	0	0	0	1580	0	0	0	0	0	1E-06	1	0.479
FIPC(+57.02)SPFSDYVY(+79.97)KR	Dpysl3	C4:1000, Y12:12.81	0	0	0	0	0	0	0	0	24300	1	1E-06	1E-06
TISASTQVQGGDFNLY(+79.97)ENMR	Dpysl5	Y16:35.27	0	0	0	0	0	0	0	0	6840	1	1E-06	1E-06
NEIMVAPDKDY(+79.97)FLIVIQNPTE	Dynlrb1	Y11:41.26	0	0	0	8190	0	0	0	0	0	1E-06	1	0.596
EHALLAY(+79.97)TLGVK	Eef1a1	Y7:11.06	0	0	0	54900	0	25100	0	48200	55500	1E-06	1E-06	0.504
LPLQDVY(+79.97)K	Eef1a1	Y7:1000.0	0	0	0	22000	26000	0	1E+05	1E+05	0	1	1E-06	0.989
LPLQDVY(+79.97)KIGGIGTVPVGR	Eef1a1	Y7:37.50	0	0	0	2E+05	0	95100	1E+05	5E+05	2E+05	1E-06	1E-06	0.069
LMEPIYLVEIQC(+57.02)PEQVVGGIY(+79.97)GVLNR	Eef2	C12:1000, Y21:77.79	0	0	0	0	0	0	2E+05	42200	2E+05	1	1E-06	1E-06
ALLELQLEPEELY(+79.97)QTFQR	Eef2	Y13:9.16	0	0	0	0	0	0	0	0	3590	1	1E-06	0.157
VSGDYGHPVYIVQEMPPQSPANIYY(+79.97)KV	Efnb1	Y25:0.00	0	0	0	1E+05	38500	16200	0	97200	5E+05	1E-06	1	0.226
VSGDYGHPVYIVQEMPPQSPANIY(+79.97)YKV	Efnb1	Y24:0.00	5.32	0	4310	15500	0	24800	7E+06	0	59300	1	1E-06	0.83
VSGDYGHPVY(+79.97)IVQEMPPQSPANIY(+79.97)YKV	Efnb1	Y10:19.48, Y24:10.11	4920	0	8440	0	0	22000	2E+05	0	3E+05	1	0.435	0.957
VSGDYGHPVYIVQEMPPQS(+79.97)PANIY(+79.97)YKV	Efnb1	S19:17.67, Y24:22.87	15200	11100	13200	3E+05	0	36900	2E+05	1E+06	0	1	1	0.242
VSGDYGHPVY(+79.97)IVQEMPPQSPANIYYK	Efnb1	Y10:25.58	0	0	0	5E+05	0	93600	3E+06	2E+06	5E+05	1E-06	1E-06	1E-06

Peptide sequence and modification (phospho-S/T/Y) & Carbamidomethylation	Gene name	Modification A-score (≥ 13 = p < 0.05)	FSBA replicates			N1-Src replicates			C-Src replicates			FSBA vs N1-Src	FSBA vs C-Src	N1-Src vs C-Src
VSGDY(+79.97)GHPVY(+79.97)IVQEMPPQSPANIYYKV	Efnb1	Y5:19.27, Y10:4.14	59800	7630	36100	1E+05	8E+05	15300	1E+06	6E+05	4E+05	0.143	0.052	0.324
VSGDY(+79.97)GHPVYIVQEMPPQSPANIYYK	Efnb1	Y5:0.00	3E+05	0	2E+05	0	0	0	0	0	0	1E-06	0.126	0.427
VSGDYGHPVY(+79.97)IVQEMPPQSPANIYYKV	Efnb1	Y10:25.58	0	63500	0	7E+05	0	51100	0	0	9910	0.288	0.234	0.262
VSGDY(+79.97)GHPVYIVQEMPPQSPANIYYKV	Efnb1	Y5:17.91	9E+05	0	6E+05	0	3E+06	0	0	9E+06	0	0.417	0.024	1E-06
VSGDYGHPVYIVQEMPPQS(+79.97)PANIYY(+79.97)KV	Efnb1	S19:7.81, Y25:11.06	0	0	0	0	0	0	82300	0	0	1	1E-06	1E-06
VSGDY(+79.97)GHPVY(+79.97)IVQEMPPQSPANIYYK	Efnb1	Y5:5.08, Y10:6.04	0	0	0	0	0	0	47800	0	0	1	1E-06	0.319
VSGDYGHPVY(+79.97)IVQDGPPQSPPNIYYKV	Efnb3	Y10:17.91	0	0	0	97300	0	2E+05	0	6E+05	2E+05	1E-06	1E-06	0.308
VSGDYGHPVYIVQDGPPQSPPNIYY(+79.97)KV	Efnb3	Y25:8.69	0	0	0	57000	0	1E+05	0	66400	5E+05	1E-06	1E-06	1E-06
VSGDY(+79.97)GHPVYIVQDGPPQSPPNIYYK	Efnb3	Y5:0.00	0	0	0	72500	1560	59700	0	2E+05	2E+05	1E-06	1E-06	0.504
VSGDYGHPVY(+79.97)IVQDGPPQSPPNIY(+79.97)YKV	Efnb3	Y10:8.81, Y24:12.28	0	0	0	0	0	0	0	24700	10700	1	1E-06	1E-06
VSGDYGHPVYIVQDGPPQS(+79.97)PPNIY(+79.97)YKV	Efnb3	S19:22.09, Y24:14.02	0	0	0	80700	2E+05	58900	8030	98400	3E+05	1E-06	1E-06	0.817
VS(+79.97)GDYGHPVYIVQDGPPQS(+79.97)PPNIY(+79.97)YKV	Efnb3	S2/Y24:0.0, S19:7.88	0	0	0	0	0	0	0	0	18700	1	1E-06	0.319
VSGDY(+79.97)GHPVYIVQDGPPQSPPNIYYKV	Efnb3	Y5:0.00	0	0	0	0	6E+05	0	0	1E+06	0	1E-06	1	1
VSGDYGHPVY(+79.97)IVQDGPPQSPPNIYYK	Efnb3	Y10:4.14	0	0	0	0	71700	0	69300	0	0	1E-06	1E-06	0.536
VISVDELEY(+79.97)RQ	Eif4enif1	Y9:36.87	0	0	0	0	0	0	0	12100	4040	1	1E-06	1E-06
SQGLSQLY(+79.97)HNQSQGLLSQLQGQSK	Eif4g2	Y8:0.00	0	0	0	1640	0	0	0	0	8470	1	1E-06	1
EALTY(+79.97)DGALLGDR	Eif4h	Y5:9.34	0	0	0	0	0	0	8120	0	0	1	1E-06	0.231
NMALLSQLY(+79.97)HSPAR	Elavl1	Y9:0.00	0	0	0	0	0	0	0	0	19300	1	1E-06	1E-06
SSQALLSQLY(+79.97)QSPNR	Elavl4	Y10:8.22	0	0	0	0	0	0	0	0	4050	1	1E-06	1E-06
AAVPSGASTGIY(+79.97)EALELRDNDK	Eno1	Y12:34.30	0	0	0	23100	1E+06	0	4E+06	1E+06	0	1E-06	1E-06	0.146
YITPDQLADLY(+79.97)K	Eno1	Y11:85.91	0	0	0	13400	0	0	7770	92400	22900	1	1E-06	1E-06
GNPTVEVDLY(+79.97)TAK	Eno1	Y10:10.11	0	0	0	0	0	0	1E+06	0	0	1	0.036	1E-06
AAVPSGASTGIY(+79.97)EALELR	Eno1	Y12:34.76	2E+05	2E+05	2E+05	5E+07	4E+07	4E+07	9E+07	2E+08	5E+07	0.247	0.097	0.171
AAVPSGAST(+79.97)GIY(+79.97)EALELR	Eno1	T9:0.00, Y12:9.75	0	0	0	3370	0	0	0	28000	0	1E-06	1	0.555
YFDSGDY(+79.97)NMAK	Ensa	Y7:28.96	0	0	0	0	42000	0	1E+05	1E+05	29300	1E-06	1E-06	0.066
TY(+79.97)VDPHTY(+79.97)EDPTQAVHEFAK	Epha3	Y2:0.00, Y8:7.21	0	0	0	93700	0	35600	0	2E+05	1E+05	1E-06	1	0.614
TYVDPHTY(+79.97)EDPTQAVHEFAK	Epha3	Y8:0.00	0	0	0	83400	0	56900	0	26000	69100	1E-06	1	0.073
EIFTGVEY(+79.97)SSC(+57.02)DTIAK	Epha3	Y8:8.14, C11:1000	3E+05	1E+05	2E+05	3E+05	2E+05	2E+05	4E+05	1E+06	2E+05	0.927	0.171	0.508
TY(+79.97)VDPHTYEDPTQAVHEFAK	Epha3	Y2:0.00	0	0	0	0	0	0	8E+05	0	0	1	1E-06	1E-06
VLEDDPEAAY(+79.97)TTR	Epha3	Y10:0.00	4540	2130	2160	4E+05	4E+05	1E+05	9E+05	1E+06	2E+05	0.129	0.089	0.194

Peptide sequence and modification (phospho-S/T/Y) & Carbamidomethylation	Gene name	Modification A-score (≥ 13 = p < 0.05)	FSBA replicates			N1-Src replicates			C-Src replicates			FSBA vs N1-Src	FSBA vs C-Src	N1-Src vs C-Src
TYVDPFTY(+79.97)EDPNQAVR	Epha4	Y8:7.65	7840	1280	0	47200	0	7240	56100	1E+05	0	0.446	0.127	0.578
NGWEEIGEVDENY(+79.97)APIHTYQVC(+57.02)K	Epha5	Y13:29.24, C22:1000.0	62900	4230	0	2700	16700	74200	0	0	1E+05	0.865	0.713	0.463
ADQEGDEELY(+79.97)FHFK	Epha7	Y10:1000.0	0	26200	0	79800	1160	73500	0	37200	58100	0.291	0.372	0.071
VIEDDPEAVY(+79.97)TTTGGKIPVR	Epha7	Y10:17.01	11200	7490	0	73400	0	70000	12000	1E+05	60700	0.157	0.233	0.802
VIEDDPEAVY(+79.97)TTTGGK	Epha7	Y10:12.28	24000	21200	11300	66300	47200	24500	2E+05	3E+05	19000	0.55	0.175	0.661
VIEDDPEAVY(+79.97)TTT(+79.97)GGKIPVR	Epha7	Y10:7.65, T13:0.00	0	0	0	0	0	0	0	19100	0	1	1E-06	1E-06
YLQDDTSDPTY(+79.97)TSSLGGK	Ephb1	Y11:17.01	13600	4330	12200	14900	17300	1510	38900	50300	11800	0.953	0.349	0.212
ADSEY(+79.97)TDKLQHYTS(+79.97)GHMTPGMK	Ephb2	Y5:7.65, S14:7.65	0	38900	0	0	0	46700	0	1E+05	99400	1E-06	1	0.406
FLEDDTSDPTY(+79.97)TSALGGKIPIR	Ephb2	Y11:17.01	0	3510	0	29500	0	33100	0	0	55500	0.094	0.162	0.991
ADSEYT(+79.97)DKLQHY(+79.97)TSGHMTPGMK	Ephb2	T6/Y12:0.00	0	0	0	0	0	0	3E+05	0	0	1	1E-06	1
IY(+79.97)IDPFTYEDPNEAVR	Ephb2	Y2:98.37	13700	4080	2830	26200	0	0	4220	29100	16200	0.535	0.646	1E-06
TYADY(+79.97)ESVNEC(+57.02)MEGVC(+57.02)K	Erh	Y5:8.26 C11/C16:1000.0	11700	4020	37000	25100	27400	11000	1E+05	3E+05	36100	0.906	0.169	0.341
HDDSSDSFC(+57.02)EVDDIQSPDAEY(+79.97)VDLLLNPER	Ero1a	C9:1000, Y21:12.35	0	0	0	0	0	0	0	0	19600	1	1E-06	0.908
FDTQYPY(+79.97)GEKQDEFKR	Erp29	Y7:27.16	0	0	0	8300	0	4200	0	0	6320	1E-06	1	0.506
NEGFY(+79.97)ADPYLYHEGR	Etl4	Y5:61.69	0	0	0	0	0	0	0	0	3990	1	1E-06	1E-06
TQDQDVPVADY(+79.97)GQVVLR	Etl4	Y11:44.17	0	0	0	0	0	0	3010	0	0	1	1E-06	0.242
QDHPSSMGVY(+79.97)GQESGGFSGPGENR	Ewsr1	Y10:35.70	0	0	0	1E+06	2E+06	7E+05	5E+06	8E+06	2E+06	1E-06	1E-06	0.294
YTDHLQSYVIY(+79.97)SLGQPLEK	Exoc1	Y11:7.21	0	0	0	0	0	0	0	0	25800	1	1E-06	1E-06
LDELGVPLY(+79.97)AVVK	Fam213a	Y9:1000.0	0	0	0	0	0	2510	0	18400	5610	1	1E-06	1E-06
EIY(+79.97)NQVNVVLK	Fam49b	Y3:1000.0	0	0	0	0	0	0	0	4450	0	1	1E-06	1E-06
MSLFY(+79.97)AEATPMLK	Fam49b	Y5:25.70	0	0	0	2640	0	0	0	0	3150	1	1E-06	0.292
NFHTFLY(+79.97)EPEWR	Fdft1	Y7:41.59	0	0	0	0	0	0	0	0	15300	1	1E-06	1E-06
Y(+79.97)WPQEAGEYAVHVLC(+57.02)NSEDIR	Flna	Y1:0.00, C15:1000	0	0	0	0	0	0	0	0	31800	1	1E-06	1E-06
SGFEPPGDFPFEDYSQHIY(+79.97)R	Fnbp1l	Y19:14.19	0	0	0	62100	60600	2E+05	3E+05	5E+05	8E+05	1E-06	1E-06	0.791
IGGDAGTS(+79.97)LNSNDY(+79.97)GYGGQKRPLEDGDQPDAK	Fubp1	S8:3.29, Y14:0.00	0	0	0	0	0	0	0	59600	11100	1	1E-06	0.948
QQAAY(+79.97)YAQTSPQGMPQHPPAPQGQ	Fubp1	Y5:0.00	0	0	0	5870	4980	0	76000	32400	3530	1E-06	1E-06	0.348
IGGDAGTSLNSNDY(+79.97)GYGGQK	Fubp1	Y14:12.81	0	3010	0	5E+05	5E+05	2E+05	2E+06	2E+06	4E+05	0.111	0.083	0.145
SVMTEEY(+79.97)KVPDGMVGFIIGR	Fubp1	Y7:0.00	0	0	0	0	0	0	0	0	24100	1	1E-06	1E-06
IGGDAGTSLNSNDYGY(+79.97)GGQK	Fubp1	Y16:10.53	0	0	0	0	0	0	1E+05	0	0	1	1E-06	1E-06
IDSIPHLNNSTPLVDPSVY(+79.97)GYGVQK	Fubp3	Y19:11.10	0	0	0	8160	0	0	0	0	0	1E-06	1	1E-06
VTSVSGESGLY(+79.97)NLPR	Gab1	Y11:28.36	0	0	0	7830	0	0	12000	40100	10500	1E-06	1E-06	1E-06
SSLTGSET(+79.97)DNEDVY(+79.97)TFK	Gab2	T8:8.87, Y14:0.0	0	0	0	0	16900	4650	10500	88000	7890	1E-06	1E-06	0.345

Peptide sequence and modification (phospho-S/T/Y) & Carbamidomethylation	Gene name	Modification A-score (≥ 13 = p < 0.05)	FSBA replicates			N1-Src replicates			C-Src replicates			FSBA vs N1-Src	FSBA vs C-Src	N1-Src vs C-Src
HNTEFKDSTY(+79.97)DLPR	Gab2	Y10:14.02	0	0	0	2E+05	4720	2E+05	5E+05	3E+05	4E+05	1E-06	1E-06	0.484
SSLTGSETDNEDVY(+79.97)TFK	Gab2	Y14:7.21	0	0	0	55100	3E+05	93000	1E+05	8E+05	3E+05	1E-06	1E-06	0.836
WGDAGAEY(+79.97)VVESTGVFTTMEK	Gapdh	Y8:67.69	0	0	0	19100	68300	6850	0	0	48100	1E-06	1E-06	0.296
LISWYDNEY(+79.97)GYSNR	Gapdh	Y9:7.32	0	0	0	9320	7590	0	0	24700	52100	1E-06	1	0.479
YKTPDFESTGLY(+79.97)SAMPR	Gatm	Y12:17.01	0	0	0	3790	0	0	0	0	5150	1E-06	1E-06	0.185
FVAISDLY(+79.97)EPIDDGSESQVFC(+57.02)SC(+57.02)SYDATTH FETTC(+57.02)NDIK	Gdi1	Y8:0.00 C21/C23/C35:1000.0	0	0	0	0	0	0	0	0	15100	1	1E-06	1E-06
SPYLYPLY(+79.97)GLGELPQGFAR	Gdi1	Y8:14.84	0	0	0	2540	0	0	0	0	0	1E-06	1	1
NY(+79.97)TAILFTHAEKIK	Gimd1	Y2:0.00	1E+06	4E+05	2E+06	6E+05	8E+05	8E+05	1E+06	0	2E+06	0.644	0.977	0.245
RTS(+79.97)SLDTITGPY(+79.97)LTGQWPR	Glcci1	S3:0.00, Y12:26.31	0	0	0	2E+05	18900	67500	84900	16300	1E+05	1E-06	1E-06	0.145
T(+79.97)SSLDTITGPY(+79.97)LTGQWPR	Glcci1	T1:0.00, Y11:5.99	0	0	0	1E+05	83400	39000	3E+05	4E+05	1E+05	1E-06	1	0.223
TSSLDTITGPY(+79.97)LTGQWPR	Glcci1	Y11:32.28	0	0	0	1E+05	36600	91300	25600	4E+05	1E+05	1E-06	1E-06	0.158
RTSSLDTITGPY(+79.97)LTGQWPR	Glcci1	Y12:26.31	0	0	0	27900	0	36400	0	0	59100	1	1E-06	0.482
RTSS(+79.97)LDTITGPY(+79.97)LTGQWPR	Glcci1	S4:0.00, Y12:17.01	0	0	0	0	0	0	5280	0	0	1	1E-06	1E-06
LLELQY(+79.97)FISR	Glg1	Y6:27.07	0	0	0	3370	0	0	0	0	5780	1E-06	1E-06	1E-06
FYQASTSELY(+79.97)GK	Gmds	Y10:28.36	0	0	0	27700	47900	2230	97400	88800	45300	1E-06	1E-06	0.225
IINEVKPTEIY(+79.97)NLGAQSHVK	Gmds	Y11:16.36	0	0	0	16800	0	0	0	0	61600	1E-06	1	0.982
IGAADY(+79.97)QPTEQDILR	Gnao1	Y6:20.70	0	0	0	2140	3660	0	0	0	7130	1E-06	1	0.048
SPLTIC(+57.02)FPEYPGSNTY(+79.97)EDAAAYIQTQFESK	Gnao1	C6:1000, Y16:0.00	0	0	0	0	0	0	0	0	40800	1	1E-06	0.344
AAADLMAY(+79.97)C(+57.02)EAHAKEDPLLTPVPASENPFR	Gng2	Y8:26.38, C9:1000	0	0	0	0	0	0	78300	5400	2E+05	1	1E-06	0.925
AAADLMTY(+79.97)C(+57.02)DAHAC(+57.02)EDPLITPVPTSENPF R	Gng3	Y8:17.01 C9/C14:1000.0	0	0	0	33500	0	5140	0	0	0	1E-06	1	0.728
LVDPLY(+79.97)SIKEK	Gnpda1	Y6:9.34	0	0	0	3E+05	39300	1E+05	48900	6E+05	3E+05	1E-06	1E-06	0.258
LVDPLY(+79.97)SIK	Gnpda1	Y6:12.28	0	0	0	2E+05	1E+05	92000	4E+05	7E+05	2E+05	1E-06	1E-06	0.172
NLDKEY(+79.97)LPIGGLADFC(+57.02)K	Got2	Y6/C16:1000.0	0	0	0	0	0	0	0	0	6650	1	1E-06	0.528
VGTSFPHESTY(+79.97)GVGNFNTFK	Gpbp1	Y11:8.14	0	0	0	3E+05	0	1E+05	3E+05	2E+05	2E+05	1E-06	1E-06	0.424
GFNKNDAPLY(+79.97)EINGDHLK	Gpc4	Y10:1000.0	0	0	0	64600	0	67900	1E+05	0	3E+05	1E-06	1E-06	0.5
NDAPLY(+79.97)EINGDHLK	Gpc4	Y6:1000.0	0	0	0	49700	5590	16400	0	94200	0	1E-06	1E-06	0.578
GFSLADIPY(+79.97)QEIAGEHLR	Gpc6	Y9:26.50	0	0	0	0	0	0	0	0	26600	1	1E-06	1E-06
GPSEGAY(+79.97)DVILPR	Gprc5c	Y7:67.69	0	0	0	2490	0	0	17900	0	7880	1	1E-06	0.295
NALPAPSDDPTALMTDPKY(+79.97)IIWSPVC(+57.02)R	Gpx1	Y19:14.58, C26:1000	0	0	0	31600	9210	23800	1E+05	78700	94300	1E-06	1	0.461
Y(+79.97)IIWSPVC(+57.02)R	Gpx1	Y1:44.28, C8:1000	0	0	0	13100	0	0	2280	65100	24500	1	1E-06	1E-06

Peptide sequence and modification (phospho-S/T/Y) & Carbamidomethylation	Gene name	Modification A-score (≥ 13 = p < 0.05)	FSBA replicates			N1-Src replicates			C-Src replicates			FSBA vs N1-Src	FSBA vs C-Src	N1-Src vs C-Src
EGYNVY(+79.97)GIESVKI	Gria2	Y6:28.70	0	0	0	18100	20700	1320	7930	86800	1E+05	1E-06	1	0.906
FDPY(+79.97)EHEALFHTPVEGK	Grpel1	Y4:37.54	0	0	0	47700	0	1E+05	5.81	0	3E+05	1E-06	1E-06	0.005
FDPY(+79.97)EHEALFHTPVEGKEPGTVALVSK	Grpel1	Y4:19.61	0	0	0	0	0	0	0	0	2E+05	1	1E-06	1E-06
GEPNVSY(+79.97)IC(+57.02)SR	Gsk3a	Y7:9.34, C9:1000.0	2E+06	1E+06	1E+06	2E+06	3E+06	5E+05	0	6E+06	1E+06	0.955	0.491	0.206
STC(+57.02)LY(+79.97)GQLPKFEDGDLTLYQSNAILR	Gstp1	C3:1000, Y5:11.12	0	0	0	0	0	0	0	0	10800	1	1E-06	0.149
FEDGDLTLY(+79.97)QSNAILR	Gstp1	Y9:26.31	0	0	0	3040	0	0	0	12000	0	1E-06	1	0.411
VVTTNYKPVANHQY(+79.97)NIEYER	Gtf2f2	Y14:7.38	0	0	0	4800	0	0	0	0	12700	1	1E-06	1E-06
WEQGQADY(+79.97)MGADSFDNIKR	Gyg1	Y8:76.17	0	0	0	33500	0	8880	0	2070	72800	1E-06	1E-06	0.741
IGGHGGEY(+79.97)GEEALQR	Hba1	Y8:1000.0	2580	0	0	2E+05	2E+05	49900	4E+05	9E+05	1E+05	0.216	0.103	0.158
TY(+79.97)FSHIDVSPGSAQVK	Hba1	Y2:0.00	79500	1E+05	63400	3E+07	2E+07	53300	5E+07	1E+08	6E+07	0.417	0.178	0.377
QPETY(+79.97)HTYTTNTPTTAR	Hcfc1	Y5:0.00	0	0	0	0	0	0	4660	4170	0	1	1E-06	1E-06
YSNDLY(+79.97)ELQASR	Hcfc1	Y6:41.96	0	0	0	14000	7030	0	32100	78000	15100	1E-06	1E-06	0.239
KNPMALY(+79.97)ILK	Hepacam	Y7:1000.0	0	0	0	18700	0	1620	3E+05	0	12400	1E-06	1E-06	0.234
ISGLIY(+79.97)EETR	Hist1h4b	Y6:9.42	0	0	0	0	2940	0	4120	12600	1510	1E-06	1E-06	0.231
KGAPGEALTQDPY(+79.97)TLSR	Hivep2	Y13:8.14	0	0	0	26200	0	4630	0	29800	18400	1	1E-06	0.299
HSPDDFYY(+79.97)GDISTLESSQK	Hmgxb4	Y8:30.46	0	0	0	7140	0	0	0	0	15000	1E-06	1E-06	0.231
ATENDIY(+79.97)NFFSPLNPVR	Hnrnph1	Y7:39.44	0	0	0	84000	0	14900	45000	21900	23400	1E-06	1E-06	0.206
GSY(+79.97)GDLGGPIITTQVTIPK	Hnrnpk	Y3:0.00	0	0	0	23400	0	0	37000	83300	14600	1E-06	1E-06	1
FNEC(+57.02)GHVLY(+79.97)ADIK	Hnrnpm	C4/Y9:1000.0	0	0	0	6400	0	0	0	0	2130	1E-06	1	1E-06
DKFNEC(+57.02)GHVLY(+79.97)ADIK	Hnrnpm	C6/Y11:1000.0	0	0	0	0	0	5830	0	0	24000	1	1E-06	0.46
NYILDQTNVY(+79.97)GSAQR	Hnrnpul1	Y10:14.04	0	0	0	0	0	0	0	32300	0	1	1E-06	1E-06
QVVIDGETC(+57.02)LLDILDTAGQEEY(+79.97)SAMR	Hras	C9:1000, Y22:0.00	0	0	0	0	0	0	48600	0	17700	1	1E-06	0.272
IIMTASASGIY(+79.97)GNFGQANYSAAK	Hsd17b4	Y11:12.35	0	0	0	13000	0	0	4470	11200	0	1E-06	1	1E-06
NPDDITNEEY(+79.97)GEFYK	Hsp90aa1	Y10:42.89	0	0	0	2E+05	3E+05	1E+05	7E+05	1E+06	4E+05	1E-06	1E-06	1E-06
NPDDITQEEY(+79.97)GEFYK	Hsp90ab1	Y10:5.26	0	0	0	0	0	0	23	0	0	1	1E-06	1E-06
NAVEEYVY(+79.97)EMRDK	Hspa4	Y8:32.28	0	0	0	0	0	0	0	0	16000	1	1E-06	1E-06
ITPSY(+79.97)VAFTPEGER	Hspa5	Y5:0.00	0	0	0	0	0	0	0	43600	6880	1	1E-06	1E-06
GPAVGIDLGTTY(+79.97)SC(+57.02)VGVFQHGK	Hspa8	Y12:8.69, C14:1000	0	0	0	2E+06	2E+06	3E+06	9E+06	1E+07	5E+06	1E-06	1E-06	0.328
TTPSY(+79.97)VAFTDTER	Hspa8	Y5:17.01	0	0	0	99600	1E+05	0	4E+05	8E+05	1E+05	1E-06	1E-06	0.197
IINEPTAAAIAY(+79.97)GLDKK	Hspa8	Y12:0.00	0	0	89600	6170	3940	6040	9980	3500	5490	0.519	0.557	0.684
GYISPY(+79.97)FINTSK	Hspd1	Y6:8.26	0	0	0	6290	1980	2370	0	22100	12200	1E-06	1	0.362

Peptide sequence and modification (phospho-S/T/Y) & Carbamidomethylation	Gene name	Modification A-score (≥ 13 = p < 0.05)	FSBA replicates			N1-Src replicates			C-Src replicates			FSBA vs N1-Src	FSBA vs C-Src	N1-Src vs C-Src
VVLDDKDY(+79.97)FLFR	Hspe1	Y8:1000.0	0	0	0	3E+05	18800	4E+05	4E+05	4E+05	8E+05	1E-06	1E-06	0.798
VVLDDKDY(+79.97)FLFRDGDILGK	Hspe1	Y8:1000.0	0	0	0	0	0	0	0	0	42900	1	1E-06	1E-06
NAVEEC(+57.02)VY(+79.97)EFR	Hsph1	C6/Y8:1000.0	0	0	0	26300	5030	0	17200	65600	11400	1E-06	1E-06	0.326
NAVEEC(+57.02)VY(+79.97)EFRDK	Hsph1	C6/Y8:1000.0	0	0	0	6E+05	70200	3E+05	5E+05	8E+05	5E+05	1E-06	1E-06	0.916
LLTETEDWLY(+79.97)EEGEDQAK	Hsph1	Y10:17.91	0	0	0	5000	0	2450	0	0	9340	1	1E-06	0.207
YLQLHDLEEDPY(+79.97)LFGNPR	Ids	Y12:47.72	0	0	0	0	0	78500	0	0	5E+05	1E-06	1E-06	0.748
EHEEPTTSEMAEETY(+79.97)SPK	Igfbp5	Y15:9.34	0	0	0	20000	7400	0	14900	1E+05	17900	1E-06	1E-06	0.678
EVQIVSTVDSSFPY(+79.97)AIYTQR	Igsf3	Y14:47.09	0	0	0	18600	0	17600	45400	2E+05	47200	0.481	1	0.262
TTHNSAFEY(+79.97)GTYAEEEGLR	Igsf3	Y9:10.75	0	0	0	0	0	0	0	0	22100	1	1E-06	1E-06
VEALPQEDLPLTKPEMFENPLY(+79.97)GSVSPFPK	Inpp5d	Y22:7.44	0	0	0	0	0	0	2E+05	0	0	1	1E-06	0.646
VAYNPYPEDY(+79.97)GDIEIGSHK	Irs2	Y10:14.15	0	0	0	2920	0	0	0	0	9790	1E-06	1	1E-06
ILESSLY(+79.97)SEEPVEYK	Itga5	Y7:14.02	0	0	0	2E+05	9900	97600	6E+05	9E+05	3E+05	1E-06	1E-06	0.145
WDTGENPIY(+79.97)K	Itgb1	Y9:36.87	0	0	0	51600	65500	20900	2E+05	3E+05	69200	1E-06	1E-06	0.692
DFGWDPC(+57.02)FQPDGYEQTY(+79.97)AEMPK	Itpa	C7:1000, Y17:17.01	0	0	0	4E+05	4E+05	2E+05	1E+06	2E+06	6E+05	1E-06	1E-06	1
DFGWDPC(+57.02)FQPDGYEQTY(+79.97)AEMPKAEK	Itpa	C7:1000, Y17:11.06	0	0	0	75200	0	1E+05	0	0	3E+05	1E-06	1E-06	0.966
TSMTEEY(+79.97)RVPDGMVGLIIGR	Khsrp	Y7:0.00	0	0	0	7290	0	9310	0	1E+05	1E+05	1	1E-06	0.668
AAAAATDPNAAWAAYYSHYY(+79.97)QQPPGPVPGPAPAPAAPPA QGEPPQPPPTGQSDYTK	Khsrp	Y20:0.00	0	0	0	7E+05	0	0	0	6E+06	8E+05	1	1E-06	1E-06
AAAAATDPNAAWAAY(+79.97)YSHYYQQPPGPVPGPAPAPAAPPA QGEPPQPPPTGQSDYTK	Khsrp	Y15:7.21	0	0	0	4E+05	4E+06	2E+05	7E+06	1E+07	6E+05	1E-06	1E-06	0.528
DSAPY(+79.97)GEYGSWYK	Klc2	Y5:25.20	0	0	0	0	5330	0	4140	19000	11200	1	1E-06	0.235
YNAELESGNQFLLY(+79.97)R	Kng1	Y14:23.64	0	0	0	16100	0	0	3160	56700	20900	1E-06	1E-06	1E-06
DGAETLY(+79.97)SFK	Kng1	Y7:14.02	0	0	0	24100	19500	4780	71600	1E+05	20900	1E-06	1E-06	0.186
HLGQSLNC(+57.02)NANVY(+79.97)MRPWENK	Kng1	C8:1000, Y13:32.94	0	0	0	0	0	0	0	0	99900	1	1E-06	0.322
TLQLLNVGEEDDGEY(+79.97)TC(+57.02)LAENSLGSAR	L1cam	Y15:10.11, C17:1000	0	0	0	39300	0	23700	0	59600	18100	1E-06	1	0.564
VTAINKY(+79.97)GPGEPS(+79.97)PVSETVVTPEAAPEK	L1cam	Y7:0.00, S13:6.63	0	0	0	0	0	0	57200	0	0	1	1E-06	0.708
AVEIY(+79.97)ASVAQLTPVDSEALESEANK	Lamc1	Y5:5.47	0	0	0	12200	0	8410	40800	70100	18700	1E-06	1	0.431
AFPNPYADY(+79.97)NK	Lancl1	Y9:28.36	0	0	0	9860	31400	0	64900	1E+05	33800	1E-06	1E-06	0.438
RPTEQQQPQPHHIPTSAPVY(+79.97)QQPQQQQVTPSYGGYKEPAA PVSIQR	Lasp1	Y20:0.00	0	0	0	0	0	25400	0	0	6E+06	1E-06	1	0.525
TQDQISNIKY(+79.97)HEEFEK	Lasp1	Y10:38.03	0	0	0	5410	0	0	0	0	19100	1	1E-06	1E-06
NS(+79.97)NNNNT(+79.97)AAAASVAAAPAGMGVRPGSGDFAY(+ 79.97)LR	Lemd3	S2/T7/Y31:0.00	0	0	0	55200	41500	69700	55600	3E+05	87100	1	1E-06	0.052

Peptide sequence and modification (phospho-S/T/Y) & Carbamidomethylation	Gene name	Modification A-score (≥ 13 = p < 0.05)	FSBA replicates			N1-Src replicates			C-Src replicates			FSBA vs N1-Src	FSBA vs C-Src	N1-Src vs C-Src
KLEEGGPVY(+79.97)SPPAQVVVKK	Letm1	Y9:11.06	0	0	0	18200	0	16800	0	30300	38000	1E-06	1	0.6
LEEGGPVY(+79.97)SPPAQVVVKK	Letm1	Y8:33.98	0	0	0	15200	0	16400	0	93100	30500	1E-06	1E-06	0.326
KLEEGGPVY(+79.97)SPPAQVVVK	Letm1	Y9:8.69	0	0	0	45900	4920	0	0	2E+05	50700	1E-06	1E-06	0.436
LEEGGPVY(+79.97)SPPAQVVVK	Letm1	Y8:10.11	0	0	0	30600	7630	13200	78100	2E+05	19000	1E-06	1E-06	0.141
LDDGHLNNSLGS(+79.97)PVQADVY(+79.97)FPR	Lgalsl	S12:22.45, Y19:57.10	0	0	0	40100	4350	4140	0	0	49100	1E-06	1	0.508
LDDGHLNNSLGSPVQADVY(+79.97)FPR	Lgalsl	Y19:79.54	0	0	0	0	0	0	5E+05	0	0	1	1E-06	1E-06
EVYEHVY(+79.97)ETVDISSSPEVR	Lin7c	Y7:15.39	0	0	0	2E+05	38700	2E+05	4E+06	3E+06	6E+05	1E-06	0.125	0.64
EVY(+79.97)EHVYET(+79.97)VDISSSPEVR	Lin7c	Y3:22.37, T9:0.00	0	0	0	8860	21600	9000	57400	15600	4080	1E-06	1E-06	0.38
EVY(+79.97)EHVY(+79.97)ETVDISSSPEVR	Lin7c	Y3:26.50, Y7:7.32	0	25400	0	6E+05	4E+05	3E+05	9E+05	2E+06	1E+06	0.063	0.047	0.527
EVY(+79.97)EHVYETVDISSSPEVR	Lin7c	Y3:6.65	0	56000	0	1E+06	4E+05	2E+06	6E+05	58400	4E+06	0.247	0.164	0.75
EVYEHVY(+79.97)ET(+79.97)VDISSSPEVR	Lin7c	Y7/T9:0.00	0	0	0	0	1870	0	13700	0	0	1	1E-06	1E-06
SLEVGDNDLVY(+79.97)ISHR	Lingo1	Y11:32.28	0	0	0	0	0	576	0	0	6500	1	1E-06	0.968
ELAPY(+79.97)DENWFYTR	LOC100362339	Y5:41.57	0	0	22800	17300	12300	14400	0	52300	49900	0.705	0.272	0.126
HKELAPY(+79.97)DENWFYTR	LOC100362339	Y7:66.06	0	0	0	0	0	0	0	0	1E+05	1	1E-06	0.216
LTESLHEVY(+79.97)EPDWYGREDVK	LOC100910792	Y9:16.56	0	0	0	0	0	7130	0	0	14600	1	1E-06	1E-06
EVPNY(+79.97)KLITPAVVSER	LOC100911337	Y5:42.68	0	0	0	1630	0	0	0	0	7230	1E-06	1	0.31
DHLNHHHY(+79.97)VAAAFK	Lrrc4b	Y8:1000.0	0	0	0	0	0	0	43500	0	0	1	1E-06	1E-06
EFEGEEEY(+79.97)LEILGITR	Lsamp	Y8:61.82	0	0	0	7540	0	0	0	6540	17300	1E-06	1	1E-06
GSDIKDLTVC(+57.02)EPPKPQC(+57.02)SLPQDPAIVQSSLGSSSSSF QSVGSY(+79.97)GPFGR	Lsm14a	C10/C17:1000.0 Y43:14.02	0	0	0	0	0	0	0	0	1E+05	1	1E-06	1E-06
SFESTVGQGSDTY(+79.97)SYIFR	M6pr	Y13:10.11	0	0	0	41100	0	20500	13300	1E+05	40800	1E-06	1E-06	0.1
IEDPVY(+79.97)GVY(+79.97)YVDHINRK	Magi1	Y6:34.30, Y9:14.02	0	0	0	54800	0	0	0	6750	30000	1E-06	1	0.393
IEDPVY(+79.97)GVY(+79.97)YVDHINR	Magi1	Y6:42.68, Y9:17.01	0	0	0	4240	0	0	0	11400	4480	1	1E-06	1E-06
IEDPVY(+79.97)GVYYVDHINR	Magi1	Y6:34.94	0	0	0	1E+06	6E+05	6E+05	25300	2E+06	1E+06	1E-06	1E-06	0.403
IEDPVY(+79.97)GVYYVDHINRK	Magi1	Y6:38.16	0	0	0	2E+05	25800	5E+05	4E+05	89300	2E+06	1E-06	1E-06	0.44
GYPLPFDPDDPNTSLVTSVAILDKEPIIVNGQETY(+79.97)DSPASHSS K	Magi1	Y35:11.06	0	0	0	0	0	0	0	0	1E+05	1	1E-06	1E-06
HNYETY(+79.97)LEYISR	Magi2	Y6:9.34	0	0	0	3E+05	0	3E+05	7E+05	2E+05	9E+05	1E-06	1E-06	0.714
IDDPIY(+79.97)GTYYVDHINR	Magi2	Y6:36.05	0	0	0	1E+05	0	34300	8E+05	54000	87600	1E-06	1E-06	0.404
IDDPIYGTY(+79.97)YVDHINRR	Magi2	Y9:7.65	0	0	0	52000	0	3E+05	0	0	1E+06	1E-06	1E-06	0.542
SDKHGSPY(+79.97)FYLLGHPK	Magi2	Y8:18.23	0	0	0	0	0	0	0	0	1E+05	1	1E-06	1E-06

Peptide sequence and modification (phospho-S/T/Y) & Carbamidomethylation	Gene name	Modification A-score (≥ 13 = p < 0.05)	FSBA replicates			N1-Src replicates			C-Src replicates			FSBA vs N1-Src	FSBA vs C-Src	N1-Src vs C-Src
HGSPY(+79.97)FYLLGHPK	Magi2	Y5:7.32	0	0	0	0	0	7000	0	0	2E+05	1	1E-06	0.472
HNYETYLEY(+79.97)ISR	Magi2	Y9:6.65	0	0	0	0	0	0	0	26500	0	1	1E-06	1E-06
IEDPQY(+79.97)GTYYVDHLNQK	Magi3	Y6:27.07	0	0	0	1E+05	3500	26500	0	1E+05	75500	1	1E-06	0.475
VLS(+79.97)PLRS(+79.97)PPLIGSESAY(+79.97)EDFLSADDK	Map1b	S3:21.51, S7:28.13 Y17:14.04	0	0	0	1E+05	79900	14400	0	2E+05	2E+05	1E-06	1	0.323
SPPLIGSESAY(+79.97)EDFLSADDKALGR	Map1b	Y11:0.00	0	0	0	0	1E+05	0	6E+05	6E+05	0	1E-06	1E-06	0.219
SSYY(+79.97)VVSGNDPAAEEPSR	Map1b	Y4:0.00	0	0	0	0	0	0	25100	27800	0	1	1E-06	1E-06
VLSPLRS(+79.97)PPLIGSESAY(+79.97)EDFLSADDK	Map1b	S7:7.69, Y17:18.53	0	0	0	5E+05	5E+05	4E+05	5E+05	2E+06	6E+05	1E-06	1E-06	0.362
SPPLIGSESAY(+79.97)EDFLSADDK	Map1b	Y11:27.16	0	0	0	3E+05	2E+05	1E+05	2E+05	1E+06	3E+05	1E-06	1E-06	0.338
DMSLY(+79.97)ASLASEK	Map1b	Y5:25.86	0	0	0	13900	40000	7860	96100	2E+05	69100	1E-06	1	0.385
QGFSDKESPVSDLTSDLY(+79.97)QDKQEEK	Map1b	Y18:19.05	0	0	0	0	0	0	0	0	8460	1	1E-06	0.307
VLS(+79.97)PLRS(+79.97)PPLIGSESAY(+79.97)EDFLSADDKALGR	Map1b	S3:0.00, S7:1.99 Y17:6.65	0	0	0	0	0	0	0	0	42000	1	1E-06	1E-06
SSTVPPGLPVY(+79.97)LDLC(+57.02)YIPNHSNSK	Map1b	Y11:7.71, C15:1000	0	0	0	0	0	0	6E+05	0	0	1	1E-06	1E-06
STGLGSDY(+79.97)Y(+79.97)ELSDSRGNAQESLDTVSPK	Map2	Y8/Y9:0.00	0	0	0	4820	4600	0	3520	0	21200	1E-06	1	0.887
SGTS(+79.97)TPTTPGSTAITPGTPPSY(+79.97)SSR	Map2	S4/Y22:0.00	0	0	0	0	0	0	18100	8270	0	1	1E-06	1E-06
STGLGSDY(+79.97)YELSDSR	Map2	Y8:12.28	0	0	0	69000	47100	29300	2E+05	3E+05	54500	1E-06	1E-06	0.329
STGLGSDYY(+79.97)ELSDSR	Map2	Y9:11.06	0	0	0	39000	7340	13000	70400	2E+05	23500	1E-06	1E-06	0.468
GEEEEIEAEGEY(+79.97)DKLLFR	Map2	Y12:1000.0	0	0	0	2410	0	0	0	0	19700	1E-06	1E-06	1
SGTSTPTTPGSTAITPGTPPSY(+79.97)SSR	Map2	Y22:8.69	0	0	0	28700	0	0	0	0	80900	1	1E-06	0.406
VKPSQSAGDINTIY(+79.97)QAPEPR	Map3k3	Y14:26.31	0	0	0	3900	0	0	0	8370	1120	1E-06	1	0.057
SLY(+79.97)SEPFKESPK	Map6	Y3:17.01	0	0	0	67000	30300	15700	39800	3E+05	77800	1E-06	1E-06	0.335
IRSLY(+79.97)S(+79.97)EPFKESPK	Map6	Y5:18.53, S6:14.84	0	0	0	8770	0	0	0	0	3310	1E-06	1	1E-06
VADPDHDHTGFLTEY(+79.97)VAT(+79.97)R	Mapk1	Y15:0.00, T18:5.81	8110	8490	0	2E+05	1610	87800	0	1E+05	64600	0.208	0.122	0.612
VADPDHDHTGFLTEY(+79.97)VATR	Mapk1	Y15:10.03	7E+05	3E+05	2E+05	2E+06	2E+05	2E+06	2E+06	1E+06	3E+06	0.361	0.299	0.399
VADPDHDHTGFLT(+79.97)EY(+79.97)VATR	Mapk1	T13:7.26, Y15:0.00	2530	0	0	0	0	0	0	0	0	1E-06	1E-06	0.908
IADPEHDHTGFLTEY(+79.97)VATR	Mapk3	Y15:9.74	0	0	0	24700	0	1E+05	0	0	1E+05	1E-06	1E-06	0.318
YTQLQYIGEGAY(+79.97)GMVSSAYDHVR	Mapk3	Y12:3.70	0	0	0	0	0	0	0	0	39400	1	1E-06	0.652
TDHGAEIVY(+79.97)KSPVVSGDT(+79.97)SPR	Mapt	Y9:22.85, T18:0.00	0	0	0	0	5800	0	31400	65500	0	1E-06	1E-06	0.935
TDHGAEIVY(+79.97)KS(+79.97)PVVSGDT(+79.97)SPR	Mapt	Y9:42.78 S11:22.05, T18:0.0	0	0	4080	8E+05	7E+05	3E+05	2E+06	3E+06	9E+05	1E-06	1E-06	6E-04
TDHGAEIVY(+79.97)KSPVVSGDTSPR	Mapt	Y9:60.92	0	0	0	3E+05	40400	3E+05	8E+05	1E+06	3E+05	1E-06	1E-06	0.08

Peptide sequence and modification (phospho-S/T/Y) & Carbamidomethylation	Gene name	Modification A-score (≥ 13 = p < 0.05)	FSBA replicates			N1-Src replicates			C-Src replicates			FSBA vs N1-Src	FSBA vs C-Src	N1-Src vs C-Src
TDHGAEIVY(+79.97)KS(+79.97)PVVS(+79.97)GDTSPR	Mapt	Y9:31.37 S11:14.15, S15:6.63	0	0	0	2E+05	1E+05	89000	2E+05	9E+05	2E+05	1E-06	1E-06	0.774
AKTDHGAEIVY(+79.97)KS(+79.97)PVVS(+79.97)GDTSPR	Mapt	Y11:28.92 S13:9.00, S17:9.42	0	0	0	1E+05	56400	47100	67300	4E+05	2E+05	1E-06	1E-06	0.325
TDHGAEIVY(+79.97)KSPVVS(+79.97)GDTSPR	Mapt	Y9:14.04, S15:3.29	9710	1E+05	0	1E+05	1770	0	2E+05	1E+05	1E+05	0.979	0.231	0.287
TDHGAEIVY(+79.97)KSPVVSGDTS(+79.97)PR	Mapt	Y9:26.31, S19:8.69	0	0	0	0	3870	0	3E+05	76600	7830	1	1E-06	0.112
AKTDHGAEIVY(+79.97)KSPVVSGDTS(+79.97)PR	Mapt	Y11:13.45, S21:0.0	0	0	0	99300	1410	1E+05	0	2E+05	0	1E-06	1	0.262
SLY(+79.97)QSSPLFGMYFSVEK	Marc2	Y3:8.22	0	0	0	0	0	0	0	0	8520	1	1E-06	1E-06
EVMLQSLEENVY(+79.97)DAPSLSR	Mast4	Y12:29.67	0	0	0	1E+05	2E+05	73400	5E+05	5E+05	2E+05	1E-06	1E-06	0.959
YLDEDTIY(+79.97)HLQPSGR	Mat2a	Y8:9.00	0	0	0	17800	0	11800	0	29000	63700	1E-06	1	0.386
EHPEQEPELGGPSTANVDSVPIATY(+79.97)GPVSPTVSFQPLPR	Mavs	Y25:0.00	0	0	0	1E+05	0	0	0	2E+05	1E+05	1	1E-06	1E-06
LPINSVY(+79.97)TGIVPSK	Mavs	Y7:10.11	0	0	0	51200	32500	24600	1E+05	3E+05	44200	1E-06	1E-06	0.238
DGESYDPY(+79.97)DFSEAER	Mcm3	Y8:19.16	0	0	0	7730	0	0	31900	49800	7020	1	1E-06	1E-06
FIY(+79.97)EAWQGVER	Mcrip1	Y3:1000.0	0	0	0	2E+06	2E+06	2E+06	3E+06	1E+07	3E+06	1E-06	1E-06	0.023
GSDTLSHSQDNGVDIY(+79.97)EPLYTQGETK	Mdga1	Y16:61.69	0	0	0	4E+05	1E+05	1E+05	5E+05	70800	4E+05	1E-06	1E-06	0.417
GSDTLSHSQDNGVDIYEPLY(+79.97)TQGETK	Mdga1	Y20:17.01	0	0	0	1E+05	52500	49400	49300	3E+05	2E+05	1E-06	1E-06	0.889
GSDTLSHSQDNGVDIY(+79.97)EPLY(+79.97)TQGETK	Mdga1	Y16:45.16, Y20:14.02	0	0	0	85100	79200	29200	3E+05	4E+05	2E+05	1	1E-06	0.406
RGSDTLSHSQDNGVDIY(+79.97)EPLY(+79.97)TQGETK	Mdga1	Y17:17.91, Y21:0.0	0	0	0	0	0	0	0	0	2640	1	1E-06	1E-06
GSDTLSHS(+79.97)QDNGVDIYEPLY(+79.97)TQGETK	Mdga1	S8/Y20:0.00	0	0	0	0	0	0	8370	0	0	1	1E-06	1
GVEIY(+79.97)EPFFTQGETK	Mdga2	Y5:37.78	0	0	0	26800	9920	4090	30800	67600	0	1	1E-06	0.499
EVGVY(+79.97)EALKDDSWLK	Mdh1	Y5:56.54	0	0	0	10200	0	32700	0	0	92300	1	1E-06	0.125
ETEC(+57.02)TY(+79.97)FSTPLLLGK	Mdh2	C4:1000.0, Y6:10.11	0	0	0	1E+06	7E+05	6E+05	2E+06	4E+06	1E+06	1E-06	1E-06	0.177
LTLY(+79.97)DIAHTPGVAADLSHIETR	Mdh2	Y4:22.85	0	0	0	0	0	0	0	0	73000	1	1E-06	0.286
SNYVSLLPDVY(+79.97)DWPESSLKPPQIPE	Me2	Y11:2.81	0	0	0	6E+05	6E+05	5E+05	1E+06	3E+06	8E+05	1E-06	1	0.213
NSHIPC(+57.02)HY(+79.97)DLLPVR	Megf10	C6:1000, Y8:72.73	0	0	0	0	0	0	0	0	13600	1	1E-06	1E-06
YSYYDESQGEIY(+79.97)R	Memo1	Y12:0.00	0	0	0	4980	0	0	15800	46000	6720	1	1E-06	1E-06
AVSPAIPSAPLY(+79.97)EEITYSGISDGLSQASC(+57.02)PLAGLDR	Mgrn1	Y12:0.0, C29:1000	0	0	0	2E+05	2E+05	1E+05	5E+05	6E+05	2E+05	1E-06	1	0.531
FELLEKDPY(+79.97)ALDVPNTAFGR	Mia2	Y9:104.80	0	0	0	0	0	0	0	0	8400	1	1E-06	1E-06
VQADQYIPEEDIY(+79.97)GEMDSIER	Micall1	Y13:45.16	0	0	0	39600	23200	18200	63800	97100	34400	1E-06	1E-06	0.229
KEEEVY(+79.97)EPNPFSK	Mlip	Y6:45.99	0	0	0	49300	6730	11400	1650	62200	23000	1E-06	1E-06	0.612
EEEVY(+79.97)EPNPFSK	Mlip	Y5:32.67	0	0	0	20600	15100	5140	73300	1E+05	12100	1	1E-06	1E-06

Peptide sequence and modification (phospho-S/T/Y) & Carbamidomethylation	Gene name	Modification A-score (≥ 13 = p < 0.05)	FSBA replicates			N1-Src replicates			C-Src replicates			FSBA vs N1-Src	FSBA vs C-Src	N1-Src vs C-Src
KSPEGDPLLEY(+79.97)STFNFWR	Mllt11	Y11:27.96	4810	0	0	0	0	0	0	0	85800	1	0.116	1E-06
NSATLFSASDY(+79.97)EVAPPEYHR	Morf4l1	Y11:18.53	0	0	0	0	0	1820	0	29800	0	1E-06	1	0.394
LFAPTLSQDDPYLSIY(+79.97)DPPVPDFTVMK	Mpi	Y16:1.10	0	0	0	0	0	0	23200	0	11500	1	1E-06	1E-06
SPPSAGSHQGPVIY(+79.97)AQLDHSGGHHSGK	Mpzl1	Y14:7.22	0	0	0	0	0	0	1E+05	0	10000	1	1E-06	0.384
SIFSGIGSTAEPVSQSTTSDY(+79.97)QWDGSR	Mtdh	Y21:8.22	0	0	0	42800	5500	34700	0	87100	0	1E-06	1	0.5
ANPY(+79.97)EC(+57.02)GFDPTSSAR	Mtnd3	Y4:50.34, C6:1000	0	0	0	9510	3240	0	49800	1E+05	0	1E-06	1	0.492
DTEELTY(+79.97)SVPYGR	Mug1	Y7:0.00	0	0	0	1E+05	3E+05	1E+05	3E+05	1E+06	3E+05	1E-06	1	0.266
RNDSIY(+79.97)EASS(+79.97)LYGISAMDGVPFTLHPR	Mvb12a	Y6:14.04, S10:0.00	0	0	0	0	0	0	0	0	10200	1	1E-06	1E-06
RNDSIY(+79.97)EASSLY(+79.97)GISAMDGVPFTLHPR	Mvb12a	Y6:6.59, Y12:13.38	0	0	0	0	0	0	0	0	33200	1	1E-06	0.362
NDSIY(+79.97)EASS(+79.97)LYGISAMDGVPFTLHPR	Mvb12a	Y5:8.22, S9:0.00	0	0	0	0	0	0	0	0	25700	1	1E-06	1E-06
NDSIY(+79.97)EASSLYGISAMDGVPFTLHPR	Mvb12a	Y5:3.64	0	0	0	0	0	0	0	0	49400	1	1E-06	0.335
NKDQGTY(+79.97)EDYVEGLR	Myl6	Y7:21.94	0	0	0	36400	7330	15000	0	87400	89700	1E-06	1E-06	0.794
SPASDTY(+79.97)IVFGEAK	Naca	Y7:11.06	0	0	0	4E+05	1E+05	2E+05	9E+05	2E+06	2E+05	1E-06	1E-06	0.597
SPASDTY(+79.97)VVFGEAK	Nacad	Y7:14.02	0	0	0	47500	14000	17600	93100	2E+05	13600	1E-06	1E-06	0.108
HHISIAEIY(+79.97)ETELVDVEK	Napa	Y9:32.28	0	0	0	0	0	0	99000	40300	0	1	1E-06	0.353
AIDIY(+79.97)EQVGTSAMDSPLLK	Napa	Y5:52.68	0	0	0	2E+05	2E+05	2E+05	1E+06	1E+06	5E+05	1E-06	1E-06	0.424
AIAHY(+79.97)EQSADYYKGEESNSSANK	Napa	Y5:11.12	0	0	0	3930	0	0	0	0	11000	1E-06	1	0.196
HHITIAEIY(+79.97)ETELVDIEK	Napb	Y9:18.53	0	0	0	0	0	0	0	25100	31800	1	1E-06	1E-06
AIEIY(+79.97)EQVGANTMDNPLLK	Napb	Y5:63.15	0	0	0	1E+05	94800	1E+05	4E+05	9E+05	4E+05	1E-06	1E-06	0.562
ADPQEAINC(+57.02)LNAAIDIY(+79.97)TDMGR	Napb	C9:1000, Y17:0.00	0	0	0	0	0	0	0	0	4350	1	1E-06	1E-06
QQQHHQQQYY(+79.97)QSLVELQQR	Nav3	Y10:20.92	0	0	0	5740	0	0	0	0	7490	1E-06	1E-06	1E-06
IGIVGGC(+57.02)QEY(+79.97)TGAPYFAGISALK	Naxd	C7:1000, Y10:17.01	0	0	0	0	0	0	0	0	17600	1	1E-06	1
YQLNLPAYPDTEC(+57.02)VY(+79.97)RLQ	Naxe	C13:1000, Y15:49.79	0	0	0	22100	0	16700	31500	63900	75700	1E-06	1E-06	0.204
SLDWNAEY(+79.97)EVY(+79.97)VVAENQQGK	Ncam1	Y8:0.00, Y11:32.47	0	0	0	0	0	0	0	38500	4470	1	1E-06	1E-06
SLDWNAEY(+79.97)EVYVVAENQQGK	Ncam1	Y8:29.06	0	0	0	1E+05	23700	1E+05	5E+05	5E+05	91000	1E-06	1E-06	0.857
NVDKNDEAEY(+79.97)VC(+57.02)IAENK	Ncam1	Y10/C12:1000.0	0	0	0	3690	0	0	0	16800	0	1E-06	1E-06	0.222
RSMIDDTY(+79.97)QC(+57.02)LTAVAGTPR	Ncdn	Y8:17.01, C10:1000	0	0	0	0	0	0	0	0	8080	1	1E-06	1E-06
SMIDDTY(+79.97)QC(+57.02)LTAVAGTPR	Ncdn	Y7:8.69, C9:1000.0	0	0	0	0	4180	0	40800	0	0	1E-06	1E-06	0.435
TESVFKEPTLVPESSDTTTY(+79.97)K	Ndufv3	Y20:12.28	0	0	0	61800	0	0	0	2E+05	79100	1E-06	1E-06	1E-06
NLQHHEY(+79.97)NAFTFLDLNLDLSK	Ndufv3	Y7:61.69	0	0	0	0	0	8990	0	87600	0	1	1E-06	0.39
YDEDAKRPY(+79.97)FTVDEAEAR	Nectin1	Y9:22.85	0	0	0	90200	3710	2E+05	1E+05	1E+05	8E+05	1E-06	1E-06	0.225

Peptide sequence and modification (phospho-S/T/Y) & Carbamidomethylation	Gene name	Modification A-score (≥ 13 = p < 0.05)	FSBA replicates			N1-Src replicates			C-Src replicates			FSBA vs N1-Src	FSBA vs C-Src	N1-Src vs C-Src
SLY(+79.97)ESFVSSSDR	Nelfe	Y3:26.31	0	0	0	12100	1960	3650	30900	80300	14900	1E-06	1E-06	0.132
MSNAAPSSDSSLY(+79.97)SAPLPEYSSC(+57.02)QPPSAPPPSYAK	N-Enah	Y13:0.0, C23:1000	0	0	0	0	9130	43400	1E+06	2E+05	0	1	1E-06	0.442
VISAPVSDAAPDY(+79.97)AVVTALPPTST(+79.97)PPT(+79.97)PPLR	N-Enah	Y13:5.14, T24:0.00 T27:5.81	0	0	0	60000	3E+05	0	3E+05	3E+05	2E+05	1E-06	1	0.7
MSNAAPSSDSSLYSAPLPEY(+79.97)SSC(+57.02)QPPSAPPPSYAK	N-Enah	Y20:0.0, C23:1000	0	0	0	0	0	76800	0	0	0	1	1	1E-06
VISAPVSDAAPDY(+79.97)AVVTALPPTSTPPTPPLR	N-Enah	Y13:11.12	0	0	0	0	8E+05	0	0	4E+06	0	1E-06	1E-06	0.514
RMSNAAPSSDSSLY(+79.97)SAPLPEYSSC(+57.02)QPPSAPPPSYAK	N-Enah	Y14:0.00 C24:1000.0	0	0	0	0	0	0	2E+05	0	0	1	1E-06	1E-06
SFAVPAIPPPGPPIY(+79.97)DPALPSTPLLSQQALNHHLHSVK	Neo1	Y15:0.00	0	0	0	0	0	0	0	0	1E+05	1	1E-06	1E-06
QQESDDSLVDYGEGGEGQFNEDGSFIGQY(+79.97)TVR	Nfasc	Y29:10.11	0	0	0	11300	0	0	0	50200	5180	1E-06	1	0.802
KDKEETEGNESSEATSPVNAIY(+79.97)SLA	Nfasc	Y22:3.61	0	0	0	4E+05	65000	2E+05	34000	7E+05	6E+05	1E-06	1E-06	0.582
IPLPGAEMLEEEPLY(+79.97)VNAK	Nfya	Y15:1000.0	0	0	0	5E+05	1E+06	4E+05	2E+06	3E+06	7E+05	1E-06	1E-06	0.314
ESFREQDIY(+79.97)LPIANVAR	Nfyb	Y9:26.08	0	0	0	50800	0	20900	0	8390	19000	1E-06	1E-06	0.272
EQDIY(+79.97)LPIANVAR	Nfyb	Y5:1000.0	0	0	0	25500	0	6530	45500	1E+05	5220	1	1E-06	0.291
GWDENVY(+79.97)YTVPLVR	Nipsnap1	Y7:17.01	0	0	0	50900	7100	29500	8350	1E+05	65300	1E-06	1E-06	0.006
SC(+57.02)AQNWIY(+79.97)E	Nme1	C2:1000, Y8:28.95	0	0	0	23300	43900	0	0	0	91500	1E-06	1	0.706
AGPY(+79.97)SSVPPPSVSLSK	Nolc1	Y4:20.00	0	0	0	14400	4380	0	0	48100	14600	1E-06	1E-06	0.412
ATGATQQDANASSLLDIY(+79.97)SFWLK	Nolc1	Y18:9.34	0	0	0	21000	19200	5580	71600	44000	56300	1E-06	1E-06	0.502
SNTGEEGEY(+79.97)FLK	Nova2	Y9:43.32	0	0	0	0	0	0	6190	0	0	1	1E-06	1E-06
LGAAPEEESAY(+79.97)VAGERR	Nsfl1c	Y11:18.53	0	0	0	16500	0	3940	501	54000	4180	1E-06	1E-06	0.379
LGAAPEEESAY(+79.97)VAGER	Nsfl1c	Y11:20.41	0	0	0	2E+05	79300	49700	8E+05	7E+05	70500	1E-06	1E-06	0.678
NTQC(+57.02)IPEGLESYY(+79.97)TEQDSSAR	Nsg1	C4:1000, Y13:17.01	0	0	0	0	0	0	0	8260	0	1	1E-06	0.472
ALAEDSTVYEYDSIY(+79.97)DEMQK	Nsrp1	Y15:18.53	0	0	0	24600	0	13300	0	1E+05	41500	1E-06	1	0.059
ALAEDSTVY(+79.97)EYDSIY(+79.97)DEMQK	Nsrp1	Y9:14.04, Y15:22.85	0	0	0	9080	36400	0	52800	2E+05	59300	1	1E-06	0.644
QENLPDEIY(+79.97)HVY(+79.97)SFALR	Ntmt1	Y9:49.79, Y12:14.02	0	0	0	55500	0	44200	0	98100	1E+05	1E-06	1E-06	0.989
QENLPDEIY(+79.97)HVYSFALR	Ntmt1	Y9:38.16	0	0	0	0	0	1E+05	6060	0	5E+05	1E-06	1	0.421
QENLPDEIYHVY(+79.97)SFALR	Ntmt1	Y12:14.02	0	0	0	4420	0	28200	0	0	91300	1E-06	1E-06	0.272
IEPPDTGLYYDEY(+79.97)LK	Nucb2	Y13:0.00	0	0	0	10500	0	0	18100	6170	0	1	1E-06	1E-06
IEPPDTGLYY(+79.97)DEYLK	Nucb2	Y10:9.34	0	0	0	2E+05	1910	44400	3E+05	6890	46000	1E-06	1	0.643
IEPPDTGLY(+79.97)YDEYLK	Nucb2	Y9:8.69	0	0	0	0	0	0	2E+05	0	0	1	1E-06	1E-06
VVDY(+79.97)SQFQESDDADEDYGR	Nucks1	Y4:7.21	0	0	0	0	0	0	14600	64500	0	1	1E-06	0.491

Peptide sequence and modification (phospho-S/T/Y) & Carbamidomethylation	Gene name	Modification A-score (≥ 13 = p < 0.05)	FSBA replicates			N1-Src replicates			C-Src replicates			FSBA vs N1-Src	FSBA vs C-Src	N1-Src vs C-Src
KVVDY(+79.97)SQFQES(+79.97)DDADEDYGR	Nucks1	Y5:12.28, S11:23.70	0	0	0	3020	0	0	21700	54400	0	1	1E-06	1E-06
IAGDLDAGAQEEEPVY(+79.97)IEMVGDVFR	Nyap1	Y16:1000.0	0	0	0	0	97500	7120	77100	1E+05	2E+05	1E-06	1E-06	0.502
SGGGLTGPPLGSGGPTPPAAADSDS(+79.97)EDSEAIY(+79.97)EEMKYPLPEETGDGR	Nyap1	S25/Y32:0.00	0	0	0	5280	1E+05	0	0	1E+05	0	1	1E-06	0.569
DSSLSQVC(+57.02)SPAADPEEEEPVY(+79.97)IEMVGNILR	Nyap2	C8:1000 , Y21:6.68	0	0	0	34100	1E+05	31400	0	2E+05	97900	1E-06	1E-06	0.26
EGQGFVSEDEY(+79.97)LEISDIKR	Opcml	Y11:33.81	0	0	0	0	0	8800	0	0	92600	1E-06	1E-06	0.647
Y(+79.97)KMGGDIANR	Pa2g4	Y1:1000.0	7E+05	9E+05	1E+06	7E+05	1E+06	1E+06	1E+06	0	1E+06	0.986	1	0.504
ADFAEY(+79.97)ASVDR	Pag1	Y6:32.28	0	0	0	0	0	0	3280	9940	0	1	1E-06	1E-06
AADGDSGPGVEGPY(+79.97)EVLK	Pag1	Y14:64.00	0	0	0	1E+05	0	42600	4E+05	8E+05	1E+05	1E-06	1E-06	0.47
DSSSQENMVEDC(+57.02)LY(+79.97)ETVK	Pag1	C12:1000, Y14:14.04	0	0	0	37900	13200	0	94100	2E+05	8710	1E-06	1E-06	0.703
RPGEEPEPDY(+79.97)EAIQTLNR	Pag1	Y10:119.54	0	0	0	2E+05	45300	1E+05	2E+05	8E+05	3E+05	1E-06	1E-06	0.962
ENDY(+79.97)ESIGDLQQGR	Pag1	Y4:17.01	0	0	0	95000	1E+05	40300	3E+05	5E+05	96900	1E-06	1E-06	0.107
DSSSQENMVEDC(+57.02)LY(+79.97)ETVKEIK	Pag1	C12:1000, Y14:18.53	0	0	0	73600	41600	47500	2E+05	2E+05	50700	1E-06	1E-06	0.234
AADGDSGPGVEGPY(+79.97)EVLKDSS(+79.97)SQENMVEDC(+57.02)LYETVK	Pag1	Y14/S21:0.00 C30:1000.0	0	0	0	64100	90900	6770	64400	2E+05	2E+05	1E-06	1	0.498
AADGDSGPGVEGPYEVLKDS(+79.97)SSQENMVEDC(+57.02)LY(+79.97)ETVK	Pag1	S20:0.0, C30:1000 Y32:5.99	0	0	0	87100	32500	0	1E+05	9E+05	76900	1	1E-06	0.139
EVY(+79.97)ELLDSPGR	Paics	Y3:39.44	0	0	0	0	2960	0	4190	33600	12200	1E-06	1E-06	0.365
TQGPY(+79.97)DVVVLPGGNLGAQNLSESALVK	Park7	Y5:4.08	0	0	0	13700	7360	5960	30600	91900	22500	1E-06	1	0.327
DVVIC(+57.02)PDTSLEEAKTQGPY(+79.97)DVVVLPGGNLGAQNLSESALVK	Park7	C5:1000, Y19:4.08	0	0	0	8490	0	0	0	0	0	1E-06	1	0.979
YSTGSDSASFPHTTPSMC(+57.02)LNPDLEGPPLEAY(+79.97)TIQGQYAIPQPDLTK	Pcbp2	C18:1000.0 Y31:2.23	0	0	0	1E+06	0	4E+05	5E+06	9E+06	3E+06	1E-06	1E-06	0.135
YSTGSDSASFPHTTPSMC(+57.02)LNPDLEGPPLEAYTIQGQY(+79.97)AIPQPDLTK	Pcbp2	C18:1000.0 Y37:22.09	0	0	0	0	2E+06	0	0	0	0	1E-06	1	1
HQVVQDLPPANTFVGTGDTTSTGSEQY(+79.97)SDYSYR	Pcdh1	Y27:9.34	0	0	0	0	13000	0	9E+05	87200	0	1E-06	1E-06	0.469
HQVVQDLPPANTFVGTGDTTSTGSEQYSDY(+79.97)SYR	Pcdh1	Y30:0.00	0	0	0	9090	0	0	0	0	0	1E-06	1	0.208
KHQVVQDLPPANTFVGTGDTTSTGSEQY(+79.97)SDYSYR	Pcdh1	Y28:14.02	0	0	0	0	0	0	0	0	22500	1	1E-06	0.607
LPDLQEIGVPLY(+79.97)ESPPGGR	Pcdh8	Y12:11.10	0	0	0	0	0	0	0	0	23700	1	1E-06	1E-06
NFDPPIEEFNDPY(+79.97)QQLVTTLIK	Pcyox1	Y13:33.54	0	0	0	0	0	0	0	24200	7940	1	1E-06	1E-06
QY(+79.97)TSPEEIDAQLQAEK	Pdap1	Y2:0.00	0	0	0	0	0	0	20300	60400	11600	1	1E-06	0.462
VRQY(+79.97)TSPEEIDAQLQAEK	Pdap1	Y4:0.00	0	0	0	2930	0	0	0	0	7680	1E-06	1E-06	0.448
MAADDVEEY(+79.97)MIERPEPEFQDLNEK	Pdcd10	Y9:1000.0	0	0	0	72700	0	5500	0	0	94900	1E-06	1E-06	0.198
EIEDAAQFATADPEPPLEELGYHIY(+79.97)SSDPPFEVR	Pdha1l1	Y25:0.00	0	0	0	4E+05	2E+05	9E+05	1E+06	2E+06	3E+06	1E-06	1E-06	0.518
MDATANDVPSPY(+79.97)EVK	Pdia3	Y12:14.04	0	0	0	3370	18800	0	38400	55400	6930	1E-06	1E-06	1E-06
HAHLTDTEIMTLVDETNMY(+79.97)EGVGR	Pfdn1	Y19:22.45	0	0	0	0	0	0	5060	17300	18700	1	1E-06	1E-06

Peptide sequence and modification (phospho-S/T/Y) & Carbamidomethylation	Gene name	Modification A-score (≥ 13 = p < 0.05)	FSBA replicates			N1-Src replicates			C-Src replicates			FSBA vs N1-Src	FSBA vs C-Src	N1-Src vs C-Src
DSLY(+79.97)VDSDC(+57.02)TMDIR	Pfn2	Y4:24.24, C9:1000	0	0	0	0	0	0	1530	6310	0	1	1E-06	1E-06
LGDVY(+79.97)VNDAFGTAHR	Pgk1	Y5:26.17	0	0	0	11800	0	6630	0	0	25300	1E-06	1E-06	0.425
FYGPEGPY(+79.97)GVFAGR	Pgrmc1	Y8:55.42	0	0	0	7E+05	84300	2E+05	7E+05	9E+05	2E+05	1E-06	1E-06	0.345
KFYGPEGPY(+79.97)GVFAGR	Pgrmc1	Y9:41.55	0	0	0	2E+05	0	1E+05	0	0	2E+05	1E-06	1E-06	0.108
FYGPAGPY(+79.97)GIFAGR	Pgrmc2	Y8:66.06	0	0	0	15000	0	0	1140	16000	11200	1	1E-06	1E-06
TTANPVY(+79.97)SGAVFEPER	Phf21a	Y7:12.79	0	0	0	0	0	0	0	0	25700	1	1E-06	1E-06
HEVTIC(+57.02)NY(+79.97)EASANPADHR	Pithd1	C6:1000, Y8:44.44	0	0	0	25900	0	12500	0	42600	34600	1E-06	1E-06	0.016
RHEVTIC(+57.02)NY(+79.97)EASANPADHR	Pithd1	C7:1000, Y9:9.42	0	0	0	0	0	0	0	0	6900	1	1E-06	0.206
HVEAIY(+79.97)IDIADR	Pitpna	Y6:1000.0	0	0	0	90700	0	2E+05	8E+05	3E+05	1E+06	1E-06	1E-06	0.372
VILPVS(+79.97)VDEYQVGQLY(+79.97)SVAEASK	Pitpna	S6:0.00, Y16:14.02	0	0	0	16600	11200	0	33200	68200	15400	1E-06	1	0.149
VILPVSVDEY(+79.97)QVGQLYSVAEASK	Pitpna	Y10:15.39	10100	9090	0	3E+05	2E+05	2E+05	9E+05	1E+06	2E+05	0.17	0.144	0.564
VILPVSVDEYQVGQLY(+79.97)SVAEASK	Pitpna	Y16:14.02	0	0	0	0	0	0	0	48600	0	1	1E-06	0.056
VVLPC(+57.02)SVQEYQVGQLY(+79.97)SVAEASK	Pitpnb	C5:1000, Y16:10.11	0	0	0	7E+05	4E+05	4E+05	2E+06	2E+06	5E+05	1E-06	1E-06	0.453
VVLPC(+57.02)SVQEY(+79.97)QVGQLYSVAEASK	Pitpnb	C5:1000, Y10:11.01	0	0	0	28300	0	0	0	0	0	1E-06	1	0.435
VVLPC(+57.02)SVQEYQVGQLY(+79.97)SVAEASKNETGGGEGIEVLK	Pitpnb	C5:1000, Y16:0.00	0	0	0	0	0	0	1E+05	0	0	1	1E-06	1E-06
AATESFASDPILY(+79.97)RPVAVALDTK	Pkm	Y13:3.75	0	0	0	0	0	3800	0	0	0	1	1	1E-06
DYVPDTY(+79.97)ADVIEALSNPIR	Plcb1	Y7:14.40	0	0	0	2E+05	1E+05	84200	8E+05	7E+05	1E+05	1E-06	1E-06	0.178
IGTAEPDY(+79.97)GALYEGR	Plcg1	Y8:15.39	0	0	0	0	0	0	2630	0	1770	1	1E-06	1E-06
DPDNELY(+79.97)FAHGLFSAK	Plcxd3	Y7:61.82	0	0	0	372	0	7710	0	0	23500	1	1E-06	0.798
VVEGEGGY(+79.97)ELGDLAR	Plppr3	Y8:1000.0	0	0	0	7150	1670	3300	12500	0	9570	1E-06	1E-06	0.991
LRNEY(+79.97)GPVLHMPTSK	Plrg1	Y5:99.62	0	0	0	6570	0	16700	0	0	81600	1E-06	1E-06	0.728
QYPANQGQDVEY(+79.97)LVTGTHPYPPGPGVALTADTK	Plrg1	Y12:0.00	0	0	0	0	0	0	4E+05	0	0	1	1E-06	1E-06
DPESSAMLDY(+79.97)ELHSDFVSSLIK	Plxna2	Y10:0.00	0	0	0	0	0	0	0	0	17600	1	1E-06	1E-06
VVQNDAY(+79.97)TAPVLPSSVR	Poldip3	Y7:17.01	0	0	0	27000	21200	0	62600	2E+05	56600	1E-06	1E-06	0.617
QNLY(+79.97)DLDEDDDIVAPVPTK	Poldip3	Y4:80.11	0	0	0	39400	24600	22600	1E+05	3E+05	1E+05	1E-06	1E-06	0.138
KGPQTVNSSSIY(+79.97)SMYLQQATPPK	Ppp1r13b	Y12:12.33	0	0	0	29500	0	5750	0	0	22700	1E-06	1	0.587
VY(+79.97)FQSPPGAAGEGPGGADDDGPVR	Ppp1r14b	Y2:12.16	0	0	0	14000	6420	0	46200	1E+05	23700	1E-06	1E-06	0.241
VY(+79.97)FQSPPGAAGEGPGGADDDGPVRR	Ppp1r14b	Y2:28.36	0	0	0	6E+05	2E+05	4E+05	2E+05	2E+06	1E+06	1E-06	1E-06	0.275
NVITEPIY(+79.97)PEAVHMFAVNMFR	Ppp2r5c	Y8:22.37	0	0	0	0	0	0	0	0	55300	1	1E-06	0.119
KSELPQDVY(+79.97)TIK	Ppp2r5d	Y9:0.00	0	0	0	26900	21000	13600	0	1E+05	75100	1E-06	1	0.358
RKS(+79.97)ELPQDVY(+79.97)TIK	Ppp2r5d	S3:66.10, Y10:0.00	0	0	0	15500	28500	9620	0	1E+05	64300	1E-06	1E-06	0.217

Peptide sequence and modification (phospho-S/T/Y) & Carbamidomethylation	Gene name	Modification A-score (≥ 13 = p < 0.05)	FSBA replicates			N1-Src replicates			C-Src replicates			FSBA vs N1-Src	FSBA vs C-Src	N1-Src vs C-Src
APPPLPPVY(+79.97)SMETETPTAEDIQLLK	Ppp2r5d	Y9:8.14	0	0	0	86800	5E+05	57900	2E+05	0	4E+05	1E-06	1	0.467
SELPQDVY(+79.97)TIK	Ppp2r5d	Y8:17.01	0	0	0	43200	1E+05	26600	1E+05	3E+05	1E+05	1E-06	1E-06	0.565
APPPLPPVY(+79.97)SMETETPTAEDIQLLKR	Ppp2r5d	Y9:7.21	0	0	0	19500	4E+05	55900	2E+05	8E+05	3E+05	1E-06	1E-06	0.379
RKSELPQDVY(+79.97)TIK	Ppp2r5d	Y10:0.00	0	0	0	0	0	0	0	0	34700	1	1E-06	0.685
EAVQPEPIY(+79.97)AESAK	Prag1	Y9:5.08	0	0	0	0	3220	0	15200	14500	0	1E-06	1E-06	0.582
LVQAFQYTDEHGEVC(+57.02)PAGWKPGSDTIKPNVDDSKEY(+79.97)FSK	Prdx2	C15:1000.0 Y36:6.13	0	0	0	0	0	0	0	0	1E+06	1	1E-06	0.615
AFQFVETHGEVC(+57.02)PANWTPESPTIKPSPTASKEY(+79.97)FEK	Prdx3	C12:1000.0 Y33:0.00	0	0	0	0	0	0	0	0	86700	1	1E-06	0.914
ENEC(+57.02)HFY(+79.97)AGGQVYPGEVSR	Prdx4	C4:1000, Y7:41.57	0	0	0	13900	0	0	0	22200	12600	1	1E-06	1E-06
TRENEC(+57.02)HFY(+79.97)AGGQVYPGEVSR	Prdx4	C6:1000, Y9:42.22	0	0	0	4370	0	0	0	0	59000	1E-06	1E-06	1E-06
DVMGSSAGAGSGEFHVY(+79.97)R	Prkrip1	Y17:47.92	0	0	0	8610	0	2020	0	34400	24300	1E-06	1E-06	1
LC(+57.02)DFGSASHVADNDITPY(+79.97)LVSR	Prpf4b	C2:1000, Y18:22.45	0	6080	10700	79100	1E+05	39100	59700	11300	2E+05	0.177	0.184	1E-06
SPDEALPGGLGSHSPY(+79.97)ALER	Prrc2b	Y16:14.04	0	0	0	64500	0	24600	0	62700	56100	1E-06	1	0.914
IASETHSEGSEY(+79.97)EELPKR	Prrc2b	Y12:5.47	0	0	0	38600	642	3990	0	54100	1970	1E-06	1E-06	0.333
RSPDEALPGGLGSHSPY(+79.97)ALER	Prrc2b	Y17:14.04	0	0	0	0	0	0	0	0	11800	1	1E-06	1E-06
LYQTDPSGTY(+79.97)HAWK	Psma7	Y10:17.81	0	0	0	22800	0	0	752	34800	18400	1	1E-06	1E-06
ADVDLY(+79.97)QVR	Psmd9	Y6:1000.0	0	0	0	11900	15100	0	66500	60700	9720	1E-06	1E-06	0.163
QLVHELDEAEY(+79.97)QEIR	Psme1	Y11:1000.0	0	0	0	61300	0	30900	0	44600	68700	1E-06	1E-06	0.798
LMTTNEIQSNIY(+79.97)T	Psmg1	Y12:0.00	0	0	0	3660	14600	0	0	91900	31400	1E-06	1	0.542
TC(+57.02)ESTY(+79.97)NLSSPFLR	Psmg1	C2:1000.0, Y6:0.00	0	0	0	6E+05	5E+05	3E+05	1E+06	2E+06	6E+05	1E-06	1E-06	1E-06
MNEETGADY(+79.97)LAPWQLAQVADGGGLGVIEESK	Ptgr2	Y9:8.26	76500	27100	40200	0	1E+05	97500	9E+05	7E+05	1E+05	0.622	0.068	0.743
LHQEDNDY(+79.97)INASLIK	Ptpn1	Y8:48.12	0	0	0	5E+05	2E+05	5E+05	7E+05	3E+06	1E+06	1E-06	1E-06	0.65
IKLHQEDNDY(+79.97)INASLIK	Ptpn1	Y10:25.70	0	0	0	4520	0	1E+05	2E+05	9440	7E+05	1	1E-06	0.269
IQNTGDY(+79.97)YDLYGGEK	Ptpn11	Y7:14.02	40100	22600	39800	87400	73100	23100	5E+05	2E+05	39900	0.656	0.205	0.564
VKEGYVPQEEVPVY(+79.97)ENKYVK	Pym1	Y14:0.00	0	0	0	1E+05	0	1E+05	0	26100	2E+05	1E-06	1E-06	1E-06
VKEGYVPQEEVPVY(+79.97)ENKY(+79.97)VK	Pym1	Y14:78.86, Y18:63.13	0	0	0	2E+05	58800	2E+05	0	7E+05	4E+05	1E-06	1E-06	0.214
EGYVPQEEVPVY(+79.97)ENKYVK	Pym1	Y12:28.70	0	0	0	5E+05	2E+05	4E+05	1E+06	2E+06	6E+05	1E-06	1E-06	0.579
EGYVPQEEVPVY(+79.97)ENKY(+79.97)VK	Pym1	Y12:22.90, Y16:31.16	0	0	0	5E+05	4E+05	3E+05	2E+06	3E+06	7E+05	1E-06	1E-06	0.624
EGYVPQEEVPVY(+79.97)ENK	Pym1	Y12:54.49	0	0	0	1E+05	1E+05	66300	3E+05	6E+05	96700	1E-06	1E-06	0.57
FADDTY(+79.97)TESYISTIGVDFK	Rab1b	Y6:11.06	0	0	0	73700	34200	35100	0	2E+05	55600	1E-06	1E-06	0.78
MGSGIQY(+79.97)GDISLR	Rab4b	Y7:47.31	0	0	0	0	0	0	2690	30100	3310	1	1E-06	1E-06

Peptide sequence and modification (phospho-S/T/Y) & Carbamidomethylation	Gene name	Modification A-score (≥ 13 = p < 0.05)	FSBA replicates			N1-Src replicates			C-Src replicates			FSBA vs N1-Src	FSBA vs C-Src	N1-Src vs C-Src
NALKQETEVELY(+79.97)NEFPEPIKLDK	Rab7a	Y12:68.60	3E+05	0	2E+05	9E+05	1E+06	5E+06	7E+06	6E+06	1E+07	0.189	0.077	0.736
NALKQETEVELY(+79.97)NEFPEPIK	Rab7a	Y12:98.37	1E+06	3E+05	1E+06	6E+06	6E+06	5E+06	2E+07	2E+07	8E+06	0.441	0.135	0.348
QETEVELY(+79.97)NEFPEPIK	Rab7a	Y8:86.16	0	0	0	0	2710	0	2060	0	0	1E-06	1	0.068
GHSSAGDAIY(+79.97)EVVSLQR	Rabgap1l	Y10:61.69	0	0	0	0	0	0	0	0	17800	1	1E-06	1E-06
DSFLY(+79.97)STWLDDSVSTTSGGSSPGLTR	Rap1gap	Y5:11.06	0	0	0	30000	0	11000	0	42000	23900	1E-06	1	0.166
LPPEPGLPDSY(+79.97)SFDYPTDVGPR	Raver1	Y11:0.00	0	0	0	36700	12000	13800	12700	2E+05	1E+05	1E-06	1	0.673
NAEDC(+57.02)LY(+79.97)ELPENIR	RGD1305178	C5/Y7:1000.0	1420	0	0	1E+06	8E+05	7E+05	3E+06	4E+06	8E+05	0.184	0.023	0.885
LEGEDNPVQLIY(+79.97)FVENQDGER	RGD1306271	Y12:1000.0	0	0	0	26200	6340	15100	44800	75600	18900	1E-06	1E-06	0.262
TGEEDKKINEELESQY(+79.97)QQSMDSK	RGD1311703	Y16:7.32	0	0	0	5E+05	77700	5E+05	2E+06	8E+05	1E+06	1E-06	1E-06	0.228
INEELESQY(+79.97)QQSMDSK	RGD1311703	Y9:14.04	0	0	0	94300	2E+05	29100	4E+05	6E+05	62000	1E-06	1E-06	0.752
WSNIY(+79.97)EDNGDDAPQNAK	RGD1560065	Y5:22.45	0	0	0	10300	6220	0	31200	0	13200	1E-06	1E-06	0.347
YLY(+79.97)TLVITDKEK	RGD1561636	Y3:17.01	0	0	0	9570	0	2750	0	31600	45400	1E-06	1	0.455
QVELALWDTAGQEDY(+79.97)DR	Rhoa	Y15:36.87	0	0	0	0	0	0	0	19100	2370	1	1E-06	0.092
SPLQLTTEDVY(+79.97)DISYVVGR	Rilpl2	Y11:48.12	0	0	0	5780	0	3280	0	0	11200	1E-06	1E-06	0.247
SAKPVGPEDMGATAVY(+79.97)ELDTEKER	Rnf113a1	Y16:49.79	0	0	0	2E+05	2E+05	90500	2E+05	93000	2E+05	1E-06	1E-06	0.42
RLEASETESFGNEIY(+79.97)TVK	Rnmt	Y15:14.02	0	0	0	0	0	759	0	0	10500	1	1E-06	1E-06
SSVSSSDGSFFTDADFAQAVAAAAEY(+79.97)AGLK	Robo1	Y26:17.81	0	0	0	0	0	3210	0	17600	0	1E-06	1	0.877
PVAVGPY(+79.97)GQSQPSC(+57.02)FDR	Romo1	Y7:9.42, C14:1000	0	0	0	2840	1410	0	10200	38000	5300	1E-06	1	0.565
IAIY(+79.97)ELLFK	Rps10	Y4:1000.0	1E+05	1E+05	2E+05	5E+06	3E+06	5E+06	1E+07	2E+07	1E+07	0.107	0.12	0.305
IAIY(+79.97)ELLFKEGVMVAK	Rps10	Y4:1000.0	0	0	0	0	0	0	0	0	35200	1	1E-06	1E-06
TY(+79.97)GIC(+57.02)GAIR	Rps21	Y2:10.11, C5:1000	0	0	0	0	0	0	37900	50600	0	1	1E-06	0.281
WSTDDVQINDISLQDY(+79.97)IAVK	Rps5	Y16:28.70	0	0	3470	0	0	0	0	0	27100	1	0.239	0.608
ADHQPLTEASY(+79.97)VNLPTIALC(+57.02)NTDSPLR	Rpsa	Y11:7.21, C20:1000	0	0	0	1E+05	0	70200	0	3E+05	84000	1E-06	1E-06	0.24
AQQLWYAIIESQTETGTPY(+79.97)MLYK	Rrm1	Y19:14.04	0	0	0	17000	9760	7600	88900	89700	0	1E-06	1E-06	0.202
TSNPFLVAVQDSEADY(+79.97)VTTDTLSK	Rtn4	Y16:26.31	0	0	0	2E+05	2E+05	63400	3E+05	2E+05	2E+05	1E-06	1E-06	0.478
DLAEFSELEY(+79.97)SEMGSSFK	Rtn4	Y10:7.21	0	0	0	51100	63400	13100	87400	1E+05	95900	1E-06	1E-06	0.021
ISLQMEEFNTAIY(+79.97)SNDDLLSSK	Rtn4	Y13:17.01	0	0	0	34500	1E+05	18300	29000	2E+05	1E+05	1E-06	1	0.817
ISLQMEEFNTAIY(+79.97)SNDDLLSSKEDK	Rtn4	Y13:17.01	0	0	0	4080	0	30800	0	0	4E+05	1E-06	1E-06	0.511
EGIKEPESFNAAVQETEAPY(+79.97)ISIAC(+57.02)DLIK	Rtn4	Y20:32.28, C25:1000	0	0	0	0	0	0	0	0	1E+05	1	1E-06	1E-06
EKISLQMEEFNTAIY(+79.97)SNDDLLSSK	Rtn4	Y15:14.02	0	0	0	0	0	0	0	0	7290	1	1E-06	1E-06
LSTEPSPDFSNY(+79.97)SEIAKFEK	Rtn4	Y12:8.22	0	0	0	0	0	0	0	0	29600	1	1E-06	1E-06

Peptide sequence and modification (phospho-S/T/Y) & Carbamidomethylation	Gene name	Modification A-score (≥ 13 = p < 0.05)	FSBA replicates			N1-Src replicates			C-Src replicates			FSBA vs N1-Src	FSBA vs C-Src	N1-Src vs C-Src
SQVSDY(+79.97)GNY(+79.97)DIIVR	S1pr1	Y6:0.00, Y9:39.44	0	0	0	11200	10200	0	39800	31700	0	1E-06	1E-06	1E-06
SQVSDY(+79.97)GNYDIIVR	S1pr1	Y6:15.21	0	0	0	31000	19600	7660	64900	1E+05	40400	1E-06	1E-06	0.778
SQVSDYGNY(+79.97)DIIVR	S1pr1	Y9:22.45	22700	6310	7990	77200	54300	26500	2E+05	2E+05	64500	0.313	0.149	0.546
VIAINVDDPDAANY(+79.97)HDISDVER	Sar1a	Y14:24.67	0	0	0	2E+05	10200	85400	3E+05	3E+05	1E+05	1E-06	1E-06	1E-06
AAPFTLEY(+79.97)R	Sar1a	Y8:12.33	0	0	0	27600	2140	4100	1E+05	2E+05	18500	1E-06	1E-06	0.933
NVPPGLDEY(+79.97)NPFSDSR	Scamp1	Y9:37.48	0	0	0	3E+05	3E+05	1E+05	1E+06	2E+06	2E+05	1E-06	1E-06	0.718
MPNVPNTQPAIMKPTEEHPAY(+79.97)TQITK	Scamp1	Y21:7.65	0	0	0	0	0	0	8E+05	0	0	1	1E-06	0.151
QQAHREES(+79.97)SPDYNPY(+79.97)QGISVPLQLK	Scg2	S8:0.00, Y15:5.55	0	0	0	86700	0	34100	0	24800	93400	1	1E-06	0.794
LLERPLDSQSIY(+79.97)QLIEISR	Scg2	Y12:36.80	0	0	0	0	0	0	0	0	28300	1	1E-06	1
QASVTYQKPDKQEEFY(+79.97)A	Sdc3	Y16:47.07	2890	0	0	3010	2E+05	0	4290	6210	0	1	0.085	0.302
LGHPPLPGAGGVYQAAQEGDVQPY(+79.97)FSQFVGIR	Sec16a	Y24:32.28	0	0	0	0	0	0	0	0	4E+05	1	1E-06	1E-06
LGHPPLPGAGGVY(+79.97)QAAQEGDVQPYFSQFVGIR	Sec16a	Y13:16.94	0	0	0	0	0	19100	0	0	63700	1	1E-06	1E-06
EASLY(+79.97)SPPSTLPR	Sema6d	Y5:17.01	0	0	0	0	1620	0	2510	24100	0	1E-06	1E-06	0.525
ESFNPETY(+79.97)ELDK	Sephs1	Y8:0.00	0	0	0	28700	13000	8760	86400	2E+05	15300	1E-06	1E-06	0.982
LATPEDKQDIDKQY(+79.97)VGFATLPNQVHR	Sept5	Y14:17.91	0	0	0	0	0	0	0	0	26100	1	1E-06	1E-06
GTEVVSGTVSEITAY(+79.97)C(+57.02)MPPVIK	Serpina10	Y15:32.28, C16:1000	0	0	0	1E+05	2E+05	21900	4E+05	3E+05	51100	1E-06	1E-06	0.971
LPLMYSHPYSQITVETEFDNPIY(+79.97)ETGETR	Sez6l	Y23:18.53	0	0	0	0	0	0	0	0	68400	1	1E-06	1E-06
SLFGFS(+79.97)GSHSYSPITVESDFSNPLY(+79.97)EAGDTR	Sez6l2	S6:0.00, Y25:4.73	0	0	0	0	0	0	0	0	19700	1	1E-06	0.1
TGDLGIPPNPEDRS(+79.97)PS(+79.97)PEPIY(+79.97)NSEGK	Sf1	S14:13.41, S16:13.18, Y21:17.01	0	0	0	0	0	0	51400	15100	0	1	1E-06	1E-06
TGDLGIPPNPEDRS(+79.97)PSPEPIY(+79.97)NS(+79.97)EGK	Sf1	S14/Y21/S23:0.00	0	0	0	0	0	0	2640	14900	0	1	1E-06	0.279
TGDLGIPPNPEDRS(+79.97)PS(+79.97)PEPIY(+79.97)NSEGKR	Sf1	S14:6.45, S16:8.15 Y21:0.00	0	0	0	58600	0	0	23000	3E+05	40100	1E-06	1E-06	1E-06
TGDLGIPPNPEDRS(+79.97)PSPEPIY(+79.97)NS(+79.97)EGKR	Sf1	S14/Y21:0.0, S23:4.54	0	0	0	11600	0	0	10600	25200	5380	1E-06	1	1E-06
T(+79.97)GDLGIPPNPEDRSPSPEPIY(+79.97)NS(+79.97)EGKR	Sf1	T1/Y21/S23:0.00	0	0	0	8970	0	0	6020	59500	5500	1	1E-06	1E-06
TGDLGIPPNPEDRSPS(+79.97)PEPIY(+79.97)NS(+79.97)EGKR	Sf1	S16/Y21/S23:0.00	0	0	0	0	0	0	0	4150	0	1	1E-06	1E-06
EKQSDDEVY(+79.97)APGLDIESSLK	Sf3a1	Y9:9.30	0	0	0	3E+05	63600	2E+05	78500	6E+05	3E+05	1E-06	1E-06	0.248
KAALDEAQGVGLDSTGYYDQEIY(+79.97)GGSDSR	Sf3b1	Y23:12.33	0	0	0	12000	11900	0	0	1E+05	3E+05	1E-06	1	0.847
AALDEAQGVGLDSTGYYDQEIY(+79.97)GGSDSR	Sf3b1	Y22:12.16	0	0	0	25700	99100	25700	0	2E+05	2E+05	1E-06	1	0.986
TATVGGAMMGSTHIY(+79.97)DMSTVMSR	Sf3b2	Y15:13.38	0	0	0	0	61000	0	0	33300	0	1E-06	1	0.577

Peptide sequence and modification (phospho-S/T/Y) & Carbamidomethylation	Gene name	Modification A-score (≥ 13 = p < 0.05)	FSBA replicates			N1-Src replicates			C-Src replicates			FSBA vs N1-Src	FSBA vs C-Src	N1-Src vs C-Src
DKLESEMEDAY(+79.97)HEHQANLLR	Sfpq	Y11:9.27	0	0	0	0	0	0	0	0	2E+05	1	1E-06	1E-06
FAQHGTFEY(+79.97)EYSQR	Sfpq	Y9:45.01	0	0	0	56300	0	15100	0	44200	0	1E-06	1E-06	0.261
DAKDKLESEMEDAY(+79.97)HEHQANLLR	Sfpq	Y14:25.65	0	0	0	0	0	0	2E+05	0	0	1	1E-06	1E-06
AIELNPANAVY(+79.97)FC(+57.02)NR	Sgta	Y11/C13:1000.0	0	0	0	0	0	0	0	13500	3480	1	1E-06	1E-06
ENNAVY(+79.97)AFLGLTAPPGSK	Sh3bgrl	Y6:78.19	0	0	0	95800	49700	59100	0	3E+05	2E+05	1E-06	1E-06	0.244
IEEFVY(+79.97)EKLDR	Sh3glb1	Y6:1000.0	0	0	0	3E+05	8510	2E+05	11400	1E+07	4E+05	1E-06	1E-06	0.548
INNPELLGQY(+79.97)MIDAGTEFGPGTAYGNALIK	Sh3glb1	Y10:33.66	0	0	0	16300	0	6930	0	0	21400	1E-06	1E-06	0.664
VEEFLY(+79.97)EKLDR	Sh3glb2	Y6:1000.0	0	0	0	80700	0	40600	0	74100	95200	1E-06	1E-06	0.309
TEPAQGEDQVDIY(+79.97)NLR	Sh3pxd2b	Y13:85.14	0	0	0	7E+05	5E+05	3E+05	2E+06	7E+05	6E+05	1E-06	1E-06	0.14
DFEDPY(+79.97)NGPGSSLR	Shb	Y6:15.57	0	0	0	3070	0	0	28500	64400	3840	1E-06	1E-06	1
DEY(+79.97)LLEEAQQR	Shroom2	Y3:1000.0	0	0	0	0	0	0	10000	0	0	1	1E-06	1E-06
RLDDQESPVY(+79.97)AAQQR	Sin3a	Y10:78.06	0	0	0	5810	1150	0	0	40900	11900	1E-06	1E-06	0.828
LDDQESPVY(+79.97)AAQQR	Sin3a	Y9:17.81	0	0	0	0	0	0	9660	15200	0	1	1E-06	1E-06
VPEPNNHTEYASIETGKLPRPEDTLTY(+79.97)ADLDMVHLNR	Sirpa	Y27:7.21	0	0	0	50000	0	0	0	4E+06	13900	1E-06	1E-06	0.139
VPEPNNHTEY(+79.97)ASIETGK	Sirpa	Y10:0.00	0	0	0	30500	12000	0	3440	2E+05	26500	1E-06	1E-06	0.344
AQPTPKPEPSFSEY(+79.97)ASVQVQR	Sirpa	Y14:22.85	0	0	0	3E+05	1E+05	5E+05	3E+05	1E+06	3E+06	1E-06	1E-06	0.238
EITQIQDTNDINDITY(+79.97)ADLNLPK	Sirpa	Y16:9.34	10000	31100	18600	3E+06	4E+06	2E+06	1E+07	1E+07	5E+06	0.194	0.104	0.355
LPRPEDTLTY(+79.97)ADLDMVHLNR	Sirpa	Y10:33.98	0	0	0	0	0	0	9E+05	7E+05	1E+06	1	1E-06	1E-06
EITQIQDTNDINDITY(+79.97)ADLNLPKEK	Sirpa	Y16:33.98	0	0	0	13600	0	21100	0	0	73900	1E-06	1	0.977
VPEPNNHTEY(+79.97)ASIETGKLPRPEDTLTY(+79.97)ADLDMVHLNR	Sirpa	Y10:4.75 Y27:6.63	0	0	0	0	0	0	0	0	2E+06	1	1E-06	1E-06
VPEPNNHTEY(+79.97)ASIETGKLPRPEDT(+79.97)LTYADLDMVHLNR	Sirpa	Y10/T24:0.00	0	0	0	0	0	0	0	0	3E+06	1	1E-06	1E-06
YPEDDPDY(+79.97)C(+57.02)VWVPPEGQSGDGR	Slc4a1ap	Y8:0.00, C9:1000.0	0	0	0	39000	10400	13400	5750	80900	3630	1E-06	1E-06	0.587
Y(+79.97)PEDDPDYC(+57.02)VWVPPEGQSGDGR	Slc4a1ap	Y1:0.00, C9:1000.0	0	0	0	96600	7110	7390	3E+05	2E+05	17500	1	1E-06	0.597
IAAAQY(+79.97)SVTGSAVAR	Snap91	Y6:20.00	0	0	0	1E+06	6E+05	2E+05	4E+06	3E+06	3E+05	1E-06	1E-06	1E-06
LTAELIEQAAQY(+79.97)TNAVR	Snrpa1	Y12:9.34	0	0	0	2E+05	39500	1E+05	3E+05	4E+05	2E+05	1E-06	1E-06	0.893
VKLTAELIEQAAQY(+79.97)TNAVR	Snrpa1	Y14:11.06	0	0	0	0	0	51500	1E+05	0	0	1E-06	1E-06	0.5
PKFY(+79.97)C(+57.02)DYC(+57.02)DTY(+79.97)LTHDSPSVR	Snrpc	Y4:9.42, Y11:7.65 C5/C8:1000.0	0	0	0	12400	0	9400	0	35500	1E+05	1E-06	1	1E-06
FYC(+57.02)DYC(+57.02)DTY(+79.97)LTHDSPSVR	Snrpc	C3/C6:1000.0 Y9:0.00	0	0	0	2E+05	1E+06	1E+05	3E+06	1E+06	4E+05	1E-06	1E-06	0.804
FYC(+57.02)DY(+79.97)C(+57.02)DT(+79.97)YLTHDSPSVR	Snrpc	C3/C6:1000.0 Y5:5.55, T8:0.00	0	0	0	39800	76100	48900	24900	4E+05	2E+05	1E-06	1	0.705

Peptide sequence and modification (phospho-S/T/Y) & Carbamidomethylation	Gene name	Modification A-score (≥ 13 = p < 0.05)	FSBA replicates			N1-Src replicates			C-Src replicates			FSBA vs N1-Src	FSBA vs C-Src	N1-Src vs C-Src
FY(+79.97)C(+57.02)DYC(+57.02)DTYLTHDSPSVR	Snrpc	Y2:0.00 C3/C6:1000.0	0	0	0	7730	14500	12100	7E+05	18200	57400	1E-06	1E-06	0.316
PKFYC(+57.02)DY(+79.97)C(+57.02)DTYLTHDSPSVR	Snrpc	C5/C8:1000.0	0	0	0	0	0	6370	0	0	0	1E-06	1	0.566
PKFYC(+57.02)DYC(+57.02)DTY(+79.97)LTHDSPSVR	Snrpc	C5/C8:1000.0 Y11:14.02	0	0	0	0	0	2E+05	0	0	7E+05	1	1E-06	1E-06
PKFY(+79.97)C(+57.02)DYC(+57.02)DTYLTHDSPSVR	Snrpc	Y4:0.00	0	0	0	0	0	35300	0	0	2E+05	1	1E-06	1E-06
FYC(+57.02)DY(+79.97)C(+57.02)DTYLTHDSPSVR	Snrpc	C3/C6:1000.0	0	0	0	0	68600	0	0	77400	0	1E-06	1E-06	1
GMDS(+79.97)GFAGGEDEIYNVY(+79.97)DQAWR	Snw1	S4:0.00, Y17:32.97	0	0	0	0	62000	5190	0	2E+05	89500	1E-06	1	0.184
GMDSGFAGGEDEIY(+79.97)NVYDQAWR	Snw1	Y14:20.11	0	0	0	2E+05	6E+05	3E+05	2E+05	8E+05	5E+05	1E-06	1E-06	0.415
GMDSGFAGGEDEIY(+79.97)NVY(+79.97)DQAWR	Snw1	Y14:0.0, Y17:20.21	0	0	0	33400	1E+05	57500	21900	3E+05	2E+05	1E-06	1	0.161
GMDSGFAGGEDEIYNVY(+79.97)DQAWR	Snw1	Y17:68.31	0	0	0	5630	15000	10400	0	0	36800	1E-06	1E-06	0.291
VPASPTLSSAAESPEGASLY(+79.97)DEVR	Sox11	Y20:12.19	0	0	0	53900	66500	50700	52800	3E+05	1E+05	1E-06	1E-06	0.557
DAAHMLQANKTY(+79.97)GC(+57.02)VPVANKR	Spag7	Y12:0.0, C14:1000	0	0	0	0	0	0	0	0	9140	1	1E-06	1E-06
STYFPTQDDVDLY(+79.97)TDSEPR	Spata2	Y13:7.65	0	0	0	0	19400	0	0	71000	61900	1E-06	1E-06	0.861
SVDAYDSY(+79.97)WESR	Spata2	Y8:8.14	0	0	0	0	0	0	4770	13800	0	1	1E-06	1E-06
VSC(+57.02)DPC(+57.02)LGAY(+79.97)HYDPC(+57.02)C(+57.02)R	Spata2	C3/C6/C15/C16:1000 Y10:14.63	0	0	0	24300	0	7000	0	0	14300	1E-06	1E-06	0.389
SVDAY(+79.97)DSYWESR	Spata2	Y5:26.31	0	0	0	0	0	0	5850	0	0	1	1E-06	0.957
DTFQSGAHVDFY(+79.97)DI	Spr	Y12:27.33	0	0	0	0	0	0	0	0	13200	1	1E-06	0.097
LIEDNEY(+79.97)TAR	Src	Y7:14.02	0	0	0	3E+05	6E+05	1E+05	2E+06	3E+06	3E+05	1E-06	1E-06	0.34
WTAPEAALY(+79.97)GR	Src	Y9:104.80	0	0	0	19200	3400	5570	11800	91700	16500	1E-06	1E-06	0.243
LVQLYAVVSEEPIY(+79.97)IVTEYMNK	Src	Y14:32.97	0	0	0	0	0	0	0	0	7940	1	1E-06	1E-06
AGPLAGGVTTFVALY(+79.97)DY(+79.97)ESRTETDLSFK	Src	Y15/Y17:0.00	0	0	0	0	0	0	0	0	14300	1	1E-06	1E-06
GEGLY(+79.97)ADPY(+79.97)GLLHEGR	Srcin1	Y5/Y9:1000.0	0	0	0	0	0	0	0	30900	11700	1	1E-06	1E-06
AGAGGPLY(+79.97)GDGYGFR	Srcin1	Y8:41.04	0	0	0	32300	27200	17500	36700	2E+05	59400	1E-06	1E-06	0.561
GEGLY(+79.97)ADPYGLLHEGR	Srcin1	Y5:28.70	0	0	0	8400	0	4600	0	0	22200	1E-06	1	0.564
AGAGGPLYGDGY(+79.97)GFR	Srcin1	Y12:16.51	0	0	0	0	0	0	10400	0	0	1	1E-06	1E-06
DTQTSITDSSAIY(+79.97)KVNNNR	Srprb	Y13:28.36	0	0	0	0	0	0	0	21400	0	1	1E-06	0.579
LAY(+79.97)INPDLALEEK	Stip1	Y3:1000.0	0	0	0	59700	17500	17700	1E+05	3E+05	0	1E-06	1E-06	0.71
ELDPTNMTY(+79.97)ITNQAAVHFEK	Stip1	Y9:0.00	0	0	0	0	36500	0	6E+05	4E+05	0	1E-06	1E-06	0.843
NINIY(+79.97)TYDDMEVK	Stmn2	Y5:0.00	0	0	0	10300	0	0	34200	71800	23600	1	1E-06	1E-06
REPLPSLEAVY(+79.97)LITPSEK	Stxbp1	Y11:19.05	0	0	0	0	0	1540	0	0	28100	1E-06	1E-06	0.204
C(+57.02)SVSGSAVY(+79.97)SLDLGR	Sugp2	C1:1000, Y9:28.36	0	0	0	39200	69200	25000	2E+05	3E+05	1E+05	1E-06	1	0.21
LFQQIY(+79.97)SDGSDEVK	Sugt1	Y6:10.11	0	0	0	0	2990	21100	85600	2E+05	18400	1E-06	1E-06	0.879

Peptide sequence and modification (phospho-S/T/Y) & Carbamidomethylation	Gene name	Modification A-score (≥ 13 = p < 0.05)	FSBA replicates			N1-Src replicates			C-Src replicates			FSBA vs N1-Src	FSBA vs C-Src	N1-Src vs C-Src
LFQQIY(+79.97)SDGSDEVKR	Sugt1	Y6:8.69	0	0	0	2E+06	2E+05	0	3E+06	2E+05	1E+06	1E-06	1E-06	0.524
IKVENQHDY(+79.97)QDITSVVAMAK	Syn3	Y9:25.70	0	0	0	11100	0	5800	0	0	51900	1	1E-06	1E-06
TLPVAQAYQDNLY(+79.97)R	Tanc2	Y13:23.70	0	0	0	0	0	0	52700	0	0	1	1E-06	0.266
ELNY(+79.97)TELQELK	Tbc1d24	Y4:7.65	0	0	0	27300	0	0	43200	45800	11500	1E-06	1	1E-06
DIGGYYGFY(+79.97)SHS	Tbr1	Y9:20.00	0	0	0	10600	2650	0	0	42400	29000	1E-06	1	0.533
SIDSSDSGIY(+79.97)EQAK	Tbr1	Y10:0.00	0	0	0	0	2310	0	10300	5000	0	1E-06	1E-06	0.769
DIGGY(+79.97)YGFYSHS	Tbr1	Y5:14.02	0	0	0	19800	7740	0	30400	61600	42900	1	1	0.592
TGDDYVAIGADEEELGSQIEEAIY(+79.97)QEIR	Tcea1	Y24:61.82	0	0	0	33300	88900	2E+05	2E+06	9E+05	4E+05	1E-06	1E-06	0.611
TGDDY(+79.97)VAIGADEEELGSQIEEAIY(+79.97)QEIR	Tcea1	Y5:0.00, Y24:27.25	0	0	0	0	7160	0	1E+05	71700	22000	1E-06	1	0.424
SSSQYY(+79.97)TSFPSNPR	Tcf3	Y6:21.94	0	0	0	644	0	0	10600	21600	0	1	1E-06	1E-06
LSEVIY(+79.97)EPFQLLSK	Tex2	Y6:31.93	0	0	0	12000	0	2230	0	0	0	1E-06	1	0.192
LPEGTTY(+79.97)EEYLGAEYLQAVGNIR	Tf	Y7:9.34	0	0	0	0	0	0	0	0	46000	1	1E-06	1E-06
GSESSKPWPDATTY(+79.97)GTGSASR	Thrap3	Y14:0.00	0	0	0	49300	83600	25400	26100	3E+05	2E+05	1	1E-06	0.364
HVLSGTLGVPEHTY(+79.97)R	Thy1	Y14:0.00	0	0	0	0	0	0	0	62	0	1	0.638	1E-06
EVDSGNDIY(+79.97)GNPIKR	Timp2	Y9:21.59	0	0	0	0	4300	0	9760	13300	0	1	1E-06	1E-06
AVSEKEVDSGNDIY(+79.97)GNPIKR	Timp2	Y14:39.44	0	0	0	4E+05	1E+05	3E+05	89200	17100	9E+05	1E-06	1E-06	0.194
LGQSDPAPLQHQVDVY(+79.97)QK	Tkt	Y16:26.38	0	0	0	13500	0	4740	0	51500	13300	1E-06	1E-06	0.452
TSRPENAIIY(+79.97)SNNEDFQVGQAK	Tkt	Y10:8.69	0	0	0	5E+05	37200	4E+05	1E+06	5840	5E+05	1E-06	1E-06	0.132
NMAEQIIQEIY(+79.97)SQVQSK	Tkt	Y11:8.14	0	0	0	5E+05	2E+05	1E+06	3E+06	4E+06	2E+06	1E-06	1E-06	0.161
LGQSDPAPLQHQVDVY(+79.97)QKR	Tkt	Y16:17.85	0	0	0	13800	0	8590	0	0	1350	1E-06	1	0.207
ILTVEDHYY(+79.97)EGGIGEAVSAVVVGEPGVTVTR	Tkt	Y9:7.65	0	0	0	0	0	34100	0	0	10100	1E-06	1	0.312
ILTVEDHY(+79.97)YEGGIGEAVSAVVVGEPGVTVTR	Tkt	Y8:6.47	0	0	0	0	0	0	0	0	53800	1	1E-06	1E-06
ISDY(+79.97)FEFAGGSGPGTSPGR	Tlk2	Y4:0.00	0	0	0	96600	36500	40400	2E+05	4E+05	97000	1E-06	1E-06	0.676
VHLDIQVGEHANDY(+79.97)AEIAAK	Tmed9	Y14:1000.0	0	0	0	0	0	6410	91500	0	3E+05	1	1E-06	1E-06
TDFSILY(+79.97)VVPSR	Tmeff1	Y7:24.67	0	0	0	8040	0	0	0	0	9570	1E-06	1	0.568
SGDVSQFPY(+79.97)VEFTGR	Tmem106b	Y9:41.50	0	0	0	2E+06	2E+06	1E+06	5E+06	9E+06	3E+06	1E-06	1E-06	0.476
KALPESAEEQPSLY(+79.97)EKAPQGK	Tmem35a	Y14:39.76	0	0	0	1E+05	9640	73200	21400	2E+05	1E+05	1E-06	1E-06	0.555
ALPESAEEQPSLY(+79.97)EK	Tmem35a	Y13:9.40	0	0	0	62100	55500	4850	3E+05	3E+05	24500	1E-06	1E-06	0.771
ALPESAEEQPSLY(+79.97)EKAPQGK	Tmem35a	Y13:39.76	2E+05	20100	58900	1E+06	6E+05	7E+05	2E+06	5E+06	1E+06	0.256	0.204	0.469
KALPESAEEQPSLY(+79.97)EK	Tmem35a	Y14:22.85	0	0	0	0	0	0	0	1990	0	1	1E-06	0.719
DVY(+79.97)VQLYLQHLTAR	Tmpo	Y3:42.68	0	0	0	0	0	0	34500	0	26700	1	1E-06	1E-06

Peptide sequence and modification (phospho-S/T/Y) & Carbamidomethylation	Gene name	Modification A-score (≥ 13 = p < 0.05)	FSBA replicates			N1-Src replicates			C-Src replicates			FSBA vs N1-Src	FSBA vs C-Src	N1-Src vs C-Src
EMFPY(+79.97)EASTPTGISASC(+57.02)R	Tmpo	Y5:34.87, C17:1000	0	0	0	34600	16300	9430	1E+05	2E+05	30200	1E-06	1E-06	0.895
IEHNQSY(+79.97)SEAGVTETEWTSGSSK	Tmpo	Y7:0.00	0	0	0	391	0	0	0	0	0	1E-06	1	1E-06
DILKEMFPY(+79.97)EASTPTGISASC(+57.02)R	Tmpo	Y9:7.77, C21:1000	0	0	0	0	0	30400	0	0	1E+05	1E-06	1	0.946
GSADPEEESVLY(+79.97)SNR	Tomm34	Y12:9.34	0	0	0	38600	42800	117	2E+05	3E+05	36200	1E-06	1E-06	0.182
KVEEVVY(+79.97)DLSIR	Tsn	Y7:101.94	0	0	0	1E+06	9E+05	1E+06	3E+06	5E+06	3E+06	1E-06	1E-06	0.342
VEEVVY(+79.97)DLSIR	Tsn	Y6:37.54	0	0	0	83900	74700	49400	2E+05	5E+05	1E+05	1E-06	1E-06	0.771
VGINY(+79.97)QPPTVVPGGDLAK	Tuba1a	Y5:28.70	0	0	0	0	0	0	840	0	0	1	1E-06	1E-06
IHFPLATY(+79.97)APVISAEK	Tuba1a	Y8:30.46	0	0	0	2E+05	49700	1E+05	5E+05	1E+05	4E+05	1E-06	1E-06	0.785
QLFHPEQLITGKEDAANNY(+79.97)AR	Tuba1a	Y19:45.63	0	0	0	0	0	0	0	0	45300	1	1E-06	1E-06
VSDTVVEPYNATLSVHQLVENTDETYC(+57.02)IDNEALY(+79.97)DI C(+57.02)FR	Tubb2b	C27/C37:1000.0 Y34:54.40	0	0	0	0	0	0	0	0	65500	1	1E-06	1E-06
FWEVISDEHGIDPSGNY(+79.97)VGDSDLQLER	Tubb3	Y17:12.33	0	0	0	0	0	15100	0	0	2E+05	1E-06	1E-06	0.467
ISY(+79.97)FTFIGTPVQATNMNDFKR	Txnl1	Y3:12.28	0	0	0	4580	0	24200	0	0	17700	1E-06	1	0.403
AAAEIY(+79.97)EEFLAAFEGSDGNK	U2surp	Y6:85.70	25600	1560	0	84200	85800	80800	2E+05	2E+05	2E+05	0.185	0.084	0.578
EDEKAAAEIY(+79.97)EEFLAAFEGSDGNK	U2surp	Y10:82.30	0	0	0	0	0	0	0	0	62500	1	1E-06	1E-06
IIPAIAT(+79.97)TTAAVVGLVC(+57.02)LELY(+79.97)K	Uba1	T7:14.02, Y21:9.05	0	0	0	0	7E+05	8E+05	5E+05	0	4E+05	1	1E-06	0.446
ALVLELC(+57.02)C(+57.02)NDESGEDVEVPY(+79.97)VR	Uba1	C7/C8:1000.0 Y20:49.35	0	0	0	15600	0	14200	27400	68900	28000	1	1E-06	0.259
VGPDTERIY(+79.97)DDDFFQNLDGVANALDNVDAR	Uba1	Y9:5.55	0	0	0	0	0	3650	0	0	1E+05	1E-06	1	0.066
SQASKPTYGNSPY(+79.97)WTN	Ubap2	Y13:21.68	0	0	0	0	4870	0	0	27200	15400	1	1E-06	1E-06
DGSLASNPY(+79.97)SGDLTK	Ubap2l	Y9:0.00	0	0	0	0	10100	0	13400	58600	13500	1	1E-06	0.378
FPLDY(+79.97)YSIPFPTPTTPLTGR	Ubap2l	Y5:10.11	0	0	0	1350	0	0	0	6570	0	1E-06	1	1E-06
NQDLALSNLESIPGGY(+79.97)NALRR	Ubqln2	Y16:0.00	0	0	0	6310	0	0	0	0	19400	1E-06	1E-06	1E-06
AFDQGADAVYDY(+79.97)INEGK	Uqcr10	Y12:14.04	0	0	0	0	0	0	13300	5030	0	1	1E-06	0.832
AFDQGADAVY(+79.97)DYINEGK	Uqcr10	Y10:32.28	16700	16600	0	2E+06	2E+06	1E+06	4E+06	8E+06	2E+06	0.211	0.208	0.583
AFDQGADAVY(+79.97)DY(+79.97)INEGK	Uqcr10	Y10/Y12:1000.0	0	0	4040	6370	13300	0	28700	48300	7900	0.444	1	0.262
YEEDKFY(+79.97)LEPYLK	Uqcrb	Y7:23.11	0	0	0	30300	0	36200	0	0	42100	1E-06	1	0.951
QGLY(+79.97)DRLPPLPVTPGMEGAGVVVAVGEGVSDR	Vat1	Y4:1.73	0	0	0	0	0	0	0	0	34300	1	1E-06	0.475
FHPDINVY(+79.97)IIEVR	Vcan	Y8:1000.0	0	0	0	0	0	0	0	0	6520	1	1E-06	0.167
AVAGNIS(+79.97)DPGLQKS(+79.97)FLDSGY(+79.97)RILGAVAK	Vcl	S7:7.03, S14:11.12 Y20:0.00	4E+05	4E+05	5E+05	4E+05	5E+05	5E+05	6E+05	0	6E+05	1	0.705	1E-06
LDQLIY(+79.97)IPLPDEK	Vcp	Y6:1000.0	0	0	0	15200	0	0	0	0	0	1E-06	1	1
RESPESEGPIY(+79.97)EGLIL	Vps35	Y11:33.54	0	0	0	0	0	0	0	0	12200	1	1E-06	1E-06

Peptide sequence and modification (phospho-S/T/Y) & Carbamidomethylation	Gene name	Modification A-score (≥ 13 = p < 0.05)	FSBA replicates			N1-Src replicates			C-Src replicates			FSBA vs N1-Src	FSBA vs C-Src	N1-Src vs C-Src
HHSAPLY(+79.97)SSYLHK	Vstm2a	Y7:9.95	0	0	0	0	0	0	0	0	2890	1	1E-06	1E-06
AAEAAASAY(+79.97)YNPGNPHNVYMPTSQPPPPPYYPPEDK	Wbp2	Y9:0.00	0	0	0	20300	0	31800	0	3E+05	1E+06	1E-06	1E-06	0.181
AAEAAASAYYNPGNPHNVY(+79.97)MPTSQPPPPPYYPPEDK	Wbp2	Y19:0.00	0	0	0	0	0	0	2E+06	2E+05	0	1	1E-06	1E-06
AAEAAASAYY(+79.97)NPGNPHNVYMPTSQPPPPPYYPPEDK	Wbp2	Y10:3.75	0	0	0	0	23700	0	0	0	0	1E-06	1	0.587
AAEDNPY(+79.97)WVSPAYSK	Wdr70	Y7:32.97	0	0	0	2E+05	2E+05	1E+05	5E+05	9E+05	2E+05	1E-06	1E-06	0.851
TLSLDEVY(+79.97)LIDSGAQYK	Xpnpep1	Y8:19.39	0	0	0	21400	0	10400	11700	63200	24700	1E-06	1E-06	0.647
DQPAFTPSGILTPY(+79.97)ALGSR	Xrn2	Y14:0.00	0	0	0	78600	49800	30200	1E+05	3E+05	85500	1E-06	1E-06	0.337
GTDYQLSKEY(+79.97)TLDVYR	Yars	Y10:11.06	0	0	0	75200	4170	42900	0	90900	99100	1E-06	1E-06	0.305
EYTLDVY(+79.97)R	Yars	Y7:47.31	0	0	0	7160	6590	0	30900	29600	0	1E-06	1E-06	0.714
HPDADSLY(+79.97)VEKIDVGEAEPR	Yars	Y8:22.85	0	0	0	0	0	2720	0	0	21400	1E-06	1E-06	0.123
NSVVEASEAAY(+79.97)KEAFEISK	Ywhah	Y11:9.85	0	0	0	0	0	0	0	0	4640	1	1E-06	1E-06
KQTIENSQGAY(+79.97)QEAFDISKK	Ywhaq	Y11:35.70	0	0	0	71100	0	75100	0	74400	1E+05	1E-06	1E-06	0.705
KQTIENSQGAY(+79.97)QEAFDISK	Ywhaq	Y11:37.48	0	0	0	6190	0	2900	0	27400	910	1E-06	1E-06	0.364
GIVDQSQQAY(+79.97)QEAFEISK	Ywhaz	Y10:0.00	0	0	0	4000	0	0	1610	21300	0	1E-06	1E-06	0.241
GIVDQSQQAY(+79.97)QEAFEISKK	Ywhaz	Y10:19.86	0	0	0	1E+05	0	78300	63100	2E+05	1E+05	1E-06	1E-06	0.484
TFTESYAARPDGDY(+79.97)TSSVNGGNIK	Zc2hc1a	Y14:9.34	0	0	0	13200	0	2460	0	37400	31900	1E-06	1	0.957
LPPPPPPSYDPDY(+79.97)IQC(+57.02)PYC(+57.02)QR	Zc2hc1a	Y13:35.03 C16/C19:1000.0	0	0	0	2E+05	2E+05	83900	1E+06	2E+06	2E+05	1E-06	1E-06	0.24
LPPPPPPSYDPDYIQC(+57.02)PY(+79.97)C(+57.02)QR	Zc2hc1a	C16/C19:1000.0 Y18:56.99	0	0	0	42000	7230	24400	2E+05	4E+05	20500	1E-06	1E-06	0.545
LPPPPPPSY(+79.97)DPDYIQC(+57.02)PYC(+57.02)QR	Zc2hc1a	Y9:0.00 C16/C19:1000.0	0	0	0	19600	19400	27800	17800	7970	2930	1E-06	1	0.312
EGGKLPPPPPPSYDPDY(+79.97)IQC(+57.02)PYC(+57.02)QR	Zc2hc1a	Y17:22.07 C20/C23:1000.0	0	0	0	0	0	0	50400	89800	12000	1	1E-06	1E-06
EGGKLPPPPPPSY(+79.97)DPDYIQC(+57.02)PYC(+57.02)QR	Zc2hc1a	Y13:0.00 C20/C23:1000.0	0	0	0	0	0	0	11400	0	0	1	1E-06	1E-06
LC(+57.02)EPEVLGSVEDTY(+79.97)SPFFR	Zc3h14	C2:1000, Y14:11.06	0	0	0	8E+05	1E+06	9E+05	1E+06	3E+06	2E+06	1E-06	1E-06	0.574
VLAAGGLGQGSSSGQSSVLSGISLY(+79.97)DPR	Zc3h4	Y25:0.00	0	0	0	5970	0	0	0	0	0	1E-06	1	1E-06
TDIELEIY(+79.97)GMEGIPEKDMDER	Zfp207	Y8:0.00	0	0	0	0	0	0	0	0	31800	1	1E-06	0.23
EAESNSITLSVY(+79.97)EPFKVR	Zfp532	Y12:32.28	0	0	0	0	0	2520	0	0	21900	1	1E-06	1E-06
AEADKVY(+79.97)TFTDNAPSPSIGSASR	Zfp608	Y7:7.65	0	0	0	6050	0	9290	0	51600	23100	1E-06	1E-06	0.298
AEADKIY(+79.97)SFTDNAPSPSIGGSSR	Zfp609	Y7:14.02	0	0	0	2E+05	11800	83700	11000	3E+05	1E+05	1E-06	1E-06	0.36

Peptide sequence and modification (phospho-S/T/Y) & Carbamidomethylation	Gene name	Modification A-score (≥ 13 = p < 0.05)	FSBA replicates			N1-Src replicates			C-Src replicates			FSBA vs N1-Src	FSBA vs C-Src	N1-Src vs C-Src
AALIY(+79.97)TC(+57.02)TVC(+57.02)R	Zfp706	Y5:11.06 C7/C10:1000.0	0	0	0	2E+05	3E+05	0	1E+06	2E+06	4E+05	1E-06	1E-06	0.524
QYYQQPTATAAAVAAAAQPQPSVAETY(+79.97)YQTAPK	Zfr	Y27:0.00	0	0	0	20600	0	0	0	60700	52500	1E-06	1	0.334
GTLDGYVY(+79.97)SC(+57.02)KEC(+57.02)DFR	Zhx3	Y8:22.09 C10/C13:1000.0	0	0	0	32700	0	29100	0	52200	1E+05	1E-06	1	0.051

Appendix 5: The *in vitro* tyrosine phosphorylation sites (rat) of the C- and N1-Src substrates in postnatal day 1 rat brain homogenates.

	Phosphorylation site			Phosphorylation site	
Protein	**N1-Src**	**C-Src**	**Protein**	**N1-Src**	**C-Src**
A1m	-	1039	Dcc	1062	-
Acp1	143	143	Dcx	350	350
Akap1	154	154	Ddx41	-	33
Alb	419, 425	419, 425	Dek	354	354, 360
Aldh2	334	334	Denr	29, 39, 42	39
Aldoc	357	357	Dlg2	737	737
Ambp	343	-	Dlg3	618	618
Apc	1076	-	Dlgap4	984	984
Apoo	-	43	Dnajc5	17	17, 149
Arhgap12	241	-	Dpysl2	290	290, 499
Arhgdia	156	156	Dpysl3	-	431
Arpc3	47	47	Eef1a1	254	254
Ashwin	53	53	Eef2	-	760
Atn1	776	776	Efnb1	328	328
Atp5o	82	35, 82	Efnb3	323, 337	323, 337
Atxn2	34	34	Eif4enif1	-	983
Atxn2l	116	116	Eno1	-	280
Cacng8	307	307	Ensa	-	70
Cadm2	-	433	Erp29	66	-
Cadm3	394	394	Ewsr1	284	284
Canx	71	71	Fam213a	-	110
Cap1	-	31	Fnbp1l	291	291
Casd1	-	213	Gab1	-	285
Casp3	32	32	Gab2	263	263
Ccdc177	131	131	Gapdh	92	-
Cdv3	213	213	Glcci1	64	64
Celf2	67	-	Gmds	159	159
Cep170b	1299	1299	Gnao1	168	-
Cct8	-	30	Gng2	-	13
Cfl1	68, 85	68, 85	Gng3	44	-
Cherp	902	902	Gpc4	50	50
Cic	1452	1452	Gprc5c	-	386
Cisd1	71	71	Gpx1	147	147
Ckap4	53	53	Gria2	876	-
Clasp1	521, 1192	521, 1192, 1282	Grpel1	173	173
Clasp2	299, 1014	299, 1014	Gyg1	315	315
Clstn1	150	-	Hcfc1	111	111
Cnpy3	76	76	Hepacam	312	312
Cnrip1	89	85,89	Hnrnph1	306	306
Cops4	-	167	Hsp90aa1	310	310
Cops7a	137	137	Hspa8	41	41
Cpd	1372	-	Hspe1	88	88
Cs	80	69, 80	Hsph1	644	644
Cxadr	318	318	Itga5	178	178
Dcbld2	744	-	Itgb1	784	784

	Phosphorylation site			Phosphorylation site	
Protein	**N1-Src**	**C-Src**	**Protein**	**N1-Src**	**C-Src**
Itpa	164	164	Pgrmc1	113	113
Klc2	-	431	Pgrmc2	-	137
Kng1	72	57, 72	Pithd1	96	96
Lancl1	13	13	Pitpna	24, 141	141
Letm1	140	140	Plcb1	803	803
Lgalsl	25	-	Plcg1	-	771
Lin7c	58	54	Plppr3	619	619
Magi1	373	373	Plrg1	52	-
Magi2	362	362	Poldip3	182, 236	182, 236
Magi3	-	356	Ppp1r14b	29	29
Map1b	1402, 1753	1402	Ppp2r5d	573	573
Map6	539	539	Prdx4	-	56
Mapt	705	705	Prkrip1	82	82
Mast4	1300	1300	Prrc2b	1496	-
Mcm3	-	706	Psma7	-	159
Mcrip1	41	41	Psmd9	70	70
Mdga1	187, 191	187, 191	Psme1	209	209
Mdga2	-	189	Ptpn1	66	66
Micall1	677	677	Pym1	45	45, 49
Mlip	788	788	Rab4b	-	189
Mtnd3	37	-	RGD1305178	-	147
Myl6	86	86	RGD1306271	1157	1157
Nacad	1316	1316	RGD1311703	84	84
Napa	185	131, 185	RGD1560065	131	131
Napb	184	131, 184	RGD1561636	43	-
Naxe	279	279	RhoA	-	66
Ncam1	680	680	Rilpl2	32	-
Nectin1	466	466	Rnf113a1	118	118
Nelfe	133	133	Rrm1	404	404
Nfya	260	260	Rtn4	506, 814	506
Nfyb	58	58	S1pr1	20, 23	20, 23
Nipsnap1	261	261	Sar1a	191	191
Nme1	151	-	Scamp1	37	37
Nolc1	299	299	Sema6d	-	926
Nsfl1c	167	167	Serpina10	400	400
Nsrp1	78	72, 78	Sf1	-	87
Ntmt1	215, 218	215, 218	Sfpq	477	-
Nyap1	215	215	Sgta	-	127
Pag1	165, 183, 381	165, 183, 224, 381, 409	Shb	-	95
Paics	-	22	Sh3bgrl	92	92
Pcyox1	-	339	Sh3glb1	80,100	80
Pdcd10	89	-	Sh3glb2	77	77
Pdia3	445	445	Sh3pxd2b	558	558
Pfdn1	-	61	Sin3a	13	13
Pfn2	-	79	Sirpa	501	477, 501
Pgk1	161	-	Snap91	15	15

	Phosphorylation site	
Protein	**N1-Src**	**C-Src**
Snw1	420, 430, 433	430
Spata2	478	-
Src	419, 439	419, 439
Srcin1	431, 496	431, 435, 496
Stip1	354	354
Sugp2	68	-
Tbr1	677	-
Tcea1	177	177
Tcf3	-	151
Tex2	299	-
Timp2	62	62
Tkt	202	202
Tmed9	-	152
Tmem106b	51	51
Tmpo	350	37, 350
Tsn	264	264
Tuba1a	272	272
Uba1	-	1052
Ubap2	-	1132
Uqcrb	90	-
Uqcr10	-	46
Wdr70	619	619
Xpnpep1	412	412
Yars	134	134
Ywhaq	149	149
Ywhaz	149	149
Zc2hc1a	119, 124	119, 124
Zfp609	796	796
Zhx3	77	-

Abbreviations

% mol; Percentage molarity

3'; Three prime

32P; Phosphorus-32

5'; Five prime

AMPA; α-amino-3-hydroxy-5-methyl-4-isoxazolepropionic acid

APS; Ammonium persulfate

ASV; Avian sarcoma virus

ATP; Adenosine triphosphate

B104; rat neuroblastoma cell line

BP; Base pair

BSA; Bovine serum albumin

cAMP; Cyclic adenosine monophosphate

°C; Degrees centigrade

C; Carboxyl

CDK5; Cyclin Dependent Kinase 5

cDNA; Complementary DNA

CEF; Chicken embryo fibroblast

CHK; Csk homologous kinase

CNS; Central nervous system

COS-7; African green monkey kidney fibroblast-like cell line

CSK; C-terminal Src kinase

CSP; Chemical shift perturbation

CTD; C-terminal domain

DCC; Deleted in colorectal carcinoma

DMEM; Dulbecco's Modified Eagle's Medium

DMSO; Dimethyl sulfoxide

DNA; Deoxyribonucleic acid

DTT; Dithiothreitol

E; Embryonic

ECL; Enhanced chemiluminescence

EDTA; Ethylenediaminetetraacetic acid

EGF; Epidermal growth factor

EGFR; Epidermal growth factor receptor

eMPAI: Exponentially modified protein abundance index

EVL; Ena/VASP-like protein

FAK; Focal adhesion kinase

FBS; Fetal bovine serum

FDR; False discovery rate

FGFR; Fibroblast growth factor receptors

GABA; Gamma-Aminobutyric Acid

GFP: Green fluorescent protein

GO; Gene ontology

GPCR; G-protein coupled receptor

GPI; Glycosylphosphatidylinositol

GST; Glutathione S-transferase

HEK; Human embryonic kidney

His; A polyhistidine-tag

HRP; Horseradish peroxidase

HSQC; Heteronuclear single quantum coherence spectroscopy

IPTG; Isopropyl β-D-1-thiogalactopyranoside

KD; Kinase domain

kDa; Kilodalton

L1-CAM; L1 cell adhesion molecule

L; Litre

LB; Lysogeny broth

LC; Liquid chromatography

LDE; Long distance element

M; Molar

Min; Minute(s)

ml; Millilitre(s)

mM; Millimolar

MS; Mass spectrometry

MW; Molecular weight

MWCO; Molecular weight cut off

nPTB; Neuronal polypyrimidine tract-binding protein

N1-Src: Neuronal Src kinase 1

N2-Src: Neuronal Src kinase 2

NB; Neuroblastoma

NMDA; N-methyl-D-aspartate

NMR; Nuclear magnetic resonance

nRTK; Non-receptor tyrosine kinase

P1: Postnatal day 1

PAI: Protein abundance index

PBS; Phosphate buffered saline

PC12; cell line derived from a pheochromocytoma of the rat adrenal medulla

PCR; Polymerase chain reaction

PDGFR; Platelet-derived growth factor receptors

PI3K: Phosphoinositide 3-kinase

PK; Pyruvate kinase

PKA; Protein kinase A

PMSF; Phenylmethanesulfonyl fluoride

PNS; Peripheral nervous system

PPII helix; Polyproline type II helix

PP1; 4-amino-5-(4-methylphenyl)-7-(t-butyl)pyrazolo-d-3,4-pyrimidine

PP2; 1-*tert*-Butyl-3-(4-chlorophenyl)-1*H*-pyrazolo[3,4-*d*]pyrimidin-4-amine

PRD; Proline rich domain

PRR; Proline rich region

PTB; Polypyrimidine tract-binding protein

PTB; Phosphotyrosine binding (PTB) domains

PTM; Post translational modification

RGC; Retinal ganglion cell

RIPA; Radioimmunoprecipitation assay buffer

RNA; Ribonucleic acid

RPM; Revolutions per minute

RSV; Rous Sarcoma virus

RTK; Receptor tyrosine kinase

SDE; Short distance element

SDS; Sodium dodecyl sulfate

SDS-PAGE; Sodium dodecyl sulphate polyacrylamide gel electrophoresis

SFK; Src family kinases

SH1; Src homology 1 domain

SH2; Src homology 2 domain

SH3; Src homology 3 domain

SH4; Src homology 4 domain

SPR; Surface plasmon resonance

TEMED; Tetramethylethylenediamine

TOCSY; Total correlation spectroscopy

µg; Microgram(s)

µM; Micromolar

v/v; Volume per volume

WT; Wild-type

w/v; Weight per volume

References

Abdelhameed, T. 2010. “Role of Src Splice Variants in Nerve Terminal Function.” The University of Edinburgh: The University of Edinburgh.

Advani, Gahana, Ya Chee Lim, Bruno Catimel, Daisy Sio Seng Lio, Nadia L. Y. Ng, Anderly C. Chüeh, Mai Tran, et al. 2017. “Csk-Homologous Kinase (Chk) Is an Efficient Inhibitor of Src-Family Kinases but a Poor Catalyst of Phosphorylation of Their C-Terminal Regulatory Tyrosine.” *Cell Communication and Signaling: CCS* 15 (1): 29.

Ahn, Seungkirl, Jihee Kim, Carmen L. Lucaveche, Mary C. Reedy, Louis M. Luttrell, Robert J. Lefkowitz, and Yehia Daaka. 2002. “Src-Dependent Tyrosine Phosphorylation Regulates Dynamin Self-Assembly and Ligand-Induced Endocytosis of the Epidermal Growth Factor Receptor.” *The Journal of Biological Chemistry* 277 (29): 26642–51.

Ahn, Seungkirl, Stuart Maudsley, Louis M. Luttrell, Robert J. Lefkowitz, and Yehia Daaka. 1999. “Src-Mediated Tyrosine Phosphorylation of Dynamin Is Required for β2-Adrenergic Receptor Internalization and Mitogen-Activated Protein Kinase Signaling.” *The Journal of Biological Chemistry* 274 (3): 1185–88.

Ahn, S., S. Maudsley, L. M. Luttrell, R. J. Lefkowitz, and Y. Daaka. 1999. “Src-Mediated Tyrosine Phosphorylation of Dynamin Is Required for beta2-Adrenergic Receptor Internalization and Mitogen-Activated Protein Kinase Signaling.” *The Journal of Biological Chemistry* 274: 1185–88.

Aitio, Olli, Maarit Hellman, Tapio Kesti, Iivari Kleino, Olga Samuilova, Kimmo Pääkkönen, Helena Tossavainen, Kalle Saksela, and Perttu Permi. 2008. “Structural Basis of PxxDY Motif Recognition in SH3 Binding.” *Journal of Molecular Biology* 382 (1): 167–78.

Amanchy, Ramars, Jun Zhong, Rosa Hong, James H. Kim, Marjan Gucek, Robert N. Cole, Henrik Molina, and Akhilesh Pandey. 2009. “Identification of c-Src Tyrosine Kinase Substrates in Platelet-Derived Growth Factor Receptor Signaling.” *Molecular Oncology* 3 (5-6): 439–50.

Amanchy, Ramars, Jun Zhong, Henrik Molina, Raghothama Chaerkady, Akiko Iwahori, Dario Eluan Kalume, Mads Grønborg, Jos Joore, Leslie Cope, and Akhilesh Pandey. 2008. “Identification of c-Src Tyrosine Kinase Substrates Using Mass Spectrometry and Peptide Microarrays.” *Journal of Proteome Research* 7 (9): 3900–3910.

Amata, Irene, Mariano Maffei, and Miquel Pons. 2014. “Phosphorylation of Unique Domains of Src Family Kinases.” *Frontiers in Genetics* 5 (June): 181.

Anggono, Victor, Karen J. Smillie, Mark E. Graham, Valentina A. Valova, Michael A. Cousin, and Phillip J. Robinson. 2006. “Syndapin I Is the Phosphorylation-Regulated Dynamin I Partner in Synaptic Vesicle Endocytosis.” *Nature Neuroscience* 9 (6): 752–60.

Ardern, Hazel, Emma Sandilands, Laura M. Machesky, Paul Timpson, Margaret C. Frame, and Valerie G. Brunton. 2006. “Src-Dependent Phosphorylation of Scar1 Promotes Its Association with the Arp2/3 Complex.” *Cell Motility and the Cytoskeleton* 63 (1): 6–13.

Ardito, Fatima, Michele Giuliani, Donatella Perrone, Giuseppe Troiano, and Lorenzo Lo Muzio. 2017. “The Crucial Role of Protein Phosphorylation in Cell Signaling and Its Use as Targeted Therapy (Review).” *International Journal of Molecular Medicine* 40 (2): 271–80.

Arold, S., R. O’Brien, P. Franken, M. P. Strub, F. Hoh, C. Dumas, and J. E. Ladbury. 1998. “RT Loop Flexibility Enhances the Specificity of Src Family SH3 Domains for HIV-1 Nef.” *Biochemistry* 37 (42): 14683–91.

Atsumi, S., K. Wakabayashi, K. Titani, Y. Fujii, and T. Kawate. 1993. “Neuronal

pp60c-Src(+) in the Developing Chick Spinal Cord as Revealed with Anti-Hexapeptide Antibody." *Journal of Neurocytology* 22 (4): 244–58.

Balsamo, Michele, Chandrani Mondal, Guillaume Carmona, Leslie M. McClain, Daisy N. Riquelme, Jenny Tadros, Duan Ma, et al. 2016. "The Alternatively-Included 11a Sequence Modifies the Effects of Mena on Actin Cytoskeletal Organization and Cell Behavior." *Scientific Reports* 6 (October): 35298.

Barker, S. C., D. B. Kassel, D. Weigl, X. Huang, M. A. Luther, and W. B. Knight. 1995. "Characterization of pp60c-Src Tyrosine Kinase Activities Using a Continuous Assay: Autoactivation of the Enzyme Is an Intermolecular Autophosphorylation Process." *Biochemistry* 34 (45): 14843–51.

Bevilaqua, L. R. M., J. I. Rossato, J. H. Medina, I. Izquierdo, and M. Cammarota. 2003. "Src Kinase Activity Is Required for Avoidance Memory Formation and Recall." *Behavioural Pharmacology* 14 (8): 649–52.

Biel, Martin, Christian Wahl-Schott, Stylianos Michalakis, and Xiangang Zong. 2009. "Hyperpolarization-Activated Cation Channels: From Genes to Function." *Physiological Reviews* 89 (3): 847–85.

Biscardi, J. S., M. C. Maa, D. A. Tice, M. E. Cox, T. H. Leu, and S. J. Parsons. 1999. "C-Src-Mediated Phosphorylation of the Epidermal Growth Factor Receptor on Tyr845 and Tyr1101 Is Associated with Modulation of Receptor Function." *The Journal of Biological Chemistry* 274 (12): 8335–43.

Black, D. L. 1992. "Activation of c-Src Neuron-Specific Splicing by an Unusual RNA Element in Vivo and in Vitro." *Cell* 69 (5): 795–807.

Bolen, J. B., and J. S. Brugge. 1997. "Leukocyte Protein Tyrosine Kinases: Potential Targets for Drug Discovery." *Annual Review of Immunology* 15: 371–404.

Bond, Charles S., and Archa H. Fox. 2009. "Paraspeckles: Nuclear Bodies Built on Long Noncoding RNA." *The Journal of Cell Biology* 186 (5): 637–44.

Boutz, Paul L., Peter Stoilov, Qin Li, Chia-Ho Lin, Geetanjali Chawla, Kristin Ostrow, Lily Shiue, Manuel Ares Jr, and Douglas L. Black. 2007. "A Post-Transcriptional Regulatory Switch in Polypyrimidine Tract-Binding Proteins Reprograms Alternative Splicing in Developing Neurons." *Genes & Development* 21 (13): 1636–52.

Briggs, S. D., and T. E. Smithgall. 1999. "SH2-Kinase Linker Mutations Release Hck Tyrosine Kinase and Transforming Activities in Rat-2 Fibroblasts." *The Journal of Biological Chemistry* 274 (37): 26579–83.

Brouns, M. R., S. F. Matheson, and J. Settleman. 2001. "p190 RhoGAP Is the Principal Src Substrate in Brain and Regulates Axon Outgrowth, Guidance and Fasciculation." *Nature Cell Biology* 3 (4): 361–67.

Brown, M. T., J. Andrade, H. Radhakrishna, J. G. Donaldson, J. A. Cooper, and P. A. Randazzo. 1998. "ASAP1, a Phospholipid-Dependent Arf GTPase-Activating Protein That Associates with and Is Phosphorylated by Src." *Molecular and Cellular Biology* 18 (12): 7038–51.

Brown, M. T., and J. A. Cooper. 1996. "Regulation, Substrates and Functions of Src." *Biochimica et Biophysica Acta* 1287 (2-3): 121–49.

Brugge, J., P. Cotton, A. Lustig, W. Yonemoto, L. Lipsich, P. Coussens, J. N. Barrett, D. Nonner, and R. W. Keane. 1987. "Characterization of the Altered Form of the c-Src Gene Product in Neuronal Cells." *Genes & Development* 1 (3): 287–96.

Brugge, J. S., P. C. Cotton, A. E. Queral, J. N. Barrett, D. Nonner, and R. W. Keane. 1985. "Neurones Express High Levels of a Structurally Modified, Activated Form of pp60c-Src." *Nature* 316 (6028): 554–57.

Brugge, J. S., A. Lustig, and A. Messer. 1987. "Changes in the Pattern of Expression of pp60c-Src in Cerebellar Mutants of Mice." *Journal of Neuroscience Research* 18 (4): 532–38.

Cabral, Estela, Henrique Soares, Hercília Guimarães, Rui Vitorino, Rita Ferreira, and Tiago Henriques-Coelho. 2017. “Prediction of Cardiovascular Risk in Preterm Neonates through Urinary Proteomics: An Exploratory Study.” *Porto Biomedical Journal* 2 (6): 287–92.

Campbell, E. J., E. McDuff, O. Tatarov, S. Tovey, V. Brunton, T. G. Cooke, and J. Edwards. 2008. “Phosphorylated c-Src in the Nucleus Is Associated with Improved Patient Outcome in ER-Positive Breast Cancer.” *British Journal of Cancer* 99 (11): 1769–74.

Cans, C., G. Neubauer, and K. Bomsztyk. 2002. “C-Src-Mediated Phosphorylation of hnRNP K Drives Translational Activation of Specifically Silenced mRNAs.” *And Cellular Biology*. http://mcb.asm.org/content/22/13/4535.short.

Cao, Hong, Jing Chen, Eugene W. Krueger, and Mark A. McNiven. 2010. “Src-Mediated Phosphorylation of Dynamin and Cortactin Regulates the ‘Constitutive’ Endocytosis of Transferrin.” *Molecular and Cellular Biology* 30 (3): 781–92.

Carmona, G., U. Perera, C. Gillett, A. Naba, A-L Law, V. P. Sharma, J. Wang, et al. 2016. “Lamellipodin Promotes Invasive 3D Cancer Cell Migration via Regulated Interactions with Ena/VASP and SCAR/WAVE.” *Oncogene*, March. https://doi.org/10.1038/onc.2016.47.

Challis, G. B., and H. J. Stam. 1990. “The Spontaneous Regression of Cancer. A Review of Cases from 1900 to 1987.” *Acta Oncologica* 29 (5): 545–50.

Chan, R. C., and D. L. Black. 1997. “The Polypyrimidine Tract Binding Protein Binds Upstream of Neural Cell-Specific c-Src Exon N1 to Repress the Splicing of the Intron Downstream.” *Molecular and Cellular Biology* 17 (8): 4667–76.

Cheadle, C., Y. Ivashchenko, V. South, G. H. Searfoss, S. French, R. Howk, G. A. Ricca, and M. Jaye. 1994. “Identification of a Src SH3 Domain Binding Motif by Screening a Random Phage Display Library.” *The Journal of Biological Chemistry* 269: 24034–39.

Cheerathodi, Mujeeburahim, James J. Vincent, and Bryan A. Ballif. 2015. “Quantitative Comparison of CrkL-SH3 Binding Proteins from Embryonic Murine Brain and Liver: Implications for Developmental Signaling and the Quantification of Protein Species Variants in Bottom-up Proteomics.” *Journal of Proteomics* 125 (July): 104–11.

Chellaiah, Meenakshi A., and Michael D. Schaller. 2009. “Activation of Src Kinase by Protein-Tyrosine Phosphatase-PEST in Osteoclasts: Comparative Analysis of the Effects of Bisphosphonate and Protein-Tyrosine Phosphatase Inhibitor on Src Activation in Vitro.” *Journal of Cellular Physiology* 220 (2): 382–93.

Chen, Min, Shirley C. Chen, and Catherine J. Pallen. 2006. “Integrin-Induced Tyrosine Phosphorylation of Protein-Tyrosine Phosphatase-α Is Required for Cytoskeletal Reorganization and Cell Migration.” *The Journal of Biological Chemistry* 281 (17): 11972–80.

Chou, M. Y., N. Rooke, C. W. Turck, and D. L. Black. 1999. “hnRNP H Is a Component of a Splicing Enhancer Complex That Activates a c-Src Alternative Exon in Neuronal Cells.” *Molecular and Cellular Biology* 19 (1): 69–77.

Collett, James W., and Robert E. Steele. 1992. “Identification and Developmental Expression of Src+ mRNAs in Xenopus Laevis.” *Developmental Biology* 152 (1): 194–98.

———. 1993. “Alternative Splicing of a Neural-Specific Src mRNA (Src+) Is a Rapid and Protein Synthesis-Independent Response to Neural Induction in Xenopus Laevis.” *Developmental Biology* 158 (2): 487–95.

Collett, J. W., and R. E. Steele. 1992. “Identification and Developmental Expression of Src+ mRNAs in Xenopus Laevis.” *Developmental Biology* 152: 194–98.

Collett, M. S., and R. L. Erikson. 1978. “Protein Kinase Activity Associated with the Avian Sarcoma Virus Src Gene Product.” *Proceedings of the National Academy of Sciences of the United States of America* 75 (4): 2021–24.

Cooper, Bret, Jian Feng, and Wesley M. Garrett. 2010. “Relative, Label-Free Protein Quantitation: Spectral Counting Error Statistics from Nine Replicate MudPIT Samples.” *Journal of the American Society for Mass Spectrometry* 21 (9): 1534–46.

Cosker, Katharina E., Sara J. Fenstermacher, Maria F. Pazyra-Murphy, Hunter L. Elliott, and Rosalind A. Segal. 2016. “The RNA-Binding Protein SFPQ Orchestrates an RNA Regulon to Promote Axon Viability.” *Nature Neuroscience* 19 (5): 690–96.

Cotton, P. C., and J. S. Brugge. 1983. “Neural Tissues Express High Levels of the Cellular Src Gene Product pp60c-Src.” *Molecular and Cellular Biology* 3: 1157–62.

Coussens, P. M., J. A. Cooper, T. Hunter, and D. Shalloway. 1985. “Restriction of the in Vitro and in Vivo Tyrosine Protein Kinase Activities of pp60c-Src Relative to pp60v-Src.” *Molecular and Cellular Biology* 5 (10): 2753–63.

Coutinho-Mansfield, Gabriela C., Yuanchao Xue, Yi Zhang, and Xiang-Dong Fu. 2007. “PTB/nPTB Switch: A Post-Transcriptional Mechanism for Programming Neuronal Differentiation.” *Genes & Development* 21 (13): 1573–77.

Craggs, G., P. M. Finan, D. Lawson, J. Wingfield, T. Perera, S. Gadher, N. F. Totty, and S. Kellie. 2001. “A Nuclear SH3 Domain-Binding Protein That Colocalizes with mRNA Splicing Factors and Intermediate Filament-Containing Perinuclear Networks.” *The Journal of Biological Chemistry* 276 (32): 30552–60.

Dadke, Shrikrishna, and Jonathan Chernoff. 2003. “Protein-Tyrosine Phosphatase 1B Mediates the Effects of Insulin on the Actin Cytoskeleton in Immortalized Fibroblasts.” *The Journal of Biological Chemistry* 278 (42): 40607–11.

Dent, Erik W., Stephanie L. Gupton, and Frank B. Gertler. 2011. “The Growth Cone Cytoskeleton in Axon Outgrowth and Guidance.” *Cold Spring Harbor Perspectives in Biology* 3 (3). https://doi.org/10.1101/cshperspect.a001800.

Dergai, M., L. Tsyba, O. Dergai, I. Zlatskii, I. Skrypkina, V. Kovalenko, and A. Rynditch. 2010. “Microexon-Based Regulation of ITSN1 and Src SH3 Domains Specificity Relies on Introduction of Charged Amino Acids into the Interaction Interface.” *Biochemical and Biophysical Research Communications* 399: 307–12.

Destaing, Olivier, Archana Sanjay, Cecile Itzstein, William C. Horne, Derek Toomre, Pietro De Camilli, and Roland Baron. 2008. “The Tyrosine Kinase Activity of c-Src Regulates Actin Dynamics and Organization of Podosomes in Osteoclasts.” *Molecular Biology of the Cell* 19 (1): 394–404.

Dowle, Adam A., Julie Wilson, and Jerry R. Thomas. 2016. “Comparing the Diagnostic Classification Accuracy of iTRAQ, Peak-Area, Spectral-Counting, and emPAI Methods for Relative Quantification in Expression Proteomics.” *Journal of Proteome Research* 15 (10): 3550–62.

Dunning, Christopher J. R., Hannah L. Black, Katie L. Andrews, Elizabeth C. Davenport, Michael Conboy, Sangeeta Chawla, Adam A. Dowle, David Ashford, Jerry R. Thomas, and Gareth J. O. Evans. 2016. “Multisite Tyrosine Phosphorylation of the N-Terminus of Mint1/X11α by Src Kinase Regulates the Trafficking of Amyloid Precursor Protein.” *Journal of Neurochemistry* 137 (4): 518–27.

Eckhart, W., M. A. Hutchinson, and T. Hunter. 1979. “An Activity Phosphorylating Tyrosine in Polyoma T Antigen Immunoprecipitates.” *Cell* 18 (4): 925–33.

Erpel, T., G. Superti-Furga, and S. A. Courtneidge. 1995. “Mutational Analysis of the Src SH3 Domain: The Same Residues of the Ligand Binding Surface Are Important for Intra- and Intermolecular Interactions.” *The EMBO Journal* 14 (5): 963.

Feng, S., J. K. Chen, H. Yu, J. A. Simon, and S. L. Schreiber. 1994. “Two Binding Orientations for Peptides to the Src SH3 Domain: Development of a General Model for SH3-Ligand Interactions.” *Science* 266 (5188): 1241–47.

Feng, S., C. Kasahara, R. J. Rickles, and S. L. Schreiber. 1995a. “Specific Interactions Outside the Proline-Rich Core of Two Classes of Src Homology 3 Ligands.”

Proceedings of the National Academy of Sciences 92 (26): 12408–15.
———. 1995b. “Specific Interactions Outside the Proline-Rich Core of Two Classes of Src Homology 3 Ligands.” *Proceedings of the National Academy of Sciences of the United States of America* 92 (26): 12408–15.
Ferguson, Shawn M., and Pietro De Camilli. 2012. “Dynamin, a Membrane-Remodelling GTPase.” *Nature Reviews. Molecular Cell Biology* 13 (2): 75–88.
Fernandez-Ballester, G., C. Blanes-Mira, and L. Serrano. 2004. “The Tryptophan Switch: Changing Ligand-Binding Specificity from Type I to Type II in SH3 Domains.” *Journal of Molecular Biology* 335: 619–29.
Ferrando, Isabel Martinez, Raghothama Chaerkady, Jun Zhong, Henrik Molina, Harrys K. C. Jacob, Katie Herbst-Robinson, Beverley M. Dancy, et al. 2012a. “Identification of Targets of c-Src Tyrosine Kinase by Chemical Complementation and Phosphoproteomics.” *Molecular & Cellular Proteomics: MCP* 11 (8): 355–69.
———. 2012b. “Identification of Targets of c-Src Tyrosine Kinase by Chemical Complementation and Phosphoproteomics.” *Molecular & Cellular Proteomics: MCP* 11 (8): 355–69.
Figge, Carina, Gabriele Loers, Melitta Schachner, and Thomas Tilling. 2012. “Neurite Outgrowth Triggered by the Cell Adhesion Molecule L1 Requires Activation and Inactivation of the Cytoskeletal Protein Cofilin.” *Molecular and Cellular Neurosciences* 49 (2): 196–204.
Fincham, V. J., and M. C. Frame. 1998. “The Catalytic Activity of Src Is Dispensable for Translocation to Focal Adhesions but Controls the Turnover of These Structures during Cell Motility.” *The EMBO Journal* 17 (1): 81–92.
Fincham, V. J., M. Unlu, V. G. Brunton, J. D. Pitts, J. A. Wyke, and M. C. Frame. 1996. “Translocation of Src Kinase to the Cell Periphery Is Mediated by the Actin Cytoskeleton under the Control of the Rho Family of Small G Proteins.” *The Journal of Cell Biology* 135: 1551–64.
Florio, M., L. K. Wilson, J. B. Trager, J. Thorner, and G. S. Martin. 1994. “Aberrant Protein Phosphorylation at Tyrosine Is Responsible for the Growth-Inhibitory Action of pp60v-Src Expressed in the Yeast Saccharomyces Cerevisiae.” *Molecular Biology of the Cell* 5 (3): 283–96.
Foda, Zachariah H., Yibing Shan, Eric T. Kim, David E. Shaw, and Markus A. Seeliger. 2015. “A Dynamically Coupled Allosteric Network Underlies Binding Cooperativity in Src Kinase.” *Nature Communications* 6 (January): 5939.
Foster-Barber, Audrey, and J. Michael Bishop. 1998. “Src Interacts with Dynamin and Synapsin in Neuronal Cells.” *Proceedings of the National Academy of Sciences of the United States of America* 95 (8): 4673–77.
Geese, Marcus, Joseph J. Loureiro, James E. Bear, Jürgen Wehland, Frank B. Gertler, and Antonio S. Sechi. 2002. “Contribution of Ena/VASP Proteins to Intracellular Motility ofListeria Requires Phosphorylation and Proline-Rich Core but Not F-Actin Binding or Multimerization.” *Molecular Biology of the Cell* 13 (7): 2383–96.
Gertler, Frank B., Kirsten Niebuhr, Matthias Reinhard, Jürgen Wehland, and Philippe Soriano. 1996. “Mena, a Relative of VASP and Drosophila Enabled, Is Implicated in the Control of Microfilament Dynamics.” *Cell* 87 (2): 227–39.
Ghose, R., A. Shekhtman, M. J. Goger, H. Ji, and D. Cowburn. 2001. “A Novel, Specific Interaction Involving the Csk SH3 Domain and Its Natural Ligand.” *Nature Structural Biology* 8 (11): 998–1004.
Gkourtsa, Areti, Janny van den Burg, Teja Avula, Frans Hochstenbach, and Ben Distel. 2016/9. “Binding of a Proline-Independent Hydrophobic Motif by the Candida Albicans Rvs167-3 SH3 Domain.” *Microbiological Research* 190: 27–36.
Gocek, Elzbieta, Anargyros N. Moulas, and George P. Studzinski. 2014. “Non-Receptor

Protein Tyrosine Kinases Signaling Pathways in Normal and Cancer Cells." *Critical Reviews in Clinical Laboratory Sciences* 51 (3): 125–37.
Goldsmith, Jeffrey F., Craig G. Hall, and T. Prescott Atkinson. 2002. "Identification of an Alternatively Spliced Isoform of the Fyn Tyrosine Kinase." *Biochemical and Biophysical Research Communications* 298 (4): 501–4.
Groveman, Bradley R., Sheng Xue, Vedrana Marin, Jindong Xu, Mohammad K. Ali, Ewa A. Bienkiewicz, and Xian-Min Yu. 2011. "Roles of the SH2 and SH3 Domains in the Regulation of Neuronal Src Kinase Functions." *The FEBS Journal* 278 (4): 643–53.
Hall, Alan, and Giovanna Lalli. 2010. "Rho and Ras GTPases in Axon Growth, Guidance, and Branching." *Cold Spring Harbor Perspectives in Biology* 2 (2): a001818.
Hamadi, A., T. B. Deramaudt, K. Takeda, and P. Rondé. 2009. "Src Activation and Translocation from Focal Adhesions to Membrane Ruffles Contribute to Formation of New Adhesion Sites." *Cellular and Molecular Life Sciences: CMLS* 66 (2): 324–38.
Hansen, Scott D., and R. Dyche Mullins. 2015. "Lamellipodin Promotes Actin Assembly by Clustering Ena/VASP Proteins and Tethering Them to Actin Filaments." *eLife* 4 (August). https://doi.org/10.7554/eLife.06585.
Harrison, Stephen C. 2003. "Variation on an Src-like Theme." *Cell* 112 (6): 737–40.
Hayashi, Takashi, and Richard L. Huganir. 2004. "Tyrosine Phosphorylation and Regulation of the AMPA Receptor by SRC Family Tyrosine Kinases." *The Journal of Neuroscience: The Official Journal of the Society for Neuroscience* 24 (27): 6152–60.
Hiipakka, Marita, and Kalle Saksela. 2007. "Versatile Retargeting of SH3 Domain Binding by Modification of Non-Conserved Loop Residues." *FEBS Letters* 581 (9): 1735–41.
Hoffmann, F. Michael, Lucille D. Fresco, Hedda Hoffman-Falk, and Ben-Zion Shilo. 1983. "Nucleotide Sequences of the Drosophila Src and Abl Homologs: Conservation and Variability in the Src Family Oncogenes." *Cell* 35 (2, Part 1): 393–401.
Huang, Yu, Mo-Chou Chen-Hwang, Georgia Dolios, Noriko Murakami, Júlio C. Padovan, Rong Wang, and Yu-Wen Hwang. 2004. "Mnb/Dyrk1A Phosphorylation Regulates the Interaction of Dynamin 1 with SH3 Domain-Containing Proteins." *Biochemistry* 43 (31): 10173–85.
Hunter, T. 1998. "The Croonian Lecture 1997. The Phosphorylation of Proteins on Tyrosine: Its Role in Cell Growth and Disease." *Philosophical Transactions of the Royal Society of London. Series B, Biological Sciences* 353 (1368): 583–605.
Hunter, T., and B. M. Sefton. 1980. "Transforming Gene Product of Rous Sarcoma Virus Phosphorylates Tyrosine." *Proceedings of the National Academy of Sciences of the United States of America* 77 (3): 1311–15.
Huse, Morgan, and John Kuriyan. 2002. "The Conformational Plasticity of Protein Kinases." *Cell* 109 (3): 275–82.
Ignelzi, Michael A., Danette R. Miller, Philippe Soriano, and Patricia F. Maness. 1994. "Impaired Neurite Outgrowth of Src-Minus Cerebellar Neurons on the Cell Adhesion Molecule L1." *Neuron* 12 (4): 873–84.
Imamoto, A., and P. Soriano. 1993. "Disruption of the Csk Gene, Encoding a Negative Regulator of Src Family Tyrosine Kinases, Leads to Neural Tube Defects and Embryonic Lethality in Mice." *Cell* 73 (6): 1117–24.
Inomata, Mika, Yoshiharu Takayama, Hiroshi Kiyama, Shigeyuki Nada, Masato Okada, and Hachiro Nakagawa. 1994. "Regulation of Src Family Kinases in the Developing Rat Brain: Correlation with Their Regulator Kinase, Csk1." *Journal of Biochemistry* 116 (2): 386–92.
Irimia, Manuel, Robert J. Weatheritt, Jonathan D. Ellis, Neelroop N. Parikshak, Thomas Gonatopoulos-Pournatzis, Mariana Babor, Mathieu Quesnel-Vallières, et al. 2014. "A Highly Conserved Program of Neuronal Microexons Is Misregulated in Autistic Brains." *Cell* 159 (7): 1511–23.

Irtegun, Sevgi, Rebecca J. Wood, Angelique R. Ormsby, Terrence D. Mulhern, and Danny M. Hatters. 2013. “Tyrosine 416 Is Phosphorylated in the Closed, Repressed Conformation of c-Src.” *PloS One* 8 (7): e71035.

Ishihama, Yasushi, Yoshiya Oda, Tsuyoshi Tabata, Toshitaka Sato, Takeshi Nagasu, Juri Rappsilber, and Matthias Mann. 2005. “Exponentially Modified Protein Abundance Index (emPAI) for Estimation of Absolute Protein Amount in Proteomics by the Number of Sequenced Peptides per Protein.” *Molecular & Cellular Proteomics: MCP* 4 (9): 1265–72.

Janoštiak, Radoslav, Ondřej Tolde, Zuzana Brůhová, Marian Novotný, Steven K. Hanks, Daniel Rösel, and Jan Brábek. 2011. “Tyrosine Phosphorylation within the SH3 Domain Regulates CAS Subcellular Localization, Cell Migration, and Invasiveness.” *Molecular Biology of the Cell* 22 (22): 4256–67.

Jeon, Chan-Young, Mi-Young Moon, Jong-Hyun Kim, Hee-Jun Kim, Jae-Gyu Kim, Yi Li, Jae-Kwang Jin, et al. 2012. “Control of Neurite Outgrowth by RhoA Inactivation.” *Journal of Neurochemistry* 120 (5): 684–98.

Jiang, Ruotian, Adeline Martz, Sophie Gonin, Antoine Taly, Lia Prado de Carvalho, and Thomas Grutter. 2010. “A Putative Extracellular Salt Bridge at the Subunit Interface Contributes to the Ion Channel Function of the ATP-Gated P2X2 Receptor.” *The Journal of Biological Chemistry* 285 (21): 15805–15.

Johnson, Sam A., and Tony Hunter. 2005. “Kinomics: Methods for Deciphering the Kinome.” *Nature Methods* 2 (1): 17–25.

Kamps, M. P., J. E. Buss, and B. M. Sefton. 1985. “Mutation of NH2-Terminal Glycine of p60src Prevents Both Myristoylation and Morphological Transformation.” *Proceedings of the National Academy of Sciences of the United States of America* 82 (14): 4625–28.

Kaneko, Tomonori, Lei Li, and Shawn S-C Li. 2008. “The SH3 Domain--a Family of Versatile Peptide- and Protein-Recognition Module.” *Frontiers in Bioscience: A Journal and Virtual Library* 13 (May): 4938–52.

Kang, H., C. Freund, J. S. Duke-Cohan, A. Musacchio, G. Wagner, and C. E. Rudd. 2000. “SH3 Domain Recognition of a Proline-Independent Tyrosine-Based RKxxYxxY Motif in Immune Cell Adaptor SKAP55.” *The EMBO Journal* 19 (12): 2889–99.

Kaplan, J. M., H. E. Varmus, and J. M. Bishop. 1990. “The Src Protein Contains Multiple Domains for Specific Attachment to Membranes.” *Molecular and Cellular Biology* 10 (3): 1000–1009.

Kärkkäinen, Satu, Marita Hiipakka, Jing-Huan Wang, Iivari Kleino, Marika Vähä-Jaakkola, G. Herma Renkema, Michael Liss, Ralf Wagner, and Kalle Saksela. 2006. “Identification of Preferred Protein Interactions by Phage-Display of the Human Src Homology-3 Proteome.” *EMBO Reports* 7 (2): 186–91.

Kasahara, Kousuke, Yuji Nakayama, Akio Kihara, Daisuke Matsuda, Kikuko Ikeda, Takahisa Kuga, Yasunori Fukumoto, Yasuyuki Igarashi, and Naoto Yamaguchi. 2007. “Rapid Trafficking of c-Src, a Non-Palmitoylated Src-Family Kinase, between the Plasma Membrane and Late Endosomes/lysosomes.” *Experimental Cell Research* 313 (12): 2651–66.

Kataoka, Y., T. Matsumura, S. Yamamoto, T. Sugimoto, and T. Sawada. 1993. “Distinct Cytotoxicity against Neuroblastoma Cells of Peripheral Blood and Tumor-Infiltrating Lymphocytes from Patients with Neuroblastoma.” *Cancer Letters* 73 (1): 11–21.

Katyal, Priya, Robbins Puthenveetil, and Olga Vinogradova. 2013. “Structural Insights into the Recognition of β3 Integrin Cytoplasmic Tail by the SH3 Domain of Src Kinase.” *Protein Science: A Publication of the Protein Society* 22 (10): 1358–65.

Keenan, Sarah. 2012. “Structure-Function Studies of the Neuronal Src Kinases.” University of York. http://etheses.whiterose.ac.uk/3294/.

Keenan, Sarah, Philip A. Lewis, Sarah J. Wetherill, Christopher J. R. Dunning, and Gareth J.

O. Evans. 2015. “The N2-Src Neuronal Splice Variant of C-Src Has Altered SH3 Domain Ligand Specificity and a Higher Constitutive Activity than N1-Src.” *FEBS Letters* 589 (15): 1995–2000.

Keenan, Sarah, Sarah J. Wetherill, Christopher I. Ugbode, Sangeeta Chawla, William J. Brackenbury, and Gareth J. O. Evans. 2017. “Inhibition of N1-Src Kinase by a Specific SH3 Peptide Ligand Reveals a Role for N1-Src in Neurite Elongation by L1-CAM.” *Scientific Reports* 7 (February): 43106.

Keenan, S., P. A. Lewis, S. J. Wetherill, and Cjr Dunning. 2015. “The N2-Src Neuronal Splice Variant of C-Src Has Altered SH3 Domain Ligand Specificity and a Higher Constitutive Activity than N1-Src.” *FEBS*. http://onlinelibrary.wiley.com/doi/10.1016/j.febslet.2015.05.033/full.

Khodosevich, Konstantin, and Hannah Monyer. 2010. “Signaling Involved in Neurite Outgrowth of Postnatally Born Subventricular Zone Neurons in Vitro.” *BMC Neuroscience* 11 (February): 18.

Kiefel, Helena, Sandra Bondong, John Hazin, Johannes Ridinger, Uwe Schirmer, Svenja Riedle, and Peter Altevogt. 2012. “L1CAM: A Major Driver for Tumor Cell Invasion and Motility.” *Cell Adhesion & Migration* 6 (4): 374–84.

Kim, Jae-Gyu, Kyoung-Chan Choi, Chang-Won Hong, Hwee-Seon Park, Eun-Kyoung Choi, Yong-Sun Kim, and Jae-Bong Park. 2017. “Tyr42 Phosphorylation of RhoA GTPase Promotes Tumorigenesis through Nuclear Factor (NF)-κB.” *Free Radical Biology & Medicine* 112 (November): 69–83.

Kinnunen, T., M. Kaksonen, J. Saarinen, N. Kalkkinen, H. B. Peng, and H. Rauvala. 1998. “Cortactin-Src Kinase Signaling Pathway Is Involved in N-Syndecan-Dependent Neurite Outgrowth.” *The Journal of Biological Chemistry* 273 (17): 10702–8.

Kleino, Iivari, Annika Järviluoma, Jussi Hepojoki, Ari Pekka Huovila, and Kalle Saksela. 2015. “Preferred SH3 Domain Partners of ADAM Metalloproteases Include Shared and ADAM-Specific SH3 Interactions.” *PloS One* 10 (3): e0121301.

Kloth, Michael T., Kristen K. Laughlin, Jacqueline S. Biscardi, Julie L. Boerner, Sarah J. Parsons, and Corinne M. Silva. 2003. “STAT5b, a Mediator of Synergism between c-Src and the Epidermal Growth Factor Receptor.” *The Journal of Biological Chemistry* 278 (3): 1671–79.

Kmiecik, Thomas E., and David Shalloway. 1987. “Activation and Suppression of pp60c-Src Transforming Ability by Mutation of Its Primary Sites of Tyrosine Phosphorylation.” *Cell* 49 (1): 65–73.

Knight, James D. R., Ruijun Tian, Robin E. C. Lee, Fangjun Wang, Ariane Beauvais, Hanfa Zou, Lynn A. Megeney, et al. 2012. “A Novel Whole-Cell Lysate Kinase Assay Identifies Substrates of the p38 MAPK in Differentiating Myoblasts.” *Skeletal Muscle* 2 (1): 5.

Knöll, Bernd, and Uwe Drescher. 2004. “Src Family Kinases Are Involved in EphA Receptor-Mediated Retinal Axon Guidance.” *The Journal of Neuroscience: The Official Journal of the Society for Neuroscience* 24 (28): 6248–57.

Knott, Gavin J., Charles S. Bond, and Archa H. Fox. 2016. “The DBHS Proteins SFPQ, NONO and PSPC1: A Multipurpose Molecular Scaffold.” *Nucleic Acids Research* 44 (9): 3989–4004.

Koch, C. A., M. F. Moran, D. Anderson, X. Q. Liu, G. Mbamalu, and T. Pawson. 1992. “Multiple SH2-Mediated Interactions in v-Src-Transformed Cells.” *Molecular and Cellular Biology* 12 (3): 1366–74.

Kokoszka, Malgorzata E., Stefanie L. Kall, Sehar Khosla, Jennifer E. McGinnis, Arnon Lavie, and Brian K. Kay. 2018. “Identification of Two Distinct Peptide-Binding Pockets in the SH3 Domain of Human Mixed-Lineage Kinase 3.” *The Journal of Biological Chemistry*, July. https://doi.org/10.1074/jbc.RA117.000262.

Korade, Zeljka, and Anne K. Kenworthy. 2008. “Lipid Rafts, Cholesterol, and the Brain.” *Neuropharmacology* 55 (8): 1265–73.

Kosako, Hidetaka, and Kohji Nagano. 2011. “Quantitative Phosphoproteomics Strategies for Understanding Protein Kinase-Mediated Signal Transduction Pathways.” *Expert Review of Proteomics* 8 (1): 81–94.

Kotani, Takenori, Nobuhiro Morone, Shigeki Yuasa, Shigeyuki Nada, and Masato Okada. 2007. “Constitutive Activation of Neuronal Src Causes Aberrant Dendritic Morphogenesis in Mouse Cerebellar Purkinje Cells.” *Neuroscience Research* 57 (2): 210–19.

Krause, Matthias, Erik W. Dent, James E. Bear, Joseph J. Loureiro, and Frank B. Gertler. 2003. “E NA /VASP P ROTEINS : Regulators of the Actin Cytoskeleton and Cell Migration.” *Annual Review of Cell and Developmental Biology* 19 (1): 541–64.

Kremer, N. E., G. D’Arcangelo, S. M. Thomas, M. DeMarco, J. S. Brugge, and S. Halegoua. 1991. “Signal Transduction by Nerve Growth Factor and Fibroblast Growth Factor in PC12 Cells Requires a Sequence of Src and Ras Actions.” *The Journal of Cell Biology* 115 (3): 809–19.

Kükenshöner, Tim, Nadine Eliane Schmit, Emilie Bouda, Fern Sha, Florence Pojer, Akiko Koide, Markus Seeliger, Shohei Koide, and Oliver Hantschel. 2017. “Selective Targeting of SH2 Domain-Phosphotyrosine Interactions of Src Family Tyrosine Kinases with Monobodies.” *Journal of Molecular Biology* 429 (9): 1364–80.

Lambrechts, A., A. V. Kwiatkowski, L. M. Lanier, J. E. Bear, J. Vandekerckhove, C. Ampe, and F. B. Gertler. 2000. “cAMP-Dependent Protein Kinase Phosphorylation of EVL, a Mena/VASP Relative, Regulates Its Interaction with Actin and SH3 Domains.” *The Journal of Biological Chemistry* 275: 36143–51.

Lamontanara, Allan Joaquim, Sandrine Georgeon, Giancarlo Tria, Dmitri I. Svergun, and Oliver Hantschel. 2014. “The SH2 Domain of Abl Kinases Regulates Kinase Autophosphorylation by Controlling Activation Loop Accessibility.” *Nature Communications* 5 (November): 5470.

Lanier, L. M., M. A. Gates, W. Witke, A. S. Menzies, A. M. Wehman, J. D. Macklis, D. Kwiatkowski, P. Soriano, and F. B. Gertler. 1999. “Mena Is Required for Neurulation and Commissure Formation.” *Neuron* 22 (2): 313–25.

Laurent, Benoit, Lv Ruitu, Jernej Murn, Kristina Hempel, Ryan Ferrao, Yang Xiang, Shichong Liu, et al. 2015. “A Specific LSD1/KDM1A Isoform Regulates Neuronal Differentiation through H3K9 Demethylation.” *Molecular Cell* 57 (6): 957–70.

Le Beau, J. M., O. D. Wiestler, and G. Walter. 1987. “An Altered Form of pp60c-Src Is Expressed Primarily in the Central Nervous System.” *Molecular and Cellular Biology* 7: 4115–17.

Lemmon, Mark A., and Joseph Schlessinger. 2010. “Cell Signaling by Receptor Tyrosine Kinases.” *Cell* 141 (7): 1117–34.

Levy, J. B., and J. S. Brugge. 1989. “Biological and Biochemical Properties of the c-Src+ Gene Product Overexpressed in Chicken Embryo Fibroblasts.” *Molecular and Cellular Biology* 9 (8): 3332–41.

Levy, J. B., T. Dorai, L. H. Wang, and J. S. Brugge. 1987. “The Structurally Distinct Form of pp60c-Src Detected in Neuronal Cells Is Encoded by a Unique c-Src mRNA.” *Molecular and Cellular Biology* 7 (11): 4142–45.

Lewis, Philip A., Isobel C. Bradley, Alastair R. Pizzey, Harry V. Isaacs, and Gareth J. O. Evans. 2017. “N1-Src Kinase Is Required for Primary Neurogenesis inXenopus Tropicalis.” *The Journal of Neuroscience: The Official Journal of the Society for Neuroscience* 37 (35): 8477–85.

Li, Chen-Hong, Qi Zhang, Bunyen Teng, S. Jamal Mustafa, Jian-Ying Huang, and Han-Gang Yu. 2008. “Src Tyrosine Kinase Alters Gating of Hyperpolarization-Activated HCN4

Pacemaker Channel through Tyr531." *American Journal of Physiology-Cell Physiology* 294 (1): C355–62.
Li, Fei, and Joe Z. Tsien. 2009. "Memory and the NMDA Receptors." *The New England Journal of Medicine* 361 (3): 302–3.
Liu, Bernard A., Karl Jablonowski, Monica Raina, Michael Arcé, Tony Pawson, and Piers D. Nash. 2006. "The Human and Mouse Complement of SH2 Domain Proteins—Establishing the Boundaries of Phosphotyrosine Signaling." *Molecular Cell* 22 (6): 851–68.
Liu, Bernard A., Karl Jablonowski, Eshana E. Shah, Brett W. Engelmann, Richard B. Jones, and Piers D. Nash. 2010. "SH2 Domains Recognize Contextual Peptide Sequence Information to Determine Selectivity." *Molecular & Cellular Proteomics: MCP* 9 (11): 2391–2404.
Liu, Qin, Donna Berry, Piers Nash, Tony Pawson, C. Jane McGlade, and Shawn Shun-Cheng Li. 2003. "Structural Basis for Specific Binding of the Gads SH3 Domain to an RxxK Motif-Containing SLP-76 Peptide: A Novel Mode of Peptide Recognition." *Molecular Cell* 11 (2): 471–81.
Liu, Y., K. Shah, F. Yang, L. Witucki, and K. M. Shokat. 1998. "A Molecular Gate Which Controls Unnatural ATP Analogue Recognition by the Tyrosine Kinase v-Src." *Bioorganic & Medicinal Chemistry* 6 (8): 1219–26.
Li, Weiquan, Jeeyong Lee, Haris G. Vikis, Seung-Hee Lee, Guofa Liu, Jennifer Aurandt, Tang-Long Shen, et al. 2004. "Activation of FAK and Src Are Receptor-Proximal Events Required for Netrin Signaling." *Nature Neuroscience* 7 (11): 1213–21.
Lowery, Laura Anne, Jamie Rubin, and Hazel Sive. 2007. "Whitesnake/sfpq Is Required for Cell Survival and Neuronal Development in the Zebrafish." *Developmental Dynamics: An Official Publication of the American Association of Anatomists* 236 (5): 1347–57.
Lukong, Kiven E., Marc-Etienne Huot, and Stéphane Richard. 2009. "BRK Phosphorylates PSF Promoting Its Cytoplasmic Localization and Cell Cycle Arrest." *Cellular Signalling* 21 (9): 1415–22.
Luo, Lin, Jing Xue, Ann Kwan, Roland Gamsjaeger, Jerome Wielens, Lisa von Kleist, Liza Cubeddu, et al. 2016. "The Binding of Syndapin SH3 Domain to Dynamin Proline-Rich Domain Involves Short and Long Distance Elements." *The Journal of Biological Chemistry*, February. https://doi.org/10.1074/jbc.M115.703108.
Lynch, S. A., J. S. Brugge, and J. M. Levine. 1986. "Induction of Altered c-Src Product during Neural Differentiation of Embryonal Carcinoma Cells." *Science* 234 (4778): 873–76.
Maffei, Mariano, Miguel Arbesú, Anabel-Lise Le Roux, Irene Amata, Serge Roche, and Miquel Pons. 2015. "The SH3 Domain Acts as a Scaffold for the N-Terminal Intrinsically Disordered Regions of c-Src." *Structure* 23 (5): 893–902.
Magee, J. C. 1998. "Dendritic Hyperpolarization-Activated Currents Modify the Integrative Properties of Hippocampal CA1 Pyramidal Neurons." *The Journal of Neuroscience: The Official Journal of the Society for Neuroscience* 18 (19): 7613–24.
———. 1999. "Dendritic Lh Normalizes Temporal Summation in Hippocampal CA1 Neurons." *Nature Neuroscience* 2 (6): 508–14.
Maness, P. F., M. Aubry, C. G. Shores, L. Frame, and K. H. Pfenninger. 1988. "C-Src Gene Product in Developing Rat Brain Is Enriched in Nerve Growth Cone Membranes." *Proceedings of the National Academy of Sciences* 85 (14): 5001–5.
Maness, P. F., and W. T. Matten. 1990. "Tyrosine Phosphorylation of Membrane-Associated Tubulin in Nerve Growth Cones Enriched in pp60c-Src." *Ciba Foundation Symposium* 150: 57–69; discussion 69–78.
Manning, G., D. B. Whyte, R. Martinez, T. Hunter, and S. Sudarsanam. 2002. "The Protein Kinase Complement of the Human Genome." *Science* 298 (5600): 1912–34.

Martinez, R., B. Mathey-Prevot, A. Bernards, and D. Baltimore. 1987. “Neuronal pp60c-Src Contains a Six-Amino Acid Insertion Relative to Its Non-Neuronal Counterpart.” *Science* 237 (4813): 411–15.

Matsunaga, Tadashi, Hiroshi Shirasawa, Masahiro Tanabe, Naomi Ohnuma, Hideyo Takahashi, and Bunsiti Simizu. 1993. “Expression of Alternatively Spliced Src Messenger RNAs Related to Neuronal Differentiation in Human Neuroblastomas.” *Cancer Research* 53 (13): 3179–85.

Matsunaga, T., H. Shirasawa, H. Enomoto, H. Yoshida, J. Iwai, M. Tanabe, K. Kawamura, T. Etoh, and N. Ohnuma. 1998. “Neuronal Src and Trk a Protooncogene Expression in Neuroblastomas and Patient Prognosis.” *International Journal of Cancer. Journal International Du Cancer* 79 (3): 226–31.

Matsunaga, T., H. Shirasawa, M. Tanabe, N. Ohnuma, K. Kawamura, T. Etoh, H. Takahashi, and B. Simizu. 1994. “Expression of Neuronal Src mRNA as a Favorable Marker and Inverse Correlation to N-Myc Gene Amplification in Human Neuroblastomas.” *International Journal of Cancer. Journal International Du Cancer* 58: 793–98.

Matsunaga, T., H. Shirasawa, M. Tanabe, N. Ohnuma, H. Takahashi, and B. Simizu. 1993. “Expression of Alternatively Spliced Src Messenger RNAs Related to Neuronal Differentiation in Human Neuroblastomas.” *Cancer Research* 53 (13): 3179–85.

Meng, Yilin, and Benoît Roux. 2014. “Locking the Active Conformation of c-Src Kinase through the Phosphorylation of the Activation Loop.” *Journal of Molecular Biology* 426 (2): 423–35.

Menzies, A. Sheila, Attila Aszodi, Scott E. Williams, Alexander Pfeifer, Ann M. Wehman, Keow Lin Goh, Carol A. Mason, Reinhard Fassler, and Frank B. Gertler. 2004. “Mena and Vasodilator-Stimulated Phosphoprotein Are Required for Multiple Actin-Dependent Processes That Shape the Vertebrate Nervous System.” *The Journal of Neuroscience: The Official Journal of the Society for Neuroscience* 24 (37): 8029–38.

Messina, Samantha, Franco Onofri, Lucilla Bongiorno-Borbone, Silvia Giovedì, Flavia Valtorta, Jean-Antoine Girault, and Fabio Benfenati. 2003. “Specific Interactions of Neuronal Focal Adhesion Kinase Isoforms with Src Kinases and Amphiphysin.” *Journal of Neurochemistry* 84 (2): 253–65.

Min, H., C. W. Turck, J. M. Nikolic, and D. L. Black. 1997. “A New Regulatory Protein, KSRP, Mediates Exon Inclusion through an Intronic Splicing Enhancer.” *Genes & Development* 11 (8): 1023–36.

Miyagi, Yohei, Tetsuji Yamashita, Masahiro Fukaya, Tomoko Sonoda, Toshiaki Okuno, Kazuyuki Yamada, Masahiko Watanabe, et al. 2002. “Delphilin: A Novel PDZ and Formin Homology Domain-Containing Protein That Synaptically Colocalizes and Interacts with Glutamate Receptor δ2 Subunit.” *The Journal of Neuroscience: The Official Journal of the Society for Neuroscience* 22 (3): 803–14.

Moarefi, I., M. LaFevre-Bernt, F. Sicheri, M. Huse, C. H. Lee, J. Kuriyan, and W. T. Miller. 1997. “Activation of the Src-Family Tyrosine Kinase Hck by SH3 Domain Displacement.” *Nature* 385 (6617): 650–53.

Moroco, Jamie A., Jodi K. Craigo, Roxana E. Iacob, Thomas E. Wales, John R. Engen, and Thomas E. Smithgall. 2014. “Differential Sensitivity of Src-Family Kinases to Activation by SH3 Domain Displacement.” *PloS One* 9 (8): e105629.

Morse, Wendy R., John G. Whitesides, Anthony-Samuel LaMantia, and Patricia F. Maness. 1998. “p59fyn and pp60c-Src Modulate Axonal Guidance in the Developing Mouse Olfactory Pathway.” *Journal of Neurobiology* 36 (1): 53–63.

Morton, C. J., D. J. Pugh, E. L. Brown, J. D. Kahmann, D. A. Renzoni, and I. D. Campbell. 1996. “Solution Structure and Peptide Binding of the SH3 Domain from Human Fyn.” *Structure* 4 (6): 705–14.

Moss, Stephen J., George H. Gorrie, Alessandra Amato, and Trevor G. Smart. 1995.

"Modulation of GABAA Receptors by Tyrosine Phosphorylation." *Nature* 377 (6547): 344–48.

Mukherjee, Abir, Lionel Arnaud, and Jonathan A. Cooper. 2003. "Lipid-Dependent Recruitment of Neuronal Src to Lipid Rafts in the Brain." *The Journal of Biological Chemistry* 278 (42): 40806–14.

Müller, André C., Roberto Giambruno, Juliane Weißer, Peter Májek, Alexandre Hofer, Johannes W. Bigenzahn, Giulio Superti-Furga, Henning J. Jessen, and Keiryn L. Bennett. 2016. "Identifying Kinase Substrates via a Heavy ATP Kinase Assay and Quantitative Mass Spectrometry." *Scientific Reports* 6 (June): 28107.

Murphy, S. M., M. Bergman, and D. O. Morgan. 1993. "Suppression of c-Src Activity by C-Terminal Src Kinase Involves the c-Src SH2 and SH3 Domains: Analysis with Saccharomyces Cerevisiae." *Molecular and Cellular Biology* 13 (9): 5290–5300.

Musacchio, Andrea, Martin Noble, Richard Pauptit, Rik Wierenga, and Matti Saraste. 1992. "Crystal Structure of a Src-Homology 3 (SH3) Domain." *Nature* 359 (6398): 851–55.

Musacchio, A., M. Saraste, and M. Wilmanns. 1994. "High-Resolution Crystal Structures of Tyrosine Kinase SH3 Domains Complexed with Proline-Rich Peptides." *Nature Structural Biology* 1 (8): 546–51.

Naganuma, Takao, Shinichi Nakagawa, Akie Tanigawa, Yasnory F. Sasaki, Naoki Goshima, and Tetsuro Hirose. 2012. "Alternative 3′-End Processing of Long Noncoding RNA Initiates Construction of Nuclear Paraspeckles." *The EMBO Journal* 31 (20): 4020–34.

Nisticò, P., and Modugno F. Di. 2011. "ENAH (enabled Homolog (Drosophila))." *Atlas of Genetics and Cytogenetics in Oncology and Haematology*, no. 7. https://doi.org/10.4267/2042/44510.

Ohnishi, H., S. Yamamori, K. Ono, K. Aoyagi, S. Kondo, and M. Takahashi. 2001. "A Src Family Tyrosine Kinase Inhibits Neurotransmitter Release from Neuronal Cells." *Proceedings of the National Academy of Sciences of the United States of America* 98 (19): 10930–35.

Ohnishi, Takafumi, Michiko Shirane, Yutaka Hashimoto, Shotaro Saita, and Keiichi I. Nakayama. 2014. "Identification and Characterization of a Neuron-Specific Isoform of Protrudin." *Genes to Cells: Devoted to Molecular & Cellular Mechanisms* 19 (2): 97–111.

Okada, Hirokazu, Akiyoshi Uezu, Frank M. Mason, Erik J. Soderblom, M. Arthur Moseley 3rd, and Scott H. Soderling. 2011. "SH3 Domain-Based Phototrapping in Living Cells Reveals Rho Family GAP Signaling Complexes." *Science Signaling* 4 (201): rs13.

Okamoto, Wataru, Isamu Okamoto, Takeshi Yoshida, Kunio Okamoto, Ken Takezawa, Erina Hatashita, Yuki Yamada, et al. 2010. "Identification of c-Src as a Potential Therapeutic Target for Gastric Cancer and of MET Activation as a Cause of Resistance to c-Src Inhibition." *Molecular Cancer Therapeutics* 9 (5): 1188–97.

Onofri, Franco, Mirko Messa, Vittoria Matafora, Giambattista Bonanno, Anna Corradi, Angela Bachi, Flavia Valtorta, and Fabio Benfenati. 2007. "Synapsin Phosphorylation by SRC Tyrosine Kinase Enhances SRC Activity in Synaptic Vesicles." *The Journal of Biological Chemistry* 282 (21): 15754–67.

Osusky, M., S. J. Taylor, and D. Shalloway. 1995. "Autophosphorylation of Purified c-Src at Its Primary Negative Regulation Site." *The Journal of Biological Chemistry* 270 (43): 25729–32.

Owen, D. J., P. Wigge, Y. Vallis, J. D. Moore, P. R. Evans, and H. T. McMahon. 1998. "Crystal Structure of the Amphiphysin-2 SH3 Domain and Its Role in the Prevention of Dynamin Ring Formation." *The EMBO Journal* 17 (18): 5273–85.

Paladino, David, Peibin Yue, Hideki Furuya, Jared Acoba, Charles J. Rosser, and James Turkson. 2016. "A Novel Nuclear Src and p300 Signaling Axis Controls Migratory and Invasive Behavior in Pancreatic Cancer." *Oncotarget* 7 (6): 7253–67.

Palmer, Amparo, Manuel Zimmer, Kai S. Erdmann, Volker Eulenburg, Annika Porthin, Rolf Heumann, Urban Deutsch, and Rüdiger Klein. 2002. “EphrinB Phosphorylation and Reverse Signaling: Regulation by Src Kinases and PTP-BL Phosphatase.” *Molecular Cell* 9 (4): 725–37.

Parker, R. C., G. Mardon, R. V. Lebo, H. E. Varmus, and J. M. Bishop. 1985. “Isolation of Duplicated Human c-Src Genes Located on Chromosomes 1 and 20.” *Molecular and Cellular Biology* 5 (4): 831–38.

Park, Sun Joo, Shiro Suetsugu, and Tadaomi Takenawa. 2005. “Interaction of HSP90 to N-WASP Leads to Activation and Protection from Proteasome-Dependent Degradation.” *The EMBO Journal* 24 (8): 1557–70.

Pellicena, P., K. R. Stowell, and W. T. Miller. 1998. “Enhanced Phosphorylation of Src Family Kinase Substrates Containing SH2 Domain Binding Sites.” *The Journal of Biological Chemistry* 273 (25): 15325–28.

Peng, Z. Y., and C. A. Cartwright. 1995. “Regulation of the Src Tyrosine Kinase and Syp Tyrosine Phosphatase by Their Cellular Association.” *Oncogene* 11 (10): 1955–62.

Pérez, Yolanda, Margarida Gairí, Miquel Pons, and Pau Bernadó. 2009. “Structural Characterization of the Natively Unfolded N-Terminal Domain of Human c-Src Kinase: Insights into the Role of Phosphorylation of the Unique Domain.” *Journal of Molecular Biology* 391 (1): 136–48.

Pérez, Yolanda, Mariano Maffei, Ana Igea, Irene Amata, Margarida Gairí, Angel R. Nebreda, Pau Bernadó, and Miquel Pons. 2013. “Lipid Binding by the Unique and SH3 Domains of c-Src Suggests a New Regulatory Mechanism.” *Scientific Reports* 3: 1295.

Pollitt, Alice Y., and Robert H. Insall. 2009. “WASP and SCAR/WAVE Proteins: The Drivers of Actin Assembly.” *Journal of Cell Science* 122 (Pt 15): 2575–78.

Pyper, J. M., and J. B. Bolen. 1989. “Neuron-Specific Splicing of C-SRC RNA in Human Brain.” *Journal of Neuroscience Research* 24 (1): 89–96.

———. 1990. “Identification of a Novel Neuronal C-SRC Exon Expressed in Human Brain.” *Molecular and Cellular Biology* 10 (5): 2035–40.

Raj, Bushra, and Benjamin J. Blencowe. 2015. “Alternative Splicing in the Mammalian Nervous System: Recent Insights into Mechanisms and Functional Roles.” *Neuron* 87 (1): 14–27.

Ramjaun, A. R., K. D. Micheva, I. Bouchelet, and P. S. McPherson. 1997. “Identification and Characterization of a Nerve Terminal-Enriched Amphiphysin Isoform.” *The Journal of Biological Chemistry* 272 (26): 16700–706.

Ratner, Nancy, Garrett M. Brodeur, Russell C. Dale, and Nina F. Schor. 2016. “The ‘Neuro’ of Neuroblastoma: Neuroblastoma as a Neurodevelopmental Disorder.” *Annals of Neurology* 80 (1): 13–23.

Raulf, F., S. M. Robertson, and M. Schartl. 1989. “Evolution of the Neuron-Specific Alternative Splicing Product of the c-Src Proto-Oncogene.” *Journal of Neuroscience Research* 24 (1): 81–88.

Refaei, Mary Anne, Al Combs, Douglas J. Kojetin, John Cavanagh, Carol Caperelli, Mark Rance, Jennifer Sapitro, and Pearl Tsang. 2011. “Observing Selected Domains in Multi-Domain Proteins via Sortase-Mediated Ligation and NMR Spectroscopy.” *Journal of Biomolecular NMR* 49 (1): 3–7.

Resh, M. D. 1993. “Interaction of Tyrosine Kinase Oncoproteins with Cellular Membranes.” *Biochimica et Biophysica Acta* 1155 (3): 307–22.

———. 1994. “Myristylation and Palmitylation of Src Family Members: The Fats of the Matter.” *Cell* 76 (3): 411–13.

———. 1999. “Fatty Acylation of Proteins: New Insights into Membrane Targeting of Myristoylated and Palmitoylated Proteins.” *Biochimica et Biophysica Acta* 1451 (1): 1–16.

Reynolds, A. B., J. Vila, T. J. Lansing, W. M. Potts, M. J. Weber, and J. T. Parsons. 1987. "Activation of the Oncogenic Potential of the Avian Cellular Src Protein by Specific Structural Alteration of the Carboxy Terminus." *The EMBO Journal* 6 (8): 2359–64.

Reynolds, C. H., C. J. Garwood, S. Wray, C. Price, S. Kellie, T. Perera, M. Zvelebil, et al. 2008. "Phosphorylation Regulates Tau Interactions with Src Homology 3 Domains of Phosphatidylinositol 3-Kinase, Phospholipase C 1, Grb2, and Src Family Kinases." *The Journal of Biological Chemistry* 283 (26): 18177–86.

Richnau, N., and P. Aspenström. 2001. "Rich, a Rho GTPase-Activating Protein Domain-Containing Protein Involved in Signaling by Cdc42 and Rac1." *The Journal of Biological Chemistry* 276 (37): 35060–70.

Rooke, Nanette, Vadim Markovtsov, Esra Cagavi, and Douglas L. Black. 2003. "Roles for SR Proteins and hnRNP A1 in the Regulation of c-Src Exon N1." *Molecular and Cellular Biology* 23 (6): 1874–84.

Roskoski, Robert, Jr. 2004. "Src Protein–tyrosine Kinase Structure and Regulation." *Biochemical and Biophysical Research Communications* 324 (4): 1155–64.

———. 2005. "Src Kinase Regulation by Phosphorylation and Dephosphorylation." *Biochemical and Biophysical Research Communications* 331 (1): 1–14.

Roskoski, Robert, Jr. 2015. "Src Protein-Tyrosine Kinase Structure, Mechanism, and Small Molecule Inhibitors." *Pharmacological Research: The Official Journal of the Italian Pharmacological Society* 94 (April): 9–25.

Ross, C. A., G. E. Wright, M. D. Resh, R. C. Pearson, and S. H. Snyder. 1988. "Brain-Specific Src Oncogene mRNA Mapped in Rat Brain by in Situ Hybridization." *Proceedings of the National Academy of Sciences of the United States of America* 85 (24): 9831.

Rouer, Evelyne. 2010. "[Neuronal isoforms of Src, Fyn and Lck tyrosine kinases: A specific role for p56lckN in neuron protection]." *Comptes rendus biologies* 333 (1): 1–10.

Rouka, Evgenia, Philip C. Simister, Melanie Janning, Joerg Kumbrink, Tassos Konstantinou, João R. C. Muniz, Dhira Joshi, et al. 2015. "Differential Recognition Preferences of the Three Src Homology 3 (SH3) Domains from the Adaptor CD2-Associated Protein (CD2AP) and Direct Association with Ras and Rab Interactor 3 (RIN3)." *The Journal of Biological Chemistry* 290 (42): 25275–92.

Roussel, R. R., S. R. Brodeur, D. Shalloway, and A. P. Laudano. 1991. "Selective Binding of Activated pp60c-Src by an Immobilized Synthetic Phosphopeptide Modeled on the Carboxyl Terminus of pp60c-Src." *Proceedings of the National Academy of Sciences* 88 (23): 10696–700.

Roux, Kyle J., Dae In Kim, Manfred Raida, and Brian Burke. 2012. "A Promiscuous Biotin Ligase Fusion Protein Identifies Proximal and Interacting Proteins in Mammalian Cells." *The Journal of Cell Biology* 196 (6): 801–10.

Ruest, P. J., N. Y. Shin, T. R. Polte, X. Zhang, and S. K. Hanks. 2001. "Mechanisms of CAS Substrate Domain Tyrosine Phosphorylation by FAK and Src." *Molecular and Cellular Biology* 21 (22): 7641–52.

Rufer, Arne C., Julia Rumpf, Max von Holleben, Sandra Beer, Katrin Rittinger, and Yvonne Groemping. 2009. "Isoform-Selective Interaction of the Adaptor Protein Tks5/FISH with Sos1 and Dynamins." *Journal of Molecular Biology* 390 (5): 939–50.

Rusanescu, G., H. Qi, S. M. Thomas, J. S. Brugge, and S. Halegoua. 1995. "Calcium Influx Induces Neurite Growth through a Src-Ras Signaling Cassette." *Neuron* 15 (6): 1415–25.

Sachdev, Sanjay, Yahao Bu, and Irwin H. Gelman. 2009. "Paxillin-Y118 Phosphorylation Contributes to the Control of Src-Induced Anchorage-Independent Growth by FAK and Adhesion." *BMC Cancer* 9 (January): 12.

Saksela, Kalle, and Perttu Permi. 2012. "SH3 Domain Ligand Binding: What's the

Consensus and Where's the Specificity?" *FEBS Letters* 586 (17): 2609–14.
Sandilands, Emma, Valerie G. Brunton, and Margaret C. Frame. 2007. "The Membrane Targeting and Spatial Activation of Src, Yes and Fyn Is Influenced by Palmitoylation and Distinct RhoB/RhoD Endosome Requirements." *Journal of Cell Science* 120 (Pt 15): 2555–64.
Sandilands, Emma, Christophe Cans, Valerie J. Fincham, Valerie G. Brunton, Harry Mellor, George C. Prendergast, Jim C. Norman, Giulio Superti-Furga, and Margaret C. Frame. 2004. "RhoB and Actin Polymerization Coordinate Src Activation with Endosome-Mediated Delivery to the Membrane." *Developmental Cell* 7 (6): 855–69.
Santiveri, Clara M., Aldo Borroto, Luis Simón, Manuel Rico, Balbino Alarcón, and M. Angeles Jiménez. 2009. "Interaction between the N-Terminal SH3 Domain of Nckα and CD3ε-Derived Peptides: Non-Canonical and Canonical Recognition Motifs." *Biochimica et Biophysica Acta (BBA) - Proteins and Proteomics* 1794 (1): 110–17.
Santoro, B., S. G. Grant, D. Bartsch, and E. R. Kandel. 1997. "Interactive Cloning with the SH3 Domain of N-Src Identifies a New Brain Specific Ion Channel Protein, with Homology to Eag and Cyclic Nucleotide-Gated Channels." *Proceedings of the National Academy of Sciences of the United States of America* 94 (26): 14815–20.
Sato, Izumi, Yuuki Obata, Kousuke Kasahara, Yuji Nakayama, Yasunori Fukumoto, Takahito Yamasaki, Kazunari K. Yokoyama, Takashi Saito, and Naoto Yamaguchi. 2009. "Differential Trafficking of Src, Lyn, Yes and Fyn Is Specified by the State of Palmitoylation in the SH4 Domain." *Journal of Cell Science* 122 (Pt 7): 965–75.
Schaefer, Andrew W., Yoshimasa Kamei, Hiroyuki Kamiguchi, Eric V. Wong, Iris Rapoport, Tomas Kirchhausen, Carol M. Beach, Gary Landreth, Sandra K. Lemmon, and Vance Lemmon. 2002. "L1 Endocytosis Is Controlled by a Phosphorylation-Dephosphorylation Cycle Stimulated by Outside-in Signaling by L1." *The Journal of Cell Biology* 157 (7): 1223–32.
Schlessinger, Joseph. 2000. "Cell Signaling by Receptor Tyrosine Kinases." *Cell* 103 (2): 211–25.
Scholz, Ralf, Sven Berberich, Louisa Rathgeber, Alexander Kolleker, Georg Köhr, and Hans-Christian Kornau. 2010. "AMPA Receptor Signaling through BRAG2 and Arf6 Critical for Long-Term Synaptic Depression." *Neuron* 66 (5): 768–80.
Schwenk, Benjamin M., Christina M. Lang, Sebastian Hogl, Sabina Tahirovic, Denise Orozco, Kristin Rentzsch, Stefan F. Lichtenthaler, et al. 2014. "The FTLD Risk Factor TMEM106B and MAP6 Control Dendritic Trafficking of Lysosomes." *The EMBO Journal* 33 (5): 450–67.
Scott, Margaret Porter, Francesca Zappacosta, Eun Young Kim, Roland S. Annan, and W. Todd Miller. 2002. "Identification of Novel SH3 Domain Ligands for the Src Family Kinase Hck: WISKOTT-ALDRICH SYNDROME PROTEIN (WASP), WASP-INTERACTING PROTEIN (WIP), AND ELMO1." *The Journal of Biological Chemistry* 277 (31): 28238–46.
Sefton, B. M., and T. Hunter. 1986. "From c-Src to v-Src, or the Case of the Missing C Terminus." *Cancer Surveys* 5 (2): 159–72.
Ségaliny, Aude I., Marta Tellez-Gabriel, Marie-Françoise Heymann, and Dominique Heymann. 2015. "Receptor Tyrosine Kinases: Characterisation, Mechanism of Action and Therapeutic Interests for Bone Cancers." *Journal of Bone Oncology* 4 (1): 1–12.
Seidel-Dugan, C., B. E. Meyer, S. M. Thomas, and J. S. Brugge. 1992. "Effects of SH2 and SH3 Deletions on the Functional Activities of Wild-Type and Transforming Variants of c-Src." *Molecular and Cellular Biology* 12 (4): 1835–45.
Shastry, P., A. Basu, and M. S. Rajadhyaksha. 2001. "Neuroblastoma Cell Lines--a Versatile in Vitro Model in Neurobiology." *The International Journal of Neuroscience* 108 (1-2): 109–26.

Shchemelinin, I., L. Sefc, and E. Necas. 2006. “Protein Kinases, Their Function and Implication in Cancer and Other Diseases.” *Folia Biologica* 52 (3): 81–100.
Shenoy, S., I. Chackalaparampil, S. Bagrodia, P. H. Lin, and D. Shalloway. 1992. “Role of p34cdc2-Mediated Phosphorylations in Two-Step Activation of pp60c-Src during Mitosis.” *Proceedings of the National Academy of Sciences of the United States of America* 89 (15): 7237–41.
Shen, Z., A. Batzer, J. A. Koehler, P. Polakis, J. Schlessinger, N. B. Lydon, and M. F. Moran. 1999. “Evidence for SH3 Domain Directed Binding and Phosphorylation of Sam68 by Src.” *Oncogene* 18 (33): 4647–53.
Shi, Yongsheng, Dafne Campigli Di Giammartino, Derek Taylor, Ali Sarkeshik, William J. Rice, John R. Yates, Joachim Frank, and James L. Manley. 2009. “Molecular Architecture of the Human Pre-mRNA 3′ Processing Complex.” *Molecular Cell* 33 (3): 365–76.
Skupien, Anna, Anna Konopka, Pawei Trzaskoma, Josephine Labus, Adam Gorlewicz, Lukasz Swiech, Matylda Babraj, et al. 2014. “CD44 Regulates Dendrite Morphogenesis through Src Tyrosine Kinase-Dependent Positioning of the Golgi Apparatus.” *Journal of Cell Science* 127 (23): 5038–51.
Smalley, M. J. 2005. “Dishevelled (Dvl-2) Activates Canonical Wnt Signalling in the Absence of Cytoplasmic Puncta.” *Journal of Cell Science* 118 (22): 5279–89.
Solomaha, Elena, Frances L. Szeto, Mohammed A. Yousef, and H. Clive Palfrey. 2005. “Kinetics of Src Homology 3 Domain Association with the Proline-Rich Domain of Dynamins SPECIFICITY, OCCLUSION, AND THE EFFECTS OF PHOSPHORYLATION.” *The Journal of Biological Chemistry* 280 (24): 23147–56.
Somani, A. K., J. S. Bignon, G. B. Mills, K. A. Siminovitch, and D. R. Branch. 1997. “Src Kinase Activity Is Regulated by the SHP-1 Protein-Tyrosine Phosphatase.” *The Journal of Biological Chemistry* 272 (34): 21113–19.
Sommese, Ruth F., and Sivaraj Sivaramakrishnan. 2016. “Substrate Affinity Differentially Influences Protein Kinase C Regulation and Inhibitor Potency.” *The Journal of Biological Chemistry* 291 (42): 21963–70.
Songyang, Z., and L. C. Cantley. 1995. “Recognition and Specificity in Protein Tyrosine Kinase-Mediated Signalling.” *Trends in Biochemical Sciences* 20 (11): 470–75.
Songyang, Z., S. E. Shoelson, M. Chaudhuri, G. Gish, T. Pawson, W. G. Haser, F. King, T. Roberts, S. Ratnofsky, and R. J. Lechleider. 1993. “SH2 Domains Recognize Specific Phosphopeptide Sequences.” *Cell* 72 (5): 767–78.
Songyang, Z., S. E. Shoelson, J. McGlade, P. Olivier, T. Pawson, X. R. Bustelo, M. Barbacid, H. Sabe, H. Hanafusa, and T. Yi. 1994. “Specific Motifs Recognized by the SH2 Domains of Csk, 3BP2, Fps/fes, GRB-2, HCP, SHC, Syk, and Vav.” *Molecular and Cellular Biology* 14 (4): 2777–85.
Sorge, J. P., L. K. Sorge, and P. F. Maness. 1985. “pp60c-Src Is Expressed in Human Fetal and Adult Brain.” *The American Journal of Pathology* 119 (1): 151–57.
Soriano, P., C. Montgomery, R. Geske, and A. Bradley. 1991. “Targeted Disruption of the c-Src Proto-Oncogene Leads to Osteopetrosis in Mice.” *Cell* 64 (4): 693–702.
Souza, Gustavo A. de, Nils A. Leversen, Hiwa Målen, and Harald G. Wiker. 2011. “Bacterial Proteins with Cleaved or Uncleaved Signal Peptides of the General Secretory Pathway.” *Journal of Proteomics* 75 (2): 502–10.
Stamenova, Svetoslava D., Michael E. French, Yuan He, Smitha A. Francis, Zachary B. Kramer, and Linda Hicke. 2007. “Ubiquitin Binds to and Regulates a Subset of SH3 Domains.” *Molecular Cell* 25 (2): 273–84.
Stein, P. L., H. Vogel, and P. Soriano. 1994. “Combined Deficiencies of Src, Fyn, and Yes Tyrosine Kinases in Mutant Mice.” *Genes & Development* 8 (17): 1999–2007.
Stover, David R., Michael Becker, Janis Liebetanz, and Nicholas B. Lydon. 1995. “Src

Phosphorylation of the Epidermal Growth Factor Receptor at Novel Sites Mediates Receptor Interaction with Src and P85α." *The Journal of Biological Chemistry* 270 (26): 15591–97.

Su, Chun-Hao, D. Dhananjaya, and Woan-Yuh Tarn. 2018. "Alternative Splicing in Neurogenesis and Brain Development." *Frontiers in Molecular Biosciences* 5. https://doi.org/10.3389/fmolb.2018.00012.

Sugimoto, Y., E. Erikson, Y. Graziani, and R. L. Erikson. 1985. "Inter- and Intramolecular Interactions of Highly Purified Rous Sarcoma Virus-Transforming Protein, pp60v-Src." *The Journal of Biological Chemistry* 260 (25): 13838–43.

Sugrue, M. M., J. S. Brugge, D. R. Marshak, P. Greengard, and E. L. Gustafson. 1990. "Immunocytochemical Localization of the Neuron-Specific Form of the c-Src Gene Product, pp60c-Src(+), in Rat Brain." *The Journal of Neuroscience: The Official Journal of the Society for Neuroscience* 10 (8): 2513–27.

Sun, Zuyue, Xiujuan Li, Sara Massena, Simone Kutschera, Narendra Padhan, Laura Gualandi, Vibeke Sundvold-Gjerstad, et al. 2012. "VEGFR2 Induces c-Src Signaling and Vascular Permeability in Vivo via the Adaptor Protein TSAd." *The Journal of Experimental Medicine* 209 (7): 1363–77.

Szklarczyk, Damian, John H. Morris, Helen Cook, Michael Kuhn, Stefan Wyder, Milan Simonovic, Alberto Santos, et al. 2016. "The STRING Database in 2017: Quality-Controlled Protein–protein Association Networks, Made Broadly Accessible." *Nucleic Acids Research* 45 (D1): D362–68.

Taylor, S. J., M. Anafi, T. Pawson, and D. Shalloway. 1995. "Functional Interaction between c-Src and Its Mitotic Target, Sam 68." *The Journal of Biological Chemistry* 270 (17): 10120–24.

Tehrani, Shandiz, Nenad Tomasevic, Scott Weed, Roman Sakowicz, and John A. Cooper. 2007. "Src Phosphorylation of Cortactin Enhances Actin Assembly." *Proceedings of the National Academy of Sciences* 104 (29): 11933–38.

Teyra, Joan, Haiming Huang, Shobhit Jain, Xinyu Guan, Aiping Dong, Yanli Liu, Wolfram Tempel, et al. 2017. "Comprehensive Analysis of the Human SH3 Domain Family Reveals a Wide Variety of Non-Canonical Specificities." *Structure* , August. https://doi.org/10.1016/j.str.2017.07.017.

Thomas-Jinu, Swapna, Patricia M. Gordon, Triona Fielding, Richard Taylor, Bradley N. Smith, Victoria Snowden, Eric Blanc, et al. 2017. "Non-Nuclear Pool of Splicing Factor SFPQ Regulates Axonal Transcripts Required for Normal Motor Development." *Neuron* 94 (2): 322–36.e5.

Thomas, J. W., B. Ellis, R. J. Boerner, W. B. Knight, G. C. White 2nd, and M. D. Schaller. 1998. "SH2- and SH3-Mediated Interactions between Focal Adhesion Kinase and Src." *The Journal of Biological Chemistry* 273 (1): 577–83.

Thomas, S. M., and J. S. Brugge. 1997. "Cellular Functions Regulated by Src Family Kinases." *Annual Review of Cell and Developmental Biology* 13: 513–609.

Tong, Michael, Jeff G. Pelton, Michelle L. Gill, Weibing Zhang, Francis Picart, and Markus A. Seeliger. 2017. "Survey of Solution Dynamics in Src Kinase Reveals Allosteric Cross Talk between the Ligand Binding and Regulatory Sites." *Nature Communications* 8 (1): 2160.

Tsyba, Liudmyla, Tetyana Gryaznova, Oleksandr Dergai, Mykola Dergai, Inessa Skrypkina, Sergiy Kropyvko, Oleksiy Boldyryev, Oleksii Nikolaienko, Olga Novokhatska, and Alla Rynditch. 2008. "Alternative Splicing Affecting the SH3A Domain Controls the Binding Properties of Intersectin 1 in Neurons." *Biochemical and Biophysical Research Communications* 372 (4): 929–34.

Tu, Chun, Cesar F. Ortega-Cava, Paul Winograd, Marissa Jo Stanton, Alagarsamy Lakku Reddi, Ingrid Dodge, Ranjana Arya, et al. 2010. "Endosomal-Sorting Complexes

Required for Transport (ESCRT) Pathway-Dependent Endosomal Traffic Regulates the Localization of Active Src at Focal Adhesions." *Proceedings of the National Academy of Sciences of the United States of America* 107 (37): 16107–12.
Underwood, Jason G., Paul L. Boutz, Joseph D. Dougherty, Peter Stoilov, and Douglas L. Black. 2005. "Homologues of the Caenorhabditis Elegans Fox-1 Protein Are Neuronal Splicing Regulators in Mammals." *Molecular and Cellular Biology* 25 (22): 10005–16.
Venkatachalan, S. P., and C. Czajkowski. 2008. "A Conserved Salt Bridge Critical for GABAA Receptor Function and Loop C Dynamics." *Proceedings of the National Academy of Sciences* 105 (36): 13604–9.
Vidaki, Marina, Frauke Drees, Tanvi Saxena, Erwin Lanslots, Matthew J. Taliaferro, Antonios Tatarakis, Christopher B. Burge, Eric T. Wang, and Frank B. Gertler. 2017. "A Requirement for Mena, an Actin Regulator, in Local mRNA Translation in Developing Neurons." *Neuron* 95 (3): 608–22.e5.
Waksman, G., S. E. Shoelson, N. Pant, D. Cowburn, and J. Kuriyan. 1993. "Binding of a High Affinity Phosphotyrosyl Peptide to the Src SH2 Domain: Crystal Structures of the Complexed and Peptide-Free Forms." *Cell* 72 (5): 779–90.
Walker, F., J. deBlaquiere, and A. W. Burgess. 1993. "Translocation of pp60c-Src from the Plasma Membrane to the Cytosol after Stimulation by Platelet-Derived Growth Factor." *The Journal of Biological Chemistry* 268 (26): 19552–58.
Wang, Jiamin, Lili Yu, and Xinmin Zheng. 2013. "PTPα-Mediated Src Activation by EGF in Human Breast Cancer Cells." *Acta Biochimica et Biophysica Sinica* 45 (4): 320–29.
Wang, Kan, John T. Hackett, Michael E. Cox, Monique Van Hoek, Jon M. Lindstrom, and Sarah J. Parsons. 2004. "Regulation of the Neuronal Nicotinic Acetylcholine Receptor by SRC Family Tyrosine Kinases." *The Journal of Biological Chemistry* 279 (10): 8779–86.
Weernink, Paschal A. Oude, and Gert Rijksen. 1995. "Activation and Translocation of c-Src to the Cytoskeleton by Both Platelet-Derived Growth Factor and Epidermal Growth Factor." *The Journal of Biological Chemistry* 270 (5): 2264–67.
Weng, Z., R. J. Rickles, S. Feng, S. Richard, A. S. Shaw, S. L. Schreiber, and J. S. Brugge. 1995. "Structure-Function Analysis of SH3 Domains: SH3 Binding Specificity Altered by Single Amino Acid Substitutions." *Molecular and Cellular Biology* 15 (10): 5627–34.
Weng, Z., J. A. Taylor, C. E. Turner, J. S. Brugge, and C. Seidel-Dugan. 1993. "Detection of Src Homology 3-Binding Proteins, Including Paxillin, in Normal and v-Src-Transformed Balb/c 3T3 Cells." *The Journal of Biological Chemistry* 268 (20): 14956–63.
Weng, Z., S. M. Thomas, R. J. Rickles, J. A. Taylor, A. W. Brauer, C. Seidel-Dugan, W. M. Michael, G. Dreyfuss, and J. S. Brugge. 1994. "Identification of Src, Fyn, and Lyn SH3-Binding Proteins: Implications for a Function of SH3 Domains." *Molecular and Cellular Biology* 14 (7): 4509–21.
Wetherill, Sarah Jane. 2016. "The Role of N1-Src in Neuronal Development." Phd, University of York. http://etheses.whiterose.ac.uk/15573/.
Wiestler, O. D., and G. Walter. 1988. "Developmental Expression of Two Forms of pp60c-Src in Mouse Brain." *Molecular and Cellular Biology* 8 (1): 502–4.
Williams, J. C., A. Weijland, S. Gonfloni, A. Thompson, S. A. Courtneidge, G. Superti-Furga, and R. K. Wierenga. 1997. "The 2.35 A Crystal Structure of the Inactivated Form of Chicken Src: A Dynamic Molecule with Multiple Regulatory Interactions." *Journal of Molecular Biology* 274 (5): 757–75.
Williamson, Mike P. 2013. "Using Chemical Shift Perturbation to Characterise Ligand Binding." *Progress in Nuclear Magnetic Resonance Spectroscopy* 73 (August): 1–16.
Worley, T. L., E. Cornel, and C. E. Holt. 1997. "Overexpression of c-Src and N-Src in the

Developing Xenopus Retina Differentially Impairs Axonogenesis." *Molecular and Cellular Neurosciences* 9 (4): 276–92.
Wu, Yibing, Lisa M. Span, Patrik Nygren, Hua Zhu, David T. Moore, Hong Cheng, Heinrich Roder, William F. DeGrado, and Joel S. Bennett. 2015. "The Tyrosine Kinase c-Src Specifically Binds to the Active Integrin αIIbβ3 to Initiate Outside-in Signaling in Platelets." *The Journal of Biological Chemistry* 290 (25): 15825–34.
Xue, Liang, Robert L. Geahlen, and W. Andy Tao. 2013. "Identification of Direct Tyrosine Kinase Substrates Based on Protein Kinase Assay-Linked Phosphoproteomics." *Molecular & Cellular Proteomics: MCP* 12 (10): 2969–80.
Xu, W., A. Doshi, M. Lei, M. J. Eck, and S. C. Harrison. 1999. "Crystal Structures of c-Src Reveal Features of Its Autoinhibitory Mechanism." *Molecular Cell* 3 (5): 629–38.
Xu, W., S. C. Harrison, and M. J. Eck. 1997. "Three-Dimensional Structure of the Tyrosine Kinase c-Src." *Nature* 385: 595–602.
Yang, M., and J. P. Leonard. 2001. "Identification of Mouse NMDA Receptor Subunit NR2A C-Terminal Tyrosine Sites Phosphorylated by Coexpression with v-Src." *Journal of Neurochemistry* 77 (2): 580–88.
Yang, Yong, Theodore W. Thannhauser, Li Li, and Sheng Zhang. 2007. "Development of an Integrated Approach for Evaluation of 2-D Gel Image Analysis: Impact of Multiple Proteins in Single Spots on Comparative Proteomics in Conventional 2-D gel/MALDI Workflow." *Electrophoresis* 28 (12): 2080–94.
Yarosh, Christopher A., Joseph R. Iacona, Carol S. Lutz, and Kristen W. Lynch. 2015. "PSF: Nuclear Busy-Body or Nuclear Facilitator?" *Wiley Interdisciplinary Reviews. RNA* 6 (4): 351–67.
Yoo, Y., H. J. Ho, C. Wang, and J-L Guan. 2010. "Tyrosine Phosphorylation of Cofilin at Y68 by v-Src Leads to Its Degradation through Ubiquitin-Proteasome Pathway." *Oncogene* 29 (2): 263–72.
Yu, H., J. K. Chen, S. Feng, D. C. Dalgarno, A. W. Brauer, and S. L. Schreiber. 1994. "Structural Basis for the Binding of Proline-Rich Peptides to SH3 Domains." *Cell* 76 (5): 933–45.
Yu, Hongtao, Michael K. Rosen, T. Bum Shin, Cynthia Seidel-Dugan, Joan S. Brugge, and Stuart L. Schreiber. 1992. "Solution Structure of the SH3 Domain of Src and Identification of Its Ligand-Binding Site." *Science* 258: 1665–1665.
Yu, H., M. K. Rosen, T. B. Shin, C. Seidel-Dugan, J. S. Brugge, and S. L. Schreiber. 1992. "Solution Structure of the SH3 Domain of Src and Identification of Its Ligand-Binding Site." *Science* 258 (5088): 1665–68.
Yu, X. M., R. Askalan, G. J. Keil 2nd, and M. W. Salter. 1997. "NMDA Channel Regulation by Channel-Associated Protein Tyrosine Kinase Src." *Science* 275 (5300): 674–78.
Zhao, Weiqin, Sebastiano Cavallaro, Pavel Gusev, and Daniel L. Alkon. 2000. "Nonreceptor Tyrosine Protein Kinase pp60c-Src in Spatial Learning: Synapse-Specific Changes in Its Gene Expression, Tyrosine Phosphorylation, and Protein–protein Interactions." *Proceedings of the National Academy of Sciences* 97 (14): 8098–8103.
Zheng, F., M. B. Gingrich, S. F. Traynelis, and P. J. Conn. 1998. "Tyrosine Kinase Potentiates NMDA Receptor Currents by Reducing Tonic Zinc Inhibition." *Nature Neuroscience* 1 (3): 185–91.
Zisch, A. H., M. S. Kalo, L. D. Chong, and E. B. Pasquale. 1998. "Complex Formation between EphB2 and Src Requires Phosphorylation of Tyrosine 611 in the EphB2 Juxtamembrane Region." *Oncogene* 16 (20): 2657–70.